



# **THE ELECTROMAGNETIC ORIGIN OF QUANTUM THEORY AND LIGHT**

*Dale M. Grimes & Craig A. Grimes*

**World Scientific**

# **THE ELECTROMAGNETIC ORIGIN OF QUANTUM THEORY AND LIGHT**

This page is intentionally left blank

# THE ELECTROMAGNETIC ORIGIN OF QUANTUM THEORY AND LIGHT

*Dale M. Grimes & Craig A. Grimes*

*The Pennsylvania State University*



**World Scientific**

*New Jersey • London • Singapore • Hong Kong*



*Published by*

World Scientific Publishing Co. Pte. Ltd.

P O Box 128, Farrer Road, Singapore 912805

*USA office:* Suite 1B, 1060 Main Street, River Edge, NJ 07661

*UK office:* 57 Shelton Street, Covent Garden, London WC2H 9HE

**British Library Cataloguing-in-Publication Data**

A catalogue record for this book is available from the British Library.

**THE ELECTROMAGNETIC ORIGIN OF QUANTUM THEORY AND LIGHT**

Copyright © 2002 by World Scientific Publishing Co. Pte. Ltd.

*All rights reserved. This book, or parts thereof, may not be reproduced in any form or by any means, electronic or mechanical, including photocopying, recording or any information storage and retrieval system now known or to be invented, without written permission from the Publisher.*

For photocopying of material in this volume, please pay a copying fee through the Copyright Clearance Center, Inc., 222 Rosewood Drive, Danvers, MA 01923, USA. In this case permission to photocopy is not required from the publisher.

ISBN 981-02-4785-0

Printed in Singapore by World Scientific Printers (S) Pte Ltd

## Foreword

Suppose that the technical knowledge bases of electromagnetic theory and the theory of electrons available in the year 2001 were available when the historic interpretation of quantum theory was constructed. Would the additional facts affect the outcome? That is, is the historic interpretation uniquely correct as constructed? Knowledge of several physical properties that would appear to play critical roles in quantum theory were discovered *after* the interpretation was completed. These include {1} the standing energy that accompanies and encompasses active, electrically small volumes, {2} the power-frequency relationships in nonlinear systems, {3} the possible directivity of modal fields, and {4} electron nonlocality. How could it be that such basic physical effects would not importantly affect the dynamic interaction between an electron and its nucleus, for both isolated atoms and atoms immersed in a plane wave?

It is indisputable that the mathematics of quantum theory coupled with the historic interpretation adequately accounts for observed physical phenomena. It is also indisputable that, in contrast with other physical disciplines, the historic interpretation requires special, indeed rather quixotic, quantum theory axioms. Perhaps the philosophically most significant result of the historic interpretation is the inherent uncertainty of physical events: The status of all physical phenomena at any instant *does not* completely specify the status an instant later. The inherent uncertainty goes against all other natural philosophy.

In addition to an inherent uncertainty of physical events, in the absence of the four physical phenomena listed above the axioms needed to satisfactorily explain quantum mechanical phenomena require rejecting selected portions of classical electromagnetism within atoms. In this book, we incorporate these four phenomena into a new interpretation, and understanding, of quantum theory. This is primarily based upon showing that both the magnitudes and the consequences of radiation reaction forces have been greatly underestimated. We find that such forces are responsible for the

inherent stability of isolated atoms and for the nonlinear, regenerative drive of transitions between eigenstates.

The interpretation that results from incorporating these physical phenomena preserves the full applicability of electromagnetic field theory within atoms and it enables calculating the complete electromagnetic solution for a photon. Furthermore, it preserves causality in the sense that the status of all physical phenomena at any instant completely specifies the status an instant later.

Detailed three-dimensional, time-dependent plots of power, energy, and electromagnetic stress in the vicinity of a radiating electric dipole, of mixed electric and magnetic dipoles, and photons near a radiating atom are maintained on website:

<<http://www.ee.psu.edu/grimes/antennas/breakthrough.htm>>

Dale M. Grimes  
Craig A. Grimes  
University Park, PA USA  
September 2001

# Table of Contents

Foreword.....	v
Prologue.....	xiii
1. Classical Electrodynamics .....	1
1.1 Introductory Comments.....	1
1.2 Space and Time Dependence upon Speed .....	2
1.3 Four-Dimensional Space Time .....	5
1.4 Newton's Laws .....	7
1.5 Electrodynamics .....	9
1.6 The Field Equations.....	12
1.7 Accelerating Charges .....	16
1.8 The Maxwell Stress Tensor.....	17
1.9 Kinematic Properties of Fields.....	22
1.10 A Lemma for Calculation of Electromagnetic Fields .....	24
1.11 The Scalar Differential Equation .....	26
1.12 Radiation Fields in Spherical Coordinates .....	30
1.13 Electromagnetic Fields in a Box.....	34
References.....	36
2. Selected Boundary Value Problems .....	37
2.1 Traveling Waves.....	37
<i>Scattering</i> .....	40
2.2 Scattering of a Plane Wave by a Sphere.....	40
2.3 Ideal Spherical Scatterers .....	47
<i>Biconical Transmitting Antennas</i> .....	52
2.4 General Comments .....	52
2.5 Fields.....	54
2.6 TEM Mode.....	57
2.7 Boundary Conditions.....	60
2.8 The Defining Integral Equations.....	65

2.9	Solution of the Biconical Antenna Problem .....	68
2.10	Power .....	75
2.11	Field Expansion for $y$ -Directed Exponential .....	78
	<i>An Incoming Plane Wave</i> .....	82
2.12	Incoming TE Fields .....	82
2.13	Incoming TM Fields .....	83
2.14	Exterior Fields, Powers, and Forces .....	86
2.15	The Cross Sections .....	91
	<i>Biconical Receiving Antennas</i> .....	95
2.16	General Comments .....	95
2.17	Fields of Receiving Antennas .....	97
2.18	Boundary Conditions .....	99
2.19	Zero Degree Solution .....	103
2.20	Non-Zero Degree Solutions .....	105
2.21	Surface Current Densities .....	106
2.22	Power .....	107
	References .....	111
3.	Antenna Q .....	113
3.1	Instantaneous and Complex Power in Circuits .....	113
3.2	Instantaneous and Complex Power in Fields .....	117
3.3	Time Varying Power in Actual Radiation Fields .....	119
3.4	Comparison of Complex and Instantaneous Powers .....	122
3.5	Radiation Q .....	127
3.6	Chu's Q Analysis, TM Fields .....	131
3.7	Chu's Q Analysis, Exact for TM Fields .....	136
3.8	Chu's Q Analysis, TE Field .....	138
3.9	Chu's Q Analysis, Collocated TM and TE Modes .....	140
3.10	Q the Easy Way, Electrically Small Antennas .....	142
3.11	Q on the Basis of Time-Dependent Field Theory .....	142
3.12	Q of a Radiating Electric Dipole .....	149
3.13	Surface Pressure on Dipolar Source .....	154
3.14	Q of Radiating Magnetic Dipoles .....	158
3.15	Q of Collocated Electric and Magnetic Dipole Pair .....	159
3.16	Q of Collocated, Perpendicular Electric Dipoles .....	164
3.17	Four Collocated Electric and Magnetic Dipoles and Multipoles .....	165
3.18	Numerical Characterization of Antennas .....	172
3.19	Experimental Characterization of Antennas .....	179

3.20 Q of Collocated Electric and Magnetic Dipoles:  
    Numerical and Experimental Characterizations.....183  
References.....190

4. Quantum Theory.....191

    4.1 Electrons .....192

    4.2 Radiation Reaction Force .....194

    4.3 The Time-Independent Schrödinger Equation .....198

    4.4 The Uncertainty Principle .....203

    4.5 The Time-Dependent Schrödinger Equation.....205

    4.6 Quantum Operator Properties .....209

    4.7 Orthogonality .....210

    4.8 Electron Angular Momentum, Central Force Fields.....212

    4.9 The Coulomb Potential Source .....215

    4.10 Hydrogen Atom Eigenfunctions .....220

    4.11 Perturbation Analysis.....223

    4.12 Non-Ionizing Transitions .....225

    4.13 Absorption and Emission of Radiation.....228

    4.14 Electric Dipole Selection Rules for One Electron Atoms.....231

    4.15 Electron Spin .....234

    4.16 Many-Electron Problems .....236

    4.17 Electron Photo Effects .....239

    References.....243

5. Photons .....245

    5.1 Power-Frequency Relationships .....245

    5.2 Length of the Wave Train and Radiation Q .....251

    5.3 Phase and Radial Dependence of Field Magnitude.....254

    5.4 Gain and Radiation Pattern .....258

    5.5 Kinematic Values of the Radiation .....260

    5.6 Telefields and Far Fields .....266

    5.7 Evaluation of Sum  $S_{12}$  on the Axes .....270

    5.8 Evaluation of Sums  $S_{22}$  and  $S_{32}$  on the Polar Axes.....273

    5.9 Evaluation of Sum  $S_{32}$  in the Equatorial Plane .....279

    5.10 Evaluation of Sum  $S_{22}$  in the Equatorial Plane.....281

    5.11 The Axial Fields, Summary .....283

    5.12 Infinite Radius Radiation Pattern.....287

    5.13 Self-Consistent Field Analysis.....290

    5.14 Power and Energy Exchange .....295

5.15 The Wave Train.....	297
5.16 Multipolar Moments.....	299
5.17 Field Stress on the Active Region .....	302
5.18 Summary.....	313
References.....	315
6. Epilogue.....	317
6.1 Historic Background.....	317
6.2 Overview.....	322
6.3 The Radiation Scenario .....	324
References.....	329
Appendix.....	331
A.1 Introduction to Tensors.....	331
A.2 Tensor Operations.....	334
A.3 Tensor Symmetry.....	336
A.4 Differential Operations on Tensor Fields .....	337
A.5 Green's Function .....	340
A.6 The Potentials .....	345
A.7 Equivalent Sources .....	346
A.8 A Series Resonant Circuit .....	351
A.9 Q of Time Varying Systems.....	354
A.10 Bandwidth.....	357
A.11 Instantaneous and Complex Power in Radiation Fields.....	358
A.12 Conducting Boundary Conditions .....	361
A.13 Uniqueness.....	364
A.14 Spherical Shell Dipole.....	365
<i>Spherical Harmonics</i> .....	367
A.15 Gamma Functions .....	367
A.16 Azimuth Angle Trigonometric Functions .....	371
A.17 Zenith Angle Legendre Functions .....	374
A.18 Legendre Polynomials.....	379
A.19 Associated Legendre Functions .....	383
A.20 Orthogonality.....	385
A.21 Recursion Relationships.....	387
A.22 Integrals of Legendre Functions .....	397
A.23 Integrals of Fractional Order Legendre Functions .....	402
<i>Spherical Bessel Functions</i> .....	405
A.24 The First Solution Form .....	405

A.25 The Second Solution Form .....410

A.26 Tables of Spherical Bessel, Neumann, and Hankel Functions  
.....414

A.27 Sums Over Spherical Bessel Functions .....423

*Multipolar Sources* .....428

A.28 Static Scalar Potentials .....428

A.29 Static Vector Potentials .....433

References.....440

Index .....441



This page is intentionally left blank

## Prologue

A radiating antenna sits in a standing energy field of its own making. Even at the shortest wavelengths for which antennas have been made, if the antenna is electrically too small, that is, if the length-to-wavelength ratio is too small, the amount of standing field energy is so large it essentially shuts off energy exchange. Yet an atom in the act of exchanging electromagnetic energy may be scaled as an electrically short antenna, and standing energy is ignored by quantum theory seemingly without consequence. Why, in one case, the energy is dominant and, in the other, it plays no role has been a mystery. The framers of the historic interpretation of quantum theory could not have accounted for the standing energy, since an analysis of it was first formulated more than twenty years after the interpretation was accomplished. Similarly, nonlocality is a significant and essential feature of eigenstate electrons, yet nonlocality played no historic role since it was discovered a half-century after the interpretation was accomplished. Similar statements apply to the power-frequency relationships of nonlinear systems and to the maximum possible gain of an electromagnetic mode.

In this book, we form a simplified and deterministic interpretation of quantum theory that accounts for standing energy in the radiation field, field directivity, the power-frequency relationships, and electron nonlocality. We find that all play integral and essential roles in atomic stability and energy exchanges. Together they form a complete electromagnetic field solution of quantum mechanical exchanges of electromagnetic energy, without the separate axioms of the historic interpretation.

Stable atoms occupy space measured on the picometer scale of dimensions and exchange energy during periods measured on the picosecond scale of time. Since this dimensional combination precludes direct observation, it is necessary to infer active atomic events from observations over much larger distances and times. Large-scale measurements led the framers of the historic interpretation to conclude that the equations of classical electromagnetism do not fully apply on an atomic scale of

shows no inherent distance or time scale limitations; derived results are independent of an observer's size and speed. A primary purpose of this book is to assist in resolving this enigma.

Although this book is primarily a monograph, early versions were used as a text for topical courses in electromagnetic theory in the Electrical Engineering Departments of the University of Michigan and the Pennsylvania State University. A later version served as a text for a topical course in theoretical physics in the Department of Physics and Astronomy of the University of Kentucky; it was after this course that we began systematic work on the book. Throughout the book, all theorems used were carefully reexamined, with the emphasis used that best met the needs of the book. For the same purpose we extract freely and without prejudice from accepted works of electrical engineering, on the one hand, and physics, on the other. Too often there is imperfect communication between these two sides of the same coin. The result is an innovative way of viewing scattering phenomena, radiation exchanges, and energy transfer by electromagnetic fields.

The equations of classical electromagnetism are derived and developed in Chapter 1. In Chapter 2 the equations are applied to a series of increasingly complex boundary value problems. The choice of solved problems is based on two criteria: First, the solution form is a general one that, when the modal coefficients are properly chosen, applies to any electromagnetic problem, and hence to atomic radiation. Second, each solution is electromagnetically complete; the solution is in the form of an infinite series of constant coefficients times products of radial, spherical and harmonic functions. Completeness is required to assure that no solution forms have been overlooked. The importance of completeness cannot be overemphasized. For example, historically the character of receiving current modes on antennas was not correctly estimated; the full complexity and beauty were not appreciated until an electromagnetically complete solution to biconical receiving antennas became available. That is to say, our modern technological culture, with its vast experience with antennas, did not understand the modes on the simplest of receiving antennas until a complete mathematical solution became available in 1982. Similarly, we cannot be sure we fully understand a radiating atom without a complete solution.

Chapter 3 deals with standing energy fields associated with electromagnetic energy exchanges. To analyze them, it is necessary to re-examine complex power and energy in radiation fields. The use of complex power is nearly universal in the analysis of electric circuits and fields. Although complex power leads to the correct power at any terminal pair,

expressions for complex power in a radiation field suppress a radius-dependent phase factor. Hence, no equation that depends upon the phase of field power versus radius can be solved using only complex power. To avoid the difficulty, we switch to a time domain description of the fields, and use it to calculate modal field energies. From them, we calculate the ratio of source-associated field energy to the average energy per radian radiated permanently away from the antenna. We confirm earlier work showing that the ratio increases so rapidly with decreasing electrical size that all modal combinations, save one, are subject to severe operational limitations. We then show the multimodal combination to which such limitations do not apply.

Chapter 4 contains a brief review of quantum theory that is conventional in most ways, but unconventional in the treatment of atomic stability. We show that the standing energy of a dipole field generated by an oscillating point electron creates an expansive radiation reaction force on the electron. That force is the same order of magnitude as the trapping Coulomb force and is three orders of magnitude larger than the commonly accepted radiation reaction force. We hypothesize it forces the electron into a charge density distributed throughout the eigenstate. As an analogy, consider a drop of oil: A small quantity of oil in isolation, and under the influence of surface tension, forms into a spherical drop, yet when placed on a pond it expands to cover the entire surface. An expanded electron is not small compared with atomic dimensions and may be formed into a non-radiating array of charge and current densities. Such an array is inherently stable and interaction between the intrinsic and orbital magnetic moments produces a continuous torque and assures continuous motion of the parts. This model and energy conservation forms an adequate basis for Schrödinger's time-independent wave equation; his time-dependent equation follows if the system remains in near-equilibrium. In this way, Schrödinger's equations are the equivalent of ensemble energy expressions in classical thermodynamics. In both places, general results are obtained without detailed knowledge of the ensemble.

Schrödinger's time-dependent equation treats state transitions by describing the initial and final states. Although answers are unquestionably correct, the approach gives no information about fields that are present during the emission and absorption process, yet clearly photon near fields must exist. The classical interpretation of quantum theory supplies no counterpart to the full field sets obtained in Chapter 2 for the transmission and reception of energy by biconical antennas.

In Chapter 5, we integrate and extend results of the preceding chapters. We begin by showing that the Manley Rowe equations, which are meaningful *only with nonlinear systems*, correctly describe the Ritz power-frequency relationships of photons; yet, the Schrödinger and Dirac equations are linear. We next impose the kinematic properties of quantized radiation as a boundary condition on a general, multimodal field expansion. The results are field expressions with a form similar to those of Chapter 2, and are closely related to multipolar expansions for plane waves. In addition, the resulting modal fields are members of the set of resonant modes for which, by Chapter 3, standing energy limitations do not apply. Hence, a rapid build-up of radiated power is expected. These results are combined and used to determine all radiated fields, near and far, during eigenstate transitions, *i.e.*, during photon exchanges. Next, we use the similarity between photon and plane wave multipolar expansions to re-express the photon fields in an expansion from infinity inward. This expansion permits the evaluation of the radiation reaction force of a photon field on its generating electron. We find that the radiation reaction pressure on the surface of a spherical, radiating atom is at least many thousands of times larger than the Coulomb attractive pressure. The reaction pressure is properly directed and phased to drive the nonlocal electron regeneratively, and nonlinearly, to a rapid buildup of exchanged power. Hence, radiation in accordance with the Manley Rowe power frequency relations occurs, and continues until all available energy is radiated.

The mathematics and the ideas presented here, summarized on a point-by-point basis in the Epilogue, combine to give a simple, electromagnetically complete, and deterministic interpretation of quantum theory.

# 1. Classical Electrodynamics

## 1.1 Introductory Comments

There are two quite disparate approaches to electromagnetic field theory. One is a deductive approach that begins with a single relativistic source potential and deduces from it the full slate of classical equations of electromagnetism. The other is an inductive approach that begins with the experimentally determined force laws and induces from them, incorporating new facts as needed, until the Maxwell equations are obtained. Although the inductive approach is the way in which the theory was developed, it is the deductive method that shows the full beauty, symmetry, and simplicity of electromagnetism.

The inductive approach is commonly used in textbooks at all levels. Coulomb's law is the usual starting point, with other effects included as needed until the full slate of measurable quantities are obtained. From this viewpoint, the potentials are but mathematical artifices that simplify force field calculations. They simplify the calculation necessary to solve for the force fields but are without intrinsic significance. The deductive approach begins with a limited axiomatic base and develops a potential theory from which, in turn, follow the force fields. In 1959 Aharonov and Bohm, using the premise that potential has a special significance, predicted an effect that was confirmed in 1960, the Aharonov-Bohm effect: Magnetic field quantization is affected by a static magnetic potential even in a region void of force fields. We conclude that the magnetic potential has a physical significance in its own right and has meaning in a way that extends beyond the calculation of force fields. There is physical significance contained in the deductive approach that is not present in the inductive one.

To begin the deductive approach, consider that the universe is totally empty of condensed matter but does contain light. What is the speed of the light? Since there is no reference frame by which to measure it, the question

is moot. Therefore, introduce an asteroid large enough to support an observer and his equipment, which determines the speed of light passing him to be  $v_A$ . Since there is nothing else in the universe, a question about the speed of the asteroid is moot. Next, introduce a second asteroid, identical to the first but many light years away from it. The asteroids are separated far enough to be independent of each other by any means of which we are currently aware. An observer on the second asteroid determines the speed of light passing him to be  $v_B$ . Will the measured values be the same? By the cosmological principle, an experiment run in one local four-space yields the same results as an identical experiment run in a different local four-space. Therefore we expect that  $v_A = v_B = c$ .

Next, bring the asteroids into the same local region. Either the speeds depend upon the magnitude of the local masses or they do not, and if they do not, there is no change in speed. However, in the local region, a relative speed between asteroids A and B may be determined. Since there is no way one asteroid can be preferred over the other in an otherwise empty universe, the two observers continue to measure the same speed. This condition requires that the speed of light be independent of the relative speed of the system on which it is measured. Next, bring in other material, bit by bit, until the universe is in its present form, and the conclusion remains the same. The speed of light is independent of the speed of the object on which it is measured, independently of the speed of other objects.

## 1.2 Space and Time Dependence upon Speed

Let a pulse of light be emitted from an origin in reference frame F and observed in reference frame F'. If the speed of light is the same in all reference frames, if the two frames are in relative motion, and if the origins coincide at the time the light is emitted, the light positions as measured in the two frames are:

$$x^2 + y^2 + z^2 - c^2 t^2 = x'^2 + y'^2 + z'^2 - c^2 t'^2 \quad (1.2.1)$$

If the relative speed is such that F' is moving at speed  $v$  in the  $z$ -direction with respect to F, then at low speeds:

$$x' = x, \quad y' = y, \quad z' = (z - vt); \quad t' = t \quad (1.2.2)$$

Since Eq. 1.2.1 isn't satisfied by Eq. 1.2.2, it follows that Eq. 1.2.2 doesn't extend to speeds that are a significantly large fraction of  $c$ . To obtain a transition that is linear in the independent variables, and that goes to Eq. 1.2.2 in the low speed limit, consider the linear transformation form:

$$x' = x; \quad y' = y; \quad z' = \gamma(z - vt); \quad t' = At + Bz \quad (1.2.3)$$

Parameters  $\gamma$ ,  $A$ , and  $B$  are undetermined but independent of both position and time. Since Eq. 1.2.3 approaches Eq. 1.2.2 in the limit of velocity  $v$  much less than  $c$ , in that limit:

$$\gamma = 1; \quad A = 1; \quad B = 0 \quad (1.2.4)$$

Since the coordinates are independent variables, combining Eqs. 1.2.1 and 1.2.3 and solving shows that:

$$\begin{aligned} z^2(\gamma^2 - 1 - c^2 B^2) &= 0 \\ t^2(c^2 + \gamma^2 v^2 - c^2 A^2) &= 0 \\ zt(\gamma^2 + ABc^2) &= 0 \end{aligned} \quad (1.2.5)$$

Solving Eq. 1.2.5 yields:

$$A = \gamma = \left(1 - v^2/c^2\right)^{-1/2}; \quad B = -\frac{\gamma v}{c^2} \quad (1.2.6)$$

Combining yields the Lorentz transformation equations:

$$x' = x; \quad y' = y; \quad z' = \gamma(z - vt); \quad t' = \gamma\left(t - \frac{vz}{c^2}\right) \quad (1.2.7)$$

This transformation preserves the speed of light in inertial frames.

Equation 1.2.7 is a sufficient basis upon which to determine results if events in one frame of reference are observed in another one. Let the observer be in the unprimed frame. A stick of length  $L_0$  as determined in the moving frame, in which it is stationary, lies along the  $z$ -axis. It moves past



the observer in the  $z$ -direction at speed  $v$ . A flash of light illuminates the region, during which time the observer determines the positions of the ends of the moving stick,  $z_1$  and  $z_2$ . It follows from Eqs. 1.2.7 that the measured positions are:

$$z'_1 = \gamma(z_1 - vt_0) \quad \text{and} \quad z'_2 = \gamma(z_2 - vt_0) \quad (1.2.8)$$

The length as measured in the stationary frame is:

$$L = (z_2 - z_1) = (z'_2 - z'_1)/\gamma = L_0/\gamma \quad (1.2.9)$$

It follows that:

$$L = L_0 \left(1 - v^2/c^2\right)^{1/2} \leq L_0 \quad (1.2.10)$$

The observed length of the stick is less than is measured in the rest frame; this fractional contraction is the Lorentz contraction.

Next pulses of light are issued at times  $t'_2$  and  $t'_1$ , again in the moving frame. When does a stationary observer see them, and what is the time interval between them? Using Eqs. 1.2.7:

$$t_2 = \gamma \left( t'_2 - vz'_2/c^2 \right) \quad \text{and} \quad t_1 = \gamma \left( t'_1 - vz'_1/c^2 \right) \quad (1.2.11)$$

From Eq. 1.2.11 the time difference in the frame at which the two sources are stationary is:

$$T_0 = t_2 - t_1 = \gamma \left[ (t'_2 - t'_1) - v(z'_2 - z'_1)/c^2 \right] = \gamma T \left( 1 - v^2/c^2 \right) \quad (1.2.12)$$

$T$  is the time measured in the stationary frame. Solving for  $T$  gives:

$$T = \gamma T_0 = \frac{T_0}{\left(1 - v^2/c^2\right)^{1/2}} \geq T_0 \quad (1.2.13)$$

The observer measures the time duration between pulses to be more than is measured in the rest frame; this time expansion is time dilatation.

### 1.3 Four-Dimensional Space Time

The equality of the speed of light in all inertial frames is the basis for a system of 4-vectors. Let  $x_1, x_2, x_3$  represent the three spatial axes  $x, y, z$  of three dimensions and  $x_4 = ict$  where  $i = \sqrt{-1}$ .

$$(x_1, x_2, x_3, x_4) \quad (1.3.1)$$

Since three of the axes determine lengths and one determines time, a three-dimensional rotation represents a change in spatial orientation and a four-dimensional rotation includes a change in time. Such four-dimensional rotations are Lorentz transformations. These transformations are usually simple and contain a high degree of symmetry. Such transformations are covariant with respect to changes in coordinate systems; that is, an equation that represents reality in one reference frame has the same form in all other inertial frames.

The imaginary property of the fourth dimension represents an essential difference from spatial ones: the squares of the space coefficients and time coefficients have different signs. For notational purposes we use Roman or Greek subscripts to indicate, respectively, three- or four-dimensional tensors. For example, the rotation matrix element in four dimensions is  $c_{\mu\nu}$  where, for velocities  $v$  directed along the  $x_1$ -axis:

$$c_{\mu\nu} = \begin{pmatrix} \gamma & 0 & 0 & i\gamma v/c \\ 0 & 1 & 0 & 0 \\ 0 & 0 & 1 & 0 \\ -i\gamma v/c & 0 & 0 & \gamma \end{pmatrix} \quad (1.3.2)$$

It follows similarly to three-dimensional direction cosines that

$$c_{\mu\nu} = c'_{\nu\mu} \quad ; \quad c_{\mu\nu}c_{\mu\rho} = \delta_{\nu\rho} \quad ; \quad \det |c_{\mu\nu}| = 1 \quad (1.3.3)$$

The Lorentz direction cosines  $c_{\mu\nu}$  are:

$$x'_\mu = c_{\mu\nu}x_\nu \quad (1.3.4)$$

The proper time interval,  $\Delta\tau$ , between two events with space-time coordinates spaced  $\Delta_\alpha$  apart is defined to be:

$$(\Delta\tau)^2 = -\frac{1}{c^2} \Delta x_\alpha \Delta x_\alpha \quad (1.3.5)$$

Using three-dimensional notation, the proper time difference is

$$(\Delta\tau)^2 = (\Delta t)^2 - \frac{(\Delta\mathbf{r})^2}{c^2} \quad (1.3.6)$$

Since  $(\Delta\tau)^2$  can be zero, positive, or negative,  $\Delta\tau$  may be zero, real, or imaginary. Since the speed of light is the same in all reference frames, by Eq. 1.2.1 the proper time is also the same in all reference frames. If it is real, it is “time-like” and if imaginary, it is “space-like”. If time-like, the proper time is the time separation of the two events in the same frame. If space-like, there is a frame in which  $c$  times the proper time is the spatial separation of the two events that are simultaneous in that frame.

With  $\tau$  as proper time, consider the 4-vector defined by the expression:

$$U_\mu = \frac{dx_\mu}{d\tau} \quad (1.3.7)$$

Since both  $x_\mu$  and  $\tau$  are independent of details of the particular inertial frame in which it is measured, so is  $U_\mu$ ;  $U_\mu$  is therefore a 4-vector with the four components:

$$\begin{aligned} U_1 &= \frac{dx}{d\tau} = \frac{dx}{dt} \frac{dt}{d\tau} = \gamma v_x \quad ; \quad U_2 = \frac{dy}{d\tau} = \frac{dy}{dt} \frac{dt}{d\tau} = \gamma v_y \\ U_3 &= \frac{dz}{d\tau} = \frac{dz}{dt} \frac{dt}{d\tau} = \gamma v_z \quad ; \quad U_4 = \frac{d(ict)}{d\tau} = \gamma ic \end{aligned} \quad (1.3.8)$$

The three-dimensional velocity components are  $v_i$  and the 4-velocity components are  $U_\mu$ .

A particle of mass  $m_0$  with 4-velocity  $U_\mu$  has 4-momentum given by:

$$P_\mu = m_0 U_\mu \quad (1.3.9)$$

Combining shows the momentum components to be:

$$p = \gamma m_0 v ; \quad p_4 = \gamma m_0 ic = iW/c ; \quad W = \gamma m_0 c^2 \quad (1.3.10)$$

The quantity  $W$ , defined by Eq. 1.3.10, is the energy associated with the moving mass.

The binomial expansion is:

$$(1 \pm a)^n = 1 \pm na + \frac{n}{2!}(n-1)a^2 \pm \dots \quad (1.3.11)$$

This equation combines with the definition of  $\gamma$ , see Eq. 1.2.6, to show that:

$$\gamma = 1 + \frac{v^2}{2c^2} + \frac{3v^4}{8c^4} + \dots \quad (1.3.12)$$

Combining Eqs. 1.3.10 and 1.3.12 shows the total energy of the particle:

$$W = m_0 c^2 \left[ 1 + \frac{v^2}{2c^2} + \frac{3v^4}{8c^4} + \dots \right] \quad (1.3.13)$$

In the rest frame  $m_0$  is the rest mass. The particle energy is:

$$W_0 = m_0 c^2 \quad (1.3.14)$$

By Eq. 1.3.14, the first term of Eq. 1.3.13 is the self-energy of the mass. The second term is the kinetic energy at low speeds and the higher order terms complete the evaluation of the kinetic energy of the mass at any speed.

## 1.4 Newton's Laws

The Minkowski force is defined to be:

$$F_{\mu} = \frac{d}{d\tau} P_{\mu} \quad (1.4.1)$$

This force is a 4-vector with the  $x$ -directed component:

$$F_1 = \frac{d}{d\tau} (m_0 U_1) = \gamma \frac{\partial}{\partial t} (\gamma m_0 v_x) \quad (1.4.2)$$

The corresponding three-dimensional force component is:

$$F_x = \frac{\partial}{\partial t} (\gamma m_0 v_x) \quad (1.4.3)$$

The factor  $\gamma$  in Eq. 1.4.3 was known before the full relativistic effect was understood. Although relativity makes it abundantly clear that the result is a space-time effect, it was historically interpreted as an increase in mass whereby the effective mass  $m$  is a function of speed:

$$m = \gamma m_0 \quad (1.4.4)$$

Even with relativity, the nomenclature remains and the effective mass of a moving particle, by definition, is equal to Eq. 1.4.4.

Since the 4-momentum is a 4-vector, it is conserved between Lorentz frames. That is,

$$W_0^2 = W^2 - p^2 c^2 \quad (1.4.5)$$

The energy is related to momentum, in any given frame, as:

$$W^2 = m_0^2 c^4 + p^2 c^2 \quad (1.4.6)$$

Since  $W$  is second order in  $v/c$ , three-momentum is constant in low speed inertial frames. Energy is also nearly conserved. However, in high-energy systems neither energy nor momentum is conserved, only the combination. This example illustrates a general characteristic of 4-tensors that at low speeds the real and imaginary parts are separately nearly conserved but at high speeds only the combined magnitude is conserved.

## 1.5 Electrodynamics

The three scalars defined so far are speed,  $c$ , time interval between events in a rest frame,  $\tau$ , and mass,  $m_0$ . A fourth is electric charge,  $q$ ; electric charge can have either sign. Just as an intrinsic part of any mass is the associated gravitational field,  $G$ , an intrinsic part of charge is the associated 4-vector potential field  $A_\mu$ . Consider that the individual charges are much smaller than other dimensions and that there are many of them. For this case choose a differential volume, with dimensions  $(x_1, x_2, x_3)$ , in which each dimension is much less than any macroscopic dimension of interest but contains large numbers of charges. If both conditions are met, the tools of calculus apply. Charge density  $\rho$  is defined to be the charge per unit volume at a point. Charge density  $\rho_0$  is defined in a frame in which the time average position is at rest. Observers in fixed and moving frames see the same total charge but, because of the Lorentz contraction, the moving observer determines the volume containing it to be smaller by a factor of  $\gamma$ . Therefore, the charge density in a moving frame is increased by the factor:

$$\rho = \gamma \rho_0 \quad (1.5.1)$$

If the charge density moves with 4-velocity  $U_\mu$ , in a way similar to three dimensions the 4-current density is defined to be:

$$J_\mu = \rho_0 U_\mu = \{\gamma \rho_0 v, \gamma i c \rho_0\} = \{\mathbf{J}, i c \rho\} \quad (1.5.2)$$

The vector terms within the curly brackets indicate the first three dimensions, and the scalar term represents the fourth dimension. The 4-divergence of the current density is:

$$\frac{\partial J_\mu}{\partial X_\mu} = \nabla \cdot \mathbf{J} + \frac{\partial \rho}{\partial t} = 0 \quad (1.5.3)$$

The first equality of Eq. 1.5.3 follows from definition of terms and the second is true if and only if net charge is neither created nor destroyed. Pair production or annihilation may occur but there is no change in the total charge. The zero 4-divergence shows that the net change in the four-current

is always equal to zero. Physically a net change in the total charge does not occur and charges are created and destroyed only in canceling pairs.

The 4-vector potential field  $A_\mu(X_\gamma)$  is defined to be the potential that satisfies the differential equation:

$$\frac{\partial^2 A_\nu}{\partial X_\beta \partial X_\beta} = -\mu J_\nu \quad (1.5.4)$$

Constant  $\mu$  is defined to be the permeability of free space; it is a dimension-determining constant and defined to equal  $4\pi/10^7$  Henrys/meter.

Taking the 4-divergence of Eq. 1.5.4 then combining with Eq. 1.5.3 gives:

$$\frac{\partial}{\partial X_\nu} \frac{\partial^2}{\partial X_\beta \partial X_\beta} A_\nu = \frac{\partial^2}{\partial X_\beta \partial X_\beta} \frac{\partial A_\nu}{\partial X_\nu} = -\mu \frac{\partial J_\nu}{\partial X_\nu} = 0$$

Combining, it follows that:

$$\partial A_\nu / \partial X_\nu = 0 \quad (1.5.5)$$

Equation 1.5.5 shows that the divergence of  $A_\nu$  is zero, from which it follows that, like charge, the total amount of 4-potential doesn't change. If transitions are made between different reference frames changes occur in the components of the potential but not in the sum over all four components.

The four-dimensional Laplacian of Eq. 1.5.4 may be integrated over all space to obtain an expression for the potential itself. By Eq. A.6.2 the potential of a moving charge is:

$$A_\alpha(X_\gamma) = \frac{\mu}{4\pi} \iiint \frac{J_\alpha(\mathbf{r}', t' - R/c)}{\left(R - \mathbf{R} \cdot \frac{\mathbf{v}}{c}\right)} dV' \quad (1.5.6)$$

The integral is over all source-bearing regions,  $dV'$  is differential volume,  $X_\gamma$  are the 4-coordinates of the field point,  $X'_\gamma$  are the 4-coordinates at the

source point,  $\mathbf{R}$  is the vector from the source point to the field point. At low speeds Eq. 1.5.6 simplifies to:

$$A_{\alpha}(X_{\gamma}) = \frac{\mu}{4\pi} \iiint \frac{J_{\alpha}(\mathbf{r}', t' - R/c)}{R(X_{\gamma}, X_{\gamma})} dV' \quad (1.5.7)$$

Substituting in the three-dimensional values of  $J_{\alpha}$  results in the three-dimensional potentials:

$$\begin{aligned} A(\mathbf{r}, t) &= \frac{\mu}{4\pi} \iiint \frac{J(\mathbf{r}', t' - R/c)}{R(\mathbf{r} - \mathbf{r}', t')} dV' \\ \Phi(\mathbf{r}, t) &= -icA_4(\mathbf{r}, t) = \frac{1}{4\pi\epsilon} \iiint \frac{\rho(\mathbf{r}', t' - R/c)}{R(\mathbf{r} - \mathbf{r}', t')} dV' \end{aligned} \quad (1.5.8)$$

Constant  $\epsilon$  is defined to be the permittivity of free space; it is a dimension determining constant and defined to be exactly equal to  $1/(\mu c^2)$  Farads/meter.

For a point charge, instead of a charge distribution, the corresponding 4-potential is:

$$A_{\alpha}(X_{\gamma}) = \frac{\mu q}{4\pi} \frac{U_{\alpha}(\mathbf{r}', t' - R/c)}{(R - \mathbf{R} \cdot \mathbf{v}/c)} \quad (1.5.9)$$

The three-dimensional potentials are:

$$\begin{aligned} A(\mathbf{r}, t) &= \frac{\mu}{4\pi} \frac{q\mathbf{v}(\mathbf{r}', t' - R/c)}{(R - \mathbf{R} \cdot \mathbf{v}/c)} \\ \Phi(\mathbf{r}, t) &= \frac{\mu}{4\pi} \frac{q(\mathbf{r}', t' - R/c)}{(R - \mathbf{R} \cdot \mathbf{v}/c)} \end{aligned} \quad (1.5.10)$$

If the charge moves at a speed much less than  $c$  Eqs. 1.5.10 are the usual three-dimensional vector and scalar potential fields of individual charges.

It is apparent from Eqs. 1.5.10 that a charge moving towards or away from a field point generates potentials with magnitudes respectively larger or smaller than the low speed value.



## 1.6 The Field Equations

If  $\rho_0$  is the charge density in an inertial reference frame in which the average speed of the charges is zero, then  $\rho = \gamma\rho_0$  is the charge density in a moving frame. The charge density and the three-dimensional current density  $J_i$  were extended to form the 4-current density, as shown by Eq. 1.5.2, from which the Laplacian of the 4-potential was defined by Eq. 1.5.4. Other useful 4-tensors follow from 4-dimensional operations on the 4-potential  $A_\alpha(X_\gamma)$ ; some especially important ones follow.

A second rank antisymmetric tensor of interest follows from the potential by the equation:

$$f_{\alpha\beta} = \frac{\partial A_\beta}{\partial X_\alpha} - \frac{\partial A_\alpha}{\partial X_\beta} \quad (1.6.1)$$

Antisymmetric 4-tensors are spatial arrays of six numbers and, in common with all antisymmetric tensors, the trace is zero:

$$f_{\alpha\alpha} = 0 \quad (1.6.2)$$

Writing out the six values that appear in the upper right portion of the 4-tensor, and using the result to define function  $\Phi$ , gives:

$$f_{12} = \frac{\partial A_2}{\partial X_1} - \frac{\partial A_1}{\partial X_2} = \frac{\partial A_y}{\partial x} - \frac{\partial A_x}{\partial y} = B_z$$

$$f_{23} = \frac{\partial A_y}{\partial z} - \frac{\partial A_z}{\partial y} = B_x$$

$$f_{31} = \frac{\partial A_x}{\partial z} - \frac{\partial A_z}{\partial x} = B_y$$

$$f_{14} = \frac{\partial A_4}{\partial X_1} - \frac{\partial A_1}{\partial X_4} = \frac{i}{c} \frac{\partial \Phi}{\partial x} - \frac{\partial A_x}{i c \partial t} = -\frac{i}{c} E_x$$

$$f_{24} = \frac{i}{c} \frac{\partial \Phi}{\partial y} - \frac{\partial A_y}{i c \partial t} = -\frac{i}{c} E_y \quad (1.6.3)$$

$$f_{34} = \frac{i}{c} \frac{\partial \Phi}{\partial z} - \frac{\partial A_z}{i c \partial t} = -\frac{i}{c} E_z$$

With the deductive approach to electromagnetism, Eqs. 1.6.3 are the defining terms for field vectors **E** and **B**. The result written in tensor form is:

$$(f) = \begin{pmatrix} 0 & B_z & -B_y & -iE_x/c \\ -B_z & 0 & B_x & -iE_y/c \\ B_y & -B_x & 0 & -iE_z/c \\ iE_x/c & iE_y/c & iE_z/c & 0 \end{pmatrix} \quad (1.6.4)$$

Differentiating  $f_{\alpha\beta}$  with respect to  $X_\beta$  results in the equality chain:

$$\frac{\partial f_{\alpha\beta}}{\partial X_\beta} = \frac{\partial}{\partial X_\beta} \left( \frac{\partial A_\beta}{\partial X_\alpha} - \frac{\partial A_\alpha}{\partial X_\beta} \right) = \frac{\partial^2 A_\beta}{\partial X_\beta \partial X_\alpha} - \frac{\partial^2 A_\alpha}{\partial X_\beta \partial X_\beta} = \mu J_\alpha \quad (1.6.5)$$

Combining terms:

$$\frac{\partial f_{\alpha\beta}}{\partial X_\beta} = \mu J_\alpha \quad (1.6.6)$$

Evaluating Eq. 1.6.6 results in:

$$\frac{\partial f_{1\beta}}{\partial X_\beta} = \frac{\partial B_z}{\partial y} - \frac{\partial B_y}{\partial z} - \frac{1}{c^2} \frac{\partial E_x}{\partial t} = \mu J_x$$

$$\frac{\partial f_{2\beta}}{\partial X_\beta} = \frac{\partial B_x}{\partial z} - \frac{\partial B_z}{\partial x} - \frac{1}{c^2} \frac{\partial E_y}{\partial t} = \mu J_y$$

$$\frac{\partial f_{3\beta}}{\partial X_\beta} = \frac{\partial B_y}{\partial x} - \frac{\partial B_x}{\partial y} - \frac{1}{c^2} \frac{\partial E_z}{\partial t} = \mu J_z \quad (1.6.7)$$

$$\frac{c}{i} \frac{\partial f_{4\beta}}{\partial X_\beta} = \frac{\partial E_x}{\partial x} + \frac{\partial E_y}{\partial y} + \frac{\partial E_z}{\partial z} = \frac{\rho}{\epsilon}$$

These are the nonhomogeneous Maxwell equations and relate fields to sources. In three-dimensional notation:

$$\nabla \times \mathbf{B} - \frac{1}{c^2} \frac{\partial \mathbf{E}}{\partial t} = \mu \mathbf{J}; \quad \epsilon \nabla \cdot \mathbf{E} = \rho \quad (1.6.8)$$

The nonhomogeneous Maxwell equations relate force field intensities  $\mathbf{E}$  and  $\mathbf{B}$  to sources  $\rho$  and  $\mathbf{J}$ . The first order terms of  $\mathbf{E}$  and  $\mathbf{B}$  are, respectively, independent of and proportional to the first power of the speed of the charge.

It follows from the definition of  $f_{\alpha\beta}$  that:

$$\frac{\partial f_{\nu\sigma}}{\partial X_\alpha} + \frac{\partial f_{\sigma\alpha}}{\partial X_\nu} + \frac{\partial f_{\alpha\nu}}{\partial X_\sigma} = 0 \quad (1.6.9)$$

Evaluation of Eq. 1.6.9 for each tensor component shows that:

$$\begin{aligned} \frac{\partial f_{12}}{\partial X_3} + \frac{\partial f_{23}}{\partial X_1} + \frac{\partial f_{31}}{\partial X_2} &= \frac{\partial B_z}{\partial z} + \frac{\partial B_x}{\partial x} + \frac{\partial B_y}{\partial y} = 0 \\ \frac{\partial f_{24}}{\partial X_1} + \frac{\partial f_{41}}{\partial X_2} + \frac{\partial f_{12}}{\partial X_4} &= \frac{1}{ic} \left( \frac{\partial E_y}{\partial x} - \frac{\partial E_x}{\partial y} + \frac{\partial B_z}{\partial t} \right) = 0 \\ \frac{\partial f_{34}}{\partial X_2} + \frac{\partial f_{42}}{\partial X_3} + \frac{\partial f_{23}}{\partial X_4} &= \frac{1}{ic} \left( \frac{\partial E_z}{\partial y} - \frac{\partial E_y}{\partial z} + \frac{\partial B_x}{\partial t} \right) = 0 \\ \frac{\partial f_{14}}{\partial X_3} + \frac{\partial f_{43}}{\partial X_1} + \frac{\partial f_{31}}{\partial X_4} &= \frac{1}{ic} \left( \frac{\partial E_x}{\partial z} - \frac{\partial E_z}{\partial x} + \frac{\partial B_y}{\partial t} \right) = 0 \end{aligned} \quad (1.6.10)$$

These are the homogeneous Maxwell equations and relate force field vectors  $\mathbf{E}$  and  $\mathbf{B}$ . In three-dimensional notation:

$$\nabla \times \mathbf{E} - \frac{\partial \mathbf{B}}{\partial t} = 0; \quad \nabla \cdot \mathbf{B} = 0 \quad (1.6.11)$$

Another useful 4-vector is the force intensity, defined by the equation

$$F_{\alpha}^{\nu} = f_{\alpha\beta} J_{\beta} \quad (1.6.12)$$

Evaluation of each component of Eq. 1.6.12 shows that:

$$\begin{aligned} F_1^{\nu} &= F_x^{\nu} = J_y B_z - J_z B_y + \rho E_x \\ F_2^{\nu} &= F_y^{\nu} = J_z B_x - J_x B_z + \rho E_y \\ F_3^{\nu} &= F_z^{\nu} = J_x B_y - J_y B_x + \rho E_z \\ F_4^{\nu} &= \frac{i}{c} (E_x J_x + E_y J_y + E_z J_z) \end{aligned} \quad (1.6.13)$$

These equations relate force and power to the interaction of the charges and the fields. In three-dimensional notation:

$$\mathbf{F}^{\nu} = \rho \mathbf{E} + \mathbf{J} \times \mathbf{B}; \quad -icF_4^{\nu} = \mathbf{E} \cdot \mathbf{J} \quad (1.6.14)$$

To assist in the interpretation of Eq. 1.6.12, consider the 4-scalar formed by taking the scalar product:

$$F_{\alpha}^{\nu} J_{\alpha} = f_{\alpha\beta} J_{\alpha} J_{\beta} = 0 \quad (1.6.15)$$

The second equality of Eq. 1.6.15 follows from the antisymmetric character of  $f_{\alpha\beta}$  and shows that the 4-vector  $F_{\alpha}^{\nu}$  is perpendicular to the 4-current density. Since the 4-current density is proportional to the 4-velocity, it follows that  $F_{\alpha}^{\nu}$  is also perpendicular to the 4-velocity. Consider the differential with respect to proper time of the square of the 4-velocity:

$$\frac{d}{d\tau} (U_{\alpha} U_{\alpha}) = 2U_{\alpha} \frac{dU_{\alpha}}{d\tau} = \frac{d}{d\tau} (-c^2) = 0 \quad (1.6.16)$$

Therefore both the 4-acceleration and  $F_{\alpha}^{\nu}$  are perpendicular to the 4-velocity. This is a necessary but insufficient requirement for  $F_{\alpha}^{\nu}$  to be the force density.

This approach to the Maxwell equations is based upon the original axiom relating a charge to its accompanying potential. The form of the source shows that only charges produce a 4-curvature of the 4-potential field. The technique is a neat way both to package the electromagnetic equations and to show that they take the same form in all inertial coordinate systems. The relationship between fields  $\mathbf{E}$  and  $\mathbf{B}$  and the potentials follows from Eq. 1.6.3. By direct comparison

$$\begin{aligned}\frac{\partial A_j}{\partial x_i} - \frac{\partial A_i}{\partial x_j} &= B_k \Rightarrow \nabla \times \mathbf{A} = \mathbf{B} \\ -\frac{\partial \Phi}{\partial x_i} - \frac{\partial A_i}{\partial t} &= E_i \Rightarrow -\left( \nabla \Phi + \frac{\partial \mathbf{A}}{\partial t} \right) = \mathbf{E}\end{aligned}\tag{1.6.17}$$

## 1.7 Accelerating Charges

The potentials surrounding electric charges in uniform motion are given by Eq. 1.5.10 and the force fields are related to the potential by Eqs. 1.6.3. The partial derivative operations of Eqs. 1.6.3 take place at the field position and time,  $(\mathbf{r}, t)$ . The position and time at the source,  $(\mathbf{r}', t')$ , do not enter into the operations. To carry out the operations it is convenient to define  $S$  by the equation:

$$S = \left( R - \frac{\mathbf{R} \cdot \boldsymbol{\nu}}{c} \right)\tag{1.7.1}$$

Operating upon the potential while keeping terms involving charge accelerations gives:

$$\begin{aligned}\mathbf{E} &= \frac{q}{4\pi\epsilon} \left\{ \frac{1}{\gamma^2 S^3} \left( \mathbf{R} - R \frac{\boldsymbol{\nu}}{c} \right) + \frac{1}{c^2 S^3} \mathbf{R} \times \left[ \left( \mathbf{R} - R \frac{\boldsymbol{\nu}}{c} \right) \times \frac{\partial}{\partial t} \boldsymbol{\nu} \right] \right\} \\ \mathbf{B} &= \frac{1}{Rc} \mathbf{R} \times \mathbf{E}\end{aligned}\tag{1.7.2}$$

Keeping only first order terms in powers of  $v/c$  leads to:

$$\mathbf{E} = \frac{q}{4\pi\epsilon R^3} \left\{ \left( \mathbf{R} - R \frac{\boldsymbol{\nu}}{c} \right) + \frac{1}{c^2} \mathbf{R} \times \left( \mathbf{R} \times \frac{\partial}{\partial t} \boldsymbol{\nu} \right) \right\} \quad (1.7.3)$$

$$\mathbf{B} = -\frac{\mu q}{4\pi R^3} \mathbf{R} \times \left( \boldsymbol{\nu} + \frac{R}{c} \frac{\partial}{\partial t} \boldsymbol{\nu} \right)$$

The equations show that: A stationary charge produces an electric field intensity that varies as the inverse square of the radius, but there is no magnetic field. If the charge is moving, both electric and magnetic field intensities exist that are proportional to the speed of the charge and that vary as the inverse square of the radius. If the charge is accelerating, both electric and magnetic field intensities exist in proportion to the acceleration of the charge and the inverse radius. Where charge distributions are applicable Eqs. 1.7.3 take the form of spatial integrals over charge bearing regions.

## 1.8 The Maxwell Stress Tensor

Another result of four-dimensional field analysis is the Maxwell stress tensor. It is defined to be the symmetric, second rank 4-tensor  $T_{\alpha\beta}$ :

$$\mu T_{\alpha\beta} = f_{\alpha\kappa} f_{\kappa\beta} + \frac{1}{4} \delta_{\alpha\beta} f_{\nu\sigma} f_{\nu\sigma} \quad (1.8.1)$$

A symmetric 4-tensor consists of an array of ten independent numbers. It may be shown, after some algebra, that the force density 4-vector of Eq. 1.6.12 is related to the Maxwell stress tensor as:

$$F_{\alpha}^{\nu} = \partial T_{\alpha\beta} / \partial X_{\beta} \quad (1.8.2)$$

The independent components of  $T_{\alpha\beta}$  follow from Eqs. 1.6.7 and 1.8.1. The result is:

$$\begin{aligned}
T_{11} &= \frac{\epsilon}{2} (E_x^2 - E_y^2 - E_z^2) + \frac{1}{2\mu} (B_x^2 - B_y^2 - B_z^2) \\
T_{12} &= \epsilon E_x E_y + \frac{1}{\mu} B_x B_y \\
T_{22} &= \frac{\epsilon}{2} (E_y^2 - E_z^2 - E_x^2) + \frac{1}{2\mu} (B_y^2 - B_z^2 - B_x^2) \\
T_{23} &= \epsilon E_y E_z + \frac{1}{\mu} B_y B_z \\
T_{33} &= \frac{\epsilon}{2} (E_z^2 - E_x^2 - E_y^2) + \frac{1}{2\mu} (B_z^2 - B_x^2 - B_y^2) \\
T_{31} &= \epsilon E_z E_x + \frac{1}{\mu} B_z B_x \\
T_{44} &= \frac{\epsilon}{2} (E_x^2 + E_y^2 + E_z^2) + \frac{1}{2\mu} (B_x^2 + B_y^2 + B_z^2) \\
T_{14} &= \frac{1}{ic\mu} (E_y B_z - E_z B_y) \\
T_{24} &= \frac{1}{ic\mu} (E_z B_x - E_x B_z) \\
T_{34} &= \frac{1}{ic\mu} (E_x B_y - E_y B_x)
\end{aligned} \tag{1.8.3}$$

The tensor may be written in the form:

$$[T] = \begin{bmatrix} T_{ij} & \frac{i}{c} N \\ \frac{i}{c} N & w \end{bmatrix} \tag{1.8.4}$$

By definition  $w = T_{44}$  is equal to:

$$T_{44} = \frac{\epsilon}{2} E^2 + \frac{1}{2\mu} B^2 \tag{1.8.5}$$

$T_{ij}$  is the 3-dimensional Maxwell stress tensor:

$$T_{ij} = \begin{pmatrix} \frac{\epsilon}{2}[E_x^2 - E_y^2 - E_z^2] & \epsilon E_x E_y + \frac{1}{\mu} B_x B_y & \epsilon E_x E_z + \frac{1}{\mu} B_x B_z \\ +\frac{1}{2\mu}[B_x^2 - B_y^2 - B_z^2] & \frac{\epsilon}{2}[E_y^2 - E_z^2 - E_x^2] & \epsilon E_y E_z + \frac{1}{\mu} B_y B_z \\ \epsilon E_y E_x + \frac{1}{\mu} B_y B_x & +\frac{1}{2\mu}[B_y^2 - B_z^2 - B_x^2] & \frac{\epsilon}{2}[E_z^2 - E_x^2 - E_y^2] \\ \epsilon E_z E_x + \frac{1}{\mu} B_z B_x & \epsilon E_z E_y + \frac{1}{\mu} B_z B_y & +\frac{1}{2\mu}[B_z^2 - B_x^2 - B_y^2] \end{pmatrix} \quad (1.8.6)$$

$\mathbf{N}$  is the 3-dimensional Poynting vector:

$$\mathbf{N} = (\mathbf{E} \times \mathbf{B})/\mu \quad (1.8.7)$$

Symmetric tensors of rank two in three dimensions reduce from six to three components by transforming to the principal axes and aligning one axis with the source field intensity. For example, if there is no magnetic field and if the electric field intensity is directed along the  $x$ -axis the tensor reduces to:

$$[T] = \frac{\epsilon}{2} \begin{bmatrix} E^2 & 0 & 0 \\ 0 & -E^2 & 0 \\ 0 & 0 & -E^2 \end{bmatrix} \quad (1.8.8)$$

To interpret the stress tensor, consider the 4-dimensional spatial integral of Eq. 1.8.2. The equation may be written:

$$\begin{aligned} & \iiint \int c'_{\sigma\alpha} F'^{\nu}_{\alpha} dX'_1 dX'_2 dX'_3 dX'_4 \\ & = \iiint \int c'_{\sigma\alpha} \frac{\partial T'_{\alpha\beta}}{\partial X'_\beta} dX'_1 dX'_2 dX'_3 dX'_4 \end{aligned} \quad (1.8.9)$$

Working with the left side:



$$\begin{aligned}
& \iiint \int c'_{\sigma\alpha} F'^{\nu}_{\sigma} dX'_1 dX'_2 dX'_3 dX'_4 \\
&= \iiint \int F^{\nu}_{\sigma} dX'_1 dX'_2 dX'_3 dX'_4 \\
&= \iiint \int F^{\nu}_{\sigma} dX_1 dX_2 dX_3 dX_4
\end{aligned}$$

Working with the right side:

$$\begin{aligned}
& \iiint \int c'_{\sigma\alpha} \frac{\partial T'_{\alpha\beta}}{\partial X'_{\beta}} dX'_1 dX'_2 dX'_3 dX'_4 \\
&= \iiint \int \frac{\partial (c'_{\sigma\alpha} T'_{\alpha\beta})}{\partial X'_{\beta}} dX'_1 dX'_2 dX'_3 dX'_4 \\
&= \iiint \int c'_{\sigma\alpha} T'_{\alpha 4} dX'_1 dX'_2 dX'_3
\end{aligned}$$

The last equality results since the integral at the limits of the spatial integrals vanish. Working with the last integral, note that

$$c'_{\alpha\beta} T_{\sigma\alpha} = c'_{\lambda\beta} c'_{\sigma\alpha} c'_{\lambda\gamma} T'_{\alpha\gamma} \quad (1.8.10)$$

Since  $c'_{\lambda\beta} c'_{\lambda\gamma} = \delta_{\beta\gamma}$  it follows that  $c'_{\alpha\beta} T_{\sigma\alpha} = c'_{\sigma\alpha} T'_{\alpha\beta}$  from which  $c'_{\sigma\alpha} T'_{\alpha 4} = c'_{\alpha 4} T_{\sigma\alpha}$ . This leaves the equality:

$$\begin{aligned}
& \iiint \int F'^{\nu}_{\sigma} dX'_1 dX'_2 dX'_3 dX'_4 \\
&= \iiint \int c'_{\alpha 4} T_{\sigma\alpha} dX'_1 dX'_2 dX'_3
\end{aligned} \quad (1.8.11)$$

Since  $c'_{\alpha 4} = U_{\alpha}/ic$  this may be written:

$$\iiint \int F'^{\nu}_{\sigma} dX'_1 dX'_2 dX'_3 dX'_4 = \frac{1}{ic} \iiint \int T_{\sigma\alpha} U_{\alpha} dX_1 dX_2 dX_3 \quad (1.8.12)$$

To change the 4-integral into a three dimensional one, differentiate by  $(ict)$  to obtain:

$$\iiint F'^{\nu}_{\sigma} dX'_1 dX'_2 dX'_3 = F_{\sigma} = -\frac{1}{c^2} \frac{\partial}{\partial t} \iiint T_{\sigma\alpha} U_{\alpha} dX_1 dX_2 dX_3 \quad (1.8.13)$$

Since all time integrals are zero at time  $t = -\infty$ , time integration has a value only at the present time.

To examine results of these equations, consider a charge moving with low speed in the  $z$ -direction. With the axis in the direction of motion, the sum  $T_{\sigma\alpha} U_{\alpha}$  takes the form:

$$T_{3\alpha} U_{\alpha} = \frac{\epsilon}{2} E^2 \nu \quad (1.8.14)$$

Combining:

$$F = \int F^{\nu} dV = \frac{d}{dt} \left\{ \frac{\nu}{c^2} \int \left( \frac{\epsilon}{2} E^2 \right) dV \right\} \quad (1.8.15)$$

The sign was changed to represent reaction of the field on its source, rather than *vice versa*. For a low speed particle undergoing differential acceleration Eq. 1.8.15 has the form:

$$F = \frac{d}{dt} (m\nu) = \frac{d\rho}{dt} \quad (1.8.16)$$

The mass is calculated as:

$$m = \frac{1}{c^2} \int \left( \frac{\epsilon}{2} E^2 \right) dV \quad (1.8.17)$$

The interpretation accorded these equations is that Eq. 1.8.16 is Newton's law for electromagnetic mass, confirming that  $F$  is a force. The expression for the mass shows that  $(\epsilon E^2/2)$  is the energy density of an electric field.

## 1.9 Kinematic Properties of Fields

To further analyze the kinematic properties of fields, begin with the four-dimensional force equation, Eq. 1.6.14:

$$\mathbf{F}^\nu = \rho \mathbf{E} + \mathbf{J} \times \mathbf{B}; \quad -icF_4^\nu = \mathbf{E} \cdot \mathbf{J} \quad (1.9.1)$$

To express this equality in a way that depends upon the fields only, it is necessary to substitute for  $\rho$  and  $\mathbf{J}$  from the nonhomogeneous Maxwell equations, Eq. 1.6.8:

$$\begin{aligned} \mathbf{F}^\nu &= \epsilon \mathbf{E} (\nabla \cdot \mathbf{E}) - \mathbf{B} \times \left( \frac{1}{\mu} \nabla \times \mathbf{B} - \epsilon \frac{\partial \mathbf{E}}{\partial t} \right) \\ -icF_4^\nu &= \mathbf{E} \cdot \left( \frac{1}{\mu} \nabla \times \mathbf{B} - \epsilon \frac{\partial \mathbf{E}}{\partial t} \right) \end{aligned} \quad (1.9.2)$$

It is helpful to add zero to each equation in the form of terms proportional to the homogeneous Maxwell equations, Eqs. 1.2.11. The added terms are:

$$\begin{aligned} &\frac{1}{\mu} \mathbf{B} (\nabla \cdot \mathbf{B}) - \epsilon \mathbf{E} \times \left( \nabla \times \mathbf{E} + \frac{\partial \mathbf{B}}{\partial t} \right) \\ \text{and} \quad &-\mathbf{B} \cdot \left( \nabla \times \mathbf{E} + \frac{\partial \mathbf{B}}{\partial t} \right) \end{aligned} \quad (1.9.3)$$

Combining gives:

$$\begin{aligned} \mathbf{F}^\nu &= \epsilon \left\{ \mathbf{E} (\nabla \cdot \mathbf{E}) - \mathbf{E} \times (\nabla \times \mathbf{E}) \right\} + \frac{1}{\mu} \left\{ \mathbf{B} (\nabla \cdot \mathbf{B}) - \mathbf{B} \times (\nabla \times \mathbf{B}) \right\} - \frac{1}{c^2} \frac{\partial \mathbf{N}}{\partial t} \\ icF_4^\nu &= \frac{\partial}{\partial t} \left( \frac{\epsilon}{2} E^2 + \frac{1}{2\mu} B^2 \right) + \nabla \cdot \mathbf{N} \end{aligned} \quad (1.9.4)$$

Writing the first of Eqs. 1.9.4 in tensor form gives:

$$F_i^\nu = \frac{\partial}{\partial x_j} \left\{ \epsilon \left( E_i E_j - \frac{1}{2} \delta_{ij} E_k E_k \right) + \frac{1}{\mu} \left( B_i B_j - \frac{1}{2} \delta_{ij} B_k B_k \right) \right\} - \frac{1}{c^2} N_i \quad (1.9.5)$$

Integrating over a closed three-dimensional volume gives:

$$\oint \left\{ \epsilon \left( E_i E_j - \frac{1}{2} \delta_{ij} E_k E_k \right) + \frac{1}{\mu} \left( B_i B_j - \frac{1}{2} \delta_{ij} B_k B_k \right) \right\} dS_j \\ = \int \left( \frac{1}{c^2} \frac{\partial N_i}{\partial t} + F_i^v \right) dV \quad (1.9.6)$$

By Eq. 1.8.16 the last term on the right is the rate of change of momentum of all charges contained within the volume,  $\mathbf{p}_{\text{charge}}$ . Therefore, the first term on the right is the rate of change of field momentum,  $\mathbf{p}_{\text{field}}$ . It follows that the left side of the equation is equal to the force on the charges and fields within the volume of integration. The results may be written as:

$$\mathbf{p}_{\text{field}} = \frac{1}{c^2} \int \mathbf{N} dV \quad \text{and} \quad \mathbf{F}^v = \rho \mathbf{E} + \mathbf{J} \times \mathbf{B} = \frac{d}{dt} \mathbf{p}_{\text{charge}} \quad (1.9.7)$$

Since  $\mathbf{F}^v$  is a force density, it follows from Eq. 1.9.7 that the electric field intensity is a force per unit charge. Since a wave travels at speed  $c$ , by the first of Eqs. 1.9.7 the momentum passing through a planar surface is:

$$\mathbf{p}_{\text{field}} = \frac{1}{c} \int \mathbf{N} \cdot d\mathbf{S} \quad (1.9.8)$$

By definition  $d\mathbf{S}$  is a differential vector area normally outward from the surface.

Integrating the second of Eqs. 1.9.1 and 1.9.4 over a three dimensional volume gives:

$$\int (\mathbf{E} \cdot \mathbf{J}) dV = \frac{d}{dt} \int \left( \frac{\epsilon}{2} E^2 + \frac{1}{2\mu} B^2 \right) dV + \oint \mathbf{N} \cdot d\mathbf{S} \quad (1.9.9)$$

Since the field intensity is a force per unit charge it follows that the left side of Eq. 1.9.9 is the rate at which energy enters the volume of integration. Therefore the volume integral on the right side must be the rate at which energy increases in the interior, and the surface integral must be the rate at

which energy exits through the surface. It follows that the energy in the electromagnetic fields is equal to:

$$W = \int \left( \frac{\epsilon}{2} E^2 + \frac{1}{2\mu} B^2 \right) dV \quad (1.9.10)$$

It also follows that the rate at which energy exits the volume through the surface is:

$$P = \oint \mathbf{N} \cdot d\mathbf{S} \quad (1.9.11)$$

A different formulation of Eq. 1.9.10 that is sometimes useful is by rewriting it in terms of the potentials. Combining Eq. 1.9.10 with Eqs. 1.6.8 and 1.6.17 results in:

$$\begin{aligned} W = & \int [\rho\Phi + \mathbf{J} \cdot \mathbf{A}] dV + \oint \left[ -\epsilon(\phi\mathbf{E}) + \frac{1}{\mu} (\mathbf{A} \times \mathbf{B}) \right] \cdot d\mathbf{S} \\ & + \epsilon \int \left[ -\mathbf{E} \cdot \frac{\partial \mathbf{A}}{\partial t} + \mathbf{A} \cdot \frac{\partial \mathbf{E}}{\partial t} \right] dV \end{aligned} \quad (1.9.12)$$

For a charge moving at a constant speed, or if the charge acceleration is small enough so the energy escaping into the far field is negligible, only the first term of Eq. 1.9.12 is significant. For that case the total field energy may also be expressed as:

$$W = \int [\rho\Phi + \mathbf{J} \cdot \mathbf{A}] dV \quad (1.9.13)$$

## 1.10 A Lemma for Calculation of Electromagnetic Fields

A lemma is needed to assist in the unrestricted and systematic calculation of electromagnetic fields about known sources. To obtain it begin with the general form for fields in a source-free region containing time-dependent fields:

$$\nabla \times \mathbf{B} - \epsilon\mu \frac{\partial \mathbf{E}}{\partial t} = 0 = \nabla \times \mathbf{E} + \epsilon\mu \frac{\partial \mathbf{B}}{\partial t} \quad (1.10.1)$$

Taking the curl of Eq. 1.10.1 and substituting as needed gives

$$\nabla \times (\nabla \times \mathbf{B}) + \epsilon\mu \frac{\partial^2 \mathbf{B}}{\partial t^2} = 0 = \nabla \times (\nabla \times \mathbf{E}) + \epsilon\mu \frac{\partial^2 \mathbf{E}}{\partial t^2} \quad (1.10.2)$$

This shows that, away from sources,  $\mathbf{E}$  and  $\mathbf{B}$  satisfy the same partial differential equation.

$$\nabla^2 \Psi - \epsilon\mu \partial^2 \Psi / \partial t^2 = 0 \quad (1.10.3)$$

This is useful because of an associated lemma that begins with the vector field  $\mathbf{F}(\mathbf{r}, t)$ , defined by

$$\mathbf{F} = \nabla \times (\mathbf{r}\Psi) \quad (1.10.4)$$

The lemma is that if  $\Psi$  satisfies Eq. 1.10.3 then  $\mathbf{F}$  satisfies the differential equation:

$$\nabla \times (\nabla \times \mathbf{F}) + \epsilon\mu \partial^2 \mathbf{F} / \partial t^2 = 0 \quad (1.10.5)$$

To verify that Eq. 1.10.5 is correct, multiply Eq. 1.10.3 by  $(-\mathbf{r})$  then take the curl:

$$-\nabla \times (\mathbf{r} \nabla^2 \Psi) + \epsilon\mu \frac{\partial^2}{\partial t^2} [\nabla \times (\mathbf{r}\Psi)] = 0 \quad (1.10.6)$$

Comparing Eqs. 1.10.4 through 1.10.6 shows that Eq. 1.10.5 is satisfied if:

$$\nabla \times \{ \nabla \times [\nabla \times (\mathbf{r}\Psi)] \} = -\nabla \times (\mathbf{r} \nabla^2 \Psi) \quad (1.10.7)$$

To confirm Eq. 1.10.7, begin with the identity for the curl of a scalar-vector product:

$$\nabla \times (\mathbf{r}\Psi) \equiv \Psi(\nabla \times \mathbf{r}) - \mathbf{r} \times \nabla \Psi \quad (1.10.8)$$

Since  $\nabla \times \mathbf{r} \equiv 0$ , it follows that:

$$\nabla \times [\nabla \times (\mathbf{r}\Psi)] = -\nabla \times (\mathbf{r} \times \nabla \Psi) \quad (1.10.9)$$

Combining Eqs. 1.10.7 and 1.10.9 gives:

$$\nabla \times [\nabla \times (\mathbf{r} \times \nabla \Psi)] - \nabla \times (\mathbf{r} \nabla^2 \Psi) = 0 \quad (1.10.10)$$

Two identities from vector analysis are:

$$\nabla(\mathbf{A} \bullet \mathbf{B}) \equiv \mathbf{A} \times (\nabla \times \mathbf{B}) + \mathbf{B} \times (\nabla \times \mathbf{A}) + (\mathbf{B} \bullet \nabla)\mathbf{A} + (\mathbf{A} \bullet \nabla)\mathbf{B} \quad (1.10.11)$$

$$\nabla \times (\mathbf{A} \times \mathbf{B}) \equiv \mathbf{A}(\nabla \bullet \mathbf{B}) - \mathbf{B}(\nabla \bullet \mathbf{A}) + (\mathbf{B} \bullet \nabla)\mathbf{A} - (\mathbf{A} \bullet \nabla)\mathbf{B}$$

Putting  $\mathbf{A} = \mathbf{r}$  and  $\mathbf{B} = \nabla \Psi$ :

$$\nabla(\mathbf{r} \bullet \nabla \Psi) \equiv (\mathbf{r} \bullet \nabla)\nabla \Psi + (\nabla \Psi \bullet \nabla)\mathbf{r} = (\mathbf{r} \bullet \nabla)\nabla \Psi + \nabla \Psi \quad (1.10.12)$$

$$\nabla \times (\mathbf{r} \times \nabla \Psi) \equiv \mathbf{r} \nabla^2 \Psi - 2\nabla \Psi + (\mathbf{r} \bullet \nabla)\nabla \Psi$$

Combining Eqs. 1.10.10 and 1.10.12:

$$\nabla \times (\mathbf{r} \times \nabla \Psi) - \mathbf{r} \nabla^2 \Psi + \nabla \Psi + \nabla(\mathbf{r} \bullet \nabla \Psi) = 0 \quad (1.10.13)$$

Since the curl of the gradient vanishes, taking the curl of Eq. 1.10.13 yields Eq. 1.10.10 and completes the proof.

## 1.11 The Scalar Differential Equation

To solve Eq. 1.10.3 it is useful to remove the time-dependent portion. For that purpose use the Fourier integral expansion:

$$\Psi(\mathbf{r}, t) = \int_{-\infty}^{\infty} \psi(\mathbf{r}, \omega) e^{i\omega t} d\omega \quad (1.11.1)$$

Substituting Eq. 1.11.1 into Eq. 1.10.3 leads to:

$$\int_{-\infty}^{\infty} (\nabla^2 \psi + k^2 \psi) e^{i\omega t} d\omega = 0 \quad (1.11.2)$$

By definition  $k^2 = \omega^2 \epsilon \mu$ . For this equation to be zero for all values of  $\omega$ , the integrand of Eq. 1.11.2 must equal zero:

$$\nabla^2 \psi + k^2 \psi = 0 \quad (1.11.3)$$

This is the Helmholtz equation, solutions of which combine with Eqs. 1.10.3 to 1.10.5 to obtain the full solution for vector fields.

Certain helpful vector operations in spherical coordinates are listed in Table 1.11.1. Using spherical coordinates with  $\theta$  the polar angle from the  $z$ -axis,  $\phi$  the azimuth angle from the  $x$ -axis, and  $r$  the radial distance from the origin, by Table 1.11.1 the Helmholtz equation is given by:

$$\frac{1}{r^2 \sin \theta} \left[ \sin \theta \frac{\partial \psi}{\partial \theta} \right] + \frac{1}{r^2 \sin^2 \theta} \frac{\partial^2 \psi}{\partial \phi^2} + \frac{1}{r^2} \frac{\partial}{\partial r} \left[ r^2 \frac{\partial \psi}{\partial r} \right] + k^2 \psi = 0 \quad (1.11.4)$$

Dividing the equation by  $k^2$  shows that the radial dependence of the solution is a function of only the product  $\sigma = kr$ , and therefore  $\psi$  may be written as  $\psi(\sigma, \theta, \phi)$ . A theorem applicable to problems using spherical coordinates is that the complete solution of Eq. 1.11.4 is obtained by summing over all possible functions  $\psi(\sigma, \theta, \phi)$  where:



---

Orthogonal Line Elements:	$dr, r d\theta, r \sin \theta d\phi$
Divergence of Vector A:	$\left\{ (\nabla \Psi)_r = \frac{\partial \Psi}{\partial r} \quad (\nabla \Psi)_\theta = \frac{1}{r} \frac{\partial \Psi}{\partial \theta} \quad (\nabla \Psi)_\phi = \frac{1}{r \sin \theta} \frac{\partial \Psi}{\partial \phi} \right\}$
Components of Curl A:	$\left\{ \begin{aligned} (\nabla \times \mathbf{A})_r &= \frac{1}{r \sin \theta} \left[ \frac{\partial (\sin \theta A_\phi)}{\partial \theta} - \frac{\partial A_\theta}{\partial \phi} \right] \\ (\nabla \times \mathbf{A})_\theta &= \frac{1}{r \sin \theta} \frac{\partial A_r}{\partial \phi} - \frac{1}{r} \frac{\partial (r A_\phi)}{\partial r} \\ (\nabla \times \mathbf{A})_\phi &= \frac{1}{r} \left[ \frac{\partial (r A_\theta)}{\partial r} - \frac{\partial A_r}{\partial \theta} \right] \end{aligned} \right\}$
Laplacian of $\Psi = \nabla^2 \Psi$ :	$\left\{ \frac{1}{r} \frac{\partial}{\partial r} \left( r^2 \frac{\partial \Psi}{\partial r} \right) + \frac{1}{r^2 \sin \theta} \frac{\partial}{\partial \theta} \left( \sin \theta \frac{\partial \Psi}{\partial \theta} \right) + \frac{1}{r^2 \sin^2 \theta} \frac{\partial^2 \Psi}{\partial \phi^2} \right\}$

---

Table 1.11.1. Vector operations, spherical coordinates

$$\psi(r, \theta, \phi) = R(\sigma) \Theta(\theta) \Phi(\phi) \quad (1.11.5)$$

To obtain  $\psi(\sigma, \theta, \phi)$ , it is necessary to begin by solving for the solutions of Eq. 1.11.5 that involve only one independent variable. After obtaining the functional forms, all possible products are formed and weighted by a constant multiplying coefficient. The coefficient is determined by matching boundary conditions. Finally, all individual product functions with appropriate coefficients are summed.

Substituting Eq. 1.11.5 into Eq. 1.11.4 and multiplying by  $r^2$  gives:

$$\frac{1}{\Theta \sin \theta} \frac{d}{d\theta} \left( \sin \theta \frac{d\Theta}{d\theta} \right) + \frac{1}{\Phi} \frac{d^2 \Phi}{d\phi^2} + \frac{1}{R} \frac{d}{d\sigma} \left( \sigma^2 \frac{dR}{d\sigma} \right) + \sigma^2 = 0 \quad (1.11.6)$$

The first two terms are independent of the radius and the last two terms are independent of the angles, yet the two sets equal each other's negative, requiring both sets to be constant. The constant is known as the separation constant. A convenient choice of separation constant is for the radial terms to equal  $v(v+1)$  and the angular terms  $-v(v+1)$ , and results in the separated, complete differential equations:

$$\frac{1}{\sigma^2} \frac{d}{d\sigma} \left( \sigma^2 \frac{dR}{d\sigma} \right) + \left( 1 - \frac{\nu(\nu+1)}{\sigma^2} \right) R = 0 \quad (1.11.7)$$

$$\frac{\Phi}{\sin\theta} \frac{d}{d\theta} \left[ \sin\theta \frac{d\Theta}{d\theta} \right] + \frac{\Theta}{\sin^2\theta} \frac{d^2\Phi}{d\phi^2} + \nu(\nu+1)\Theta\Phi = 0 \quad (1.11.8)$$

The radial equation is a differential equation with one independent variable. The angular equation may be written as:

$$\frac{\sin\theta}{\Theta} \frac{d}{d\theta} \left[ \sin\theta \frac{d\Theta}{d\theta} \right] + \nu(\nu+1) \sin^2\theta + \frac{1}{\Phi} \frac{d^2\Phi}{d\phi^2} = 0 \quad (1.11.9)$$

The first two terms of Eq. 1.11.9 are functions of  $\theta$  only and the third is a function of  $\phi$  only, yet the terms equal each other's negative. Again, both sets are constant. Putting the first two terms equal to  $m^2$ , where  $m$  is the second separation constant, results in two separated equations, each involving only one independent variable:

$$\frac{1}{\sin\theta} \frac{d}{d\theta} \left( \sin\theta \frac{d\Theta}{d\theta} \right) + \left( \nu(\nu+1) - \frac{m^2}{\sin^2\theta} \right) \Theta = 0 \quad (1.11.10)$$

$$\frac{d^2\Phi}{d\phi^2} + m^2\Phi = 0 \quad (1.11.11)$$

Solutions of the separated differential equations and tabulated functions are in the Appendix.

Solutions of the radial equation are spherical Bessel, Neumann, and Hankel functions, respectively,  $j_\nu(\sigma)$ ,  $y_\nu(\sigma)$ , and  $h_\nu(\sigma)$ . A particularly important linear combination is Hankel functions of the second kind and integer order:  $h_\ell(\sigma)$  where “ $\ell$ ” represents any integer value of “ $\nu$ ”. Solutions of the zenith angle equation are associated Legendre functions; solutions are, in some instances, of integer order and in others of noninteger order. In all cases, the orders of the radial and zenith angle solutions are the same. Trigonometric functions form the solutions of the azimuth angle equation:

$\sin\phi$ ,  $\cos\phi$ , and  $\exp(\pm im\phi)$ . Since all solutions to be considered extend over the full range of azimuth angle, zero through  $2\pi$ , only integer values of degree  $m$ , are present. With exponential notation, the exponent may have either sign. With symbol  $z_v(\sigma)$  representing a linear combination of possible radial solution forms, rather than writing the solution as two separate sums it is rewritten as:

$$\psi_v^m(r, \theta, \phi) = z_v(\sigma) \Theta_v^m(\theta) e^{-im\phi} \quad (1.11.12)$$

With this notation, completeness requires  $m$  to include the full set of positive and negative integers, however the degree of the Legendre function is always positive.

## 1.12 Radiation Fields in Spherical Coordinates

Replacing  $\mathbf{B}$  by  $\mu\mathbf{H}$  more closely matches common usage. For what lies ahead we are concerned only with free space and there  $\mu$  is merely a unit-determining parameter that measures the magnetic field in amperes per meter instead of webers per square meter.

The field calculation procedure is due to Hansen, and begins with the vector theorem that a field with zero divergence is completely specified by its curl. It is, therefore, helpful to introduce the two independent field sets:

$$\eta\mathbf{H}_1 = \mathbf{r} \times \nabla\Psi_1 \quad \text{and} \quad \mathbf{E}_2 = \mathbf{r} \times \nabla\Psi_2 \quad (1.12.1)$$

Since the free space divergence of both vectors are zero, solutions of Eqs. 1.12.1 provide the complete set of possible values for vectors  $\mathbf{H}_1$  and  $\mathbf{E}_2$ . The remaining field solutions,  $\mathbf{H}_2$  and  $\mathbf{E}_1$ , may be obtained from Eqs. 1.12.1 using the Maxwell curl equations. The total fields,  $(\mathbf{E}_1 + \mathbf{E}_2)$  and  $(\mathbf{H}_1 + \mathbf{H}_2)$ , are then complete. If the boundary conditions are matched, the fields are also unique.

In what follows we use the notation that time dependence is  $\exp(i\omega t)$  and azimuth angle dependence is  $\exp(-jm\phi)$ , where  $i^2 = j^2 = -1$ . The reasons for separate notation are that it permits separation of polarization and time dependencies and it permits restriction of separation constant  $m$  to the field

of positive integers, without loss of generality. With Hansen's method the defining terms for phasor fields are, see Eq. 1.10.4:

$$\eta \tilde{\mathbf{H}}_1 = \mathbf{r} \times \nabla \psi_1 \quad \text{and} \quad \tilde{\mathbf{E}}_2 = \mathbf{r} \times \nabla \psi_2 \quad (1.12.2)$$

A tilde over a vector indicates that it is a phasor. It is required that the scalar functions satisfy the Helmholtz equation, Eq. 1.11.3. For integer modes, the results are solutions in the form of Eq. 1.11.12:

$$\begin{aligned} \psi_1 &= F(\ell, m) z_\ell(\sigma) \Theta_\ell^m e^{-jm\phi} \\ \psi_2 &= \mathcal{J}G(\ell, m) z_\ell(\sigma) \Theta_\ell^m e^{-jm\phi} \end{aligned} \quad (1.12.3)$$

The order is not restricted to integer values and the radial function  $z_\ell(\sigma)$  may be any linear combination of spherical Bessel and Neumann functions. The zenith angle function may be any linear combination of associated Legendre functions. Both the applicable functions and the constant multiplying coefficients  $F(\ell, m)$  and  $G(\ell, m)$  are determined by the boundary conditions.

Applying the operation of Eq. 1.12.2 to Eqs. 1.12.3 gives the result:

$$\mathbf{r} \times \nabla \psi = -\frac{\hat{\theta}}{\sin \theta} \frac{\partial \psi}{\partial \phi} + \hat{\phi} \frac{\partial \psi}{\partial \theta} \quad (1.12.4)$$

Combining gives:

$$\begin{aligned} \eta \tilde{\mathbf{H}}_1 &= F(\ell, m) z_\ell(\sigma) \left[ \mathcal{J} \hat{\theta} \frac{m \Theta_\ell^m}{\sin \theta} + \hat{\phi} \frac{d\Theta_\ell^m}{d\theta} \right] e^{-jm\phi} \\ \tilde{\mathbf{E}}_2 &= \mathcal{J}G(\ell, m) z_\ell(\sigma) \left[ \hat{\theta} \frac{m \Theta_\ell^m}{\sin \theta} + \hat{\phi} \frac{d\Theta_\ell^m}{d\theta} \right] e^{-jm\phi} \end{aligned} \quad (1.12.5)$$

Taking the curl of the second of Eqs. 1.12.5 then applying the Maxwell curl equation leads to:

$$\eta \tilde{\mathbf{H}}_2 = -\mathcal{J}G(\ell, m) e^{-jm\phi} \left\{ j\ell(\ell+1) \frac{z_\ell}{\sigma} \Theta_\ell^m \hat{\mathbf{r}} + z_\ell \left( j \frac{d\Theta_\ell^m}{d\theta} \hat{\theta} + \frac{m \Theta_\ell^m}{\sin \theta} \hat{\phi} \right) \right\} \quad (1.12.6)$$

Carat “ $\hat{\cdot}$ ” indicates a unit vector, and:

$$\mathbf{z}_\ell^\bullet(\sigma) = \frac{1}{\sigma} \frac{d}{d\sigma} [\sigma \mathbf{z}_\ell(\sigma)] \quad (1.12.7)$$

Taking the curl of the first of Eqs. 1.12.5 then applying the Maxwell curl equation leads to:

$$\tilde{\mathbf{E}}_1 = rF(\ell, m)e^{-jm\phi} \left\{ \ell(\ell+1) \frac{\mathbf{z}_\ell}{\sigma} \Theta_\ell^m \hat{\mathbf{r}} + \mathbf{z}_\ell^\bullet \left( \frac{d\Theta_\ell^m}{d\theta} \hat{\theta} - j \frac{m\Theta_\ell^m}{\sin\theta} \hat{\phi} \right) \right\} \quad (1.12.8)$$

The total fields are the sum of Eqs. 1.12.5, 1.12.6 and 1.12.8. They may be written as:

$$\begin{aligned} \tilde{\mathbf{E}}_r &= i \sum_{\ell=0}^{\infty} \sum_{m=0}^{\ell} i^{-\ell} F(\ell, m) \ell(\ell+1) \frac{\mathbf{z}_\ell(\sigma)}{\sigma} \Theta_\ell^m(\cos\theta) e^{-jm\phi} \\ \eta \tilde{\mathbf{H}}_r &= -ij \sum_{\ell=0}^{\infty} \sum_{m=0}^{\ell} i^{-\ell} G(\ell, m) \ell(\ell+1) \frac{\mathbf{z}_\ell(\sigma)}{\sigma} \Theta_\ell^m(\cos\theta) e^{-jm\phi} \\ \tilde{\mathbf{E}}_\theta &= \sum_{\ell=0}^{\infty} \sum_{m=0}^{\ell} i^{-\ell} \left[ rF(\ell, m) \mathbf{z}_\ell^\bullet \frac{d\Theta_\ell^m}{d\theta} - G(\ell, m) \mathbf{z}_{zv} \frac{m\Theta_\ell^m}{\sin\theta} \right] e^{-jm\phi} \\ \eta \tilde{\mathbf{H}}_\phi &= \sum_{\ell=0}^{\infty} \sum_{m=0}^{\ell} i^{-\ell} \left[ F(\ell, m) \mathbf{z}_\ell \frac{d\Theta_\ell^m}{d\theta} - rG(\ell, m) \mathbf{z}_\ell^\bullet \frac{m\Theta_\ell^m}{\sin\theta} \right] e^{-jm\phi} \\ \tilde{\mathbf{E}}_\phi &= -j \sum_{\ell=0}^{\infty} \sum_{m=0}^{\ell} i^{-\ell} \left[ rF(\ell, m) \mathbf{z}_\ell^\bullet \frac{m\Theta_\ell^m}{\sin\theta} - G(\ell, m) \mathbf{z}_\ell \frac{d\Theta_\ell^m}{d\theta} \right] e^{-jm\phi} \\ \eta \tilde{\mathbf{H}}_\theta &= j \sum_{\ell=0}^{\infty} \sum_{m=0}^{\ell} i^{-\ell} \left[ F(\ell, m) \mathbf{z}_\ell \frac{m\Theta_\ell^m}{\sin\theta} - rG(\ell, m) \mathbf{z}_\ell^\bullet \frac{d\Theta_\ell^m}{d\theta} \right] e^{-jm\phi} \end{aligned} \quad (1.12.9)$$

Without loss of generality, the phases of constants  $F(\ell, m)$  and  $G(\ell, m)$  and the multiplying factor  $i^{-\ell}$  have been picked for later convenience. Coefficients  $F(\ell, m)$  multiply the radial component of the electric field terms and are TM (transverse magnetic) fields and modes, where “T” indicates transverse to

the radial direction. Coefficients  $G(\ell, m)$  multiply the radial component of the magnetic field and are TE (transverse electric) fields and modes. Terms with  $\ell = m = 0$  have no radial fields and are the TEM (transverse electric and magnetic) fields and mode. This result is valid for all possible electromagnetic field solutions.

Keeping only the real or only the imaginary part with respect to “ $j$ ” provides, respectively,  $x$  or  $y$  polarization of the electric field intensity. The fields are right or left circularly polarized, respectively, with  $j = i$  or  $j = -i$ . Since this result is applicable to all time-dependent outgoing waves, it follows that it also applies when the rate of change is arbitrarily small. Hence, it describes fields in the limit as the frequency goes to zero, a static charge distribution. Because of this general result, it is helpful to obtain a physical view of what constitutes field sources. The sources of coefficients  $F(\ell, m)$  and  $G(\ell, m)$  for static fields are discussed in the appendix, Sections A.28 and A.29.

Consider a few special cases of Eqs. 1.12.9. If the described fields are contained within a source-free region of space, and if that space is loss free, solutions have positive, integer values of orders and integer values of degrees. Spherical Bessel functions, which have no singularities, form the radial portion of the solution; spherical Neumann functions, which have singularities, are not present. Associated Legendre functions of the first kind, and of integer order, which have no singularities, form the angular portion of the solution; fractional order associated Legendre functions and those of the second kind, which have singularities, are not present.

In the main, if the fields originate at a point and support an outward flow of energy from that point, the radial portion of the solution consists of spherical Hankel functions of the second kind. A solution within an enclosed space that excludes the  $z$ -axis, but has rotational symmetry, is described by associated Legendre functions of both the first and second kind, with noninteger, positive-real orders and integer degrees.

In all cases, if the medium in which the fields exist is lossy, the separation constants are complex numbers with a positive real part. Since all cases of interest in this book concern lossless medium and a full  $2\pi$  spatial rotation about the  $z$ -axis, both the order and degree are real and degrees have only integer values.

### 1.13 Electromagnetic Fields in a Box

To analyze a later radiation problem, it is helpful to know the number of independent field solutions that can exist within a prescribed volume. For example, consider all possible electromagnetic field modes that can exist inside an otherwise empty, rectangular cavity confined by walls of infinite conductivity. With sinusoidal field excitation, the Maxwell equations have the form:

$$\eta \tilde{\mathbf{H}} = \frac{i}{k} \nabla \times \tilde{\mathbf{E}} \quad \tilde{\mathbf{E}} = -\frac{i}{k} \nabla \times (\eta \tilde{\mathbf{H}}) \quad (1.13.1)$$

Assign axial directions to each side of the box; the cavity length in the  $x$ -direction is  $a$ , in the  $y$ -direction is  $b$ , and in the  $z$ -direction is  $d$ .

Application of conducting boundary conditions requires the  $z$ -component of the electric field intensity to equal zero at  $x = 0$  and  $a$ , and at  $y = 0$  and  $b$ . If both the electric and magnetic fields at  $z = 0$  and  $d$  are equal to zero the result is the trivial one of no fields at all. Application of the boundary conditions also requires the  $z$ -component of the magnetic field intensity to equal zero at  $z = 0$  and  $d$  and to have zero slope at the  $x$ - and  $y$ -directed boundaries. The result is that the most general forms of normalized field solutions have the  $z$ -components:

$$\begin{aligned} \eta H_z(x, y, z, t) &= \cos\left(\frac{\ell\pi x}{a}\right) \cos\left(\frac{m\pi y}{b}\right) \sin\left(\frac{n\pi z}{d}\right) e^{i\omega t} \\ E_z(x, y, z, t) &= \sin\left(\frac{\ell\pi x}{a}\right) \sin\left(\frac{m\pi y}{b}\right) \cos\left(\frac{n\pi z}{d}\right) e^{i\omega t} \end{aligned} \quad (1.13.2)$$

Symbols  $\ell$ ,  $m$ , and  $n$  indicate positive integers.

For the case of  $E_z(x, y, z, t) = 0$ , the complete set of remaining fields is:

$$\begin{aligned} \eta H_z(x, y, z, t) &= \cos\left(\frac{\ell\pi x}{a}\right) \cos\left(\frac{m\pi y}{b}\right) \sin\left(\frac{n\pi z}{d}\right) \sin(\omega t) \\ \eta H_x(x, y, z, t) &= -\frac{1}{k_c^2} \left(\frac{\ell\pi}{a}\right) \left(\frac{m\pi}{d}\right) \sin\left(\frac{\ell\pi x}{a}\right) \cos\left(\frac{m\pi y}{b}\right) \cos\left(\frac{n\pi z}{d}\right) \sin(\omega t) \\ \eta H_y(x, y, z, t) &= -\frac{1}{k_c^2} \left(\frac{m\pi}{b}\right) \left(\frac{n\pi}{d}\right) \cos\left(\frac{\ell\pi x}{a}\right) \sin\left(\frac{m\pi y}{b}\right) \cos\left(\frac{n\pi z}{d}\right) \sin(\omega t) \end{aligned} \quad (1.13.3)$$

$$E_x(x, y, z, t) = \frac{k}{k_c^2} \left( \frac{m\pi}{b} \right) \cos\left(\frac{\ell\pi x}{a}\right) \sin\left(\frac{m\pi y}{b}\right) \sin\left(\frac{n\pi z}{d}\right) \cos(\omega t)$$

$$E_y(x, y, z, t) = -\frac{k}{k_c^2} \left( \frac{\ell\pi}{a} \right) \sin\left(\frac{\ell\pi x}{a}\right) \cos\left(\frac{m\pi y}{b}\right) \sin\left(\frac{n\pi z}{d}\right) \cos(\omega t)$$

In Eq. 1.13.3 the definition  $k = \omega/c$  is used, and:

$$k^2 = \left( \frac{\ell\pi}{a} \right)^2 + \left( \frac{m\pi}{b} \right)^2 + \left( \frac{n\pi}{d} \right)^2 \quad (1.13.4)$$

$$k_c^2 = \left( \frac{\ell\pi}{a} \right)^2 + \left( \frac{m\pi}{b} \right)^2 \quad (1.13.5)$$

The field energy is given by:

$$W = \frac{1}{2} \int (\epsilon E^2 + \mu H^2) dV \quad (1.13.6)$$

Substituting Eqs. 1.13.3 into 1.13.6 gives the result:

$$W = \epsilon \frac{abd}{16} \left\{ 1 + \frac{\left( \frac{\ell\pi}{a} \right)^2 \left( \frac{m\pi}{d} \right)^2 + \left( \frac{m\pi}{b} \right)^2 \left( \frac{n\pi}{d} \right)^2}{\left[ \left( \frac{\ell\pi}{a} \right)^2 + \left( \frac{m\pi}{b} \right)^2 \right]^2} \right\} \quad (1.13.7)$$

Evaluating the energy of solutions with  $H_z(x, y, z, t) = 0$  yields dual solutions and the same energy form.

Of interest with a problem to come is the number of possible separate solutions for electromagnetic fields in a box of dimensions  $a, b, d$ . Unit lengths along the  $x$ -,  $y$ - and  $z$ -axes in  $k$ -space are, respectively,  $\pi/a$ ,  $\pi/b$  and  $\pi/d$ . Since each point in the upper right quadrant of  $k$ -space corresponds to a separate solution to each of Eqs. 1.13.2 the number of separate solutions is just twice the volume of the upper right quadrant. If the box is very large the line spacing is vanishingly small.



## References

- R. Becker, *Electromagnetic Fields and Interactions*, Blaisdell Publishing Co. and Blackie and Son (1964), reprinted by Dover Publications (1982)
- W.W. Hansen, "A New Type of Expansion in Radiation Problems," *Phys. Rev.*, vol. 47, pp.139-143 (1935)
- J.D. Jackson, *Classical Electrodynamics*, 2<sup>nd</sup> ed., John Wiley (1975)
- L.D. Landau, E.M. Lifshitz, *The Classical Theory of Fields*, trans. by H. Hamermesh, Addison-Wesley (1951)
- W.K.H. Panofsky, M. Phillips, *Classical Electricity and Magnetism*, 2<sup>nd</sup> ed., Addison-Wesley (1961)
- A. Sommerfeld, *Electrodynamics*, Academic Press (1952)
- J.A. Stratton, *Electromagnetic Theory*, McGraw-Hill (1941)
- J.B. Westgard, *Electrodynamics: A Concise Introduction*, Springer-Verlag (1997)

## 2. Selected Boundary Value Problems

### 2.1 Traveling Waves

It is helpful in many ways to have an expression for a plane wave although, since they extend infinitely in two directions normal to the direction of propagation, they do not exist. Plane waves are used to describe the interaction of a wave with an object much smaller than the region over which the wave approximates a plane wave. Spherical waves do exist and so long as the radius of curvature of the sphere is much larger than other dimensions of interest a plane wave analysis is justified. The criterion is simply that the non-planar nature of the wave be negligible at the problem of interest.

The electric and magnetic fields of a unit magnitude,  $x$ -polarized,  $z$ -directed plane wave expressed in rectangular coordinates are:

$$\tilde{\mathbf{E}} = \hat{x}e^{-ikz} \quad \text{and} \quad \eta\tilde{\mathbf{H}} = \hat{y}e^{-ikz} \quad (2.1.1)$$

The same fields expressed in spherical coordinates are:

$$\begin{aligned} \tilde{\mathbf{E}} &= e^{-i\sigma \cos\theta} \left\{ \sin\theta \cos\phi \hat{r} + \cos\theta \cos\phi \hat{\theta} - \sin\phi \hat{\phi} \right\} \\ \eta\tilde{\mathbf{H}} &= e^{-i\sigma \cos\theta} \left\{ \sin\theta \sin\phi \hat{r} + \sin\theta \sin\phi \hat{\theta} + \cos\phi \hat{\phi} \right\} \end{aligned} \quad (2.1.2)$$

The fields of Eqs. 1.12.9 may, of course, be used to describe plane waves; it is only necessary to obtain appropriate values for the coefficients  $F(\ell, m)$  and  $G(\ell, m)$ , and to evaluate the different mathematical functions. To do so it is most convenient to work with the radial field components only. The radial component of the electric field intensity of Eqs. 1.12.9 is:

$$\tilde{E}_r = i \sum_{\ell=0}^{\infty} \sum_{m=0}^{\ell} i^{-\ell} F(\ell, m) \ell(\ell+1) \frac{z_{\ell}(\sigma)}{\sigma} \Theta_{\ell}^m(\cos \theta) e^{-jm\phi} \quad (2.1.3)$$

Since a plane wave has no singularities neither does the radial function of Eq. 2.1.3; it follows that only spherical Bessel functions form part of the solution, with  $z_{\ell}(\sigma)$  replaced by  $j_{\ell}(\sigma)$ . Since the wave occupies all values of azimuth angles  $\phi$ , degree  $m$  must be an integer. Since the  $z$ -axes are included in the solution only integer order associated Legendre functions of the first kind,  $P_{\ell}^m(\cos \theta)$ , are present. Applying these conditions and equating Eq. 2.1.3 with the radial component of Eq. 2.1.2 gives:

$$\sin \theta \cos \phi e^{-i\sigma \cos \theta} = i \sum_{\ell=0}^{\infty} \sum_{m=0}^{\ell} i^{-\ell} F(\ell, m) \ell(\ell+1) \frac{j_{\ell}(\sigma)}{\sigma} P_{\ell}^m(\cos \theta) e^{-jm\phi} \quad (2.1.4)$$

The azimuth dependence of Eq. 2.1.4 shows that only coefficients of degree one,  $F(\ell, 1)$ , are different from zero, as are all imaginary parts with respect to “ $j$ ”. This leaves the equality:

$$e^{-i\sigma \cos \theta} = \frac{i}{\sigma} \sum_{\ell=1}^{\infty} i^{-\ell} F(\ell, 1) \ell(\ell+1) j_{\ell}(\sigma) \frac{P_{\ell}^1(\cos \theta)}{\sin \theta} \quad (2.1.5)$$

Another expansion for the exponential is listed in the appendix, Table A.27.1.2:

$$e^{-i\sigma \cos \theta} = \frac{i}{\sigma} \sum_{\ell=1}^{\infty} i^{-\ell} (2\ell+1) j_{\ell}(\sigma) \frac{P_{\ell}^1(\cos \theta)}{\sin \theta} \quad (2.1.6)$$

Equating the two expressions shows that the coefficient is:

$$F(\ell, 1) = \frac{(2\ell+1)}{\ell(\ell+1)} \quad (2.1.7)$$

Entering these results into Eq. 2.1.3 gives:

$$\tilde{E}_r = i \sum_{\ell=1}^{\infty} r^{-\ell} (2\ell+1) \frac{j_{\ell}(\sigma)}{\sigma} P_{\ell}^1(\cos\theta) \cos\phi \quad (2.1.8)$$

Working with TE modes in a similar way results in the equalities:

$$G(\ell,1) = -\frac{(2\ell+1)}{\ell(\ell+1)} \quad (2.1.9)$$

$$\eta \tilde{H}_r = i \sum_{\ell=1}^{\infty} r^{-\ell} (2\ell+1) \frac{j_{\ell}(\sigma)}{\sigma} P_{\ell}^1(\cos\theta) \sin\phi \quad (2.1.10)$$

The angular field components follow from the radial components and the form of Eqs. 1.12.9:

$$\begin{aligned} \tilde{E}_{\theta} &= \sum_{\ell=1}^{\infty} r^{-\ell} \frac{(2\ell+1)}{\ell(\ell+1)} \left[ j_{\ell}^{\bullet}(\sigma) \frac{dP_{\ell}^1}{d\theta} + j_{\ell}(\sigma) \frac{P_{\ell}^1}{\sin\theta} \right] \cos\phi \\ \eta \tilde{H}_{\phi} &= \sum_{\ell=1}^{\infty} r^{-\ell} \frac{(2\ell+1)}{\ell(\ell+1)} \left[ j_{\ell}(\sigma) \frac{dP_{\ell}^1}{d\theta} + j_{\ell}^{\bullet}(\sigma) \frac{P_{\ell}^1}{\sin\theta} \right] \cos\phi \\ \tilde{E}_{\phi} &= -\sum_{\ell=1}^{\infty} r^{-\ell} \frac{(2\ell+1)}{\ell(\ell+1)} \left[ j_{\ell}(\sigma) \frac{dP_{\ell}^1}{d\theta} + j_{\ell}^{\bullet}(\sigma) \frac{P_{\ell}^1}{\sin\theta} \right] \sin\phi \\ \eta \tilde{H}_{\theta} &= \sum_{\ell=1}^{\infty} r^{-\ell} \frac{(2\ell+1)}{\ell(\ell+1)} \left[ j_{\ell}^{\bullet}(\sigma) \frac{dP_{\ell}^1}{d\theta} + j_{\ell}(\sigma) \frac{P_{\ell}^1}{\sin\theta} \right] \sin\phi \end{aligned} \quad (2.1.11)$$

Equations 2.1.8, 2.1.10, and 2.1.11 are the electric and magnetic fields of a unit magnitude,  $x$ -polarized,  $z$ -directed plane wave expressed in spherical coordinates using spherical functions.

## *Scattering*

### 2.2 Scattering of a Plane Wave by a Sphere

A spherical object of radius  $a$  is immersed in the plane wave described by Eqs. 2.1.8, 2.1.10, and 2.1.11. Analysis of the interaction between the sphere and the plane wave is done by separating the procedure into steps. In the first step energy and momentum is extracted from the wave and applied to the sphere; these are extinction values of energy and momentum. In the second step the extinction values separate into parts. The scatterer permanently retains the absorbed energy and the scattered energy goes back into space. To determine the scattered fields everywhere, note that all possible fields are expressible in the form of Eqs. 1.12.9. Problem solution is simplified if three characteristics of the scattered field are noted. First, since scattered fields exist on the  $z$ -axis and since only associated Legendre polynomials of integer order converge on that axis the zenith angle dependence varies as associated Legendre polynomials of integer order. Second, the total scattered power is constant in the limit of infinite radius and constant power requires outgoing fields to vary with distance as  $e^{-i\sigma}/\sigma$ . Only spherical Hankel functions of the second kind have the needed limiting form and satisfy the spherical Bessel differential equation. Third, the scattered field possesses only the symmetries of the scatterer and the input field. Therefore, only fields of degree one are present.

To solve for the magnitudes and phases of the scattered modes it is convenient to multiply each set of modes by sets of complex constant coefficients:  $\alpha_\ell$  for TE modes and  $\beta_\ell$  for TM modes. With this definition the radial components of the scattered fields are:

$$\begin{aligned}\tilde{E}_r &= i \sum_{\ell=1}^{\infty} i^{-\ell} (2\ell+1) \frac{\beta_\ell h_\ell(\sigma)}{\sigma} P_\ell^1(\cos\theta) \cos\phi \\ \eta \tilde{H}_r &= i \sum_{\ell=1}^{\infty} i^{-\ell} (2\ell+1) \frac{\alpha_\ell h_\ell(\sigma)}{\sigma} P_\ell^1(\cos\theta) \sin\phi\end{aligned}\tag{2.2.1}$$

Problem solution requires evaluation of each value of  $\alpha_\ell$  and  $\beta_\ell$ . With "•" defined by Eq. 1.12.7, the sum of plane and scattered fields is:

$$\begin{aligned}
\sigma \tilde{E}_r &= i \sum_{\ell=1}^{\infty} i^{-\ell} (2\ell+1) (j_\ell + \beta_\ell h_\ell) P_\ell^1(\cos\theta) \cos\phi \\
\sigma \eta \tilde{H}_r &= i \sum_{\ell=1}^{\infty} i^{-\ell} (2\ell+1) (j_\ell + \alpha_\ell h_\ell) P_\ell^1(\cos\theta) \sin\phi \\
\tilde{E}_\theta &= \sum_{\ell=1}^{\infty} i^{-\ell} \frac{2\ell+1}{\ell(\ell+1)} \left[ \alpha j_\ell^\bullet + \beta h_\ell^\bullet \frac{dP_\ell^1}{d\theta} + (j_\ell + \alpha_\ell h_\ell) \frac{P_\ell^1}{\sin\theta} \right] \cos\phi \\
\eta \tilde{H}_\phi &= \sum_{\ell=1}^{\infty} i^{-\ell} \frac{2\ell+1}{\ell(\ell+1)} \left[ (j_\ell + \beta_\ell h_\ell) \frac{dP_\ell^1}{d\theta} + \alpha j_\ell^\bullet + \alpha_\ell h_\ell^\bullet \frac{P_\ell^1}{\sin\theta} \right] \cos\phi \\
\tilde{E}_\phi &= - \sum_{\ell=1}^{\infty} i^{-\ell} \frac{2\ell+1}{\ell(\ell+1)} \left[ (j_\ell + \alpha_\ell h_\ell) \frac{dP_\ell^1}{d\theta} + \alpha j_\ell^\bullet + \beta h_\ell^\bullet \frac{P_\ell^1}{\sin\theta} \right] \sin\phi \\
\eta \tilde{H}_\phi &= \sum_{\ell=1}^{\infty} i^{-\ell} \frac{2\ell+1}{\ell(\ell+1)} \left[ \alpha j_\ell^\bullet + \alpha_\ell h_\ell^\bullet \frac{dP_\ell^1}{d\theta} + (j_\ell + \beta_\ell h_\ell) \frac{P_\ell^1}{\sin\theta} \right] \sin\phi
\end{aligned} \tag{2.2.2}$$

By Poynting's theorem the time-average power,  $P_{av}$ , on a spherical, virtual surface of radius  $\sigma/k$  circumscribing the scatterer is equal to the real part of the surface integral of the radial component of complex Poynting vector  $N_{cr} = (\tilde{E} \times \tilde{H})_r / 2$ , see Eq. A.11.5:

$$P_{av} = \frac{\sigma^2}{\eta k^2} \int_0^{2\pi} d\phi \int_0^\pi \sin\theta d\theta \operatorname{Re}(N_{cr}) \tag{2.2.3}$$

Using Eqs. 2.2.2 to evaluate the radial component, and “\*” indicating complex conjugate, the complex Poynting vector is:

$$N_{cr} = \operatorname{Re} \frac{\sigma^2}{2\eta k^2} \sum_{\ell=1}^{\infty} \sum_{n=1}^{\infty} i^{n-\ell} \left( \frac{(2\ell+1)}{\ell(\ell+1)} \right) \left( \frac{(2n+1)}{n(n+1)} \right) \times$$

$$\left\{ \begin{aligned} & i \left[ \begin{aligned} & \left( j_n + \beta_n^* h_n^* \right) \left( j_\ell^* + \beta_\ell h_\ell^* \right) \left( \frac{dP_\ell^1}{d\theta} \frac{dP_n^1}{d\theta} \cos^2 \phi + \frac{P_\ell^1 P_n^1}{\sin^2 \theta} \sin^2 \phi \right) \\ & - \left( j_\ell + \alpha_\ell h_\ell \right) \left( j_n^* + \alpha_n^* h_n^{**} \right) \left( \frac{dP_\ell^1}{d\theta} \frac{dP_n^1}{d\theta} \sin^2 \phi + \frac{P_\ell^1 P_n^1}{\sin^2 \theta} \cos^2 \phi \right) \end{aligned} \right] \\ & + \left[ \begin{aligned} & \left( j_\ell + \alpha_\ell h_\ell \right) \left( j_n + \beta_n^* h_n^* \right) \left( \frac{dP_\ell^1}{d\theta} \frac{P_n^1}{\sin \theta} \sin^2 \phi + \frac{P_\ell^1}{\sin \theta} \frac{dP_n^1}{d\theta} \cos^2 \phi \right) \\ & + \left( j_n^* + \alpha_n^* h_n^{**} \right) \left( j_\ell^* + \beta_\ell h_\ell^* \right) \left( \frac{dP_\ell^1}{d\theta} \frac{P_n^1}{\sin \theta} \cos^2 \phi + \frac{P_\ell^1}{\sin \theta} \frac{dP_n^1}{d\theta} \sin^2 \phi \right) \end{aligned} \right] \end{aligned} \right\} \quad (2.2.4)$$

Inserting Eq. 2.2.4 into the integral of Eq. 2.2.3 and integrating over the azimuth angle gives:

$$P_{av} = \int_0^\pi \sin \theta d\theta \left\{ \begin{aligned} & \text{Re} \frac{\pi \sigma^2}{2\eta k^2} \sum_{\ell=1}^{\infty} \sum_{n=1}^{\infty} i^{n-\ell} \left( \frac{(2\ell+1)}{\ell(\ell+1)} \right) \left( \frac{(2n+1)}{n(n+1)} \right) \times \\ & \left\{ i \left[ \left( j_n + \beta_n^* h_n^* \right) \left( j_\ell^* + \beta_\ell h_\ell^* \right) - \left( j_\ell + \alpha_\ell h_\ell \right) \left( j_n^* + \alpha_n^* h_n^{**} \right) \right] \right. \\ & \times \left[ \frac{dP_\ell^1}{d\theta} \frac{dP_n^1}{d\theta} + \frac{P_\ell^1 P_n^1}{\sin^2 \theta} \right] \\ & + \left[ \left( j_\ell^* + \beta_\ell h_\ell^* \right) \left( j_n^* + \alpha_n^* h_n^{**} \right) + \left( j_\ell + \alpha_\ell h_\ell \right) \left( j_n + \beta_n^* h_n^* \right) \right] \\ & \times \left[ \frac{1}{\sin \theta} \frac{d(P_n^1 P_\ell^1)}{d\theta} \right] \end{aligned} \right\} \quad (2.2.5)$$

Using integrals in Table A.22.1.3 and A.22.1.6 to evaluate the integrals of Eq. 2.2.5 gives:

$$P_{av} = \frac{\pi \sigma^2}{\eta k^2} \text{Re} \sum_{\ell=1}^{\infty} d(2\ell+1) \left[ \left( j_\ell + \beta_\ell^* h_\ell^* \right) \left( j_\ell^* + \beta_\ell h_\ell^* \right) - \left( j_\ell + \alpha_\ell h_\ell \right) \left( j_\ell^* + \alpha_\ell^* h_\ell^{**} \right) \right] \quad (2.2.6)$$

In the limit as the radius becomes many times larger than either radius  $a$  or wavelength  $\lambda$ , Eq. 2.2.6 simplifies to:

$$P_{av} = \frac{\pi}{\eta k^2} \sum_{\ell=1}^{\infty} (2\ell+1) \left[ \operatorname{Re}(\alpha_{\ell} + \beta_{\ell}) + (\alpha_{\ell} \alpha_{\ell}^* + \beta_{\ell} \beta_{\ell}^*) \right] \quad (2.2.7)$$

Energy and momentum are transported into the system on the plane wave; both are transferred to the scatterer. The input power is equal to the term proportional to  $\operatorname{Re}(\alpha_{\ell} + \beta_{\ell})$ . The total power first extracted from the beam is defined as extinction power, and is always positive. Changing the sign to conform with this usage, the extinction power is:

$$P_{EX} = -\frac{\pi}{\eta k^2} \operatorname{Re} \sum_{\ell=1}^{\infty} (2\ell+1) (\alpha_{\ell} + \beta_{\ell}) \quad (2.2.8)$$

The power scattered back into the field is equal to:

$$P_{SC} = \frac{\pi}{\eta k^2} \sum_{\ell=1}^{\infty} (2\ell+1) (\alpha_{\ell} \alpha_{\ell}^* + \beta_{\ell} \beta_{\ell}^*) \quad (2.2.9)$$

Absorbed power, the negative of Eq. 2.2.7, does not reappear in the field but may be calculated by subtracting the scattered power from the extinction power. Lossless scatterers have no absorbed power and, therefore, for them Eq. 2.2.7 is equal to zero.

The critical scattering parameters are commonly normalized to a value that is independent of the magnitude of the plane wave. Define scattering cross section,  $C_{SC}$ , to equal the scattered power-to-incoming power density ratio. With a unit magnitude electric field intensity the incoming power density is  $1/(2\eta)$ , see Eqs. 2.1.1 and A.11.5. Values are sometimes also normalized with respect to the geometric cross section. Cross section has the dimensions of an area, and normalization with respect to the geometric cross sectional area gives a measure of size the scatterer appears to be versus the size it would appear with zero wavelength optics. Define geometric cross section,  $C_{GE}$ , to be the area the scatterer presents to the plane wave. For example, the geometric cross sectional area of a spherical scatterer of radius  $a$  is  $C_{GE} = \pi a^2$ . Combining the definition with Eqs. 2.1.11 and Eq. 2.12.9 shows the scattering-to-geometric cross section ratio to be:



$$\frac{C_{SC}}{C_{GE}} = \frac{2}{k^2 a^2} \sum_{\ell=1}^{\infty} (2\ell+1) [\alpha_{\ell} \alpha_{\ell}^* + \beta_{\ell} \beta_{\ell}^*] \quad (2.2.10)$$

Similarly, the extinction cross section,  $C_{EX}$ , is defined to equal the extinction power-to-incoming power density ratio. Combining the definition with Eqs. 2.1.11 and Eq. 2.2.8 shows the extinction-to-geometric cross section ratio to be:

$$\frac{C_{EX}}{C_{GE}} = -\frac{2}{k^2 a^2} \sum_{\ell=1}^{\infty} (2\ell+1) \text{Re}(\alpha_{\ell} + \beta_{\ell}) \quad (2.2.11)$$

A third cross section that is often of interest is radar cross section. Define the radar cross section,  $C_{RCS}$ , to equal the quotient of the power that would be scattered if the power density were everywhere equal to its value at  $\theta = \pi$  divided by the incoming power density. It is a measure of the power returned towards a single interrogating radar antenna. By definition, the power scattered in direction  $\theta = \pi$  is the back-scattered power. To determine the radar cross section, evaluate Eq. 2.2.4 at  $\theta = \pi$ . The angular functions at that angle are equal to:

$$\frac{dP_{\ell}^1}{d\theta} = -\frac{P_{\ell}^1}{\sin\theta} = \frac{1}{2} \ell(\ell+1)(-1)^{\ell} \quad (2.2.12)$$

Carrying out the calculation then normalizing by both the incoming power density and the geometric cross section results in the normalized radar cross section:

$$\frac{C_{RCS}}{C_{GE}} = \frac{1}{k^2 a^2} \sum_{\ell=1}^{\infty} \sum_{n=1}^{\ell} (2\ell+1)(2n+1)(-1)^{\ell+n} U(\ell-n) [\alpha_{\ell} - \beta_{\ell}](\alpha_n^* - \beta_n^*) \quad (2.2.13)$$

Function  $U(\ell-n)$  is the step function:

$$U(\ell - n) = \begin{cases} 1 & \ell > n \\ 1/2 & \ell = n \\ 0 & \ell < n \end{cases} \quad (2.2.14)$$

As shown by Eq. 1.9.8 the fields carry momentum as well as energy, and momentum transfer from the field to the scatterer constitutes an applied force. The momentum transferred to the scatterer by the extinction energy is in the direction of the incoming wave and, by Eq. 1.9.8, is equal to the energy divided by  $c$ . The scattered power transfers momentum in proportion to the cosine of the angle between the incident and scattering directions. The back-scattered and forward-scattered portions of the power produce momentum respectively into or away from the direction of the beam. The sign of the total transferred momentum depends upon which type dominates, and that depends upon details of the specific scatterer. Although the resulting force is too small to be significant in most macro-scale applications, nonetheless it exists and affects all scatterers and receiving antennas.

It is also possible to calculate the force on a scatterer because of the scattered field,  $F_{SC}$ . The physical origin of the force is that the surface currents move, at least partially in phase with the incident field, in the  $x$ -direction. The incident magnetic field intensity is  $y$ -directed. It interacts with the  $x$ -directed current density to form a  $z$ -directed force. However, this is not the way to calculate the force. For purposes of calculation, note that the momentum density is directly proportional to the power density, differing only by a factor of  $c$ . The force is most easily calculated by taking the  $z$ -component of the scattered power, which is equal to the integral of the product of the Poynting vector and the cosine of the scattering angle. With the help of Eq. 1.9.7 the expression for the force in the direction of the plane wave is:

$$F_{SC} = -\frac{\sigma^2}{2ck^2} \int_0^{2\pi} \int_0^{\pi} \sin\theta \cos\theta d\theta d\phi \operatorname{Re}(N_r) \quad (2.2.15)$$

Substituting the scattered fields of Eqs. 2.2.1 into Eq. 2.2.15 and integrating

$$F_{SC} = -\int_0^\pi \sin\theta d\theta \left\{ \frac{\pi\epsilon\sigma^2}{2k^2} \operatorname{Re} \sum_{\ell=1}^{\infty} \sum_{n=1}^{\infty} i^{n-\ell} \left( \frac{(2\ell+1)}{\ell(\ell+1)} \right) \left( \frac{(2n+1)}{n(n+1)} \right) \times \right. \\ \left. \left[ \beta_\ell \beta_n^* h_n^* h_\ell^\bullet - \alpha_\ell \alpha_n^* h_\ell h_n^* \right] \left[ \frac{dP_\ell^1}{d\theta} \frac{dP_n^1}{d\theta} + \frac{P_\ell^1 P_n^1}{\sin^2\theta} \right] \cos\theta \right. \\ \left. + \left[ \alpha_\ell \beta_n^* h_n h_\ell^* + \alpha_n^* \beta_\ell h_\ell^\bullet h_n^* \right] \left[ \frac{1}{\sin\theta} \frac{d(P_\ell^1 P_n^1)}{d\theta} \right] \cos\theta \right\} \quad (2.2.16)$$

Inserting the integrals of Table A.22.1.4 and A.22.1.7 into Eq. 2.2.16 gives:

$$F_{SC} = \left\{ \frac{\pi\epsilon\sigma^2}{k^2} \operatorname{Re} \sum_{\ell=1}^{\infty} \left( \frac{\ell(\ell+2)}{(\ell+1)} \right) \left[ \alpha_\ell \alpha_{\ell+1}^* h_{\ell+1}^* h_\ell^\bullet - \beta_\ell \beta_{\ell+1}^* h_\ell h_{\ell+1}^* \right] \right. \\ \left. - \frac{\pi\epsilon\sigma^2}{k^2} \operatorname{Re} \sum_{\ell=1}^{\infty} \left( \frac{(\ell-1)(\ell+1)}{\ell} \right) \left[ \beta_\ell \beta_{\ell-1}^* h_{\ell-1}^* h_\ell^\bullet - \alpha_\ell \alpha_{\ell-1}^* h_\ell h_{\ell-1}^* \right] \right. \\ \left. - \frac{\pi\epsilon\sigma^2}{k^2} \operatorname{Re} \sum_{\ell=1}^{\infty} \left( \frac{(2\ell+1)}{\ell(\ell+1)} \right) \left[ \alpha_\ell \beta_\ell^* h_\ell^\bullet h_\ell^* + \alpha_\ell^* \beta_\ell h_\ell h_\ell^* \right] \right\} \quad (2.2.17)$$

In the far field Eq. 2.2.17 goes to:

$$F_{SC} = -\frac{\epsilon\pi}{k^2} \sum_{\ell=1}^{\infty} \left\{ \frac{\ell(\ell+2)}{(\ell+1)} \left( \alpha_\ell \alpha_{\ell+1}^* + \alpha_\ell^* \alpha_{\ell+1} + \beta_\ell \beta_{\ell+1}^* + \beta_\ell^* \beta_{\ell+1} \right) \right. \\ \left. + \frac{(2\ell+1)}{\ell(\ell+1)} \left( \alpha_\ell \beta_\ell^* + \alpha_\ell^* \beta_\ell \right) \right\} \quad (2.2.18)$$

Using Eq. 2.2.11, the force due to reception of the extinction power, the extinction force,  $F_{EX}$  is in the direction of the incoming field. Normalizing  $F_{EX}$  by the incoming power density determines the normalized force,  $f_{EX}$ . Normalizing it by the geometric cross section gives:

$$\frac{f_{EX}}{C_{GE}} = -\frac{2}{ck^2 a^2} \sum_{\ell=1}^{\infty} (2\ell+1) \operatorname{Re}(\alpha_\ell + \beta_\ell) \quad (2.2.19)$$

Summing Eq. 2.2.18 and Eq. 2.2.19 gives the normalized total force on the scatterer:

$$\frac{(f_{SC} + f_{EX})}{C_{GE}} = -\frac{2}{ck^2 a^2} \sum_{\ell=1}^{\infty} \left\{ \begin{aligned} &(2\ell+1)\text{Re}(\alpha_{\ell} + \beta_{\ell}) \\ &\frac{\ell(\ell+2)}{(\ell+1)} (\alpha_{\ell} \alpha_{\ell+1}^* + \alpha_{\ell}^* \alpha_{\ell+1} + \beta_{\ell} \beta_{\ell+1}^* + \beta_{\ell}^* \beta_{\ell+1}) \\ &+ \frac{(2\ell+1)}{\ell(\ell+1)} (\alpha_{\ell} \beta_{\ell}^* + \alpha_{\ell}^* \beta_{\ell}) \end{aligned} \right\} \quad (2.2.20)$$

Although the energy absorbed by a lossless scatterer is zero the momentum transferred is not. Even lossless scatterers are accelerated in the direction of an incoming plane wave. Although the effect is small enough so that the effect of sunlight on atmospheric molecules is less significant than normal thermal unbalance, in other cases it can be significant. For example, the impulse electromagnetic wave produced by a nuclear blast results in forces of major significance.

## 2.3 Ideal Spherical Scatterers

The form of electromagnetic fields produced by a spherical scatterer immersed in a plane wave depends upon the symmetry of the scatterer, and the scattering coefficients  $\alpha_n$  and  $\beta_n$  depend upon its electromagnetic characteristics. The special case of a perfectly conducting sphere is important since it approximates many natural objects, it is convenient to analyze, and yet it demonstrates a full range of solution characteristics. The solution procedure is to apply the boundary condition that the tangential component of the total field intensities are equal on either side of the  $r = a$  boundary, see Section A.12. On the exterior this is the sum of the incident plane and scattered waves; with an ideally conducting scatterer the tangential component of the interior field is zero. Therefore, the following sums are equal to zero:

$$\sum_{n=1}^{\infty} \left( \frac{E_{\theta}(a, \theta, \phi)}{\cos \phi} \frac{dP_n^1}{d\theta} - \frac{E_{\phi}(a, \theta, \phi)}{\sin \phi} \frac{P_n^1}{\sin \theta} \right) = 0 \quad (2.3.1)$$

$$\sum_{n=1}^{\infty} \left( \frac{E_{\theta}(a, \theta, \phi)}{\cos \phi} \frac{P_n^1}{\sin \theta} - \frac{E_{\phi}(a, \theta, \phi)}{\sin \phi} \frac{dP_n^1}{d\theta} \right) = 0$$

Use of Eq. 2.2.2 shows that Eqs. 2.3.1 may be expressed as:

$$\sum_{\ell=1}^{\infty} i^{-\ell} \frac{(2\ell+1)}{\ell(\ell+1)} \left\{ \begin{aligned} & i \left[ j_{\ell}^{\bullet}(ka) + \beta_{\ell} h_{\ell}^{\bullet}(ka) \right] \left[ \frac{dP_{\ell}^1}{d\theta} \frac{dP_n^1}{d\theta} + \frac{P_{\ell}^1 P_n^1}{\sin^2 \theta} \right] \\ & + \left[ j_{\ell}(ka) + \alpha_{\ell} h_{\ell}(ka) \right] \left[ \frac{1}{\sin \theta} \frac{d(P_{\ell}^1 P_n^1)}{d\theta} \right] \end{aligned} \right\} = 0 \quad (2.3.2)$$

$$\sum_{\ell=1}^{\infty} i^{-\ell} \frac{(2\ell+1)}{\ell(\ell+1)} \left\{ \begin{aligned} & \left[ j_{\ell}(ka) + \alpha_{\ell} h_{\ell}(ka) \right] \left[ \frac{dP_{\ell}^1}{d\theta} \frac{dP_n^1}{d\theta} + \frac{P_{\ell}^1 P_n^1}{\sin^2 \theta} \right] \\ & + i \left[ j_{\ell}^{\bullet}(ka) + \beta_{\ell} h_{\ell}^{\bullet}(ka) \right] \left[ \frac{1}{\sin \theta} \frac{d(P_{\ell}^1 P_n^1)}{d\theta} \right] \end{aligned} \right\} = 0 \quad (2.3.3)$$

Next, form the integrals:

$$\int_0^{\pi} \sin \theta d\theta \sum_{n=1}^{\infty} \left( \frac{E_{\theta}(a, \theta, \phi)}{\cos \phi} \frac{dP_n^1}{d\theta} - \frac{E_{\phi}(a, \theta, \phi)}{\sin \phi} \frac{P_n^1}{\sin \theta} \right) = 0 \quad (2.3.4)$$

$$\int_0^{\pi} \sin \theta d\theta \sum_{n=1}^{\infty} \left( \frac{E_{\theta}(a, \theta, \phi)}{\cos \phi} \frac{P_n^1}{\sin \theta} - \frac{E_{\phi}(a, \theta, \phi)}{\sin \phi} \frac{dP_n^1}{d\theta} \right) = 0$$

Inserting the needed integral forms from Table A.22.1 into Eq. 2.3.4 gives, after simplifying:

$$\begin{aligned} j_{\ell}^{\bullet}(ka) + \beta_{\ell} h_{\ell}^{\bullet}(ka) &= 0 \\ j_{\ell}(ka) + \alpha_{\ell} h_{\ell}(ka) &= 0 \end{aligned} \quad (2.3.5)$$

Solving for the coefficients:

$$\alpha_\ell(ka) = -\frac{j_\ell(ka)}{h_\ell(ka)} \quad \text{and} \quad \beta_\ell(ka) = -\frac{j_\ell^*(ka)}{h_\ell^*(ka)} \quad (2.3.6)$$

An important special case is a scatterer with a small radius-to-wavelength ratio; for this case incorporating the values of the spherical Bessel functions in the limit as  $ka \Rightarrow 0$  gives:

$$\begin{aligned} \alpha_1(ka) &= -\frac{(ka)/3}{(ka)/3 + i/(ka)^2} \cong \frac{i(ka)^3}{3} \\ \beta_1(ka) &= -\frac{2/3}{2/3 - i/(ka)^3} \cong \frac{2(ka)^3}{3i} \end{aligned} \quad (2.3.7)$$

The cross sections and normalized forces are:

$$\begin{aligned} \frac{C_{EX}}{C_{GE}} = \frac{C_{SC}}{C_{GE}} = \frac{\mathcal{C}_{EX}}{C_{GE}} &= \frac{10(ka)^4}{3} \\ \frac{C_{RCS}}{C_{GE}} &= 9(ka)^4; \quad \frac{\mathcal{C}_{SC}}{C_{GE}} = \frac{4(ka)^4}{3} \end{aligned} \quad (2.3.8)$$

As always,  $c$  represents the speed of light.

Figure 2.3.1 shows the normalized extinction cross section for a conducting scatterer as a function of  $ka$ , for scatterers of any physical size. Since the incoming power is fully directed, Fig. 2.3.1 also shows the momentum transferred to the scatterer; Eq. 2.3.8 shows that for small scatterers it varies as  $(ka)^4$ . The largest normalized extinction cross section occurs at  $ka \cong 1.2$ , and is equal to 2.28. For larger values of  $ka$  the total cross section oscillates towards a limit of twice the geometric cross section, in the limit of infinite radius.

In the lossless case the extinction and scattering cross sections are equal and the total force on the illuminated sphere is the extinction plus scattered forces,  $(F_{EX} + F_{SC})$ . The force on the scatterer because of the scattered field is shown in Fig. 2.3.2. Electrically small objects scatter predominantly back

into the direction from which the wave came, increasing the thrust in the direction of the wave. Electrically large objects scatter predominantly in the direction of the incoming wave, decreasing the thrust on the scatterer. The sign of the scattering force changes at about  $ka \cong 1.38$ . The largest forward magnitude is about 0.257 and occurs at  $ka \cong 1.12$ .

The extinction momentum is in the direction of the incoming wave. All interacting energy forms part of the extinction momentum but, upon re-radiation, it may either add or subtract momentum from the scatterer. Since the subtracted momentum cannot exceed the extinction momentum, it follows that:

$$\frac{\text{Absorbed Energy}}{\text{Absorbed Momentum}} \leq c \quad (2.3.9)$$

Scatterers are commonly divided into groupings that depend upon the radius-to-wavelength ratio. The Rayleigh region is over frequencies for which  $ka \ll 1$ , the Mie region is over frequencies for which  $ka$  is on the order of one, and the optical region is over frequencies for which  $ka \gg 1$ .

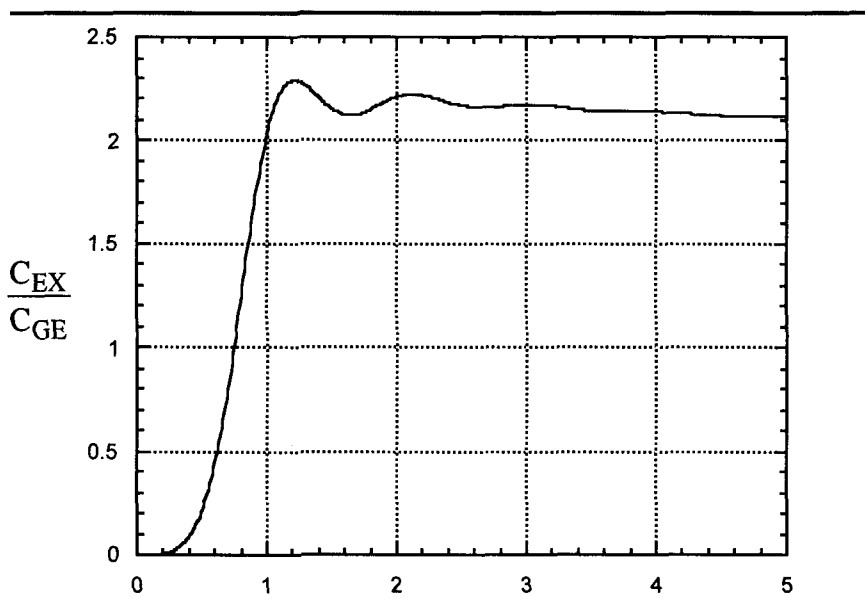


Figure 2.3.1 Extinction Cross Section Versus  $ka$  for a Conducting Sphere of Radius  $a$

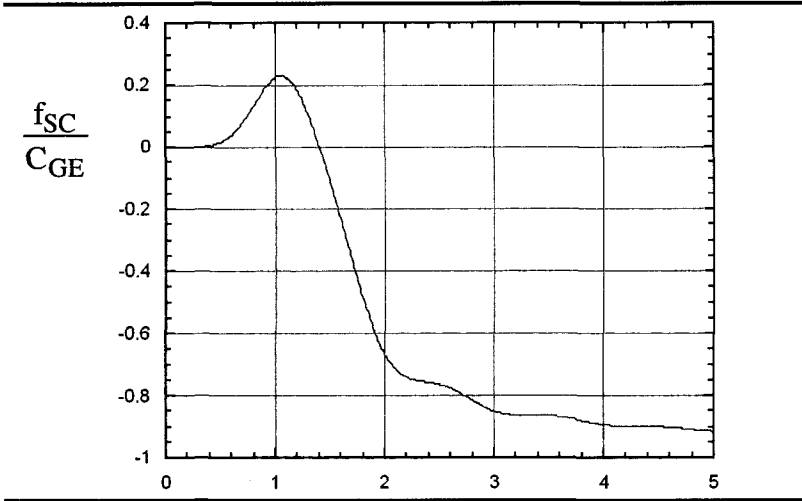


Figure 2.3.2 Normalized Scattering Force Versus  $ka$  for a Conducting Sphere of Radius  $a$

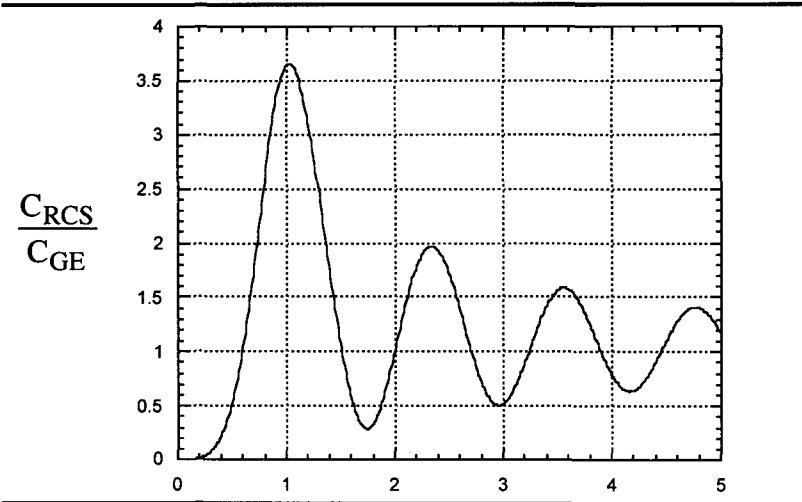


Figure 2.3.3 Radar Cross Section Versus  $ka$  for a Conducting Sphere of Radius  $a$

The normalized radar cross section is shown in Fig. 2.3.3. Since conducting spheres that are the right size to be held in a person’s hand have radar cross sections that are convenient to measure, the curve of Fig. 2.3.3 is often used as a laboratory calibration standard.



Optical scattering results determine the optical properties of the sky. A clear atmosphere of gaseous nitrogen and oxygen, without suspended particulate matter, scatters a portion of the light that passes through it. Since the molecules are much smaller than a wavelength of visible light, the scattering process selectively acts more on the shorter wavelengths than longer ones and more blue than red light is scattered. When the sun is directly overhead the sky away from the directly incoming beam is illuminated by scattered light, which is dominantly blue. Some of that dominantly blue light is scattered to the earth, giving the sky its characteristically blue color. The removal of selected wavelengths makes the sun appear yellow.

At sunrise and sunset the sun's light travels farther through the atmosphere than it does at noon and more light is scattered. The remaining direct sunlight, therefore, is dominantly red. If particulate matter, such as dust, about the size of an optical wavelength is present, scattering is insensitive to the wavelength and the sky appears to be dark.

## ***Biconical Transmitting Antennas***

### **2.4 General Comments**

A biconical antenna is illustrated in Fig. 2.4.1. The input power is applied across a sphere of radius  $b$ , centered at the apices of the cones. The cones extend from radius  $b$  to radius  $a$ , the length of the cones, at angle  $\psi$  as measured from the  $z$ -axis. All surfaces are ideal conductors. Source radius  $b$  is much smaller than either  $a$  or wavelength  $\lambda$ .

Biconical antennas are unique in that they are amenable to a rigorous and complete electromagnetic analysis and are shaped similarly to many practical antennas. Any solution with fields that satisfy the Maxwell equations and for which the fields match the boundary conditions is both a unique solution, see Section A.13, and a complete solution. Completeness assures that all solution terms are present, in contrast with numerical solutions that begin with an assumed symmetry and obtain an iterative answer. For those cases, the output solution contains only symmetries

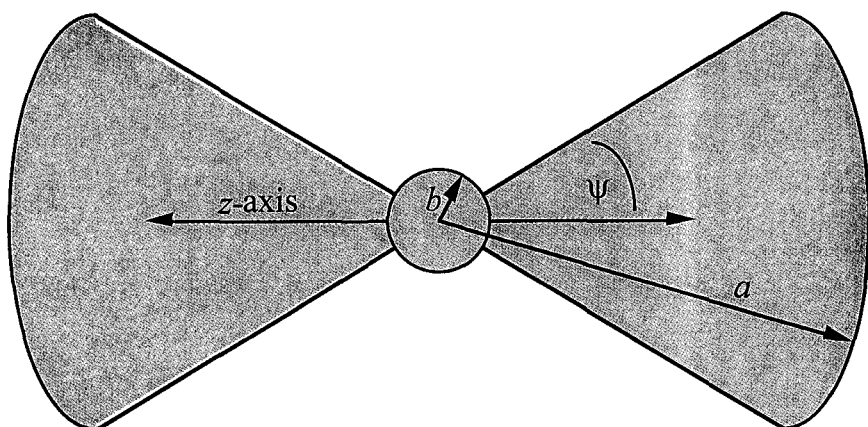


Figure 2.4.1 Schematic Illustration of a Biconical Antenna

*The antenna arms are conical sections that extend from  $b$  and  $a$ , expansion half angles  $\psi$  are measured from the  $z$ -axis, and the outer termination of the cone is capped by a spherical segment of radius  $a$ .*

present in the initial input and hence the solution is only as complete as the initial input.

Transmitting antennas include an energy source that applies a sinusoidal steady state voltage or current to source region  $b$ . The two cones, although oriented in opposite directions from the center sphere, act as a transmission line and direct the energy through the inner region, radius  $b$  to radius  $a$ , as a TEM mode. The energy then passes through the open aperture at  $r = a$  and enters the outer region. All radiation has rotational symmetry about the antenna axis and many wavelengths from the antenna the electric field intensity is linearly polarized in the direction of the conical axis. The impedance that the antenna presents to the source is determined by details of the antenna structure: cone angles, cone length, and the wavelength of the radiation. The outgoing waves undergo a discontinuity in the wave admittance (impedance) at the open aperture that results in infinite sets of TM modes in both the interior and exterior regions. Both inner and outer modes support standing energy and a steady state outward energy flow. Solution of the transmitting antenna problem requires solving for the input admittance, the coefficients of each of the infinite sets of interior and exterior TM modes as well as the TEM mode, and the radiation pattern.

Analysis is simplified by dividing space in the following way:

Source region

$$r < b ; \quad 0 \leq \theta \leq \pi; \quad 0 \leq \phi \leq 2\pi \quad (2.4.1)$$

Interior region

Arms

$$b < r < a ; \quad 0 \leq \theta < \psi \text{ and } \pi - \psi < \theta \leq \pi; \quad 0 \leq \phi \leq 2\pi \quad (2.4.2)$$

Space

$$b < r < a ; \quad \psi < \theta < \pi - \psi; \quad 0 \leq \phi \leq 2\pi \quad (2.4.3)$$

Exterior region

$$r > a ; \quad 0 \leq \theta \leq \pi; \quad 0 \leq \phi \leq 2\pi \quad (2.4.4)$$

Aperture

$$r = a ; \quad \psi \leq \theta \leq \pi - \psi; \quad 0 \leq \phi \leq 2\pi \quad (2.4.5)$$

## 2.5 Fields

The first objective is to obtain an expression for all fields. The procedure begins with the general expansion, Eqs. 1.12.9, and imposes boundary conditions specific to the biconical structure of Fig. 2.4.1. As was the case for the analysis of scatterers, field determination is greatly simplified by incorporating general field properties before matching the boundary conditions. General field properties are: (1) Since the antenna has rotational symmetry about the  $z$ -axis there is no dependence upon azimuth angle  $\phi$  and only functions with degree  $m$  equal to zero form part of the solution. All coefficients  $F(v, m)$  and  $G(v, m)$  are equal to zero for  $m$  greater than zero. This changes the sums over orders and degrees of Eqs. 1.12.9 to a sum over orders only. (2) The source drives straight currents that produce no current loops. Since TE coefficients are generated by current loops all coefficients  $G(v, 0)$  are equal to zero. (3) A source located evenly between the two cones drives surface current density with the symmetry  $I(r, \psi) = I(r, \pi - \psi)$  and surface charge density with the symmetry  $\rho(r, \psi) = -\rho(r, \pi - \psi)$ . By Eqs. 1.12.9, and with  $v = \ell$  an integer,  $E_\theta$  is proportional to  $dP_\ell(\cos\theta)/d\theta$ . It is shown in Section A.18 that Legendre functions have either even or odd

symmetry as  $\ell$  is even or odd. Consider a Legendre function of order  $\ell$  containing terms with the symmetry of  $\cos^\ell \theta$ . For that term:

$$\text{If } P_\ell(\cos \theta) \approx \cos^\ell \theta \text{ then } E_\theta \approx \frac{dP_\ell(\cos \theta)}{d\theta} \approx \ell \cos^{\ell-1} \theta \sin \theta \quad (2.5.1)$$

For  $\ell$  odd Eq. 2.5.1 shows that  $E_\theta(\sigma, \theta) = E_\theta(\sigma, \pi - \theta)$  and for  $\ell$  even  $E_\theta(\sigma, \theta) = -E_\theta(\sigma, \pi - \theta)$ . Since the source drives only even symmetry electric fields, it follows that only odd symmetry Legendre functions appear in the field solution. Therefore, the coefficients of all even order Legendre functions are equal to zero.

The exterior region: (4) Since the  $z$ -axis is included in the field region all terms have null coefficients except Legendre functions of the first kind. (5) In the limit as the radius approaches infinity, energy conservation requires the radial dependence to be  $\exp[i(\omega t - \sigma)]/\sigma$  which, in turn, requires the coefficients of all radial functions except Hankel functions of the second kind to be zero.

After incorporating the five constraints into Eqs. 1.12.9 and making the notational shift:

$$F_\ell = i^{1-\ell} F(\ell, 0)$$

The most general possible set of exterior field components is:

$$E_\theta = \sum_{\ell=1;\infty} F_\ell h_\ell(\sigma) \frac{dP_\ell(\cos \theta)}{d\theta} \quad (2.5.2)$$

$$\eta H_\phi = -i \sum_{\ell=1;\infty} F_\ell h_\ell(\sigma) \frac{dP_\ell(\cos \theta)}{d\theta}$$

$$\sigma E_r = \sum_{\ell=1;\infty} \ell(\ell+1) F_\ell h_\ell(\sigma) P_\ell(\cos \theta)$$

The symbol  $\ell = 1; \infty$  indicates the sum begins with  $\ell = 1$  and is over odd integers only. The constants  $F_\ell$  form an infinite set of unknown but constant field coefficients. Complete problem solution requires obtaining a solution for each of them.

The interior region: (6) Since the cones exclude fields from the  $z$ -axis modal orders need not be integers. Since symmetry requirement (3) requires null coefficients for even functions by Eq. A.17.26 the coefficients of the even parity portion of Legendre functions,  $L_v(\cos\theta)$ , are equal to zero. This restricts solutions to odd parity Legendre functions,  $M_v(\cos\theta)$ . It follows in the same way that the zero order Legendre function,  $P_0(\cos\theta)$ , has a null coefficient but, by Eqs. A.18.14 and A.18.15, zero order Legendre function of the second kind,  $Q_0(\cos\theta)$ , does not; the derivative of the zero order Legendre function of the second kind remains finite on cone surfaces. (7) Both the source voltage and the source current are finite. The voltage and current are, respectively, proportional to  $\sigma$  times the electric and magnetic field intensity and the radial functions approach zero as  $j_v(\sigma) \Rightarrow \sigma^v$  and  $y_v(\sigma) \Rightarrow \sigma^{-(v+1)}$ , see Eqs. A.24.9 and A.24.1. Therefore the input voltage and current values remain finite only if the coefficients of all spherical Neumann functions except  $v = \ell = 0$  are equal to zero.

Incorporating these constraints into Eqs. 1.12.9 and separately denoting the zero order TEM mode shows that the general forms of the interior field components are:

$$\begin{aligned}
 E_r &= \sum_{v>0}^{\infty} \Gamma_v v(v+1) \frac{j_v(\sigma)}{\sigma} M_v(\cos\theta) \\
 E_\theta &= \sum_{v>0}^{\infty} \Gamma_v j_v \frac{dM_v}{d\theta} + i [c_0 j_0(\sigma) + d_0 y_0(\sigma)] \frac{dQ_0(\cos\theta)}{d\theta} \\
 \eta H_\phi &= -i \sum_{v>0}^{\infty} \Gamma_v j_v \frac{dM_v}{d\theta} + [c_0 j_0(\sigma) + d_0 y_0(\sigma)] \frac{dQ_0(\cos\theta)}{d\theta}
 \end{aligned} \tag{2.5.3}$$

Coefficients of noninteger order modes,  $F(v,0)$  of Eq. 1.12.9, are denoted by  $\Gamma_v$  and coefficients of zero order spherical Bessel and Neumann functions respectively by the constants  $c_0$  and  $d_0$ .

## 2.6 TEM Mode

The TEM mode may be reformulated in terms of measurable antenna parameters. Consider properties of  $Q_0(\cos\theta)$ , see Section A.18:

$$Q_0(\cos\theta) = \ln \left[ \cot \left( \frac{\theta}{2} \right) \right] = \frac{1}{2} \left[ \ln \left( \frac{1 + \cos\theta}{1 - \cos\theta} \right) \right] \quad (2.6.1)$$

Differentiating:

$$\frac{dQ_0}{d\theta} = -\frac{1}{\sin\theta} \quad (2.6.2)$$

The zero order spherical Bessel, Neumann and related functions are:

$$j_0(\sigma) = \frac{\sin \sigma}{\sigma}; \quad y_0(\sigma) = -\frac{\cos \sigma}{\sigma}; \quad \dot{j}_0(\sigma) = \frac{\cos \sigma}{\sigma}; \quad \dot{y}_0(\sigma) = \frac{\sin \sigma}{\sigma} \quad (2.6.3)$$

Substituting  $v = 0$  and Eqs. 2.6.2 and 2.6.3 into Eq. 1.12.9 give:

$$\begin{aligned} E_r &= 0 \\ \sigma E_\theta &= \frac{1}{i \sin\theta} (c_0 \cos \sigma + d_0 \sin \sigma) \\ \sigma \eta H_\phi &= \frac{1}{\sin\theta} (d_0 \cos \sigma - c_0 \sin \sigma) \end{aligned} \quad (2.6.4)$$

The voltage difference between equal radii positions on the two antenna arms is a measurable quantity. It may be calculated from knowledge of the antenna structure and the electric field intensity using Eqs. 2.6.3:

$$V(r) = \frac{\sigma}{k} \int_{\psi}^{\pi-\psi} E_\theta d\theta = \frac{1}{ik} (c_0 \cos \sigma + d_0 \sin \sigma) \int_{\psi}^{\pi-\psi} \frac{d\theta}{\sin\theta} \quad (2.6.5)$$

Integrating Eq. 2.6.2 shows that:

$$\int_{\psi}^{\pi-\psi} \frac{d\theta}{\sin \theta} = 2 \ln \left[ \cot \left( \frac{\psi}{2} \right) \right]$$

It is useful in what lies ahead to define the line admittance of the transmission line formed by the two antenna arms to be  $G(\psi)$  where:

$$G(\psi) = \frac{\pi}{\eta \ln \left[ \cot \left( \frac{\psi}{2} \right) \right]} \quad (2.6.6)$$

Combining Eq. 2.6.5 and 2.6.6 shows voltage  $V(r)$  to be:

$$V(r) = \frac{2\pi}{ik\eta G(\psi)} (c_0 \cos \sigma + d_0 \sin \sigma) \quad (2.6.7)$$

Substituting Eq. 2.6.7 into the TEM component of the electric field intensity, Eq. 2.5.3, shows the zero order electric field intensity to be:

$$E_{\theta} = \frac{\eta k V(r) G(\psi)}{2\pi \sigma \sin \theta} \quad (2.6.8)$$

Since the magnetic field intensity is directed around the cone arms, the current on the antenna arms is radially directed. Use of Eq. 2.6.3 gives the relationship:

$$I(r) = \frac{\sigma}{k} \sin \theta \int_0^{2\pi} H_{\phi} d\phi = \frac{2\pi}{\eta k} (d_0 \cos \sigma - c_0 \sin \sigma) \quad (2.6.9)$$

Substituting Eq. 2.6.9 into the TEM component of the magnetic field intensity term of Eq. 2.5.3 shows the zero order magnetic field intensity to be:

$$H_{\phi} = \frac{k I(r)}{2\pi \sigma \sin \theta} \quad (2.6.10)$$

Defining position  $r = a$  to be the terminus, the voltage and current there follow from Eqs. 2.6.7 and Eq. 2.6.10:

$$\begin{aligned} V(a) &= \frac{2\pi}{\eta G i k} \{c_0 \cos(ka) + d_0 \sin(ka)\} \\ I(a) &= \frac{2\pi}{\eta k} \{d_0 \cos(ka) - c_0 \sin(ka)\} \end{aligned} \quad (2.6.11)$$

Inverting Eqs. 2.6.11 to obtain the field coefficients in terms of terminator voltage and current gives:

$$\begin{aligned} c_0 &= \frac{\eta k}{2\pi} \{iGV(a)\cos(ka) - I(a)\sin(ka)\} \\ d_0 &= \frac{\eta k}{2\pi} \{I(a)\cos(ka) + iGV(a)\sin(ka)\} \end{aligned} \quad (2.6.12)$$

Next, define  $Y(a)$  to be the terminator admittance:

$$Y(a) = I(a)/V(a)$$

Rearranging gives the voltage between, and the current on, the cone arms as a function of  $Y(a)$ :

$$\begin{aligned} V(r) &= \frac{V(a)}{G} \{G \cos[k(a-r)] + iY(a) \sin[k(a-r)]\} \\ I(r) &= V(a) \{Y(a) \cos[k(a-r)] + iG \sin[k(a-r)]\} \end{aligned} \quad (2.6.13)$$

In terms of the terminator and line admittances, the admittance at each radius along the cones is:

$$Y(r) = G \frac{Y(a) \cos[k(a-r)] + iG \sin[k(a-r)]}{G \cos[k(a-r)] + iY(a) \sin[k(a-r)]} \quad (2.6.14)$$

Use Eq. 2.6.14 to define the antenna input admittance  $Y(0)$  then put it equal to  $Y_0$ , the admittance at  $r = b$  in the limit as  $b$  approaches zero. Also, define the input voltage,  $V(0)$ , and current,  $I(0)$ , to be:



$$V(0) = \lim_{b \Rightarrow 0} V(b); \quad I(0) = \lim_{b \Rightarrow 0} I(b) \quad (2.6.15)$$

The input admittance is:

$$Y_0 = G \left\{ \frac{Y(a) \cos(ka) + iG \sin(ka)}{G \cos(ka) + iY(a) \sin ka} \right\} \quad (2.6.16)$$

The radial dependence of the admittance as a function of the input and line admittances is:

$$Y(\sigma) = G \left\{ \frac{Y_0 \cos \sigma - iG \sin \sigma}{G \cos \sigma - iY_0 \sin \sigma} \right\} \quad (2.6.17)$$

The line admittance equations have the exact form of admittance transfer along a TEM transmission line and show that the cone arms jointly act as a constant admittance line guiding the TEM mode from the source to the terminus. Quite differently from a parallel wire transmission line in which the guiding conductors remain equally spaced along the length of the line, here the guiding conductors are oppositely directed on either side of the source. Like many transmission lines the line impedance is constant, see Eq. 2.6.6. Voltage is measured between equal radius points on the cone arms and the current is measured along each arm.

## 2.7 Boundary Conditions

Packaging the TEM results of Section 2.6 into the interior field equations shows that the general form of the interior fields is:

$$\begin{aligned} E_r &= \sum_{v>0} \Gamma_v v(v+1) \frac{j_v(\sigma)}{\sigma} M_v(\cos \theta) \\ E_\theta &= \sum_{v>0} \Gamma_v j_v \frac{dM_v(\cos \theta)}{d\theta} + \frac{\eta k G V(\sigma)}{2\pi \sigma \sin \theta} \\ \eta H_\phi &= -i \sum_{v>0} \Gamma_v j_v \frac{dM_v(\cos \theta)}{d\theta} + \frac{A(\sigma)}{2\pi \sigma \sin \theta} \end{aligned} \quad (2.7.1)$$

The infinite set of multiplying coefficients  $\Gamma_v$  and the input admittance  $Y(0)$  are unknown and to be determined.

Since the magnetic field is entirely  $\phi$ -directed, all currents on the cones are directed along the length of the cones. The total current consists of the sum of currents associated with the TM modes and the TEM mode. Define the TM modal current  $I'(\sigma)$  to be the complementary current and the TEM modal current  $I(\sigma)$  to be the principal current. The total current is the sum:

$$I_T(\sigma) = I'(\sigma) + I(\sigma) \quad (2.7.2)$$

The first term in the expression for  $H_\phi$  shows that the complementary current, in amperes, is:

$$I'(\sigma, \psi) = \frac{2\pi\sigma}{\hbar\eta k} \sum_{v>0}^{\infty} \Gamma_v j_v(\sigma) \frac{dM_v(\cos\theta)}{d\theta} \Big|_{\theta=\psi} \quad (2.7.3)$$

Since  $j_v(\sigma)$  varies as  $\sigma^v$  for small radii, where  $v > 0$ , it follows that the complementary current vanishes in that limit:

$$\lim_{\sigma \Rightarrow 0} I'(0) = 0 \quad (2.7.4)$$

The principal current at the origin follows from Eqs. 2.6.9 and 2.6.12, and is:

$$\lim_{\sigma \Rightarrow 0} I(0) = I(a)\cos(ka) + i GV(a)\sin(ka) \quad (2.7.5)$$

Since only the principal current exists at the source, only it can support the energy flow away from the source. Since the time average power supported by the TEM mode does not depend upon the radius, it follows that the time average power is guided through the region by the principal current.

Application of the conducting boundary conditions to the exterior fields of Eqs. 2.5.2 shows that the field intensities on the caps are related to the surface charges and currents as:

$$0 \leq \theta < \psi \quad \text{and} \quad \pi - \psi < \theta \leq \pi;$$

$$\begin{aligned} \epsilon E_r(ka, \theta, \phi) &= \frac{\epsilon}{\sigma} \sum_{\ell=1;0}^{\infty} \ell(\ell+1) F_{\ell} h_{\ell}(ka) P_{\ell}(\cos \theta) = \rho(ka, \theta, \phi) \\ E_{\theta}(ka, \theta, \phi) &= \sum_{\ell=1;0}^{\infty} F_{\ell} h_{\ell}^{\bullet}(ka) \frac{dP_{\ell}(\cos \theta)}{d\theta} = 0 \\ H_{\phi}(ka, \theta, \phi) &= -\frac{i}{\eta} \sum_{\ell=1;0}^{\infty} F_{\ell} h_{\ell}(ka) \frac{dP_{\ell}(\cos \theta)}{d\theta} = -I_{\theta}(ka, \theta, \phi) \end{aligned} \quad (2.7.6)$$

Symbol  $\rho(ka, \theta, \phi)$  indicates the surface charge density on the caps in coulombs per square meter and symbol  $I_{\theta}(ka, \theta, \phi)$  indicates surface current density on the caps in amperes per meter. Application of the conducting boundary conditions to the interior field components of Eqs. 2.7.1 shows that the interior field intensities on the arms are subject to the constraints:

$$kb \leq \sigma \leq ka$$

$$\begin{aligned} E_r(\sigma, \psi, \phi) &= \sum_v^{\infty} v(v+1) F_v \frac{j_v(\sigma)}{\sigma} M_v(\cos \psi) = 0 \\ \epsilon E_{\theta}(\sigma, \psi, \phi) &= \frac{\eta k G V(\sigma)}{2\pi\sigma \sin \psi} + \epsilon \sum_{v>0}^{\infty} \Gamma_v j_v^{\bullet} \frac{dM_v(\cos \theta)}{d\theta} \Big|_{\theta=\psi} = \rho(\sigma, \psi, \phi) + \rho'(\sigma, \psi, \phi) \\ \eta H_{\phi}(\sigma, \psi, \phi) &= -i \sum_{v>0}^{\infty} \Gamma_v j_v \frac{dM_v(\cos \theta)}{d\theta} \Big|_{\theta=\psi} + \frac{A(\sigma)}{2\pi\sigma \sin \theta} = I_r(\sigma, \psi, \phi) + I'_r(\sigma, \psi, \phi) \end{aligned} \quad (2.7.7)$$

Symbols with and without the primes indicate, respectively, principal and complimentary surface charge and current densities on the cone arms.

The null value of the radial field component at the conical surfaces is only satisfied by a nontrivial solution if for every value of  $v$ :

$$M_v(\cos \psi) = 0 \quad (2.7.8)$$

Equation 2.7.8 determines an infinite and unique set of positive-real eigenvalues of  $v$ . Plots of  $v$  versus angle  $\psi$  for which Eq. 2.7.8 is satisfied

are shown in Fig. 2.7.1 for the first through the fifth sequence of roots. Function  $M_\nu(\cos\theta)$  is plotted versus  $\nu$  in Fig. 2.7.2, showing the first 24 zeros. Plots of  $M_\nu(\cos\theta)$  versus  $\theta$  at the first two roots of  $M_\nu[\cos(5^\circ)]$  are illustrated by Figure 2.7.3.

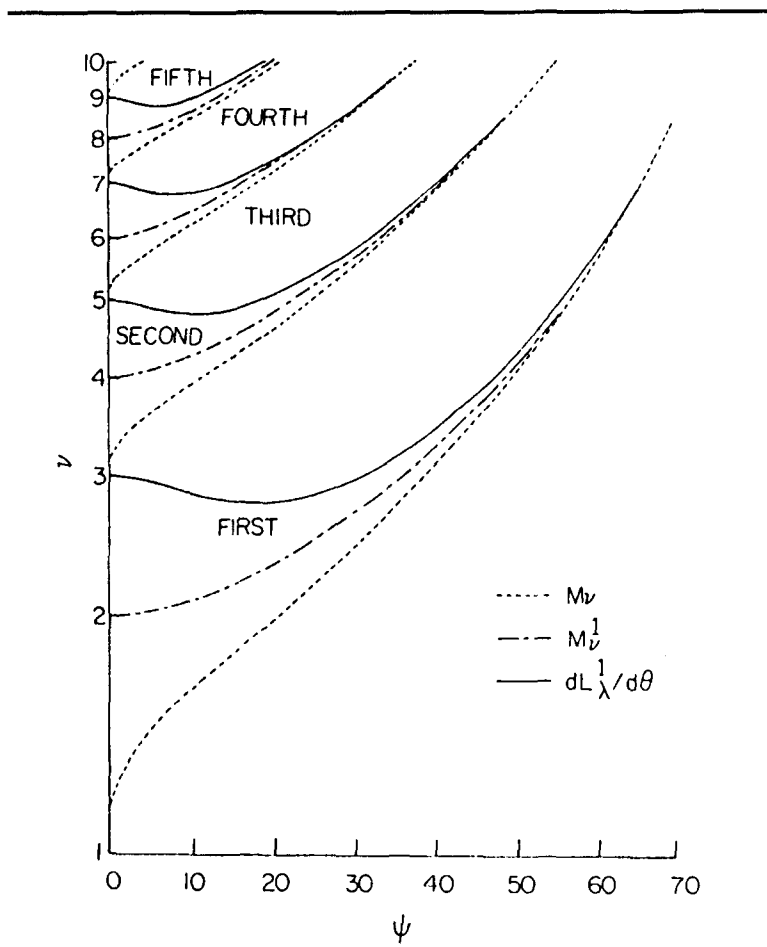


Figure 2.7.1 Root Values, Noninteger Legendre Functions  
 Plot showing values of  $\nu$  for which the three functions  $M_\nu(\cos\psi)$ ,  $M_\nu^1(\cos\psi)$ , and  $dL_\nu^1(\cos\theta)/d\theta|_{\theta=\psi}$ , are equal to zero versus cone angle  $\psi$ . Cardinal numbers indicate root order.

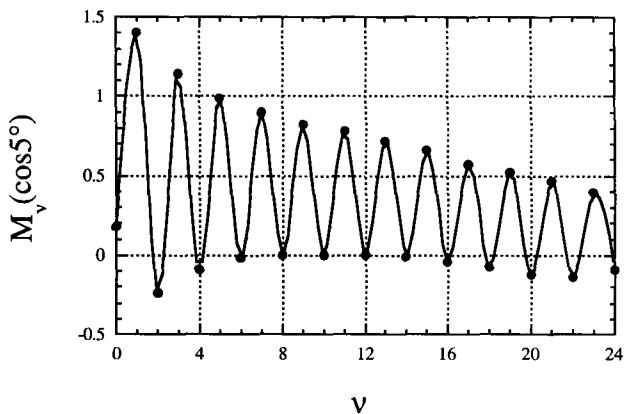


Figure 2.7.2 The function  $M_v[\cos(5^\circ)]$  plotted versus  $v$ .

On the aperture, virtual boundary conditions apply, see Eqs. A.12.6, and all field components are continuous through the boundary. Imposing these conditions on Eqs. 2.5.2 and 2.7.1 give the constraining equations:

$$\psi < \theta < \pi - \psi;$$

$$\sigma E_r(ka, \theta, \phi) = \sum_{\ell=1, \infty}^{\infty} \ell(\ell+1) F_{\ell} h_{\ell}^{\bullet}(ka) P_{\ell}(\cos \theta) = \sum_{v>0}^{\infty} v(v+1) \Gamma_v j_v^{\bullet}(ka) M_v(\cos \theta) \quad (2.7.9)$$

$$\psi < \theta < \pi - \psi;$$

$$E_{\theta}(ka, \theta, \phi) = \sum_{\ell=1, \infty}^{\infty} F_{\ell} h_{\ell}^{\bullet}(ka) \frac{dP_{\ell}(\cos \theta)}{d\theta} = \sum_v^{\infty} \Gamma_v j_v^{\bullet}(ka) \frac{dM_v(\cos \theta)}{d\theta} + \frac{\eta k G V(a)}{2\pi \sigma \sin \theta} \quad (2.7.10)$$

$$\psi < \theta < \pi - \psi;$$

$$\eta H_{\phi}(ka, \theta, \phi) = -i \sum_{\ell=1, \infty}^{\infty} F_{\ell} h_{\ell}(ka) \frac{dP_{\ell}(\cos \theta)}{d\theta} = -i \sum_v^{\infty} \Gamma_v j_v(ka) \frac{dM_v(\cos \theta)}{d\theta} + \frac{kV(a)}{2\pi \sigma \sin \theta} \quad (2.7.11)$$

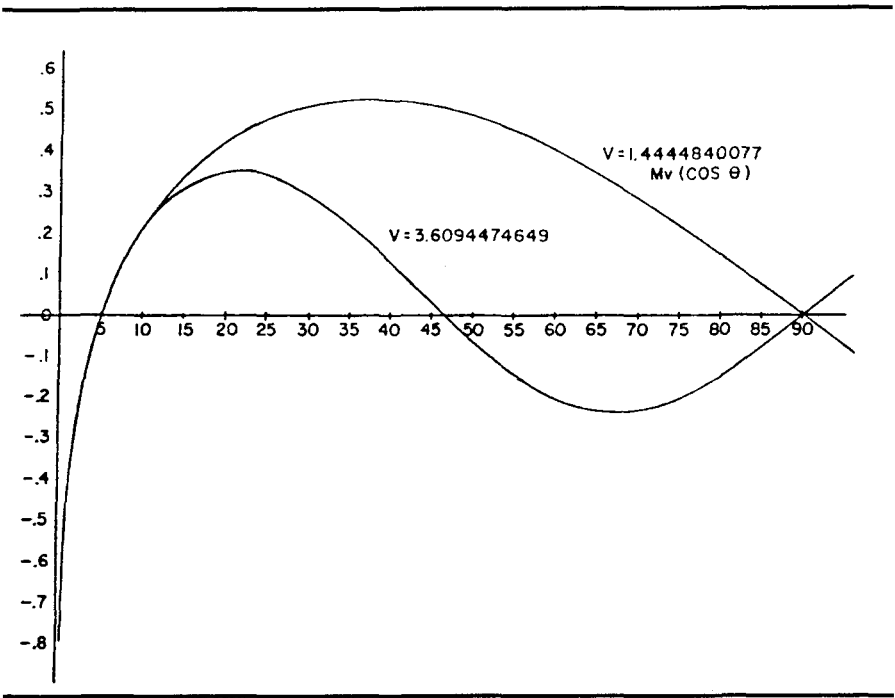


Figure 2.7.3 Two lowest order functions  $M_V(\cos\theta)$  vs.  $\theta$ ;  $M_V[\cos(5^\circ)] = 0$

These are the field values on the interface between interior and exterior regions. This completes the discussion of the field equations at a point as boundary conditions.

### 2.8 The Defining Integral Equations

In the preceding sections, the general forms of the boundary conditions are obtained as infinite sums over radial and harmonic functions. The exact form of the functions and the relationships between them is specified. In each case what remains are sums over an infinite set of modal orders and it remains to separate out the coefficients, one by one. In all but one case this is accomplished using the orthogonality of the Legendre functions. Sets of orthogonal integrals are formed and evaluated that change the equalities

involving Legendre functions of the preceding sections into linear algebraic equations. The algebraic equations are used to solve for the coefficients.

The first algebraic equation is obtained without using orthogonality. Operating on Eq. 2.7.11 to evaluate the line integrals of the expression for  $H_\phi$  around the periphery of the antenna arm on both sides of the  $r = a$  boundary gives:

$$\begin{aligned} \int_{\psi}^{\pi-\psi} a H_\phi d\phi &= -i \frac{a}{\eta} \sum_{\ell=1}^{\infty} F_\ell h_\ell(ka) P_\ell(\cos \theta) \Big|_{\psi}^{\pi-\psi} \\ &= -i \frac{a}{\eta} \sum_v \Gamma_v j_v(ka) M_v(\cos \theta) \Big|_{\psi}^{\pi-\psi} + \frac{I(a)}{\eta G} \end{aligned} \quad (2.8.1)$$

The condition that  $M_v(\cos \psi) = 0$  removes the sum over  $v$ . Collecting the remaining terms and making the substitution that  $I(a) = Y(a)V(a)$  gives the interior line admittance at the terminus as a function of the exterior coefficients:

$$Y(a) = \frac{2ia}{V(a)} \sum_{\ell=1}^{\infty} F_\ell h_\ell(ka) P_\ell(\cos \psi) \quad (2.8.2)$$

Under the summation sign of Eq. 2.8.2, symbol  $\ell_{0;1}$  indicates that  $\ell$  represents the field of odd integers with the lowest value of one. This equation, the first of the algebraic equations, equates the applied voltage and the admittance to a sum over odd order, exterior modes.

The next algebraic equation is obtained using the orthogonality of integer order Legendre functions. Multiplying Eq. 2.7.10 by  $\sin \theta d\theta dP_n(\cos \theta)/d\theta$  and integrating over the aperture gives:

$$\int_0^\pi \sin \theta d\theta \frac{dP_n}{d\theta} \sum_{\ell=1}^{\infty} F_\ell h_\ell(ka) \frac{dP_\ell}{d\theta} = \int_{\psi}^{\pi-\psi} \sin \theta d\theta \frac{dP_n}{d\theta} \left\{ \sum_{v>0} \Gamma_v j_v(ka) \frac{dM_v}{d\theta} + \frac{\eta G V(a)}{2\pi a \sin \theta} \right\} \quad (2.8.3)$$

Although with the problem as stated the limits on both integrals are from  $\psi$  to  $\pi - \psi$ , it follows from Eq. 2.7.6 that the sum on the left side of Eq. 2.8.3 is equal to zero over the caps. Therefore, the range of integration of the left side may be extended to the full range 0 to  $\pi$  without affecting the value of the integral. Use the extended angular range and use the definitions of Tables A.22.1 and A.23.1 that:

$$I_{\ell\ell} = \frac{2}{2\ell+1} \quad \text{and} \quad I_{\ell v} = \int_{\psi}^{\pi-\psi} P_{\ell}(\cos\theta) M_v(\cos\theta) \sin\theta d\theta \quad (2.8.4)$$

Symbol 'I' with two subscripts indicates an integral and with one subscript indicates current. Evaluating Eq. 2.8.3 by incorporating Eq. 2.8.4, Table A.22.1.6, and Table A.23.1.1 gives:

$$\ell(\ell+1)F_{\ell}h_{\ell}^*(ka)I_{\ell\ell} = \ell(\ell+1)\sum_{v>0}^{\infty} \Gamma_v j_v^*(ka)I_{\ell v} - \frac{\eta GV(a)}{\pi a} P_{\ell}(\cos\psi) \quad (2.8.5)$$

Equation 2.8.5 is the second algebraic expression that equates individual exterior modal coefficients to a sum over interior modal coefficients.

The third algebraic equation uses the orthogonality of fractional order Legendre functions. Begin by multiplying Eq. 2.7.11 by  $\sin\theta d\theta dM_{\mu}(\cos\theta)/d\theta$  and integrating over the aperture:

$$\begin{aligned} & \int_{\psi}^{\pi-\psi} \sin\theta d\theta \sum_{\ell \geq 1}^{\infty} F_{\ell} h_{\ell}(ka) \frac{dP_{\ell}}{d\theta} \frac{dM_{\mu}}{d\theta} \\ &= \int_{\psi}^{\pi-\psi} \sin\theta d\theta \frac{dM_{\mu}}{d\theta} \left\{ \sum_v^{\infty} \Gamma_v j_v(ka) \frac{dM_v}{d\theta} + \frac{\eta GV(a)}{2\pi a \sin\theta} \right\} \end{aligned} \quad (2.8.6)$$

Evaluating the integrals of Eq. 2.8.6 using integral A.23.1.5 with A.23.1.1 and integral A.23.1.7 with A.23.1.6 gives:

$$\mu(\mu+1)I_{\mu\mu}\Gamma_{\mu}j_{\mu}(ka) = \sum_{\ell \geq 1}^{\infty} \ell(\ell+1)F_{\ell}h_{\ell}(ka)I_{\ell\mu} \quad (2.8.7)$$



Equation Eq. 2.8.7 is an algebraic expression that equates individual interior modal coefficients to a sum over exterior modes.

## 2.9 Solution of the Biconical Antenna Problem

The result of applying the orthogonality of Legendre functions to point equations is an expression for individual exterior or interior modal magnitudes as sums over interior or exterior modes, respectively. The equations are:

$$F_\ell h_\ell^\bullet(ka) = -\frac{V(a)}{a} \frac{\eta G}{\pi} \frac{P_\ell(\cos \psi)}{\ell(\ell+1)I_{\ell\ell}} + \sum_{v>0}^{\infty} \Gamma_v j_v^\bullet(ka) \frac{I_{\ell v}}{I_{\ell\ell}} \quad (2.9.1)$$

$$\Gamma_v j_v(ka) = \frac{1}{v(v+1)} \sum_{\ell=0;1}^{\infty} F_\ell h_\ell(ka) \ell(\ell+1) \frac{I_{\ell v}}{I_{vv}} \quad (2.9.2)$$

Each equation contains an infinite number of linear algebraic equations. The zero order interior mode is:

$$Y(a) = \frac{2ia}{V(a)} \sum_{\ell=0;1}^{\infty} F_\ell h_\ell(ka) P_\ell(\cos \psi) \quad (2.9.3)$$

It remains to solve the three equations for the individual coefficients.

After some manipulation, including multiplying through by  $h_\ell(\sigma)/h_\ell^\bullet(\sigma)$ , Eqs. 2.9.1 and 2.9.2 combine to form the equality:

$$\begin{aligned} F_\ell h_\ell(ka) - \sum_{n=1}^{\infty} F_n h_n(ka) \sum_{v>0}^{\infty} \frac{n(n+1)}{v(v+1)} \frac{I_{\ell v} I_{nv}}{I_{\ell\ell} I_{vv}} \frac{j_v^\bullet(ka) h_\ell(ka)}{j_v(ka) h_\ell^\bullet(ka)} \\ = -\frac{\eta G}{\pi} \frac{V(a)}{a} \frac{P_\ell(\cos \psi)}{\ell(\ell+1)I_{\ell\ell}} \frac{h_\ell(ka)}{h_\ell^\bullet(ka)} \end{aligned} \quad (2.9.4)$$

Equation 2.9.4 represents an infinite set of linear equations, one for each coefficient  $F_\ell$ , and has the form:

$$x_\ell + \sum_{n=1}^{\infty} N_{\ell n} x_n = B_\ell \quad (2.9.5)$$

Because the magnitudes of coefficients  $F_\ell$  decrease rapidly with increasing modal number, and to keep the magnitude within available computer range, it is helpful to solve the problem with the initial variable  $x_\ell$  equal to  $F_\ell h_\ell(ka)$ .

After solving for  $x_\ell$  and knowing  $h_\ell(ka)$ , solve for  $F_\ell$ .

Although an equation of the form of Eq. 2.9.5 may be readily solved using matrix techniques, doing so requires the series to be truncated and truncation produces errors. The solution procedure is to: (1) pick an arbitrary but specific value for the ratio  $V(a)/a$ , our choice was one, (2) use the matrix solution to solve for the product  $F_\ell h_\ell(ka)$ , (3) divide by  $h_\ell(ka)$  to obtain  $F_\ell$ . The procedure determines as many of the previously unknown exterior coefficients as needed, and is limited only by the capability of available computers. This completes the calculation of the exterior coefficients. Knowing  $F_\ell h_\ell(ka)$ , Eq. 2.9.2 may be truncated and solved for  $F_v$ , and Eq. 2.9.3 may be truncated and solved for the admittance  $Y(a)$ :

$$Y(a) = \frac{2\pi G}{V(a)/a} \sum_{\ell=1}^{\infty} F_\ell h_\ell(ka) \quad (2.9.6)$$

All quantities on the right side are known. Since for each mode  $F_\ell h_\ell(ka)$  is proportional to  $V(a)/a$ , the magnitudes in the numerator and denominator of Eq. 2.9.6 cancel and the value of  $Y(a)$  are correct for any applied voltage.

To change the field normalization to the more conveniently determined value  $V(0)/a = 1$ , enter the value into the first of Eqs. 2.6.13 to obtain:

$$\frac{V(a)}{a} = \frac{G}{G \cos(ka) + iY(a) \sin(ka)} \quad (2.9.7)$$

Use of Eq. 2.9.7 to re-normalize  $F_\ell$  completes the numerical analysis of biconical transmitting antennas.

Badii, Tomiyama, and Grimes used The Pennsylvania State University main frame computer, programmed for quadrupole precision, to do numerical analyses of several biconical antennas through 12-place accuracy. The analyses included series truncation with 17 external (maximum modal number of 33) and 16 internal modes. Table 2.9.1 lists, with six place accuracy, values of  $F_\ell h_\ell(ka)$  and  $\Gamma_v j_v(ka)$  for an antenna with  $\psi = 5^\circ$  and  $ka = 2$ , external modes one through 17 and internal modes 1.444 through 16.391. Table 2.9.2 lists the first six figures of  $F_\ell$  and  $\Gamma_v$  for the same antenna. The table values illustrate that the magnitudes of  $F_\ell$  and  $\Gamma_v$  respectively decrease and increase rapidly with increasing modal number. The coefficients and Eq. 2.9.7 determine the terminal admittance,  $Y(a)$ .  $Y(a)$  and Eq. 2.6.14 determine the antenna input impedance  $Y(0)$ .

$\ell$	$F_\ell h_\ell(ka)$	$v$	$\Gamma_v j_v(ka)$
1	(1.50924- <i>i</i> 2.40989)D-01	0	
3	(5.42697- <i>i</i> 1.70419)D-02	1.444 4840	(4.33823- <i>i</i> 17.5963)D-02
5	(21.95628- <i>i</i> 6.98844)D-03	3.609 4475	(3.68170- <i>i</i> 2.37137)D-02
7	(12.5283- <i>i</i> 3.81076)D-03	5.754 8721	(2.23379- <i>i</i> 1.17634)D-02
9	(8.18028- <i>i</i> 2.93358)D-03	7.887 3272	(2.59971- <i>i</i> 1.27571)D-02
11	(5.72681- <i>i</i> 2.11622)D-03	10.016 937	(-10.8348+ <i>i</i> 5.10427)D-02
13	(4.17152- <i>i</i> 1.57614)D-03	12.143 571	(-8.89611+ <i>i</i> 4.07774)D-03
15	(3.10771- <i>i</i> 1.19513)D-03	14.268 228	(-3.57476+ <i>i</i> 1.60594)D-03
17	(23.4057- <i>i</i> 9.13644)D-04	16.391 498	(-19.5095+ <i>i</i> 8.62755)D-04

Table 2.9.1 Constants for  $\psi = 5^\circ$ ,  $ka = 2$

Figure 2.9.1 shows the input resistance and reactance as a function of arm length for  $5^\circ$  cones. The mark at about  $-i450$  ohms shows the input impedance of an antenna with  $ka = 0.5$ ; succeeding marks are spaced at intervals of cones made longer by  $\Delta(ka) = 0.5$ . Figure 2.9.2 shows the input impedance of an antenna with  $\psi = 5^\circ$  as a function of arm length. Note that the initial resonance is much sharper than succeeding ones; peaks are centered at about  $ka \cong 1.11, 4.06$ , and  $7.14$ .

$\ell$	$F_\ell$	$\nu$	$\Gamma_\nu$
1	$(-6.00998-i50.5094)D-02$	0	
3	$(-9.96861-i36.9686)D-03$	1.444484	$(1.32836-i5.387966)D-01$
5	$(-3.75732-i11.81043)D-04$	3.609448	$(14.3649-i9.25205)D-01$
7	$(-6.96510-i20.3034)D-06$	5.754872	$(3.36507-i1.77209)D+01$
9	$(-7.74256-i21.5902)D-08$	7.887327	$(3.04273-i1.49310)D+03$
11	$(-5.7288-i15.5031)D-10$	10.01694	$(-16.5306+i7.78756)D+05$
13	$(-3.01440-i7.97810)D-12$	12.14357	$(-2.67294+i1.22520)D+07$
15	$(-1.18075-i3.07030)D-14$	14.26823	$(-2.98297+i1.34009)D+09$
17	$(-1.22586-i9.11817)D-18$	16.39150	$(-6.07222+i2.68528)D+11$

Table 2.9.2 Constants for  $\psi = 5^\circ$ ,  $ka = 2$  (cont.)

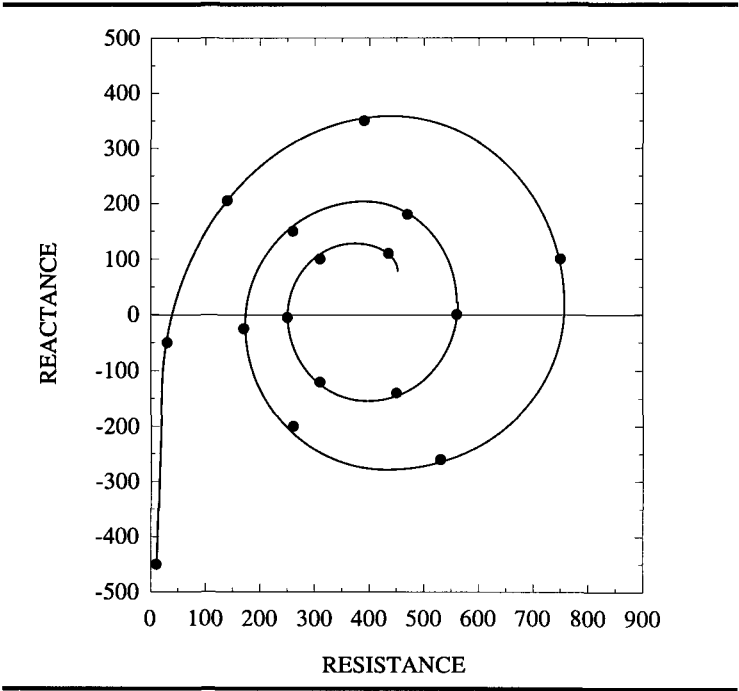


Figure 2.9.1 Input impedance of a biconical antenna

*Input Impedance of a biconical antenna, with  $\psi = 5^\circ$ , as a function of arm length. Zero reactance values are at  $ka = 1.11, 2.59, 4.06, 5.51, 7.14$ . The first mark is at  $ka = 0.5$ , each succeeding mark increases  $ka$  by  $0.5$ .*

By Eq. 2.7.6, each modal contribution to the total magnetic field intensity at the aperture is equal to  $F_\ell h_\ell(ka) dP_\ell \cos(\theta)/d\theta$ ; the magnitude of  $F_\ell h_\ell(ka)$  is listed in Table 2.9.1. From the theory of Legendre polynomials, see Table A.18.1:

$$\left. \frac{d}{d\theta} P_\ell \cos(\theta) \right|_{\pi/2} = (-1)^{(\ell-1)/2} \frac{(\ell)!!}{(\ell-1)!!} \quad (2.9.8)$$

Values of the ratio of the modal contribution to  $H_\phi$  to that of the exterior dipole mode at  $\phi = \pi/2$  are listed in Table 2.9.3. At the aperture, the modal magnitudes decrease so slowly with increasing modal number that a reasonably accurate description of interface affects requires a large number of modes. In the far field, on the other hand, only the first few modes determine the fields.

$\ell$	Aperture Ratio	Far Field Ratio	$v$	Factorial Ratio	Interior Ratio
1	1	1			
3	2.0005D-01	7.5275D-02	1.4444840	3.2498	2.0713
5	8.1033D-02	2.4366D-03	3.6094475	3.6529	5.6258D-01
7	4.6052D-02	4.2199D-05	5.7548721	3.8350	3.4050D-01
9	3.0563D-02	4.5092D-07	7.8873272	3.9504	4.0232D-01
11	2.1471D-02	3.2493D-09	10.016937	6.8083D-02	2.8677D-02
13	1.5682D-02	1.6767D-11	12.143571	3.8859D-01	1.1845D-03
15	1.1710D-02	6.4671D-14	14.268228	9.6692D-01	1.8995D-04
17	8.8363D-03	1.8087D-17	16.391498	1.6152	3.4457D-03

Table 2.9.3 Magnetic Field Modal Magnitudes

Modal magnitudes of  $H_\phi(ka, \pi/2)$  for exterior and interior orders. All ratios are normalized by the magnitude of the exterior dipole mode. The first three columns refer to exterior fields: the first is modal number, the second the modal-to-dipole field ratio at the aperture and the third the modal-to-dipole field ratio at far field. The next three columns refer to interior fields: the first is modal number, the second the magnitude of Eq. 2.9.9, and the third modal-to-aperture field ratio.

In the interior region, modal magnitudes of  $H_\phi(ka, \pi/2)$  at  $\phi = \pi/2$  are equal to:

$$\Gamma_{vjv}(ka) \frac{(v)!!}{(v-1)!!} \quad (2.9.9)$$

Values of the ratio of factorials and the ratio-magnitude product for each mode are listed in Table 2.9.3. The ratio is a measure of the rate of convergence of the field expressions with increasing order. Although the external modes are monotone decreasing with increasing modal number, the internal modes are not; the interior modes decrease but not monotonically with increasing modal number. The difference is because interior-to-exterior modal coupling depends upon the numerical difference between the interior modal orders and odd integers, as well as the magnitudes of the modes.

Field values determine the charge and current densities on the antenna surfaces. Results are summarized as:

Cap:  $\sigma = ka$ ,  $0 \leq \theta < \psi$ ;  $\pi - \psi < \theta \leq \pi$

$$\rho(ka, \theta) = \epsilon \sum_{\ell=0,1}^{\infty} \ell(\ell+1) F_\ell \frac{h_\ell(ka)}{ka} P_\ell(\cos \theta) \frac{\text{coulombs}}{\text{meter}^2} \quad (2.9.10)$$

$$I_\theta(ka, \theta) = \frac{i}{\eta} \sum_{\ell=0,1}^{\infty} F_\ell h_\ell(ka) \frac{dP_\ell(\cos \theta)}{d\theta} \frac{\text{amperes}}{\text{meter}}$$

Cones:  $b < r < a$ ,  $\theta = \psi$

$$\begin{aligned} \rho(\sigma, \psi) &= \left\{ \epsilon \sum_{v>0}^{\infty} \Gamma_{vjv}(\sigma) \frac{dM_v(\cos \theta)}{d\theta} \Big|_{\theta=\psi} + \frac{KGV(r)}{2\pi\sigma \sin \psi} \right\} \frac{\text{coulombs}}{\text{meter}^2} \\ I_r(\sigma, \psi) + I_r(r, \psi) &= \left\{ -\frac{K(r)}{2\pi\sigma \sin \psi} + \frac{i}{\eta} \sum_{v>0}^{\infty} \Gamma_{vjv}(\sigma) \frac{dM_v(\cos \theta)}{d\theta} \Big|_{\theta=\psi} \right\} \frac{\text{amperes}}{\text{meter}} \end{aligned} \quad (2.9.11)$$

On the cones the surface current density is radially directed and on the caps it is zenith angle directed. The two currents have quite different dependencies upon radius and zenith angle and therefore the current is not continuous through the cone-cap junction. A loop of charge accumulates at

the junction with a sign and magnitude that depends upon antenna structural details and the radiated wavelength. The resulting ring charge is:

$$Q(ka, \psi) = \frac{2\pi a}{\kappa\omega} \left( \sum_{\ell=0,1}^{\infty} \beta_{\ell} h_{\ell}(ka) \frac{dP_{\ell}(\cos \psi)}{d\psi} + \sum_{\nu>0}^{\infty} \Gamma_{\nu} j_{\nu}(ka) \frac{dM_{\nu}(\cos \psi)}{d\psi} \right) + \frac{i I(a)}{\omega \sin \psi} \quad (2.9.12)$$

Similarly, charge densities on the cap and cone have quite different dependencies upon radius and zenith angle. The electric field intensity on the cone and cap are, respectively  $\theta$  and  $r$  directed, and just off an ideal  $90^{\circ}$  junction the field is directed at an angle of  $45^{\circ}$  as measured from both the cone and cap.

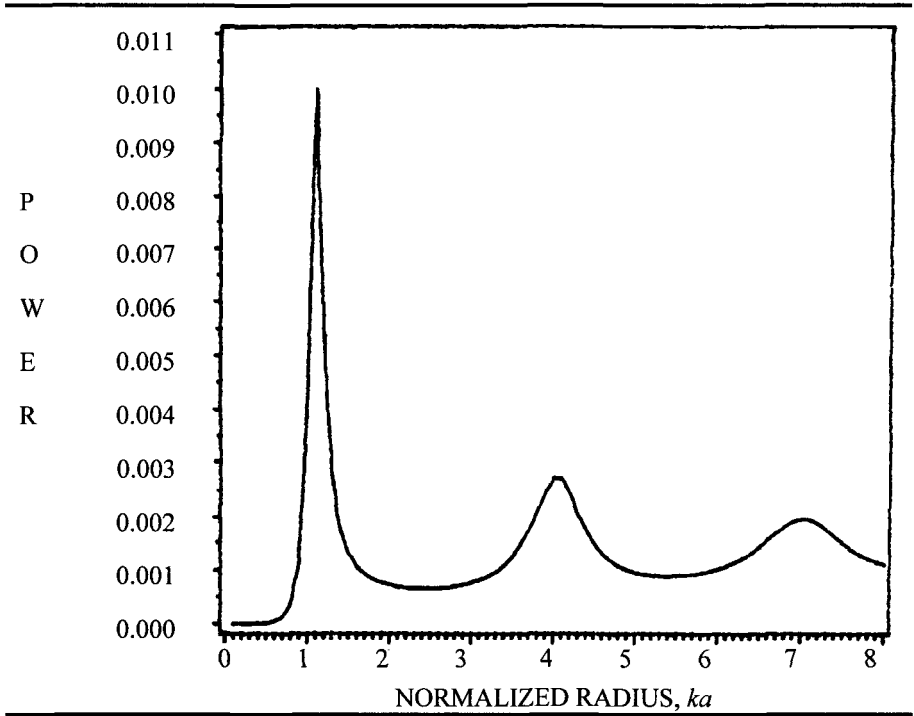


Figure 2.9.2 Output power versus  $ka$  for a  $5^{\circ}$ , biconical, transmitting antenna. Antenna with  $5^{\circ}$  cone angles and a constant input voltage, showing radiated power peaks at  $ka = 1.11, 4.06, 7.14$ .

## 2.10 Power

For a transmitting antenna, the time average power in the interior and exterior regions follow by use of the fields of Eqs. 2.7.1 and 2.5.2, respectively. In the interior region, the time average real power satisfies the transmission line rules between radii  $b$  and  $a$ . The input impedance and the radiated power are strong functions of the physical location of the standing energy wave, and it depends upon the antenna arm length.

The time average power produced by an antenna is equal to the integral of the real part of the radial component of the complex Poynting vector at the surface of a virtual sphere which, for ease in calculation, is made concentric with the antenna. The fields of Eqs. 2.5.2 show that the time average output power is:

$$P_{av} = \frac{\sigma^2}{2\eta k^2} \operatorname{Re} \left\{ \int_0^{2\pi} d\phi \int_0^\pi \sin\theta d\theta \sum_{\ell=1}^{\infty} \sum_{n=1}^{\infty} F_\ell F_n^* h_\ell^*(\sigma) h_n^*(\sigma) \frac{dP_\ell}{d\theta} \frac{dP_n}{d\theta} \right\} \quad (2.10.1)$$

Replacing the Hankel functions by their far field values and evaluating the integral gives:

$$P_{av} = \frac{1}{\eta k^2} \sum_{\ell=1}^{\infty} \frac{\ell(\ell+1)}{(2\ell+1)} [F_\ell F_\ell^*] \quad (2.10.2)$$

Since all terms on the right side are known, Eq. 2.10.2 is sufficient to evaluate the output power.

The time average power input,  $P_{in}$ , to the antenna is:

$$P_{in} = \frac{1}{2} \operatorname{Re} [V(0) I^*(0)] \quad (2.10.3)$$

By Eq. 2.6.13 the TEM voltage and current in the interior region are:

$$\begin{aligned} V(r) &= \frac{V(a)}{G} \{ G \cos[k(a-r)] + r Y(a) \sin[k(a-r)] \} \\ I(r) &= V(a) \{ Y(a) \cos[k(a-r)] + r G \sin[k(a-r)] \} \end{aligned} \quad (2.10.4)$$

Combining Eqs. 2.10.3 and 2.10.4 gives:



$$P_{\text{in}} = \frac{1}{2} \text{Re} [V(a) V^*(a)] Y^*(a) \quad (2.10.5)$$

Since  $V(a)$  and  $Y(a)$  are known, Eq. 2.10.5 is sufficient to evaluate the input power.

In a lossless antenna:

$$P_{\text{in}} = P_{\text{av}} \quad (2.10.6)$$

The equality serves as a check on all procedures.

The complex power,  $P_c$ , on a concentric sphere of normalized radius  $\sigma$  is:

$$kb < \sigma < ka$$

$$P_c(\sigma) = \int_0^\pi \sin \theta d\theta \left\{ \frac{i\pi}{2} \sum_v \Gamma_v \Gamma_v^* j_v j_v^* \left( \frac{dM_v}{d\theta} \right)^2 + \frac{\eta k^2 G}{2\pi \sigma^2 \sin^2 \theta} V(r) I^*(r) \right\} \quad (2.10.7)$$

$$\sigma > ka$$

$$P_c(\sigma) = \frac{\pi \sigma^2}{\eta k^2} \int_0^\pi \left( \frac{dP_\ell}{d\theta} \right)^2 \sin \theta d\theta \sum_{\ell=1}^{\infty} F_\ell F_\ell^* h_\ell^*(\sigma) h_\ell(\sigma)$$

With biconical antennas, the electric field intensity just off the surface of the caps has only a radial component. Therefore there is no normally directed Poynting vector and no energy is exchanged between the cap and the field. Since all aperture fields are continuous through the aperture, the total complex power is a continuous function of radius between positions  $a-\delta$  and  $a+\delta$ , where  $\delta$  is a differential radial length. Since all fields are continuous through the aperture, so is the energy density. Adjacent to the caps, the radial component of the electric field intensity and the azimuth component of the magnetic field intensity are not equal to zero. Therefore the energy per unit length as a function of radius is discontinuous between positions  $a-\delta$  and  $a+\delta$ . The magnitude of the discontinuity increases with increasing cone angle.

Figures 2.10.1-2.10.3 describe the complex powers about three antennas with normalized arms lengths of  $ka = 0.70$ , 1.28, and 2.00; all have cone

angles of  $1^\circ$ . The antennas are, respectively, electrically short, resonant, and electrically long. In all cases the real power,  $P_{\text{real}}$ , is constant.

The normalized complex power about an electrically short antenna,  $ka = 0.7$ , is shown in Fig. 2.10.1; the real power is small and the terminal impedance is capacitive. The peak reactive power is capacitive and occurs at approximately  $kr = 0.1$ . From there, the power decreases slowly with decreasing radius until reaching the terminals,  $kr = 0$ . For increasing radius it decreases more rapidly until reaching  $kr = ka$ , where it drops abruptly, then decreases slowly to zero with increasing radius for  $kr > ka$ .

The normalized complex power about a resonant antenna,  $ka = 1.28$  is shown in Fig. 2.10.2; the real power is large and the terminal impedance is resistive. The capacitively phased reactive power peak of Fig. 2.10.1 has moved outward to about  $kr = 0.8$ . From there it decreases slowly with decreasing radius to zero at the terminals. For increasing radius it behaves very similarly to Fig. 2.10.1.

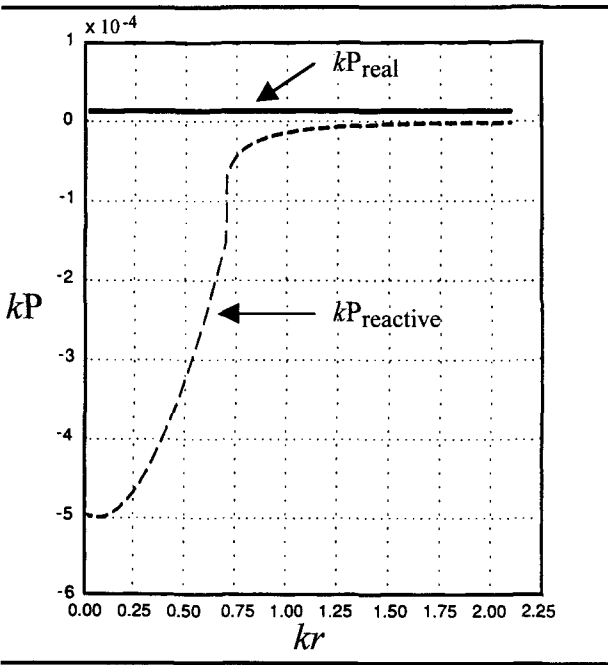


Figure 2.10.1 Normalized real and reactive powers versus  $kr$  for a biconical transmitting antenna.

Applied voltage  $V(0) = a$ , cone angle  $\psi = 1^\circ$ , and  $ka = 0.70$ .

The normalized complex power about an electrically long antenna,  $ka = 2.00$ , is shown in Fig. 2.10.3; the real power is less than that of Fig. 2.10.2 and the terminal impedance is inductive. The capacitively phased reactive power peak has moved outward to about  $kr = 1.6$ . From there it decreases slowly with decreasing radius, passes through zero and becomes inductively phased at the terminals. For increasing radius it behaves very similarly to Figs. 2.10.1 and 2.10.2.

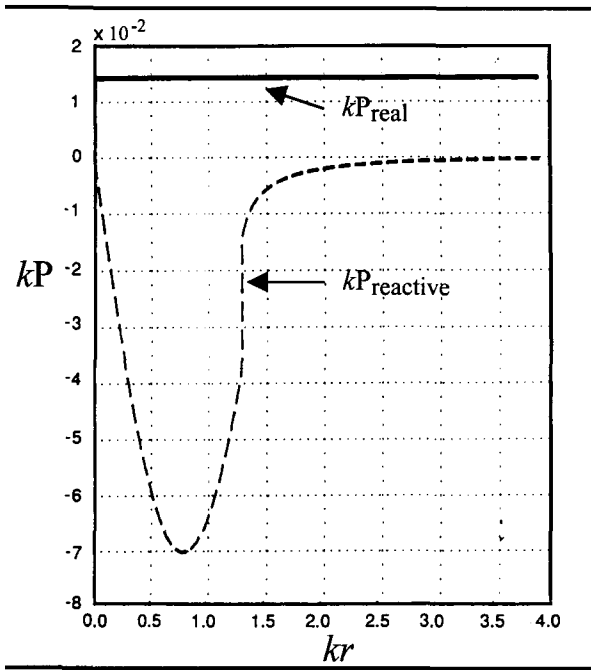


Figure 2.10.2 Real and reactive powers versus  $kr$  for a biconical transmitting antenna.

Applied voltage  $V(0) = a$ , cone angle  $\psi = 1^\circ$ , and  $ka = 1.28$ .

### 2.11 Field Expansion for $y$ -Directed Exponential

For a receiving antenna to function it is necessary that a component of the electric field intensity be aligned parallel with the antenna axis; optimum operation is with full alignment. With plane waves, the directions of polarization and propagation are perpendicular and, in the analysis of

scattering from a sphere, the incoming plane wave propagated in the  $z$ -direction. To analyze scattering from a receiving antenna it is convenient for the antenna axis to lie along the  $z$ -axis. It is necessary, therefore, to analyze a  $z$ -polarized plane wave and, with  $z$ -polarization, it must propagate somewhere in the  $xy$ -plane. We make the arbitrary choice that the plane wave propagates in the  $y$ -direction. It is, therefore, necessary to expand a  $y$ -directed wave in spherical coordinates. Such an expansion is done in a way similar to the way it was done for a  $z$ -directed plane wave, see Section 2.1. The desired exponential is:

$$e^{j(\omega t - ky)} = e^{j(\omega t - \sigma \sin \theta \sin \phi)} \tag{2.11.1}$$

Since Eq. 2.11.1 has no singularities, the spherical coordinate expansion can contain no spherical Neumann functions, no fractional order Legendre functions, and no Legendre functions of the second kind. Only spherical Bessel functions and associated Legendre polynomials remain. The most general form for the expansion is:

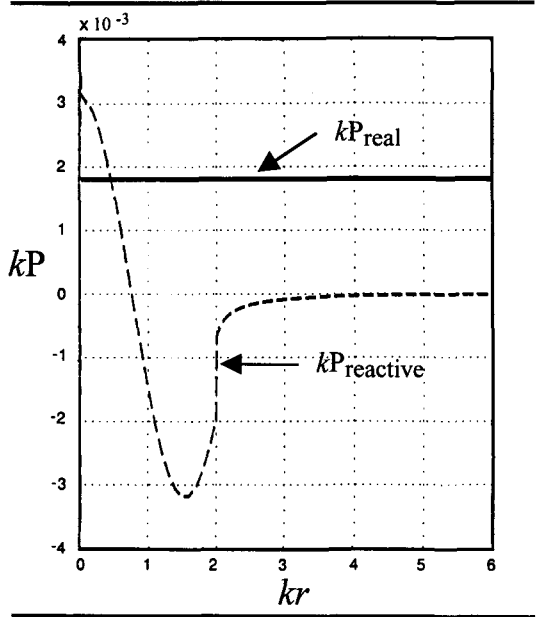


Figure 2.10.3 Real and reactive powers versus  $kr$  for a biconical transmitting antenna.

Applied voltage  $V(0) = a$ , cone angle  $\psi = 1^\circ$ , and  $ka = 2.00$ .

$$e^{-i\sigma \sin \theta \sin \phi} = \sum_{\ell=0}^{\infty} \sum_{m=0}^{\ell} \left[ {}^c G_{\ell}^m \cos m\phi - i {}^s G_{\ell}^m \sin m\phi \right] \frac{\ell(\ell+1)}{m} j_{\ell}(\sigma) P_{\ell}^m(\cos \theta) \quad (2.11.2)$$

To complete the description it is necessary to evaluate both infinite sets of coefficients  ${}^c G_{\ell}^m$  and  ${}^s G_{\ell}^m$ . The reverse superscripts “c” and “s” indicate coefficients of cosine and sine, respectively, and the multiplying factor  $\ell(\ell+1)/m$  is chosen for later convenience. As written Eq. 2.11.2 is in the form of two sums over infinite sets of coefficients. In order to evaluate the coefficients it is necessary to reformulate the equation as a doubly infinite number of separate algebraic equations, each of which provides a definite value for one coefficient.

From the theory of spherical Bessel functions, Eq. A.24.9:

$$j_{\ell}(\sigma) = \frac{\sigma^{\ell}}{(2\ell+1)!!} + \text{higher order terms} \quad (2.11.3)$$

Substitute Eq. 2.11.3 into the right side of Eq. 2.11.2; take  $\ell$  differentials of both sides with respect to  $\sigma$ , then go to the limit as  $\sigma$  goes to zero. The result is the equality:

$$(-i)^{\ell} \sin^{\ell} \theta \sin^{\ell} \phi = \sum_{\ell=0}^{\infty} \sum_{m=0}^{\ell} \left[ {}^c G_{\ell}^m \cos m\phi - i {}^s G_{\ell}^m \sin m\phi \right] \frac{\ell(\ell+1)}{m} \frac{\ell!}{(2\ell+1)!!} P_{\ell}^m(\cos \theta) \quad (2.11.4)$$

The left side of Eq. 2.11.4 involves powers of trigonometric functions. Identities that convert powers to multiples of the angles are:

n even

$$\sin^n \phi = \frac{2}{2^n} \left\{ \sum_{k=0}^{n/2-1} (-1)^{n/2-k} \frac{(n)!}{(n-k)!k!} \cos[(n-2k)\phi] + \frac{(n)!}{(n/2)!^2} \right\} \quad (2.11.5)$$

n odd

$$\sin^n \phi = \frac{2}{2^n} \left\{ \sum_{k=0}^{(n-1)/2} (-1)^{(n-1)/2-k} \frac{(n)!}{(n-k)!k!} \sin[(n-2k)\phi] \right\}$$

Substitute Eqs. 2.11.5 into Eq. 2.11.4 then multiply by  $\cos(q\phi)$ , where  $q$  is an integer, and integrate over the azimuth angle. Next, multiply by  $\sin(q\phi)$  and repeat the procedure. The results, where the  $\delta$  represents Kronecker delta functions and  $s$  represents an integer, are:

$$\begin{aligned} \frac{{}^c G_\ell^q}{q} \frac{\ell(\ell+1)}{(2\ell+1)!!} P_\ell^q(\cos\theta) &= \frac{(-i)^{(\ell-q)} \delta(q, 2s)}{(q/2)![(\ell-q)/2]!} \sin^\ell \theta \\ \frac{{}^s G_\ell^q}{q} \frac{\ell(\ell+1)}{(2\ell+1)!} P_\ell^q(\cos\theta) &= \frac{(-i)^{(\ell-q)} \delta(q, 2s+1)}{(q/2)![(\ell-q)/2]!} \sin^\ell \theta \end{aligned} \quad (2.11.6)$$

By Eq. 2.11.6,  ${}^c G_\ell^q$  is equal to zero if  $q$  is odd and  ${}^s G_\ell^q$  is equal to zero if  $q$  is even. This reduces the total number of nonzero coefficients by half.

Next, multiply the top of Eqs. 2.11.6 by  $P_\ell^q(\cos\theta)$  and integrate over the zenith angle. Integral forms are Eqs. 1 and 10 of Table A.22.1. Results are:

$q$  even

$$\frac{2^{\ell+1} \ell!(\ell+q)!}{(q/2)![(\ell-q)/2]!(2\ell+1)!} \delta(\ell+q, 2s) = \frac{{}^c G_\ell^q}{q} \frac{\ell(\ell+1)}{(2\ell+1)!!} \frac{2}{(2\ell+1)} \frac{(\ell+q)!}{(\ell-q)!} \quad (2.11.7)$$

By Eq. 2.11.7,  ${}^c G_\ell^q$  is equal to zero if  $\ell+q$  is odd. Since  $q$  is even, it follows that  $\ell$  is also even. Conducting the same operation on the bottom of Eqs. 2.11.6 shows that  ${}^s G_\ell^q$  is also equal to zero if  $\ell+q$  is odd. Since, for this case,  $q$  is odd, it follows that  $\ell$  is also odd. Therefore the two groups of coefficients form non-overlapping sets and the distinction may be dropped:  $G_\ell^q$  represent both sets of functions. This reduces the set of non-zero coefficients to one-fourth of the original number in Eq. 2.11.2.

Simplifying results shows that:

$$G_\ell^m = \frac{2m(2\ell+1)(\ell-m)!\delta(\ell+m, 2q)}{2^\ell \ell(\ell+1) \left(\frac{\ell+m}{2}\right)! \left(\frac{\ell-m}{2}\right)!} = \frac{2m(2\ell+1)(\ell-m)!\delta(\ell+m, 2q)}{\ell(\ell+1)(\ell+m)! (\ell-m)!} \quad (2.11.8)$$

This equation is correct for all modal combinations. Combining Eqs. 2.11.2 and 2.11.8 shows that the spherical coordinate expansion for a  $y$ -directed,  $z$ -polarized plane wave is:

$$e^{-i\sigma \sin \theta \sin \phi} = \left\{ \sum_{\ell=0;\infty}^{\infty} \sum_{m\pi}^{\ell} \cos(m\phi) - i \sum_{\ell=1;\infty}^{\infty} \sum_{m0}^{\ell} \sin(m\phi) \right\} \frac{\ell(\ell+1)}{m} G_{\ell}^m j_{\ell}(\sigma) P_{\ell}^m(\cos \theta) \quad (2.11.9)$$

## *An Incoming Plane Wave*

### 2.12 Incoming TE Fields

To find the expression for the radial magnetic field component,  $H_r$ , of a  $y$ -directed plane wave with the electric field intensity  $z$ -directed, begin by noting that:

$$\eta H_r = \sin \theta \cos \phi e^{-i\sigma \sin \theta \sin \phi} = \frac{i}{\sigma} \frac{\partial}{\partial \phi} e^{-i\sigma \sin \theta \sin \phi} \quad (2.12.1)$$

The first equality in Eq. 2.12.1 is by definition. Using the derivative operation of Eq. 2.12.1 on the spherical coordinate expression for the exponential form of Eq. 2.11.9 gives:

$$\eta H_r = \left[ \sum_{\ell=1;\infty}^{\infty} \sum_{m0}^{\ell} \cos(m\phi) - i \sum_{\ell=2;\infty}^{\infty} \sum_{m\pi}^{\ell} \sin(m\phi) \right] \ell(\ell+1) G_{\ell}^m \frac{j_{\ell}(\sigma)}{\sigma} P_{\ell}^m(\cos \theta) \quad (2.12.2)$$

Combining Eq. 2.12.2 with the same field component of Eq. 1.12.9 determines the constant field coefficients. Knowledge of the constant field coefficients and the component forms of Eq. 1.12.9 are sufficient to obtain the full set of TE modes.

## 2.13 Incoming TM Fields

A longer procedure is necessary to obtain the coefficients for TM modes. It is convenient to define  $E_r$  in a way analogous with Eq. 2.12.2, using Eq. 2.13.1 to define coefficients  ${}^cF_\ell^m$  and  ${}^sF_\ell^m$ , then solve for the constants. The general form for the field is:

$$E_r = \sum_{\ell=0}^{\infty} \sum_{m=0}^{\ell} \left[ {}^cF_\ell^m \cos(m\phi) - i {}^sF_\ell^m \sin(m\phi) \right] \ell(\ell+1) \frac{j_\ell(\sigma)}{\sigma} P_\ell^m(\cos \theta) \quad (2.13.1)$$

The radial component of the  $y$ -directed plane wave is:

$$E_r = \cos \theta e^{-i\sigma \sin \theta \sin \phi} = \frac{i}{\sigma \sin \phi} \frac{\partial}{\partial \theta} e^{-i\sigma \sin \theta \sin \phi} \quad (2.13.2)$$

Using the derivative operation of Eq. 2.13.2 on the spherical coordinate expression for the exponential form of Eq. 2.11.9 gives:

$$E_r = \frac{i}{\sin \phi} \left[ \sum_{\ell e; 0}^{\infty} \sum_{me}^{\ell} \cos(m\phi) - i \sum_{\ell o; 1}^{\infty} \sum_{mo}^{\ell} \sin(m\phi) \right] \times \frac{\ell(\ell+1)}{m} G_\ell^m \frac{j_\ell(\sigma)}{\sigma} \frac{dP_\ell^m(\cos \theta)}{d\theta} \quad (2.13.3)$$

Symbols  $\ell e; 0$  and  $\ell o; 1$  indicate sums respectively over even integers starting at zero, and over odd integers starting at one. Symbols  $me$  and  $mo$  indicate sums respectively over even and odd integers. A trigonometric identity that puts Eq. 2.13.3 in a more useful form is:

$$\frac{1}{\sin \phi} \equiv 2 \sum_{s=0}^{\infty} \sin[(2s+1)\phi] \quad (2.13.4)$$

Combining Eqs. 2.13.3 and 2.13.4 results in:



$$E_r = 2 \sum_{s=0}^{\infty} \left[ i \sum_{\ell \in 0}^{\infty} \sum_{m \in \ell}^{\ell} \cos m\phi + \sum_{\ell \in 1}^{\infty} \sum_{m \in 0}^{\ell} \sin m\phi \right] \sin[(2s+1)\phi] \quad (2.13.5)$$

$$\times \frac{\ell(\ell+1)}{m} G_{\ell}^m \frac{j_{\ell}(\sigma)}{\sigma} \frac{dP_{\ell}^m(\cos\theta)}{d\theta}$$

Other useful trigonometric identities are:

$$2 \sin m\phi \sin(2s+1)\phi \equiv \cos[(m-2s-1)\phi] - \cos[(m+2s+1)\phi] \quad (2.13.6)$$

$$2 \cos m\phi \sin(2s+1)\phi \equiv \sin[(m+2s+1)\phi] - \sin[(m-2s-1)\phi]$$

The procedure is to substitute Eqs. 2.13.6 into Eq. 2.13.5, equate Eqs. 2.13.1 and 2.13.5, differentiate both  $(\ell-1)$  times by  $\sigma$ , then go to the limit as  $\sigma$  goes to zero. The result, for  $\ell$  odd, is:

$$\sum_{s=0}^{\infty} \left[ \sum_{m \in 0}^{\ell} \{ \cos[(m-2s-1)\phi] - \cos[(m+2s+1)\phi] \} \right] \frac{G_{\ell}^m}{m} \frac{dP_{\ell}^m(\cos\theta)}{d\theta} \quad (2.13.7)$$

$$= \sum_{n=0}^{\ell} \left[ {}^c F_{\ell}^n \cos(m\phi) - i {}^s F_{\ell}^n \sin(m\phi) \right] P_{\ell}^n(\cos\theta)$$

Next multiply Eq. 2.13.7 by  $\cos(q\phi)$ , where  $q$  is an integer, and integrate over the full range  $\phi = 0$  to  $2\pi$ . This shows that  ${}^s F_{\ell}^n$  is equal to zero for odd values of  $\ell$ ; it follows in a similar way that  ${}^c F_{\ell}^n$  is equal to zero for even values of  $\ell$ . Therefore the coefficients form non-overlapping sets and, again, the notation may be simplified by dropping the reverse superscript, with  $F_{\ell}^n$  representing both sets of coefficients. This reduces the set of non-zero coefficients to one-fourth of the original number in Eq. 2.13.1. The resulting equality is

$$\sum_{n=0}^{\ell} \delta(q, n) F_{\ell}^n P_{\ell}^n(\cos\theta) \quad (2.13.8)$$

$$= \sum_{s=0}^{\infty} \sum_{m \in \ell}^{\ell} \{ \delta(q, |m-2s-1|) - \delta(q, m+2s+1) \} \frac{G_{\ell}^m}{m} \frac{dP_{\ell}^m(\cos\theta)}{d\theta}$$

Evaluating the delta functions and collecting terms gives, after some algebra, and with  $U(q)$  representing a step function of  $q$ :

$$F_{\ell}^q P_{\ell}^q(\cos \theta) = 2U(q) \sum_{s=0}^{(\ell-q-1)/2} \frac{G_{\ell}^{q+2s+1}}{q+2s+1} \frac{dP_{\ell}^{q+2s+1}(\cos \theta)}{d\theta} \quad (2.13.9)$$

With the aid of Table A.21.1.1, Eq. 2.13.9 may be rewritten as:

$$F_{\ell}^q P_{\ell}^q(\cos \theta) = U(q) \sum_{s=0}^{(\ell-q-1)/2} \frac{G_{\ell}^{q+2s+1}}{q+2s+1} \times \left[ (\ell+q+2s+1)(\ell-q-2s)P_{\ell}^{q+2s} - P_{\ell}^{q+2s+2} \right] \quad (2.13.10)$$

Multiply Eq. 2.13.10 by  $P_{\ell}^q(\cos \theta)$  and integrate over  $\theta$  using the integrals of Table A.22.1.2. After simplifying, the result is:

$$F_{\ell}^q = 2\ell(\ell-q)! \sum_{s=0}^{(\ell-q-1)/2} \frac{G_{\ell}^{q+2s+1}}{(q+2s+1)} \frac{(-1)^s U(q)}{(\ell-q-2s-1)!} \quad (2.13.11)$$

Combining Eqs. 2.11.9 and 2.13.11, with  $n$  equal to any of the full set of positive integers, gives:

$$F_{\ell}^q = \frac{4(2\ell+1)}{(\ell+1)} (\ell-q)! \sum_{s=0}^{(\ell-q-1)/2} \frac{(-1)^s U(q) \delta(\ell+q, 2n+1)}{(\ell-q-2s-1)! (\ell+q+2s+1)!} \quad (2.13.12)$$

The sum of Eq. 2.13.12 is listed in Table A.15.1.8. Incorporating the sum, replacing  $q$  by  $m$  to give the same dummy index as Eq. 2.11.9, and letting  $n$  denote any of the full set of possible integers, the two coefficient sets  $F_{\ell}^m$  and  $G_{\ell}^m$  are equal to:

$$F_{\ell}^m = \frac{2(2\ell+1)}{\ell(\ell+1)} \frac{U(m)(\ell-m)! \delta(\ell+m, 2n+1)}{(\ell+m-1)! (\ell-m-1)!} \quad (2.13.13)$$

$$G_{\ell}^m \equiv \frac{2(2\ell+1)}{\ell(\ell+1)} \frac{m(\ell-m)! \delta(\ell+m, 2n)}{(\ell+m)! (\ell-m)!}$$

Coefficients  $F_\ell^m$  and  $G_\ell^m$  have opposite parity in that  $F_\ell^m$  is other than zero only if  $\ell + m$  is odd and  $G_\ell^m$  is other than zero only if  $\ell + m$  is even. At degree  $m = 0$  coefficients  $F_\ell^m$  have the maximum value and coefficients  $G_\ell^m$  are equal to zero. Values through the first five orders are listed in Table 2.13.1.

---

$F_1^0 = \frac{3}{2}$	$G_1^1 = \frac{3}{2}$				
	$F_2^1 = \frac{5}{6}$	$G_2^2 = \frac{5}{12}$			
$F_3^0 = \frac{7}{8}$	$G_3^1 = \frac{7}{72}$	$F_3^2 = \frac{7}{48}$	$G_3^3 = \frac{7}{96}$		
	$F_4^1 = \frac{9}{160}$	$G_4^2 = \frac{3}{160}$	$F_4^3 = \frac{3}{160}$	$G_4^4 = \frac{3}{320}$	
$F_5^0 = \frac{11}{16}$	$G_5^1 = \frac{11}{240}$	$F_5^2 = \frac{11}{240}$	$G_5^3 = \frac{11}{1920}$	$F_5^4 = \frac{11}{5760}$	$G_5^5 = \frac{11}{11520}$

---

Table 2.13.1 Values of field coefficients for a y-directed, z-polarized plane wave

## 2.14 Exterior Fields, Powers, and Forces

The radial field components of a y-directed, z-polarized plane wave are given by the combination of Eqs. 2.12.2, 2.13.1, and 2.13.13:

$$\begin{aligned}
 E_r &= \left\{ \sum_{\ell \geq 1} \sum_{m \in}^{\ell} \cos(m\phi) - i \sum_{\ell \geq 2} \sum_{m \in}^{\ell} \sin(m\phi) \right\} \ell(\ell+1) F_\ell^m \frac{j_\ell(\sigma)}{\sigma} P_\ell^m(\cos\theta) \\
 \eta H_r &= \left\{ \sum_{\ell \geq 1} \sum_{m \in}^{\ell} \cos(m\phi) - i \sum_{\ell \geq 2} \sum_{m \in}^{\ell} \sin(m\phi) \right\} \ell(\ell+1) G_\ell^m \frac{j_\ell(\sigma)}{\sigma} P_\ell^m(\cos\theta)
 \end{aligned}
 \tag{2.14.1}$$

The angularly directed field components follow from Eqs. 2.14.1.

One of the two differences between the field forms of the incoming plane wave and the scattered waves is that in the limit of infinite radius the

scattered wave varies with distance as  $\exp[i(\omega t - \sigma)]/\sigma$ . This functional form requires the radial dependent functions to be spherical Hankel functions of the second kind. It is, therefore, necessary to replace the spherical Bessel functions by spherical Hankel functions. Similar to a spherical scatterer, different modes scatter with different magnitudes and different phases. To account for these changes introduce two new infinite sets of field constants,  $\alpha_\ell^m$  and  $\beta_\ell^m$ , as part of the scattered fields. Let  $\alpha_\ell^m$  be the coefficient of TE modes and  $\beta_\ell^m$  be the coefficient of TM modes. Incorporating these results into the radial components of the scattered field gives:

$$\begin{aligned} E_r &= \left[ \sum_{\ell=0}^{\infty} \sum_{m\ell}^{\ell-1} \cos(m\phi) - i \sum_{\ell=2}^{\infty} \sum_{m\ell}^{\ell-1} \sin(m\phi) \right] \ell(\ell+1) \beta_\ell^m F_\ell^m \frac{h_\ell(\sigma)}{\sigma} P_\ell^m(\cos \theta) \\ \eta H_r &= \left[ \sum_{\ell=0}^{\infty} \sum_{m\ell}^{\ell} \cos(m\phi) - i \sum_{\ell=2}^{\infty} \sum_{m\ell}^{\ell} \sin(m\phi) \right] \ell(\ell+1) \alpha_\ell^m G_\ell^m \frac{h_\ell(\sigma)}{\sigma} P_\ell^m(\cos \theta) \end{aligned} \quad (2.14.2)$$

Problem solution requires evaluation of the full parameter sets  $\alpha_\ell^m$  and  $\beta_\ell^m$ . As with the spherical scatterer, the total field is the sum of the incoming plane wave fields and the outwardly directed scattered fields. Summing the radial field components of Eqs. 2.14.1 and 2.14.2 gives the total radial field components. The angular field components follow directly from the radial ones, see Eqs. 1.12.9, and are:

$$\begin{aligned} E_\theta &= \left[ \sum_{\ell=0}^{\infty} \sum_{m\ell}^{\ell-1} \cos(m\phi) - i \sum_{\ell=2}^{\infty} \sum_{m\ell}^{\ell-1} \sin(m\phi) \right] F_\ell^m \left( j_\ell + \beta_\ell^m h_\ell \right) \frac{dP_\ell^m}{d\theta} \\ &\quad - \left[ \sum_{\ell=2}^{\infty} \sum_{m\ell}^{\ell} \cos(m\phi) - i \sum_{\ell=0}^{\infty} \sum_{m\ell}^{\ell} \sin(m\phi) \right] G_\ell^m \left( j_\ell + \alpha_\ell^m h_\ell \right) \frac{mP_\ell^m}{\sin \theta} \\ \eta H_\phi &= -i \left[ \sum_{\ell=0}^{\infty} \sum_{m\ell}^{\ell-1} \cos(m\phi) - i \sum_{\ell=2}^{\infty} \sum_{m\ell}^{\ell-1} \sin(m\phi) \right] F_\ell^m \left( j_\ell + \beta_\ell^m h_\ell \right) \frac{dP_\ell^m}{d\theta} \\ &\quad - i \left[ \sum_{\ell=2}^{\infty} \sum_{m\ell}^{\ell} \cos(m\phi) - i \sum_{\ell=0}^{\infty} \sum_{m\ell}^{\ell} \sin(m\phi) \right] G_\ell^m \left( j_\ell + \alpha_\ell^m h_\ell \right) \frac{mP_\ell^m}{\sin \theta} \end{aligned}$$

$$\begin{aligned}
 -E_\phi = i & \left[ \sum_{\ell e;2}^{\infty} \sum_{m\phi}^{\ell-1} \cos(m\phi) - i \sum_{\ell o;3}^{\infty} \sum_{m\epsilon}^{\ell-1} \sin(m\phi) \right] F_\ell^m \left( j_\ell^\bullet + \beta_\ell^m h_\ell^\bullet \right) \frac{mP_\ell^m}{\sin\theta} \\
 & - i \left[ \sum_{\ell o;1}^{\infty} \sum_{m\phi}^{\ell} \cos(m\phi) - i \sum_{\ell e;2}^{\infty} \sum_{m\epsilon}^{\ell} \sin(m\phi) \right] G_\ell^m \left( j_\ell + \alpha_\ell^m h_\ell \right) \frac{dP_\ell^m}{d\theta}
 \end{aligned} \quad (2.14.3)$$

$$\begin{aligned}
 \eta H_\theta = & \left[ \sum_{\ell e;2}^{\infty} \sum_{m\phi}^{\ell-1} \cos(m\phi) - i \sum_{\ell o;3}^{\infty} \sum_{m\epsilon}^{\ell-1} \sin(m\phi) \right] F_\ell^m \left( j_\ell + \beta_\ell^m h_\ell \right) \frac{mP_\ell^m}{\sin\theta} \\
 & + \left[ \sum_{\ell o;1}^{\infty} \sum_{m\phi}^{\ell} \cos(m\phi) - i \sum_{\ell e;2}^{\infty} \sum_{m\epsilon}^{\ell} \sin(m\phi) \right] G_\ell^m \left( j_\ell^\bullet + \alpha_\ell^m h_\ell^\bullet \right) \frac{dP_\ell^m}{d\theta}
 \end{aligned}$$

Power on a circumscribing virtual sphere of radius greater than  $a$  is obtained from the radial component of the complex Poynting vector. Substituting Eqs. 2.14.3 into Eq. 2.2.3 and breaking the resulting vector into four parts gives:

$$N_{r11} = \frac{\text{Re}}{2\eta} \left\{ \begin{aligned} & \left( \sum_{\ell o}^{\infty} \sum_{m\epsilon}^{\ell-1} \cos(m\phi) - i \sum_{\ell e}^{\infty} \sum_{m\phi}^{\ell-1} \sin(m\phi) \right) \left( \sum_{no}^{\infty} \sum_{pe}^{n-1} \cos(p\phi) + i \sum_{ne}^{\infty} \sum_{po}^{n-1} \sin(p\phi) \right) \\ & \times i F_\ell^m F_n^p \left( j_\ell^\bullet + \beta_\ell^m h_\ell^\bullet \right) \left( j_n + \beta_n^p h_n^* \right) \left( \frac{dP_\ell^m}{d\theta} \frac{dP_n^p}{d\theta} \right) \\ & \left( \sum_{\ell e}^{\infty} \sum_{m\phi}^{\ell-1} \cos(m\phi) - i \sum_{\ell o}^{\infty} \sum_{m\epsilon}^{\ell-1} \sin(m\phi) \right) \left( \sum_{ne}^{\infty} \sum_{po}^{n-1} \cos(p\phi) + i \sum_{no}^{\infty} \sum_{pe}^{n-1} \sin(p\phi) \right) \\ & \times i F_\ell^m F_n^p \left( j_\ell^\bullet + \beta_\ell^m h_\ell^\bullet \right) \left( j_n + \beta_n^p h_n^* \right) \left( \frac{mP_\ell^m}{\sin\theta} \frac{pP_n^p}{\sin\theta} \right) \end{aligned} \right\} \quad (2.14.4)$$

$$N_{r12} = -\frac{\text{Re}}{2\eta} \left\{ \begin{aligned} & \left( \sum_{\ell o}^{\infty} \sum_{m o}^{\ell} \cos(m\phi) - i \sum_{\ell e}^{\infty} \sum_{m e}^{\ell} \sin(m\phi) \right) \left( \sum_{no}^{\infty} \sum_{po}^n \cos(p\phi) + i \sum_{ne}^{\infty} \sum_{pe}^n \sin(p\phi) \right) \\ & \times \kappa G_{\ell}^m G_n^p (j_{\ell} + \alpha_{\ell}^m h_{\ell}) (j_n^{\bullet} + \alpha_n^{p*} h_n^{\bullet*}) \left( \frac{dP_{\ell}^m}{d\theta} \frac{dP_n^p}{d\theta} \right) \\ & \left( \sum_{\ell e}^{\infty} \sum_{m e}^{\ell} \cos(m\phi) - i \sum_{\ell o}^{\infty} \sum_{m o}^{\ell} \sin(m\phi) \right) \left( \sum_{ne}^{\infty} \sum_{pe}^n \cos(p\phi) + i \sum_{no}^{\infty} \sum_{po}^n \sin(p\phi) \right) \\ & \times \kappa G_{\ell}^m G_n^p (j_{\ell} + \alpha_{\ell}^m h_{\ell}) (j_n^{\bullet} + \alpha_n^{p*} h_n^{\bullet*}) \left( \frac{mP_{\ell}^m}{\sin\theta} \frac{pP_n^p}{\sin\theta} \right) \end{aligned} \right\} \quad (2.14.5)$$

$$N_{r21} = \frac{\text{Re}}{2\eta} \left\{ \begin{aligned} & \left( \sum_{\ell o}^{\infty} \sum_{m e}^{\ell-1} \cos(m\phi) - i \sum_{\ell e}^{\infty} \sum_{m o}^{\ell-1} \sin(m\phi) \right) \left( \sum_{ne}^{\infty} \sum_{pe}^n \cos(p\phi) + i \sum_{no}^{\infty} \sum_{po}^n \sin(p\phi) \right) \\ & \times i F_{\ell}^m G_n^p (j_{\ell}^{\bullet} + \beta_{\ell}^m h_{\ell}^{\bullet}) (j_n^{\bullet} + \alpha_n^{p*} h_n^{\bullet*}) \left( \frac{pP_n^p}{\sin\theta} \frac{dP_{\ell}^m}{d\theta} \right) \\ & + \left( \sum_{\ell e}^{\infty} \sum_{m o}^{\ell-1} \cos(m\phi) - i \sum_{\ell o}^{\infty} \sum_{m e}^{\ell-1} \sin(m\phi) \right) \left( \sum_{no}^{\infty} \sum_{po}^n \cos(p\phi) + i \sum_{ne}^{\infty} \sum_{pe}^n \sin(p\phi) \right) \\ & \times i F_{\ell}^m G_n^p (j_{\ell}^{\bullet} + \beta_{\ell}^m h_{\ell}^{\bullet}) (j_n^{\bullet} + \alpha_n^{p*} h_n^{\bullet*}) \left( \frac{mP_{\ell}^m}{\sin\theta} \frac{dP_n^p}{d\theta} \right) \end{aligned} \right\} \quad (2.14.6)$$

$$N_{r22} = -\frac{\text{Re}}{2\eta} \left\{ \begin{aligned} & \left( \sum_{\ell e}^{\infty} \sum_{m e}^{\ell} \cos(m\phi) - i \sum_{\ell o}^{\infty} \sum_{m o}^{\ell} \sin(m\phi) \right) \left( \sum_{no}^{\infty} \sum_{pe}^{n-1} \cos(p\phi) + i \sum_{ne}^{\infty} \sum_{po}^{n-1} \sin(p\phi) \right) \\ & \times i F_{\ell}^m G_n^p (j_{\ell} + \alpha_{\ell}^m h_{\ell}) (j_n + \beta_n^{p*} h_n^*) \left( \frac{mP_{\ell}^m}{\sin\theta} \frac{dP_n^p}{d\theta} \right) \\ & + \left( \sum_{\ell o}^{\infty} \sum_{m o}^{\ell} \cos(m\phi) - i \sum_{\ell e}^{\infty} \sum_{m e}^{\ell} \sin(m\phi) \right) \left( \sum_{ne}^{\infty} \sum_{po}^{n-1} \cos(p\phi) + i \sum_{no}^{\infty} \sum_{pe}^{n-1} \sin(p\phi) \right) \\ & \times i F_{\ell}^m G_n^p (j_{\ell} + \alpha_{\ell}^m h_{\ell}) (j_n + \beta_n^{p*} h_n^*) \left( \frac{pP_n^p}{\sin\theta} \frac{dP_{\ell}^m}{d\theta} \right) \end{aligned} \right\} \quad (2.14.7)$$

The total surface power is equal to the surface integral of Eqs. 2.14.4 to 2.14.7. Integrating over the azimuth angle gives a Kronecker delta function of  $m$  and  $p$ , decreasing the number of sums by one. Results are shown in Eqs. 2.14.8 and 2.14.9:

$$\begin{aligned} \int_0^{2\pi} d\phi (N_{r11} + N_{r12}) = \text{Re} & \left[ \left( \sum_{\ell o} \sum_{n o} \sum_{m e} + \sum_{\ell e} \sum_{n e} \sum_{m o} \right) i F_{\ell}^m F_n^m \left( j_{\ell}^{\bullet} + \beta_{\ell}^m h_{\ell}^{\bullet} \right) \left( j_n + \beta_n^{m*} h_n^* \right) \right. \\ & \left. - \left( \sum_{\ell o} \sum_{n o} \sum_{m o} + \sum_{\ell e} \sum_{n e} \sum_{m e} \right) i G_{\ell}^m G_n^m \left( j_{\ell} + \alpha_{\ell}^m h_{\ell} \right) \left( j_n + \alpha_n^{m*} h_n^{**} \right) \right] \\ & \times \frac{\pi}{2\eta} [1 + \delta(m, 0)] \left( \frac{dP_{\ell}^m}{d\theta} \frac{dP_n^m}{d\theta} + \frac{m^2 P_{\ell}^m P_n^m}{\sin^2 \theta} \right) \end{aligned} \quad (2.14.8)$$

$$\begin{aligned} \int_0^{2\pi} d\phi (N_{r21} + N_{r22}) = \text{Re} & \left[ \left( \sum_{\ell e} \sum_{n o} \sum_{m o} + \sum_{\ell o} \sum_{n e} \sum_{m e} \right) i F_{\ell}^m G_n^m \left( j_{\ell}^{\bullet} + \beta_{\ell}^m h_{\ell}^{\bullet} \right) \left( j_n^{\bullet} + \alpha_n^{m*} h_n^{**} \right) \right. \\ & \left. - \left( \sum_{\ell e} \sum_{n o} \sum_{m e} + \sum_{\ell o} \sum_{n e} \sum_{m o} \right) i F_{\ell}^m G_n^m \left( j_{\ell} + \alpha_{\ell}^m h_{\ell} \right) \left( j_n + \beta_n^{m*} h_n^* \right) \right] \\ & \times \frac{\pi}{\eta} \frac{m}{\sin \theta} \left( P_{\ell}^m P_n^m \right) \end{aligned} \quad (2.14.9)$$

To complete the evaluation it is necessary to integrate Eqs. 2.14.8 and 2.14.9 over the zenith angle. The integral of Eq. 2.14.9 gives a null result. Evaluating the integral of Eq. 2.14.8 and replacing the coefficients by the values of Eqs. 2.13.13 gives:

$$\begin{aligned} P_{av} = \frac{4\pi\sigma^2}{\eta k^2} \text{Re} & \left[ \sum_{\ell o}^{\infty} \sum_{m e}^{\ell-1} + \sum_{\ell e}^{\infty} \sum_{m o}^{\ell-1} \right] \frac{U(m)(2\ell+1)(\ell-m)!!(\ell+m)!!}{\ell(\ell+1)(\ell-m-1)!!(\ell+m-1)!!} i \left( j_{\ell}^{\bullet} + \beta_{\ell}^m h_{\ell}^{\bullet} \right) \left( j_{\ell} + \beta_{\ell}^{m*} h_{\ell}^* \right) \Bigg\} \\ & - \frac{4\pi\sigma^2}{\eta k^2} \text{Re} \left[ \sum_{\ell o}^{\infty} \sum_{m o}^{\ell} + \sum_{\ell e}^{\infty} \sum_{m e}^{\ell} \right] \frac{m^2(2\ell+1)(\ell-m-1)!!(\ell+m-1)!!}{\ell(\ell+1)(\ell-m)!!(\ell+m)!!} i \left( j_{\ell} + \alpha_{\ell}^m h_{\ell} \right) \left( j_{\ell}^{\bullet} + \alpha_{\ell}^{m*} h_{\ell}^{**} \right) \Bigg\} \end{aligned} \quad (2.14.10)$$

In the limit of infinite radius, Eq. 2.14.10 goes to:

$$\begin{aligned}
P_{av} = & \frac{4\pi}{\eta k^2} \left\{ \left[ \sum_{\ell o}^{\infty} \sum_{m e}^{\ell-1} + \sum_{\ell e}^{\infty} \sum_{m o}^{\ell-1} \right] \frac{U(m)(2\ell+1)(\ell-m)!!(\ell+m)!!}{\ell(\ell+1)!!(\ell-m-1)!!(\ell+m-1)!!} \left( \text{Re}\beta_{\ell}^m + \beta_{\ell}^m \beta_{\ell}^{m*} \right) \right\} \\
& + \frac{4\pi}{\eta k^2} \left\{ \left[ \sum_{\ell o}^{\infty} \sum_{m o}^{\ell} + \sum_{\ell e}^{\infty} \sum_{m e}^{\ell} \right] \frac{m^2(2\ell+1)(\ell-m-1)!!(\ell+m-1)!!}{\ell(\ell+1)(\ell-m)!!(\ell+m)!!} \left( \text{Re}\alpha_{\ell}^m + \alpha_{\ell}^m \alpha_{\ell}^{m*} \right) \right\}
\end{aligned}
\tag{2.14.11}$$

The terms are interpreted similarly to those of Eq. 2.2.7 for scattering from a sphere: terms proportional to both  $\alpha_n^m \alpha_n^{m*}$  and  $\beta_n^m \beta_n^{m*}$  describe time-average power scattered away from the antenna; each term is positive. Terms proportional to  $\text{Re}\alpha_n^m$  and  $\text{Re}\beta_n^m$  are negative and describe inwardly directed power; the time integral of Eq. 2.14.11 is the negative of the extinction (absorbed plus scattered) energy. For an ideal antenna with shorted terminals, the two sets of terms have equal magnitude and opposite sign and sum to zero.

## 2.15 The Cross Sections

The purpose of this section is to compare and contrast the scattering properties of spheres with those of a biconical receiving antenna. One view of a receiving antenna is as a lossy scatterer. Cross sections were defined in Section 2.2. Analogously with Eq. 2.2.10, the scattering cross section  $C_{SC}$  is defined to equal the ratio of scattered power to the input power density. The geometric cross section is equal to the cross sectional area of the scatterer. Using Eq. 2.14.11 to determine the scattered power, for a spherical scatterer of radius  $a$  the scattering-to-geometric cross section ratio is:

$$\begin{aligned}
\frac{C_{SC}}{C_{GE}} = & \frac{8}{k^2 a^2} \left\{ \left[ \sum_{\ell o}^{\infty} \sum_{m e}^{\ell-1} + \sum_{\ell e}^{\infty} \sum_{m o}^{\ell-1} \right] \frac{U(m)(2\ell+1)(\ell-m)!!(\ell+m)!!}{\ell(\ell+1)(\ell-m-1)!!(\ell+m-1)!!} \left( \beta_{\ell}^m \beta_{\ell}^{m*} \right) \right\} \\
& + \frac{8}{k^2 a^2} \left\{ \left[ \sum_{\ell o}^{\infty} \sum_{m o}^{\ell} + \sum_{\ell e}^{\infty} \sum_{m e}^{\ell} \right] \frac{m^2(2\ell+1)(\ell-m-1)!!(\ell+m-1)!!}{\ell(\ell+1)(\ell-m)!!(\ell+m)!!} \left( \alpha_{\ell}^m \alpha_{\ell}^{m*} \right) \right\}
\end{aligned}
\tag{2.15.1}$$



The normalized extinction cross section  $C_{EX}$  is equal to the ratio of the total power extracted from the incoming plane wave to the geometric cross sectional area of the scatterer. For a spherical scatterer of radius  $a$  and using Eq. 2.14.11 to determine the total power extracted from the wave, the extinction-to-geometric cross section ratio is:

$$\begin{aligned} \frac{C_{EX}}{C_{GE}} = & -\frac{4}{k^2 a^2} \left\{ \left[ \sum_{\ell o}^{\infty} \sum_{m \epsilon}^{\ell-1} + \sum_{\ell e}^{\infty} \sum_{m o}^{\ell-1} \right] \frac{U(m)(2\ell+1)(\ell-m)!!(\ell+m)!!}{\ell(\ell+1)(\ell-m-1)!!(\ell+m-1)!!} \left( \text{Re} \beta_{\ell}^m \right) \right\} \\ & - \frac{8}{k^2 a^2} \left\{ \left[ \sum_{\ell o}^{\infty} \sum_{m o}^{\ell} + \sum_{\ell e}^{\infty} \sum_{m \epsilon}^{\ell} \right] \frac{m^2 (2\ell+1)(\ell-m-1)!!(\ell+m-1)!!}{\ell(\ell+1)(\ell-m)!!(\ell+m)!!} \left( \text{Re} \alpha_{\ell}^m \right) \right\} \end{aligned} \quad (2.15.2)$$

The absorption cross section,  $C_{AB}$ , is equal to the absorbed power-to-cross sectional area of the scatterer ratio. Using Eq. 2.14.11, the value is:

$$\begin{aligned} \frac{C_{AB}}{C_{GE}} = & -\frac{4}{k^2 a^2} \left\{ \left[ \sum_{\ell o}^{\infty} \sum_{m \epsilon}^{\ell-1} + \sum_{\ell e}^{\infty} \sum_{m o}^{\ell-1} \right] \frac{(2\ell+1)(\ell-m)!!(\ell+m)!!}{\ell(\ell+1)(\ell-m-1)!!(\ell+m-1)!!} \left( \text{Re} \beta_{\ell}^m - \beta_{\ell}^{m o} \beta_{\ell}^{m*} \right) \right\} \\ & - \frac{8}{k^2 a^2} \left\{ \left[ \sum_{\ell o}^{\infty} \sum_{m o}^{\ell} + \sum_{\ell e}^{\infty} \sum_{m \epsilon}^{\ell} \right] \frac{m^2 (2\ell+1)(\ell-m-1)!!(\ell+m-1)!!}{\ell(\ell+1)(\ell-m)!!(\ell+m)!!} \left( \text{Re} \alpha_{\ell}^m - \alpha_{\ell}^{m o} \alpha_{\ell}^{m*} \right) \right\} \end{aligned} \quad (2.15.3)$$

The thrust on the antenna from the total power absorbed is  $c$  times the value of extinction power, Eq. 2.15.2. The thrust on the antenna from the scattered power is equal to the component of scattered wave in the direction of the incoming field integrated over a virtual surface:

$$F_{ySC} = -\frac{\sigma^2}{2\eta k^2} \int_0^{2\pi} \sin \phi d\phi \int_0^{\pi} \sin^2 \theta d\theta \text{Re}(N_r) \quad (2.15.4)$$

Inserting the scattered field terms of Eqs. 2.14.3 into Eq. 2.15.4 gives:

$$\begin{aligned}
\int_0^{2\pi} N_r \sin \phi d\phi = & \frac{\pi \text{Re}}{4\eta} \left\{ \sum_{\ell o} \sum_{n e} \sum_{m e} \left( F_\ell^m F_n^{m+1} \beta_\ell^m \beta_n^{m+1} h_\ell^* h_n^* \right) [1 + \delta(m)] \right. \\
& \left. + \sum_{\ell e} \sum_{n o} \sum_{m o} \left( F_\ell^m F_n^{m-1} \beta_\ell^m \beta_n^{m-1} h_\ell^* h_n^* \right) [1 + \delta(m-1)] \right\} \\
& \times \left\{ \left( \frac{dP_\ell^m}{d\theta} \frac{dP_n^{m+1}}{d\theta} + \frac{m(m+1)}{\sin^2 \theta} P_\ell^m P_n^{m+1} \right) \right. \\
& \left. - \left( \frac{dP_\ell^m}{d\theta} \frac{dP_n^{m-1}}{d\theta} + \frac{m(m-1)}{\sin^2 \theta} P_\ell^m P_n^{m-1} \right) \right\} \\
- \frac{\pi \text{Re}}{4\eta} & \left\{ \sum_{\ell o} \sum_{n e} \sum_{m o} \left( G_\ell^m G_n^{m+1} \alpha_\ell^m \alpha_n^{m+1} h_\ell h_n^* \right) \left( \frac{dP_\ell^m}{d\theta} \frac{dP_n^{m+1}}{d\theta} + \frac{m(m+1)}{\sin^2 \theta} P_\ell^m P_n^{m+1} \right) \right. \\
& \left. + \sum_{\ell e} \sum_{n o} \sum_{m e} \left( G_\ell^m G_n^{m-1} \alpha_\ell^m \alpha_n^{m-1} h_\ell h_n^* \right) \left( \frac{dP_\ell^m}{d\theta} \frac{dP_n^{m-1}}{d\theta} + \frac{m(m-1)}{\sin^2 \theta} P_\ell^m P_n^{m-1} \right) \right\} \\
+ \frac{\pi \text{Re}}{4\eta} & \left\{ \sum_{\ell o} \sum_{n o} \sum_{m e} \left( G_\ell^{m+1} F_\ell^m \alpha_n^{m+1} \beta_\ell^m h_\ell^* h_n^* \right) [1 + \delta(m)] \right. \\
& \left. + \sum_{\ell e} \sum_{n e} \sum_{m o} \left( G_\ell^{m-1} F_\ell^m \alpha_n^{m-1} \beta_\ell^m h_\ell^* h_n^* \right) \left( \frac{m P_\ell^m}{\sin \theta} \frac{dP_n^{m+1}}{d\theta} + \frac{(m+1) P_n^{m+1}}{\sin \theta} \frac{dP_\ell^m}{d\theta} \right) \right. \\
& \left. - G_n^{m-1} F_\ell^m \alpha_n^{m-1} \beta_\ell^m h_\ell^* h_n^* \left( \frac{m P_\ell^m}{\sin \theta} \frac{dP_n^{m-1}}{d\theta} + \frac{(m-1) P_n^{m-1}}{\sin \theta} \frac{dP_\ell^m}{d\theta} \right) \right\} \\
+ \frac{\pi \text{Re}}{4\eta} & \left\{ \sum_{\ell o} \sum_{n o} \sum_{m o} \left( G_\ell^m F_n^{m-1} \alpha_\ell^m \beta_n^{m-1} h_\ell h_n^* \right) [1 + \delta(m-1)] \right. \\
& \left. + \sum_{\ell e} \sum_{n e} \sum_{m e} \left( G_\ell^m F_n^{m+1} \alpha_\ell^m \beta_n^{m+1} h_\ell h_n^* \right) \left( \frac{m P_\ell^m}{\sin \theta} \frac{dP_n^{m-1}}{d\theta} + \frac{(m-1) P_n^{m-1}}{\sin \theta} \frac{dP_\ell^m}{d\theta} \right) \right. \\
& \left. - G_\ell^m F_n^{m+1} \alpha_\ell^m \beta_n^{m+1} h_\ell h_n^* \left( \frac{m P_\ell^m}{\sin \theta} \frac{dP_n^{m+1}}{d\theta} + \frac{(m+1) P_n^{m+1}}{\sin \theta} \frac{dP_\ell^m}{d\theta} \right) \right\}
\end{aligned}
\tag{2.15.5}$$

Next, integrate Eq. 2.15.4 to find the directed power through a virtual circumscribing sphere, with the aid of Table A.22.1.8, 22.1.9, 22.1.11, and 22.1.12. In the limit where the scattered waves extend to infinite radius, the normalized  $y$ -directed force due to the scattered field is:

$$\frac{\alpha_{JSC}}{C_{GE}} = -\frac{4}{k^2 a^2} \left\{ \left( \sum_{\ell o} \sum_{m c} + \sum_{\ell e} \sum_{m o} \right) \left( \begin{aligned} &+ \left( \beta_{\ell}^m \beta_{\ell+1}^{m+1*} + \beta_{\ell}^{m*} \beta_{\ell+1}^{m+1} \right) \frac{U(m)(\ell-m)!!(\ell+2)!!}{(\ell+1)^2(\ell-m-1)!!(\ell+m-1)!!} \\ &+ \left( \beta_{\ell}^m \beta_{\ell-1}^{m+1*} + \beta_{\ell}^{m*} \beta_{\ell-1}^{m+1} \right) \frac{U(m)(\ell-m)!!(\ell+m)!!}{(\ell)^2(\ell-m-3)!!(\ell+m-1)!!} \end{aligned} \right) \right. \\ \left. + \left( \sum_{\ell o} \sum_{m o} + \sum_{\ell e} \sum_{m c} \right) \left( \begin{aligned} &+ \left( \alpha_{\ell}^m \alpha_{\ell+1}^{m+1*} + \alpha_{\ell}^{m*} \alpha_{\ell+1}^{m+1} \right) \frac{m(m+1)(\ell-m-1)!!(\ell+m+1)!!}{(\ell+1)^2(\ell-m)!!(\ell+m)!!} \\ &+ \left( \alpha_{\ell}^m \alpha_{\ell-1}^{m+1*} + \alpha_{\ell}^{m*} \alpha_{\ell-1}^{m+1} \right) \frac{m(m+1)(\ell-m-1)!!(\ell+m+1)!!}{(\ell)^2(\ell-m-2)!!(\ell+m)!!} \end{aligned} \right) \right. \\ \left. + \left( \sum_{\ell o} \sum_{m c} + \sum_{\ell e} \sum_{m o} \right) \left( \alpha_{\ell}^{m+1*} \beta_{\ell}^m + \alpha_{\ell}^{m+1} \beta_{\ell}^{m*} \right) \left( \frac{(m+1)(2\ell+1)(\ell-m)!!(\ell+m)!!}{\ell^2(\ell+1)^2(\ell-m-1)!!(\ell+m-1)!!} \right) \right. \\ \left. - \left( \sum_{\ell o} \sum_{m o} + \sum_{\ell e} \sum_{m c} \right) \left( \alpha_{\ell}^m \beta_{\ell}^{m+1*} + \alpha_{\ell}^{m*} \beta_{\ell}^{m+1} \right) \left( \frac{m(2\ell+1)(\ell-m-1)!!(\ell+m+1)!!}{\ell^2(\ell+1)^2(\ell-m-2)!!(\ell+m)!!} \right) \right\} \quad (2.15.6)$$

The normalized force due to the extinction power is:

$$\frac{\alpha_{JEX}}{C_{GE}} = -\frac{8}{k^2 a^2} \left\{ \left[ \sum_{\ell o} \sum_{m c}^{\infty \ell-1} + \sum_{\ell e} \sum_{m o}^{\infty \ell-1} \right] \frac{U(m)(2\ell+1)(\ell-m)!!(\ell+m)!!}{\ell(\ell+1)(\ell-m-1)!!(\ell+m-1)!!} \text{Re} \beta_{\ell}^m \right. \\ \left. + \left[ \sum_{\ell o} \sum_{m o}^{\infty \ell} + \sum_{\ell e} \sum_{m c}^{\infty \ell} \right] \frac{m^2(2\ell+1)(\ell-m-1)!!(\ell+m-1)!!}{\ell(\ell+1)(\ell-m)!!(\ell+m)!!} \text{Re} \alpha_{\ell}^m \right\} \quad (2.15.7)$$

To compare results obtained using  $y$ - and  $z$ -directed incoming plane waves, consider scattering by an ideally conducting sphere. For a  $z$ -directed wave, the coefficients are given by Eq. 2.3.5 and 2.3.6; for a  $y$ -directed wave, the boundary conditions follow from Eqs. 2.15.3, and are:

$$j_{\ell}^{\bullet}(ka) + \beta_{\ell}^m h_{\ell}^{\bullet}(ka) = 0 \quad j_{\ell}(ka) + \alpha_{\ell}^m h_{\ell}(ka) = 0 \quad (2.15.8)$$

These lead to:

$$\beta_{\ell}^m(ka) = -\frac{j_{\ell}^{\bullet}(ka)}{h_{\ell}^{\bullet}(ka)} \quad \alpha_{\ell}^m(ka) = -\frac{j_{\ell}(ka)}{h_{\ell}(ka)} \quad (2.15.9)$$

These equations show that the coefficients are independent of degree. For the case where the scatterer radius is much less than a wavelength the dipole coefficients are:

$$\beta_1^0(ka) = -\frac{2/3}{2/3 - i/(ka)^3} \cong \frac{2(ka)^3}{3i} \quad \alpha_1^1(ka) = -\frac{(ka)/3}{(ka)/3 + i/(ka)^2} \cong \frac{i(ka)^3}{3} \quad (2.15.10)$$

The cross sections and normalized forces are:

$$\frac{C_{EX}}{C_{GE}} = \frac{C_{SC}}{C_{GE}} = \frac{cf_{EX}}{C_{GE}} = \frac{10(ka)^4}{3} \quad (2.15.11)$$

These results are equal to those of Eqs. 2.3.7 and 2.3.8.

## *Biconical Receiving Antennas*

### **2.16 General Comments**

Biconical receiving antennas are of special significance for the same reasons biconical transmitting antennas are. Namely, only biconical and ellipsoidal shapes closely represent three-dimensional antennas and only for them do mathematically complete solutions exist. The list of practical antennas that biconical shapes approach is longer than the list for ellipsoidal ones. The receiving antenna problem is a scattering problem. The antenna is immersed in an otherwise steady state plane wave. Some of the incoming energy, the extinction energy, is transferred to the scatterer and the rest continues unperturbed; part of the extinction energy is absorbed and the rest is radiated away as a scattered field. The objective is to analyze a biconical receiving antenna of arbitrary cone length and half angle and with an arbitrary value of impedance attached to the terminals. A full analysis requires knowing all fields at all points in space. This is obtained by matching the full sets of possible field forms in the external and internal regions, see Fig. 2.4.1, to conducting boundary conditions at the antenna surfaces and to virtual

boundary conditions in the open aperture. The extinction energy and momentum, the scattered energy and momentum, and the surface charge and current densities may be evaluated once the fields are known. The absorbed power and the impedance at the antenna terminals follow from the surface currents and the interior fields.

For transmission, either voltage  $V(0)$  from a constant voltage source or current  $I(0)$  from a constant current source is applied between the terminals of the cones at  $r = b$ . There are no incident fields. For reception, the power sink at  $r < b$  is a passive, isotropic energy absorber. Extinction power is extracted from an incident,  $y$ -directed plane wave; some is scattered and some is absorbed. It is convenient to break space into regions similar to those of transmitting antennas. The regions are:

Sink

$$r < b ; \quad 0 \leq \theta \leq \pi; \quad 0 \leq \phi \leq 2\pi \quad (2.16.1)$$

Interior

Arms

$$b < r < a ; \quad 0 \leq \theta < \psi; \quad \pi - \psi < \theta \leq \pi; \quad 0 \leq \phi \leq 2\pi \quad (2.16.2)$$

Space

$$b < r < a ; \quad \psi < \theta < \pi - \psi; \quad 0 \leq \phi \leq 2\pi \quad (2.16.3)$$

Exterior

$$r > a ; \quad 0 \leq \theta \leq \pi; \quad 0 \leq \phi \leq 2\pi \quad (2.16.4)$$

The spherical coordinate expansion for a  $y$ -directed plane wave, Eqs. 2.14.2 and 2.14.3, contains products of trigonometric functions, harmonic spherical functions, and spherical Bessel functions of integer order, with orders ranging from one to infinity. Although exterior and interior modal products of different degrees are orthogonal, exterior and interior modes of different orders are not: Each exterior order contributes to all interior orders of the same degree. Interior modes are associated with surface current and charge densities on the cones. All driven antenna modes absorb energy and momentum from the plane wave, some of each is absorbed and some of each is scattered away. The zero degree plane wave modes excite TM scattering modes and TM and TEM interior modes similar to the transmitter modes; modes known as transmitter modes. Higher degree exterior modes excite both TM and TE scattered and interior modes. With

these modes the extinction and scattered energies are equal and result in the absorption of momentum but not energy from the wave; these are the receiver modes.

As an example of receiver modes, at low enough frequencies a surface current flows along the illuminated face of the antenna; it is largest near the caps. (Detailed sketches are shown in Fig. 2.21.1). Going toward the conical apices at each differential length some of the current terminates on local electric charge densities, until it disappears entirely at the terminals. At the cone-cap junction, some charge is stored and some passes through onto the cap. Since the currents into and out of the cone-cap junctions are not necessarily equal, an oscillating ring of charge resides there. A similar current distribution is repeated, but oppositely directed, on the shadowed side of the antenna. The current pattern generates a magnetic dipole moment; the cross sectional area of the dipole is the geometrical cross section of the cones perpendicular both to the incoming wave and to the antenna axis, in this case the  $x$ -direction. By Lenz's law, the phase of the generated magnetic moment is opposite that of the incoming magnetic field and results in a scattered wave.

Just as for transmission, the charge and current densities on the cones are functions of the interior fields and those on the caps are functions of the exterior fields. The signs of adjacent arm and cap surface and line charge densities may or may not be the same. The current that flows from the cone to the cone-cap junction is not necessarily equal to the current that flows from the junction to the cap and, as noted, differences result in a ring of charge at the junction.

## 2.17 Fields of Receiving Antennas

Combining Eqs. 2.13.13 and 2.14.3 shows the TM and TE modes respectively to be proportional  $\delta(\ell + m, 2n+1)$  and  $\delta(\ell + m, 2n)$ , and expresses the condition that the associated Legendre polynomials satisfy the symmetry conditions:

$$\begin{array}{ll} \text{TM modes} & P_\ell^m(\cos\theta) = -P_\ell^m(-\cos\theta) \\ \text{TE modes} & P_\ell^m(\cos\theta) = P_\ell^m(\cos\theta) \end{array} \quad (2.17.1)$$

The total exterior field, the modal fields of the plane and scattered waves, are equal to the sum of Eqs. 2.14.1, 2.14.2 and 2.14.3. A complete field evaluation requires evaluation of the scattering field coefficients.

The interior modal structure of a receiving antenna depends upon the symmetries both of the driving field and the antenna. For the antenna axis parallel with the direction of polarization, the antenna implementation retains the symmetry of the external fields in the internal region. As was the case for a transmitting antenna, finite interior fields require the multiplying coefficient of all functions  $y_v(\sigma)$  to be equal to zero for  $v > 0$ . Coefficients of the  $j_v(\sigma)$  functions are nonzero for both TM and TE modes. The symmetry of the interior TM and TE modes remains the same as the exterior symmetry, with undetermined coefficients respectively defined to be  $\Gamma_v^m$  and  $\Lambda_v^m$ . A full solution requires evaluation of the functional relationships between internal coefficients  $\Gamma_v^m$  and  $\Lambda_v^m$  and the scattering coefficients  $\alpha_\ell^m$  and  $\beta_\ell^m$ .

Combining all the above for the interior fields, the zero degree terms have the same form as the transmitter terms, Eqs. 2.7.1, and combine with the higher degree terms requirements to provide the expanded equation set:

$$\begin{aligned}
 E_r &= \sum_{v>0} \left[ \sum_{m\in}^{\infty} \cos m\phi - i \sum_{m0}^{\infty} \sin m\phi \right] v(v+1) \Gamma_v^m \frac{j_v(\sigma)}{\sigma} M_v^m(\cos \theta) \\
 \eta H_r &= \sum_{v>0} \left[ \sum_{m0}^{\infty} \cos m\phi - i \sum_{m\in}^{\infty} \sin m\phi \right] v(v+1) \Lambda_v^m \frac{j_v(\sigma)}{\sigma} L_v^m(\cos \theta) \\
 E_\theta &= \frac{\eta G V(r)}{2\pi r \sin \theta} + \sum_{v>0} \left[ \sum_{m\in}^{\infty} \cos m\phi - i \sum_{m0}^{\infty} \sin m\phi \right] \Gamma_v^m j_v(\sigma) \frac{dM_v^m}{d\theta} \\
 &\quad - \sum_{v>0} \left[ \sum_{m\in}^{\infty} \cos m\phi - i \sum_{m0}^{\infty} \sin m\phi \right] \Lambda_v^m j_v(\sigma) \frac{m L_v^m}{\sin \theta} \\
 \eta H_\phi &= \frac{\eta I(r)}{2\pi r \sin \theta} - i \sum_{v>0} \left[ \sum_{m\in}^{\infty} \cos m\phi - i \sum_{m0}^{\infty} \sin m\phi \right] \Gamma_v^m j_v(\sigma) \frac{dM_v^m}{d\theta} \\
 &\quad - i \sum_{v>0} \left[ \sum_{m\in}^{\infty} \cos m\phi - i \sum_{m0}^{\infty} \sin m\phi \right] \Lambda_v^m j_v(\sigma) \frac{m L_v^m}{\sin \theta}
 \end{aligned} \tag{2.17.2}$$

$$\begin{aligned}
E_\phi &= -i \sum_{\nu>0} \left[ \sum_{m0}^{\infty} \cos m\phi - i \sum_{m\epsilon}^{\infty} \sin m\phi \right] \Gamma_\nu^m j_\nu(\sigma) \frac{m M_\nu^m}{\sin \theta} \\
&\quad + \sum_{\nu>0} \left[ \sum_{m0}^{\infty} \cos m\phi - i \sum_{m\epsilon}^{\infty} \sin m\phi \right] \Lambda_\nu^m j_\nu(\sigma) \frac{dL_\nu^m}{d\theta} \\
\eta H_\theta &= \sum_{\nu>0} \left[ \sum_{m0}^{\infty} \cos m\phi - i \sum_{m\epsilon}^{\infty} \sin m\phi \right] \Gamma_\nu^m j_\nu(\sigma) \frac{m M_\nu^m}{\sin \theta} \\
&\quad + \sum_{\nu>0} \left[ \sum_{m0}^{\infty} \cos m\phi - i \sum_{m\epsilon}^{\infty} \sin m\phi \right] \Lambda_\nu^m j_\nu(\sigma) \frac{dL_\nu^m}{d\theta}
\end{aligned}$$

As was the case for transmission, in the limit as  $b$  goes to zero the only nonzero terms just off the  $r = b$  surface are the TEM components of  $E_\theta$  and  $H_\phi$ . The TEM fields guide the energy through the interior region. Repeating the procedure of Eq. 2.9.6, evaluate the integral using Eq. 2.17.2:

$$\int_{-\psi}^{\psi} d\theta H_\phi \Big|_{m=0}$$

The result is the algebraic equation:

$$\frac{V(a)}{a} = \frac{2\lambda G}{Y_R(a)} \sum_{\ell} D_{\ell}^0(j_{\ell} + \beta_{\ell}^0 h_{\ell}) \quad (2.17.3)$$

## 2.18 Boundary Conditions

Several boundary conditions have been built into field Eqs. 2.14.2 and 2.14.3: Rotational symmetry requires  $m$  to be an integer and regularity of the zenith angle functions on the exterior axes,  $r > a$ , requires integer order Legendre functions of the first kind. The limiting condition as the radius becomes infinite requires spherical Hankel functions of the second kind. In the interior, regularity of the functions at  $r = b$  requires the



coefficients of all negative order Bessel functions to be zero. The boundary conditions still to be applied are:

1. Interior region,  $b < r < a$ ,  $\theta = \psi$  and  $\theta = \pi - \psi$

On the cone arms the tangential components of the electric field intensity,  $E_r$  and  $E_\phi$ , and the normal component of the magnetic field intensity,  $H_\theta$ , are zero.

2. Exterior region,  $r = a$ ,  $\theta < \psi$  and  $\theta > \pi - \psi$ .

The tangential components of the electric field intensity,  $E_\theta$  and  $E_\phi$ , and the normal component of the magnetic field intensity,  $H_r$ , are zero.

3. Boundary,  $r = a$ ,  $\psi < \theta < \pi - \psi$

All fields are continuous through the virtual interface between internal and external regions.

To satisfy the first boundary condition, note that the tangential component of the electric field and the normal component of the magnetic field are equal to zero at the surface of the cone. From Eqs. 2.17.2, the sums are equal to zero for all interior radii only if:

$$M_v^m(\cos \psi) = 0 \quad \text{and} \quad dL_v^m(\cos \theta) / d\theta \big|_{\theta=\psi} = 0 \quad (2.18.1)$$

For each degree, an infinite number of orders satisfy Eq. 2.18.1. Figure 2.7.1 includes plots of the first few values of  $v$  and  $\psi$  for functions with  $m = 1$  that satisfy these boundary conditions. In the limit as  $\psi$  approaches zero the first solutions for the odd and even functions occur respectively at  $v = 2$  and  $3$ .

To satisfy the second boundary condition from Eq. 2.14.3 it is necessary that:

$$\begin{aligned} \theta < \psi \quad \text{and} \quad \theta > \pi - \psi \\ E_\theta(ka, \theta, \phi) = 0 \quad \text{and} \quad E_\phi(ka, \theta, \phi) = 0 \end{aligned} \quad (2.18.2)$$

To satisfy the third boundary condition, with  $\delta$  a vanishingly small positive number, it is necessary that:

$$\psi < \theta < \pi - \psi$$

$$E(ka - \delta, \theta, \phi) = E(ka + \delta, \theta, \phi) \quad (2.18.3)$$

$$H(ka - \delta, \theta, \phi) = H(ka + \delta, \theta, \phi)$$

The fields on the left side of Eq. 2.18.3 are those of Eqs. 2.17.2. The fields on the right side of Eq. 2.18.3 are the sum of Eqs. 2.14.1, 2.14.2, and 2.14.3.

Desired algebraic equations are most easily obtained using the second and third boundary conditions to construct the four integral equalities of Eqs. 2.18.4 through 2.18.7. In addition to these four equalities, the process is to be repeated with a similar set of integral equations after replacing  $\sin m\phi$  by  $\cos m\phi$  and  $\cos m\phi$  by  $-\sin m\phi$ . Although the zenith angle limits on both integrals would be  $\psi$  to  $\pi - \psi$  the second boundary condition permits changing the limits to 0 to  $\pi$  for the electric field components.

$$\begin{aligned} & \int_{\psi}^{\pi-\psi} \sin \theta d\theta \int_0^{2\pi} d\phi \left\{ E_{\theta} \frac{dP_{\ell}^m}{d\theta} \cos(m\phi) - E_{\phi} \frac{mP_{\ell}^m}{\sin \theta} \sin(m\phi) \right\} \Bigg|_{\sigma=ka-\delta} \\ &= \int_0^{\pi} \sin \theta d\theta \int_0^{2\pi} d\phi \left\{ E_{\theta} \frac{dP_{\ell}^m}{d\theta} \cos(m\phi) - E_{\phi} \frac{mP_{\ell}^m}{\sin \theta} \sin(m\phi) \right\} \Bigg|_{\sigma=ka+\delta} \end{aligned} \quad (2.18.4)$$

$$\begin{aligned} & \int_{\psi}^{\pi-\psi} \sin \theta d\theta \int_0^{2\pi} d\phi \left\{ H_{\phi} \frac{dM_{\nu}^m}{d\theta} \cos(m\phi) + H_{\theta} \frac{mM_{\nu}^m}{\sin \theta} \sin(m\phi) \right\} \Bigg|_{\sigma=ka-\delta} \\ &= \int_{\psi}^{\pi-\psi} \sin \theta d\theta \int_0^{2\pi} d\phi \left\{ H_{\phi} \frac{dM_{\nu}^m}{d\theta} \cos(m\phi) + H_{\theta} \frac{mM_{\nu}^m}{\sin \theta} \sin(m\phi) \right\} \Bigg|_{\sigma=ka+\delta} \end{aligned} \quad (2.18.5)$$

$$\begin{aligned} & \int_{\psi}^{\pi-\psi} \sin \theta d\theta \int_0^{2\pi} d\phi \left\{ E_{\theta} \frac{mP_{\ell}^m}{\sin \theta} \cos(m\phi) - E_{\phi} \frac{dP_{\ell}^m}{d\theta} \sin m\phi \right\} \Bigg|_{\sigma=ka-\delta} \\ &= \int_0^{\pi} \sin \theta d\theta \int_0^{2\pi} d\phi \left\{ E_{\theta} \frac{mP_{\ell}^m}{\sin \theta} \cos(m\phi) - E_{\phi} \frac{dP_{\ell}^m}{d\theta} \sin m\phi \right\} \Bigg|_{\sigma=ka+\delta} \end{aligned} \quad (2.18.6)$$

$$\begin{aligned}
& \int_{\psi}^{\pi-\psi} \sin\theta d\theta \int_0^{2\pi} d\theta \left\{ H_{\phi} \frac{mL_v^m}{\sin\theta} \cos(m\phi) + H_{\theta} \frac{dL_v^m}{d\theta} \sin(m\phi) \right\}_{\sigma=ka-\delta} \\
& = \int_{\psi}^{\pi-\psi} \sin\theta d\theta \int_0^{2\pi} d\theta \left\{ H_{\phi} \frac{mL_v^m}{\sin\theta} \cos(m\phi) + H_{\theta} \frac{dL_v^m}{d\theta} \sin(m\phi) \right\}_{\sigma=ka+\delta}
\end{aligned} \quad (2.18.7)$$

Carrying out the integral operations of Eqs. 2.18.4 through 2.18.7 with the similar set obtained by replacing  $\sin m\phi$  by  $\cos m\phi$  and  $\cos m\phi$  by  $-\sin m\phi$  results in the four linear equations:

$$\begin{aligned}
& \ell(\ell+1)j_{\ell}^{\bullet}F_{\ell}^m I_{\ell\ell} + \ell(\ell+1)\beta_{\ell}^m h_{\ell}^{\bullet}F_{\ell}^m I_{\ell\ell} \\
& = \ell(\ell+1) \sum_{\nu_0}^{\infty} \Gamma_{\nu}^m j_{\nu}^{\bullet} K_{\ell\nu} - \frac{\eta G V(a)}{\pi a} P_{\ell} \delta(m, 0) + 2m P_{\ell}^m \sum_{\rho}^{\infty} \Lambda_{\rho}^m j_{\rho} L_{\rho}^m
\end{aligned} \quad (2.18.8)$$

$$\nu(\nu+1)\Gamma_{\nu}^m j_{\nu} K_{\nu\nu} = \sum_n^{\infty} n(n+1)F_n^m j_n K_{n\nu} + \sum_n^{\infty} n(n+1)F_n^m \beta_n^m h_n K_{n\nu} \quad (2.18.9)$$

$$\ell(\ell+1)G_{\ell}^m j_{\ell} I_{\ell\ell} + \ell(\ell+1)G_{\ell}^m \alpha_{\ell}^m h_{\ell} I_{\ell\ell} = \sum_{\rho}^{\infty} \rho(\rho+1)\Lambda_{\rho}^m j_{\rho} I_{\ell\rho} \quad (2.18.10)$$

$$\begin{aligned}
\rho(\rho+1)\Lambda_{\rho}^m j_{\rho}^{\bullet} I_{\rho\rho} & = \rho(\rho+1) \sum_r^{\infty} G_r^m j_r^{\bullet} I_{r\rho} + \rho(\rho+1) \sum_r^{\infty} G_r^m \alpha_r^m h_r^{\bullet} I_{r\rho} \\
& - 2m L_{\rho}^m \sum_n^{\infty} F_n^m j_n P_n^m - 2m L_{\rho}^m \sum_n^{\infty} F_n^m \beta_n^m h_n P_n^m
\end{aligned} \quad (2.18.11)$$

All but five terms are known in Eq. 2.18.8 - 2.18.11:  $V(a)$ ,  $\alpha_{\ell}^m$ ,  $\beta_{\ell}^m$ ,  $\Lambda_{\rho}^m$ , and  $\Gamma_{\nu}^m$ . Problem solution requires evaluation of each of them. With transmission there were but three unknowns:  $Y_T(a)$ ,  $\beta_{\ell}$ , and  $\Gamma_{\nu}$ .

## 2.19 Zero Degree Solution

Since only the zero degree modes carry absorbed power, as discussed in Sec. 2.7 it is convenient to analyze them first. Equation 2.17.3 and the  $m = 0$  portion of Eqs. 2.18.8 through 2.18.11 are

$$\begin{aligned} \frac{V(a)}{a} &= \frac{2\pi G}{Y_R(a)} \sum_{n0} F_n^0 (j_n + \beta_n^0 h_n) \\ \ell(\ell+1)F_\ell^0 \beta_\ell^0 h_\ell^* I_{\ell\ell} &= -\ell(\ell+1)F_\ell^0 j_\ell^* I_{\ell\ell} - \frac{\eta G V(a)}{\pi a} P_\ell + \ell(\ell+1) \sum_v \Gamma_v j_v^* K_{\ell v} \\ v(v+1)\Gamma_v j_v K_{vv} &= \sum_{n0} n(n+1)F_n^0 j_n K_{nv} + \sum_{n0} n(n+1)F_n^0 \beta_n^0 h_n K_{nv} \end{aligned} \quad (2.19.1)$$

The transmitter coefficients  $\beta_\ell$  and the receiver products  $F_\ell^0 \beta_\ell^0$  play similar roles: both sets of coefficients multiply TM fields that emanate from the antenna. Although Eq. 2.19.1 and Eqs. 2.9.1 to 2.9.3 are similar in form, a different approach to problem solution is helpful.

A case of special interest is an equated load. For this case, the receiver antenna load impedance equals the input impedance the transmitter antenna applies to incoming power. To analyze the case, adjust the driving field so  $V(0) = a$ . The antenna parameters given in Eqs. 2.19.1 are then the same as those of the transmitter case of Eqs. 2.9.1 to 2.9.3. Since identical equations give identical solutions:

$$\frac{\beta_\ell h_\ell}{F_\ell^0} = j_\ell + \beta_\ell^0 h_\ell \quad (2.19.2)$$

Equation 2.19.2 shows that the relative phases and magnitudes of the transmitted and scattered fields per mode,  $\ell$ , are not the same. Several coefficient values are tabulated in Table 2.19.3. Values are calculated using the numerical results of Table 2.9.1 and Eq. 2.19.2 for the special case  $Y_R(a) = Y_T(a)$ ,  $ka = 2$ ,  $\psi = 5^\circ$ , and  $V(0) = a$ .

$\ell$	real part, $\beta_\ell^0$	imaginary part, $\beta_\ell^0$	$\times$ order of magnitude
1	-1.0073	+0.15175	1
3	-1.3064	-0.14110	$10^{-2}$
5	-5.4652	-1.5762	$10^{-3}$
7	-1.1887	-3.4642	$10^{-5}$

Table 2.19.1 Values of  $\beta_\ell^0$  for the special case of an equated load,  $ka = 2$ ,  $\psi = 5^\circ$ , and  $V(0) = a$

Comparison of the transmitting and receiving equations shows that

$$\Gamma_V^0 = \Gamma_V \quad (2.19.3)$$

That is, the internal field coefficients for the two cases are the same. Equations 2.19.2 and 2.19.3 contrast the relationships between the transmission and reception coefficients. Comparing Eqs. 2.9.6 and 2.19.1 shows that the termination admittances  $Y(a)$  for the two cases are identical. Equation 2.6.16 translates the admittance  $Y(r)$  to the terminals and confirms that the terminal impedances of the antenna as a transmitter and as a receiver are identical.

$$Y_R(0) = Y_T(0) \quad (2.19.4)$$

For an arbitrary but known load impedance, the solution procedure is to use Eq. 2.6.17 to solve for  $Y(a)$  then combine with Eqs. 2.19.1 to 2.19.3 to obtain the linear equation

$$\beta_\ell^0 h_\ell = \frac{h_\ell}{F_\ell^0 h_\ell^* I_{\ell\ell}} \left\{ -F_\ell^0 j_\ell^* I_{\ell\ell} - \frac{2\eta \kappa G^2 P_\ell}{\pi \ell(\ell+1) Y_R(a)} \sum_{n=0}^{\infty} F_n^0 j_n + \sum_v \sum_{n=0}^{\infty} F_n^0 \frac{n(n+1) j_v^* j_n K_{\ell v} K_{nv}}{v(v+1) j_v K_{vv}} \right. \\ \left. - \frac{2\eta \kappa G^2 P_\ell}{\pi \ell(\ell+1) Y_R(a)} \sum_{n=0}^{\infty} F_n^0 \beta_n^0 h_n + \sum_v \sum_{n=0}^{\infty} F_n^0 \frac{n(n+1) j_v^* K_{\ell v} K_{nv}}{v(v+1) j_v K_{vv}} \beta_n^0 h_n \right\} \quad (2.19.5)$$

Symbols  $I_{\ell\ell}$  and  $K_{\ell v}$  *et al.* represent integrals listed in Tables A.22.1 and A.23.1. The equation form is the same as Eq. 2.9.5, and the solution technique is the same. Since all terms in Eq. 2.19.5 are known except  $\beta_\ell^0$  it may be solved first for  $\beta_\ell^0 h_\ell$  and then for  $\beta_\ell^0$ . Once the  $\beta_\ell^0$  are known, Eq. 2.19.1 may be used to solve for  $V(a)$ . The value of  $\Gamma_v^0$  may be obtained using Eq. 2.19.3. The zero degree solution is then complete.

## 2.20 Non-Zero Degree Solutions

To find the solution for  $m > 0$  solve for the exterior field parameters  $\alpha_\ell^m$  and  $\beta_\ell^m$  using Eqs. 2.18.8 through 2.18.11. This is most easily done by rewriting them in the forms:

$$(\beta_\ell^m h_\ell) = \frac{h_\ell}{\ell(\ell+1)h_\ell^* F_\ell^m I_{\ell\ell}} \left\{ \begin{aligned} & -\ell(\ell+1)F_\ell^m j_\ell^* I_{\ell\ell} + \ell(\ell+1) \sum_v \sum_n F_n^m \frac{n(n+1)j_n j_v^* K_{nv} K_{lv}}{\sqrt{(v+1)}j_v K_{vv}} \\ & 2mP_\ell^m \sum_\rho \sum_r G_r^m \frac{j_\rho j_r^* L_\rho^m I_{\rho\ell}}{j_\rho^* I_{\rho\rho}} - 4m^2 P_\ell^m \sum_\rho \sum_n F_n^m \frac{j_\rho j_n (L_\rho^m)^2 P_n^m}{\rho(\rho+1)j_\rho^* I_{\rho\rho}} \\ & + 2mP_\ell^m \sum_\rho \sum_r G_r^m \frac{j_\rho h_r^* L_\rho^m I_{\rho\ell}}{j_\rho^* h_r I_{\rho\rho}} (\alpha_r^m h_r) - 4m^2 P_\ell^m \sum_\rho \sum_n F_n^m \frac{j_\rho (L_\rho^m)^2 P_n^m}{\rho(\rho+1)j_\rho^* I_{\rho\rho}} (\beta_n^m h_n) \\ & + \ell(\ell+1) \sum_v \sum_n F_n^m \frac{n(n+1)j_v^* K_{nv} K_{lv}}{\sqrt{(v+1)}j_v K_{vv}} (\beta_n^m h_n) \end{aligned} \right\} \quad (2.20.1)$$

$$(\alpha_\ell^m h_\ell) = \frac{1}{\ell(\ell+1)G_\ell^m I_{\ell\ell}} \left\{ \begin{aligned} & -\ell(\ell+1)G_\ell^m j_\ell I_{\ell\ell} + \sum_\rho \sum_r G_r^m \frac{\rho(\rho+1)j_\rho j_r^* I_{\rho\ell} I_{\ell\rho}}{j_\rho^* I_{\rho\rho}} \\ & - 2m \sum_\rho \sum_n F_n^m \frac{j_\rho j_n I_{\ell\rho} L_\rho^m P_n^m}{j_\rho^* I_{\rho\rho}} \\ & \sum_\rho \sum_r G_r^m \frac{\rho(\rho+1)j_\rho h_r^* I_{\rho\ell} I_{\ell\rho}}{j_\rho^* h_r I_{\rho\rho}} (\alpha_r^m h_r) - 2m \sum_\rho \sum_n F_n^m \frac{j_\rho I_{\ell\rho} L_\rho^m P_n^m}{j_\rho^* I_{\rho\rho}} (\beta_n^m h_n) \end{aligned} \right\} \quad (2.20.2)$$

Equations 2.20.1 and 2.20.2 have the general algebraic form:

$$\begin{aligned}
 x_\ell + \sum_n^\infty N_{\ell n} x_n + \sum_r^\infty M_{\ell r} y_r &= B_\ell \\
 y_\ell + \sum_n^\infty S_{\ell n} x_n + \sum_r^\infty R_{\ell r} y_r &= A_\ell
 \end{aligned}
 \tag{2.20.3}$$

All needed integrals are listed in Tables A.22.1 and A.23.1 and all other parameters are known. The sums of Eq. 2.20.1 and 2.20.2 may be truncated and solved concurrently for coefficients  $\alpha_\ell^m$  and  $\beta_\ell^m$ , from which  $\Gamma_v^m$  and  $\Lambda_v^m$  follow directly. Knowledge of these four parameters provides the total solution of the fields around a receiving antenna.

Although the integral of products of Legendre functions of integer and noninteger orders,  $M_v(\cos\theta)P_\ell(\cos\theta)$  for example, are largest if  $v$  is nearly equal to  $\ell$ , none of them vanish. Therefore cross coupling exists between all modes of the same degree,  $m$ . Coupling between  $\alpha_\ell^m$  and  $\beta_\ell^m$  terms show that all modes, even and odd, of the same degree are coupled. That is, each TM mode interacts with all other TM and TE modes, and *vice versa*: Each value of  $\beta_\ell^m$  and  $\alpha_\ell^m$  depends both upon all values of  $\beta_\lambda^m$  and  $\alpha_\lambda^m$ , but are independent of  $\beta_\ell^p$  and  $\alpha_\ell^p$  for  $m \neq p$ .

Since for  $m = 0$  and  $\psi$  approaching zero the order approaches an integer value quite slowly, the integrals of cross modal terms remain significantly large, and, therefore, coupling is significantly large even for  $\psi$  near zero.

## 2.21 Surface Current Densities

A conducting boundary condition is that the surface current density,  $\tilde{\mathbf{I}}$ , in amperes per meter is related to the magnetic field adjacent to it by the vector-phasor relationship

$$\tilde{\mathbf{I}} = n \times \tilde{\mathbf{H}} \tag{2.21.1}$$

Unit vector  $n$  is normal to and outbound from the conductor. Knowledge of the field coefficients permits the calculation of all antenna currents. Figure 2.21.1 illustrates surface current patterns for the lowest order exterior

modes,  $(\ell, m) = (1, 0)$  and  $(1, 1)$  and the three lowest order interior ones, modes  $(\nu, m) = (0, 0)$ ,  $(1+, 0)$ , and  $(2+, 1)$ . The exact interior modal number depends upon the value of  $\psi$ : with  $5^\circ$  cones the modal numbers  $1+$  and  $2+$  are respectively 1.444 484 and 2.022 029. The figure depicts current patterns for a small antenna,  $a < \pi/4$ . A plane wave is incident from the left, with a  $z$ -directed electric field intensity. In the interior the TEM mode fields, see Eq. 2.7.1, are maximum at  $r = b$ . The current of mode  $(1+, 0)$  has rotational symmetry around the cones. The current of mode  $(2+, 1)$  is in phase with mode  $(1+, 0)$  on the front face and out of phase on the back face; it is equal to zero in between. Both are TM modes, both are zero at the origin, both are large near  $r = a$ , and both are zero at the sink. The current of mode  $(1+, 0)$  produces a  $z$ -directed electric dipole moment. The current of mode  $(2+, 1)$  produces a  $y$ -directed magnetic dipole mode, with a magnetic field phased according to Lenz's law. In the exterior, the currents of the two lowest modes,  $(1, 0)$  and  $(2, 1)$ , produce respectively TM and TE fields. The cap current density of mode  $(1, 0)$  is  $\theta$ -directed and zero at the center, and the current density of mode  $(2, 1)$  is  $x$ -directed and maximum at the center.

## 2.22 Power

The time average power on the surface of a virtual surface of radius  $\sigma/k$  that circumscribes the antenna is

$$P = \frac{\sigma^2}{k^2} \int_0^{2\pi} d\phi \int_0^\pi \sin\theta d\theta \operatorname{Re}(N_r) \quad (2.22.1)$$

For receiving antennas, the time average received power is equal to the negative of the real part of Eq. 2.22.1, after inserting the coefficients evaluated in Sections 2.19 and 2.20. The power and the cross sections were calculated in Sections 2.14 and 2.15. The normalized absorption cross section  $C_{AB}/C_{GE}$ , see Eq. 2.15.3, is:



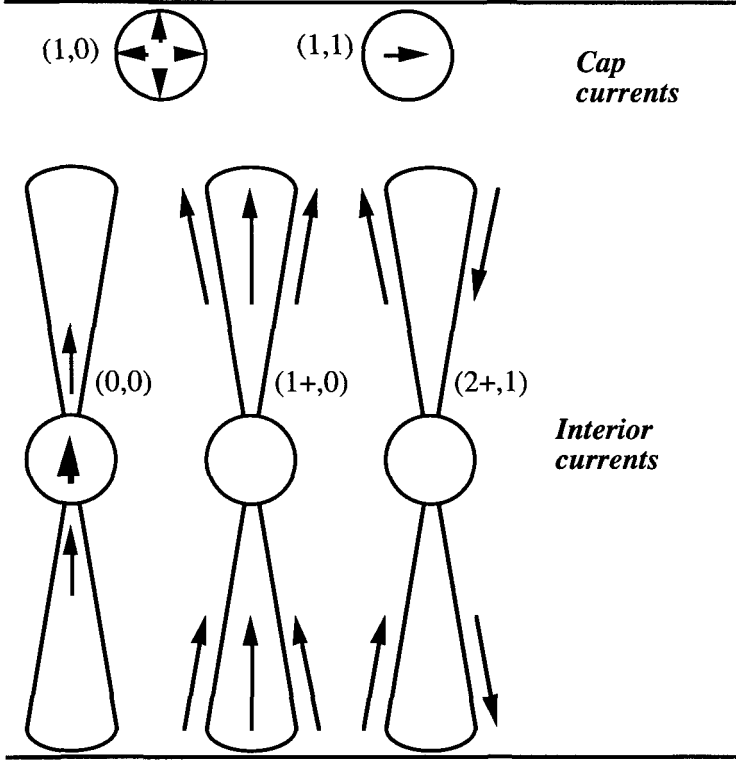


Figure 2.21.1 Receiving Modal Surface Currents, Wave Incoming from Left. In the interior region the  $(0,0)$  current is maximum and the  $(1+,0)$  and  $(2+,1)$  currents are zero at  $r = 0$ . The  $(1+,0)$  current is unidirectional and rotationally symmetric around the arms. The  $(2+,1)$  current is bi-directional, creating a magnetic moment directed in accordance with Lenz's law. In the exterior, the  $(1,0)$  cap currents are  $\theta$  directed, rotationally symmetric and zero at the midpoint. The  $(2,1)$  currents are  $x$ -directed with a maximum at the midpoints.

$$\frac{C_{AB}}{C_{GE}} = -\frac{4}{k^2 a^2} \left\{ \left[ \sum_{\ell=0}^{\infty} \sum_{m\ell}^{\ell-1} + \sum_{\ell=0}^{\infty} \sum_{m\ell}^{\ell-1} \right] \frac{(2\ell+1)(\ell-m)!!(\ell+m)!!}{\ell(\ell+1)(\ell-m-1)!!(\ell+m-1)!!} \left[ \text{Re}(\beta_{\ell}^m) + \beta_{\ell}^m \beta_{\ell}^{m*} \right] \right\} \\ - \frac{8}{k^2 a^2} \left\{ \left[ \sum_{\ell=0}^{\infty} \sum_{m\ell}^{\ell} + \sum_{\ell=0}^{\infty} \sum_{m\ell}^{\ell} \right] \frac{m^2 (2\ell+1)(\ell-m-1)!!(\ell+m-1)!!}{\ell(\ell+1)(\ell-m)!!(\ell+m)!!} \left[ \text{Re}(\alpha_{\ell}^m) + \alpha_{\ell}^m \alpha_{\ell}^{m*} \right] \right\} \quad (2.22.2)$$

As was shown for a sphere, Sections 2.2 and 2.3, the portion of Eq. 2.22.2 proportional to  $-\text{Re}(\alpha_\ell^m + \beta_\ell^m)$  represents the extinction power extracted from the wave, and the portion proportional to  $\alpha_\ell^m \alpha_\ell^{m*}$  and  $\beta_\ell^m \beta_\ell^{m*}$  represents power scattered away from the antenna. The sum, expressed by Eq. 2.22.2, is the power absorbed by the antenna.

The incoming wave transfers both momentum and energy to the antenna. Since the incoming plane wave is  $y$ -directed, linear momentum is transferred to the antenna in that direction. The force on the scatterer is related to the momentum transferred as:

$$F_y = \frac{d}{dt}(\text{linear momentum}) \quad (2.22.3)$$

The net force applied to the antenna follows from the rate of momentum absorption and scattering, and is equal to:

$$F_y = \frac{\sigma^2}{ck^2} \int_0^{2\pi} \sin\phi d\phi \int_0^\pi N_r \sin^2\theta d\theta \quad (2.22.4)$$

By Eq. 2.15.7 the normalized force due to the extinction power is:

$$\frac{cf_{\text{EX}}}{C_{\text{GE}}} = -\frac{8\epsilon}{k^2 a^2} \left\{ \left[ \sum_{\ell=0}^{\infty} \sum_{m\epsilon}^{\ell-1} + \sum_{\ell e}^{\infty} \sum_{m\epsilon}^{\ell-1} \right] \frac{U(m)(2\ell+1)(\ell-m)!!(\ell+m)!!}{\ell(\ell+1)(\ell-m-1)!!(\ell+m-1)!!} \text{Re}(\beta_\ell^m) \right\} \\ + \left[ \sum_{\ell=0}^{\infty} \sum_{m\epsilon}^{\ell} + \sum_{\ell e}^{\infty} \sum_{m\epsilon}^{\ell} \right] \frac{m^2(2\ell+1)(\ell-m-1)!!(\ell+m-1)!!}{\ell(\ell+1)(\ell-m)!!(\ell+m)!!} \text{Re}(\alpha_\ell^m) \right\} \quad (2.22.5)$$

By Eq. 2.15.6 the normalized scattering force is:

$$\frac{cf_{jSC}}{C_{GE}} = -\frac{4}{k^2 a^2} \left\{ \begin{aligned} & \left( \sum_{\ell o} \sum_{m e} + \sum_{\ell e} \sum_{m o} \right) \left( \left( \beta_{\ell}^m \beta_{\ell+1}^{m+1*} + \beta_{\ell}^{m*} \beta_{\ell+1}^{m+1} \right) \frac{U(m)(\ell-m)!!(\ell+m+2)!!}{(\ell+1)^2(\ell-m-1)!!(\ell+m-1)!!} \right. \\ & \quad \left. + \left( \beta_{\ell}^m \beta_{\ell-1}^{m+1*} + \beta_{\ell}^{m*} \beta_{\ell-1}^{m+1} \right) \frac{U(m)(\ell-m)!!(\ell+m)!!}{\ell^2(\ell-m-3)!!(\ell+m-1)!!} \right) \\ & + \left( \sum_{\ell o} \sum_{m o} + \sum_{\ell e} \sum_{m e} \right) \left( \left( \alpha_{\ell}^m \alpha_{\ell+1}^{m+1*} + \alpha_{\ell}^{m*} \alpha_{\ell+1}^{m+1} \right) \frac{m(m+1)(\ell-m-1)!!(\ell+m+1)!!}{(\ell+1)^2(\ell-m)!!(\ell+m)!!} \right. \\ & \quad \left. + \left( \alpha_{\ell}^m \alpha_{\ell-1}^{m+1*} + \alpha_{\ell}^{m*} \alpha_{\ell-1}^{m+1} \right) \frac{m(m+1)(\ell-m-1)!!(\ell+m+1)!!}{\ell^2(\ell-m-2)!!(\ell+m)!!} \right) \\ & + \left( \sum_{\ell o} \sum_{m e} + \sum_{\ell e} \sum_{m o} \right) \left( \alpha_{\ell}^{m+1*} \beta_{\ell}^m + \alpha_{\ell}^{m+1} \beta_{\ell}^{m*} \right) \left( \frac{(m+1)(2\ell+1)(\ell-m)!!(\ell+m)!!}{\ell^2(\ell+1)^2(\ell-m-1)!!(\ell+m-1)!!} \right) \\ & - \left( \sum_{\ell o} \sum_{m o} + \sum_{\ell e} \sum_{m e} \right) \left( \alpha_{\ell}^m \beta_{\ell}^{m+1*} + \alpha_{\ell}^{m*} \beta_{\ell}^{m+1} \right) \left( \frac{m(2\ell+1)(\ell-m-1)!!(\ell+m+1)!!}{\ell^2(\ell+1)^2(\ell-m-2)!!(\ell+m)!!} \right) \end{aligned} \right\} \quad (2.22.6)$$

For the special case  $m = 0$ , the scattering cross section and normalized force terms are:

$$\frac{C_{SC}}{C_{GE}} = \frac{4}{k^2 a^2} \sum_{\ell o}^{\infty} \frac{(2\ell+1)\ell!!^2}{\ell(\ell+1)[(\ell-1)!!]^2} \beta_{\ell}^0 \beta_{\ell}^{0*} \quad (2.22.7)$$

$$\frac{cf_{jSC}}{C_{GE}} = -\frac{2}{k^2 a^2} \sum_{\ell o} \left\{ \begin{aligned} & + \left( \beta_{\ell}^0 \beta_{\ell+1}^{1*} + \beta_{\ell}^{0*} \beta_{\ell+1}^1 \right) \frac{\ell!!(\ell+2)!!}{(\ell+1)^2[(\ell-1)!!]^2} \\ & + \left( \beta_{\ell}^0 \beta_{\ell-1}^{1*} + \beta_{\ell}^{0*} \beta_{\ell-1}^1 \right) \frac{\ell!!^2}{\ell^2(\ell-3)!!(\ell-1)!!} \\ & + \left( \alpha_{\ell}^{1*} \beta_{\ell}^0 + \alpha_{\ell}^1 \beta_{\ell}^{0*} \right) \frac{2(2\ell+1)\ell!!^2}{\ell^2(\ell+1)^2[(\ell-1)!!]^2} \end{aligned} \right\} \quad (2.22.8)$$

If the antenna is electrically small and only the dipole terms are significantly large, Eq. 2.22.8 shows that:

$$\frac{cf_{jSC}}{C_{GE}} = -\frac{3}{k^2 a^2} \left( \alpha_1^{1*} \beta_1^0 + \alpha_1^1 \beta_1^{0*} \right) \quad (2.22.9)$$

Although the energy density-to-linear momentum density in the incoming plane wave is  $c$ , as discussed in Section 2.3 the received energy-to-momentum ratio satisfies the relationship:

$$\frac{\text{Received Energy}}{\text{Received Momentum}} \leq c \quad (2.22.10)$$

This is in contrast with a transmitting antenna. When transmitting, power is radiated over a spread of angles and the average value of the cosine of the angle can never be greater than one. Therefore, the transmitted energy-to-momentum ratio obeys the relationship:

$$\frac{\text{Transmitted Energy}}{\text{Transmitted Momentum}} \geq c \quad (2.22.11)$$

## References

- D.M. Grimes, "Biconical Receiving Antennas," *J. Math. Phys.*, vol. 23, pp. 897-914 (1982)
- D.M. Grimes, C. A. Grimes, "Transmission and Reception of Power by Antennas," in T. W. Barrett, D. M. Grimes, *Advanced Electromagnetism: Foundations, Theory and Applications*, World Scientific Publishing (1995) pp. 763-791
- H. Hertz, *Electric Waves: Researches on the Propagation of Electric Action with Finite Velocity Through Space* (1893) Translated by D. E. Jones, Dover Publications (1962)
- G. Mie, "A Contribution to Optical Extinction by Metallic Colloidal Suspensions," *Ann. Physik.* vol. 25, p. 377 (1908)
- W.K.H. Panofsky, M. Phillips, *Classical Electricity and Magnetism*, 2<sup>nd</sup> ed., Addison-Wesley (1962)
- S.A. Schelkunoff, *Advanced Antenna Theory*, John Wiley (1952)
- S.A. Schelkunoff, *Applied Mathematics for Engineers and Scientists*, 2<sup>nd</sup> ed., Van Nostrand (1965)
- W.R. Smythe, *Static and Dynamic Electricity*, 3<sup>rd</sup> ed., McGraw-Hill (1968)
- H.C. Van de Hulst, *Light Scattering by Small Particles*, John Wiley (1957)

This page is intentionally left blank

### 3. Antenna Q

#### 3.1 Instantaneous and Complex Power in Circuits

It is commonplace to discuss power and energy in radiation fields using complex numbers. To make a critical examination of the procedure, since one-dimensional electrical circuits are simpler systems than three-dimensional electromagnetic fields, we begin with electrical circuits. Consider the time-varying power and energy of an electrical circuit that is driven by a sinusoidal, steady state source. With  $\chi$  and  $\zeta$  representing circuit-dependent phase constants, the input voltage and current to an electrical circuit are:

$$v(t) = V_0 \cos(\omega t - \chi) \quad \text{and} \quad i(t) = I_0 \cos(\omega t - \zeta) \quad (3.1.1)$$

With this notation, either  $V_0$  or  $I_0$  can be the independent variable with the other being the dependent variable. Both are real, time-independent quantities. The power at the terminals follows from the force laws, and is the simple product:

$$\begin{aligned} p(t) &= v(t)i(t) \\ &= \frac{1}{2} V_0 I_0 \{ \cos(\zeta - \chi) + \cos(\zeta + \chi) \cos(2\omega t) + \sin(\zeta + \chi) \sin(2\omega t) \} \end{aligned} \quad (3.1.2)$$

Trigonometric identities may be used to transform Eq. 3.1.2 into the more useful form:

$$p(t) = \frac{1}{2} V_0 I_0 \{ \cos(\zeta - \chi) [1 + \cos(2\omega t - 2\xi)] + \sin(\zeta - \chi) \sin(2\omega t - 2\xi) \} \quad (3.1.3)$$

Although either a plus or minus sign could be placed in front of the  $\sin(\zeta-\chi)$  term, a positive sign is convenient and leads to no loss of generality.

It follows from Eq. 3.1.3 that the three numbers needed to characterize the power are the product  $V_0 I_0$ , the phase difference  $(\zeta-\chi)$ , and the phase angle  $\xi$ . The equation also shows that the term proportional to  $\cos(\zeta-\chi)[1+\cos(2\omega t-2\xi)]$  is zero twice each field cycle, it is never negative, and it describes the time average energy flow into the circuit. The term proportional to  $\sin(\zeta-\chi)\sin(2\omega t-2\xi)$  is in time-quadrature with the first term and changes sign twice each power cycle; it describes the lossless, oscillatory energy flow between the circuit and the energy source and is not associated with a time average energy flow. In many cases, instantaneous phase  $\xi$  is irrelevant and appears only as unwanted clutter. For such cases, the quantities  $\zeta-\chi$  and  $V_0 I_0$  determine the important properties of the power and no other information is either needed or desired. For such cases, phase factor  $\xi$  is suppressed and real power,  $p_r(t)$ , and reactive power,  $p_x(t)$ , are defined by the equations:

$$\begin{aligned} p_r(t) &= \frac{1}{2} V_0 I_0 \cos(\zeta - \chi) [1 + \cos(2\omega t)] \\ p_x(t) &= \frac{1}{2} V_0 I_0 \sin(\zeta - \chi) \sin(2\omega t) \end{aligned} \quad (3.1.4)$$

Since only two pieces of information are included and since complex numbers have two places available to carry information, this power may be conveniently described by complex numbers.

To restate the same physical situation using complex numbers, write the input voltage and current in phasor form:

$$V(t) = V_0 e^{j(\omega t - \chi)} \quad I(t) = I_0 e^{j(\omega t - \zeta)} \quad (3.1.5)$$

Equations 3.1.5 differ from Eqs. 3.1.1 in that virtual terms, the imaginary parts of Eqs. 3.1.5, have been added to the phase of each variable. The real parts of Eqs. 3.1.5 are equal to the actual values of Eqs. 3.1.1. Equations 3.1.5 are used to form the product:

$$P_c = \frac{1}{2} V(t) I(t)^* \quad (3.1.6)$$

The real part,  $P_r$ , and imaginary part,  $P_i$ , of Eq. 3.1.6 are:

$$\begin{aligned} P_c &= P_r + iP_i = \frac{1}{2} V_0 I_0 e^{i(\zeta - \chi)} \\ &= \frac{1}{2} V_0 I_0 [\cos(\zeta - \chi) + i \sin(\zeta - \chi)] \end{aligned} \quad (3.1.7)$$

Comparison of Eq. 3.1.3 with Eq. 3.1.7 shows that the latter contains all information except the suppressed phase factor. The real part is equal to the magnitude of the time-average input power and the imaginary part is equal to the magnitude of the oscillating power. In this case, both real and imaginary parts of the power represent actual quantities. The phase-quadrature difference between real and reactive powers is indicated by an “ $i$ ” in Eq. 3.1.7. Equations 3.1.4 and 3.1.7 are but different notations for the same physics. Neither contains information about phase angle  $\xi$ .

By definition the Thévenin circuit input impedance elements are

$$R = \frac{V_0}{I_0} \cos(\zeta - \chi) \quad \text{and} \quad X = \frac{V_0}{I_0} \sin(\zeta - \chi) \quad (3.1.8)$$

Combining Eqs. 3.1.7 and 3.1.8 shows that the complex power may be expressed as:

$$P_c = \frac{1}{2} I_0 I_0^* (R + iX) \quad (3.1.9)$$

With Eq. 3.1.9,  $I_0$  has been modified to a complex number that includes factor  $\exp(-i\zeta)$ .

Consider next the case of two isolated electrical circuits. It is easy to show that the total power is the simple sum of the power in each circuit, as described by Eqs. 3.1.2. The sum is:



$$\begin{aligned}
 p(t) &= \sum_{k=1}^2 v_k(t) i_k(t) \\
 &= \frac{1}{2} \sum_{k=1}^2 V_k I_k \{ \cos(\zeta_k - \chi_k) + \cos(\zeta_k + \chi_k) \cos(2\omega t) + \sin(\zeta_k + \chi_k) \sin(2\omega t) \}
 \end{aligned}
 \tag{3.1.10}$$

To learn how to express the information contained in Eq. 3.1.10 using complex notation begin by rewriting it in a form similar to that of Eq. 3.1.3:

$$p(t) = \frac{1}{2} \sum_{k=1}^2 [V_k I_k \cos(\zeta_k - \chi_k)] [1 + \cos(2\omega t - \xi)] + K_{12} \sin(2\omega t - \xi)
 \tag{3.1.11}$$

Insisting that Eqs. 3.1.10 and 3.1.11 be identical and solving for  $K_{12}$  results in the equality:

$$\begin{aligned}
 K_{12}^2 &= V_1^2 I_1^2 \sin^2(\zeta_1 - \chi_1) + V_2^2 I_2^2 \sin^2(\zeta_2 - \chi_2) \\
 &\quad + 2V_1 V_2 [-\sin(\chi_1 - \chi_2) \sin(\zeta_1 - \zeta_2) + \sin(\zeta_1 - \chi_2) \sin(\zeta_2 - \chi_1)]
 \end{aligned}
 \tag{3.1.12}$$

Consider the special case where one of the two equalities apply:

$$\zeta_1 = \zeta_2 \quad \text{or} \quad \chi_1 = \chi_2
 \tag{3.1.13}$$

For either case, Eq. 3.1.12 simplifies to:

$$K_{12} = V_1 I_1 \sin(\zeta_1 - \chi_1) + V_2 I_2 \sin(\zeta_2 - \chi_2)
 \tag{3.1.14}$$

Combining Eqs. 3.1.14 with Eq. 3.1.11 shows that:

$$p(t) = \frac{1}{2} \sum_{k=1}^2 V_k I_k \{ \cos(\zeta_k - \chi_k) [1 + \cos(2\omega t - \xi)] + \sin(\zeta_k - \chi_k) \sin(2\omega t - \xi) \}
 \tag{3.1.15}$$

According to Eq. 3.1.15 if either of the two conditions of Eq. 3.1.13 is met the powers of the two circuits combine by simple addition. Within interconnected electric circuits, the Kirchhoff circuit laws assure that one of the conditions of Eq. 3.1.13 is met, either between circuit nodes or along circuit branches. For these special cases, the complex power is the simple sum over the power of the different circuit elements:

$$P_c = \frac{1}{2} \sum_k V_k I_k e^{j(\zeta_k - \chi_k)} \quad (3.1.16)$$

As we shall see, different modes of multimodal radiation fields do not meet the conditions of Eq. 3.1.13 and therefore Eq. 3.1.16 does not apply.

## 3.2 Instantaneous and Complex Power in Fields

To analyze power and energy about an antenna it is enough to consider only antennas with rotational symmetry about the  $z$ -axis. With this choice the field solutions are of degree zero and there is no dependence on the azimuth angle. Since, as will be shown, the essential points of interest depend only upon the radial field functions, and since the radial field functions are independent of degree, results are general and apply to a full multipolar expansion. Written in phasor form, but keeping the retarded time phase dependence, in terms of the letter functions of Appendix A.26, the general form of the field expansion terms, Eq. 1.12.9, is:

$$\begin{aligned} \sigma^2 \tilde{E}_r &= \sum_{\ell=1}^{\infty} F_{\ell} \ell (\ell+1) [B_{\ell}(\sigma) + iA_{\ell}(\sigma)] P_{\ell}(\cos \theta) e^{-i\sigma} \\ \sigma^2 \eta \tilde{H}_r &= - \sum_{\ell=1}^{\infty} G_{\ell} \ell (\ell+1) [B_{\ell}(\sigma) + iA_{\ell}(\sigma)] P_{\ell}(\cos \theta) e^{-i\sigma} \\ \sigma \hat{E}_{\theta} &= \sum_{\ell=1}^{\infty} F_{\ell} [D_{\ell}(\sigma) + iC_{\ell}(\sigma)] \frac{dP_{\ell}(\cos \theta)}{d\theta} e^{-i\sigma} \\ \sigma \eta \hat{H}_{\phi} &= \sum_{\ell=1}^{\infty} F_{\ell} [A_{\ell}(\sigma) - iB_{\ell}(\sigma)] \frac{dP_{\ell}(\cos \theta)}{d\theta} e^{-i\sigma} \end{aligned} \quad (3.2.1)$$

$$\sigma \tilde{E}_\phi = \sum_{\ell=1}^{\infty} G_\ell [A_\ell(\sigma) - iB_\ell(\sigma)] \frac{dP_\ell(\cos\theta)}{d\theta} e^{-i\sigma}$$

$$\sigma \eta \tilde{H}_\theta = - \sum_{\ell=1}^{\infty} G_\ell [D_\ell(\sigma) + iC_\ell(\sigma)] \frac{dP_\ell(\cos\theta)}{d\theta} e^{-i\sigma}$$

Every possible radiating antenna field with rotational symmetry about the  $z$ -axis may be fully described by picking appropriate choices of multiplying coefficients  $F_\ell$  and  $G_\ell$ .

After making use of Eq. 3.2.1 and Table A.22.1.6, the surface integral of the complex Poynting vector evaluated on a circumscribing, spherical surface of radius  $\sigma/k$  is:

$$P_c(\sigma) = \oint N_c \cdot d\mathbf{S} = \frac{\pi}{\eta k^2} \sum_{\ell=1}^{\infty} \frac{\ell(\ell+1)}{(2\ell+1)} \left\{ \begin{aligned} & \left( F_\ell F_\ell^* + G_\ell G_\ell^* \right) [A_\ell(\sigma) D_\ell(\sigma) - B_\ell(\sigma) C_\ell(\sigma)] \\ & + i \left( F_\ell F_\ell^* - G_\ell G_\ell^* \right) [A_\ell(\sigma) C_\ell(\sigma) + B_\ell(\sigma) D_\ell(\sigma)] \end{aligned} \right\} \quad (3.2.2)$$

The absence of cross product terms between TM and TE modes shows that the two modal types act independently. The sign of the imaginary term depends upon whether the field is TE or TM; if both are present and of equal magnitude the net is zero. Since each modal coefficient is multiplied by its own complex conjugate, a phase difference between sources has no affect and all modal phase factors are suppressed.

Examination of Eq. 3.2.2 shows that the two numbers needed to evaluate the modal power are weighted sums over  $(A_\ell D_\ell - B_\ell C_\ell)$  and  $(A_\ell C_\ell + B_\ell D_\ell)$ . By Table A.26.2.8,  $(A_\ell D_\ell - B_\ell C_\ell)$  is equal to one for all orders. The second term is defined to be:

$$\gamma_\ell(\sigma) = A_\ell(\sigma) C_\ell(\sigma) + B_\ell(\sigma) D_\ell(\sigma) \quad (3.2.3)$$

Values of  $\gamma_\ell(\sigma)$  are listed in Table 3.2.1.

Table 3.2.1 shows that the magnitude of  $\gamma_\ell(\sigma)$  increases precipitously with small and decreasing values of  $\sigma$  and with increasing modal number  $\ell$ . All signs in Table 3.2.1 are the same and  $\gamma_\ell(\sigma)$  is a monotone decreasing

function of  $\sigma$ . Taking  $\gamma_\ell(\sigma)$  as a measure of reactive power, the surface reactance has the same sign for all radii: capacitive for TM modes and inductive for TE modes. This is in marked contrast with the numerical analysis of center-driven biconical antennas where the sign of the reactance of a TM antenna at the input terminals is primarily a function of normalized cone length. This emphasizes, see Fig. 2.9.1, that changes in the sign of the input reactance versus antenna radius for TM sources are due to the transmission line character of the antenna arms and not to intrinsic properties of the radiating surface.

---

$\gamma_1(\sigma) = -\frac{1}{\sigma^3}$
$\gamma_2(\sigma) = -\frac{18}{\sigma^5} - \frac{3}{\sigma^3}$
$\gamma_3(\sigma) = -\frac{675}{\sigma^7} - \frac{90}{\sigma^5} - \frac{6}{\sigma^3}$
$\gamma_4(\sigma) = -\frac{44100}{\sigma^9} - \frac{4725}{\sigma^7} - \frac{270}{\sigma^5} - \frac{10}{\sigma^3}$
$\gamma_5(\sigma) = -\frac{4465125}{\sigma^{11}} - \frac{396900}{\sigma^9} - \frac{18900}{\sigma^7} - \frac{630}{\sigma^5} - \frac{15}{\sigma^3}$
$\gamma_6(\sigma) = -\frac{648,336,150}{\sigma^{13}} - \frac{49,116,375}{\sigma^{11}} - \frac{1984500}{\sigma^9} - \frac{56700}{\sigma^7} - \frac{1260}{\sigma^5} - \frac{21}{\sigma^3}$

---

Table 3.2.1 Radial Dependence of  $\gamma_\ell(\sigma)$

### 3.3 Time Varying Power in Actual Radiation Fields

The actual fields, from which the phasor fields of Eqs. 3.2.1 follow, are listed in Eq. 3.3.1. The driving source varies with time as  $\cos(\omega t)$ . If the constant coefficients of Eqs. 3.2.1 are entirely real or entirely imaginary, respectively the upper or lower set of terms within the square brackets in each field component of Eq. 3.3.1 applies. Although the absolute phases of the elements are not important to our results, the phase differences between modes are. Since by proper adjustment of the time origin all phase

relationships are expressible as sums over the upper and lower terms results of analyzing this set of field equations are general.

$$\begin{aligned}
 \sigma^2 E_r &= \sum_{\ell=1}^{\infty} F_{\ell} \ell(\ell+1) \begin{bmatrix} B_{\ell} \cos(\omega t_R) - A_{\ell} \sin(\omega t_R) \\ A_{\ell} \cos(\omega t_R) + B_{\ell} \sin(\omega t_R) \end{bmatrix} P_{\ell}(\cos \theta) \\
 \sigma^2 \eta H_r &= - \sum_{\ell=1}^{\infty} G_{\ell} \ell(\ell+1) \begin{bmatrix} B_{\ell} \cos(\omega t_R) - A_{\ell} \sin(\omega t_R) \\ A_{\ell} \cos(\omega t_R) + B_{\ell} \sin(\omega t_R) \end{bmatrix} P_{\ell}(\cos \theta) \\
 \sigma E_{\theta} &= \sum_{\ell=1}^{\infty} F_{\ell} \begin{bmatrix} D_{\ell} \cos(\omega t_R) - C_{\ell} \sin(\omega t_R) \\ C_{\ell} \cos(\omega t_R) + D_{\ell} \sin(\omega t_R) \end{bmatrix} \frac{dP_{\ell}(\cos \theta)}{d\theta} \\
 \sigma \eta H_{\phi} &= \sum_{\ell=1}^{\infty} F_{\ell} \begin{bmatrix} A_{\ell} \cos(\omega t_R) + B_{\ell} \sin(\omega t_R) \\ -B_{\ell} \cos(\omega t_R) + A_{\ell} \sin(\omega t_R) \end{bmatrix} \frac{dP_{\ell}(\cos \theta)}{d\theta} \\
 \sigma E_{\phi} &= \sum_{\ell=1}^{\infty} G_{\ell} \begin{bmatrix} A_{\ell} \cos(\omega t_R) + B_{\ell} \sin(\omega t_R) \\ -B_{\ell} \cos(\omega t_R) + A_{\ell} \sin(\omega t_R) \end{bmatrix} \frac{dP_{\ell}(\cos \theta)}{d\theta} \\
 \sigma \eta H_{\theta} &= \sum_{\ell=1}^{\infty} G_{\ell} \begin{bmatrix} -D_{\ell} \cos(\omega t_R) + C_{\ell} \sin(\omega t_R) \\ -C_{\ell} \cos(\omega t_R) - D_{\ell} \sin(\omega t_R) \end{bmatrix} \frac{dP_{\ell}(\cos \theta)}{d\theta}
 \end{aligned} \tag{3.3.1}$$

Using Eqs. 3.3.1 to evaluate the radial component of the time-dependent Poynting vector then integrating over a constant radius surface centered at the origin gives the surface power:

$$p(\sigma, t_R) = \oint \mathbf{N} \cdot d\mathbf{S} = \frac{\pi}{\eta k^2} \sum_{\ell=1}^{\infty} \frac{\ell(\ell+1)}{(2\ell+1)} [F_{\ell}^2 + G_{\ell}^2] \left\{ A_{\ell} D_{\ell} [1 \pm \cos(2\omega t_R)] - B_{\ell} C_{\ell} [1 \mp \cos(2\omega t_R)] \right\} \left\{ \mp (A_{\ell} C_{\ell} - B_{\ell} D_{\ell}) \sin(2\omega t_R) \right\} \tag{3.3.2}$$

The upper or lower signs respectively apply to the upper or lower terms in the square brackets of Eqs. 3.3.1. The sign choice depends upon the phase of the modes but does not depend upon the TM or TE character of the modes. Hence, in contrast with results obtained using phasor fields, Eq. 3.3.2 depends upon the relative phases of the driving modes.

Examination of Eq. 3.3.2 shows that it contains three separate parameters: weighted sums over  $A_{\ell} D_{\ell}$ ,  $B_{\ell} C_{\ell}$ , and  $A_{\ell} C_{\ell} - B_{\ell} D_{\ell}$ . For what follows it is necessary to work with functions with a zero asymptotic limit at infinity. For that purpose, define  $\alpha_{\ell}(\sigma)$  and  $\beta_{\ell}(\sigma)$  to be:

$$\begin{aligned}\alpha_\ell(\sigma) &= (A_\ell D_\ell + B_\ell C_\ell) - (-1)^\ell \\ \beta_\ell(\sigma) &= (A_\ell C_\ell - B_\ell D_\ell)\end{aligned}\quad (3.3.3)$$

Combining Eq. 3.3.2 with Eq. 3.3.3 shows that:

$$p(\sigma, t_R) = \frac{\pi}{\eta k^2} \sum_{\ell=1}^{\infty} \frac{\ell(\ell+1)}{(2\ell+1)} \left[ F_\ell^2 + G_\ell^2 \right] \left\{ \begin{aligned} & \left[ 1 \pm (-1)^\ell \cos(2\omega t_R) \right] \\ & \pm \left[ \alpha_\ell(\sigma) \cos(2\omega t_R) - \beta_\ell(\sigma) \sin(2\omega t_R) \right] \end{aligned} \right\} \quad (3.3.4)$$

Within the curly brackets of Eq. 3.3.4, the envelope of the first term is independent of distance from the antenna. Functions  $\alpha_\ell(\sigma)$  and  $\beta_\ell(\sigma)$  are represented by alternating series and oscillating functions of distance. Functional values of  $\alpha_\ell(\sigma)$  and  $\beta_\ell(\sigma)$  are listed in Tables 3.3.1 and 3.3.2 for  $\ell = 1$  through 6.

The first term in Eq. 3.3.4 is the real power  $p_r(\sigma, t_R)$  where:

$$p_r(\sigma, t_R) = \frac{\pi}{\eta k^2} \sum_{\ell=1}^{\infty} \frac{\ell(\ell+1)}{(2\ell+1)} \left[ F_\ell^2 + G_\ell^2 \right] \left[ 1 \pm (-1)^\ell \cos(2\omega t_R) \right] \quad (3.3.5)$$

This equation describes power that travels ever outward at speed  $c$  in the form of periodic, trigonometric pulses. There is no time-independent, radius-dependent phase term and the magnitude does not approach a limit at infinite radius.

The distance dependent power terms in Eq. 3.3.4 are given by  $p_i(\sigma, t_R)$  where:

$$p_i(\sigma, t_R) = \pm \frac{\pi}{\eta k^2} \sum_{\ell=1}^{\infty} \frac{\ell(\ell+1)}{(2\ell+1)} \left[ F_\ell^2 + G_\ell^2 \right] \left[ \alpha_\ell(\sigma) \cos(2\omega t_R) - \beta_\ell(\sigma) \sin(2\omega t_R) \right] \quad (3.3.6)$$

As may be seen from Tables 3.3.1 and 3.3.2, the maximum of the envelope for each term occurs at the antenna surface and goes asymptotically to zero at infinite radius.

---


$$\alpha_1(\sigma) = \frac{2}{\sigma^2}$$

$$\alpha_2(\sigma) = \frac{36}{\sigma^4} - \frac{18}{\sigma^2}$$

$$\alpha_3(\sigma) = \frac{1350}{\sigma^6} - \frac{720}{\sigma^4} + \frac{72}{\sigma^2}$$

$$\alpha_4(\sigma) = \frac{88200}{\sigma^8} - \frac{49350}{\sigma^6} + \frac{6000}{\sigma^4} - \frac{200}{\sigma^2}$$

$$\alpha_5(\sigma) = \frac{8,930,250}{\sigma^{10}} - \frac{5,159,700}{\sigma^8} + \frac{699,300}{\sigma^6} - \frac{31,500}{\sigma^4} + \frac{450}{\sigma^2}$$

$$\alpha_6(\sigma) = \frac{1,296,672,300}{\sigma^{12}} - \frac{766,215,450}{\sigma^{10}} + \frac{111,370,140}{\sigma^8} - \frac{5,900,580}{\sigma^6} + \frac{123,480}{\sigma^4} - \frac{882}{\sigma^2}$$


---

Table 3.3.1 Radial Dependence of  $\alpha_\ell(\sigma)$ 

---


$$\beta_1(\sigma) = -\frac{1}{\sigma^3} + \frac{2}{\sigma}$$

$$\beta_2(\sigma) = -\frac{18}{\sigma^5} + \frac{33}{\sigma^3} - \frac{6}{\sigma}$$

$$\beta_3(\sigma) = -\frac{675}{\sigma^7} + \frac{1250}{\sigma^5} - \frac{276}{\sigma^3} + \frac{12}{\sigma}$$

$$\beta_4(\sigma) = -\frac{44100}{\sigma^9} + \frac{83475}{\sigma^7} - \frac{20220}{\sigma^5} + \frac{1300}{\sigma^3} - \frac{20}{\sigma}$$

$$\beta_5(\sigma) = -\frac{4,465,125}{\sigma^{11}} + \frac{8,533,350}{\sigma^9} - \frac{2,201,850}{\sigma^7} + \frac{169,470}{\sigma^5} - \frac{4425}{\sigma^3} + \frac{30}{\sigma}$$

$$\beta_6(\sigma) = -\frac{648,336,150}{\sigma^{13}} + \frac{1,247,555,935}{\sigma^{11}} - \frac{335,975,850}{\sigma^9} + \frac{28,797,930}{\sigma^7} - \frac{961,380}{\sigma^5} + \frac{122,010}{\sigma^3} - \frac{42}{\sigma}$$


---

Table 3.3.2 Radial Dependence of  $\beta_\ell(\sigma)$ 

### 3.4 Comparison of Complex and Instantaneous Powers

In the discussion to follow only TM modes are analyzed. The result carries over in the same form with TE modes, only the sign of the imaginary part changes.

With electric circuits, the complex power form of Eq. 3.1.4 is determined by Eq. 3.1.3 and, conversely, Eq. 3.1.3 is partially determined by Eq. 3.1.4. In a similar way, the time-dependent field power of Eq. 3.3.2 leads to the complex power of Eqs. 3.2.2. Equation 3.3.2 may be put in the form:

$$P_c(\sigma, t_R) = \frac{\pi}{\eta k^2} \sum_{\ell=1}^{\infty} \frac{\ell(\ell+1)}{(2\ell+1)} F_{\ell}^2 \left\{ [1 \pm \cos(2\omega t_R - 2\xi)] + \gamma_{\ell}(\sigma) \sin(2\omega t_R - 2\xi) \right\} \quad (3.4.1)$$

The instantaneous power expression for the identical set of electromagnetic fields is given by Eq. 3.3.4, and repeated here for TM modes only:

$$p(\sigma, t_R) = \frac{\pi}{\eta k^2} \sum_{\ell=1}^{\infty} \frac{\ell(\ell+1)}{(2\ell+1)} F_{\ell}^2 \left\{ \begin{aligned} & \left[ 1 \pm (-1)^{\ell} \cos(2\omega t_R) \right] \\ & \left[ \pm [\alpha_{\ell}(\sigma) \cos(2\omega t_R) - \beta_{\ell}(\sigma) \sin(2\omega t_R)] \right] \end{aligned} \right\} \quad (3.4.2)$$

With these two descriptions of the same energy flow, Eqs. 3.4.1 and 3.4.2, the curly brackets of the two equations are multiplied by identical factors but contain, respectively, two and three time-dependent terms.

The first term of Eq. 3.4.1 is the real part of the complex power. It does not go to a limit at infinite radius, it is equal to zero twice each field cycle, and it is never negative; it describes a unidirectional energy flow away from the source. The gamma power term of Eq. 3.4.1 is in phase quadrature with the real power and, by definition, is the reactive part of the complex power. It goes to zero in the limit of infinite radius; at each point it oscillates between equal negative and positive values and hence describes radially directed, alternating power. The time-dependent terms contain identical mode- or radius-dependent, time-independent phase factors.

The first term of Eq. 3.4.2 is the real power. Like its counterpart in Eq. 3.4.1, it does not go to a limit at infinite radius, it is equal to zero twice each field cycle, and it is never negative. It, too, describes a unidirectional energy flow away from the source. The real power and  $\alpha_{\ell}(\sigma)$  power are in time phase, and both are in time quadrature with  $\beta_{\ell}(\sigma)$  power. Both  $\alpha_{\ell}(\sigma)$  and  $\beta_{\ell}(\sigma)$  powers go to zero in the limit of infinite radius; at each point both oscillate between equal negative and positive parts and hence both describe radially-directed, alternating power. There are no mode- or radius-dependent, time-independent phase factors.



The phases of the real part of the complex power and the real power differ by a radius-dependent phase factor. Since the instantaneous power represents an actual physical entity, it follows that the real part of the complex power does not. A quantitative expression for phase angle  $\xi_\ell(\sigma)$  may be obtained by equating Eqs. 3.4.1 and 3.4.2. The result is:

$$\tan(2\xi_\ell) = \frac{A_\ell B_\ell}{A_\ell^2 - B_\ell^2} \quad (3.4.3)$$

It follows from Eq. 3.4.1 that the group velocity of the real part of the complex power is:

$$v_{gp} = \frac{c}{1 + d\xi_\ell/d\sigma} \quad (3.4.4)$$

It may be verified using Table A.26.2.20 that:

$$\frac{d}{d\sigma} \left( \frac{A_\ell B_\ell}{A_\ell^2 - B_\ell^2} \right) \leq 0 \quad (3.4.5)$$

Combining Eqs. 3.4.3 and 3.4.5 with functional properties of the tangent gives:

$$d\xi_\ell/d\sigma \leq 0 \quad (3.4.6)$$

Combining Eq. 3.4.4 with 3.4.6 shows that the real part of the complex power, Eq. 3.4.1, propagates faster than the speed of light. A basic tenet of physics is that the speed of electromagnetic energy is never greater than  $c$ . This also suggests that the complex power is not a physical entity and it does not describe an actual energy flow. In contrast, the first term of Eq. 3.4.2 does travel at the speed of light and does describe actual energy flow.

It follows from Eq. 3.4.1 that if the calculus operations of differentiating or integrating complex power with respect to the radius is done, the calculation must include operations on the function  $\xi_\ell(\sigma)$ . Yet with complex power, knowledge of  $\xi_\ell(\sigma)$  is suppressed and unavailable. Therefore, it is not possible to carry out such operations from knowledge of only complex power.

$\xi_\ell(\sigma)$	$\ell = 1$	$\ell = 2$	$\ell = 3$
0	0	0	0
$-\pi/2$	0.618	0.777	0.785
$-\pi$	1	1.414	1.566
$-3\pi/2$	1.618	1.882	2.221
$-2\pi$	$\infty$	2.449	2.739
$-5\pi/2$		4.104	3.289
$-3\pi$		$\infty$	4.310
$-7\pi/2$			7.852
$-4\pi$			$\infty$

Table 3.4.1 Radius for Which Selected Values of Phase Angle Occur, Three Lowest Modes

If suppressed phase angle  $\xi_\ell(\sigma)$  of mode  $\ell$  is assigned a value of zero at a vanishingly small radius, the value decreases with increasing radius to equal  $-(\ell+1)\pi$  at infinite radius. Table 3.4.1 lists values of  $\sigma$  for which the phase angle reaches selected values as a function of radius and modal number.

Since the use of complex power is uncompromised in electric circuits, the complex power expression of Eq. 3.4.1, re-expressed as Eq. 3.4.7, applies to the driving circuitry, including the input side of the radiating surface,  $\sigma = ka$ :

$$P_c(\sigma, t_R) = \frac{\pi}{\eta k^2} \sum_{\ell=1}^{\infty} \frac{\ell(\ell+1)}{(2\ell+1)} F_\ell^2 \left\{ \begin{aligned} & [A_\ell D_\ell - B_\ell C_\ell] [1 \pm \cos(2\omega t_R - 2\xi_\ell)] \\ & \mp [A_\ell C_\ell + B_\ell D_\ell] \sin(2\omega t_R - 2\xi_\ell) \end{aligned} \right\} \quad (3.4.7)$$

The time-dependent power expression of Eq. 3.4.2, re-expressed as Eq. 3.4.8, applies to the external region, including the output side of the radiating surface  $\sigma = ka$ :

$$p(\sigma, t_R) = \frac{\pi}{\eta k^2} \sum_{\ell=1}^{\infty} \frac{\ell(\ell+1)}{(2\ell+1)} F_\ell^2 \left\{ \begin{aligned} & [A_\ell D_\ell - B_\ell C_\ell] \pm [A_\ell D_\ell + B_\ell C_\ell] \cos(2\omega t_R) \\ & \mp [A_\ell C_\ell - B_\ell D_\ell] \sin(2\omega t_R) \end{aligned} \right\} \quad (3.4.8)$$

The mean square value of the time varying portions are respectively given by:

$$[A_\ell D_\ell - B_\ell C_\ell]^2 + [A_\ell C_\ell + B_\ell D_\ell]^2 = [A_\ell D_\ell + B_\ell C_\ell]^2 + [A_\ell C_\ell - B_\ell D_\ell]^2 \quad (3.4.9)$$

It follows by inspection that Eq. 3.4.9 is an identity. Therefore, the total power is continuous through the interface. The left side terms are the magnitudes of the real plus imaginary parts of the input complex power on the source side. On the right side, the first term applies to the time variation of the real power and the in-phase oscillatory power. The second term represents the out-of-phase oscillatory power.

The first two terms inside the curly brackets of Eq. 3.4.8 may be written as:

$$\begin{aligned} & [A_\ell D_\ell - B_\ell C_\ell] \pm [A_\ell D_\ell + B_\ell C_\ell] \cos(2\omega t_R) \\ &= [A_\ell D_\ell - B_\ell C_\ell] \left[ 1 \pm (-1)^\ell \cos(2\omega t_R) \right] \pm [A_\ell D_\ell + B_\ell C_\ell - (-1)^\ell] \cos(2\omega t_R) \end{aligned} \quad (3.4.10)$$

Comparison of Eq. 3.4.7 and 3.4.8 as modified by Eq. 3.4.10 at  $\sigma = ka$  shows that the real power undergoes a phase discontinuity of  $2\xi_\ell$  as it passes through the antenna. The absolute phase is determined by the phase of the source and the antenna circuit impedances.

In summary, although the total time-dependent power is continuous through the interface between the source and field regions, the separation of that power into constituent parts is different. On the source side, the power separates into real and reactive parts the time varying portions of which are in time quadrature. Power that is in phase with the input power represents power loss from the system. On the field side, power that is in phase with the real power does not represent power loss; some oscillatory power is in phase with the real power and some is in phase quadrature.

At the surface of a radiating sphere, it is correct to write the complex power in the form of Eq. 3.2.2 as:

$$P_c(ka) = \oint N_c \cdot dS = \frac{\pi}{\eta k^2} \sum_{\ell=1}^{\infty} \frac{\ell(\ell+1)}{(2\ell+1)} \left\{ \left( F_\ell F_\ell^* + G_\ell G_\ell^* \right) [A_\ell(ka)D_\ell(ka) - B_\ell(ka)C_\ell(ka)] \right. \\ \left. + i \left( F_\ell F_\ell^* - G_\ell G_\ell^* \right) [A_\ell(ka)C_\ell(ka) + B_\ell(ka)D_\ell(ka)] \right\} \quad (3.4.11)$$

The equation is correct only at radius  $a$ . The equality does not extend to larger radii for the imaginary part.

### 3.5 Radiation Q

Consider a series electric circuit consisting of all three passive circuit elements: inductance, capacitance, and resistance. Let the circuit be driven by time-dependent voltage  $v(t)$  that produces current flow  $i(t)$ . The integro-differential equation the circuit satisfies is:

$$L \frac{di(t)}{dt} + Ri(t) + \frac{1}{C} \int i(t) dt = v(t) \quad (3.5.1)$$

The homogeneous equation has the form of the harmonic oscillator equation:

$$\frac{d^2 i(t)}{dt^2} + \frac{R}{L} \frac{di(t)}{dt} + \frac{1}{LC} i(t) = 0 \quad (3.5.2)$$

The current as a function of time is equal to:

$$i(t) = I_0 e^{st} \quad (3.5.3)$$

Substituting Eq. 3.5.3 into 3.5.2 shows that:

$$s = -\frac{R}{2L} \pm \sqrt{\frac{R^2}{4L^2} - \frac{1}{LC}} \quad (3.5.4)$$

Introduce the notation that:

$$\alpha = R/2L \quad \text{and} \quad \omega_0 = 1/\sqrt{LC} \quad (3.5.5)$$

Combining shows the homogeneous current to be:

$$i(t) = I_0 e^{-\alpha t} e^{\pm i t \sqrt{\alpha^2 - \omega_0^2}} \quad (3.5.6)$$

The character of the solution depends upon the relative sizes of  $\alpha$  and  $\omega_0$ . Consider first the special case where:

$$\omega_0 > \alpha \quad (3.5.7)$$

Combining Eq. 3.5.7 with Eq. 3.5.6 gives:

$$i(t) = I_0 e^{-\alpha t} e^{\pm i t \sqrt{\omega_0^2 - \alpha^2}} \quad (3.5.8)$$

The energy of the system is proportional to:

$$W(t) \approx i(t) i^*(t) = I_0 I_0^* e^{-2\alpha t} \quad (3.5.9)$$

The power out, the rate of energy decay, is:

$$P(t) \approx \frac{d}{dt} [i(t) i^*(t)] = -2\alpha I_0 I_0^* e^{-2\alpha t} \quad (3.5.10)$$

A dimensionless quantity that measures the quality of an oscillating system is:

$$Q = \left| \frac{\omega W_{pk}(t)}{P_{av}(t)} \right| = \frac{\omega}{2\alpha} \quad (3.5.11)$$

$Q$ , the quality factor of the oscillating system, measures the rate of the decay of the envelope of energy  $W(t)$ , which is equal to the peak value  $W_{pk}(t)$ .  $P(t)$  is the time-average rate of energy dissipation.

Bandwidth is inversely proportional to  $Q$ . This may be shown by noting that the input impedance of the RLC circuit is:

$$Z(\omega) = R + i\omega L \left( 1 - \omega_0^2 / \omega^2 \right) \quad (3.5.12)$$

The bandwidth of any system is defined to be the frequency difference between half-power points. In this case the lowest impedance occurs for frequency  $\omega = \omega_0$ , at which frequency the impedance is purely resistive and equal to  $R$ . Half power points occur when the magnitude of the impedance is equal to the square root of two times  $R$ , and this happens when the real and reactive parts are equal. If  $\omega_1$  is the frequency at a half power point, it follows that:

$$R = \omega_1 L \left( 1 - \omega_0^2 / \omega_1^2 \right) \quad (3.5.13)$$

Expanding the equation shows that:

$$(\omega_1 - \omega_0)(\omega_1 + \omega_0) = \frac{\omega_1 R}{L} \quad (3.5.14)$$

Bandwidth is particularly useful if it is reasonably small, and if it is small, Eq. 3.5.14 is approximately equal to:

$$\delta\omega = R/2L$$

The substitution has been made that  $\delta\omega = \pm(\omega_1 - \omega_0)$ , the frequency difference between one of the half-power points and the resonance frequency. With the definitions of Eqs. 3.5.5 and 3.5.11, the total bandwidth,  $B$ , normalized to the actual frequency is:

$$B = \delta\omega / \omega_0 = 1/Q \quad (3.5.15)$$

It follows that in a low-loss, series resonant system  $Q$  is a direct measure of and inversely proportional to the bandwidth.

A special case is the case of a lossy inductor. Although  $Q$  follows from Eq. 3.5.11, because of the importance of the case consider another viewpoint. The steady state input impedance for a lossy inductor driven at frequency  $\omega$  is:

$$Z = R + j\omega L \quad (3.5.16)$$

If the current is  $I_0 \cos(\omega t)$  the energy stored in the inductance and the power loss in the resistance are:

$$\begin{aligned} W(t) &= \frac{1}{4} L I_0^2 [1 + \cos(2\omega t)] \\ P(t) &= \frac{1}{2} R I_0^2 [1 + \cos(2\omega t)] \end{aligned} \quad (3.5.17)$$

Combining the definition of Eq. 3.5.11 with Eq. 3.5.17 shows that:

$$Q = \frac{\omega L}{R} = \tan \zeta \quad (3.5.18)$$

Angle  $\zeta$  is the phase angle of the impedance. A similar expression holds for lossy capacitors. This is a convenient measure of  $Q$  when operating far from the resonant frequency.

Radiation  $Q$  is important with antennas since it is often necessary to radiate a certain amount of time-average power at a given frequency. It follows that the peak standing energy that must be present in the local fields about the antenna is:

$$W_{pk} = \frac{P_{av}}{\omega} Q \quad (3.5.19)$$

The larger the standing energy the larger will be the antenna surface currents, the ohmic loss, and the amount of energy that returns to the source twice each field cycle. If  $Q$  is large enough, the magnitude of standing energy required may be more than the source can supply.

Although antenna  $Q$  is important, calculation is made difficult because the energy radiated permanently away from the antenna is not absorbed. With circuits, energy once absorbed is no longer a factor. With fields, all energy remains. In the steady state the source has, ideally, been active since time  $t = -\infty$  and there is an infinite amount of field energy. Since only energy that returns to the source affects it, the critical question in  $Q$  calculations is how to separate energy that returns to the source from energy that does not.

### 3.6 Chu's Q Analysis, TM Fields

Chu was the first to quantify the relationship between Q and the electric size of an antenna. In his work, he analyzed zero degree, phasor field equations with TM sources, the same fields analyzed in Sections 3.2, 3.3, and 3.4. For this case the phasor field components are:

$$\begin{aligned}\sigma^2 \tilde{E}_r &= \sum_{\ell=1}^{\infty} \ell(\ell+1) F_{\ell} (B_{\ell} + i A_{\ell}) P_{\ell}(\cos \theta) e^{-i\sigma} \\ \sigma \tilde{E}_{\theta} &= \sum_{\ell=1}^{\infty} F_{\ell} (D_{\ell} + i C_{\ell}) \frac{d}{d\theta} P_{\ell}(\cos \theta) e^{-i\sigma} \\ \sigma \eta \tilde{H}_{\phi} &= \sum_{\ell=1}^{\infty} F_{\ell} (A_{\ell} - i B_{\ell}) \frac{d}{d\theta} P_{\ell}(\cos \theta) e^{-i\sigma}\end{aligned}\tag{3.6.1}$$

He analyzed the frequency behavior of the input impedance of an antenna producing these fields and, for each field mode, was able to connect the frequency dependence with radiation Q.

To keep the work general it is necessary to separate the analysis from a specific antenna. For this purpose he constructed the smallest virtual sphere that just circumscribed the antenna and replaced the antenna with equivalent surface sources producing identical external fields, see Section A.7. He analyzed only the field energy external to the sphere. Since he ignored interior energies, the calculated Q is the least possible value for any antenna that can fit inside the virtual sphere. That is, with an antenna of length  $2a$  Chu's results are based upon exterior fields only. Interior field energy will add an undetermined amount to Q.

The complex power on the surface of the virtual sphere follows from the complex Poynting theorem:

$$P_c = \frac{2\pi}{\eta k^2} \sum_{\ell=1}^{\infty} F_{\ell} F_{\ell}^* \frac{\ell(\ell+1)}{(2\ell+1)} (A_{\ell} + i B_{\ell}) (D_{\ell} + i C_{\ell})\tag{3.6.2}$$

Chu next introduced voltage  $V_{\ell}$  and current  $I_{\ell}$ , respectively proportional to  $E_{\theta}$  and  $H_{\phi}$ , as a generalized force and flow. The complex surface power for each mode of Eq. 3.6.2 may be written as:



$$P_{c\ell} = \frac{2\pi}{\eta k^2} F_\ell F_\ell^* \frac{\ell(\ell+1)}{(2\ell+1)} (A + i B)(D + i C) = \frac{V_\ell I_\ell^*}{2} \quad (3.6.3)$$

Since, for each mode, the angular electric-to-magnetic field ratio does not depend upon either zenith or azimuth angle, defining modal impedance  $Z_\ell(\sigma)$  to equal the ratio  $E_{\theta\ell}/H_{\phi\ell}$  gives the result:

$$Z_\ell(\sigma) = \frac{E_{\theta\ell}}{H_{\phi\ell}} = \frac{V_\ell}{I_\ell} = \eta \left[ \frac{D_\ell(\sigma) + i C_\ell(\sigma)}{A_\ell(\sigma) - i B_\ell(\sigma)} \right] \quad (3.6.4)$$

Equations 3.6.3 and 3.6.4 are both satisfied if:

$$V_\ell = \frac{F_\ell}{k} \sqrt{\frac{4\pi\ell(\ell+1)}{3(2\ell+1)}} (D_\ell + i C_\ell) e^{-i\sigma} \quad (3.6.5)$$

$$I_\ell = \frac{F_\ell}{\eta k} \sqrt{\frac{4\pi\ell(\ell+1)}{3(2\ell+1)}} (A_\ell - i B_\ell) e^{-i\sigma}$$

The modal impedance of Eq. 3.6.4 may be used to synthesize equivalent circuits that simulate the affect of the antenna upon its source. To do so break the quotient into partial fractions. For the dipole case,  $\ell = 1$ , the impedance has the form:

$$Z_{1E}(\sigma) = \frac{\frac{\eta}{i\sigma^2} + \frac{\eta}{\sigma} + i\eta}{\frac{1}{\sigma} + i} = \frac{\eta}{i\sigma} + \frac{1}{\frac{1}{i\eta\sigma} + \frac{1}{\eta}} \quad (3.6.6)$$

To evaluate the impedance at the spherical surface  $r = a$ , replace  $k$  by  $\omega/c$  and simplify:

$$Z_{1E}(ka) = \frac{i}{\omega\epsilon a} + \frac{1}{\frac{1}{\eta} + \frac{i}{\omega\mu a}} \quad (3.6.7)$$

The circuit with the impedance characteristics of Eq. 3.6.7 consists of a capacitor of  $(\epsilon a)$  farads in series with a shunt configuration of an inductor of  $(\mu a)$  henries and a resistor of  $\eta$  ohms. For small values of  $ka$ , the input impedance is large and dominated by the capacitive reactance. Power to the far field is represented by power dissipated in the resistor.

The quotient of Eq. 3.6.4 using partial fractions is valid for each value of  $\ell$ . The resulting circuit is shown in Figure 3.6.1. The circuit is a reactive ladder network with a single terminating resistor. Each additional modal number adds an additional L-C pair to the circuit ladder. Power in the ladder network represents power flows made necessary by the changing geometry of the field as the radius increases. For electrically small antennas the input impedance is dominated by the first capacitor in series with the first inductor. The input reactance is dominantly capacitive so long as  $\ell(2\ell-1) \gg k^2 a^2$ .

Turning to field properties, the impedance of a virtual shell of arbitrary radius,  $r = \sigma/k$ , may be expressed as:

$$Z_{\ell E}(\sigma) = R_{\ell}(\sigma) + iX_{\ell}(\sigma) \quad (3.6.8)$$

Inserting the letter functions of the spherical Bessel and Neumann functions shows that:

$$\begin{aligned} R_{\ell}(\sigma) &= \eta \left[ \frac{A_{\ell}(\sigma)D_{\ell}(\sigma) - B_{\ell}(\sigma)C_{\ell}(\sigma)}{A_{\ell}(\sigma)^2 + B_{\ell}(\sigma)^2} \right] \\ X_{\ell}(\sigma) &= \eta \left[ \frac{A_{\ell}(\sigma)C_{\ell}(\sigma) + B_{\ell}(\sigma)D_{\ell}(\sigma)}{A_{\ell}(\sigma)^2 + B_{\ell}(\sigma)^2} \right] \end{aligned} \quad (3.6.9)$$

Values of both numerators and the denominator are listed in Table 3.6.1 for several modes; there are no resonances and the reactance is negative for all values of  $\sigma$ . No resonances are expected since, as illustrated by biconical antennas, resonance occurs when the combination of antenna arms, acting as transmission lines, and the surface impedance resonate. It is not because of impedance changes on the spherical surface. Rather than evaluate Q separately for each modal equivalent circuit, Chu stated that the work involved would be "tedious" and sought approximate values that were easier

to calculate. Since he was interested in electrically small antennas, he approximated the equivalent circuit as a series circuit then added a lossless inductor needed to make the system resonant. Therefore his resonance arises quite differently from one dependent upon length of the antenna arms.

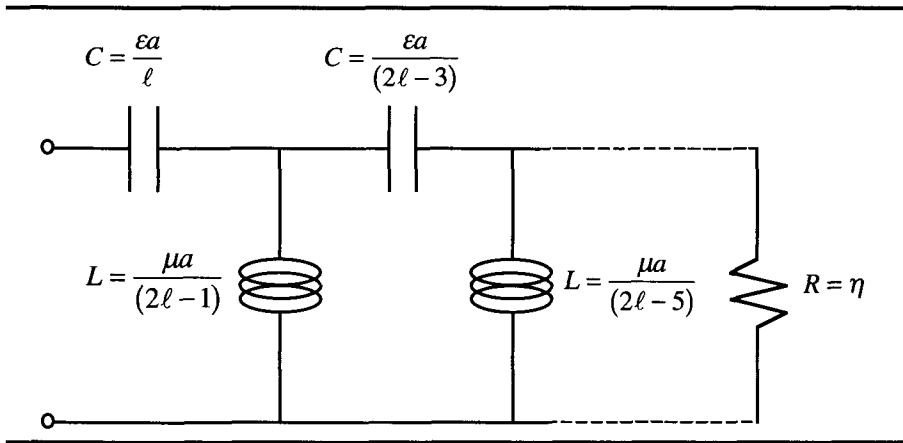


Figure 3.6.1 TM Multipolar Equivalent Circuit.  
*This circuit has the same input impedance as a spherical shell of radius  $a$  radiating an electric multipole mode of order  $\ell$ .*

$\ell$	$A_\ell C_\ell + B_\ell D_\ell$	$A_\ell^2 + B_\ell^2$
1	$-\frac{1}{\sigma^3}$	$1 + \frac{1}{\sigma^2}$
2	$-\frac{3}{\sigma^3} - \frac{18}{\sigma^5}$	$1 + \frac{3}{\sigma^2} + \frac{9}{\sigma^4}$
3	$-\frac{6}{\sigma^3} - \frac{75}{\sigma^5} - \frac{675}{\sigma^7}$	$1 + \frac{6}{\sigma^2} + \frac{45}{\sigma^4} + \frac{225}{\sigma^6}$
4	$-\frac{10}{\sigma^3} - \frac{220}{\sigma^5} - \frac{4725}{\sigma^7} - \frac{44100}{\sigma^9}$	$1 + \frac{10}{\sigma^2} + \frac{135}{\sigma^4} + \frac{1575}{\sigma^6} + \frac{11025}{\sigma^8}$
5	$-\frac{15}{\sigma^3} - \frac{630}{\sigma^5} - \frac{18900}{\sigma^7} - \frac{396900}{\sigma^9} - \frac{4465125}{\sigma^{11}}$	$1 + \frac{15}{\sigma^2} + \frac{305}{\sigma^4} + \frac{6300}{\sigma^6} + \frac{99285}{\sigma^8} + \frac{893025}{\sigma^{10}}$

Table 3.6.1 Table of Functions Needed for Equivalent Impedances;  
 $A_\ell D_\ell - B_\ell C_\ell = 1$

Since at resonance the time-average values of electric and magnetic energy are equal, he took the stored energy to be twice the time-average stored electric energy. With a series RLC circuit, the relationships between the input reactance and the reactive elements,  $L_\ell$  and  $C_\ell$ , are:

$$X_\ell = \left( \omega L_\ell - \frac{1}{\omega C_\ell} \right) \text{ and } \frac{dX_\ell}{d\omega} = \frac{1}{\omega} \left( \omega L_\ell + \frac{1}{\omega C_\ell} \right) \quad (3.6.10)$$

Solving for the values of the elements as a function of the reactance gives:

$$C_\ell = \frac{2}{\omega^2} \left( \frac{dX_\ell}{d\omega} - \frac{X_\ell}{\omega} \right)^{-1}; \quad L_\ell = \frac{1}{2} \left( \frac{dX_\ell}{d\omega} + \frac{X_\ell}{\omega} \right) \quad (3.6.11)$$

Chu put the time-average radiated power equal to that dissipated in the resistor. Combining the above shows that:

$$P_\ell = \frac{1}{2} R_\ell I_\ell I_\ell^* = \frac{\eta}{2(A_\ell^2 + B_\ell^2)} I_\ell I_\ell^* \quad (3.6.12)$$

Using Eqs. 3.6.8 and 3.6.11, the time average stored electric energy is:

$$\mathcal{W}_\ell = \frac{1}{4\omega^2 C_\ell} I_\ell I_\ell^* = \frac{I_\ell I_\ell^*}{8} \left( \frac{dX_\ell}{d\omega} - \frac{X_\ell}{\omega} \right) \quad (3.6.13)$$

Using Eq. 3.6.7, the calculated modal value of Q is:

$$Q_{\ell E} = \frac{\omega}{2\eta} \left( \frac{dX_\ell}{d\omega} - \frac{X_\ell}{\omega} \right) (A_\ell^2 + B_\ell^2) \quad (3.6.14)$$

For the special case  $\ell = 1$ ,

$$A_1^2 + B_1^2 = \frac{1 + (ka)^2}{(ka)^2} \quad \text{and} \quad X_1 = - \frac{\eta}{(ka) [1 + (ka)^2]} \quad (3.6.15)$$

$$Q_{1E} = \frac{1}{(ka)^3} \left[ \frac{1 + 2(ka)^2}{1 + (ka)^2} \right] \quad (3.6.16)$$

In the limit of electrically small antennas:

$$\lim_{ka \Rightarrow 0} Q_{1E} = \frac{1}{(ka)^3} + \frac{1}{(ka)} \quad (3.6.17)$$

Chu stated that this result is adequate for practical antennas.

### 3.7 Chu's Q Analysis, Exact for TM Fields

Although Chu's technique for approximating the value of  $Q$  for each equivalent circuit is adequate for practical purposes, a more exact analysis is needed if critical comparisons with other analytical techniques are to be made. For this purpose we make an exact analysis of the dipole circuit of Fig. 3.6.1,  $\ell = 1$ , and from the analysis obtain an exact value of antenna  $Q$ .

Let  $i_1(t)$  and  $i_2(t)$  be the currents respectively through the capacitor and the inductor; the current through the resistor is  $i_1(t) - i_2(t)$ . Then:

$$R i_1(t) = L \frac{d i_2(t)}{dt} + R i_2(t) \quad (3.7.1)$$

The instantaneous energies stored in the capacitor and inductor are:

$$w_C(t) = \frac{q_1^2(t)}{2C} \quad \text{and} \quad w_L(t) = \frac{L i_2^2(t)}{2} \quad (3.7.2)$$

The power dissipated in the resistor is:

$$p(t) = R [i_1(t) - i_2(t)]^2 \quad (3.7.3)$$

For sinusoidal steady state operation, introduce:

$$i_2(t) = I_2 \cos(\omega t) \quad (3.7.4)$$

Combining shows the charge on the capacitor to be:

$$q_1(t) = \int i_1(t) dt = \frac{I_2}{\omega} \left[ \sin(\omega t) + \frac{\omega L}{R} \cos(\omega t) \right] \quad (3.7.5)$$

Resulting energies and power are:

$$w_C(t) = \frac{I_2^2}{4\omega} \left\{ \left( \frac{1}{\omega C} + \frac{\omega L^2}{CR^2} \right) - \left( \frac{1}{\omega C} - \frac{\omega L^2}{CR^2} \right) \cos(2\omega t) + \frac{2L}{CR} \sin(2\omega t) \right\} \quad (3.7.6)$$

$$w_L(t) = \frac{I_2^2}{4\omega} \omega L [1 + \cos(2\omega t)] \quad (3.7.7)$$

$$p(t) = \frac{\omega^2 L^2}{2R} I_2^2 [1 - \cos(2\omega t)] \quad (3.7.8)$$

Use of component values from Fig. 3.6.1 in Eqs. 3.7.6-3.7.8 gives:

$$w_C(t) = \frac{\eta I_2^2}{4\omega} \left\{ \left( \frac{1}{(ka)} + (ka) \right) - \left( \frac{1}{(ka)} - (ka) \right) \cos(2\omega t) + 2 \sin(2\omega t) \right\} \quad (3.7.9)$$

$$w_L(t) = \eta I_2^2 \frac{(ka)}{4\omega} [1 + \cos(2\omega t)] \quad (3.7.10)$$

$$p(t) = \eta I_2^2 \frac{(ka)^2}{2} [1 - \cos(2\omega t)] \quad (3.7.11)$$

The total reactive energy is the sum of Eqs. 3.7.9 and 3.7.10:

$$w_X(t) = \frac{\eta I_2^2}{4\omega} \left\{ \left( \frac{1}{(ka)} + 2(ka) \right) - \left( \frac{1}{(ka)} - 2(ka) \right) \cos(2\omega t) + 2 \sin(2\omega t) \right\} \quad (3.7.12)$$

The cyclical peak of stored energy is:

$$W_{pk} = \frac{\eta I_2^2}{4\omega} \left\{ \left( \frac{1}{(ka)} + 2(ka) \right) + \frac{1}{(ka)} \sqrt{1 + 4(ka)^4} \right\} \quad (3.7.13)$$

The time average output power is:

$$P_{av} = \eta I_2^2 \frac{(ka)^2}{2} \quad (3.7.14)$$

Combining:

$$Q = \frac{\omega W_{pk}}{P_{av}} \geq \frac{1}{2(ka)^3} \left( 1 + \sqrt{1 + 4(ka)^4} \right) + \frac{1}{(ka)} \quad (3.7.15)$$

This is the exact expression for the  $Q$  of the circuit of Fig. 3.6.1 for the special case  $\ell = 1$ . In the limit as  $ka$  goes to zero Eqs. 3.7.15 is equal to Eq. 3.6.17.

### 3.8 Chu's Q Analysis, TE Field

The fields about a  $z$ -directed magnetic multipole follow from Eq. 3.2.1:

$$\begin{aligned} \sigma^2 \eta H_r &= - \sum_{\ell=1}^{\infty} \ell(\ell+1) G_{\ell} [B_{\ell}(\sigma) + i A_{\ell}(\sigma)] P_{\ell}(\cos \theta) \\ \sigma \eta H_{\theta} &= - \sum_{\ell=1}^{\infty} G_{\ell} [D_{\ell}(\sigma) + i C_{\ell}(\sigma)] \frac{d}{d\theta} P_{\ell}(\cos \theta) \\ \sigma E_{\phi} &= \sum_{\ell=1}^{\infty} G_{\ell} [A_{\ell}(\sigma) - i B_{\ell}(\sigma)] \frac{d}{d\theta} P_{\ell}(\cos \theta) \end{aligned} \quad (3.8.1)$$

Following the procedure used for TM modes, for the TE modes introduce a generalized force and flow as a voltage and a current, this time proportional respectively to  $E_{\phi}$  and  $-H_{\theta}$ . Each mode then satisfies the power equation:

$$P_c = \frac{2\pi}{\eta k^2} G_\ell G_\ell^* \frac{\ell(\ell+1)}{(2\ell+1)} [A_\ell(\sigma) - i B_\ell] [D_\ell(\sigma) - i C_\ell] = \frac{1}{2} V_\ell I_\ell^* \quad (3.8.2)$$

Like TM modes, for each TE mode the angular electric-to-magnetic field ratio depends upon radius, not angle. Defining modal admittance  $Y_\ell$  to equal the ratio  $H_{\theta\ell}/E_{\phi\ell}$ , it follows that:

$$Y_{\ell M}(\sigma) = -\frac{H_{\theta\ell}}{E_{\phi\ell}} = \frac{I_\ell}{V_\ell} = \frac{1}{\eta} \left[ \frac{D_\ell(\sigma) + i C_\ell(\sigma)}{A_\ell(\sigma) - i B_\ell(\sigma)} \right] \quad (3.8.3)$$

Both Eqs. 3.8.2 and 3.8.3 are satisfied if:

$$V_\ell = \frac{G_\ell}{k} \sqrt{\frac{4\pi\ell(\ell+1)}{3(2\ell+1)}} [A_\ell(\sigma) - i B_\ell(\sigma)] e^{-i\sigma} \quad (3.8.4)$$

$$I_\ell = \frac{G_\ell}{\eta k} \sqrt{\frac{4\pi\ell(\ell+1)}{3(2\ell+1)}} [D_\ell(\sigma) + i C_\ell(\sigma)] e^{-i\sigma}$$

Comparison of Eq. 3.6.4 and 3.8.4 shows that:

$$Y_{\ell M}(\sigma) = \frac{1}{\eta^2} Z_{\ell E}(\sigma) \quad (3.8.5)$$

Repeating the procedure used to evaluate the TM equivalent circuits gives the equivalent circuits for TE modes. The resulting circuit is shown in Figure 3.8.1; it is the dual of Figure 3.6.1.

Since the circuits are exact duals, each power and energy of Section 3.6 has an exact counterpart in Section 3.8, though what is capacitive becomes inductive, and *vice versa*. For example, the input impedance of electrically small electric dipoles is equal to the large input admittance of electrically small magnetic dipoles. If the circuit used to calculate Q is a parallel capacitor, inductor, and resistor the magnitudes of energies are unchanged, though the forms are reversed. Q therefore is the same:



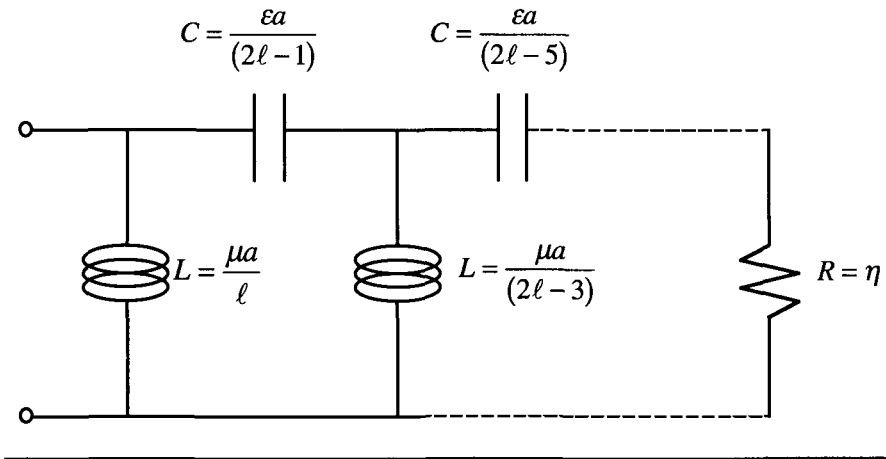


Figure 3.8.1 TE Multipolar Equivalent Circuit

*This circuit has the same input impedance as a spherical shell of radius  $a$  radiating magnetic multipole mode of order  $\ell$ .*

$$Q_{1M} \geq \frac{1}{2(ka)^3} \left( 1 + \sqrt{1 + 4(ka)^4} \right) + \frac{1}{ka} \quad (3.8.6)$$

In the limit of electrically small antennas:

$$\lim_{ka \Rightarrow 0} Q_{1M} \geq \frac{1}{(ka)^3} + \frac{1}{(ka)} \quad (3.8.7)$$

### 3.9 Chu's Q Analysis, Collocated TM and TE Modes

In addition to analyzing individual moments, Chu also analyzed superimposed (TE + TM) modes of the same order, phased to produce circular polarization. A basic difficulty is that to add modal powers it is necessary to account for phase differences, yet phase information is not contained in the complex power expressions. There are, however, other ways to account for the phase difference; Chu did this by requiring circular polarization. With both modes present and the field circularly polarized, the standing energy oscillates between the radiation fields of the two dipoles.

The average standing electric energy in the TM mode is the capacitive energy obtained using Eq. 3.6.10. Since the TE mode is its exact dual, the magnetic energy stored in the TE mode is equal to the electric energy in the TM mode. Therefore the total standing electric energy is:

$$W_{\ell}(\sigma) = \frac{1}{4\omega^2 C_{\ell}} I_{\ell} I_{\ell}^* + \frac{L_{\ell}}{4} I_{\ell} I_{\ell}^* = \frac{1}{4} I_{\ell} I_{\ell}^* \frac{dX_{\ell}}{d\omega} \quad (3.9.1)$$

The time average radiated power is twice that of Eq. 3.6.12:

$$P_{\ell} = R_{\ell} I_{\ell} I_{\ell}^* = \eta I_{\ell} I_{\ell}^* \frac{(ka)^2}{1 + (ka)^2} \quad (3.9.2)$$

The reactance is given by Eq. 3.6.10. For radiating dipoles the derivative is:

$$\frac{dX_{\ell}}{d\omega} = \frac{(ka)}{\omega} \frac{dX_{\ell}}{d(ka)} = \frac{\eta}{\omega} \frac{[1 + 3(ka)^2]}{(ka)[1 + (ka)^2]^2}$$

Combining the above gives the dipole Q:

$$Q \geq \frac{1 + 3(ka)^2}{2(ka)^3 [1 + (ka)^2]} \cong \frac{1}{2(ka)^3} + \frac{1}{ka} \quad (3.9.3)$$

For electrically small antennas, this Q is approximately half that of either dipole acting alone. The interpretation is that since the standing energy simply moves back and forth between reactive elements the total value is nearly the same as for either dipole acting alone and the radiated energy is twice that of a single dipole. Therefore, Q is reduced by an approximate factor of two.

### 3.10 Q the Easy Way, Electrically Small Antennas

It is possible to solve for  $Q$  from the impedance most easily by use of Chu's equivalent circuits. For antennas electrically small enough so  $\ell(2\ell-1) \gg k^2 a^2$ , the input reactance is dominated by the first reactive element, a capacitor for TM modes and an inductor for TE modes, and  $Q$  is very nearly equal to:

$$Q_\ell = \tan[\zeta_\ell(\sigma)] \quad (3.10.1)$$

Combining Eq. 3.10.1, Chu's equivalent circuits, and the impedance results of Section 3.2 shows that the modal  $Q$ s of electrically small antennas are, very nearly:

$$Q_\ell \geq |\gamma_\ell| \quad (3.10.2)$$

Values of  $\gamma_\ell$  are listed in Table 3.2.1. Keeping only the lead term gives:

$$Q \geq \frac{\ell[(2\ell-1)!!]^2}{(ka)^{2\ell+1}} \quad (3.10.3)$$

### 3.11 Q on the Basis of Time-Dependent Field Theory

The analytical works that follow are based upon the analysis of an idealized radiating sphere. Experimental or numerical confirmation, however, requires actual or numerical embodiments and, in the main, embodiments are made of straight wires and wire loops, not spheres. The analyses to come assume no source coupling between modes and therefore the desired modes, and only those modes, exist.

With this analysis, as with Chu's, only fields at a radius greater than the radius of the virtual, source-containing sphere of radius  $a$  are considered. Ignoring fields at smaller radii has the great advantage that results are not specific to a particular antenna. However, although the interior volume for an electrically small antenna is small, for a fixed moment the field magnitude increases rapidly enough with decreasing radius so the interior

energy remains a significant portion of the total standing energy. As examples, for the spherical shell dipole analyzed in Section A.14 the interior energy is half that of the exterior energy. For biconical transmitting antennas, see Eqs. 2.7.1, the TEM mode and an infinite number of TM modes are included. For biconical receiving antennas, see Eqs. 2.17.2, the TEM mode and infinite numbers both of TM and TE modes are included. Nonetheless, to keep the results general it is necessary to ignore interior fields.

To calculate the Q of a multiport antenna, an antenna driven by more than one terminal pair, it is necessary to account for suppressed phase angles. Since phase angles are an integral part of actual fields, we begin with a general multipolar expansion for phasor fields and then transform phasor fields into actual fields. The phasor form of the multipolar field expansion is:

$$\begin{aligned}
 \tilde{E}_r &= i \sum_{\ell=0}^{\infty} \sum_{m=0}^{\ell} i^{-\ell} F(\ell, m) \ell(\ell+1) \frac{h_{\ell}(\sigma)}{\sigma} P_{\ell}^m(\cos \theta) e^{-i\sigma - jm\phi} \\
 \eta \tilde{H}_r &= -j \sum_{\ell=0}^{\infty} \sum_{m=0}^{\ell} i^{-\ell} G(\ell, m) \ell(\ell+1) \frac{h_{\ell}(\sigma)}{\sigma} P_{\ell}^m(\cos \theta) e^{-i\sigma - jm\phi} \\
 \tilde{E}_{\theta} &= \sum_{\ell=0}^{\infty} \sum_{m=0}^{\ell} i^{-\ell} \left[ i F(\ell, m) h_{\ell}^*(\sigma) \frac{d}{d\theta} P_{\ell}^m(\cos \theta) - G(\ell, m) h_{\ell}(\sigma) \frac{m}{\sin \theta} P_{\ell}^m(\cos \theta) \right] e^{-i\sigma - jm\phi} \\
 \eta \tilde{H}_{\phi} &= \sum_{\ell=0}^{\infty} \sum_{m=0}^{\ell} i^{-\ell} \left[ F(\ell, m) h_{\ell}(\sigma) \frac{d}{d\theta} P_{\ell}^m(\cos \theta) - i G(\ell, m) h_{\ell}^*(\sigma) \frac{m}{\sin \theta} P_{\ell}^m(\cos \theta) \right] e^{-i\sigma - jm\phi} \\
 \tilde{E}_{\phi} &= -j \sum_{\ell=0}^{\infty} \sum_{m=0}^{\ell} i^{-\ell} \left[ i F(\ell, m) h_{\ell}^*(\sigma) \frac{m}{\sin \theta} P_{\ell}^m(\cos \theta) - G(\ell, m) h_{\ell}(\sigma) \frac{d}{d\theta} P_{\ell}^m(\cos \theta) \right] e^{-i\sigma - jm\phi} \\
 \eta \tilde{H}_{\theta} &= j \sum_{\ell=0}^{\infty} \sum_{m=0}^{\ell} i^{-\ell} \left[ F(\ell, m) h_{\ell}(\sigma) \frac{m}{\sin \theta} P_{\ell}^m(\cos \theta) - i G(\ell, m) h_{\ell}^*(\sigma) \frac{d}{d\theta} P_{\ell}^m(\cos \theta) \right] e^{-i\sigma - jm\phi}
 \end{aligned} \tag{3.11.1}$$

We examine the Q of different modes and modal combinations by considering a series of examples.

The first example is the set of TM modes of degree zero. For this case, Chu's "omnidirectional" case, all coefficients except  $F(\ell, 0)$  are equal to zero and, for simplicity in notation, the arbitrary normalizing equality is made that  $F(\ell, 0) \ell^{1-\ell} = 1$ . After replacing Hankel functions by equivalent letter

functions, see Appendix A.26, and accounting for the suppressed time dependence, in terms of retarded time,  $t_R$ , the actual field terms are:

$$\begin{aligned}
 \sigma^2 E_r &= \sum_{\ell=1}^{\infty} \ell(\ell+1) [B_{\ell}(\sigma) \cos(\omega t_R) - A_{\ell}(\sigma) \sin(\omega t_R)] P_{\ell}(\cos \theta) \\
 \sigma E_{\theta} &= \sum_{\ell=1}^{\infty} [D_{\ell}(\sigma) \cos(\omega t_R) - C_{\ell}(\sigma) \sin(\omega t_R)] \frac{d}{d\theta} P_{\ell}(\cos \theta) \\
 \sigma \eta H_{\phi} &= \sum_{\ell=1}^{\infty} [A_{\ell}(\sigma) \cos(\omega t_R) + B_{\ell}(\sigma) \sin(\omega t_R)] \frac{d}{d\theta} P_{\ell}(\cos \theta)
 \end{aligned} \tag{3.11.2}$$

The total energy density,  $w_T$ , at each point in the field is:

$$w_T = \frac{\epsilon}{2} \mathbf{E} \cdot \mathbf{E} + \frac{\mu}{2} \mathbf{H} \cdot \mathbf{H} \tag{3.11.3}$$

Substituting the field forms of Eq. 3.11.2 into the energy density expression shows that for each mode:

$$w_T = \frac{\epsilon}{4} \left[ \frac{\ell^2(\ell+1)^2}{\sigma^4} \left[ (A_{\ell}^2 + B_{\ell}^2) - (A_{\ell}^2 - B_{\ell}^2) \cos(2\omega t_R) - 2A_{\ell}B_{\ell} \sin(2\omega t_R) \right] [P_{\ell}(\cos \theta)]^2 \right. \\
 \left. + \frac{1}{\sigma^2} \left[ (A_{\ell}^2 + B_{\ell}^2 + C_{\ell}^2 + D_{\ell}^2) + (A_{\ell}^2 - B_{\ell}^2 - C_{\ell}^2 + D_{\ell}^2) \cos(2\omega t_R) \right] \left[ \frac{dP_{\ell}(\cos \theta)}{d\theta} \right]^2 \right] \tag{3.11.4}$$

For brevity, the dependence of the letter functions upon  $\sigma$  is suppressed. The right side, top row of Eq. 3.11.4 is the energy of the radial component of the electric field intensity. The remaining terms are the combined energies of the angular field components. The first and second lines have different parity with respect to the zenith angle.

The modal components of the Poynting vector are:

$$\begin{aligned}
N_r &= \frac{1}{2\eta\sigma^2} \left\{ \frac{(A_\ell D_\ell - B_\ell C_\ell) + (A_\ell D_\ell + B_\ell C_\ell) \cos(2\omega t_R)}{-(A_\ell C_\ell - B_\ell D_\ell) \sin(2\omega t_R)} \right\} \left( \frac{dP_\ell(\cos\theta)}{d\theta} \right)^2 \\
N_\theta &= -\frac{\ell(\ell+1)}{2\eta\sigma^3} \left\{ 2A_\ell B_\ell \cos(2\omega t_R) - (A_\ell^2 - B_\ell^2) \sin(2\omega t_R) \right\} P_\ell(\cos\theta) \frac{dP_\ell(\cos\theta)}{d\theta} \\
N_\phi &= 0
\end{aligned} \tag{3.11.5}$$

The continuity equation describes energy conservation in the field, and is:

$$\nabla \bullet \mathbf{N} + \frac{\partial w_T}{\partial t} = 0 \tag{3.11.6}$$

The equality of Eq. 3.11.6 is readily verified by substituting Eqs. 3.11.4 and 3.11.5 and solving.

We seek to separate the total energy density into a part that travels with the wave on its outbound journey and a part that separates from the wave, remaining within the local region of the antenna. Separated power may be calculated by riding with the wave and determining, at each point, the rate at which energy departs from the wave. For this purpose note that the divergence of the power at constant retarded time is equal to the negative rate at which energy per unit volume separates from the wave:

$$\nabla_R \bullet \mathbf{N} = -\frac{\partial w_S}{\partial t_R} \tag{3.11.7}$$

Symbol  $w_S$  indicates the energy density at each point that separates from the outbound wave and oscillates over a distance of  $\lambda/2$ ; we define it to be standing energy density. Symbol  $\nabla_R$  operates at constant retarded time.

The divergence operation of Eq. 3.11.7 is aided by values obtained by taking the derivatives of Table A.26.2.13 and A.26.2.14. The results are:

$$\nabla_R \bullet \mathbf{N}_\theta = \frac{\ell\ell(\ell+1)}{2\eta\sigma^4} \left[ 2A_\ell B_\ell \cos(2\omega t_R) - (A_\ell^2 - B_\ell^2) \sin(2\omega t_R) \right] \left\{ \frac{\ell(\ell+1) [P_\ell(\cos\theta)]^2}{-\left[ \frac{d}{d\theta} P_\ell(\cos\theta) \right]^2} \right\}$$

$$\nabla_R \bullet \mathbf{N}_r = \frac{k}{2\eta\sigma^2} \left[ \frac{d}{d\theta} P_\ell(\cos\theta) \right]^2$$

$$\times \left\{ \begin{aligned} & \left[ 2 \frac{\ell(\ell+1)}{\sigma^2} A_\ell B_\ell - 2(A_\ell - D_\ell)(B_\ell + C_\ell) \right] \cos(2\omega t_R) \\ & - \left[ \frac{\ell(\ell+1)}{\sigma^2} (A_\ell^2 - B_\ell^2) - (A_\ell^2 - B_\ell^2 - C_\ell^2 - D_\ell^2) \right] \sin(2\omega t_R) \\ & + 2(A_\ell D_\ell + B_\ell C_\ell) \end{aligned} \right\} \quad (3.11.8)$$

Summing the components of Eq. 3.11.8 then taking the indefinite integral with respect to retarded time gives:

$$w_S = \frac{\epsilon K}{4} + \frac{\epsilon}{4} \left\{ -\frac{\ell^2(\ell+1)^2}{\sigma^4} \left\{ (A_\ell^2 - B_\ell^2) \cos(2\omega t_R) + 2A_\ell B_\ell \sin(2\omega t_R) \right\} [P_\ell(\cos\theta)]^2 \right. \\ \left. + \frac{1}{\sigma^2} \left\{ [(A_\ell - D_\ell)^2 - (B_\ell + C_\ell)^2] \cos(2\omega t_R) \right\} \left[ \frac{dP_\ell(\cos\theta)}{d\theta} \right]^2 \right. \\ \left. + 2(A_\ell - D_\ell)(B_\ell + C_\ell) \sin(2\omega t_R) \right\} \quad (3.11.9)$$

K is a constant of integration, with dimensions chosen for later convenience. There are two requirements on K: Since it is an energy density it can never be negative and it must appear in the  $w_T$  expression. This is the equivalent of requiring that both zenith angle parities in Eq. 3.11.9 be everywhere greater than or equal to zero. Evaluating K and entering it into Eq. 3.11.9 gives:

$$w_S = \frac{\epsilon}{4} \left\{ \frac{\ell^2(\ell+1)^2}{\sigma^4} \left\{ (A_\ell^2 + B_\ell^2) - (A_\ell^2 - B_\ell^2) \cos(2\omega t_R) - 2A_\ell B_\ell \sin(2\omega t_R) \right\} [P_\ell(\cos\theta)]^2 \right. \\ \left. + \frac{1}{\sigma^2} \left\{ [(A_\ell - D_\ell)^2 + (B_\ell + C_\ell)^2] \right. \right. \\ \left. \left. + [(A_\ell - D_\ell)^2 - (B_\ell + C_\ell)^2] \cos(2\omega t_R) \right. \right. \\ \left. \left. + 2(A_\ell - D_\ell)(B_\ell + C_\ell) \sin(2\omega t_R) \right\} \left[ \frac{dP_\ell(\cos\theta)}{d\theta} \right]^2 \right\} \quad (3.11.10)$$

This is the source-associated energy density. It is separate from the traveling wave and oscillates about a fixed position in the field. The top row of

Eq. 3.11.4 is the energy density of the radial field component and the other terms are the energy densities of the angular field components. Comparison of Eq. 3.11.4 with 3.11.10 shows that the top lines are identical: all energy of the radial field component remains attached to the source. Some energy of the angular field components remains attached to the source and the rest does not.

Subtracting  $w_s$  from  $w_T$  gives the energy that remains part of the traveling wave: the field-associated energy density  $w_\delta$ .

$$w_\delta = \frac{\epsilon}{2\sigma^2} \left[ \frac{(A_\ell D_\ell - B_\ell C_\ell) + (A_\ell D_\ell + B_\ell C_\ell) \cos(2\omega t_R)}{-(A_\ell C_\ell - B_\ell D_\ell) \sin(2\omega t_R)} \right] \left[ \frac{dP_\ell(\cos\theta)}{d\theta} \right]^2 \quad (3.11.11)$$

The expressions for  $N_r$  and  $w_\delta$  differ by a multiplicative factor equal to the speed of light,  $c$ . A characteristic of traveling energy is that power is equal to the product of the energy density and the speed of travel. The movement of  $w_\delta$  produces the radially directed power density. Its value at the generating surface  $r = a$  determines the antenna input impedance. Both  $w_T$  and  $w_s$  are positive real, physical entities, but  $w_\delta$  connotes power and hence can be negative.

For single modes, an alternative and simpler derivation of the standing energy is to divide the radial component of the Poynting vector by  $c$  and subtract the result, Eq. 3.11.11, from the total energy density expression, Eq. 3.11.4. The result repeats the source associated energy density, Eq. 3.11.10. Although the technique is arguably correct for single modes, the process does not generalize to multi-modal situations.

Consider what happens if the source is suddenly disconnected. Since nothing travels outward faster than the speed of light, the originally outbound portion of the field continues without change, and energy  $W_\delta$  is transported on out into free space. Energy  $W_s$  is fixed in position. As the fields at radius less than  $r$  collapse, the energy density exterior to that radius becomes larger than those nearer, producing an inward pressure on the field. We presume, therefore, that energy  $W_s$  returns to the source.

During steady state operation, it is helpful to determine energies at the time a given wave is emitted. In a form of the ergodic theorem this is equal



to energy calculated by summing over the curve in its outward journey. In such terms the total standing energy is equal to the volume integral of  $w_S$ :

$$W_S = \frac{1}{k^3} \int_{ka}^{\infty} \sigma^2 d\sigma \int_0^{2\pi} d\phi \int_0^{\pi} \sin\theta d\theta w_S(\sigma, t_R) \quad (3.11.12)$$

Substituting Eq. 3.11.10 into 3.11.12 and integrating over the full solid angle leaves:

$$W_S = \frac{\pi\epsilon}{k^3} \frac{\ell(\ell+1)}{(2\ell+1)} \int_{ka}^{\infty} d\sigma \left\{ \begin{aligned} &4A_\ell(A_\ell - D_\ell) + \frac{d}{d\sigma}(A_\ell C_\ell + B_\ell D_\ell + 2A_\ell B_\ell) \\ &-\frac{d}{d\sigma}(A_\ell C_\ell - B_\ell D_\ell) \cos(2\omega t_R) \\ &-\frac{d}{d\sigma}(A_\ell D_\ell + B_\ell C_\ell - (-1)^\ell) \sin(2\omega t_R) \end{aligned} \right\} \quad (3.11.13)$$

The radial integrals can be done with the assistance of Table A.26.2.11 through A.26.2.14. Doing the integrals shows the standing energy to be:

$$W_S = \frac{\pi\epsilon}{k^3} \frac{\ell(\ell+1)}{(2\ell+1)} \left\{ \begin{aligned} &-(A_\ell C_\ell + B_\ell D_\ell + 2A_\ell B_\ell) + 4 \int_{\infty}^{ka} d\sigma A_\ell(A_\ell - D_\ell) \\ &+(A_\ell C_\ell - B_\ell D_\ell) \cos(2\omega t_R) \\ &+(A_\ell D_\ell + B_\ell C_\ell - (-1)^\ell) \sin(2\omega t_R) \end{aligned} \right\} \quad (3.11.14)$$

In Eq. 3.11.14, the letter functions are evaluated at  $r = a$ . The peak energy value is:

$$W_{Spk} = \frac{\pi\epsilon}{k^3} \frac{\ell(\ell+1)}{(2\ell+1)} \left\{ \begin{aligned} &-(A_\ell C_\ell + B_\ell D_\ell + 2A_\ell B_\ell) + 4 \int_{\infty}^{ka} d\sigma A_\ell(A_\ell - D_\ell) \\ &+ \sqrt{(A_\ell^2 + B_\ell^2)(C_\ell^2 + D_\ell^2) - 2(-1)^\ell(A_\ell D_\ell + B_\ell C_\ell) + 1} \end{aligned} \right\} \quad (3.11.15)$$

The total output power on the antenna surface is obtained by taking the surface integral of  $N_r$ :

$$P = \frac{\sigma^2}{k^2} \int_0^{2\pi} d\phi \int_0^\pi \sin\theta d\theta N_r(\sigma, t_R) \quad (3.11.16)$$

$$= \frac{\ell(\ell+1)}{\eta k^2(2\ell+1)} \{1 + (A_\ell D_\ell + B_\ell C_\ell) \cos(2\omega t_R) - (A_\ell C_\ell - B_\ell D_\ell) \sin(2\omega t_R)\}$$

By Eq. 3.5.11, the ratio of the peak of Eq. 3.11.15 to the time average of Eq. 3.11.16 determines Q:

$$Q \geq \frac{\omega \mathcal{H}_S|_{\text{peak}}}{P|_{\text{average}}} \quad (3.11.17)$$

Combining Eqs. 3.11.15 with the values of Eq. 3.11.16 and Eq. 3.11.17 to give an expression for the Q of arbitrary mode  $\ell$  of radiation:

$$Q_\ell \geq \frac{1}{2} \left\{ \frac{-(A_\ell C_\ell + B_\ell D_\ell + 2A_\ell B_\ell) + 4 \int_0^{ka} d\sigma A_\ell (A_\ell - D_\ell)}{\sqrt{(A_\ell^2 + B_\ell^2)(C_\ell^2 + D_\ell^2)} - 2(-1)^\ell (A_\ell D_\ell + B_\ell C_\ell) + 1} \right\} \quad (3.11.18)$$

### 3.12 Q of a Radiating Electric Dipole

The actual fields of a time-varying, z-directed electric dipole follow from Eq. 3.11.1. With coefficient  $F(1,0)$  equal to one and with all others equal to zero the fields are:

$$\sigma^2 E_r = -2 \left[ \cos(\omega t_R) + \frac{1}{\sigma} \sin(\omega t_R) \right] \cos\theta$$

$$\sigma E_\theta = \left[ -\frac{1}{\sigma} \cos(\omega t_R) + \left( 1 - \frac{1}{\sigma^2} \right) \sin(\omega t_R) \right] \sin\theta \quad (3.12.1)$$

$$\sigma \eta H_\phi = \left[ -\frac{1}{\sigma} \cos(\omega t_R) + \sin(\omega t_R) \right] \sin\theta$$

The energy densities follow from Eqs. 3.11.4, 3.11.10, and 3.11.11:

$$w_T = \frac{\epsilon}{4} \left\{ \left\{ \frac{4}{\sigma^4} [1 + \cos(2\omega t_R)] + \frac{8}{\sigma^5} \sin(2\omega t_R) + \frac{4}{\sigma^6} [1 - \cos(2\omega t_R)] \right\} \cos^2 \theta \right. \\ \left. + \left\{ \left( \frac{2}{\sigma^2} + \frac{1}{\sigma^6} \right) [1 - \cos(2\omega t_R)] + \frac{4}{\sigma^4} \cos(2\omega t_R) - \left( \frac{4}{\sigma^3} - \frac{2}{\sigma^5} \right) \sin(2\omega t_R) \right\} \sin^2 \theta \right\} \quad (3.12.2)$$

$$w_S = \frac{\epsilon}{4} \left\{ \left\{ \frac{4}{\sigma^4} [1 + \cos(2\omega t_R)] + \frac{8}{\sigma^5} \sin(2\omega t_R) + \frac{4}{\sigma^6} [1 - \cos(2\omega t_R)] \right\} \cos^2 \theta \right. \\ \left. + \frac{1}{\sigma^6} [1 - \cos(2\omega t_R)] \sin^2 \theta \right\} \quad (3.12.3)$$

$$w_S(t_R) = \frac{\epsilon}{2} \left\{ \frac{1}{\sigma^2} [1 - \cos(2\omega t_R)] + \frac{2}{\sigma^4} \cos(2\omega t_R) - \left( \frac{2}{\sigma^3} - \frac{1}{\sigma^5} \right) \sin(2\omega t_R) \right\} \sin^2 \theta \quad (3.12.4)$$

The energy density described by the first lines of Eqs. 3.12.2 and 3.12.3 is centered on the antenna axis and is the energy of the radially directed component of the electric field intensity. The second lines are centered at  $\theta = \pi/2$ ; in Eq. 3.12.2, it is the energy of the angularly directed field components and, in Eq. 3.12.3, it is the energy of the nearest radial field term. Plots of  $w_S$  at four different times are shown in Fig. 3.12.1 for  $ka = 0.1$ ; note the changes of scale.

The components of the Poynting vector follow from Eq. 3.11.5:

$$N_r = \frac{1}{2\eta} \left\{ \frac{1}{\sigma^2} [1 - \cos(2\omega t_R)] + \frac{2}{\sigma^4} \cos(2\omega t_R) - \left( \frac{2}{\sigma^3} - \frac{1}{\sigma^5} \right) \sin(2\omega t_R) \right\} \sin^2 \theta \quad (3.12.5)$$

$$N_\theta = \frac{1}{2\eta} \left\{ -\frac{4}{\sigma^4} \cos(2\omega t_R) + \left( \frac{2}{\sigma^3} - \frac{2}{\sigma^5} \right) \sin(2\omega t_R) \right\} \sin \theta \cos \theta \quad (3.12.6)$$

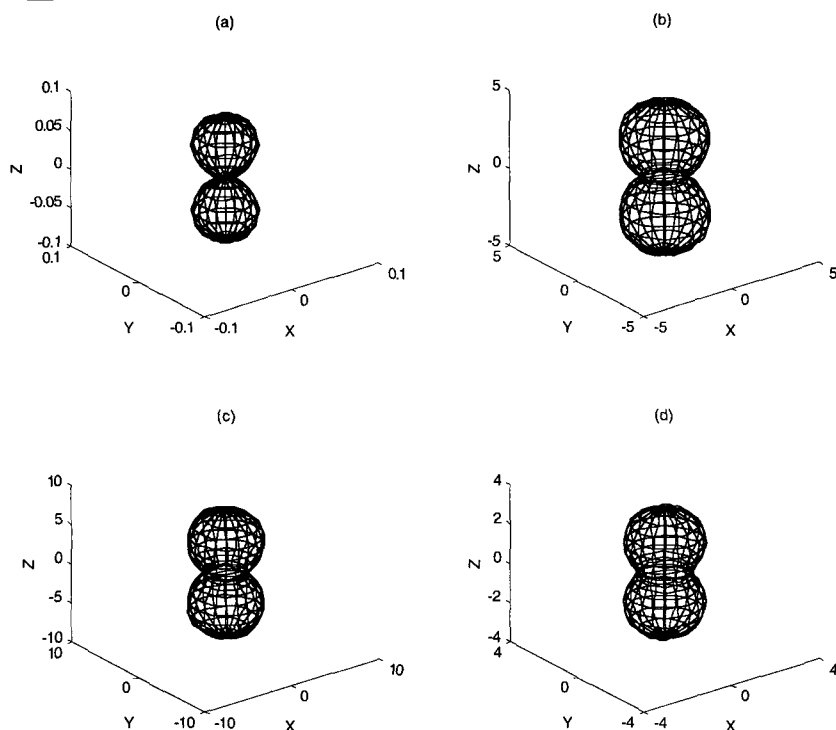


Figure 3.12.1 Standing energy density of a z-directed electric dipole.

Plots are shown at the four times  $2\omega t_R =$  (a) 0, (b)  $\pi/2$ , (c)  $\pi$ , and (d)  $3\pi/2$  at the range  $ka = 0.1$ . Note change of scale on axes. The standing energy density is centered on the z-axis and the far field radiation pattern is centered on the equator. For more detailed plots see:

<http://www.ee.psu.edu/grimes/antennas/breakthrough.htm>

Substituting values of the letter functions into Eq. 3.11.14 gives:

$$W_S = \frac{2\pi\epsilon}{3k^3} \left\{ \frac{2}{(ka)} [1 + \cos(2\omega t_R)] + \frac{2}{(ka)^2} \sin(2\omega t_R) + \frac{1}{(ka)^3} [1 - \cos(2\omega t_R)] \right\} \quad (3.12.7)$$

Similarly evaluating Eq. 3.11.16 gives:

$$p = \frac{4\pi}{3\eta k^2} \left\{ \left[ 1 - \cos(2\omega t_R) \right] + \frac{2}{(ka)^2} \cos(2\omega t_R) - \left( \frac{2}{(ka)} - \frac{1}{(ka)^3} \right) \sin(2\omega t_R) \right\} \quad (3.12.8)$$

To relate Eq. 3.12.8 to the input impedance, rewrite it in the form of time-dependent complex power:

$$P_c = \frac{4\pi}{3\eta k^2} \left\{ \left[ 1 - \cos(2\omega t_R - 2\xi(\sigma)) \right] + \frac{1}{(ka)^3} \sin(2\omega t_R - 2\xi(\sigma)) \right\} \quad (3.12.9)$$

Since the radius of the generating surface is fixed and there is but a single mode, the value of  $\xi(\sigma)$  is unimportant. The complex power follows from Eq. 3.12.9 and is:

$$P_c(\sigma) = \frac{4\pi}{3\eta k^2} \left[ 1 + \frac{i}{(ka)^3} \right] \quad (3.12.10)$$

The antenna input impedance follows from Eq. 3.12.10.

Substituting values of the letter functions into Eq. 3.11.18 gives:

$$Q \geq \frac{1}{2(ka)^3} \left[ 1 + \sqrt{1 + 4(ka)^4} \right] + \frac{1}{(ka)} \quad (3.12.11)$$

This is the same value obtained using the exact analysis of Chu's equivalent circuit, Eq. 3.7.15. In the electrically small limit  $Q$  goes to:

$$Q \geq \frac{1}{(ka)^3} + \frac{1}{(ka)} \quad (3.12.12)$$

Analytical results are summarized in Table 3.12.1.

To examine the effect of coordinate rotation, rotate the dipole from the  $z$ - to the  $x$ -direction. This illustrates the role of antenna rotations that appear in the more complicated modal structures. The force fields of an  $x$ -directed electric dipole follow from Eq. 3.11.1 with  $F(1,1) = 1$ , all other coefficients equal zero, and keeping only the real part with respect to  $j$ , are given by

Eq. 3.12.13. Analytical results are summarized in Table 3.12.2. Power maximum occurs at  $\theta = \pi/2$ .

$$\begin{aligned}
 \sigma^2 E_r &= 2[B \cos(\omega t_R) - A \sin(\omega t_R)] \sin \theta \cos \phi \\
 \sigma E_\theta &= [D \cos(\omega t_R) - C \sin(\omega t_R)] \cos \theta \cos \phi \\
 \sigma \eta H_\phi &= [A \cos(\omega t_R) + B \sin(\omega t_R)] \cos \theta \cos \phi \\
 \sigma E_\phi &= -[D \cos(\omega t_R) - C \sin(\omega t_R)] \sin \phi \\
 \sigma \eta H_\phi &= [A \cos(\omega t_R) + B \sin(\omega t_R)] \sin \phi
 \end{aligned} \tag{3.12.13}$$

---


$$\begin{aligned}
 w_T(t_R) &= \frac{\epsilon}{4} \left\{ \left\{ \frac{4}{\sigma^6} [1 - \cos(2\omega t_R)] + \frac{8}{\sigma^5} \sin(2\omega t_R) + \frac{4}{\sigma^4} [1 + \cos(2\omega t_R)] \right\} \cos^2 \theta \right. \\
 &\quad \left. + \left\{ \left( \frac{2}{\sigma^2} + \frac{1}{\sigma^6} \right) [1 - \cos(2\omega t_R)] + \frac{4}{\sigma^4} \cos(2\omega t_R) - \left( \frac{4}{\sigma^3} - \frac{2}{\sigma^5} \right) \sin(2\omega t_R) \right\} \sin^2 \theta \right\} \\
 w_S(t_R) &= \frac{\epsilon}{4} \left\{ \left\{ \frac{4}{\sigma^6} [1 - \cos(2\omega t_R)] + \frac{8}{\sigma^5} \sin(2\omega t_R) + \frac{4}{\sigma^4} [1 + \cos(2\omega t_R)] \right\} \cos^2 \theta \right. \\
 &\quad \left. + \left\{ \frac{1}{\sigma^6} [1 - \cos(2\omega t_R)] \right\} \sin^2 \theta \right\} \\
 w_\delta(t_R) &= \frac{\epsilon}{2} \left\{ \frac{1}{\sigma^2} [1 - \cos(2\omega t_R)] - \left( \frac{2}{\sigma^3} - \frac{1}{\sigma^5} \right) \sin(2\omega t_R) + \frac{2}{\sigma^4} \cos(2\omega t_R) \right\} \sin^2 \theta \\
 N_r(t_R) &= \frac{1}{2\eta} \left\{ \frac{1}{\sigma^2} [1 - \cos(2\omega t_R)] - \left( \frac{2}{\sigma^3} - \frac{1}{\sigma^5} \right) \sin(2\omega t_R) + \frac{2}{\sigma^4} \cos(2\omega t_R) \right\} \sin^2 \theta \\
 N_\theta(t_R) &= \frac{1}{2\eta} \left[ -\frac{4}{\sigma^4} \cos(2\omega t_R) + \left( \frac{2}{\sigma^3} - \frac{2}{\sigma^5} \right) \sin(2\omega t_R) \right] \sin \theta \cos \theta \\
 N_\phi(t_R) &= 0 \\
 W_S &= \frac{2\pi\epsilon}{3k^3} \left\{ \frac{1}{(ka)^3} [1 - \cos(2\omega t_R)] + \frac{2}{(ka)^2} \sin(2\omega t_R) + \frac{2}{(ka)} [1 + \cos(2\omega t_R)] \right\} \\
 p &= \frac{4\pi}{3\eta k^3} \left\{ [1 - \cos(2\omega t_R)] - \left( \frac{2}{(ka)} - \frac{1}{(ka)^3} \right) \sin(2\omega t_R) + \frac{2}{(ka)^2} \cos(2\omega t_R) \right\} \\
 Q &\geq \frac{1}{2(ka)^3} \left( 1 + \sqrt{1 + 4(ka)^4} \right) + \frac{1}{(ka)} \quad \text{Gain} = \frac{3}{2}
 \end{aligned}$$


---

Table 3.12.1 Radiating, z-Directed Electric Dipole

The force fields of this table result if  $F(1,1) = 1$ , all other coefficients are equal to zero, and only the real part with respect to  $j$  is retained.

---


$$\begin{aligned}
 w_T(t_R) &= \frac{\epsilon}{4} \left\{ 4 \left[ \frac{1}{\sigma^6} [1 - \cos(2\omega t_R)] + \frac{2}{\sigma^5} \sin(2\omega t_R) + \frac{1}{\sigma^4} [1 + \cos(2\omega t_R)] \right] \sin^2 \theta \cos^2 \phi \right. \\
 &\quad \left. + \left[ \left( \frac{2}{\sigma^2} + \frac{1}{\sigma^6} \right) [1 - \cos(2\omega t_R)] + \frac{4}{\sigma^4} \cos(2\omega t_R) - \left( \frac{4}{\sigma^3} - \frac{2}{\sigma^5} \right) \sin(2\omega t_R) \right] \right. \\
 &\quad \left. \times (\cos^2 \theta \cos^2 \phi + \sin^2 \phi) \right\} \\
 w_S(t_R) &= \frac{\epsilon}{4} \left\{ 4 \left[ \frac{1}{\sigma^6} [1 - \cos(2\omega t_R)] + \frac{2}{\sigma^5} \sin(2\omega t_R) + \frac{1}{\sigma^4} [1 + \cos(2\omega t_R)] \right] \sin^2 \theta \cos^2 \phi \right. \\
 &\quad \left. + \frac{1}{\sigma^6} [1 - \cos(2\omega t_R)] (\cos^2 \theta \cos^2 \phi + \sin^2 \phi) \right\} \\
 w_8(t_R) &= \frac{\epsilon}{2} \left\{ \frac{1}{\sigma^2} [1 - \cos(2\omega t_R)] - \left( \frac{2}{\sigma^3} - \frac{1}{\sigma^5} \right) \sin(2\omega t_R) + \frac{2}{\sigma^4} \cos(2\omega t_R) \right\} (\cos^2 \theta \cos^2 \phi + \sin^2 \theta) \\
 N_r(t_R) &= \frac{1}{2\eta} \left\{ \frac{1}{\sigma^2} [1 - \cos(2\omega t_R)] - \left( \frac{2}{\sigma^3} - \frac{1}{\sigma^5} \right) \sin(2\omega t_R) + \frac{2}{\sigma^4} \cos(2\omega t_R) \right\} (\cos^2 \theta \cos^2 \phi + \sin^2 \theta) \\
 N_\theta(t_R) &= \frac{1}{2\eta} \left\{ -\frac{4}{\sigma^4} \cos(2\omega t_R) + \left( \frac{2}{\sigma^3} - \frac{2}{\sigma^5} \right) \sin(2\omega t_R) \right\} \sin \theta \cos \theta \cos^2 \phi \\
 N_\phi(t_R) &= \frac{1}{2\eta} \left\{ -\frac{4}{\sigma^4} \cos(2\omega t_R) + \left( \frac{2}{\sigma^3} - \frac{2}{\sigma^5} \right) \sin(2\omega t_R) \right\} \sin \theta \sin \phi \cos \phi \\
 W_S &= \frac{2\pi\epsilon}{3k^2} \left\{ \frac{1}{(ka)^3} [1 - \cos(2\omega t_R)] + \frac{2}{(ka)^2} \sin(2\omega t_R) + \frac{2}{(ka)} \cos(2\omega t_R) \right\} \\
 p &= \frac{4\pi}{3\eta k^2} \left\{ [1 - \cos(2\omega t_R)] - \left( \frac{2}{ka} - \frac{1}{(ka)^3} \right) \sin(2\omega t_R) + \frac{2}{(ka)^2} \cos(2\omega t_R) \right\} \\
 Q &\geq \frac{1}{2(ka)^3} \left( 1 + \sqrt{1 + 4(ka)^4} \right) + \frac{1}{(ka)}
 \end{aligned}$$


---

Table 3.12.2 Summary of Results, x-Directed Electric Dipole.

### 3.13 Surface Pressure on Dipolar Source

Radiated fields carry with them the kinematic properties of energy, momentum, and angular momentum. These kinematic properties produce both a pressure on the radiating surface, and, in certain special cases, a shear. Consider the pressure on a spherical surface generating the electric dipole field of Eq. 3.12.1. The calculation technique is based upon the three spatial dimensions of Eq. 1.8.2. For a resting sphere, the equation is:

$$F_i^v = \partial T_{ij} / \partial x_j \quad (3.13.1)$$

$\mathbf{F}^v$ , the force per unit volume, is given by Eq. 1.6.14 and the Maxwell stress tensor,  $T_{ij}$ , is given by Eq. 1.8.6. Changing from rectangular to spherical coordinates may be done directly or by extension. The result is equal to:

$$|T_{ij}| = \begin{vmatrix} \left( \frac{\epsilon}{2} [E_r^2 - E_\theta^2 - E_\phi^2] + \frac{\mu}{2} [H_r^2 - H_\theta^2 - H_\phi^2] \right) & (\epsilon E_r E_\theta + \mu H_r H_\theta) & (\epsilon E_r E_\phi + \mu H_r H_\phi) \\ (\epsilon E_\theta E_r + \mu H_\theta H_r) & \left( \frac{\epsilon}{2} [E_\theta^2 - E_\phi^2 - E_r^2] + \frac{\mu}{2} [H_\theta^2 - H_\phi^2 - H_r^2] \right) & (\epsilon E_\theta E_\phi + \mu H_\theta H_\phi) \\ (\epsilon E_\phi E_r + \mu H_\phi H_r) & (\epsilon E_\phi E_\theta + \mu H_\phi H_\theta) & \left( \frac{\epsilon}{2} [E_\phi^2 - E_r^2 - E_\theta^2] + \frac{\mu}{2} [H_\phi^2 - H_r^2 - H_\theta^2] \right) \end{vmatrix} \quad (3.13.2)$$

The off-diagonal terms describe surface shear. Matrix element  $T_{rr}$  describes the surface radiation reaction tension; the net pressure on a radial surface is equal to the difference between exterior and interior surface values of  $T_{rr}$ . Let the generating source be a conducting sphere of radius  $a$  that supports the surface charge and current densities that generate the exterior fields. The exterior fields are those of Eq. 3.12.1, and there are no interior fields. For that case the surface radiation reaction pressure is:

$$T_{rr}(t_R) = \frac{\epsilon}{2} [E_r^2 - E_\theta^2 - E_\phi^2] + \frac{\mu}{2} [H_r^2 - H_\theta^2 - H_\phi^2] = p(t_R) \quad (3.13.3)$$

The expression for  $T_{rr}(t_R)$  at the surface is most easily evaluated from the expression for energy  $w_T(t_R)$  of Table 3.12.1 by reversing the sign of the angular field terms and replacing  $\sigma$  by  $ka$ :



$$p(r) = \frac{\epsilon}{4} \left\{ \begin{aligned} & \left\{ \frac{4}{(ka)^6} [1 - \cos(2\omega t)] + \frac{8}{(ka)^5} \sin(2\omega t) + \frac{4}{(ka)^4} [1 + \cos(2\omega t)] \right\} \cos^2 \theta \\ & - \left\{ \left( \frac{2}{(ka)^2} + \frac{1}{(ka)^6} \right) [1 - \cos(2\omega t)] + \frac{4}{(ka)^4} \cos(2\omega t) \right\} \sin^2 \theta \\ & - \left( \frac{4}{(ka)^3} - \frac{2}{(ka)^5} \right) \sin(2\omega t) \end{aligned} \right\} \quad (3.13.4)$$

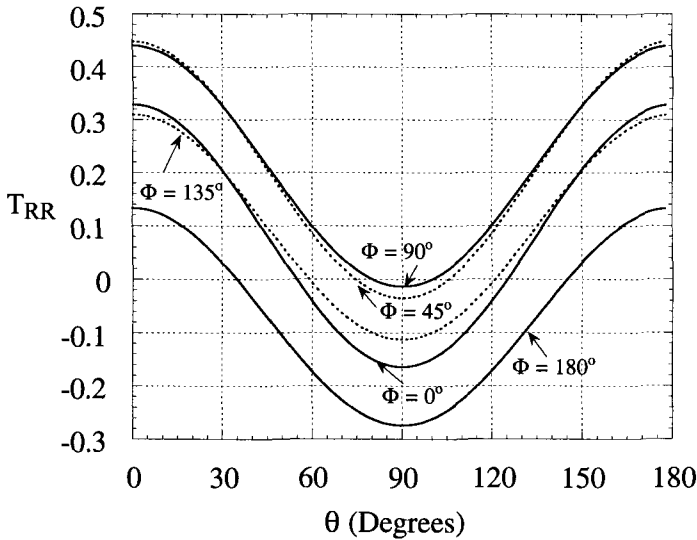


Figure 3.13.1 Surface pressure on a virtual sphere producing a z-directed electric dipole radiation field

$ka = \pi/2$ ,  $\Phi = 2\omega t$ ; all fields at  $ka < \pi/2$  are equal to zero.

A special case of interest is  $ka = \pi/2$ . The pressure on the surface of the virtual sphere for several phases is shown in Fig. 3.13.1. The figure shows pressure,  $p(t)$ , in Pascals as a function of zenith angle at several time phases. The pressure on the z-axis,  $\theta = 0$  and  $\pi$ , is expansive and fluctuates between about 0.13 and 0.45 Pa; the pressure in the  $xy$  plane,  $\theta = \pi/2$ , is compressive

and fluctuates between about 0.02 and 0.27 Pa. At  $\theta = \pi/4$  the pressure alternates between compressive and expansive. Although the figure represents actual pressure on a spherical, conducting surface, for virtual surfaces the pressure is given by Eq. 3.13.1. Commonly, electric dipole antennas are driven from a point source at the origin through a transmission line of approximate length  $\lambda/2$ ; the figure applies to such an antenna with hemispherical, radiating caps; an example is a wide angle biconical antenna.

Since, as Eq. 3.13.4 shows, for antennas with  $ka$  much less than one the surface pressure varies as the sixth power of the product  $ka$ , so does the net force on the radiator. A plot of radiation reaction pressure versus zenith angle for  $ka = 0.1$  is shown in Fig. 3.13.2. The extreme expansive pressure on the z-axis is 2 MPa, and the extreme compressive pressure in the  $xy$ -plane is 0.5 MPa. Whether an electrically small, radiating sphere distorts to become a needle is determined by the relative sizes of these pressures and the physical strength of the source.

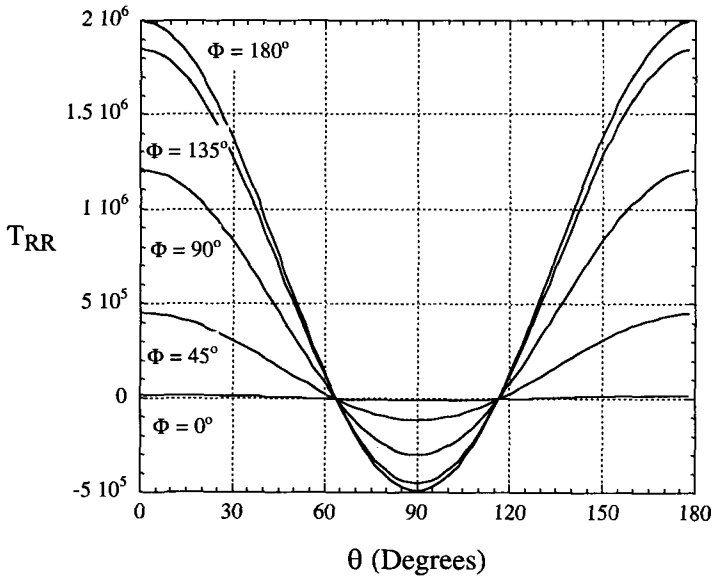


Figure 3.13.2 Surface pressure on a virtual sphere producing a z-directed electric dipole radiation field

$ka = 0.1$ ,  $\Phi = 2\omega t$ ; all fields at  $ka < 0$  are equal to zero.

We conclude that a substantial radiation reaction pressure exists on the surface of an electrically small sphere generating electric dipole radiation from surface sources. The pressure acts to extend the length in the direction of the electric moment and to compress the center region.

Detailed three-dimensional, time-dependent plots of power, energy, and electromagnetic stress in the vicinity of a radiating electric dipole, and of mixed electric and magnetic dipoles are maintained on website:

<<http://www.ee.psu.edu/grimes/antennas/breakthrough.htm>>.

### 3.14 Q of Radiating Magnetic Dipoles

Consider zero degree TE modes. Although the electric dipole fields are the dual of magnetic dipole fields, the sources are physically quite different. Sources of TM and TE fields, see Sections A.28 and A.29, are respectively linear currents and current loops. To obtain the fields, put all coefficients of Eq. 3.11.1 except  $G(\ell, 0)$  equal to zero and, for simplicity in notation, make the arbitrary choice that  $G(\ell, 0)j^{\ell-1} = -1$ . After putting  $j = i$ , replacing Hankel functions by letter functions, and accounting for the suppressed time dependence the actual values of the remaining field terms are:

$$\begin{aligned}\sigma^2 \eta H_r &= \sum_{\ell=1}^{\infty} \ell(\ell+1) [A_{\ell}(\sigma) \cos(\omega t_R) + B_{\ell}(\sigma) \sin(\omega t_R)] P_{\ell}(\cos \theta) \\ \sigma E_{\phi} &= - \sum_{\ell=1}^{\infty} [B_{\ell}(\sigma) \cos(\omega t_R) - A_{\ell}(\sigma) \sin(\omega t_R)] \frac{d}{d\theta} P_{\ell}(\cos \theta) \\ \sigma \eta H_{\theta} &= - \sum_{\ell=1}^{\infty} [C_{\ell}(\sigma) \cos(\omega t_R) + D_{\ell}(\sigma) \sin(\omega t_R)] \frac{d}{d\theta} P_{\ell}(\cos \theta)\end{aligned}\tag{3.14.1}$$

Results of a radiating, z-directed magnetic dipole are tabulated in Tables 3.14.1; magnitudes are identical with the electric dipole case and only the phases of the time-dependent terms differ. The force fields of this table result from Eq. 3.14.1 for case  $\ell = 1$ .

---


$$\begin{aligned}
 w_T(\epsilon_R) &= \frac{\epsilon}{4} \left\{ \left\{ \frac{4}{\sigma^6} [1 + \cos(2\omega\epsilon_R)] - \frac{8}{\sigma^5} \sin(2\omega\epsilon_R) + \frac{4}{\sigma^4} [1 - \cos(2\omega\epsilon_R)] \right\} \cos^2 \theta \right. \\
 &\quad \left. + \left\{ \left( \frac{2}{\sigma^2} + \frac{1}{\sigma^6} \right) [1 + \cos(2\omega\epsilon_R)] - \frac{4}{\sigma^4} \cos(2\omega\epsilon_R) + \left( \frac{4}{\sigma^3} - \frac{2}{\sigma^5} \right) \sin(2\omega\epsilon_R) \right\} \sin^2 \theta \right\} \\
 w_S(\epsilon_R) &= \frac{\epsilon}{4} \left\{ \left\{ \frac{4}{\sigma^6} [1 + \cos(2\omega\epsilon_R)] - \frac{8}{\sigma^5} \sin(2\omega\epsilon_R) + \frac{4}{\sigma^4} [1 - \cos(2\omega\epsilon_R)] \right\} \cos^2 \theta \right. \\
 &\quad \left. + \left\{ \frac{1}{\sigma^6} [1 + \cos(2\omega\epsilon_R)] \right\} \sin^2 \theta \right\} \\
 w_\delta(\epsilon_R) &= \frac{\epsilon}{2} \left\{ \frac{1}{\sigma^2} [1 + \cos(2\omega\epsilon_R)] + \left( \frac{2}{\sigma^3} - \frac{1}{\sigma^5} \right) \sin(2\omega\epsilon_R) - \frac{2}{\sigma^4} \cos(2\omega\epsilon_R) \right\} \sin^2 \theta \\
 N_r(\epsilon_R) &= \frac{1}{2\eta} \left\{ \frac{1}{\sigma^2} [1 + \cos(2\omega\epsilon_R)] + \left( \frac{2}{\sigma^3} - \frac{1}{\sigma^5} \right) \sin(2\omega\epsilon_R) - \frac{2}{\sigma^4} \cos(2\omega\epsilon_R) \right\} \sin^2 \theta \\
 N_\theta(\epsilon_R) &= \frac{1}{2\eta} \left\{ -\frac{4}{\sigma^4} \cos(2\omega\epsilon_R) + \left( \frac{2}{\sigma^3} - \frac{2}{\sigma^5} \right) \sin(2\omega\epsilon_R) \right\} \sin \theta \cos \theta \\
 &\quad - \frac{1}{\eta} \left\{ \frac{1}{\sigma^6} [1 - \cos(2\omega\epsilon_R)] + \frac{2}{\sigma^4} \cos(2\omega\epsilon_R) - \left( \frac{1}{\sigma^3} - \frac{2}{\sigma^5} \right) \sin(2\omega\epsilon_R) \right\} \sin \theta \\
 N_\phi(\epsilon_R) &= 0 \\
 W_S &= \frac{2\pi\epsilon}{3k^3} \left\{ \frac{1}{(ka)^3} [1 + \cos(2\omega\epsilon_R)] - \frac{2}{(ka)^2} \sin(2\omega\epsilon_R) + \frac{2}{(ka)} [1 - \cos(2\omega\epsilon_R)] \right\} \\
 p &= \frac{4\pi}{3\eta k^3} \left\{ [1 + \cos(2\omega\epsilon_R)] + \left( \frac{2}{(ka)} - \frac{1}{(ka)^3} \right) \sin(2\omega\epsilon_R) - \frac{2}{(ka)^2} \cos(2\omega\epsilon_R) \right\} \\
 Q &\geq \frac{1}{2(ka)^3} \left( 1 + \sqrt{1 + 4(ka)^4} \right) + \frac{1}{(ka)} \quad \text{Gain} = \frac{3}{2}
 \end{aligned}$$


---

Table 3.14.1 Radiating, z-Directed Magnetic Dipole

### 3.15 Q of Collocated Electric and Magnetic Dipole Pair

Since the TE and TM field components of z-directed antennas do not overlap, when evaluating the energy densities it is necessary to determine the integration constants for each solution *before* summing over the vector fields. The vector field equations for  $F(1,0) = -G(1,0) = 1$ , all other coefficients are equal to zero, and  $j = i$  are shown in Eqs. 3.15.1.

$$\begin{aligned}
\sigma^2 E_r &= -2 \left[ \cos(\omega t_R) + \frac{1}{\sigma} \sin(\omega t_R) \right] \cos \theta \\
\sigma^2 \eta H_r &= 2 \left[ -\frac{1}{\sigma} \cos(\omega t_R) + \sin(\omega t_R) \right] \cos \theta \\
\sigma E_\theta &= \left[ -\frac{1}{\sigma} \cos(\omega t_R) + \left( 1 - \frac{1}{\sigma^2} \right) \sin(\omega t_R) \right] \sin \theta \\
\sigma \eta H_\phi &= \left[ -\frac{1}{\sigma} \cos(\omega t_R) + \sin(\omega t_R) \right] \sin \theta \\
\sigma E_\phi &= - \left[ \cos(\omega t_R) + \frac{1}{\sigma} \sin(\omega t_R) \right] \sin \theta \\
\sigma \eta H_\theta &= \left[ \left( 1 - \frac{1}{\sigma^2} \right) \cos(\omega t_R) + \frac{1}{\sigma} \sin(\omega t_R) \right] \sin \theta
\end{aligned} \tag{3.15.1}$$

The far field is circularly polarized. A table of dynamic values similar to those of Tables 3.12.1 and 3.14.1 is given in Table 3.15.1. The three energy densities and the radial component of the Poynting vector are all time-independent. Since there are two sources, each of which produces the same average output power as listed in Tables 12.1 and 13.1, the time-average value for this case is double that of the previous cases. The zenith and azimuth components of the Poynting vector respectively are and are not equal to zero. The gain and pattern are the same as for individual dipoles. Since the total standing energy of both dipoles is nearly equal to the peak value of either,  $Q$  is about half that of an isolated dipole.

If the phase of the magnetic dipole of Table 3.15.1 is shifted by  $\pi/2$ , so  $G(1,0) = -i$ , the TM modal terms are the same as listed in Eq. 3.12.1 and the TE modal terms are given by Eq. 3.15.2:

---


$$\begin{aligned}
 w_T &= \frac{\varepsilon}{2} \left\{ \left( \frac{4}{\sigma^6} + \frac{4}{\sigma^4} \right) \cos^2 \theta + \left( \frac{2}{\sigma^2} + \frac{1}{\sigma^6} \right) \sin^2 \theta \right\} \\
 w_S &= \frac{\varepsilon}{2} \left\{ \left( \frac{4}{\sigma^6} + \frac{4}{\sigma^4} \right) \cos^2 \theta + \frac{1}{\sigma^6} \sin^2 \theta \right\}; & w_D &= \frac{\varepsilon}{\sigma^2} \sin^2 \theta \\
 N_r(t_R) &= \frac{1}{\eta \sigma^2} \sin^2 \theta; & N_\theta(t_R) &= 0; & N_\phi(t_R) &= -\frac{2}{\eta \sigma^3} \sin \theta \cos \theta \\
 W_S &= \frac{8\pi\varepsilon}{3k^3} \left[ \frac{1}{2(ka)^3} + \frac{1}{(ka)} \right]; & p &= \frac{8\pi}{3\eta k^2} \\
 Q &\geq \frac{1}{2(ka)^3} + \frac{1}{(ka)} & \text{Gain} &= \frac{3}{2}
 \end{aligned}$$


---

Table 3.15.1 Collocated, Radiating z-Directed Electric and Magnetic Dipoles Producing Circularly Polarized Fields

$$\sigma^2 \eta H_r = 2 \left[ \cos(\omega t_R) + \frac{1}{\sigma} \sin(\omega t_R) \right] \cos \theta$$

$$\sigma E_\phi = - \left[ \frac{1}{\sigma} \cos(\omega t_R) - \sin(\omega t_R) \right] \sin \theta \quad (3.15.2)$$

$$\sigma \eta H_\theta = \left[ \frac{1}{\sigma} \cos(\omega t_R) - \left( 1 - \frac{1}{\sigma^2} \right) \sin(\omega t_R) \right] \sin \theta$$

The powers and energies produced by the electric and magnetic moments are in phase. Time-dependent powers sum to twice the values of Table 3.12.1. Both gain and Q are equal to those of Table 3.12.1.

Although the integration constant is introduced quite differently in collocated parallel and crossed moments, the calculated Q is the same.

Next consider collocated x-directed electric dipole and y-directed magnetic dipole sources. For this configuration the fields strongly overlap and the integration constant is determined *after* summing over the vector fields. Fields with  $F(1,1) = 1$ ,  $G(1,1) = -i$ , all other coefficients are equal to zero, and  $j = i$  are listed in Eq. 3.15.3:

$$\begin{aligned}
\sigma^2 E_r &= -2 \left[ \cos(\omega t_R) + \frac{1}{\sigma} \sin(\omega t_R) \right] \sin \theta \cos \phi \\
\sigma^2 \eta H_r &= -2 \left[ \cos(\omega t_R) + \frac{1}{\sigma} \sin(\omega t_R) \right] \sin \theta \sin \phi \\
\sigma E_\theta &= \left\{ \left[ \frac{1}{\sigma} \cos(\omega t_R) - \sin(\omega t_R) \right] \right. \\
&\quad \left. + \left[ \frac{1}{\sigma} \cos(\omega t_R) - \left( 1 - \frac{1}{\sigma^2} \right) \sin(\omega t_R) \right] \cos \theta \right\} \cos \phi \\
\sigma E_\phi &= - \left\{ \left[ \frac{1}{\sigma} \cos(\omega t_R) - \sin(\omega t_R) \right] \cos \theta \right. \\
&\quad \left. + \left[ \frac{1}{\sigma} \cos(\omega t_R) - \left( 1 - \frac{1}{\sigma^2} \right) \sin(\omega t_R) \right] \right\} \sin \phi \\
\eta H_\phi &= -E_\phi \cot \phi; \quad \eta H_\theta = E_\phi \tan \phi
\end{aligned} \tag{3.15.3}$$

Far fields are linearly polarized. Dynamic values are listed in Table 3.15.2. As in the case of Eq. 3.15.2 the energy and power terms are in phase, the energy and power terms are doubled, and  $Q$  is equal to that of either dipole radiating in isolation. The radial and zenith portions of the Poynting vector contain factors that are proportional, respectively, to  $\cos \theta$  and  $\sin \theta$ . The terms are suppressed in the Table since they do not affect the total energies.

If the relative phasing of the dipoles is  $F(1,1) = 1$ ,  $G(1,1) = -1$ , all other coefficients are equal to zero, and  $j = i$  the fields of Eq. 3.15.4 result

$$\begin{aligned}
\sigma^2 E_r &= 2[B \cos(\omega t_R) - A \sin(\omega t_R)] \sin \theta \cos \phi \\
\sigma^2 \eta H_r &= 2[A \cos(\omega t_R) + B \sin(\omega t_R)] \sin \theta \sin \phi \\
\sigma E_\theta &= \{[D \cos(\omega t_R) - C \sin(\omega t_R)] \cos \theta - [B \cos(\omega t_R) - A \sin(\omega t_R)]\} \cos \phi \\
\eta \sigma H_\phi &= \{[A \cos(\omega t_R) + B \sin(\omega t_R)] \cos \theta + [C \cos(\omega t_R) + D \sin(\omega t_R)]\} \cos \phi \\
\sigma E_\phi &= -\{[D \cos(\omega t_R) - C \sin(\omega t_R)] - [B \cos(\omega t_R) - A \sin(\omega t_R)] \cos \theta\} \sin \phi \\
\eta \sigma H_\theta &= \{[A \cos(\omega t_R) + B \sin(\omega t_R)] + [C \cos(\omega t_R) + D \sin(\omega t_R)] \cos \theta\} \sin \phi
\end{aligned} \tag{3.15.4}$$

---


$$\begin{aligned}
 w_T(\iota_R) &= \frac{\epsilon}{4} \left\{ \left\{ \frac{4}{\sigma^6} [1 - \cos(2\omega\iota_R)] + \frac{8}{\sigma^5} \sin(2\omega\iota_R) + \frac{4}{\sigma^4} [1 + \cos(2\omega\iota_R)] \right\} \sin^2 \theta \right. \\
 &\quad \left. + \left\{ \left( \frac{2}{\sigma^2} + \frac{1}{\sigma^6} \right) [1 - \cos(2\omega\iota_R)] \right. \right. \\
 &\quad \left. \left. + \frac{4}{\sigma^4} \cos(2\omega\iota_R) - \left( \frac{4}{\sigma^3} - \frac{2}{\sigma^5} \right) \sin(2\omega\iota_R) \right\} (1 + \cos^2 \theta) \right\} \\
 w_S(\iota_R) &= \frac{\epsilon}{4} \left\{ \left\{ \frac{4}{\sigma^6} [1 - \cos(2\omega\iota_R)] + \frac{8}{\sigma^5} \sin(2\omega\iota_R) + \frac{4}{\sigma^4} [1 + \cos(2\omega\iota_R)] \right\} \sin^2 \theta \right. \\
 &\quad \left. + \left\{ \frac{1}{\sigma^6} [1 - \cos(2\omega\iota_R)] \right\} (1 + \cos^2 \theta) \right\} \\
 w_8(\iota_R) &= \frac{\epsilon}{2} \left\{ \frac{1}{\sigma^2} [1 - \cos(2\omega\iota_R)] + \frac{2}{\sigma^4} \cos(2\omega\iota_R) - \left( \frac{2}{\sigma^3} - \frac{1}{\sigma^5} \right) \sin(2\omega\iota_R) \right\} (1 + \cos^2 \theta) \\
 N_r(\iota_R) &= \frac{1}{2\eta} \left\{ \frac{1}{\sigma^2} [1 - \cos(2\omega\iota_R)] + \frac{2}{\sigma^4} \cos(2\omega\iota_R) - \left( \frac{2}{\sigma^3} - \frac{1}{\sigma^5} \right) \sin(2\omega\iota_R) \right\} (1 + \cos^2 \theta)^2 \\
 N_\theta(\iota_R) &= \frac{1}{\eta} \left[ \frac{2}{\sigma^4} \cos(2\omega\iota_R) - \left( \frac{1}{\sigma^3} - \frac{1}{\sigma^5} \right) \sin(2\omega\iota_R) \right] \sin \theta \cos \theta; \quad N_\phi(\iota_R) = 0 \\
 W_S(\iota) &= \frac{4\pi\epsilon}{3k^3} \left\{ \frac{1}{(ka)^3} [1 - \cos(2\omega\iota_R)] + \frac{2}{(ka)^2} \sin(2\omega\iota_R) + \frac{2}{(ka)} [1 + \cos(2\omega\iota_R)] \right\} \\
 p &= \frac{8\pi}{3\eta\kappa^3} \left\{ [1 - \cos(2\omega\iota_R)] - \left( \frac{2}{(ka)} - \frac{1}{(ka)^3} \right) \sin(2\omega\iota_R) + \frac{2}{(ka)^2} \cos(2\omega\iota_R) \right\} \\
 Q &\geq \frac{1}{2(ka)^3} \left( 1 + \sqrt{1 + 4(ka)^4} \right) + \frac{1}{(ka)} \quad \text{Gain} = 3
 \end{aligned}$$


---

Table 3.15.2 Collocated, Radiating z-Directed Electric and Magnetic Dipoles  
Producing Linearly Polarized Fields

Output power is centered on the positive  $z$ -axis and is equal to zero on the negative  $z$ -axis. The far field is circularly polarized. Dynamic values are listed in Table 3.15.3; again power and energy terms proportional to  $\cos \theta$  are ignored.  $Q$  is reduced below that of Table 3.15.1. This is because some of the energy that is source-associated with parallel radiating elements becomes field-associated with orthogonal elements.



---


$$\begin{aligned}
 w_r(t_R) &= \frac{\varepsilon}{2} \left\{ \left( \frac{2}{\sigma^4} + \frac{2}{\sigma^6} \right) \sin^2 \theta + \left[ \left( \frac{2}{\sigma^4} - \frac{2}{\sigma^6} \right) \cos(2\omega t_R) + \frac{4}{\sigma^5} \sin(2\omega t_R) \right] \sin^2 \theta \cos(2\phi) \right. \\
 &\quad \left. + \left( \frac{1}{\sigma^2} + \frac{1}{2\sigma^6} \right) (1 + \cos^2 \theta) \right. \\
 &\quad \left. + \left[ \left( \frac{1}{\sigma^2} - \frac{2}{\sigma^4} + \frac{1}{2\sigma^6} \right) \cos(2\omega t_R) + \left( \frac{2}{\sigma^3} - \frac{1}{\sigma^5} \right) \sin(2\omega t_R) \right] \sin^2 \theta \cos(2\phi) \right\} \\
 w_s(t_R) &= \frac{\varepsilon}{2} \left\{ \left( \frac{2}{\sigma^4} + \frac{2}{\sigma^6} \right) \sin^2 \theta + \left[ \left( \frac{2}{\sigma^4} - \frac{3}{2\sigma^6} \right) \cos(2\omega t_R) + \frac{4}{\sigma^5} \sin(2\omega t_R) \right] \sin^2 \theta \cos(2\phi) \right\} \\
 w_\delta(t_R) &= \frac{\varepsilon}{2} \left\{ \left( \frac{1}{\sigma^2} + \frac{1}{2\sigma^6} \right) (1 + \cos^2 \theta) \right. \\
 &\quad \left. + \left[ \left( \frac{1}{\sigma^2} - \frac{2}{\sigma^4} \right) \cos(2\omega t_R) + \left( \frac{2}{\sigma^3} - \frac{1}{\sigma^5} \right) \sin(2\omega t_R) \right] \sin^2 \theta \cos(2\phi) \right\} \\
 N_r &= \frac{1}{2\eta} \left\{ \frac{1}{\sigma^2} (1 + \cos^2(\theta)) + \left[ \left( \frac{1}{\sigma^2} - \frac{2}{\sigma^4} \right) \cos(2\omega t) + \left( \frac{2}{\sigma^3} - \frac{1}{\sigma^5} \right) \sin(2\omega t) \right] \sin^2(\theta) \cos(2\phi) \right\} \\
 N_\theta &= \frac{1}{\eta} \left\{ \frac{2}{\sigma^4} \cos(2\omega t_R) - \left( \frac{1}{\sigma^3} - \frac{1}{\sigma^5} \right) \sin(2\omega t_R) \right\} \sin \theta \cos \theta \cos(2\phi) \\
 N_\phi &= \frac{1}{\eta} \left\{ -\frac{1}{\sigma^3} \cos \theta + \left[ -\frac{2}{\sigma^4} \cos(2\omega t_R) + \left( \frac{1}{\sigma^3} - \frac{1}{\sigma^5} \right) \sin(2\omega t_R) \right] \right\} \sin \theta \sin(2\phi) \\
 W_s &= \frac{8\pi\varepsilon}{3k^3} \left[ \frac{1}{3(ka)^3} + \frac{1}{(ka)} \right]; \quad p = \frac{8\pi}{3\eta k^2} \\
 Q &\geq \frac{1}{3(ka)^3} + \frac{1}{(ka)}
 \end{aligned}$$


---

Table 3.15.3 Collocated, Radiating z-Directed Electric and Magnetic Dipole Pair Producing Circularly Polarized Fields

### 3.16 Q of Collocated, Perpendicular Electric Dipoles

This example is two collocated, perpendicularly directed electric dipoles driven  $\pi/2$  out of phase. These force fields, Eq. 3.16.1, result if coefficient  $F(1,1) = 1$ , all others are zero, and  $j = i$ . Output power is centered at  $\theta = \pi/2$  and circularly polarized. As with the perpendicular electric and magnetic dipoles of Table 3.15.2, since the field components strongly overlap energy

densities are combined before the integration constant is evaluated. The result is similar to in-phase electric and magnetic moments in that the standing energy of the two dipoles peak out of phase, and the peak standing energy is about equal to that of a single dipole. Since the output power is twice that of a single dipole, Q is reduced by about a factor of two. This is similar to, and for the same reason as, the reduction in Q shown in Table 3.15.1.

$$\begin{aligned}
 \sigma^2 E_r &= 2[B_1 \cos(\omega t_R - \phi) - A_1 \sin(\omega t_R - \phi)] \sin \theta \\
 \sigma E_\theta &= [D_1 \cos(\omega t_R - \phi) - C_1 \sin(\omega t_R - \phi)] \cos \theta \\
 \sigma \eta H_\phi &= [A_1 \cos(\omega t_R - \phi) + B_1 \sin(\omega t_R - \phi)] \cos \theta \\
 \sigma E_\phi &= [C_1 \cos(\omega t_R - \phi) + D_1 \sin(\omega t_R - \phi)] \\
 \sigma \eta H_\theta &= [B_1 \cos(\omega t_R - \phi) - A_1 \sin(\omega t_R - \phi)]
 \end{aligned} \tag{3.16.1}$$

The azimuth energy flow produces a z-directed angular momentum. Results are listed in Table 3.16.1. Different from the previous electric dipole cases, but like the counterpart of Table 3.15.3, a term proportional to  $\sigma^{-6}$  appears as part of the outgoing energy. It forms part of the standing energy in other special cases; among the results is that the  $w_\delta/N_r$  ratio is no longer equal to  $c$ . The energy shifts position from standing to traveling energy and results in Q being further reduced, to the value of Table 3.15.3.

### 3.17 Four Collocated Electric and Magnetic Dipoles and Multipoles

#### *Dipoles*

Table 3.17.1 tabulates results of four collocated electric and magnetic dipoles generating equal time-average output powers. The electric dipoles have the same orientation and phasing as the example of Table 3.16.1. The magnetic dipoles have the same orientation and phasing as the electric ones, and produce the dual results of Table 3.16.1. Electric and magnetic dipole pairs lie along both the  $x$ - and  $y$ -axes. Two pairs of electric and magnetic dipoles are formed into two units and driven in phase quadrature. Since the resulting circularly polarized field components overlap, the energy densities

$$\begin{aligned}
w_T(t_R) &= \frac{\epsilon}{4} \left\langle \left\{ \left[ \frac{4}{\sigma^6} [1 - \cos(2\omega t_R - 2\phi)] + \frac{8}{\sigma^5} \sin(2\omega t_R - 2\phi) + \frac{4}{\sigma^4} [1 + \cos(2\omega t_R - 2\phi)] \right] \sin^2 \theta \right\} \right. \\
&\quad \left. + \left\{ \left( \frac{2}{\sigma^2} + \frac{1}{\sigma^6} \right) (1 + \cos^2 \theta) \right. \right. \\
&\quad \left. \left. + \left[ \left( \frac{2}{\sigma^2} - \frac{4}{\sigma^4} + \frac{1}{\sigma^6} \right) \cos(2\omega t_R - 2\phi) + \left( \frac{4}{\sigma^3} - \frac{2}{\sigma^5} \right) \sin(2\omega t_R - 2\phi) \right] \sin^2 \theta \right\} \right\rangle \\
w_S(t_R) &= \frac{\epsilon}{4} \left\{ \frac{1}{\sigma^6} [4 - 3\cos(2\omega t_R - 2\phi)] + \frac{8}{\sigma^5} \sin(2\omega t_R - 2\phi) + \frac{4}{\sigma^4} [1 + \cos(2\omega t_R - 2\phi)] \right\} \sin^2 \theta \\
w_8(t_R) &= \frac{\epsilon}{2} \left\{ \left( \frac{1}{\sigma^2} + \frac{1}{2\sigma^6} \right) (1 + \cos^2 \theta) \right. \\
&\quad \left. + \left[ \left( \frac{1}{\sigma^2} - \frac{2}{\sigma^4} \right) \cos(2\omega t_R - 2\phi) + \left( \frac{2}{\sigma^3} - \frac{1}{\sigma^5} \right) \sin(2\omega t_R - 2\phi) \right] \sin^2 \theta \right\} \\
N_r(t_R) &= \frac{1}{2\eta} \left\{ \frac{1}{\sigma^2} (1 + \cos^2 \theta) + \left[ \left( \frac{1}{\sigma^2} - \frac{2}{\sigma^4} \right) \cos(2\omega t_R - 2\phi) + \left( \frac{2}{\sigma^3} - \frac{1}{\sigma^5} \right) \sin(2\omega t_R - 2\phi) \right] \sin^2 \theta \right\} \\
N_\theta(t_R) &= \frac{1}{\eta} \left\{ \frac{2}{\sigma^4} \cos(2\omega t_R - 2\phi) - \left( \frac{1}{\sigma^3} - \frac{1}{\sigma^5} \right) \sin(2\omega t_R - 2\phi) \right\} \sin \theta \cos \theta \\
N_\phi(t_R) &= \frac{1}{\eta} \left\{ \left( \frac{1}{\sigma^3} + \frac{1}{\sigma^5} \right) + \left( \frac{1}{\sigma^3} - \frac{1}{\sigma^5} \right) \cos(2\omega t_R - 2\phi) + \frac{2}{\sigma^4} \sin(2\omega t_R - 2\phi) \right\} \sin \theta \\
W_S &= \frac{8\pi\epsilon}{3k^3} \left[ \frac{1}{3(ka)^3} + \frac{1}{(ka)} \right] \quad p = \frac{8\pi}{3\eta k^2} \\
Q &\geq \left[ \frac{1}{3(ka)^3} + \frac{1}{(ka)} \right] \quad \text{Gain} = \frac{3}{2}
\end{aligned}$$

Table 3.16.1 Radiating x- and y-Directed Electric Dipoles, Circular Polarization

are combined before the integration constant is evaluated. Since no net energy leaves the traveling wave in its journey from the antenna surface to infinity, there is no source associated standing energy. The vector fields are:

$$\begin{aligned}
\sigma^2 E_r &= 2[B_1 \cos(\omega t_R - \phi) - A_1 \sin(\omega t_R - \phi)] \sin \theta \\
\sigma^2 \eta H_r &= -2[A_1 \cos(\omega t_R - \phi) + B_1 \sin(\omega t_R - \phi)] \sin \theta \\
\sigma E_\theta &= \{[D_1 \cos(\omega t_R - \phi) - C_1 \sin(\omega t_R - \phi)] \cos \theta + [A_1 \cos(\omega t_R - \phi) + B_1 \sin(\omega t_R - \phi)]\} \\
\sigma \eta H_\theta &= \{[A_1 \cos(\omega t_R - \phi) + B_1 \sin(\omega t_R - \phi)] \cos \theta + [D_1 \cos(\omega t_R - \phi) - C_1 \sin(\omega t_R - \phi)]\} \\
\sigma E_\phi &= \{-[B_1 \cos(\omega t_R - \phi) - A_1 \sin(\omega t_R - \phi)] \cos \theta + [C_1 \cos(\omega t_R - \phi) + D_1 \sin(\omega t_R - \phi)]\} \\
\sigma \eta H_\phi &= \{-[C_1 \cos(\omega t_R - \phi) + D_1 \sin(\omega t_R - \phi)] \cos \theta + [B_1 \cos(\omega t_R - \phi) - A_1 \sin(\omega t_R - \phi)]\}
\end{aligned} \tag{3.17.1}$$

Resonance depends upon the equality of the field coefficients  $F(1,1)$  and  $-G(1,1)$ . If the criterion  $F(1,1) = -G(1,1)$  is met, and  $j = i$ , the input equivalent circuit is a simple resistor and  $Q$  is equal to zero.

The pressure on a virtual sphere generating these field modes follows in the same way as the example of Section 3.13. The radial field component of the Maxwell stress tensor follows from the expression for  $w_T(t_R)$ , and is:

$$T_{rr} = \frac{\epsilon}{2} \left\{ \left( \frac{4}{\sigma^4} + \frac{4}{\sigma^6} \right) \sin^2 \theta - \left( \frac{2}{\sigma^2} + \frac{1}{\sigma^6} \right) (1 + \cos^2 \theta) - \frac{4}{\sigma^2} \cos \theta \right\} \quad (3.17.2)$$

---


$$w_T = \frac{\epsilon}{2} \left\{ \left( \frac{4}{\sigma^4} + \frac{4}{\sigma^6} \right) \sin^2 \theta + \left( \frac{2}{\sigma^2} + \frac{1}{\sigma^6} \right) (1 + \cos^2 \theta) + \frac{4}{\sigma^2} \cos \theta \right\}$$

$$w_S = 0$$

$$w_\delta = \frac{\epsilon}{2} \left\{ \left( \frac{4}{\sigma^4} + \frac{4}{\sigma^6} \right) \sin^2 \theta + \left( \frac{2}{\sigma^2} + \frac{1}{\sigma^6} \right) (1 + \cos^2 \theta) + \frac{4}{\sigma^2} \cos \theta \right\}$$

$$N_r = \frac{1}{\eta \sigma^2} \left\{ (1 + \cos^2 \theta) + \left( 2 + \frac{1}{\sigma^4} \right) \cos \theta \right\}$$

$$N_\theta = \frac{2}{\eta \sigma^6} \sin \theta$$

$$N_\phi = \frac{2}{\eta} \left[ \frac{1}{\sigma^3} \cos \theta + \left( \frac{1}{\sigma^3} + \frac{1}{\sigma^5} \right) \right] \sin \theta$$

$$w_S = 0 \quad p = \frac{16\pi}{3\eta k^2}$$

$$Q \geq 0 \quad \text{Gain} = 3$$


---

Table 3.17.1 Four superimposed  $x$ - and  $y$ -directed electric and magnetic dipoles, circular polarization

This equation shows the surface pressure to be independent of time. In free space, all fields are continuous across virtual boundaries and the pressure gradient is given by the spatial directional derivative of Eq. 3.17.2.

Figures 3.17.1-3.17.3 show the radiation reaction pressure, Eq. 3.17.2, on virtual spheres of radii  $ka = 5, 1$ , and  $0.1$  if all fields at smaller values of

radius are equal to zero. The radiation reaction pressure is expansive in the direction of the moments,  $\theta = \pi/2$ , and compressive along the  $z$ -axis. In both cases the pressure decreases rapidly with increasing radius.

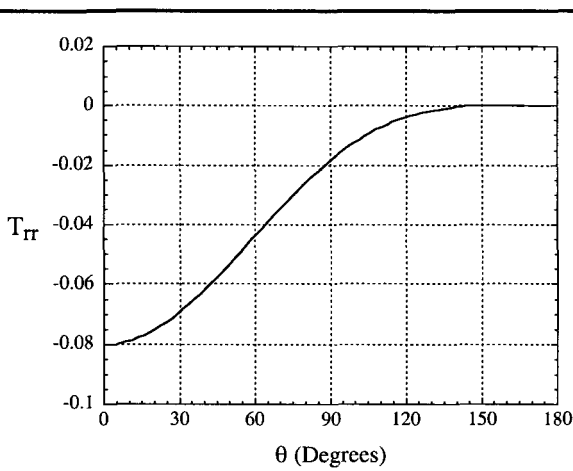


Figure 3.17.1 Radiation reaction pressure on a virtual, conducting sphere of electrical radius  $ka = 5$ , if all interior fields are equal to zero.

Although the total pressure in the  $xy$ -plane is time independent, the fields that produce it and the sources upon which they act are not. For example, the radial tensor components due to the electric and magnetic fields are:

$$\begin{aligned} \frac{\epsilon}{2} E_r^2 &= \frac{2\epsilon}{(ka)^4} \left\{ \left( 1 + \frac{1}{(ka)^2} \right) + \left( 1 + \frac{1}{(ka)^2} \right) \cos(2\omega t_R) + \frac{2}{(ka)} \sin(2\omega t_R) \right\} \\ \frac{\mu}{2} H_r^2 &= \frac{2\epsilon}{(ka)^4} \left\{ \left( 1 + \frac{1}{(ka)^2} \right) - \left( 1 + \frac{1}{(ka)^2} \right) \cos(2\omega t_R) - \frac{2}{(ka)} \sin(2\omega t_R) \right\} \end{aligned} \quad (3.17.3)$$

Although the sum of the electric and magnetic field terms, which is equal to the total pressure, is constant, the electric field acts only on electric charge densities and the magnetic field acts only on the current densities. On a rigid surface the difference is not significant. However, on a surface sufficiently

flexible to respond to local pressures, differences may produce source turbulence.

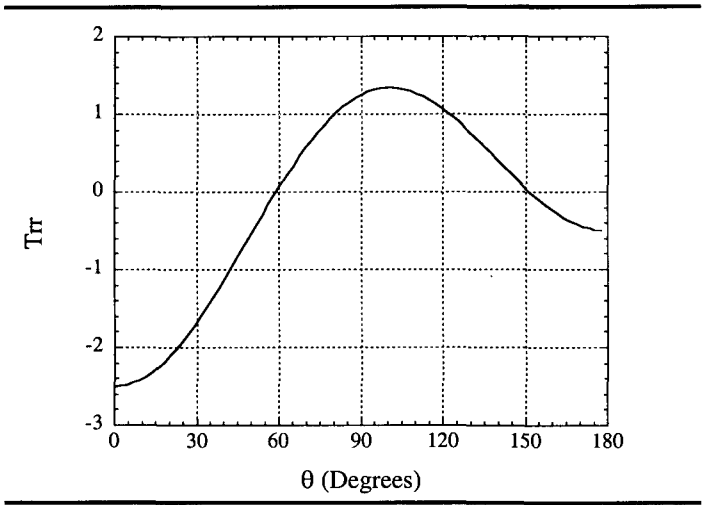


Figure 3.17.2 Radiation reaction pressure on a virtual, conducting sphere of electrical radius  $ka = 1$ , if all interior fields are equal to zero, see Eq 3.17.2.

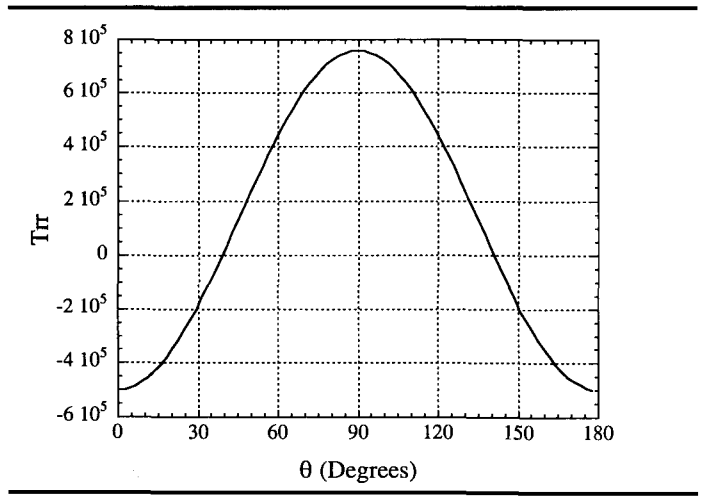


Figure 3.17.3 Radiation reaction pressure on a virtual, conducting sphere of electrical radius  $ka = 0.1$ , if all interior fields are equal to zero, see Eq 3.17.2.

To examine the significance of a zero  $Q$ , note the peak value of standing energy about any radiator is equal to:

$$W_{pk} = \frac{QP_{av}}{\omega} \quad (3.17.4)$$

This energy returns to the antenna when, for example, a shift in frequency or source shutdown occurs. By Eq. 3.17.5 no matter how large an amount of energy is available for storage in the field and no matter how small is the acceptable time average power, there is a minimum acceptable value of  $Q$ . Applications that appear to be impractical for dipole antennas because of the magnitude of required energy include radiative decay of atomic states and very low frequency communication. Quite differently, the lower limit on  $Q$  tabulated in Tables 3.17.1 and 3.17.2 shows that with  $Q$  equal to zero, energy, once radiated, never returns to the source. There is no lower limit on the antenna diameter-to-wavelength ratio and the full amount of field energy, once radiated, ultimately continues on to the far field. This does not imply that during steady state operation, at a fixed time-average output power, there is less local field energy; it implies all standing energy will ultimately travel outward to the far field, and not return to affect the source.

### *Multipoles*

An expanded antenna is obtained by replacing the dipoles of Table 3.17.1 by omnidirectional modes of arbitrary order. The modes are located, oriented, and phased similarly to those of Table 3.17.1. The resulting vector fields if coefficients  $F(\ell, 1) = 1$ ,  $G(\ell, 1) = -1$ , all others are equal to zero, and  $j = i$ , are:

$$\text{Let} \quad S_\ell = P_\ell^1(\cos\theta)/\sin\theta \quad \text{and} \quad T_\ell = dP_\ell^1(\cos\theta)/d\theta$$

$$\sigma^2 E_r = \ell(\ell+1)[B_\ell \cos(\omega t_R - \phi) - A_\ell \sin(\omega t_R - \phi)]S_\ell \sin\theta$$

$$\sigma^2 \eta H_r = -\ell(\ell+1)[A_\ell \cos(\omega t_R - \phi) + B_\ell \sin(\omega t_R - \phi)]S_\ell \sin\theta$$

$$(3.17.5)$$

$$\begin{aligned}
\sigma E_\theta &= \{ [D_\ell \cos(\omega t_R - \phi) - C_\ell \sin(\omega t_R - \phi)] T_\ell + [A_\ell \cos(\omega t_R - \phi) + B_\ell \sin(\omega t_R - \phi)] S_\ell \} \\
\sigma H_\phi &= \{ [A_\ell \cos(\omega t_R - \phi) + B_\ell \sin(\omega t_R - \phi)] T_\ell + [D_\ell \cos(\omega t_R - \phi) - C_\ell \sin(\omega t_R - \phi)] S_\ell \} \\
\sigma E_\phi &= \{ -[B_\ell \cos(\omega t_R - \phi) - A_\ell \sin(\omega t_R - \phi)] T_\ell + [C_\ell \cos(\omega t_R - \phi) + D_\ell \sin(\omega t_R - \phi)] S_\ell \} \\
\sigma H_\theta &= \{ -[C_\ell \cos(\omega t_R - \phi) + D_\ell \sin(\omega t_R - \phi)] T_\ell + [B_\ell \cos(\omega t_R - \phi) - A_\ell \sin(\omega t_R - \phi)] S_\ell \}
\end{aligned}$$


---

$$w_T = \frac{\epsilon}{2} \left\{ \frac{\ell(\ell+1)}{\sigma^4} (A_\ell^2 + B_\ell^2) S_\ell^2 \sin^2 \theta + \frac{1}{\sigma^2} (A_\ell^2 + B_\ell^2 + C_\ell^2 + D_\ell^2) (S_\ell^2 + T_\ell^2) + \frac{4}{\sigma^2} S_\ell T_\ell (A_\ell D_\ell - B_\ell C_\ell) \right\}$$

$$w_S = 0$$

$$w_\delta = \frac{\epsilon}{2} \left\{ \frac{\ell(\ell+1)}{\sigma^4} (A_\ell^2 + B_\ell^2) S_\ell^2 \sin^2 \theta + \frac{1}{\sigma^2} (A_\ell^2 + B_\ell^2 + C_\ell^2 + D_\ell^2) (S_\ell^2 + T_\ell^2) + \frac{4}{\sigma^2} S_\ell T_\ell (A_\ell D_\ell - B_\ell C_\ell) \right\}$$

$$N_r = \frac{1}{\eta \sigma^2} \{ (A_\ell D_\ell - B_\ell C_\ell) (S_\ell^2 + T_\ell^2) + (A_\ell^2 + B_\ell^2 + C_\ell^2 + D_\ell^2) S_\ell T_\ell \}$$

$$N_\theta = -\frac{\ell(\ell+1)}{\eta \sigma^3} (A_\ell C_\ell + B_\ell D_\ell) S_\ell^2 \sin \theta$$

$$N_\phi = \frac{\ell(\ell+1)}{\eta \sigma^3} \{ (A_\ell D_\ell - B_\ell C_\ell) S_\ell T_\ell + (A_\ell^2 + B_\ell^2) S_\ell^2 \} \sin \theta$$

$$W_S = 0 \quad p = \frac{16\pi}{3\eta k^2}$$

$$Q \geq 0 \quad \text{Gain} = \frac{3}{4} \ell^2 (\ell+1)^2$$


---

Table 3.17.2 Four superimposed x- and y-oriented electric and magnetic multipoles  
*Power and energy results, tabulated in Table 3.17.2, show that the zero-Q aspect extends through all modal orders.*

Table 3.17.2 confirms that the zero-Q aspect extends through all orders. Since modes of different orders operate independently, any combination of such modes will have a net Q of zero.



### 3.18 Numerical Characterization of Antennas

In an effort to confirm the  $Q$  model presented within this chapter, the radiation properties of a radiating spherical surface have been numerically modeled using finite difference time domain (FDTD). Accurate numerical modeling requires the properties of the radiating sphere to be retained, while eliminating properties of the driving network, a network which for the multipole source includes power splitters, cables, and possibly multiple phase shifters. Source  $Q$  is based upon Eq. 3.5.11:

$$Q = \frac{\omega W_{pk}}{P} \quad (3.18.1)$$

This equation is applicable to any antenna design, independently of its complexity.

The technique makes possible determination of the energy that returns from the standing energy field back to the antenna. The measurement begins by driving the antenna to steady state. Time average output power  $P$  is numerically obtained by integrating over a virtual sphere that circumscribes the source. After steady state operation has been reached, the voltage source is turned off, after which the local standing energy field collapses. The source-associated portion of the standing energy returns to the antenna from which, in turn, it is either reflected back into space or absorbed by the antenna. In the numerical model, the antenna is driven by a  $50\ \Omega$  source that absorbs returning energy. The absorbed and reflected energies are summed to obtain  $W_{pk}$ .

The time domain technique avoids spurious errors due to unwanted power reflections within the feed network. For example, when two antennas are driven by a single generator, through a power splitter and a feed network in which one arm has a  $\pi/2$  voltage phase shift, the waves reflected from the antennas back to the generator are  $\pi$  out of phase and cancel. No reflected power is measured. This null result does not mean that the  $Q$  of the antenna is zero, or that the antenna input impedance is purely real. Rather it indicates that techniques for determining  $Q$  are required that separate transmission line effects from antenna performance.

The analytical techniques used to determine the radiation  $Q$  of a source necessarily solve for the steady state fields external to a virtual sphere enclosing the radiation source. Doing so ignores standing energy at radii less than the length of the antenna arms, hence the analytic expressions for the

standing energy are inherently too small. In contrast, the numerical technique accounts for all standing energy in the near field. It forms a check on analytic techniques and a guide for experimental implementation. The total energy returned to the antenna is a simple sum over the energies returned and reflected by each element.

The numerical method for determining Q begins by determining the power that passes through a large radius, circumscribing sphere. That power is put equal to P in Eq. 3.18.1. After source turn-off the voltage across the source resistor,  $V_{in}$ , is determined and used to calculate the source current,  $I_{in}$ . These values are combined and integrated over time to obtain the returned energy:

$$W_{\text{returned}} = \int I_{in}(t)V_{in}(t)dt = \int [I_{in}(t)]^2 R_S dt \quad (3.18.2)$$

$R_S$  is the 50  $\Omega$  source resistor.  $I_{in}$  is the current that flows through the resistor and  $V_{in}$  is the voltage across the antenna terminals. Both voltage and current are determined using FDTD, then the time integral of Eq. 3.18.2 is evaluated and entered as the energy portion of the numerator of Eq. 3.18.1. The portion of the original (at source turn-off) standing energy that escapes outward is obtained by calculating the instantaneous power on the surface of an encompassing virtual sphere of radius R at times  $t > R/c$ , integrating over both the surface and time. Details of the finite difference time domain (FDTD) code used in this work are given in the two references by Liu *et al.*

For certain antennas the standing energy varies with time, hence use of Eq. 3.18.1 to determine Q requires repeating the calculation process over a range of turn-off phase angles to obtain the peak value  $W_{\text{Spk}}$ . However for other antennas, such as a turnstile antenna with the two dipoles driven in phase quadrature, the source-associated standing energy is time independent.

### *Biconical Dipole Antennas*

A field-based analysis of a single electric dipole is given in Section 3.12; Q is listed in Table 3.12.1. A terminal-based analysis of the same antenna is shown in Section 3.7 and listed in Eq. 3.7.15. Results are identical and equal to:

$$Q = \frac{1}{2(ka)^3} \left[ 1 + \sqrt{1 + 4(ka)^4} \right] + \frac{1}{(ka)} \quad (3.18.3)$$

A 5° arm angle biconical dipole antenna was the basis for a numerical analysis. The dipole was divided into 13 discrete radial segments; for  $ka = 6$  each radial segment length is  $0.073 \lambda$ . To ensure steady state operation the dipole was driven for eleven time-periods before the source voltage was turned-off. During steady state operation power on a spherical surface of radius  $R$  about the source was determined and entered as the denominator of Eq. 3.18.1. For the first standing energy measurement, turn-off was done at the most negative value of input power, point A of Figure 3.18.1. At each field point for time  $t > R/c$  the fields collapsed. Some of what was standing energy moves outward away from the antenna and some moves inward toward it. Some of the collapsing power is dissipated in the source resistor and some is reflected back into space. The returned energy is measured then the process is repeated with a different cyclical turn-off phase until the maximum returned energy is obtained. The maximum energy is substituted into the numerator of Eq. 3.18.1.

The instantaneous power at the antenna terminals,  $P_{in}$ , is calculated and plotted as the dashed curve of Figure 3.18.1, where outwardly and inwardly directed power is respectively positive and negative. It has the form:

$$p(\sigma, t) = P[1 + \gamma(\sigma)\cos(2\omega t_R)] \quad (3.18.4)$$

The steady state portion of the curve is dominated by the reactive term. For the first iteration the source is turned off at time  $t = A$ , at which time there is a maximum rate of reactive energy return to the antenna. After turn-off the terminal power drops abruptly then takes what appears to be an exponentially damped, oscillatory form. Oscillations occur at a wavelength less than that of the driven field.

The instantaneous power at the surface of an encompassing, virtual sphere one wavelength in radius is also calculated and plotted as the solid curve of Figure 3.18.1. In the steady state regime since magnitude  $\gamma(\sigma) = 1/\sigma^3$  is a monotone, rapidly decreasing function of radius the peak-to-peak magnitude is much less at the field point than it is at the terminals.

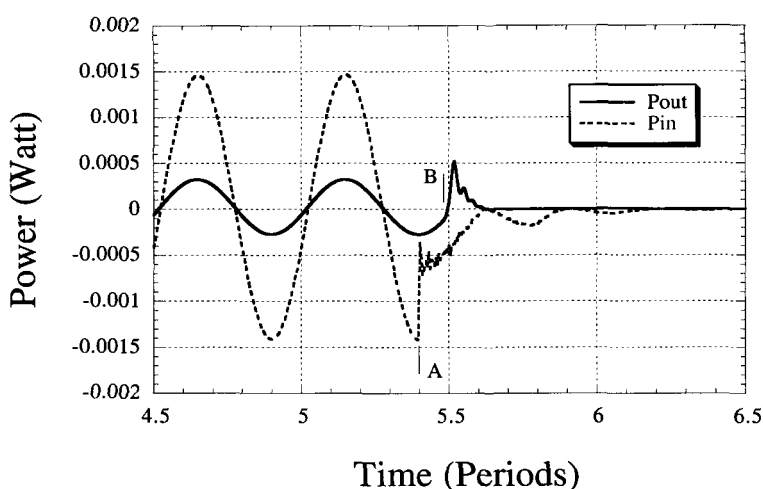


Figure 3.18.1 Time analysis of a single biconical TM dipole.

$P_{in}$  is the instantaneous power at the antenna terminals and  $P_{out}$  is the power on the surface of the encompassing, virtual sphere one wavelength in diameter, shown at the same retarded time. Source turn-off occurs at the most negative value of  $P_{in}$ , time  $t = A$ . Some standing energy travels inward and is absorbed by the input resistor and some travels outward. At time  $B$  the field collapse reaches radius  $R$  surrounding the antenna.

After source turn-off the output power remains continuous then becomes increasingly positive until reaching a positive value larger than the maximum steady state value, then decays to zero. The figure verifies that there is continued emission of energy after the source has been discontinued, and such energy can come only from what was once standing energy.

Since the source-associated standing energy of a single dipole is time dependent, the measured  $Q$  depends upon the phase at which the source is turned off. The numerically determined variation in source-associated standing energy of a biconical TM dipole of electrical size  $ka = 0.6$  is shown in Figure 3.18.2 with  $t = 0$  defined to be when  $P_{in}$  is at its most negative point.

Comparative values of  $Q$  calculated using Eq. 3.18.1 and obtained numerically using the described technique are shown in Figure 3.18.3. As expected, in all cases the numerically calculated values are slightly larger: the analytic expressions do not consider the standing energy contained at

radii less than the antenna arm length and the numerical calculations do. Furthermore for  $ka > 1.1$  octupole moment radiation becomes important. Such effects are accounted for in the numerical analyses but not in the analytical curves. The octupolar moment introduces oscillations in the powers and energies and result in the oscillatory Q behavior of Figure 3.18.3.

### Turnstile Antennas

A turnstile antenna consist of two collocated and spatially orthogonal electrical dipoles. A turnstile antenna is the simplest multi-element antenna for which theory shows that Q is dependent upon inter-element phasing. When the two dipoles are driven in phase the far field is linearly polarized and Q is the same as for a single electric dipole, Eq. 3.18.3. However when the dipoles are driven in phase-quadrature, see Section 3.16, the fields are circularly polarized and Q is given by:

$$Q = \frac{1}{3(ka)^3} + \frac{1}{(ka)} \quad (3.18.5)$$

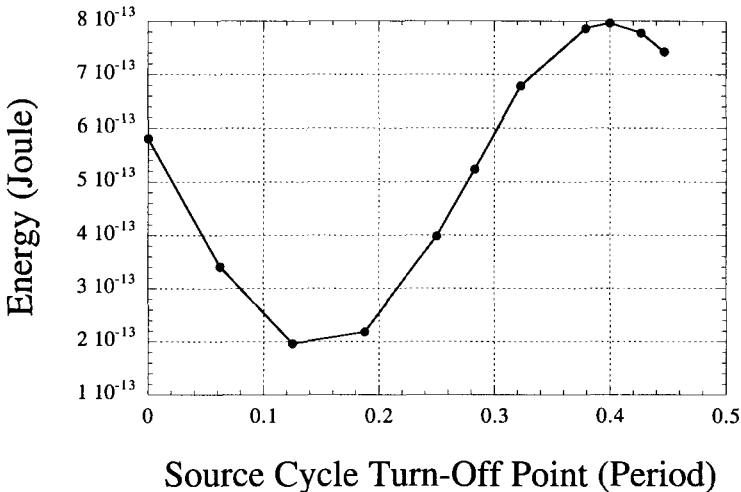


Figure 3.18.2 Source-associated standing energy for a biconical TM dipole The dipole is of electrical length  $ka = 0.6$  and the plot is a function of source turn-off point. The time reference zero point is the minimum value of  $P_{in}$ .

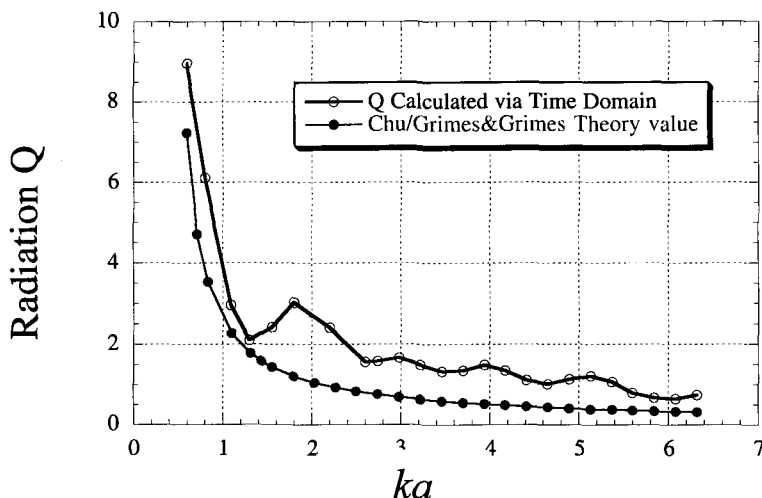


Figure 3.18.3 Numerically (open dots) and theoretically (solid dots) determined radiation  $Q$  of a biconical antenna versus electrical length  $ka$ .

In the electrically small limit, the relative phasing of the dipoles produces a factor of three difference in  $Q$ . The difference serves as an important test case for the different models.

To make a comparative numerical analysis each biconical electric dipole was divided into 13 discrete radial segments; when  $ka = 6$ , each radial segment is equivalent to about  $0.073 \lambda$ . Plots of numerically determined  $Q$  versus relative electrical size,  $ka$ , for a turnstile antenna when the dipoles are in phase and out of phase are shown in Figure 3.18.4. The data show that the relative phasing between the two dipoles affects  $Q$ . Since the analytic solutions do not account for standing energy within the inner region of the antenna calculated  $Q$  values are expected to be larger than the theoretical predictions and Figure 3.18.4 shows that to be the case. Also as expected the largest fractional reduction in  $Q$  occurs with a phase difference of  $90^\circ$ . As with a single biconical antenna when the turnstile antenna supports linear polarization the standing energy is time varying. It is, therefore, necessary to determine the source turn-off point that produces the largest calculated  $Q$ . This point was determined to be the same point it was for a single biconical antenna. A plot of  $Q$  reduction in switching from in-phase to phase quadrature as a function of  $ka$  is shown in Figure 3.18.5.

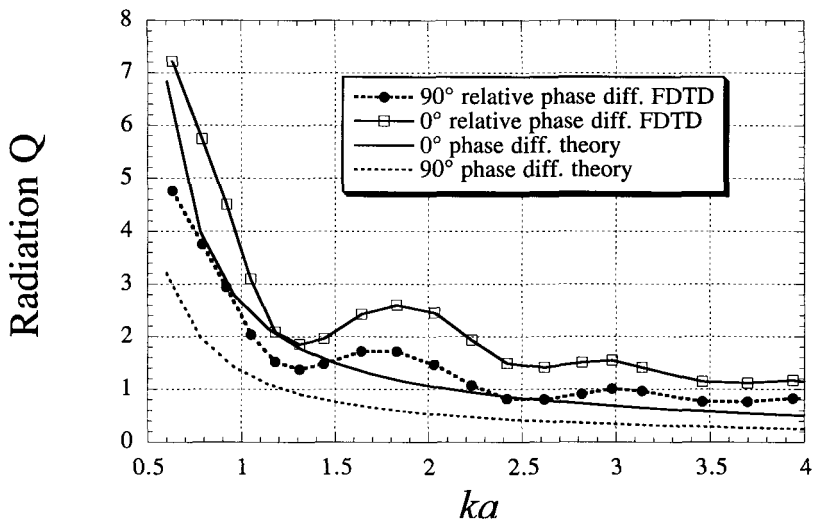


Figure 3.18.4 Numerical and analytical values of radiation  $Q$  versus  $ka$  for a turnstile antenna, when phased to support linear polarization and when phased to support circular polarization.

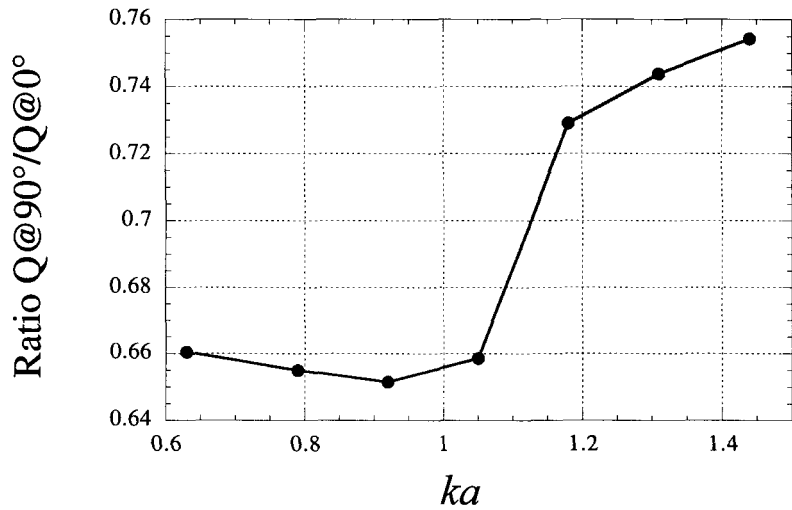


Figure 3.18.5 Fractional reduction in  $Q$  versus  $ka$  obtained by shifting the relative phase between dipoles of turnstile antenna from  $0^\circ$  to  $90^\circ$ .

The figures show that the relative phasing between the dipoles affects the radiation  $Q$  of turnstile antennas. This change in  $Q$  is due to a change in field structure that, in turn, affects the fraction of the standing energy that returns to the radiating source.

### 3.19 Experimental Characterization of Antennas

#### *Biconical Dipole Antennas*

A technique similar to the numerical one may be used to experimentally determine antenna  $Q$ . The block diagram of the experimental system for a single port antenna is shown in Figure 3.19.1. A wave generator drives a circulator that in turn drives the antenna. The return from the antenna passes back to the circulator and from it to an integrating oscilloscope; the portion of the power reflected from the antenna back into space is unknown. The experimental procedure is to obtain steady state operation, determine the real power  $P$  using a network analyzer, then switch off the generator. Energy returned from the antenna after source turn-off is directed by the circulator to the transient-capturing oscilloscope, put equal to the source-associated standing energy and entered in the numerator of Eq. 3.18.1. The  $Q$  measurement technique isolates antenna performance from the feed network and enables characterization of the antenna itself.

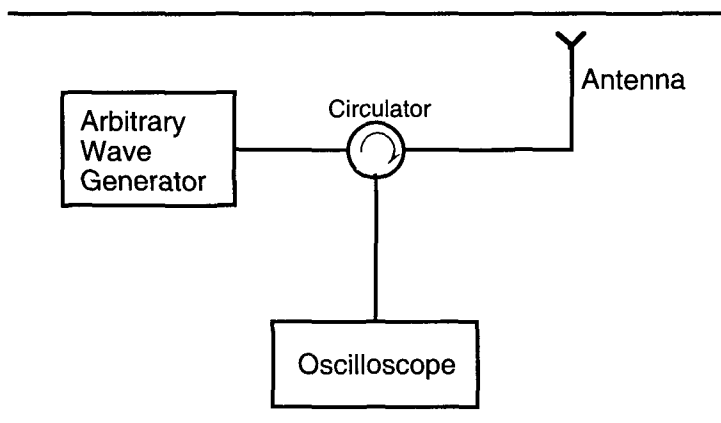


Figure 3.19.1 Experimental set-up for determining the radiation  $Q$  of a single antenna.



As detailed in the C. A. Grimes *et al.* references, a Tektronix 500 MHz arbitrary waveform generator (AWG610), which is able to terminate the waveform virtually without a measurable transient, was used as the source generator. The antenna was suspended in an anechoic chamber, driven from the AWG610 through a circulator, with the reflected waveform captured with an oscilloscope through the other circulator port. A HP 54845A oscilloscope with a sampling rate of 8 G samples/second and an advanced triggering option that capture waveforms up to 1.5 GHz was used to capture the transient signal returning from the antenna after source turn-off. All components in the experimental setup were 50  $\Omega$  devices. The generator output power in steady state was determined from the measured voltage and found to be about 7.1 mW (8.5 dBm). The circulator effectively divided the input and reflected signals so the generator always saw the network as a 50  $\Omega$  load and delivered the same power.

Using the programming capabilities of the AWG610, a waveform of frequency 450 MHz was generated and delivered to the antenna. The duration of the source signal was pre-selected, the antenna was driven until it reached the steady state, and then switched off. There was no detectable transient response. It was found that signals of 25 ns duration, about 12 periods at 450 MHz, were enough to reach steady state. After the waveform was turned off the power returned from the antenna to the oscilloscope was measured and time integrated to obtain the source-associated energy. A typical reflected power waveform for a wire dipole of length  $0.2\lambda$  is shown in Figure 3.19.2. All oscillations after turn-off are due to returned power.

The time-average power radiated by the antenna was measured indirectly. The scattering parameters of the three port network of Figure 3.19.1 without the generator, oscilloscope, and antenna were measured with a HP8753D network analyzer. The antenna was then connected to the system and the network analyzer was used to determine the input impedance. This was sufficient to permit calculation of the voltage and currents at the terminals of each port when the generator produces its measured voltage, the antenna presents its measured impedance, and the oscilloscope supplies a fifty-ohm load. The calculated real power at the antenna terminals is equal to the radiated power. The power reflected and captured with the oscilloscope was also calculated. Calculated and measured values of reflected power were the same.

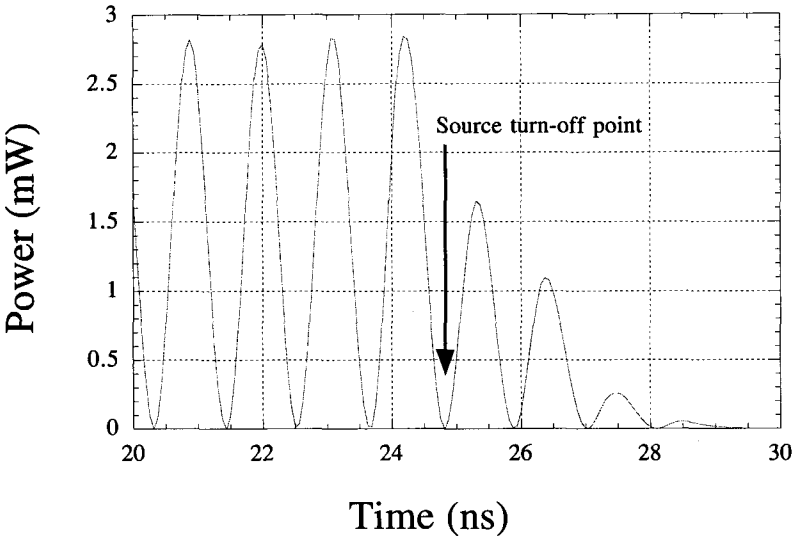


Figure 3.19.2 Measured values of reflected power for a  $0.2\lambda$  -electric dipole antenna.

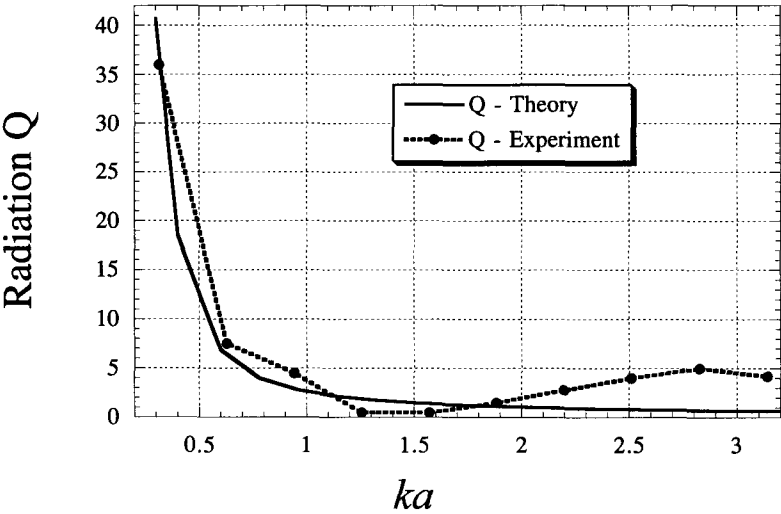


Figure 3.19.3 Experimentally determined Q versus electrical length of thin-wire electric dipoles.

### Turnstile Antennas

The radiation  $Q$  of the turnstile antenna is measured in a way that is similar to antennas with a single input port. The network needed to characterize a turnstile antenna is shown in Figure 3.19.4. A hybrid 3 dB-splitter forwards equal power to each dipole, a phase shifter adjusts the phase difference between the dipole drives, an attenuator compensates for the loss in the phase shifter, and circulators separate incoming from reflected signals. The antenna is a two-port system, the scattering parameters of which are measured by the network analyzer. The scattering parameters of a five-port network (six with the hybrid port connected to a  $50\ \Omega$  resistor) were measured. Then using network theory the power radiated by the turnstile antenna was determined. This approach accounts for parasitic coupling between the two dipoles. The oscilloscope captured the reflected waveforms and the reflected powers were determined from them. The source-associated standing energy of the turnstile antenna was determined by summing the time integrals of reflected powers from the two dipoles.

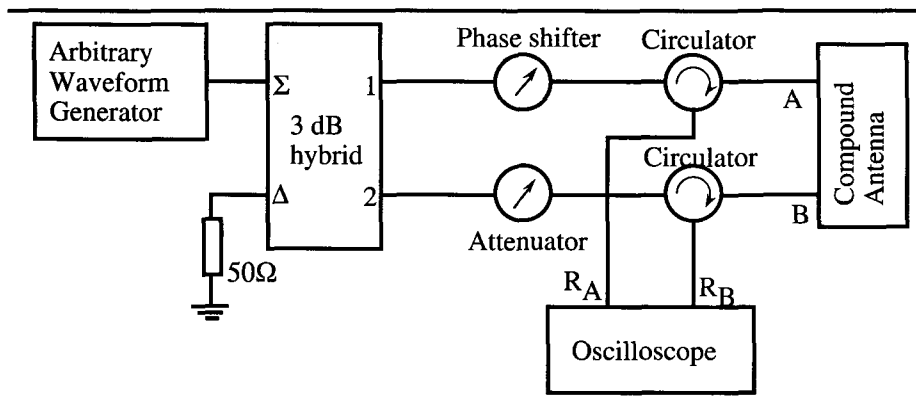


Figure 3.19.4 Experimental setup for measuring  $Q$  of the turnstile antenna.

A turnstile antenna was implemented using thin wire, equal length dipoles and measured using the setup described in Figure 3.19.4.  $Q$  was determined with both the drives in phase (linear polarization) and the drives in phase quadrature (circular polarization.) Measured values of  $Q$  versus the electrical length of the lines are plotted in Figure 3.19.5. Results confirm that the radiation  $Q$  of this antenna is a function of the difference of driving phase between the two dipoles.

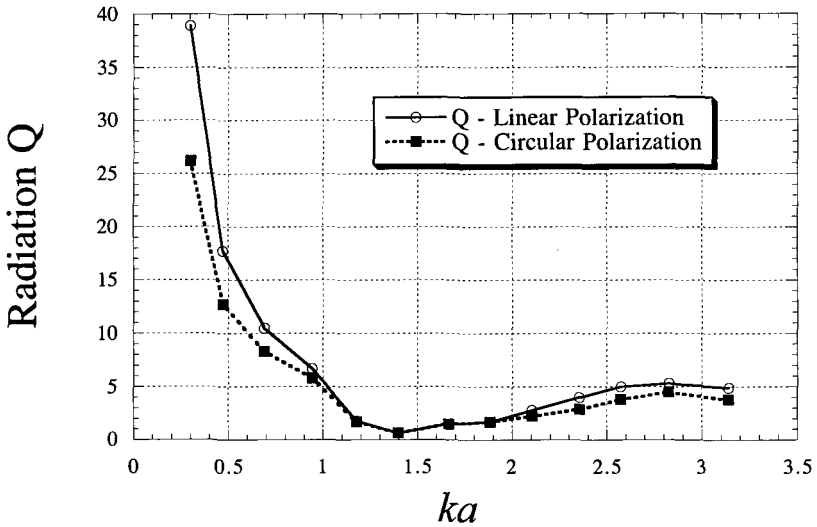


Figure 3.19.5  $Q$  of a thin-wire, turnstile antenna versus electrical length of the dipoles, for in-phase drives and phase quadrature drives.

### 3.20 $Q$ of Collocated Electric and Magnetic Dipoles: Numerical and Experimental Characterizations

The antenna discussed in Section 3.17 consists of four collocated dipoles; an electric and magnetic dipole pair radiating equal powers is oriented parallel with the  $x$ -axis and an identical pair is oriented along the  $y$ -axis. The configuration is depicted in Figure 3.20.1. The electric moments are implemented as straight wires and the magnetic moments as rectangular loops. The magnetic loops are positioned to the side of the electric dipoles in a way that produces strong coupling between the  $x$ -directed electric moment and the  $y$ -directed magnetic moment, and symmetrically between the other pair. By the analysis of Section 3.17 if driven with the proper phases the lower limit on radiation  $Q$  is equal to or greater than zero.

Early attempts to characterize this antenna design used separate feeds for each dipole and were unsuccessful due to unwanted and interfering power transfer between dipole feeds. This implementation uses two separate dipole-pair elements, with equal power from the electric and magnetic moments. With this design rather than interfering, the coupling appears to contribute to

the desired outputs. The radiation  $Q$  of the antenna system is determined using the numerical and experimental techniques detailed in Section 3.19.  $Q$  values were measured as functions of the phasing between the dipole pairs and the relative electrical size,  $ka$ .

Two things determine the relative phasing of the different radiators: the driving phase and local coupling. Similarly directed dipoles are driven by the same set of terminals and by the strong local field interaction between the  $x$ -directed electric moment and  $y$ -directed magnetic moment, as well as between the other two of elements. It is found that if the two driving ports are in phase the radiation is similar to that of Table 3.15.2 and  $Q$  is given by Eq. 3.18.3. With the driving ports in phase quadrature, the generated radiation is similar to that of Table 3.17.1, for which  $Q$  has no analytical lower limit.

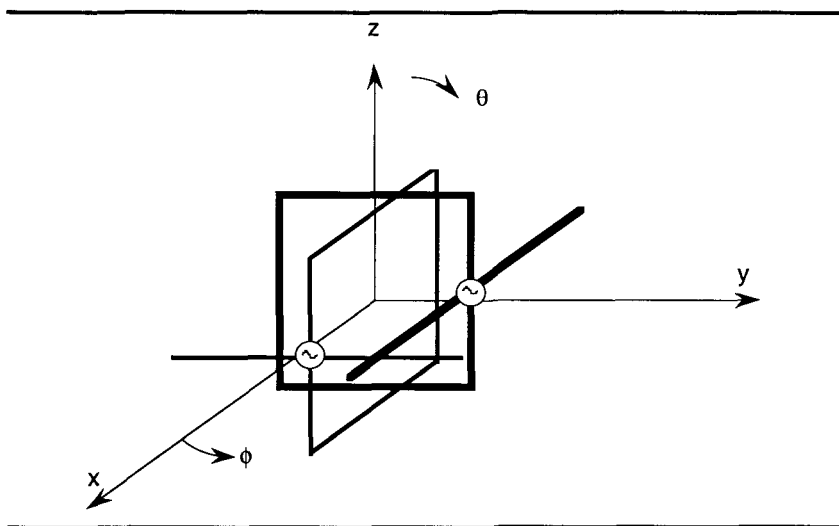


Figure 3.20.1 Implementation sketch of antenna comprised of two dipole-pair elements, each element provides equal TE and TM power.  
*Lines of different thickness differentiate the two sets of dipole-pair elements.*

The single dipole pair embodiment is shown in Figure 3.20.2. A Method of Moments (MoM) analysis was done to ensure that the elements radiate equal TE and TM power. The fields on the surface of the smallest virtual sphere that circumscribes the radiating elements were computed using NEC4 MoM. Using the technique described in Section 3.18 the calculated fields were equated to the equivalent terms in a multipolar field expansion to

determine the TM dipole field coefficient  $F$  and the TE dipole field coefficient  $G$ , see Eq. 3.11.1. Figure 3.20.3 shows the calculated TE/TM power ratio plot for the structure of Figure 3.20.2 with loop sides  $a = \ell/2 = 12$  cm. As shown in Figure 3.20.3 for these dimensions the element radiates equal TE and TM power at 166.67 MHz. Since the dimensions scale linearly with frequency for loop side  $a = \ell/2 = 4$  cm the equal power frequency is 500 MHz.

The four-dipole source was modeled numerically. Since straight-wire elements were used for the antenna implementation, FDTD computations were made using a rectangular, three-dimensional computer code based on the Yee cell. The problem space was chosen as  $120 \times 120 \times 120$  cells, with cell dimension  $\Delta x = \Delta y = \Delta z = 5$  mm; a perfectly matched absorbing boundary layer was used to terminate the computational space. Each radiating element consisted of a square loop and a straight-wire electric dipole. For the numerical computations, the dimensions of the antenna were held constant at loop side length 12 cm and electric dipole length 24 cm. The operational frequency was varied above and below 166.67 MHz, the frequency at which the TE and TM time-average powers were equal. For experimental characterization a thin-wire antenna of loop side  $a = \ell/2 = 4$  cm was built and tested in an anechoic chamber.

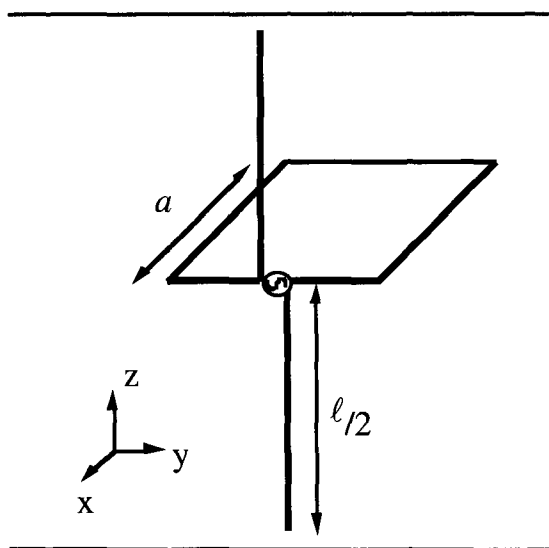


Figure 3.20.2 A Single Electric and Magnetic Dipole Pair

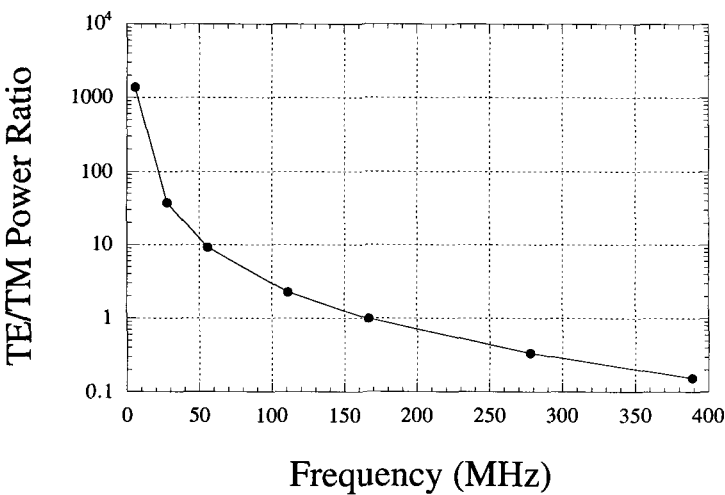


Figure 3.20.3 The TE/TM power ratio versus frequency from the single dipole-pair element pair shown in Figure 3.20.2, with dimensions  $a = \ell/2 = 12$  cm.

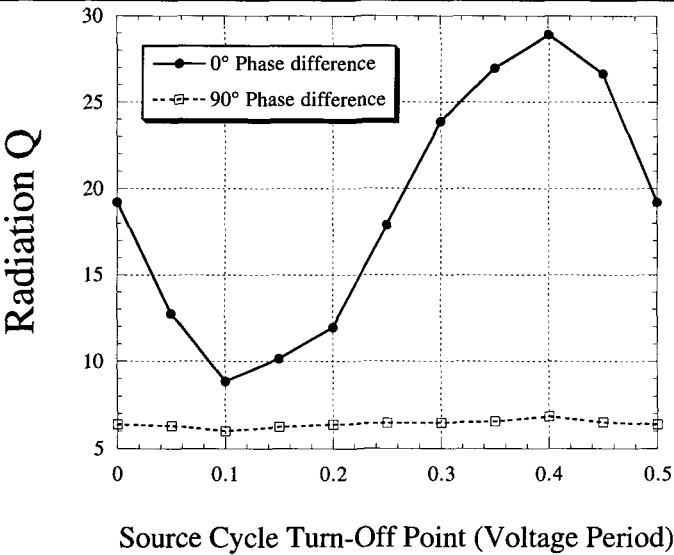


Figure 3.20.4 Numerically determined  $Q$  as a function of source-turn off point. Referenced to the input power minimum, for dipole-pair elements in phase and phased to support circular polarization;  $ka = 0.42$ .

The FDTD-determined radiation Q of the antenna for which  $ka = 0.42$  versus the source turn-off point is shown in Figure 3.20.4, relative to the minimum input power point. Theory indicates that the source-associated standing energy is time varying for all relative phases except  $90^\circ$ , when the dipole pairs support circular polarization. As seen in Figure 3.20.4, Q is independent of source turn-off point when circular polarization is maintained. However for other relative phases, Q varies with source turn-off point; the correct value of Q is the largest value that is determined when the source-associated standing energy is a maximum.

The numerically and experimentally determined radiation Q of the antenna at  $ka = 0.42$  versus phase difference between elements is shown in Figure 3.20.5. In agreement with theory, the radiation Q is dependent upon relative phasing between the antenna elements. When driven in phase Q is approximately that of an electric dipole of the same size. When driven out of phase antenna Q is reduced by an approximate factor of 4.5 from the in-phase results. For this relative electrical size, the measured Q value is approximately a factor of three below the minimum Q value determined by Chu for an antenna of the same electrical size.

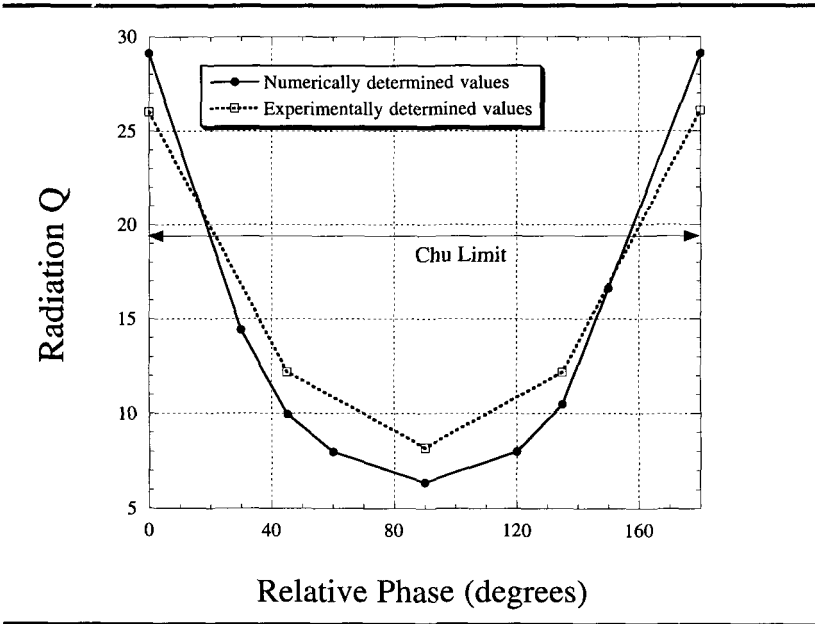


Figure 3.20.5 Numerically and experimentally determined Q versus relative phase between dipole-pair elements;  $ka = 0.42$ .



The sensitivity of  $Q$  to distance along the  $z$ -axis between the elements is shown in Figure 3.20.6. Using antennas for which  $ka = 0.42$  the antennas were displaced in steps of 5 mm for the numerical model with dimensions of  $a = \ell/2 = 12$  cm. Steps of 1.67 mm were taken for the experimental work with dimensions of  $a = \ell/2 = 4$  cm. With  $90^\circ$  relative phasing between the dipole-pair elements the radiation  $Q$  is respectively small and large when the displacement is small and large. In contrast, when the four dipoles are in phase the radiation  $Q$  is approximately that of an electric dipole of the same  $ka$  independently of the spacing. Experiments moving the dipole-pairs relative to each other in the other two dimensions showed similar results; the  $Q$  of  $90^\circ$  phased dipole-pair is sensitive to relative location, *i.e.*, modal coupling, and the  $Q$  of the in-phase dipole pairs is not.

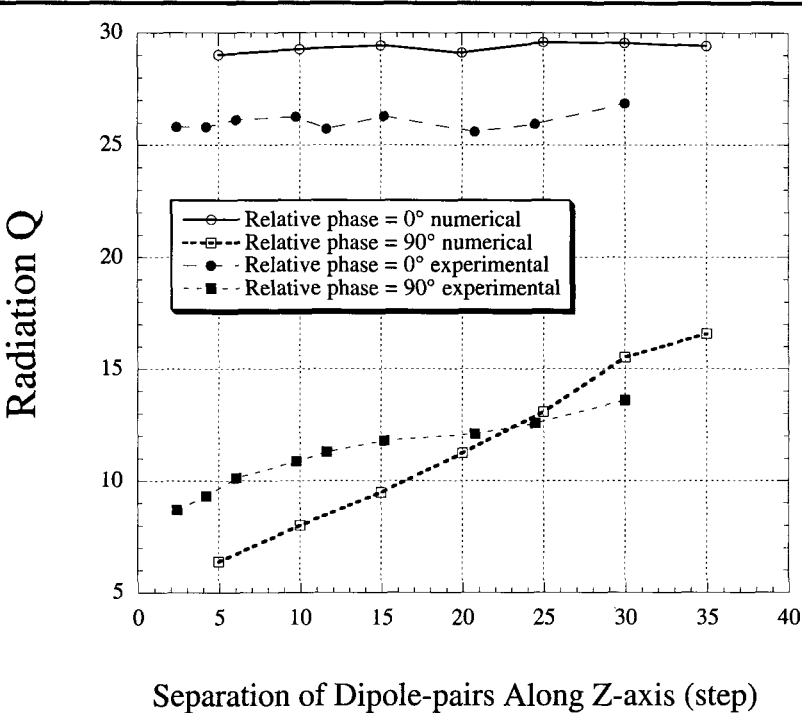


Figure 3.20.6 Numerically and experimentally determined  $Q$  as a function of spacing between dipole-pair elements.  
*Step size was 5 mm with the numerical model and 1.67 mm with the experimental model,  $ka = 0.42$ .*

The numerically determined Q versus the relative electrical size of the antenna is shown for in-phase drives and for phase quadrature drives in Figure 3.20.7. The trends shown by the numerical work were confirmed experimentally over the more limited range of  $ka = 0.37$  to  $ka = 0.42$ ; the circuit devices, not the antenna, determined the frequency limits. The circulators imposed the low frequency limit and the Tektronix Arbitrary Wave Generator AWG610 imposed the high frequency limit.

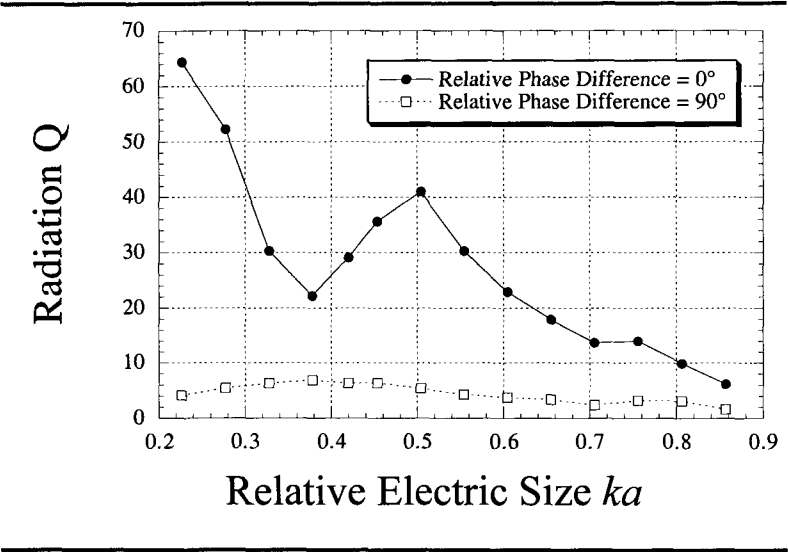


Figure 3.20.7 Numerically determined Q of antenna. Dimensions  $a = \ell/2 = 12\text{ cm}$ , shows effect of relative phasing between dipole-pair elements and electrical size  $ka$ .

At  $ka = 0.23$  the Q of the circularly polarized antenna is more than a factor of 20 below Chu’s limit. The oscillations seen in the in-phase Q results are due to higher order modes that cause variations in the outbound real power. The in-phase results show the familiar  $1/(ka)^3$  dependence of Q as the antenna becomes electrically small. In contrast, with the two dipole-pair elements phased to support circular polarization Q is relatively insensitive to frequency. The frequency response seen in Figure 3.20.7 is indicative that the current and charge distributions on the dipole-pair elements self-adjust to support radiation fields that minimize source-associated standing energy and hence Q.

We conclude that the numerical and experimental results support the analytical  $Q$  results within the limits imposed by our irreducible differences between among analytical, numerical, and experimental embodiments.

## References

- L.J. Chu, "Physical Limitations of Omni-Directional Antennas," J. Appl. Phys., vol. 19, 1163-1175 (1948)
- C.A. Grimes, G. Liu, F. Tefiku, D.M. Grimes, "Time Domain Measurement of Antenna  $Q$ ," Microwave and Optical Technology Letters, vol. 25, pp. 95-100 (2000).
- C.A. Grimes, G. Liu, D.M. Grimes, K.G. Ong, "Characterization of a Wideband, Low- $Q$ , Electrically Small Antenna," Microwave and Optical Technology Letters, vol. 27, pp. 53-58 (2000)
- D.M. Grimes, C.A. Grimes, "Power in modal radiation fields: Limits of the complex Poynting theorem and the potential for electrically small antennas," J. Electro. Waves and Appl., Vol. 11, 1721-1747 (1997)
- D.M. Grimes, C.A. Grimes, "Radiation  $Q$  of Dipole-Generated Fields," Radio Science, Vol. 34, 281-296 (1999)
- D.M. Grimes, C.A. Grimes, "Minimum  $Q$  of Electrically Small Antennas: A Critical Review," Microwave and Optical Technology Letters, vol. 28, pp. 172-177 (2001)
- R.F. Harrington, "Effect of Antenna Size on Gain, Bandwidth, and Efficiency," J. Research, Nat. Bureau of Standards, Vol. 64D, pp. 1-12, 1960.
- G. Liu, C.A. Grimes, D.M. Grimes, "A Time Domain Technique For Determining Antenna  $Q$ ," Microwave and Optical Technology Letters, vol. 21, pp. 395-398 (1999)
- G. Liu, K. G. Ong, C.A. Grimes, D.M. Grimes, "Comparison of Time and Frequency Domain Numerical Modeling of Outbound And Local Power From Two Perpendicularly Oriented, Electrically Small TM Dipoles," Int. J. of Numerical Modeling, vol. 12, pp. 229-241, (1999)

## 4. Quantum Theory

This chapter contains a review of quantum theory that is conventional in many ways, but dramatically different in key concepts. It has been known for over seventy years that electrons exhibit both particle and wave properties, and for twenty years that they are nonlocal. Although wave-particle duality plays an integral role in conventional quantum theory, the full affect of nonlocality has not been developed. In this work nonlocality is an integral part of the theory. Furthermore the full applicability of the equations of classical electromagnetic theory is retained. It is important to emphasize that the historic radiation reaction force on radiating charges is based upon energy radiated permanently away from the charge; the resulting reaction force acts to slow the motion of the charge and is much smaller than the Coulomb force. However, an oscillating charge is enmeshed in a standing electromagnetic energy field of its own making. As we show, although the radiation reaction of the standing energy does not affect the velocity of the radiator, it acts to distort and distend it; the magnitude is  $(1/ka)^3$  times larger than the radiation reaction force as it has been historically considered, and it is not small compared with the Coulomb force. There is no accounting for this large radiation reaction force in the equations of quantum theory.

Consider a point-electron as it nears an atomic nucleus. The forces acting on it include both Coulomb and centrifugal forces. By the classical laws, a point electron with an appropriate value of angular momentum will form a temporary elliptical orbit, with the nucleus at one of the foci, then two things happen to the orbit. First, the intrinsic and orbital magnetic moments interact in a way that produces a continuous torque, and thus rotation of the orbit. Second, orbiting objects accelerate and by the laws of classical electromagnetism, Eqs. 1.7.3, accelerating charges radiate energy permanently away from the system. Based on these laws, a point charge will lose energy and spiral into the nucleus, where it will be annihilated. However, electrons do not spiral into the nucleus. Instead, as Dirac points out, there is a "remarkable stability of atoms and molecules."

To further assess the “remarkable stability,” consider the reactive energy that accompanies far-field radiation. As discussed in Chapter 3, reactive energy plays a dominant role in determining the properties of electrically small antennas. Yet, although the atomic diameter-to-optical wavelength ratio is on the order of  $1/1000$ , the conventional quantum theory of radiation ignores reactive energy. Neither does it supply the full and complete set of electromagnetic fields that support the radiation process, as expressed in Chapter 2 for scatterers and biconical antennas. The quantum theory explanation is simply incomplete. This chapter contains the basis for an examination of quantum radiation that includes effects of reactive energy. The final explanation requires no special hypotheses and provides the full, steady state radiation solution, including all fields.

In this chapter, we combine electron nonlocality with the full radiation reaction force to construct an electron model. The model violates no physical laws and no experimental facts, yet it permits us to develop a view of quantum physics based upon electromagnetic field theory and the conservation of energy. We postulate that an eigenstate electron is not a particle, but extends throughout the state as a charged cloud. The exclusion principle results if, on a fine enough scale of dimensions, the cloud consists of granular units of charge. The units are minute compared with the total electron charge and are in dynamic equilibrium. Each eigenstate electron is modeled as an ensemble of such units. The mathematical results are the same as those of the historically accepted quantum theory, but the philosophical implications are not. Differences are discussed in this and the next chapter and reviewed in the epilogue.

## 4.1 Electrons

An isolated, static array of point electric charges cannot be held in equilibrium by electrostatic forces alone. Opposite charges collapse upon themselves and like charges forever repel. For a charge distribution to be stable something other than electrostatic forces must be at work. Since an electron contains at least a dominantly negative charge and since it is stable it follows that something other than electrostatic forces are present.

An electron’s physical extent has important repercussions. An early attempt to determine the size of an electron equated the electrostatic energy to its mass using Eq. 1.3.14,  $W = m_0 c^2$ . By classical electrostatics the energy of a virtual shell of radius  $R$  carrying charge  $e$  is:

$$W = \frac{e^2}{4\pi R} \quad (4.1.1)$$

The energy relationship results in radius  $R_L$ :

$$R_L = \left( \frac{e^2}{m_0} \right) \times 10^{-7} \cong 2.82 \times 10^{-15} \text{ m} \quad (4.1.2)$$

The result, the Lorentz radius of an electron, is the radius an electron would have if only electrostatic energies were present.

There have been many experimental and theoretical attempts to determine electron size. One method is based upon accurately determining the ratio between intrinsic values of magnetic moment and angular momentum: g-factor data. Such measurements show the electron radius is not more than about  $10^{-22}$  m. Scattering experiments show that electrons have no internal structure on the smallest scale of dimensions at which measurements are possible, about  $10^{-18}$  m. Theoretical quantum electrodynamic arguments point to a structureless particle with a vanishingly small radius, and string theory modifies the quantum electrodynamic result to the order of  $10^{-35}$  m. It is generally agreed, therefore, that whatever size an electron may be, since atoms are typically about  $10^{-10}$  m in diameter, free electrons are much smaller than atoms.

An electron with a diameter much less than  $10^{-10}$  m trapped within the confines of an atom will either be captured by the nucleus or undergo acceleration. Classical electromagnetic theory, see Eqs. 1.7.3, requires an accelerating electron to radiate energy into the far field, yet the energy of confined atomic electrons is fixed: it does not radiate. Both the requirement and the absence of radiation are indisputable. It is widely believed, therefore, that classical electromagnetic theory is not consistent with atomic stability. Paul A. M. Dirac stated it succinctly: the forces known in classical electrodynamics are “inadequate for the explanation of the remarkable stability of atoms and molecules.” A primary motivation for this work is to show that atomic stability, atomic absorption, and atomic emission processes do not conflict with classical electrodynamics but rather result from Maxwell’s equations and energy and momentum conservation.

## 4.2 Radiation Reaction Force

To examine the fields produced by an accelerating, point electron of charge  $e$  being captured as it spirals into an atomic nucleus, turn to the fields of Eqs. 1.7.3. To keep the model as simple as possible, require the electron velocity,  $\mathbf{v}$ , to remain much less than the speed of light,  $c$ . In that event, the radiation fields simplify to:

$$\mathbf{E} = \frac{\mu e}{4\pi r} \left[ \hat{\mathbf{r}} \times \left( \hat{\mathbf{r}} \times \frac{\partial \mathbf{v}}{\partial t} \right) \right] \quad \mathbf{H} = \frac{e}{4\pi c r} \left( \frac{\partial \mathbf{v}}{\partial t} \times \hat{\mathbf{r}} \right) \quad (4.2.1)$$

The distance from an origin located at the center of mass of the system to the point electron and its velocity are, respectively,  $\mathbf{r}$  and  $\mathbf{v}$ . To further simplify the algebra, although the acceleration is radially directed consider it to be  $\pm z$ -directed; a more realistic radial acceleration model complicates matters and adds nothing essential. With  $\pm z$ -directed acceleration the generated force fields are:

$$\mathbf{E} = \frac{\mu e}{4\pi r} \frac{\partial v}{\partial t} \sin \theta \quad \mathbf{H} = \frac{e}{4\pi c r} \frac{\partial v}{\partial t} \sin \theta \quad (4.2.2)$$

The radial component of the Poynting vector is:

$$N_r = \frac{\mu}{c} \left[ \frac{e}{4\pi R} \frac{\partial v}{\partial t} \right]^2 \sin^2 \theta \quad (4.2.3)$$

It follows that the radiated power is:

$$P = \frac{\mu e^2}{6\pi c} \left[ \frac{\partial v}{\partial t} \right]^2 \quad (4.2.4)$$

For energy to be conserved it is necessary that the time-average radiated and generated power be equal. This in turn requires a radiation reaction braking force,  $F_{RR}$ , acting on the electron to satisfy the condition:

$$\int_0^{\tau} \mathbf{F}_{\text{RR}} \cdot \mathbf{v} dt + \frac{\mu e^2}{6\pi c} \int_0^{\tau} \left[ \frac{\partial \mathbf{v}}{\partial t} \right]^2 dt = 0 \quad (4.2.5)$$

Time  $\tau$  is the period required for an integer number of rotations of the electron about the nucleus. Doing the integral by parts leads to:

$$\int_0^{\tau} \left( \mathbf{F}_{\text{RR}} - \frac{\mu e^2}{6\pi c} \frac{\partial^2 \mathbf{v}}{\partial t^2} \right) \cdot \mathbf{v} dt = \frac{\mu e^2}{6\pi c} \frac{\partial \mathbf{v}}{\partial t} \cdot \mathbf{v} \quad (4.2.6)$$

With oscillatory motion, such as an electron orbiting an atomic nucleus, the right side is equal to zero, leaving the integral equal to zero. With  $\mathbf{p}$  equal to the electron momentum, the integrand is equal to zero:

$$\mathbf{F}_{\text{RR}}|_{\text{real}} = \frac{\mu e^2}{6\pi c} \frac{\partial^2 \mathbf{v}}{\partial t^2} = \frac{\mu e}{6\pi c} \frac{\partial^3 \mathbf{p}}{\partial t^3} = \frac{\mu e \omega^3}{6\pi c} \mathbf{p} \quad (4.2.7)$$

Equation 4.2.7 expresses the time-average value of the radiation reaction force on the electron due to dipole-radiated energy, as it permanently leaves the system. This radiation reaction force is a braking force that acts on the entire charge, and has no affect on the shape of the electron.

Results of Chapter 3 include that a dipole radiating from within an electrically small region of radius  $a$  supports a reactive power that is larger than the real power by a factor of about  $1/(ka)^3$ . In the mid-optical frequency range and with an atom of radius 0.1 nm the factor is on the order of  $1/(ka)^3 \cong 10^9$ . It follows that the reactive radiation reaction force is  $10^9$  times larger than the braking force of Eq. 4.2.7. Multiplying Eq. 4.2.7 by  $1/(ka)^3$  shows that the radiation reaction force due to the reactive energy is:

$$\mathbf{F}_{\text{RR}}|_{\text{reactive}} = \frac{e}{6\pi \epsilon a^3} \mathbf{p} \quad (4.2.8)$$

Equation 4.2.8 expresses the time-average value of the reactive radiation reaction force on the electron. It is the same order of magnitude as the



Coulomb attractive force, and it is ignored by radiation analyses based upon the historic interpretation of quantum theory.

A more formal derivation of the reactive radiation reaction force of Eq. 4.2.8 follows by viewing a radiating electron as an electric dipole and using the radiation impedance of Eq. 3.6.4. After substituting for the letter functions and doing the long division, the impedance of Eq. 3.6.4 on a virtual sphere of radius  $r = \sigma/k$  may be written:

$$\begin{aligned}
 Z &= \eta \frac{D_1 + iC_1}{A_1 - iB_1} = \frac{\frac{\eta}{\sigma^2} + \frac{i\eta}{\sigma} - \eta}{\frac{i}{\sigma} - 1} \\
 &= \frac{\eta}{i\sigma} + i\eta\sigma + \eta\sigma^2 - i\eta\sigma^3 - \eta\sigma^4 + i\eta\sigma^5 + \dots
 \end{aligned} \tag{4.2.9}$$

Defining a generalized voltage and current leads directly from Eq. 4.2.9 to the voltage-current relationship:

$$V_1 = \left( \frac{\eta}{i\sigma} + i\eta\sigma + \eta\sigma^2 - i\eta\sigma^3 - \eta\sigma^4 + i\eta\sigma^5 + \dots \right) I_1$$

Replacing  $\sigma$  by  $(ka)$  gives, on the radiating surface:

$$V_1 = \mu \left( \frac{c^2}{i\omega a} + i\omega a + \omega^2 \frac{a^2}{c} - i\omega^3 \frac{a^3}{c^2} - \omega^4 \frac{a^4}{c^3} + i\omega^5 \frac{a^5}{c^4} + \dots \right) I_1 \tag{4.2.10}$$

After the second term, each succeeding term is  $(ka)$  times the previous one. Therefore the magnitude of each succeeding term is down by a factor of about 1000 in the mid-optical frequency range and the series converges rapidly. Odd and even powers of  $(ka)$  respectively describe oscillatory and outgoing energy. In this model of generalized force and flow the voltage is proportional to the driving force and the current is proportional to the magnitude of the dipole moment. To go from generalized parameters to specific ones introduce unknown constant  $K$  by the relationship:

$$V_1 = KF_1 \text{ and } I_1 = i\omega p_1 \quad (4.2.11)$$

By definition,  $F_1$  is the total dipolar radiation reaction force and  $p_1$  is the electric dipole moment. Combining Eqs. 4.2.10 and 4.2.11, then switching to time notation by replacing  $i\omega$  with a time derivative shows that:

$$F_1(t) = \frac{\mu}{K} \left( \frac{c^2}{a} p_1(t) + a \frac{d^2}{dt^2} p_1(t) - \frac{a^2}{c} \frac{d^3}{dt^3} p_1(t) + \frac{a^3}{c^2} \frac{d^4}{dt^4} p_1(t) - \frac{a^4}{c^3} \frac{d^5}{dt^5} p_1(t) + \dots \right) \quad (4.2.12)$$

The third term within the round brackets of Eq. 4.2.12 is the first term that contributes to energy loss from the oscillator; it is equivalent to Eq. 4.2.7. Making the equality shows that:

$$K = \frac{6\pi a^2}{e}$$

Substituting K back into Eq. 4.2.12 gives:

$$F_1(t) = \frac{ep_1(t)}{6\pi\epsilon a^3} + \frac{e}{6\pi\epsilon ac^2} \frac{d^2}{dt^2} p_1(t) - \frac{e}{6\pi\epsilon c^3} \frac{d^3}{dt^3} p_1(t) + \frac{ea}{6\pi\epsilon c^4} \frac{d^4}{dt^4} p_1(t) - \dots \quad (4.2.13)$$

Equation 4.2.13 is the complete expression for the radiation reaction force. Terms with an even or odd number of time derivatives, respectively, represent reactive energy exchange or resistive energy loss. The first term is a restoring force due to the local standing energy field. The second term is the mass of the standing energy field. The third term is the first term that leads to an energy loss from the system, *etc.*

The lead term of Eq. 4.2.13 is not small compared with other forces. It may be written as:

$$F_1(t) = \frac{e}{6\pi\epsilon R^3} p_1(t) = \frac{e^2 z}{6\pi\epsilon R^3} \Rightarrow \frac{e^2}{6\pi\epsilon R^2} \quad (4.2.14)$$

The last term applies at full extension of the oscillation, where force magnitude varies as the inverse square of the distance of oscillation. The force is expansive on the charge itself, and acts to extend it to an ever-larger size; it vanishes only if the charge is restructured to be nonradiating. If the charge oscillates through a region on the order of several times the electronic radii of Sec. 4.1, the expansive force is astronomical. This large force acts until or unless the electron becomes large enough to encircle the nucleus. Once that size the force rends the previously small electron into a stable, dynamic, and evolving ensemble of charge and current densities that is not small compared with atomic sizes and that is spread over the full eigenstate. For a hydrogen atom the reactive radiation reaction force and Coulomb force differ in magnitude by only a factor of  $2/3$ . As an analogy, consider an oil droplet: If isolated from external forces, surface tension acts to form it into a spherical, liquid drop. If placed on the surface of a pond, the surface tension force no longer dominates and the drop distributes itself over the surface.

We arrive at the following picture: as a point electron approaches an attracting nucleus, it begins to orbit and, under the influence of orbital acceleration, radiates. Radiation onset produces a radiation reaction force that converts the point charge into an extended ensemble of charge and current densities, the smallest size of which is determined by how finely the electron charge is subdivided. Local forces, within and about the trapped state, distribute the ensemble throughout the region. Internal forces also require the ensemble to remain in continual motion. Several studies show that there are an infinite number of stable arrays, see Kim and Wolf. Evidence to support this electron model is discussed in both preceding and coming sections.

### **4.3 The Time-Independent Schrödinger Equation**

An integral part of the science of statistical mechanics is the analysis of large numbers of identical, interacting particles taken as a single ensemble. The state of the ensemble is specified by the positions and velocities of the particles, and is sufficient information to determine the kinetic and potential energies of the system. With particles modeled as realistically as possible, there is little or no difficulty interpreting an experiment that measures the ensemble-average of a kinematic variable. The state of an isolated ensemble at any instant determines its future values. Since large ensembles contain too many degrees of freedom to detail, no attempt is made to make precise and

detailed calculations. Instead, most probable values averaged over all particles are calculated and assigned as ensemble-average values.

A single electron trapped by the Coulomb force of a positive nucleus accelerates. By the arguments of Section 4.2, the electron is transformed into an ensemble of charge and current densities. Since our present knowledge does not permit solving for the exact array, in common with statistical mechanics, it is necessary to consider each eigenstate electron on a statistical basis. Physical properties are calculated by imposing conservation laws on the ensemble. A primary result of imposing energy conservation on such an ensemble is the Schrödinger equation. First published in 1926, it is a mathematical description of the quantum character of electrons. Schrödinger discovered the usefulness of the differential equation that now bears his name:

$$-\frac{\hbar^2}{2m}\nabla^2 U(\mathbf{r}) + \Lambda(\mathbf{r})U(\mathbf{r}) = \mathcal{W}U(\mathbf{r}) \quad (4.3.1)$$

In this equation  $2\pi\hbar$  is Planck's constant,  $\Lambda(\mathbf{r})$  is the electrostatic potential, and  $U(\mathbf{r})$  is the wave function. The time average value of electric charge density at each point in space is:

$$\rho(\mathbf{r}) = eU^*(\mathbf{r})U(\mathbf{r}) \quad (4.3.2)$$

Although Schrödinger discovered that solutions of his equation correctly described the actions of electrons, he was not led to the result by first principles. The equation is invaluable for describing atomic level phenomena but solutions are statistical in character and there is no way to directly determine a unique physical basis for the equation. For example, the equation is no help in determining whether  $eU(\mathbf{r})U^*(\mathbf{r})$  represents an actual static charge density, the fraction of the time a point electron occupies a particular differential volume, or something in between. It is only known that solving Eq. 4.3.1 for  $U(\mathbf{r})$  then evaluating  $eU(\mathbf{r})U^*(\mathbf{r})$  gives the correct time-average spatial charge distribution.

Since Schrödinger first presented the equation, it has been shown that many different postulate sets yield it as a derived result. Since the interpretation depends upon the nature of the model used to derive it no single result is a sufficient basis for deciding if a particular model is correct. This section derives the Schrödinger equation using a thermodynamic

approach, and results are interpreted accordingly. A precise description of an extended, moving, bound charge density trapped by an electrostatic force and coupled to its own magnetic field is beyond our capability; we simply don't know enough about electrons. Therefore, in a way similar to thermodynamics, we seek an energy function from which follows general ensemble properties without detailed knowledge of the ensemble. The approach is adequate to obtain time-average values of kinematic properties, *i.e.*, expectation values.

The approach begins by noting that a dynamic charge distribution supports time-average values of charge and current densities, respectively  $\rho(\mathbf{r})$  and  $\rho(\mathbf{p})$ , within the spatial range  $\mathbf{r}$  and  $\mathbf{r}+d\mathbf{r}$  and the momentum range  $\mathbf{p}$  and  $\mathbf{p}+d\mathbf{p}$ . Momentum densities are directly proportional to current densities. Let an electron occupy a single eigenstate and let the charge density be everywhere the same sign. The constraint is expressed by introducing complex functions  $U(\mathbf{r})$  and  $\Gamma(\mathbf{p})$ , defined by the relationships

$$eU^*(\mathbf{r})U(\mathbf{r})=\rho(\mathbf{r}) \quad \text{and} \quad e\Gamma^*(\mathbf{p})\Gamma(\mathbf{p})=\rho(\mathbf{p}) \quad (4.3.3)$$

$U(\mathbf{r})$  and  $\Gamma(\mathbf{p})$  are complex functions and, by definition, are wave functions. It follows that

$$\int U^*(\mathbf{r})U(\mathbf{r})dV=1=\int \Gamma^*(\mathbf{p})\Gamma(\mathbf{p})dV_p \quad (4.3.4)$$

Differentials  $dV$  and  $dV_p$  represent, respectively, differential volume in space and momentum coordinates.

Since  $U(\mathbf{r})$  and  $\Gamma(\mathbf{p})$  describe the same dynamic charge distribution, they are relatable. Each position in coordinate space receives contributions from the full range of momenta in proportion to the value of  $\Gamma(\mathbf{p})$  at each velocity, and *vice versa*. Therefore we seek a linear transformation between the two coordinate systems that satisfies the conditions:

$$U(\mathbf{r})=L\{\Gamma(\mathbf{p})\} \quad \text{and} \quad \Gamma(\mathbf{p})=L^{-1}\{U(\mathbf{r})\} \quad (4.3.5)$$

$L$  is a linear operator and  $L^{-1}$  its inverse. A general linear function that meets these requirements is the Fourier integral transform pair:

$$\begin{aligned}
 U(\mathbf{r}) &= \left[ \frac{1}{2\pi\hbar} \right]^{3/2} \int \Gamma(\mathbf{p}) \exp\left( \frac{i\mathbf{r} \cdot \mathbf{p}}{\hbar} \right) dV_p \\
 \Gamma(\mathbf{p}) &= \left[ \frac{1}{2\pi\hbar} \right]^{3/2} \int U(\mathbf{r}) \exp\left( \frac{i\mathbf{r} \cdot \mathbf{p}}{\hbar} \right) dV
 \end{aligned}
 \tag{4.3.6}$$

The constant  $\hbar$  is a dimension-determining constant; its magnitude must be determined by experiment. Dropping to one dimension for simplicity, Eqs. 4.3.6 take the form:

$$\begin{aligned}
 U(x) &= \left[ \frac{1}{2\pi\hbar} \right]^{1/2} \int \Gamma(p) \exp\left( \frac{ixp}{\hbar} \right) dp \\
 \Gamma(p) &= \left[ \frac{1}{2\pi\hbar} \right]^{1/2} \int U(x) \exp\left( \frac{xp}{i\hbar} \right) dx
 \end{aligned}
 \tag{4.3.7}$$

The expectation value of momentum,  $p$ , is given by the equation:

$$\langle p \rangle = \int p \Gamma^*(p) \Gamma(p) dp
 \tag{4.3.8}$$

The same value may be calculated using  $U(x)$ . To do so, substitute  $\Gamma(p)$  from the second of Eqs. 4.3.7 into Eq. 4.3.8. The result is:

$$\langle p \rangle = \left( \frac{1}{2\pi\hbar} \right)^{1/2} \int_{-\infty}^{\infty} p \Gamma^*(p) \int_{-\infty}^{\infty} U(x) \exp\left( \frac{xp}{i\hbar} \right) dx
 \tag{4.3.9}$$

Integrating the second integral by parts gives:

$$\langle p \rangle = \left( \frac{1}{2\pi\hbar} \right)^{1/2} \int_{-\infty}^{\infty} \Gamma^*(p) \left\{ i\hbar U(x) \Big|_{-\infty}^{\infty} - i\hbar \int_{-\infty}^{\infty} \frac{\partial U(x)}{\partial x} \exp\left( \frac{xp}{i\hbar} \right) dx \right\}$$

Since an acceptable wave function is equal to zero at infinity, the first term within the brackets vanishes. Substituting the complex conjugate of the first

of Eqs. 4.3.7 into the second term and reversing the order of integration gives:

$$\langle p \rangle = \int_{-\infty}^{\infty} U^*(x) \left[ \frac{\hbar}{i} \frac{\partial U(x)}{\partial x} \right] dx \quad (4.3.10)$$

Equation 4.3.10 is an example of the general case: A dynamic variable in momentum space may be replaced by an operation in dimensional space, and *vice versa*. Letting  $O$  indicate that the variable is written in operator form, in three dimensions the momentum operator is:

$$O(p) = \frac{\hbar}{i} \nabla \quad (4.3.11)$$

It is understood that the operator acts on wave function  $U(r)$ . Repeating the above procedure for  $p^n$  shows, after 'n' partial integrations, that the result generalizes to:

$$O(p^n) = \left( \frac{\hbar}{i} \right)^n \nabla^n \quad (4.3.12)$$

A significant result is that it is not necessary to solve for both  $U(r)$  and  $\Gamma(p)$  to solve a kinematic problem. It is only necessary to work with one functional type, typically  $U(r)$ , and express conjugate variables in operator form.

The conservation law of primary importance is the low speed energy of an electron with total energy  $W$ . The sum of kinetic plus potential energies is:

$$W = \frac{1}{2m} \int dV_p [p^2 \Gamma^*(p) \Gamma(p)] + \int dV [V(r) U^*(r) U(r)] \quad (4.3.13)$$

An arbitrary constant, such as the self-energy of the electron, may be added without affecting results to follow. Applying Eq. 4.3.12 to Eq. 4.3.13 gives the result:

$$\int dV U^*(\mathbf{r}) \left\{ -\frac{\hbar^2}{2m} \nabla^2 U(\mathbf{r}) + [\Lambda(\mathbf{r}) - W] U(\mathbf{r}) \right\} = 0 \quad (4.3.14)$$

Although only the integral is required to equal zero, the more stringent condition that the integrand equal zero at all points within the region may also be applied. Doing so returns Eq. 4.3.1, the time-independent Schrödinger wave equation. Function  $U(\mathbf{r})$  is a wave function that provides the time average charge density of the electron of interest at each point.

The above development shows that the Schrödinger equation is a statement of energy conservation; Planck's constant appears as a phase-determining normalization constant in the scalar product between velocity and position vectors, see Eq. 4.3.6. The Schrödinger equation is correct only at electron speeds much less than  $c$  and it does not account for electron spin; it is necessary to add electron spin separately to the wave equation. In contrast, Dirac's equations apply in all inertial systems and spin is an integral part of the whole. Although Dirac's work is of singular importance to quantum theory, it does not assist in resolving basic issues of photon exchanges considered here. Therefore, it is not discussed in this work.

## 4.4 The Uncertainty Principle

By the uncertainty principle, it is not possible to determine simultaneously the exact value of conjugate variables, such as position and momentum. The more accurately the position of a point electron is known the less accurately the momentum can be known, and *vice versa*. As a simple example, consider the case of an electron described by a Gaussian wave function. That is,  $U(x)$  is proportional to  $\exp(-x^2/B)$ , where  $B$  is undetermined but constrained to be positive:

$$0 < B < \infty \quad (4.4.1)$$

The electron is confined to position zero only if  $B$  increases without limit and the smaller the value of  $B$  the larger the physical extent of the charge distribution. The system is normalized if the probability density at each point is:



$$U^*(x)U(x) = \sqrt{\frac{2}{\pi B}} \exp\left(-\frac{2x^2}{B}\right) \quad (4.4.2)$$

The expectation value of  $x^2$  may be calculated using the integrals of Table 4.4.1:

$$\langle x^2 \rangle = \sqrt{\frac{2}{\pi B}} \int_{-\infty}^{\infty} \exp\left(-\frac{2x^2}{B}\right) x^2 dx = \frac{B}{4} \quad (4.4.3)$$

---


$$\begin{aligned} \int_0^{\infty} \exp(-a^2 x^2) dx &= \frac{\sqrt{\pi}}{2a} \\ \int_0^{\infty} x^2 \exp(-x^2) dx &= \frac{\sqrt{\pi}}{4} \\ \int_0^{\infty} \exp(-a^2 x^2) \cos(bx) dx &= \frac{\sqrt{\pi}}{2a} \exp\left(-\frac{b^2}{4a^2}\right) \end{aligned}$$


---

Table 4.4.1. Short Table of Gaussian Integrals

Substituting  $U(x)$  into the second of Eqs. 4.3.7 results in the momentum space form of the wave function:

$$\Gamma(p) = \left(\frac{B}{2\pi\hbar^2}\right)^{1/4} \exp\left(-\frac{B}{4\hbar^2} p^2\right) \quad (4.4.4)$$

Using Eq. 4.4.4 to calculate the mean-square value of momentum gives:

$$\langle p^2 \rangle = \left(\frac{B}{2\pi\hbar^2}\right)^{1/2} \int_{-\infty}^{\infty} \exp\left(-\frac{Bp^2}{2\hbar^2}\right) p^2 dp = \frac{\hbar^2}{B} \quad (4.4.5)$$

Recalculating  $\langle p^2 \rangle$  in coordinate space using operator notation gives, after some calculation:

$$\langle p^2 \rangle = -\hbar^2 \left( \frac{2}{\pi B} \right)^{1/2} \int_{-\infty}^{\infty} \exp\left(-\frac{x^2}{B}\right) \frac{d^2}{dx^2} \left[ \exp\left(-\frac{x^2}{B}\right) \right] dx = \frac{\hbar^2}{B} \quad (4.4.6)$$

The r.m.s. values of position and momentum satisfy the parabolic relationship:

$$\sqrt{\langle x^2 \rangle \langle p^2 \rangle} = \frac{\hbar}{2} \quad (4.4.7)$$

By Eq. 4.4.7 it is not possible to know position and momentum more accurately than  $\Delta x \Delta p \approx \hbar$ , where  $\Delta x$  and  $\Delta p$  are, respectively, uncertainty in the measurement of position and momentum. This is a quantitative statement of the uncertainty principle. It results from the properties of the Fourier integral transform relationships relating the wave functions in momentum and coordinate space. The same is true for all conjugate pairs, *i.e.*, pairs related by Fourier transforms; they satisfy the parabolic uncertainty relationship of Eq. 4.4.7.

It may be shown that a Gaussian wave function provides the least possible uncertainty; all other wave functions provide a greater uncertainty than that of Eq. 4.4.7.

By the electron model of Section 4.2, the uncertainty is due to incomplete information available about the intra-electron ensemble. Were the structure adequately known, in principle the exact solution could be used to obtain full knowledge of any physical result.

## 4.5 The Time-Dependent Schrödinger Equation

Solutions of the time-independent Schrödinger equation describe time-average values of the kinematic parameters and, of course, time-average values are constant. However, the time-average expectation values occur over time intervals that are long only when compared with changes in the electron configuration within the state. Time variation of solutions over

much longer periods of time, but still short compared with events in the macroscopic world, are often of interest. In this section, we examine changes during times that are longer than needed for electron configuration changes but short compared with macroscopic times. The result determines the initial variation of expectation values away from equilibrium positions by calculating changes that occur slowly enough so ensemble averages always remain in near-equilibrium conditions. If the potential changes too rapidly, or if the potential change is too large, the near-equilibrium condition is violated and the Schrödinger equation ceases to apply. In summary, the Schrödinger time-dependent equation applies only if the ensemble remains in a near-equilibrium condition.

From Eq. 4.3.2 the time-average charge density at a point due to total charge  $e$  is:

$$\rho(\mathbf{r}) = eU^*(\mathbf{r})U(\mathbf{r}) \quad (4.5.1)$$

Since the current density is real, it may be written as:

$$\mathbf{J}(\mathbf{r}) = \frac{1}{m}\rho(\mathbf{r})\mathbf{p} = \frac{\hbar e}{im}U^*(\mathbf{r})\nabla U(\mathbf{r}) \Rightarrow \frac{\hbar e}{2im}[U^*(\mathbf{r})\nabla U(\mathbf{r}) - U(\mathbf{r})\nabla U^*(\mathbf{r})] \quad (4.5.2)$$

To describe the time dependence introduce notation similar to that of Eq. 4.5.1:

$$\rho(\mathbf{r}, t) = e\psi^*(\mathbf{r}, t)\psi(\mathbf{r}, t) \quad (4.5.3)$$

By extension

$$\mathbf{J}(\mathbf{r}, t) = \frac{\hbar e}{2im}[\psi^*(\mathbf{r}, t)\nabla\psi(\mathbf{r}, t) - \psi(\mathbf{r}, t)\nabla\psi^*(\mathbf{r}, t)] \quad (4.5.4)$$

The rate of change of the charge density is:

$$\frac{\partial\rho(\mathbf{r}, t)}{\partial t} = e\left[\psi^*(\mathbf{r}, t)\frac{\partial}{\partial t}\psi(\mathbf{r}, t) + \psi(\mathbf{r}, t)\frac{\partial}{\partial t}\psi^*(\mathbf{r}, t)\right] \quad (4.5.5)$$

The divergence of the current density is:

$$\nabla \cdot \mathbf{J}(\mathbf{r}, t) = \frac{\hbar e}{2im} \left[ \psi^*(\mathbf{r}, t) \nabla^2 \psi(\mathbf{r}, t) - \psi(\mathbf{r}, t) \nabla^2 \psi^*(\mathbf{r}, t) \right] \quad (4.5.6)$$

The continuity equation is:

$$\nabla \cdot \mathbf{J}(\mathbf{r}, t) + \frac{\partial \rho(\mathbf{r}, t)}{\partial t} = 0 \quad (4.5.7)$$

Substituting Eqs. 4.5.5 and 4.5.6 into Eq. 4.5.7, multiplying by  $(\hbar/ie)$ , and adding and subtracting potential term  $\Lambda(\mathbf{r})$  gives:

$$\begin{aligned} & \psi^*(\mathbf{r}, t) \left[ -\frac{\hbar^2}{2m} \nabla^2 \psi(\mathbf{r}, t) + \Lambda(\mathbf{r}) \psi(\mathbf{r}, t) + \frac{\hbar}{i} \frac{\partial}{\partial t} \psi(\mathbf{r}, t) \right] \\ & - \psi(\mathbf{r}, t) \left[ -\frac{\hbar^2}{2m} \nabla^2 \psi^*(\mathbf{r}, t) + \Lambda(\mathbf{r}) \psi^*(\mathbf{r}, t) - \frac{\hbar}{i} \frac{\partial}{\partial t} \psi^*(\mathbf{r}, t) \right] = 0 \end{aligned} \quad (4.5.8)$$

To connect with the time-independent equation, we seek wave function  $\psi(\mathbf{r}, t)$  that, as the time dependence becomes vanishingly slow, goes to:

$$\begin{aligned} & U^*(\mathbf{r}) \left[ -\frac{\hbar^2}{2m} \nabla^2 U(\mathbf{r}) + \Lambda U(\mathbf{r}) - \mathcal{W} U(\mathbf{r}) \right] \\ & - U(\mathbf{r}) \left[ -\frac{\hbar^2}{2m} \nabla^2 U^*(\mathbf{r}) + \Lambda U^*(\mathbf{r}) - \mathcal{W} U^*(\mathbf{r}) \right] = 0 \end{aligned} \quad (4.5.9)$$

Since each line of Eq. 4.5.9 is equal to zero, so are the two lines of Eq. 4.5.8 in the low speed limit. Therefore, the satisfactory, time-dependent wave function is:

$$\int \psi^*(\mathbf{r}, t) \left[ -\frac{\hbar^2}{2m} \nabla^2 \psi(\mathbf{r}, t) + \Lambda(\mathbf{r}) \psi(\mathbf{r}, t) + \frac{\hbar}{i} \frac{\partial}{\partial t} \psi(\mathbf{r}, t) \right] dV = 0 \quad (4.5.10)$$

Insisting that not just the integral but also the integrand be equal to zero results in the equality:

$$-\frac{\hbar}{i} \frac{\partial}{\partial t} \psi(\mathbf{r}, t) = H\psi(\mathbf{r}, t) = W\psi(\mathbf{r}, t) \quad (4.5.11)$$

Equation 4.5.11 is the Schrödinger time-dependent equation. The Hamiltonian operator,  $H$ , is defined to be the operator that acts on the wave function to produce the time dependence and state energy of Eq. 4.5.11. From the first equality of Eq. 4.5.11:

$$H\psi(\mathbf{r}, t) = -\frac{\hbar^2}{2m} \nabla^2 \psi(\mathbf{r}, t) + \Lambda(\mathbf{r})\psi(\mathbf{r}, t) \quad (4.5.12)$$

From the second equality of Eq. 4.5.11:

$$\psi(\mathbf{r}, t) = \psi(\mathbf{r}, t_0) \exp\left(\frac{iW}{\hbar} t\right) \quad (4.5.13)$$

The initial value of the wave function is the equilibrium value:

$$\psi(\mathbf{r}, t_0) = U(\mathbf{r}) \quad (4.5.14)$$

An important result of Eq. 4.5.13 is that the frequency of an eigenstate is related to the energy as:

$$\omega = W/\hbar \quad (4.5.15)$$

The time-independent Schrödinger equation has the character of a thermodynamic equation in that only time-average values taken over times long compared with the periods of possible intra-state electron movements are known. Detailed charge and current densities remain unknown. Although Eq. 4.5.11 provides correct average values, it does not imply a time-line of actual events. It only applies to initial changes at the onset of instability, not to the full transition.

## 4.6 Quantum Operator Properties

An extension of the logic that supported the use of operators to calculate momentum generalizes to include functions of momentum. To make the generalization consider the integral:

$$I = \int_{-\infty}^{\infty} [\Gamma_R^*(p) p \Gamma_S(p)] dV_p \quad (4.6.1)$$

$\Gamma_R(p)$  and  $\Gamma_S(p)$  represent two eigenfunction solutions of the same differential equation. For each function  $\Gamma_R(p)$ , there exists a Fourier integral transform function in coordinate space,  $U_R(r)$ . To rewrite the integral of Eq. 4.6.1 using spatial functions, repeat the procedure used going from Eq. 4.3.8 to Eq. 4.3.10. Taking the gradient in the direction of the momentum and working with the “S” functions, the integral of Eq. 4.6.1 becomes:

$$I = \int_{-\infty}^{\infty} U_R^*(r) \left[ \frac{\hbar}{i} \nabla U_S(r) \right] dV \quad (4.6.2)$$

Similarly, working with the “R” functions gives:

$$I = \int_{-\infty}^{\infty} U_S(r) \left[ \frac{\hbar}{i} \nabla U_R(r) \right]^* dV \quad (4.6.3)$$

Since all physical results are real, Eq. 4.6.3 is equal to its own complex conjugate:

$$\int_{-\infty}^{\infty} U_S^*(r) \left[ \frac{\hbar}{i} \nabla U_R(r) \right] dV = \int_{-\infty}^{\infty} U_S(r) \left[ -\frac{\hbar}{i} \nabla U_R^*(r) \right] dV \quad (4.6.4)$$

Combining Eqs. 4.6.2 and 4.6.4 gives:

$$\int_{-\infty}^{\infty} U_R^*(\mathbf{r}) \left[ \frac{\hbar}{i} \nabla U_S(\mathbf{r}) \right] dV = \int_{-\infty}^{\infty} U_S(\mathbf{r}) \left[ \frac{\hbar}{i} \nabla U_R(\mathbf{r}) \right]^* dV \quad (4.6.5)$$

The result generalizes to:

$$\int_{-\infty}^{\infty} U_R^*(\mathbf{r}) O[U_S(\mathbf{r})] dV = \int_{-\infty}^{\infty} U_S(\mathbf{r}) \langle O[U_S(\mathbf{r})] \rangle^* dV \quad (4.6.6)$$

The symbol “O” indicates any quantum mechanical operator. An operator that satisfies Eq. 4.6.6 is, by definition, a Hermitian operator.

## 4.7 Orthogonality

To examine the orthogonality properties of wave function  $\psi(\mathbf{r}, t)$ , let O be a quantum theory operator, let  $\psi_R(\mathbf{r}, t)$  and  $\psi_S(\mathbf{r}, t)$  be time-dependent eigenfunctions, and let  $I_R$  and  $I_S$  be the corresponding state values. That is:

$$O\psi_R(\mathbf{r}, t) = I_R\psi_R(\mathbf{r}, t) \quad \text{and} \quad O\psi_S(\mathbf{r}, t) = I_S\psi_S(\mathbf{r}, t) \quad (4.7.1)$$

Functions  $\psi_R(\mathbf{r}, t)$  that satisfy this equation are eigenfunctions and constants  $I_R$  are state values. Multiplying the left equation by  $\psi_S^*(\mathbf{r}, t)$ , the right equation by  $\psi_R^*(\mathbf{r}, t)$ , subtracting one from the other, and integrating over the volume gives:

$$\int [\psi_R^* I_S \psi_S - \psi_S^* I_R \psi_R] dV = \int [\psi_R^* O\psi_S - \psi_S (O\psi_R)^*] dV = (I_S - I_R) \int \psi_R^* \psi_S dV \quad (4.7.2)$$

It follows from Eq. 4.6.6 that:

$$\int [\psi_R^* (O\psi_S) - \psi_S (O\psi_R)^*] dV = 0 \quad (4.7.3)$$

Combining Eqs. 4.7.2 and 4.7.3 gives:

$$(I_S - I_R) \int \psi_R^* \psi_S dV = 0 \quad (4.7.4)$$

If a system has more than one eigenfunction with the same state energy, the system is degenerate; the number of solutions that produce the same state energy is the degree of degeneracy. A conclusion from Eq. 4.7.4 is that if the states are not degenerate the functions are orthogonal; if the state energies are equal the functions are degenerate and may or may not be orthogonal.

Wherever solutions of a single operator result in many eigenfunctions,  $\psi_S(r,t)$ , the physical result is a sum, weighted by constants  $a_S$ , over all possible eigenfunctions:

$$\Psi(r,t) = \sum_{S=1}^{\infty} a_S \psi_S(r,t) \quad (4.7.5)$$

$\psi_S(r,t)$  are normalized values of the wave functions. Requiring that the total wave function be normalized gives:

$$\int \Psi^* \Psi dV = \sum_{R=1}^{\infty} \sum_{S=1}^{\infty} a_R a_S^* \int \psi_R \psi_S^* dV = \sum_{R=1}^{\infty} a_R a_R^* = 1 \quad (4.7.6)$$

Equation 4.7.6 shows that the sum over the magnitudes of all coefficients is one. This leads to the conclusion that:

$$\langle O \rangle = \int \Psi^* O \Psi dV = \sum_{R=1}^{\infty} \sum_{S=1}^{\infty} a_R a_S^* \int \psi_S^* O \psi_R dV = \sum_{R=1}^{\infty} I_R a_R a_R^* \quad (4.7.7)$$

In words, the expectation value of any dynamic function “O” is the sum over the probabilities that the electron occupies a particular state multiplied by the state value. For any particular measurement, the use of operator  $\langle O \rangle$  produces only the particular value  $a_R a_R^*$ . With a linear system, a single electron in a single atom forms partial solutions over each wave function. That is, an electron is distributed in a statistical way over the possible eigenstates. With nonlinear systems, and if the nonlinearity is required for



movements between eigenstates, mixtures of nondegenerate states do not occur within individual atoms. Either way, if the measurements are repeated enough times, the different state values appear with a probability equal to the square of the eigenfunction coefficients.

The initial rate of change of an expectation value follows. Differentiating the first equality of Eq. 4.7.7 with respect to time gives:

$$\frac{d}{dt}\langle O \rangle = \int \left( \frac{\partial \psi^*}{\partial t} O \psi + \psi^* O \frac{\partial \psi}{\partial t} \right) dV \quad (4.7.8)$$

Using Eq. 4.5.11, this may be written as:

$$\frac{d}{dt}\langle O \rangle = -\frac{i}{\hbar} \int \left( \psi^* O (H\psi) - (H\psi)^* (O\psi) \right) dV \quad (4.7.9)$$

Incorporating Eq. 4.6.6:

$$\frac{d}{dt}\langle O \rangle = -\frac{i}{\hbar} \int \psi^* (OH - HO) \psi dV \quad (4.7.10)$$

For the special case where  $I = r$ :

$$\langle p \rangle = m \frac{d}{dt} \langle r \rangle = \frac{\hbar m}{\hbar} (Hr - rH) \quad (4.7.11)$$

The bracket on the right side of Eq. 4.7.11 is defined to be the commutator of the indicated variable. This particular bracket is the commutator of position.

## 4.8 Electron Angular Momentum, Central Force Fields

By definition, the angular momentum,  $I$ , in kinematic and operator forms is:

$$I \equiv r \times p = \frac{\hbar}{i} r \times \nabla \quad (4.8.1)$$

The first equality follows from classical mechanics and the second using quantum theory operator notation. By Eq. 4.8.1 the operator form of the angular momentum components about each of the three axes is:

$$\begin{aligned} L_x &= \frac{\hbar}{i} \left( y \frac{\partial}{\partial z} - z \frac{\partial}{\partial y} \right) = -\frac{\hbar}{i} \left( \sin \phi \frac{\partial}{\partial \theta} + \cot \theta \cos \phi \frac{\partial}{\partial \phi} \right) \\ L_y &= \frac{\hbar}{i} \left( z \frac{\partial}{\partial x} - x \frac{\partial}{\partial z} \right) = \frac{\hbar}{i} \left( \cos \phi \frac{\partial}{\partial \theta} - \cot \theta \sin \phi \frac{\partial}{\partial \phi} \right) \\ L_z &= \frac{\hbar}{i} \left( x \frac{\partial}{\partial y} - y \frac{\partial}{\partial x} \right) = \frac{\hbar}{i} \left( \frac{\partial}{\partial \phi} \right) \end{aligned} \quad (4.8.2)$$

The first set of equalities in Eq. 4.8.2 follow directly from Eq. 4.8.1 and the second follows after changing to spherical coordinates.

Another quantity of interest is the magnitude of the angular momentum. The operator form of the square of the angular momentum follows from Eq. 4.8.2; evaluation gives:

$$L_x^2 + L_y^2 = -\hbar^2 \left( \frac{\partial^2}{\partial \theta^2} + \cot^2 \theta \frac{\partial^2}{\partial \phi^2} + \cot \theta \frac{\partial}{\partial \theta} \right) \quad L_z^2 = -\hbar^2 \left( \frac{\partial^2}{\partial \phi^2} \right)$$

The sum is:

$$L^2 = L_x^2 + L_y^2 + L_z^2 = -\hbar^2 \left( \frac{1}{\sin \theta} \frac{\partial}{\partial \theta} \left[ \sin \theta \frac{\partial}{\partial \theta} \right] + \frac{1}{\sin^2 \theta} \frac{\partial^2}{\partial \phi^2} \right) \quad (4.8.3)$$

The electrostatic force fields about atomic nuclei have spherical symmetry. With spherical symmetry the potential is a function only of the magnitude of the radius and there is no angular dependence. For this case the Schrödinger equation has the form:

$$-\frac{\hbar^2}{2m} \nabla^2 U(\mathbf{r}) + \Lambda(\mathbf{r})U(\mathbf{r}) = \mathcal{W}U(\mathbf{r}) \quad (4.8.4)$$

Introducing the Laplacian operator in spherical coordinates and rearranging terms gives:

$$\begin{aligned}
& \frac{1}{\sin\theta} \frac{\partial}{\partial\theta} \left[ \sin\theta \frac{\partial U(r,\theta,\phi)}{\partial\theta} \right] + \frac{1}{\sin^2\theta} \left[ \frac{\partial^2 U(r,\theta,\phi)}{\partial\phi^2} \right] \\
& = -\frac{\partial}{\partial r} \left[ r^2 \frac{\partial U(r,\theta,\phi)}{\partial r} \right] + \frac{2m}{\hbar^2} [W + \Lambda(r)] r^2 U(r,\theta,\phi)
\end{aligned} \tag{4.8.5}$$

To solve the Laplacian, break function  $U(r,\theta,\phi)$  into functions of a single variable; that is, put  $U(r,\theta,\phi)$  equal to product function  $R(r)\Theta(\theta)\Phi(\phi)$  then sum over all possible solutions:

$$U(r,\theta,\phi) = \sum R(r)\Theta(\theta)\Phi(\phi) \tag{4.8.6}$$

Substituting the single function product form into Eq. 4.8.5 then multiplying by the inverse results in the equality:

$$\frac{1}{\Theta \sin\theta} \frac{d}{d\theta} \left( \sin\theta \frac{d\Theta}{d\theta} \right) + \frac{1}{\Phi \sin^2\theta} \left( \frac{d^2\Phi}{d\phi^2} \right) = -\frac{d}{R dr} \left( r^2 \frac{dR}{dr} \right) + \frac{2m}{\hbar^2} [W + \Lambda(r)] r^2 \tag{4.8.7}$$

Since the left side of the equation is only a function of angles and the right side is only a function of radius, each side is constant. It is most convenient to put the separation constant equal to  $-\ell(\ell+1)$ . In a similar way, with separation constant  $m$ , the terms on the left side of Eq. 4.8.7 break into functions of  $\theta$  alone and  $\phi$  alone. The result is two complete differential equations:

$$\begin{aligned}
& \frac{d^2\Phi}{d\phi^2} + m^2\Phi = 0 \\
& \frac{1}{\sin\theta} \frac{d}{d\theta} \left[ \sin\theta \frac{d\Theta}{d\theta} \right] + \left[ \ell(\ell+1) - \frac{m^2}{\sin^2\theta} \right] \Theta = 0
\end{aligned} \tag{4.8.8}$$

The  $\phi$  solutions may be written either as

$$\Phi(\phi) = A_m \cos(m\phi) + B_m \sin(m\phi) \quad \text{or} \quad C_m e^{im\phi} + D_m e^{-im\phi} \tag{4.8.9}$$

Since solutions that describe physical reality cannot be multivalued,  $m$  must be an integer. If the solution is proportional to either  $A_m$  or  $B_m$ , by the third of Eqs. 4.8.2 the  $z$ -component of angular momentum is zero; if the solution is proportional to  $C_m$  or  $D_m$  the  $z$ -component of angular momentum,  $l_z$ , is:

$$l_z = \pm m\hbar \quad (4.8.10)$$

Combining Eqs. 4.8.3 with the  $\theta$ -dependent part of Eq. 4.8.8 shows that the angular momentum satisfies the equation:

$$l^2 = \ell(\ell + 1)\hbar^2 \quad (4.8.11)$$

The  $\theta$ -equation provides a physically real solution only if  $\ell$  is an integer and solutions with integer values of  $\ell$  are associated Legendre functions.

The two separation constants,  $\ell$  and  $m$ , are both integers and in the equations of quantum theory are called quantum numbers. The ranges in which such solutions exist are:

$$0 \leq \ell < \infty \quad \text{and} \quad -\ell \leq m \leq \ell \quad (4.8.12)$$

Comparison of the above shows that under all circumstances:

$$l^2 > l_z^2 \quad (4.8.13)$$

Therefore the entire angular momentum is never about a single axis. This point supports electron configurational aspects discussed in later sections.

## 4.9 The Coulomb Potential Source

Let point charge  $+Ze$  attract an electron of charge  $-e$ . The resulting potential energy is:

$$\Lambda(r) = -\frac{Ze^2}{4\pi\epsilon r} \quad (4.9.1)$$

Combining Eq. 4.9.1 and the radial portion of Eq. 4.8.7 results in:

$$-\frac{\hbar^2}{2m} \frac{1}{r^2} \frac{d}{dr} \left( r^2 \frac{dR}{dr} \right) - \frac{Ze^2}{4\pi\epsilon r} R + \frac{\ell(\ell+1)\hbar^2}{2mr^2} R = WR \quad (4.9.2)$$

The total energy  $W$  is less than or greater than zero respectively for bound or free electrons. This equation is most easily solved by introducing the parameter  $\alpha$  and variable  $\rho$  where, by definition:

$$\rho = \alpha r \quad (4.9.3)$$

It is helpful to introduce the additional definitions:

$$\alpha^2 = \frac{8m|W|}{\hbar^2} \quad \text{and} \quad n = \frac{Ze^2}{4\pi\epsilon\hbar} \sqrt{\frac{m}{2|W|}} = \frac{Ze^2 m}{2\pi\epsilon\alpha\hbar^2} \quad (4.9.4)$$

If the electron energy is negative, substituting  $\rho$  back into Eq. 4.9.2 and using Eqs. 4.9.4 gives:

$$\frac{1}{\rho^2} \frac{d}{d\rho} \left( \rho^2 \frac{dR}{d\rho} \right) - \frac{\ell(\ell+1)}{\rho^2} R + \frac{nR}{\rho} - \frac{R}{4} = 0 \quad (4.9.5)$$

To solve Eq. 4.9.5 begin with the asymptotic limit at infinity. As  $\rho$  increases without limit the asymptotic differential equation is:

$$\frac{d^2 R}{d\rho^2} - \frac{R}{4} = 0 \quad (4.9.6)$$

The solution of Eq. 4.9.6 is:

$$R(\rho) = F(\rho)e^{-\rho/2} + G(\rho)e^{\rho/2} \quad (4.9.7)$$

The conditions on Eq. 4.9.6 are that, in the asymptotic limit of large radius,  $F(\rho)$  and  $G(\rho)$  must change much more slowly with  $\rho$  than the exponential terms and, since the total charge is finite, function  $R(\rho)$  must vanish at infinity. It follows that since a non-zero value of function  $G(\rho)$  does not

represent physical reality it is multiplied by zero. Substituting the remaining form  $F(\rho)e^{-\rho/2}$  into Eq. 4.9.5 results in the differential equation:

$$\frac{d^2 F}{d\rho^2} + \left(\frac{2}{\rho} - 1\right) \frac{dF}{d\rho} + \left(\frac{n-1}{\rho} - \frac{\ell(\ell+1)}{\rho^2}\right) F = 0 \quad (4.9.8)$$

A convenient solution method for Eq. 4.9.8 is a power series expansion. The solution procedure begins by forming the summation:

$$F(\rho) = \rho^s \sum_{j=0}^{\infty} a_j \rho^j \quad (4.9.9)$$

Solution requires that  $a_0 \neq 0$  and  $a_j \geq 0$ . Substituting Eq. 4.9.9 into Eq. 4.9.8 results in the sum:

$$\begin{aligned} & [s(s+1) - \ell(\ell+1)] \rho^{-2} \\ & + \sum_{j=0}^{\infty} \{[(s+j+1)(s+j+2) - \ell(\ell+1)]a_{j+1} - (s+j+1-n)a_j\} \rho^{j-1} = 0 \end{aligned} \quad (4.9.10)$$

Since  $a_0$  is not equal to zero, the first term of Eq. 4.9.10 requires that either  $s = \ell$  or  $s = -(\ell+1)$ . Since the latter is singular at the origin, it cannot represent physical reality. Substituting  $s = \ell$  into Eq. 4.9.10 results in the coefficient ratio:

$$\frac{a_{j+1}}{a_j} = \frac{j+1+\ell-n}{(j+1)(j+2\ell+2)} \quad (4.9.11)$$

As index 'j' increases without limit Eq. 4.9.11 goes asymptotically to the index of the expansion for  $e^{\rho}$ . Combining this with Eq. 4.9.7 shows that the radial function is proportional to  $e^{\rho/2}$  in the limit of very large  $\rho$ , a physically unacceptable result. Hence a nontrivial solution of  $F(\rho)$  exists if and only if

the series terminates, and the series terminates only if  $n$  is an integer. For that case, Eq. 4.9.4 shows that state energy  $W_n$  is equal to:

$$W_n = -\frac{mZ^2 e^4}{32\pi^2 \epsilon^2 n^2 \hbar^2} \quad (4.9.12)$$

This result shows that an infinite number of energy state values exist, that the energy is independent of quantum numbers  $\ell$  and  $m$ , and that the state energy varies as the inverse square of quantum number  $n$ .

It is helpful to define radius  $r_0$  as:

$$r_0 = \frac{2Z}{n\alpha} \quad \text{hence} \quad r_0 = \frac{4\pi\epsilon\hbar^2}{me^2} \quad (4.9.13)$$

Evaluating Eq. 4.9.13 shows that:

$$r_0 = 5.29172 \times 10^{-11} \text{ m} \quad (4.9.14)$$

By definition,  $r_0$  is the Bohr radius. The electrostatic energy may also be written as:

$$W_n = \frac{Ze^2}{8\pi\epsilon} \langle 1/r \rangle \quad (4.9.15)$$

Combining Eqs. 4.9.12, 4.9.13, and 4.9.15 shows that:

$$\langle 1/r \rangle = Z / (n^2 r_0) \quad (4.9.16)$$

In the limit of large values of  $n$ , the energy goes to zero and the expectation value of the radius of the electron state becomes infinite: the electron is distributed over all space.

To solve for the radial function, rewrite Eq. 4.9.11 as:

$$a_{j+1} = \frac{(j + \ell + 1 - n)}{(j + 2\ell + 2)(j + 1)} a_j \quad (4.9.17)$$

From Eq. 4.9.17, each coefficient gives:

$$a_j = (-1)^j \left( \frac{(n - \ell - 1)!(2\ell + 1)!}{(n - j - \ell - 1)!j!(2\ell + j + 1)!} \right) a_0$$

To put this notation in agreement with common usage, define  $a_0$  to be:

$$a_0 = -\frac{(n + \ell)!^2}{(n - \ell - 1)!(2\ell + 1)!}$$

Combining gives:

$$a_j = (-1)^{j+1} \left\{ \frac{(n + \ell)!^2}{(n - j - \ell - 1)!j!(2\ell + j + 1)!} \right\} \quad (4.9.18)$$

It follows that:

$$\ell < n \quad (4.9.19)$$

Combining all results shows that  $R(\rho)$  depends upon both quantum numbers  $n$  and  $\ell$ , and is equal to:

$$R_n^\ell(\rho) = \rho^\ell e^{-\rho/2} \sum_{j=0}^{n-\ell-1} (-1)^{j+1} \frac{(n + \ell)!^2 \rho^j}{(n - j - \ell - 1)!j!(2\ell + j + 1)!} \quad (4.9.20)$$

Functional values for  $n = 1$  through 4 are listed in Table 4.9.1.

Wave function normalization follows from Eq. 4.9.20, and the integral result:



	$\ell = 1$	$\ell = 2$	$\ell = 3$	$\ell = 4$
$R_n^0(\sigma)$	$-e^{-\rho/2}$	$-(2)!(2-\rho)e^{-\rho/2}$	$-3(6-6\rho+\rho^2)e^{-\rho/2}$	$-24\left(\begin{matrix} 4-6\rho \\ +2\rho^2-\rho^3 \end{matrix}\right)e^{-\rho/2}$
$R_n^1(\sigma)$		$-(3)!\rho e^{-\rho/2}$	$-(4)!(4-\rho)\rho e^{-\rho/2}$	$-60\left(\begin{matrix} 20-10\rho \\ +3\rho^2 \end{matrix}\right)\rho e^{-\rho/2}$
$R_n^2(\sigma)$			$-(5)!\rho^2 e^{-\rho/2}$	$-(6)!(6-\rho)\rho^2 e^{-\rho/2}$
$R_n^3(\sigma)$				$-(7)!\rho^3 e^{-\rho/2}$

Table 4.9.1 Values of  $R_n^\ell(\sigma)$  for  $n = 1-4$

$$I_n^\ell = \int_0^\infty \rho^2 d\rho R_n^\ell(\rho) R_q^\ell(\rho) = \frac{2n(n+\ell)!^3}{(n-\ell-1)!} \delta(n,q)$$

(4.9.21)

The first row of Table 4.9.1 shows that the largest value of the function occurs at the origin. Including the origin, there are a total of  $\ell$  maxima as a function of radius. The remaining rows show that each function is multiplied by the radius raised to power  $\ell$ . Therefore the value is equal to zero at the origin for all except  $\ell = 0$  and the radius of the region with a negligibly small value of charge increases with increasing values of  $\ell$ .

4.10 Hydrogen Atom Eigenfunctions

The full expression for an eigenfunction of a spherical potential source is:

$$U_{n\ell m}(r,\theta,\phi) = A_{n\ell m} R_n^\ell(\alpha_n r) P_\ell^m(\cos\theta) e^{-im\phi}$$

(4.10.1)

It was shown in Sections 4.8 and 4.9 that both quantum numbers  $n$  and  $\ell$  are integers. A separate requirement that  $\ell$  and  $m$  be integers follows from the requirement that the full range of solid angle be available for angular

solutions. Also since the full range of angles are available the coefficients of Legendre functions of the second kind are all equal to zero. From the theory of Legendre polynomials:

$$\int_0^\pi \sin\theta d\theta \left[ P_\ell^m(\cos\theta) \right]^2 = \frac{4\pi}{(2\ell+1)} \frac{(\ell+m)!}{(\ell-m)!} \quad (4.10.2)$$

Using Eqs. 4.9.21 and 4.10.2 to solve for the total probability of each state, then normalizing that value to unity, permits solving for the constant coefficients of Eq. 4.10.1. The result is:

$$|A_{n\ell m}| = \left\{ \frac{\alpha_n^3}{4\pi n} \frac{(n-\ell-1)!}{(n+\ell)!^3} \frac{(2\ell+1)(\ell-m)!}{(\ell+m)!} \right\}^{0.5} \quad (4.10.3)$$

Each wave function has  $(n-\ell)$  zeros, including infinity, and undergoes  $(n-\ell)$  nodes (functional maxima) as a function of radius. Several complete eigenfunctions are listed in Table 4.10.1.

The energy levels of Eq. 4.9.12 show that the energy depends upon quantum number  $n$  but not upon quantum numbers  $\ell$  and  $m$ . In common with other boundary value problems only eigenfunction solutions can exist. Parameter  $r_0$  of Eq. 4.9.13 is a normalizing radial factor that shows atomic radii to be on the order of 0.1 nm.

Since wave functions with  $m = 0$  have spherical symmetry the charge density associated with it produces monopole electrostatic fields. There is a charge density node at the origin and  $(n-1)$  others at increasing values of radius. Wave functions with  $m = 1$  have bilateral symmetry. There is a null in the charge density at the origin and  $(n-1)$  nodes. Wave functions with  $m = 2$  have quadrilateral symmetry. There is a charge density null at the origin and  $(n-2)$  nodes, *etc.*

For  $n = 1$ , both  $\ell$  and  $m$  are equal to zero and there is but one eigenfunction; there is no degeneracy. For  $n = 2$  there are two types of solutions: one is  $\ell = 1$  with an accompanying triplet of state values of  $m$ :  $m = -1, 0, +1$ . The other is the singlet  $\ell = 0$  with an accompanying singlet state value of  $m$ :  $m = 0$ . Since the energy depends only upon  $n$ , and since for

---

$U_{100} = \sqrt{\frac{1}{\pi}} \left( \frac{Z}{r_0} \right)^{3/2} e^{-Zr/r_0}$	$\frac{1}{\langle 1/r \rangle} = \frac{r_0}{Z}$
$U_{200} = \frac{1}{\sqrt{32\pi}} \left( \frac{Z}{r_0} \right)^{3/2} \left( 2 - \frac{Zr}{r_0} \right) e^{-Zr/2r_0}$	$\frac{1}{\langle 1/r \rangle} = \frac{4r_0}{Z}$
$U_{210} = \frac{1}{\sqrt{32\pi}} \left( \frac{Z}{r_0} \right)^{3/2} \left( \frac{Zr}{r_0} \right) e^{-Zr/2r_0} \cos \theta$	
$U_{21\pm 1} = \frac{1}{8\sqrt{\pi}} \left( \frac{Z}{r_0} \right)^{3/2} \left( \frac{Zr}{r_0} \right) e^{-Zr/2r_0} \sin \theta e^{\pm i\phi}$	
$U_{300} = \frac{1}{81\sqrt{3\pi}} \left( \frac{Z}{r_0} \right)^{3/2} \left( 27 - 18 \frac{Zr}{r_0} + 2 \frac{Z^2 r^2}{r_0^2} \right) e^{-Zr/3r_0}$	$\frac{1}{\langle 1/r \rangle} = \frac{9r_0}{Z}$
$U_{310} = \frac{\sqrt{2}}{81\sqrt{\pi}} \left( \frac{Z}{r_0} \right)^{3/2} \left( 6 - \frac{Zr}{r_0} \right) \left( \frac{Zr}{r_0} \right) e^{-Zr/3r_0} \cos \theta$	
$U_{31\pm 1} = \frac{1}{81\sqrt{\pi}} \left( \frac{Z}{r_0} \right)^{3/2} \left( 6 - \frac{Zr}{r_0} \right) \left( \frac{Zr}{r_0} \right) e^{-Zr/3r_0} \sin \theta e^{\pm i\phi}$	
$U_{320} = \frac{1}{81\sqrt{6\pi}} \left( \frac{Z}{r_0} \right)^{3/2} \left( \frac{Z^2 r^2}{r_0^2} \right) e^{-Zr/3r_0} (3 \cos^2 \theta - 1)$	
$U_{32\pm 1} = \frac{1}{81\sqrt{\pi}} \left( \frac{Z}{r_0} \right)^{3/2} \left( \frac{Z^2 r^2}{r_0^2} \right) e^{-Zr/3r_0} \sin \theta \cos \theta e^{\pm i\phi}$	
$U_{32\pm 2} = \frac{1}{162\sqrt{\pi}} \left( \frac{Z}{r_0} \right)^{3/2} \left( \frac{Z^2 r^2}{r_0^2} \right) e^{-Zr/3r_0} \sin^2 \theta e^{\pm i2\phi}$	

---

Table 4.10.1 Hydrogen atom eigenfunctions for  $n = 1$  through 3  
 $(1/\langle r \rangle)$  depends upon quantum number  $n$  only.

each value of  $\ell$  there are  $(2\ell + 1)$  values of  $m$ , the result is a  $(2\ell + 1)$  fold energy degeneracy. For each value of  $n$  there are  $n-1$  values of  $\ell$ . Hence the total energy degeneracy is:

$$\sum_{\ell=1}^{n-1} (2\ell + 1) = n^2 \quad (4.10.4)$$

That is, there are  $n^2$  possible solutions for each value of energy.

The degeneracy is lifted if the electron system is immersed in a static electric or magnetic field. The  $m = 0$  states are more closely tied to the nucleus than are the  $m = \pm 1$  states, which extend further outward from the nucleus. Therefore a static electric field affects the different states differently and removes the degeneracy. This is the Stark effect. The  $m = 0$  states support no angular momentum and produce no net magnetic moment. The  $m = \pm 1$  states do support angular momentum and do produce a magnetic moment. Hence, the states respond differently to an applied static magnetic field. The different response energy removes the energy degeneracy and the result is the Zeeman effect.

## 4.11 Perturbation Analysis

Consider an atom to be immersed in an external force field. So long as the applied field and its gradient are much less than those of the trapping potential the wave functions retain their original character and solutions entail a re-scrambling of the occupied states. As an example, consider the special case of an atom immersed in static, externally applied electric field of a magnitude small compared with the Coulomb field. Modifications result in a change of occupational probability of the original eigenfunctions.

To show that this is true, let the Hamiltonian operator  $H_0$  characterize the energy of an isolated electron system. The resulting total eigenfunction is a sum over wave functions that are solutions of the Schrödinger equation with operator  $H_0$ . Let one possible eigenfunction be  $U_{n0}$ . The possible eigenfunctions and the corresponding energies  $W_{n0}$  are known and each satisfies the relationship:

$$\int (U_{n0}^* H_0 U_{n0}) dV = W_{n0} \int U_{n0}^* U_{n0} dV \quad (4.11.1)$$

A small external force field is applied that modifies the Hamiltonian to the operational form:

$$H = H_0 + H_1 \quad (4.11.2)$$

Since the external field is controllable by external means, for example the intensity of an applied laser beam, the actual operational form may be written as:

$$H = H_0 + \alpha H_1 \quad (4.11.3)$$

An experimenter may control the value of  $\alpha$  from zero to one. The eigenfunctions and energies are functions of  $\alpha$ . If the applied force is small enough a power series in powers of  $\alpha$  will converge, with the result that:

$$\begin{aligned} U_n &= U_{n0} + \alpha U_{n1} + \alpha^2 U_{n2} + \dots = \sum_r \alpha^r U_{nr} \\ W_n &= W_{n0} + \alpha W_{n1} + \alpha^2 W_{n2} + \dots = \sum_s \alpha^s W_{ns} \end{aligned} \quad (4.11.4)$$

The “0” subscripts form the total solution in the absence of the external field, the “1” subscripts describe the first order correction, the “2” subscripts describe the second order correction, *etc.* For small fields, only the correction terms that are first order in  $\alpha$  are large enough to be of interest and terms proportional to  $\alpha^2$  may be ignored. The first order terms are:

$$\begin{aligned} &\int \left\{ (U_{n0}^* + \alpha U_{n1}^*) (H_0 + \alpha H_1) (U_{n0} + \alpha U_{n1}) \right\} dV \\ &= \int \left\{ (U_{n0}^* + \alpha U_{n1}^*) (W_{n0} + \alpha W_{n1}) (U_{n0} + \alpha U_{n1}) \right\} dV \\ &\equiv \int \left\{ U_{n0}^* H_0 U_{n0} + \alpha [U_{n1}^* H_0 U_{n0} + U_{n0}^* H_1 U_{n0} + U_{n0}^* H_0 U_{n1}] \right\} dV \\ &= \int \left\{ W_{n0} U_{n0}^* U_{n0} + \alpha [W_{n0} U_{n1}^* U_{n0} + W_{n1} U_{n0}^* U_{n0} + W_{n0} U_{n0}^* U_{n1}] \right\} dV \end{aligned} \quad (4.11.5)$$

Confining attention to the last equality of Eq. 4.11.5, the first terms are equal and may be subtracted out. The procedure may be repeated for the first terms within the square brackets. Applying the Hermitian property of quantum operators to the last terms within the square brackets shows that they too are equal and they, too, may be subtracted out of the equation. Eliminating these three terms leaves the center terms within the square brackets:

$$\int U_{n0}^* H_1 U_{n0} dV = W_{n1} \int U_{n0}^* U_{n0} dV = W_{n1} \quad (4.11.6)$$

This is the first order correction term. Equation 4.11.6 shows that it is not necessary to know the corrected wave function to calculate first order energy changes. It is only necessary to know how the first order Hamiltonian correction affects unperturbed eigenfunctions.

## 4.12 Non-Ionizing Transitions

Let an electron in an unperturbed atom be described by the Hamiltonian operator  $H_0$ , eigenfunctions  $\psi_n$ , and energies  $W_n$ . Schrödinger's equation is:

$$H_0 \psi_n(r_1, t) = W_n \psi_n(r_1, t) \quad (4.12.1)$$

The total wave function is a weighted sum over all possible wave functions:

$$\Psi(r_1, t) = \sum_n a_n \psi_n(r_1, t) \quad (4.12.2)$$

Next, let a second electron be attached to the same atom, affected by the same Hamiltonian operator, and have the same set of eigenfunctions and energies but a different set of coefficients:

$$\Psi(r_2, t) = \sum_n b_n \psi_n(r_2, t) \quad (4.12.3)$$

Make the definitions:

$$\Psi_{mn}(\mathbf{r}, t) = \Psi_m(\mathbf{r}_1, t) \Psi_n(\mathbf{r}_2, t)$$

$$U_{mn}(\mathbf{r}) = u_m(\mathbf{r}_1) u_n(\mathbf{r}_2)$$

$$W_{mn} = W_m + W_n$$

The equation that describes both electrons is:

$$\Psi(\mathbf{r}, t) = \sum_m \sum_n c_{mn} \Psi_{mn}(\mathbf{r}, t) = \sum_m \sum_n a_m b_n U_{mn}(\mathbf{r}_1, \mathbf{r}_2) \exp\left(\frac{iW_{mn}t}{\hbar}\right) \quad (4.12.4)$$

If a perturbing field is applied that changes the Hamiltonian operator from  $H_0$  to  $H_0 + H_1$ , the wave functions remain unaltered and the probability coefficients,  $c_{mn}$ , become time dependent. To show this, write Eq. 4.12.4 in the form:

$$(H_0 + H_1) \sum_m \sum_n c_{mn}(t) \Psi_{mn}(\mathbf{r}, t) = \frac{\hbar}{i} \frac{\partial}{\partial t} \sum_m \sum_n c_{mn}(t) \Psi_{mn}(\mathbf{r}, t) \quad (4.12.5)$$

Writing out the equation term by term gives:

$$\begin{aligned} & \sum_m \sum_n [c_{mn}(t) H_0 \Psi_{mn} + c_{mn}(t) H_1 \Psi_{mn}] \\ &= \sum_m \sum_n \left[ \frac{\hbar}{i} c_{mn}(t) \frac{\partial \Psi_{mn}(t)}{\partial t} + \frac{\hbar}{i} \frac{\partial c_{mn}(t)}{\partial t} \Psi_{mn} \right] \end{aligned} \quad (4.12.6)$$

The first terms on either side are equal; subtracting them leaves the equality:

$$\sum_m \sum_n c_{mn}(t) H_1 \Psi_{mn}(\mathbf{r}, t) = \frac{\hbar}{i} \sum_m \sum_n \frac{\partial c_{mn}(t)}{\partial t} \Psi_{mn}(\mathbf{r}, t) \quad (4.12.7)$$

Multiplying through by  $\Psi_{pq}^*(\mathbf{r}, t)$  and integrating over all space gives:

$$\frac{d}{dt}c_{pq}(t) = \frac{i}{\hbar} \sum_m \sum_n c_{mn}(t) \int \psi_{pq}^* H_1 \psi_{mn} dV \quad (4.12.8)$$

The integral is over the volume occupied by both electrons. Make the definition:

$$\langle pq | H_1 | mn \rangle = \int \psi_{pq}^* H_1 \psi_{mn} dV \quad (4.12.9)$$

The terms of Eq. 4.12.9 are, by definition, the matrix elements of interaction potential  $H_1$ . With the aid of Eq. 4.5.13, Eq. 4.12.8 may be written in the form:

$$\frac{dc_{pq}(t)}{dt} = \frac{i}{\hbar} \sum_m \sum_n c_{mn} \langle pq | H_1 | mn \rangle \exp \left[ \frac{i (W_m + W_n - W_p - W_q)t}{\hbar} \right] \quad (4.12.10)$$

As a special case suppose that at time  $t = 0$  the electrons are in states  $m$  and  $n$  and find the probability, as a function of time, that they will occupy states  $p$  and  $q$ . The initial condition is that

$$\frac{dc_{pq}(t)}{dt} = \frac{i}{\hbar} \langle pq | H_1 | mn \rangle \exp \left[ \frac{i (W_p + W_q - W_m - W_n)t}{\hbar} \right] \quad (4.12.11)$$

Coefficient  $c_{mn}$  is equal to one at time  $t = 0$ , when all other coefficients are equal to zero. Make the definition that:

$$\Delta W = W_p + W_q - W_m - W_n$$

Restricting analyses to times short enough so that  $c_{mn}$  remains nearly equal to one, the integral over time shows the initial time dependence of the coefficient to be:



$$c_{pq}(t) = \langle pq | H_1 | mn \rangle \frac{\exp(i\Delta W t / \hbar) - 1}{\Delta W} \quad (4.12.12)$$

The probability of state (p,q) being occupied is:

$$c_{pq}^* c_{pq} = 4 \langle pq | H_1 | mn \rangle^2 \frac{\sin^2(\Delta W t / 2\hbar)}{(\Delta W)^2} \quad (4.12.13)$$

Equation 4.12.13 shows that the probability that a particular transition will occur is proportional to the square of the matrix element. The magnitude of the matrix element depends upon both sets of quantum numbers, pq and mn. Transitions are “forbidden” if the matrix element is equal to zero. Since the ratio  $\sin^2(x)/x^2$  has maximum magnitude at  $x = 0$ , it follows that energy conservation requires that the most probable value of  $\Delta W$  be zero.

### 4.13 Absorption and Emission of Radiation

The purpose of this section is to describe the absorption and emission of radiation by an atom with a full complement of electrons. The atom is immersed within an externally applied plane wave of radian frequency  $\omega$  where the wavelength is much greater than the initial size of an atom.

The calculation begins with the relationships between the Hamiltonian,  $H$ , the state energy written in operator form, and the time dependence of the applied field as described by the time-dependent Schrödinger equation. The relationships are, see Eq. 4.5.11:

$$\frac{\hbar}{i} \frac{\partial}{\partial t} \psi_n(r, t) = H \psi_n(r, t) = W_n \psi_n(r, t) \quad (4.13.1)$$

It follows from Eqs. 4.5.13 and 4.5.14 that the time-dependent eigenfunctions are related to the time-independent ones as:

$$\psi_n(r, t) = U_n(r) e^{iW_n t / \hbar} \quad (4.13.2)$$

The complete wave function  $\Psi(\mathbf{r}, t)$  is a weighted sum over all possible eigenfunctions:

$$\Psi(\mathbf{r}, t) = \sum_n c_n(t) U_n(\mathbf{r}) e^{i\omega_n t} \quad (4.13.3)$$

As in Section 4.12, it is possible that the probability coefficients are time dependent. Substituting the first order perturbation equation, Eq. 4.11.6, into Eq. 4.13.1 and Eq. 4.13.3 gives the differential equation that describes the rate of change of the coefficients as a function of the coefficients themselves:

$$\frac{\hbar}{i} \sum_n \frac{\partial c_n(t)}{\partial t} U_n(\mathbf{r}) e^{i\omega_n t} = \sum_n c_n(t) H_1 U_n(\mathbf{r}) e^{i\omega_n t} \quad (4.13.4)$$

Symbol  $H_1$  represents the operator form of the modification to the Hamiltonian due to the perturbation. This equation shows that the primary affect of the applied field is to make the state coefficients time dependent.

The electric field intensity in the perturbing plane wave is  $\mathbf{E}(\mathbf{r}, t)$  and it varies with time as  $\cos(\omega t)$ . Although  $\mathbf{E}(\mathbf{r}, t)$  is a real function, it is convenient to rewrite it in complex terms as the sum of complex conjugate functions:

$$\mathbf{E}(\mathbf{r}, t) = \mathbf{E}_0 e^{i(\omega t - \mathbf{k} \cdot \mathbf{r})} + \text{c.c.} \quad (4.13.5)$$

For atoms of diameter much less than a wavelength, the perturbing energy is approximately equal to:

$$H_1 = -e\mathbf{E}(t) \cdot \mathbf{r}(t) \quad (4.13.6)$$

Combining Eq. 4.13.6 with 4.13.4 gives:

$$\sum_n \frac{\partial c_n(t)}{\partial t} e^{i\omega_n t} U_n(\mathbf{r}) = -\frac{ie}{\hbar} \sum_n \left\{ e^{i(\omega_n t + \omega t - \mathbf{k} \cdot \mathbf{r})} + e^{i(\omega_n t - \omega t + \mathbf{k} \cdot \mathbf{r})} \right\} c_n(t) \mathbf{E}_0 \cdot \mathbf{r} U_n(\mathbf{r}) \quad (4.13.7)$$

To determine the affect of interaction between states  $n$  and  $k$ , multiply Eq. 4.13.7 through by  $U_k(r)$  and integrate over all space. The result is:

$$\frac{\partial c_k(t)}{\partial t} = -\frac{ie}{\hbar} \sum_n c_n(t) \left\{ e^{ik \cdot r} e^{i(\omega_n - \omega_k - \omega)t} + e^{-ik \cdot r} e^{i(\omega_n - \omega_k + \omega)t} \right\} E_0 \cdot \langle U_k | r | U_n \rangle \quad (4.13.8)$$

Symbol  $\langle U_k | r | U_n \rangle$  is defined in Eq. 4.12.9. To simplify the problem consider as a boundary condition that at initial time  $t = 0$  only the single state 'n' is occupied by an electron. Therefore only  $c_n$  is different from zero and it is equal to one. Doing the time integral of Eq. 4.13.8 under these circumstances gives the initial solution:

$$c_k(t) = -\frac{ie}{\hbar} \left\{ e^{ik \cdot r} \left[ \frac{e^{i(\omega_n - \omega_k - \omega)t} - 1}{(\omega_n - \omega_k - \omega)} \right] + e^{-ik \cdot r} \left[ \frac{e^{i(\omega_n - \omega_k + \omega)t} - 1}{(\omega_n - \omega_k + \omega)} \right] \right\} E_0 \cdot \langle U_k | r | U_n \rangle \quad (4.13.9)$$

The exponential phase factor may be expanded as  $[e^{-ik \cdot r} \approx 1 - ik \cdot r + \dots]$ . The first order value, one, is sufficient since atomic sizes are much less than a wavelength. Making the replacement shows that the square of the magnitude of Eq. 4.13.9 may be written as:

$$|c_k(t)|^2 = (2eE_0)^2 \langle U_k | r | U_n \rangle^2 \left\{ \frac{\sin^2 \left[ \frac{1}{2\hbar} (\mathcal{W}_n - \mathcal{W}_k \pm \hbar\omega)t \right]}{(\mathcal{W}_n - \mathcal{W}_k \pm \hbar\omega)^2} \right\} \quad (4.13.10)$$

The term within the curly brackets of Eq. 4.13.10 is significantly different from zero only if the argument of the sine is equal to zero. This requires that:

$$\omega_k = \omega_n \pm \omega \quad (4.13.11)$$

Multiplying Eq. 4.13.11 through by  $\hbar$  shows that  $(W_k - W_n) = \pm \hbar\omega$ . If  $(W_k > W_n)$  energy  $\hbar\omega$  is added to the system and the transition is associated with energy absorption. If  $(W_k < W_n)$  energy  $\hbar\omega$  is removed from the system and the transition is associated with energy emission. Therefore, it seems reasonable to ascribe the upper or lower sign of Eq. 4.13.11 respectively to energy absorption or emission by the electron. Equation 4.13.11 also shows that the transition probabilities for emission and absorption are the same. . For simplicity, the development is carried out with the restriction that Eq. 4.13.10 is valid only over times so small that  $c_n(t)$  remains nearly equal to one and all other values  $c_k(t)$  remain much less than one.

If the radius of the atom is equal to the first Bohr orbit, see Eq. 4.9.14, and the wavelength is at the center of the optical band, 500 nm:

$$2kr = 6.65 \times 10^{-4} (n^2/Z) \quad (4.13.12)$$

If  $n$  is small enough so the magnitude of Eq. 4.13.12 is much less than one, the perturbation expansion of Eqs. 4.11.4 converges rapidly and calculated results may be limited to the first correction term only.

## 4.14 Electric Dipole Selection Rules for One Electron Atoms

To obtain the probability of an energy exchange by absorption or emission of radiation it is necessary to evaluate the matrix element. For an atom with only one electron, the wave functions are given by Eq. 4.10.1 and in Table 4.10.1. The components of the matrix elements directed along the three rectangular coordinate axes are:

$$\begin{aligned} X &= \int_0^\infty r^2 dr \int_0^\pi \sin \theta d\theta \int_0^{2\pi} U_{n'\ell'm'}^* U_{n\ell m} r \sin \theta \cos \phi d\phi \\ Y &= \int_0^\infty r^2 dr \int_0^\pi \sin \theta d\theta \int_0^{2\pi} U_{n'\ell'm'}^* U_{n\ell m} r \sin \theta \sin \phi d\phi \end{aligned} \quad (4.14.1)$$

$$Z = \int_0^{\infty} r^2 dr \int_0^{\pi} \sin \theta d\theta \int_0^{2\pi} U_{n'\ell'm'}^* U_{n\ell m} r \cos \theta d\phi$$

The total wave function is related to the individual functions as:

$$U_{n\ell m}(r, \theta, \phi) = A_{n\ell m} R_n^{\ell}(\alpha_n r) P_{\ell}^m(\cos \theta) e^{-im\phi} \quad (4.14.2)$$

Combining the first of Eqs. 4.14.1 with 4.14.2 gives:

$$X = A_{n'\ell'm'}^* A_{n\ell m} \int_0^{\infty} R_{n'}^{\ell'} R_n^{\ell} r^3 dr \int_0^{\pi} P_{\ell'}^{m'} P_{\ell}^m \sin^2 \theta d\theta \int_0^{2\pi} e^{i(m'-m)\phi} \cos \phi d\phi \quad (4.14.3)$$

Evaluation of the azimuth angle integral gives: g

$$\int_0^{2\pi} d\phi \cos \phi [\cos(m'-m)\phi + i \sin(m'-m)\phi] = \pi \delta(m', m \pm 1) \quad (4.14.4)$$

Incorporating Eq. 4.14.4 then using the identity of Table A.21.1.7, gives:

$$\begin{aligned} \sin^2 \theta P_{\ell'}^{m+1} P_{\ell}^m &= \frac{1}{2\ell+1} \sin \theta (P_{\ell+1}^{m+1} - P_{\ell-1}^{m+1}) P_{\ell}^{m+1} \\ \sin^2 \theta P_{\ell'}^{m-1} P_{\ell}^m &= \frac{1}{2\ell'+1} \sin \theta (P_{\ell'+1}^m - P_{\ell'-1}^m) P_{\ell}^m \end{aligned} \quad (4.14.5)$$

Combining Eqs. 4.14.3 and 4.14.5 shows that for both values of  $m$  the zenith angle integral of Eq. 4.14.3 has the form:

$$\frac{1}{2\ell+1} \int_0^{\pi} \sin \theta (P_{\ell+1}^{m+1} - P_{\ell-1}^{m+1}) P_{\ell}^{m+1} d\theta$$

Consider the integral:

$$\int_0^\pi P_{\ell'}^{m'} P_{\ell}^m \sin^2 \theta d\theta \int_0^{2\pi} \cos \phi e^{i(m'-m)\phi} d\phi =$$

$$\frac{2\pi \delta(m', m \pm 1)}{(2\ell + 1)} \left\{ \frac{1}{(2\ell + 3)} \frac{(\ell + m + 2)!}{(\ell - m)!} \delta(\ell', \ell + 1) - \frac{1}{(2\ell - 1)} \frac{(\ell + m)!}{(\ell - m - 2)!} \delta(\ell', \ell - 1) \right\} \quad (4.14.6)$$

The integral is different from zero only if:

$$\ell' = \ell \pm 1 \quad (4.14.7)$$

Combining the second of Eqs. 4.14.1 with Eq. 4.14.2 gives similar results. Combining the last of Eqs. 4.14.1 with Eq. 4.14.2 gives:

$$Z = A_{n\ell' m'}^* A_{n\ell m} \int_0^\infty R_{n\ell'}^{\ell'} R_{n\ell}^{\ell} r^3 dr \int_0^\pi P_{\ell'}^{m'} P_{\ell}^m \sin \theta \cos \theta d\theta \int_0^{2\pi} e^{i(m'-m)\phi} d\phi \quad (4.14.8)$$

Table A.21.1.4, shows that:

$$\sin \theta \cos \theta P_{\ell'}^{m'} P_{\ell}^m = \frac{1}{2\ell + 1} \sin \theta \left[ (\ell - m + 1) P_{\ell+1}^m - (\ell + m) P_{\ell-1}^m \right] P_{\ell'}^m \quad (4.14.9)$$

Combining with the zenith angle integral of Eq. 4.14.7 leaves the form:

$$\frac{1}{2\ell + 1} \int_0^\pi \sin \theta \left[ (\ell - m + 1) P_{\ell+1}^m - (\ell + m) P_{\ell-1}^m \right] P_{\ell'}^m d\theta \quad (4.14.10)$$

Consider the integrals:

$$\begin{aligned}
& \frac{1}{(2\ell+1)} \int_0^\pi \sin\theta \left[ (\ell-m+1)P_{\ell+1}^m - (\ell+m)P_{\ell-1}^m \right] P_{\ell'}^m d\theta \int_0^{2\pi} d\phi e^{i(m-m')\phi} = \\
& \frac{4\pi\delta(m',0)}{(2\ell+1)} \left\{ (\ell-m+1) \frac{(\ell+m+1)!}{(\ell-m+1)!} \delta(\ell', \ell+1) - (\ell+m) \frac{(\ell+m-1)!}{(\ell-m-1)!} \delta(\ell', \ell-1) \right\}
\end{aligned}
\tag{4.14.11}$$

Like Eqs. 4.14.6, Eq. 4.14.11 is different from zero only if Eq. 4.14.7 is satisfied. Since the radial integer provides no restrictions on  $n$ , electric dipole transitions occur only if:

$$\Delta\ell = \pm 1 \quad \text{and} \quad \Delta m = \pm 1 \text{ or } 0 \tag{4.14.12}$$

The interpretation of Eqs. 4.8.10 and 4.14.12 is that the  $z$ -component of radiated angular momentum is equal to zero or to  $\hbar$ . Since the angular momentum of the source changes by that amount, it must be carried by the radiation.

## 4.15 Electron Spin

It was known before Schrödinger's equation was known that a complete description of electronic events requires four quantum numbers. An integral part of Dirac's equations is that electron characteristics include more than charge and mass: there is a permanent angular momentum and a permanent magnetic dipole moment.

The angular momentum of a particle in terms of its mass and velocity is:

$$\mathbf{l} = m \mathbf{r} \times \mathbf{v} \tag{4.15.1}$$

By definition  $\mathbf{l}$  is the angular momentum,  $\mathbf{r}$  the radius about a fixed point, and  $\mathbf{v}$  the velocity of the point mass. If the mass also supports charge  $q$ , the magnetic moment is:

$$\mathbf{\Omega} = q\mathbf{r} \times \mathbf{v}/2 \tag{4.15.2}$$

Comparison of Eqs. 4.15.1 and 4.15.2 shows that

$$\Omega = q\hbar/2m \quad (4.15.3)$$

Thus the expected relationship between an electron's magnetic and mechanical moments, Eq. 4.15.3, is equal to:

$$\Omega = -e\hbar/2m \quad (4.15.4)$$

However, the proportionality between spin magnetic moment and angular momentum is twice as large as the ratio of the intrinsic magnetic moment and angular momentum.

It is found that the intrinsic angular momentum obeys rules similar to those of orbital motion about a central force field, Eq. 4.8.10 and 4.8.11, except that with spin the only allowed quantum numbers are plus and minus one half. That is, the total angular momentum is:

$$\mathbf{s} \cdot \mathbf{s} = s(s+1)\hbar^2 \quad (4.15.5)$$

The component along a particular axis is:

$$s_z = m_s \hbar \quad (4.15.6)$$

Quantum numbers  $m_s$  are equal to either  $\pm 1/2$ . Combining terms shows that the magnetic moment can have either of the two values:

$$\Omega_z = \pm e\hbar/2m \quad (4.15.7)$$

The absolute value of the moment is called the Bohr magneton, and of value:

$$\Omega_z = 9.274 \times 10^{-24} \text{ J/T} \quad (4.15.8)$$

These relationships may be put in appropriate quantum theory terms by considering  $S$  to be an eigenfunction,  $\hat{s}_z$  an operator, and writing:



$$\hat{s}_z S = \pm \hbar S / 2 \quad (4.15.9)$$

The total spin wave function combines the functions with coefficients as:

$$S(s_z) = c_+ S_+(s_z) + c_- S_-(s_z) \quad (4.15.10)$$

The wave functions are orthogonal and normalized.

## 4.16 Many-Electron Problems

To examine a multi-electron atom note that the Hamiltonian operator of a system of  $n$  electrons may depend in a complicated way on the internal structure of each electron. Regardless of what the complications may be, a property of critical importance is that electrons are physically indistinguishable: all results are invariant upon interchange of electrons. That is, all energies, including both electron-nucleus and electron-electron interactions, are symmetrical with respect to an interchange of electrons.

Since the energy of an electron is proportional to the square of its wave function, symmetric energies occur with both symmetric and antisymmetric wave functions. To examine the symmetry of a wave function break it into the sum of symmetric and antisymmetric parts, respectively:

$$\psi^{\text{Sy}}(\mathbf{r}) = \psi^{\text{Sy}}(-\mathbf{r}) \text{ and } \psi^{\text{As}}(\mathbf{r}) = -\psi^{\text{As}}(-\mathbf{r}) \quad (4.16.1)$$

Any physically real function of time can be expressed as the sum of symmetric and antisymmetric functions of time. For the case of wave functions:

$$\psi(\mathbf{r}) = \psi^{\text{Sy}}(\mathbf{r}) + \psi^{\text{As}}(\mathbf{r}) \quad (4.16.2)$$

The energy density is proportional to the probability density and it is equal to:

$$\begin{aligned} \psi(\mathbf{r})^* \psi(\mathbf{r}) = & \left[ \psi^{\text{Sy}*}(\mathbf{r}) \psi^{\text{Sy}}(\mathbf{r}) + \psi^{\text{As}*}(\mathbf{r}) \psi^{\text{As}}(\mathbf{r}) \right] \\ & + \left[ \psi^{\text{Sy}*}(\mathbf{r}) \psi^{\text{As}}(\mathbf{r}) + \psi^{\text{As}*}(\mathbf{r}) \psi^{\text{Sy}}(\mathbf{r}) \right] \end{aligned} \quad (4.16.3)$$

The first term of Eq. 4.16.2 is invariant with respect to the interchange of electrons and the second term is not. It follows that the second term of Eq. 4.16.3 is equal to zero. Therefore the wave function may be either symmetric or antisymmetric but it cannot be a mixture.

The simplest possible multi-electron system has two electrons, say electron “*a*” and electron “*b*”. Let  $P_{ab}$  be a permutation operator that interchanges the electrons. It follows that:

$$P_{ab} \psi(a, b) = \psi(b, a) \text{ and } P_{ab} P_{ab} \psi(a, b) = \psi(a, b) \quad (4.16.4)$$

In turn, it follows from Eq. 4.16.4 that:

$$P_{ab} P_{ab} = 1 \text{ and } P_{ab} = \pm 1 \quad (4.16.5)$$

It follows that

$$P_{ab} U^{\text{As}}(\mathbf{r}) = -U^{\text{As}}(\mathbf{r}) \quad P_{ab} U^{\text{Sy}}(\mathbf{r}) = U^{\text{Sy}}(\mathbf{r}) \quad (4.16.6)$$

Since taking operations with respect to time in quantum theory does not affect positional symmetry, time does not affect symmetry: A state that is initially symmetric or antisymmetric before a quantum mechanical operation has the same symmetry after the operation. Whatever symmetry the wave function has at time  $t = 0$ , it keeps that symmetry for all time. This argument generalizes to include an arbitrary number of electrons. The conclusion is that either there is but one type of symmetry in nature, with all wave functions of the other symmetry everywhere equal to zero, or there are two separate types of physical reality. If two types of reality exist, one type of reality would be constructed of electrons with symmetric wave functions and the other would be constructed of electrons with antisymmetric wave functions. Consider a two-electron atom for which the total and individual wave functions satisfy the relationships:

$$\begin{aligned}
 \Psi(\mathbf{r}', \mathbf{r}'') &= \psi_a(\mathbf{r}')\psi_b(\mathbf{r}'') \\
 &= \frac{1}{2}[\psi_a(\mathbf{r}')\psi_b(\mathbf{r}'') + \psi_b(\mathbf{r}')\psi_a(\mathbf{r}'')] + \frac{1}{2}[\psi_a(\mathbf{r}')\psi_b(\mathbf{r}'') - \psi_b(\mathbf{r}')\psi_a(\mathbf{r}'')]
 \end{aligned}
 \tag{4.16.7}$$

Introduce the notation that:

$$\begin{aligned}
 \Gamma_{ab}(\mathbf{r}', \mathbf{r}'') &= [\psi_a(\mathbf{r}')\psi_b(\mathbf{r}'') + \psi_b(\mathbf{r}')\psi_a(\mathbf{r}'')] \\
 \Psi_{ab}(\mathbf{r}', \mathbf{r}'') &= [\psi_a(\mathbf{r}')\psi_b(\mathbf{r}'') - \psi_b(\mathbf{r}')\psi_a(\mathbf{r}'')]
 \end{aligned}
 \tag{4.16.8}$$

Since both electrons occupy all points, examine conditions for  $\mathbf{r}' = \mathbf{r}''$ :

$$\begin{aligned}
 \Gamma_{ab}(\mathbf{r}', \mathbf{r}') &= 2\psi_a(\mathbf{r}')\psi_b(\mathbf{r}') \\
 \Psi_{ab}(\mathbf{r}', \mathbf{r}') &= 0
 \end{aligned}
 \tag{4.16.9}$$

The electrostatic interaction energy between the two electrons is:

$$W_{ab} = \frac{e^2}{4\pi\epsilon} \int \left( \frac{1}{|\mathbf{r}' - \mathbf{r}''|} \right) \Psi_{ab}(\mathbf{r}', \mathbf{r}'') \Psi_{ab}^*(\mathbf{r}', \mathbf{r}'') dV
 \tag{4.16.10}$$

If the electron charge density is a continuous function of position, Eq. 4.16.10 gives a physically acceptable result with either electron symmetry. As expected from Eq. 4.16.9, the energy with symmetric functions is larger than that with antisymmetric functions. However, the definite integral of Eq. 4.16.10 correctly represents the system energy if and only if the wave functions are continuous functions of position. If there is a dimensional scale below which the charge density is granular, on that scale of dimensions it is necessary to replace the integration by a sum over interaction energies. With symmetric wave functions, by Eq. 4.16.9 the granular charges are adjacent or overlapping and the sum is singular; there is no parallel with antisymmetric wave functions since the overlapping densities vanish. It follows that if there is a dimensional scale on which the charge density is granular, only antisymmetric wave functions exist. The Exclusion Principle, first formulated by Pauli, states that only antisymmetric

wave functions exist. On the basis of the above argument, it also suggests that, on an appropriate dimensional scale, electron charge distributions are granular.

## 4.17 Electron Photo Effects

Hertz discovered in 1887 that a spark jumps a small gap between conductors more easily when the conductors are illuminated than when in the dark. He found that the effect becomes more pronounced as the light spectrum goes from blue to ultraviolet, is most pronounced with clean and smooth terminals, and cathodes are more active than anodes. The result is a photocurrent due to the forcible ejection of electrons from the cathode.

Experimentally determined characteristics of photocurrents are:

- a) Define the stopping potential  $V_0$  to be the voltage difference between the two plates that just causes the current to cease. The electron stream continues so long as the electrons have sufficient energy to make the transit. It must be, therefore, that the actual voltage  $V$  satisfies the condition

$$V > V_0 \quad (4.17.1)$$

- b) Each type of metal has a characteristic frequency,  $\omega_0$ . A photocurrent exists only with light of that or a higher frequency  $\omega$ . That is:

$$\omega > \omega_0 \quad (4.17.2)$$

- c) Photocurrent magnitude is proportional to the intensity of the light:

$$I = I(E_0^2) \quad (4.17.3)$$

The symbol  $E_0$  indicates the electric field intensity within the light.

- d) Photocurrent magnitude is independent of frequency for frequencies greater than the characteristic frequency:

- e) Photocurrent onset occurs without a measurable time delay after onset of illumination.
- f) Expressed in terms of the above symbols, the maximum kinetic energy per electron is:

$$W = \hbar(\omega - \omega_0) \quad (4.17.4)$$

Einstein analyzed the photocurrent problem by treating light as if it consisted of particles. His argument was sufficiently convincing to persuade most physicists of the correctness of his model, and, for the analysis, he was awarded the 1921 Nobel Prize in Physics.

However, it is not necessary to imagine that light consists of particles to explain the effect. It can be explained in terms of the interaction between electrons in quantized energy states and an engulfing plane wave. Let the source metal be sized much larger than atomic dimensions. Inside the metal electrons are trapped in quantized energy states. Since the skin depth of a good conductor in the mid-optical range is on the order of 10 nm, the light penetrates the metal deeply enough to interact with the conducting band electrons. Let an electron in eigenstate  $n$  with energy  $W_n$  interact with an applied plane wave of frequency  $\omega$ . Define the work function of the metal,  $W_0$ , to be the additional energy an electron must have to exit the metal. Then:

$$W_0 = \hbar\omega \quad (4.17.5)$$

It follows from Section 1.13 that there are electromagnetic cavity solutions of energy  $E_k$  within the containing box. As the size of the box,  $L$ , becomes large, the possible energy levels form a quasi-continuum. The transition equations of Eq. 4.13.10 are repeated here:

$$|c_k(t)|^2 = (2eE_0)^2 \langle U_k | r | U_n \rangle^2 \left\{ \frac{\sin^2 \left[ \frac{1}{2\hbar} (W_n - W_k \pm \hbar\omega) t \right]}{(W_n - W_k \pm \hbar\omega)^2} \right\} \quad (4.17.6)$$

Let  $\Phi$  be the energy of the first state of the quasi-continuous spectrum. Photoelectron emission occurs because of a transition from state  $n$  to state  $k$ . Let the kinetic energy of the ejected electron be  $T_k$ . The relationship between the energies follows and is equal to:

$$W_k - W_n = \Phi + T_k \quad (4.17.7)$$

Rearranging and rewriting in terms of frequencies:

$$T_k = \hbar(\omega - \omega_0) \quad (4.17.8)$$

The voltage required to stop all emission follows from the above and is given by:

$$V_0 = \frac{\hbar}{e}(\omega - \omega_0) \quad (4.17.9)$$

Combining Eq. 4.17.6 with Eqs. 4.17.7 and 4.17.8 gives an expression for the coefficient magnitude as a function of the electron kinetic energy and the applied frequency:

$$|c_k(t)|^2 = (2eE_0)^2 \langle U_k | \mathcal{H} | U_n \rangle^2 \left\{ \frac{\sin^2 \left[ \frac{1}{2\hbar} (T_k - \hbar\omega) t \right]}{(T_k - \hbar\omega)^2} \right\} \quad (4.17.10)$$

To determine the rate of electron ejection it is necessary to integrate Eq. 4.17.10 over the full range of kinetic energies which, in turn, requires summing over the quasi-continuum states. Since it is a quasi-continuum, replace the summation with the integral shown:

$$P(t) = \sum_k |c_k(t)|^2 \Rightarrow (2eE_0)^2 \langle U_k | \mathcal{H} | U_n \rangle^2 \int_0^\infty \left\{ \frac{\sin^2 \left[ \frac{1}{2\hbar} (T - \hbar\omega) t \right]}{(T - \hbar\omega)^2} \right\} dT \quad (4.17.11)$$

$P(t)$  is the probability that emission has occurred. The integral may be rewritten as a Dirac delta function using the relationship:

$$\left\{ \frac{\sin^2 \left[ \frac{1}{2\hbar} (T - \hbar\omega) t \right]}{\left( \frac{t}{2\hbar} \right)^2 (T - \hbar\omega)^2} d\left( \frac{tT}{2\hbar} \right) \right\} = \delta(x - x_0) dx \quad (4.17.12)$$

Combining Eq. 4.17.11 with Eq. 4.17.12 and integrating over all possible kinetic energies gives:

$$P(t) = \frac{2e^2 E_0^2}{\hbar} \langle U_k | r | U_n \rangle^2 t \quad (4.17.13)$$

This probability of emission, Eq. 4.17.13, is directly proportional to time and, therefore, with a constant light intensity electrons are ejected at a constant rate. There is no time delay between onset of the light and the onset of electron emission and the rate of electron ejection is proportional to the intensity of the illuminating field atomic states. The analysis of Sections 4.12 and 4.13 contained the approximation that  $c_n(t)$  remained constant, a result that served as a preliminary to generalized cases with  $c_n(t)$  a variable. In this case, since the active electrons lie initially near the Fermi level and the conduction band is part of a quasi-continuum, the constancy is a reality.

This analysis shows that the photoelectric effect may result from an interaction between a classical radiation field and a quantized electron. It appears to be a historic accident that radiation fields as particles acquired its strongest early support from Einstein's considerations of the photoelectric effect.

## References

- D. Bohm, *Quantum Theory*, Prentice Hall, Princeton NJ (1951)
- K. Kim, E. Wolf, "Non-Radiating Monochromatic Sources and their Fields," *Optics Communication*, vol. 59, pp. 1-6, (1986)
- P.A.M. Dirac, *The Principles of Quantum Mechanics*, 4<sup>th</sup> ed., Oxford (1958)
- G. Greenstein, A.G. Zajonc, *The Quantum Challenge: Modern Research on the Foundations of Quantum Mechanics*, Jones and Bartlett Publishers (1997)
- W.E. Lamb, M.O. Scully, "The Photoelectric Effect Without Photons," in *Polarization, Matter and Radiation*, Presses Universitaires de France (1969) pp. 363-369
- L.D. Landau, E.M. Lifshitz, *Quantum Mechanics: Non-Relativistic Theory*, Addison-Wesley, Reading MA (1958)
- A. Messiah, *Quantum Mechanics*, vol. 1, trans. by G.M. Temmer, John Wiley, New York (1966)
- R. Omnès, *Understanding Quantum Mechanics*, Princeton University Press (1999)
- L.I. Schiff, *Quantum Mechanics*, McGraw-Hill Book Co., New York (1949)
- F. Schwabl, *Quantum Mechanics*, 2<sup>nd</sup> ed., Springer, New York (1995)
- R.C. Tolman, *The Principles of Statistical Mechanics* (1938), reprinted by Dover Publications (1979)



This page is intentionally left blank

## 5. Photons

This chapter discusses an electron transitioning between eigenstates. It is based upon the atomic model of Chapter 4 in which the Schrödinger equation applies during periods of electron equilibrium and near-equilibrium, but not during transitions. During transitions a unique resonant electromagnetic field set exists that consists of properly phased TE and TM modes of equal magnitudes. The mixed TE and TM radiation also produces a regenerative radiation reaction force that drives all higher order modes of the same degree. This nonlinear and regenerative force drives the radiation until all available energy is radiated or received.

We first determine that the radiated power-frequency relationships obey the Manley Rowe equations. Next we examine the radiation kinematics and find that they are the same as photon kinematics. We use the kinematics as a boundary condition on a multimodal field expansion to determine the full set of fields present during steady state photon radiation. Finally, we show that the radiation reaction pressure of the near fields is many orders of magnitude larger than the Coulomb trapping pressure and that it is directed and phased to drive the source regeneratively.

### 5.1 Power-Frequency Relationships

To address classical power-frequency relationships in a closed system, consider an equilibrated, charged system that supports an internal electromagnetic oscillation at radian frequency  $\omega_s$ . The system is immersed in and perturbed by a plane wave of frequency  $\omega$ . If the system is linear, in the sense that doubling an applied force doubles the system response, only the two frequencies  $\omega$  and  $\omega_s$  will exist inside the system. If the system response is not linear, there are additional responses at difference and sum frequencies. The system response may be written as:

$$S(t) = [A \cos(\omega_s t) + B \cos(\omega t)]^p \quad (5.1.1)$$

A, B, and  $p$  are constant, system-specific parameters. The system response may be expanded as a polynomial of trigonometric functions. An especially important example of a nonlinear response is the case of  $p = 2$ , for which:

$$\begin{aligned} S(t) = & \frac{A^2 + B^2}{2} + AB \{ \cos[(\omega_s - \omega)t] + \cos[(\omega_s + \omega)t] \} \\ & + \frac{1}{2} \{ A^2 \cos(2\omega_s t) + B^2 \cos(2\omega t) \} \end{aligned} \quad (5.1.2)$$

The constant term is unimportant for present purposes. The generated frequencies,  $[(\omega_s \pm \omega), 2\omega_s, 2\omega]$ , remain within the system and, being part of it, also drive it and thereby produce additional frequencies. The ultimate series of generated frequencies continues and includes all frequencies of the form  $(m\omega + n\omega_s)$ , where  $m$  and  $n$  are integers. The result is true for all values of  $p$  greater than one.

Energy is conserved in lossless systems independently of the degree of nonlinearity. Let  $P_{m,n}$  represent the time average power out of a system at frequency  $(m\omega + n\omega_s)$ . For lossless systems, energy conservation requires that:

$$\sum_{m=-\infty}^{\infty} \sum_{n=-\infty}^{\infty} P_{m,n} = 0 \quad (5.1.3)$$

It is helpful for what lies ahead to rewrite Eq. 5.1.3 as:

$$\omega \sum_{m=-\infty}^{\infty} \sum_{n=-\infty}^{\infty} \frac{m P_{m,n}}{m\omega + n\omega_s} + \omega_s \sum_{m=-\infty}^{\infty} \sum_{n=-\infty}^{\infty} \frac{n P_{m,n}}{m\omega + n\omega_s} = 0 \quad (5.1.4)$$

Equation 5.1.4 contains redundant information since with integer pair  $(m_0, n_0)$  the sums are identical to the sums obtained using  $(-m_0, -n_0)$ . The redundancy is removed yet all information retained by writing the sums as:

$$\omega \sum_{m=0}^{\infty} \sum_{n=-\infty}^{\infty} \frac{mP_{m,n}}{m\omega + n\omega_s} + \omega_s \sum_{m=-\infty}^{\infty} \sum_{n=0}^{\infty} \frac{nP_{m,n}}{m\omega + n\omega_s} = 0 \quad (5.1.5)$$

For example, an ideal, nonlinear capacitor is an example of a lossless, reactive system; other reactive systems may be analyzed in a parallel way. The charge on the capacitor may be expressed as:

$$q(t) = \frac{1}{2} \sum_{m=-\infty}^{\infty} \sum_{n=-\infty}^{\infty} Q_{m,n} \exp[i(m\omega + n\omega_s)t] \quad (5.1.6)$$

The value of  $Q_{m,n}$  depends upon such parameters as the capacitor size, shape, permittivity, and the supported voltage but does not depend upon frequency of operation. Since  $q(t)$  is real, the condition  $Q_{-m,-n}^* = Q_{m,n}$  follows. Similarly the voltage,  $v(t)$ , across the capacitor is:

$$v(t) = \frac{1}{2} \sum_{m=-\infty}^{\infty} \sum_{n=-\infty}^{\infty} V_{m,n} \exp[i(m\omega + n\omega_s)t] \quad (5.1.7)$$

Like  $Q_{m,n}$ ,  $V_{m,n}$  depends upon the capacitor parameters of size, shape, permittivity, and the contained charge but not frequency. The capacitive current  $i(t)$  is equal to the rate of change of charge, and may be written

$$\begin{aligned} i(t) &= \frac{1}{2} \sum_{m=-\infty}^{\infty} \sum_{n=-\infty}^{\infty} I_{m,n} \exp[i(m\omega + n\omega_s)t] \\ &= \frac{i}{2} \sum_{m=-\infty}^{\infty} \sum_{n=-\infty}^{\infty} (m\omega + n\omega_s) Q_{m,n} \exp[i(m\omega + n\omega_s)t] \end{aligned} \quad (5.1.8)$$

The second equality follows by differentiation of Eq. 5.1.6 with respect to time and shows that, differently from either the charge or voltage, current  $I_{m,n}$  does depend upon the frequency. The time average power into the capacitor is:

$$-P_{m,n} = -\frac{1}{2} \operatorname{Re}(V_{m,n} I_{m,n}^*) = \frac{1}{2} (m\omega + n\omega_s) \operatorname{Re}(i V_{m,n} Q_{m,n}^*) \quad (5.1.9)$$

It follows that

$$\frac{P_{m,n}}{(m\omega + n\omega_s)} = -\frac{1}{2} \text{Re}(i V_{m,n} Q_{m,n}^*) \quad (5.1.10)$$

Since the right side of Eq. 5.1.10 depends upon the product of  $Q_{m,n}$  and  $V_{m,n}$  which are not frequency dependent, the right side is independent of frequency. It follows that the left side is also independent of frequency. The parallel argument follows if the roles of  $m$  and  $n$  are reversed. Hence, Eq. 5.1.5 has the general algebraic form:

$$c_1\omega + c_2\omega_s = 0 \quad (5.1.11)$$

The coefficients  $c_1$  and  $c_2$  are independent of frequency. Therefore the two frequencies are independent variables and both  $c_1$  and  $c_2$  are equal to zero. Applying this result to Eq. 5.1.5 shows that the sums are separately equal to zero:

$$\begin{aligned} \sum_{m=0}^{\infty} \sum_{n=-\infty}^{\infty} \frac{mP_{m,n}}{m\omega + n\omega_m} &= 0 \\ \sum_{m=-\infty}^{\infty} \sum_{n=0}^{\infty} \frac{nP_{m,n}}{m\omega + n\omega_s} &= 0 \end{aligned} \quad (5.1.12)$$

To illustrate the use of this equation, consider a system in which one of two possible atomic states is occupied by an electron. The state frequencies are  $\omega_{\text{initial}}$  and  $\omega_{\text{final}}$ , for initially occupied and initially empty states. The ensemble is then enmeshed in a plane wave of frequency  $\omega$  where the frequency of the applied wave satisfies the relationship

$$\omega = |\omega_{\text{initial}} - \omega_{\text{final}}| \quad (5.1.13)$$

With linear systems only the driven frequency,  $\omega$ , and the system frequency,  $\omega_{\text{initial}}$ , are present. With nonlinear systems, all frequencies

$(m\omega_{\text{initial}} + n\omega)$  are driven and are potentially present. If the system is somehow restricted to support only  $\omega_{\text{initial}}$  and  $\omega_{\text{final}}$ , only the three frequencies  $\omega$ ,  $\omega_{\text{initial}}$ , and  $\omega_{\text{final}}$  are present. Consider the case of a nonlinear system that supports only frequencies  $\omega_{\text{initial}}$  and  $\omega_{\text{final}}$  and is driven at frequency  $\omega$ .

For that case, if  $\omega_{\text{initial}} > \omega$  and  $\omega_{\text{initial}} > \omega_{\text{final}}$ , Eq. 5.1.12 is satisfied for integer pairs  $(m = 1, n = 0)$  and  $(m = 1, n = -1)$ ; if  $\omega_{\text{initial}} > \omega$  and  $\omega_{\text{initial}} < \omega_{\text{final}}$ , Eq. 5.1.12 is satisfied for integer pairs  $(m = 0, \pm n = 1)$  and  $(m = -1, \pm n = 1)$ . Changing the power subscripts to match the frequency ones, for these special cases Eqs. 5.1.12 go to:

$$\frac{P_{\text{initial}}}{\omega_{\text{initial}}} + \frac{P_{\text{final}}}{\omega_{\text{final}}} = 0 \quad \text{and} \quad \frac{P_{\text{initial}}}{\omega_{\text{initial}}} \pm \frac{P}{\omega} = 0 \quad (5.1.14)$$

In the second equation, the sign is respectively positive or negative if  $\omega_{\text{initial}}$  is greater or less than  $\omega_{\text{final}}$ . The energy flows are illustrated in Fig. 5.1.1.

By definition the energy that goes into the final state is:

$$W_{\text{final}} = \int P_{\text{final}} dt \quad (5.1.15)$$

Combining Eqs. 5.1.14 and 5.1.15 shows that:

$$\left| \frac{W_{\text{initial}}}{\omega_{\text{initial}}} \right| = \left| \frac{W_{\text{final}}}{\omega_{\text{final}}} \right| = \left| \frac{W}{\omega} \right| \quad (5.1.16)$$

$W_{\text{final}}$  is the energy that goes into the final state and  $W$  is the energy exchanged between the remote field and the electron as it undergoes a change of state. The energy-frequency ratio of Eq. 5.1.16 is independent of system parameters, therefore of system details and, consequently, the ratio is constant. For eigenstates that constant is Planck's constant,  $\hbar$ . It follows that

$$W_{\text{final}} = -\hbar\omega_{\text{final}} \quad W_{\text{initial}} = \hbar\omega_{\text{initial}} \quad W = \pm\hbar\omega \quad (5.1.17)$$

The upper sign applies if  $\omega_{\text{initial}} > \omega_{\text{final}}$ , and *vice versa*.

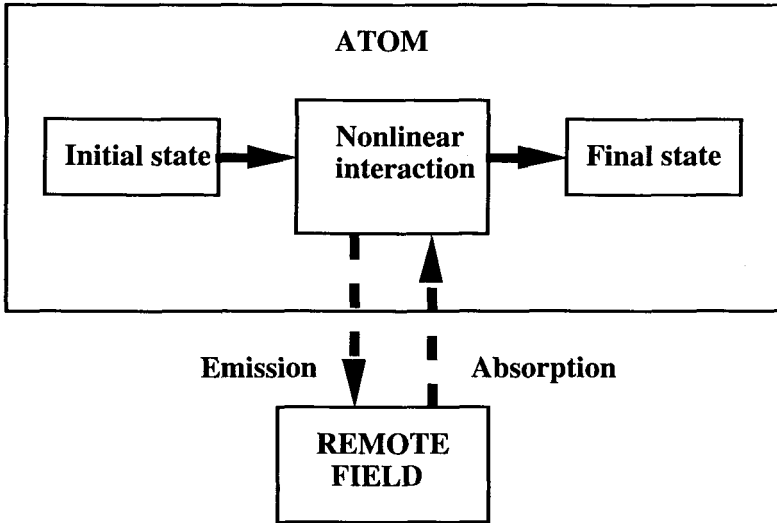


Figure 5.1.1 Diagram illustrating power flows in a nonlinear source. *Initial and remote field energies interact nonlinearly resulting in an energy flow from the initial state to the final state and either into or from the remote field.*

The results are that if the energy in the initial eigenstate is quantized into energy  $\hbar\omega$  the energy exchanged among the radiation field and the initial and final energy eigenstates all have the same energy-to-frequency ratio.

Although Eqs. 5.1.1 through 5.1.14 apply to both linear and nonlinear systems, energy flow at the sum or difference frequencies is equal to zero for linear ones. Therefore, Eqs. 5.1.15 through 5.1.17 have meaning only for nonlinear systems. We conclude that the power-frequency relationships accompanying electron transitions are unique to nonlinear transitions, not to quantum effects.

## 5.2 Length of the Wave Train and Radiation Q

An important property of photons is the length of the coherent wave train. The purpose of this section is to estimate that length for optical frequency photons. We begin by expressing the time varying electromagnetic power in a plane wave as a function of the magnitude and the frequency dependence of fields. For this purpose, let the electric and magnetic field intensities of a plane wave be expressed as integrals over all possible frequencies:

$$\mathbf{E}(t) = \int_{-\infty}^{\infty} \tilde{\mathbf{E}}(\omega) e^{i\omega t} d\omega \quad \text{and} \quad \mathbf{H}(t) = \int_{-\infty}^{\infty} \tilde{\mathbf{H}}(\omega) e^{i\omega t} d\omega \quad (5.2.1)$$

The rate at which energy passes through a unit area of surface follows from the Poynting theorem. With both fields perpendicular to the surface normal:

$$\begin{aligned} \int_{-\infty}^{\infty} N(t) dt &= \frac{1}{2} \text{Re} \int_{-\infty}^{\infty} \tilde{\mathbf{E}}(\omega) d\omega \int_{-\infty}^{\infty} \tilde{\mathbf{H}}(\omega')^* d\omega' \int_{-\infty}^{\infty} e^{i(\omega - \omega')t} dt \\ &= \pi \text{Re} \int_{-\infty}^{\infty} \tilde{\mathbf{E}}(\omega) d\omega \int_{-\infty}^{\infty} \tilde{\mathbf{H}}(\omega')^* d\omega' \delta(\omega - \omega') \\ &= 2\pi \text{Re} \int_{-\infty}^{\infty} \tilde{\mathbf{E}}(\omega) \tilde{\mathbf{H}}^*(\omega) d\omega \end{aligned} \quad (5.2.2)$$

The electric and magnetic frequency dependencies are related by:

$$\eta |H(\omega)| = |E(\omega)| \quad (5.2.3)$$

Combining shows that the power through the surface is:

$$\int_{-\infty}^{\infty} N(t) dt = \frac{2\pi}{\eta} \int_0^{\infty} |\tilde{\mathbf{E}}(\omega)|^2 d\omega \quad (5.2.4)$$

If the plane wave is turned on at time  $t = 0$  and terminated at time  $t = \tau$ , the result is a wave train of length  $l = \tau c$ . The relationship between the length



of a wave train and the measured width of the frequency spectrum follows in a way similar to that used to demonstrate the uncertainty principle. Consider the special case where frequency  $\omega'$  is turned on at time  $-\tau/2$  and off at time  $\tau/2$ , and let  $|\omega - \omega'| = \Delta\omega$ . The resulting electric field intensity is:

$$\begin{aligned} \mathbf{E}(t) &= \tilde{\mathbf{E}}_0 e^{i\omega' t} & |t| \leq \tau/2 \\ &= 0 & |t| \geq \tau/2 \end{aligned} \quad (5.2.5)$$

For this case

$$\tilde{\mathbf{E}}(\omega) = \frac{\tilde{\mathbf{E}}_0}{2\pi} \int_{-\tau/2}^{\tau/2} e^{i(\omega' - \omega)t} dt = \frac{\tau \tilde{\mathbf{E}}_0}{2\pi} \left[ \frac{\sin\left(\frac{\Delta\omega\tau}{2}\right)}{\left(\frac{\Delta\omega\tau}{2}\right)} \right] \quad (5.2.6)$$

The first zero of Eq. 5.2.6, half the width of the frequency pulse, occurs when the argument of the sine term is  $\pi$ . For that case:

$$\tau\Delta\omega = 2\pi \quad (5.2.7)$$

Substituting the length of the pulse train,  $l = c\tau$ , into Eq. 5.2.7 gives:

$$\frac{l}{\lambda} = n = \frac{\omega}{\Delta\omega} = Q \quad (5.2.8)$$

By definition  $n$  is the number of wavelengths in the wave train and the ratio  $\Delta\omega/\omega$  is the fractional bandwidth. With  $\lambda$  equal to the wavelength and for a fixed value of  $Q$  the minimum duration of a pulse is:

$$\tau = \frac{2\pi Q}{\omega} = \frac{Q\lambda}{c} \quad (5.2.9)$$

Feynman's estimate of the  $Q$  of a photon begins with the definition of Eq. 3.5.11, and is repeated here:

$$Q = \frac{\omega W}{P_{av}} \quad (5.2.10)$$

Let a point electron oscillate between positions at  $\pm z_0$ , thereby producing electric dipole radiation. When oscillating at frequency  $\omega$  the maximum energy of the electron is:

$$W = \frac{1}{2} m \omega^2 z_0^2 \quad (5.2.11)$$

The power output of an electric dipole radiator is listed in Table 3.12.1, with unit normalization. The normalization factor,  $-k^3 e z_0 / 4\pi\epsilon$ , follows by comparing the radial component of the electric field intensity with that listed in the table. Substituting the actual values shows that:

$$P_{av} = \frac{e^2 \omega^4 z_0^2}{12\pi\epsilon c^3} \quad (5.2.12)$$

Hence, the calculated  $Q$ , using Eq. 5.2.10, is approximately:

$$\frac{1}{Q} = \frac{e^2 \omega}{6\pi\epsilon m c^3} = \left( \frac{4\pi}{3\lambda} \right) \left( \frac{e^2}{4\pi\epsilon m c^2} \right) \quad (5.2.13)$$

The last bracket in Eq. 5.2.13 is the Lorentz radius of the electron,  $2.82 \times 10^{-15}$  m. At the center of the optical spectrum the wavelength is on the order of  $\lambda = 530$  nm, corresponding to a frequency of about  $5.7 \times 10^{14}$  Hz and a period of about 1.75 fs. Substituting these values into Eq. 5.2.13 shows that:

$$Q \approx 4.5 \times 10^7 \quad (5.2.14)$$

Such an oscillator would need to radiate some  $4.5 \times 10^7$  radians, or some  $7 \times 10^6$  oscillations, before dropping to  $1/e$  of its original intensity. With a resulting decay time of about 10 ns, it follows that the wave train is about

3 m long. With wave trains of this length, transient effects are not expected to be significant.

It was shown earlier that the field energy also contributes to  $Q$ . For an electrically small dipole the approximate  $Q$  due to the field energy is:

$$Q \cong 1/(ka)^3 \quad (5.2.15)$$

At the radius of the first Bohr orbit,  $5.29 \times 10^{-11}$  m, and at the same frequency:

$$ka \cong 6.27 \times 10^{-4} \quad (5.2.16)$$

Combining Eqs. 5.2.15 with Eq. 5.2.16:

$$Q \approx 4.0 \times 10^9 \quad (5.2.17)$$

The  $Q$  of the dipole field energy is approximately 100 times larger than the  $Q$  calculated using the kinetic energy of a point electron generating a dipole mode. Therefore, the radiation  $Q$  of atomic radiation is significant, yet it is ignored in analyses of quantum mechanical transitions.

### 5.3 Phase and Radial Dependence of Field Magnitude

The equation set that describes a circularly polarized,  $z$ -directed plane wave is given by Eqs. 2.1.8, 2.1.10, and 2.1.11 and repeated here:

$$\begin{aligned} \tilde{\mathbf{E}} = \sum_{\ell=1}^{\infty} r^{-\ell} \frac{(2\ell+1)}{\ell(\ell+1)} & \left\{ \begin{aligned} & i\ell(\ell+1) \frac{j_{\ell}(\sigma)}{\sigma} P_{\ell}^1(\cos\theta) \hat{r} \\ & + \left[ j_{\ell}(\sigma) \frac{P_{\ell}^1(\cos\theta)}{\sin\theta} + j_{\ell}^{\bullet}(\sigma) \frac{dP_{\ell}^1(\cos\theta)}{d\theta} \right] \hat{\theta} \\ & - j_{\ell}(\sigma) \frac{dP_{\ell}^1(\cos\theta)}{d\theta} + j_{\ell}^{\bullet}(\sigma) \frac{P_{\ell}^1(\cos\theta)}{\sin\theta} \end{aligned} \right\} \hat{\phi} \exp(-j\Phi) \\ \eta \tilde{\mathbf{H}} = j \tilde{\mathbf{E}} & \quad (5.3.1) \end{aligned}$$

The primary concern is radiation triggered by the plane wave. In the scattering cases considered earlier, the phases of the scattered modes are determined by the phase of the incoming plane wave and the phase angle of the scattering coefficients.

Table 3.17.1 shows the radiation fields produced by four radiating, collocated electric and magnetic dipoles, all of degree one. One electric and one magnetic dipole are oriented along the  $x$ -axis and an identical pair is oriented along the  $y$ -axis. As discussed in Section 3.17 the two sets of pairs radiate  $\pi/2$  out of phase. The calculation procedure shows there is no source-associated standing energy and the radiation  $Q$  is low, possibly as low as zero. The phasor multipolar fields that generate Table 3.17.2 are:

$$\tilde{\mathbf{E}} = \sum_{\ell=1}^{\infty} i^{-\ell} F_{\ell} \left\{ \begin{aligned} & i\ell(\ell+1) \frac{h_{\ell}(\sigma)}{\sigma} P_{\ell}^1(\cos\theta) \hat{r} \\ & + \left[ h_{\ell}(\sigma) \frac{P_{\ell}^1(\cos\theta)}{\sin\theta} + h_{\ell}^{\bullet}(\sigma) \frac{dP_{\ell}^1(\cos\theta)}{d\theta} \right] \hat{\theta} \\ & - j \left[ h_{\ell}(\sigma) \frac{dP_{\ell}^1(\cos\theta)}{d\theta} + h_{\ell}^{\bullet}(\sigma) \frac{P_{\ell}^1(\cos\theta)}{\sin\theta} \right] \hat{\phi} \end{aligned} \right\} \exp(-j\phi)$$

$$\eta \tilde{\mathbf{H}} = j \tilde{\mathbf{E}} \quad (5.3.2)$$

As is the case for Eq. 2.2.1, the modal phases are the same as that of a plane wave. In accordance with the requirements of Table 3.17.1, but differently from Eq. 2.2.1, the magnitudes of the TM and TE modes are equal. The question we address here is: if the fields of Eq. 5.3.1 trigger a metastable source within the circumscribed sphere, what are the expected values of  $F_{\ell}$ ?

The first step in seeking an answer is to examine the phases of the field components. On the positive  $z$ -axis the angular functions, see Table A.18.1, are given by:

$$P_{\ell}^1(1) = 0$$

$$\left. \frac{P_{\ell}^1(\cos\theta)}{\sin\theta} \right|_{\theta=0} = \left. \frac{dP_{\ell}^1(\cos\theta)}{d\theta} \right|_{\theta=0} = \frac{\ell(\ell+1)}{2}$$

$$P_\ell^1(-1) = 0 \quad (5.3.3)$$

$$\frac{P_\ell^1(\cos\theta)}{\sin\theta} \Big|_{\theta=0} = - \frac{dP_\ell^1(\cos\theta)}{d\theta} \Big|_{\theta=\pi} = (-1)^{\ell+1} \frac{\ell(\ell+1)}{2}$$

From Eqs. A.24.9 and A.24.13, the expressions for the radial spherical and related functions are:

$$\begin{aligned} j_\ell(\sigma) &= \sum_{s=0}^{\infty} \frac{(-1)^s \sigma^{\ell+2s}}{(2s)!!(2\ell+2s+1)!!} \\ j_\ell^\bullet(\sigma) &= \sum_{s=0}^{\infty} \frac{(-1)^s \sigma^{\ell+2s-1}}{(2s)!!(2\ell+2s-1)!!} \\ y_\ell(\sigma) &= - \sum_{s=0}^{\ell-1} \frac{(2\ell-2s-1)!!}{(2s)!! \sigma^{\ell+1-2s}} - \sum_{s=0}^{\infty} \frac{(-1)^s}{(2s-1)!!} \frac{\sigma^{\ell-1+2s}}{(2\ell+2s)!!} \\ y_\ell^\bullet(\sigma) &= \sum_{s=0}^{\ell-1} \frac{(2\ell-2s-1)!!}{(2s)!! \sigma^{\ell+2-2s}} (\ell-2s) - \sum_{s=0}^{\infty} \frac{(-1)^s}{(2s-1)!!} \frac{\sigma^{\ell-2+2s}}{(2\ell+2s)!!} (\ell+2s) \end{aligned} \quad (5.3.4)$$

Combining Eqs. 5.3.2 through 5.3.4 shows the relative modal phases. With terms in square brackets indicating phase only and using the zenith angle electric field component as an example, on the positive z-axis:

$$E_\theta \approx r^{-\ell} \left\{ [h_\ell(\sigma)] + i [h_\ell^\bullet(\sigma)] \right\} = r^{-\ell} [j_\ell(\sigma) + y_\ell^\bullet(\sigma)] - i^{1-\ell} [y_\ell(\sigma) - j_\ell^\bullet(\sigma)] \quad (5.3.5)$$

The first terms in each of the square brackets of Eq. 5.3.5 are due to TM modes. The phases of the first term on the right side of Eq. 5.3.5 may be written as

$$r^{-\ell} [j_\ell(\sigma) + y_\ell^\bullet(\sigma)] = r^{-\ell} (-1)^s \sigma^{\ell+2s} - r^{-\ell} (-1)^s \sigma^{\ell+2s-2} + r^{-\ell} \sigma^{-\ell-2+2s}$$

$\ell$  odd

$$\ell = 1; \approx \left\{ -i[\sigma] + i[\sigma^3] - i[\sigma^5] + i[\sigma^7] \dots \right\} + \left\{ i[\sigma^{-1}] - i[\sigma] + i[\sigma^3] - i[\sigma^5] + i[\sigma^7] \dots \right\} - i\sigma^{-3}$$

$$\ell = 3; \approx \left\{ i[\sigma^3] - i[\sigma^5] + i[\sigma^7] \dots \right\} + \left\{ -i[\sigma] + i[\sigma^3] - i[\sigma^5] + i[\sigma^7] \dots \right\} + i \left\{ [\sigma^{-5}] + [\sigma^{-3}] + [\sigma^{-1}] \right\}$$

$\ell$  even

$$\begin{aligned}\ell = 2; & \approx \{-[\sigma^2] + [\sigma^4] - [\sigma^6] + [\sigma^8] \dots\} + \{[1] - [\sigma^2] + [\sigma^4] - [\sigma^6] + [\sigma^8] \dots\} - \{[\sigma^{-4}] + [\sigma^{-2}]\} \\ \ell = 4; & \approx \{[\sigma^4] - [\sigma^6] + [\sigma^8] \dots\} + \{-[\sigma^2] + [\sigma^4] - [\sigma^6] + [\sigma^8] \dots\} + \{[\sigma^{-6}] + [\sigma^{-4}] + [\sigma^{-2}] + [1]\}\end{aligned}\quad (5.3.6)$$

The results contained in Eq. 5.3.6 show that for powers of  $\sigma$  greater than or equal to zero the phase of each power of the radius is the same for all moments. Therefore, along the positive  $z$ -axis, and in the near field, driving one dipole moment drives the corresponding far-field radial components of all odd, higher order modes. Quite differently for powers of  $\sigma$  less than zero, higher order terms have opposite signs and act to cancel the total near-field radial field component.

The second term on the right side of Eq. 5.3.5 is due to TE modes, and may be written as:

$$i^{-\ell} [y_{\ell}(\sigma) - j_{\ell}^{\bullet}(\sigma)] = 2i^{1-\ell} (-1)^s \sigma^{\ell-1+2s} + i^{1-\ell} \sigma^{-\ell-1+2s}$$

$\ell$  odd

$$\begin{aligned}\ell = 1; & \approx 2\{[1] - [\sigma^2] + [\sigma^4] - [\sigma^6] \dots\} + [\sigma^{-2}] \\ \ell = 3; & \approx 2\{-[\sigma^2] + [\sigma^4] - [\sigma^6] \dots\} - \{[\sigma^{-4}] + [\sigma^{-2}] + [1]\}\end{aligned}\quad (5.3.7)$$

$\ell$  even

$$\begin{aligned}\ell = 2; & \approx 2i \{-[\sigma] + [\sigma^3] - [\sigma^5] + [\sigma^7] \dots\} - i \{[\sigma^{-3}] + [\sigma^{-1}]\} \\ \ell = 4; & \approx 2i \{[\sigma^3] - [\sigma^5] + [\sigma^7] \dots\} + i \{[\sigma^{-5}] + [\sigma^{-3}] + [\sigma^{-1}] + [\sigma]\}\end{aligned}$$

Since the results of Eq. 5.3.7 are the same as those of Eq. 5.3.6, driving the magnetic dipole moments also drives the corresponding far-field radial components of all odd, higher order modes. For negative powers of  $\sigma$  the terms have opposite signs and act to cancel the total near-field radial field component. The relative phases of the two equations show that the dipole far-field terms of Eq. 5.3.6 produce the same phase, even order terms as does Eq. 5.3.7, and the dipole far-field terms of Eq. 5.3.7 produce the same phase odd order terms as does Eq. 5.3.6. In this way, the system is phased so the dipole terms drive all higher order terms.

On the negative  $z$ -axis both TM and TE modes contain alternate signs of the expansion modes, with canceling phases and no field buildup.

We conclude that a buildup of a term proportional to  $\sigma^n$ , where  $n \geq 0$ , by any mode builds the magnitudes of the far-fields for all modes for  $z > 0$  and, at the same time, reduces the magnitudes of the near-fields. This condition lends itself to a regenerative buildup of field magnitudes.

## 5.4 Gain and Radiation Pattern

The gain of an antenna is a power ratio; it is the ratio of the product of the maximum power density on the surface of a virtual, circumscribing sphere and the surface area to the average surface power. In mathematical terms:

$$G(\sigma) = \lim_{\sigma \Rightarrow \infty} \frac{4\pi\sigma^2}{k^2} \frac{[N_r]_{\max}}{P_{av}} \quad (5.4.1)$$

Both Einstein and Planck referred to the “spherical symmetry” of radiation modes. It was surely this idea that was the basis for Einstein’s comment that the full directivity of quantized radiation made a quantum theory of radiation “almost unavoidable” Certain radiation modes do, however, carry linear momentum. Harrington quantified the maximum gain in 1960, about four decades after both Einstein’s 1917 paper on directivity and Planck’s 1920 Nobel prize paper that addressed the issue.

Consider the gain of fields described by Eqs. 5.3.2, after making the equality  $i = j$ . For this case the maximum value of  $N_r(\sigma, \theta, \phi)$  occurs at angle  $\theta = 0$ . Making this substitution and using Table A.18.1 from the Appendix gives the fields:

$$\begin{aligned} \mathbf{E}(\sigma, 0) &= \frac{1}{2} \sum_{\ell=1}^{\infty} i^{-\ell} F_{\ell}(\ell+1) \left[ \mathbf{h}_{\ell}(\sigma) + i \mathbf{h}_{\ell}^{\bullet}(\sigma) \right] \left[ \hat{\theta} - i \hat{\phi} \right] e^{-i\phi} \\ \eta \mathbf{H}(\sigma, 0) &= \frac{1}{2} \sum_{\ell=1}^{\infty} i^{1-\ell} F_{\ell}(\ell+1) \left[ \mathbf{h}_{\ell}(\sigma) + i \mathbf{h}_{\ell}^{\bullet}(\sigma) \right] \left[ \hat{\theta} - i \hat{\phi} \right] e^{-i\phi} \end{aligned} \quad (5.4.2)$$

The radial component of the Poynting vector is:

$$\eta N_r(\sigma, 0) = \frac{1}{2i} \sum_{\ell=1}^{\infty} i^{-\ell} F_{\ell} \ell(\ell+1) \left[ h_{\ell}(\sigma) + h_{\ell}^*(\sigma) \right] \times \sum_{n=1}^{\infty} i^n F_n n(n+1) \left[ h_n(\sigma) + h_n^*(\sigma) \right]^* \quad (5.4.3)$$

Limiting forms of spherical Hankel functions are given in the Appendix: Eqs. A.25.17 and A.26.4. Making the substitution gives the maximum value of the radial component of the Poynting vector:

$$N_r(\sigma, 0) = \frac{1}{\eta \sigma^2} \left[ \sum_{\ell=1}^{\infty} F_{\ell} \ell(\ell+1) \right]^2 \quad (5.4.4)$$

Using the fields of Eqs. 5.3.2, the output power on a virtual sphere of limitlessly large radius is:

$$P_{av} = \frac{\sigma^2}{2\eta k^2} \sum_{\ell=1}^{\infty} \int_0^{2\pi} d\phi \int_0^{\pi} \sin\theta d\theta i^{-\ell} [F_{\ell}]^2 \left\{ \frac{e^{i\ell(\ell+1)}}{\sigma} \left[ \frac{P_{\ell}^1}{\sin\theta} + \frac{dP_{\ell}^1}{d\theta} \right] [\hat{\theta} - \hat{\phi}] \right\} \quad (5.4.5)$$

$$\times i^{\ell} \left\{ \frac{e^{-i\ell(\ell+1)}}{\sigma} \left[ \frac{P_{\ell}^1}{\sin\theta} + \frac{dP_{\ell}^1}{d\theta} \right] [\hat{\theta} + \hat{\phi}] \right\}$$

Evaluation gives:

$$P_{av} = \frac{4\pi}{\eta k^2} \sum_{\ell=1}^{\infty} \frac{[F_{\ell}]^2}{2\ell+1} [\ell(\ell+1)]^2 \quad (5.4.6)$$

Substituting Eqs. 5.4.4 and 5.4.6 into 5.4.1 gives:

$$G(\sigma) = \frac{\left[ \sum_{\ell=1}^{\infty} F_{\ell} \ell(\ell+1) \right]^2}{\sum_{\ell=1}^{\infty} F_{\ell}^2 \frac{\ell^2(\ell+1)^2}{2\ell+1}} \quad (5.4.7)$$

A particularly interesting special case is if the modal coefficients satisfy the relationship:



$$F_\ell = \frac{(2\ell+1)}{\ell(\ell+1)} \quad (5.4.8)$$

For this special case the gain is:

$$G = \sum_{\ell=1}^{\infty} (2\ell+1) \quad (5.4.9)$$

This expression for gain, first derived and published by Harrington in 1960, vividly demonstrates that the radiation of spherical modes can be arranged to support power that does not possess circular symmetry. That is, a net transfer of linear momentum is possible.

## 5.5 Kinematic Values of the Radiation

Radiation from electrically small sources is dominated, in the main, by the moment with the lowest power of  $ka$ . A primary reason is that the Qs of electrically small antennas producing single modes increase rapidly with increasing order, *i.e.*, as  $|\gamma(\sigma)|$  of Table 3.2.1. However it was shown in Section 3.18 that a multimodal source generating the fields of Eqs. 5.3.2 does not necessarily extract a returnable standing energy from the source. By Eq. A.28.12 and Eq. A.29.18, the magnitudes of electric and magnetic multipolar fields of order  $\ell$  are respectively proportional to  $(ka)^\ell$  and  $(ka)^{\ell+1}$ . The magnitude of fields scattered by a passive, electrically small object will, therefore, decrease rapidly with increasing modal order, see Eq. 2.3.6. For the case of interest here, however, the scatterer is not a passive object but an excited, eigenstate electron. The host atom is immersed within a  $z$ -directed, circularly polarized plane wave that triggers a nonlinear, radiating transition to a lower energy eigenstate. We seek to find radiation details that apply during the transition.

With  $p_z$  and  $l_z$  representing respectively linear and angular momentum, the kinematic properties of atomic radiation, *i.e.*, photons, are:

$$\mathcal{W}/p_z = c \quad \mathcal{W}/l_z = \omega \quad p_z/l_z = k \quad (5.5.1)$$

To examine the radiation fields using classical field theory consider the equation set of Eq. 5.3.2 and examine the rate at which energy, linear momentum, and angular momentum exit through the surface of a sphere of radius  $\sigma/k$  circumscribing the atomic source. The rates are:

Energy:

Use of Eq. 1.9.11 shows that the rate of energy loss through a spherical shell is:

$$\frac{dW}{dt} = \frac{\sigma^2}{k^2} \int_0^{2\pi} d\phi \int_0^{\pi} \text{Re}[N_r] \sin\theta d\theta \quad (5.5.2)$$

Linear Momentum:

By Eq. 1.9.7, the momentum contained within a volume is equal to  $1/c^2$  times the volume integral of the Poynting vector:

$$\mathbf{p} = \frac{1}{c^2 k^3} \int \sigma^2 d\sigma \int_0^{2\pi} d\phi \int_0^{\pi} \text{Re}[\mathbf{N}] \sin\theta d\theta \quad (5.5.3)$$

Since the equality holds for every volume in space the rate at which the  $z$ -component of momentum exits a closed volume is equal to  $c$  times the surface integral of the  $z$ -component of momentum:

$$\frac{dp_z}{dt} = \frac{\sigma^2}{ck^2} \int_0^{2\pi} d\phi \int_0^{\pi} \text{Re}[N_r \cos\theta - N_\theta \sin\theta] \sin\theta d\theta \quad (5.5.4)$$

Angular Momentum:

Angular momentum is related to linear momentum by Eq. 4.8.1; the rate at which  $z$ -directed angular momentum exits a closed volume is:

$$\frac{dJ_z}{dt} = \frac{\sigma^3}{ck^3} \int_0^{2\pi} d\phi \int_0^{\pi} \text{Re}[N_\phi] \sin^2\theta d\theta \quad (5.5.5)$$

Using the fields of Eq. 5.3.2, treating the coefficients  $F_\ell$  as unknowns, and putting  $j = i$  shows the Poynting vector to be:

$$N_r = \frac{\text{Re}}{2\eta} \sum_{\ell=1}^{\infty} \sum_{n=1}^{\infty} F_{\ell} F_n^* \ell^{n-\ell} \left\{ \begin{aligned} &\left( h_{\ell} h_n^* + h_{\ell}^* h_n \right) \left( \frac{P_{\ell}^1}{\sin \theta} \frac{dP_n^1}{d\theta} + \frac{P_n^1}{\sin \theta} \frac{dP_{\ell}^1}{d\theta} \right) \\ &- \left( h_{\ell} h_n^* - h_{\ell}^* h_n \right) \left( \frac{P_{\ell}^1}{\sin \theta} \frac{P_n^1}{\sin \theta} + \frac{dP_{\ell}^1}{d\theta} \frac{dP_n^1}{d\theta} \right) \end{aligned} \right\} \quad (5.5.6)$$

$$N_{\theta} = -\frac{\text{Re}}{2\sigma\eta} \sum_{\ell=1}^{\infty} \sum_{n=1}^{\infty} F_{\ell} F_n^* \ell^{n-\ell} \left[ n(n+1) h_n^* h_{\ell}^* + \ell(\ell+1) h_{\ell} h_n^* \right] \frac{P_{\ell}^1 P_n^1}{\sin \theta} \quad (5.5.7)$$

$$N_{\phi} = \frac{\text{Re}}{2\sigma\eta} \sum_{\ell=1}^{\infty} \sum_{n=1}^{\infty} F_{\ell} F_n^* \ell^{n-\ell} \left\{ \begin{aligned} &\left( n(n+1) h_n^* h_{\ell}^* P_n^1 \frac{dP_{\ell}^1}{d\theta} - \ell(\ell+1) h_{\ell} h_n^* P_{\ell}^1 \frac{dP_n^1}{d\theta} \right) \\ &- \left( \left[ \ell(\ell+1) + n(n+1) \right] h_{\ell} h_n^* \frac{P_{\ell}^1 P_n^1}{\sin \theta} \right) \end{aligned} \right\} \quad (5.5.8)$$

Substituting these values into Eqs. 5.5.2, 5.5.4, and 5.5.5, evaluating the integrals using Table A.22.1, and replacing the spherical radial functions by letter functions gives:

$$\frac{dW}{dt} = \sum_{\ell=1}^{\infty} \frac{4\pi}{\eta k^2} \frac{\ell^2 (\ell+1)^2}{(2\ell+1)} F_{\ell} F_{\ell}^* \quad (5.5.9)$$

$$\frac{dp_z}{dt} = \text{Re} \sum_{\ell=1}^{\infty} \frac{2\pi}{\eta c k^2} \left\{ \begin{aligned} &F_{\ell} F_{\ell}^* \frac{\ell(\ell+1)}{(2\ell+1)} (A_{\ell}^2 + B_{\ell}^2 + C_{\ell}^2 + D_{\ell}^2) - F_{\ell} F_{\ell}^* \frac{2\ell^2 (\ell+1)^2}{\sigma(2\ell+1)} (A_{\ell} C_{\ell} + B_{\ell} D_{\ell}) \\ &+ F_{\ell} F_{\ell+1}^* \frac{\ell^2 (\ell+1)(\ell+2)^2}{(2\ell+1)(2\ell+3)} (A_{\ell} C_{\ell+1} - A_{\ell+1} C_{\ell} + B_{\ell} D_{\ell+1} - B_{\ell+1} D_{\ell}) \\ &- 2F_{\ell} F_{\ell+1}^* \frac{2\ell^2 (\ell+1)^2 (\ell+2)^2}{(2\ell+1)(2\ell+3)\sigma} (A_{\ell} C_{\ell+1} + B_{\ell} D_{\ell+1}) \\ &+ F_{\ell} F_{\ell-1}^* \frac{(\ell-1)^2 \ell(\ell+1)^2}{(2\ell+1)(2\ell-1)} (A_{\ell-1} C_{\ell} - A_{\ell} C_{\ell-1} + B_{\ell-1} D_{\ell} - B_{\ell} D_{\ell-1}) \\ &- 2F_{\ell} F_{\ell-1}^* \frac{2(\ell-1)^2 \ell^2 (\ell+1)^2}{(2\ell+1)(2\ell-1)\sigma} (A_{\ell} C_{\ell-1} + B_{\ell} D_{\ell-1}) \end{aligned} \right\} \quad (5.5.10)$$

$$\frac{dL_z}{dt} = \frac{4\pi\sigma^2}{\eta\omega k^2} \operatorname{Re} \sum_{\ell=1}^{\infty} \left\{ \begin{aligned} & F_{\ell} F_{\ell}^* \frac{\ell^2(\ell+1)^2}{(2\ell+1)} (A_{\ell}^2 + B_{\ell}^2) \\ & - \left( F_{\ell} F_{\ell-1}^* - F_{\ell-1} F_{\ell}^* \right) \frac{(\ell-1)^2 \ell^2 (\ell+1)^2}{2(2\ell+1)(2\ell-1)} \left[ \frac{(A_{\ell} C_{\ell-1} + B_{\ell} D_{\ell-1})}{-i(A_{\ell} D_{\ell-1} - B_{\ell} C_{\ell-1})} \right] \\ & - \left( F_{\ell+1} F_{\ell}^* - F_{\ell} F_{\ell+1}^* \right) \frac{\ell^2(\ell+1)^2(\ell+2)^2}{2(2\ell+1)(2\ell+3)} \left[ \frac{(A_{\ell} C_{\ell+1} + B_{\ell} D_{\ell+1})}{-i(A_{\ell} D_{\ell+1} - B_{\ell} C_{\ell+1})} \right] \end{aligned} \right\} \quad (5.5.11)$$

In the limit as the radius becomes infinite:

$$\begin{aligned} \frac{dW}{dt} &= \frac{4\pi}{\eta k^2} \sum_{\ell=1}^{\infty} F_{\ell} F_{\ell}^* \frac{\ell^2(\ell+1)^2}{(2\ell+1)} \\ \frac{dp_z}{dt} &= \frac{4\pi}{\eta c k^2} \sum_{\ell=1}^{\infty} \frac{\ell(\ell+1)}{(2\ell+1)} \left\{ F_{\ell} F_{\ell}^* + F_{\ell} F_{\ell+1}^* \frac{\ell(\ell+2)^2}{(2\ell+3)} + F_{\ell} F_{\ell-1}^* \frac{(\ell-1)^2(\ell+1)}{(2\ell-1)} \right\} \quad (5.5.12) \\ \frac{dL_z}{dt} &= \frac{4\pi}{\eta\omega k^2} \sum_{\ell=1}^{\infty} F_{\ell} F_{\ell}^* \frac{\ell^2(\ell+1)^2}{(2\ell+1)} \end{aligned}$$

Equations 5.5.12 show that both the energy-to-angular momentum ratio and the energy-to-linear momentum ratio depend upon the magnitude of recursion relation  $F_{\ell}$ . Before solving for  $F_{\ell}$ , it is necessary to consider some additional factors.

To examine properties of a field described by Eqs. 5.3.2 note that sums over spherical Neumann functions can be put in closed form only at very large and at very small radii. For a very large radius note from Eq. A.24.15 that the limiting values of functions are:

$$\begin{aligned} \lim_{\sigma \Rightarrow \infty} j_{\ell}(\sigma) &= \frac{1}{\sigma} \cos \left[ \sigma - \frac{\pi}{2}(\ell+1) \right] \\ \lim_{\sigma \Rightarrow \infty} y_{\ell}(\sigma) &= \frac{1}{\sigma} \sin \left[ \sigma - \frac{\pi}{2}(\ell+1) \right] = \frac{1}{\sigma} \cos \left[ \sigma - \frac{\pi}{2}(\ell+2) \right] \end{aligned} \quad (5.5.13)$$

The two functions differ in phase by  $\pi/2$ . Next, multiply the Neumann functions by  $(\pm i)$ , as is done in the formation of spherical Hankel functions.

This changes the phase by another  $\pi/2$  and brings the functional form to either the same phase or  $\pi$  out of phase, depending upon whether the phase shifts add or subtract. The result is that in the limit of infinite radius changing spherical Bessel functions to spherical Hankel functions results in the far field sum of Bessel and Neumann parts either doubling the field terms or summing to zero.

In the limit of small radius, the two functions are equal to:

$$\lim_{\sigma \Rightarrow 0} j_\ell(\sigma) = \frac{\sigma^\ell}{(2\ell+1)!!} \quad \text{and} \quad \lim_{\sigma \Rightarrow 0} y_\ell(\sigma) = -\frac{(2\ell-1)!!}{\sigma^{\ell+1}} \quad (5.5.14)$$

Bessel function solutions are continuous through all orders at the origin but Neumann function solutions undergo an  $(\ell+1)$ -order singularity. Spherical Neumann functions therefore play an essential role in the description of scattered and generated fields. In a step we support during the rest of this chapter we assert that the correct recursion relationship is:

$$F_\ell = \frac{(2\ell+1)}{\ell(\ell+1)} F \quad (5.5.15)$$

$F$  is real and independent of  $\ell$ . Substituting the relationship back into field Eqs. 5.3.2 repeats Eqs. 5.3.1 except spherical Bessel functions are replaced by spherical Hankel functions; of course with Hankel functions, the limit values obtained using Eqs. 5.5.13 and 5.5.14 apply.

$$\tilde{\mathbf{E}} = \sum_{\ell=1}^{\infty} r^{-\ell} \frac{(2\ell+1)}{\ell(\ell+1)} \left\{ \begin{aligned} & i\ell(\ell+1) \frac{h_\ell(\sigma)}{\sigma} P_\ell^1(\cos\theta) \hat{r} \\ & + \left[ h_\ell(\sigma) \frac{P_\ell^1(\cos\theta)}{\sin\theta} + h_\ell^\bullet(\sigma) \frac{dP_\ell^1(\cos\theta)}{d\theta} \right] \hat{\theta} \\ & - \left[ h_\ell(\sigma) \frac{dP_\ell^1(\cos\theta)}{d\theta} + h_\ell^\bullet(\sigma) \frac{P_\ell^1(\cos\theta)}{\sin\theta} \right] \hat{\phi} \end{aligned} \right\} \exp(-j\phi)$$

$$\eta \tilde{\mathbf{H}} = j \tilde{\mathbf{E}} \quad (5.5.16)$$

Since the source is much smaller than a wavelength, the rules of geometric optics apply in the region where the wave interacts with the source. There the phase of the Neumann function undergoes a step change of  $\pi$  and, in optical terms, is a caustic. It is expected, therefore, that if the Bessel and Neumann contributions to the teledistant terms are in phase along the positive  $z$ -axis they will be  $\pi$  out of phase along the negative  $z$ -axis, and *vice versa*.

Substituting Eq. 5.5.16 into Eqs. 5.5.12 gives:

$$\begin{aligned} \lim_{\sigma \Rightarrow \infty} \frac{dW}{dt} &= \frac{4\pi F^2}{\eta k^2} \sum_{\ell=1}^{\infty} (2\ell + 1) \\ \lim_{\sigma \Rightarrow \infty} \frac{dp_z}{dt} &= \frac{4\pi F^2}{\eta c k^2} \sum_{\ell=1}^{\infty} (2\ell + 1) \\ \lim_{\sigma \Rightarrow \infty} \frac{dl_z}{dt} &= \frac{4\pi F^2}{\eta \omega k^2} \sum_{\ell=1}^{\infty} (2\ell + 1) \end{aligned} \quad (5.5.17)$$

It follows from Eqs. 5.5.17 that:

$$\begin{aligned} \lim_{\sigma \Rightarrow \infty} \frac{dW}{dt} \bigg/ \frac{dp_z}{dt} &= c \\ \lim_{\sigma \Rightarrow \infty} \frac{dW}{dt} \bigg/ \frac{dl_z}{dt} &= \omega \\ \lim_{\sigma \Rightarrow \infty} \frac{dp_z}{dt} \bigg/ \frac{dl_z}{dt} &= k \end{aligned} \quad (5.5.18)$$

Since the time-variation of the three kinematic properties is identical, Eq. 5.5.18 leads directly to Eq. 5.5.1. Therefore, the kinematic properties of this radiation are the same as the kinematic properties of photons and there is no dichotomy between the kinematic properties of photons and classical field theory. All three parameters are proportional to the gain, see Eq. 5.4.9.

Next, consider what requires Eq. 5.5.15 to be uniquely correct. The requirements of resonance and zero  $Q$  are met by Eq. 5.3.2. As discussed in Section 5.3 the phase portion of Eq. 5.5.16 uniquely defines fields for which equal powers of  $\sigma$  have equal phases in all modal orders, creating

regenerative feedback. The near fields are properly phased to cancel. To consider the relationship further it is necessary to examine the full set of photon fields.

## 5.6 Telefields and Far Fields

The field intensities of a circularly polarized, z-directed plane wave are expressed in spherical coordinates in Eq. 5.3.1, and by:

$$\mathbf{E} = e^{-i\sigma \cos\theta} (\hat{r} \sin\theta + \hat{\theta} \cos\theta - i \hat{\phi}) e^{-i\phi}; \quad \eta \mathbf{H} = i \mathbf{E} \quad (5.6.1)$$

Since the magnitudes of the field terms are independent of distance, define them to be telefield terms. For comparison, far field terms are proportional to  $1/\sigma$ , inverse square terms are proportional to  $1/\sigma^2$ , and near field terms are proportional to  $1/\sigma^n$  where  $n > 2$ . Since the electric and magnetic field intensities are related as described by Eq. 5.6.1, it is sufficient to solve for the electric field.

The Uniqueness Theorem requires Eqs. 5.6.1 and 5.3.1 to be identical. By Section 5.5 the external radiation fields produced during state decay is obtained by inserting Eq. 5.5.15 into Eq. 5.3.2. The result is:

$$\tilde{\mathbf{E}} = \sum_{\ell=1}^{\infty} i^{-\ell} \frac{(2\ell+1)}{\ell(\ell+1)} \left\{ \begin{aligned} & i\ell(\ell+1) \frac{h_{\ell}(\sigma)}{\sigma} P_{\ell}^1(\cos\theta) \hat{r} + \left[ h_{\ell}(\sigma) \frac{P_{\ell}^1(\cos\theta)}{\sin\theta} + h_{\ell}^*(\sigma) \frac{dP_{\ell}^1(\cos\theta)}{d\theta} \right] \hat{\theta} \\ & - i \left[ h_{\ell}(\sigma) \frac{dP_{\ell}^1(\cos\theta)}{d\theta} + h_{\ell}^*(\sigma) \frac{P_{\ell}^1(\cos\theta)}{\sin\theta} \right] \hat{\phi} \end{aligned} \right\} e^{-i\phi} \quad (5.6.2)$$

To obtain more useful expressions for the near field terms it is helpful to evaluate the sums of Eq. 5.6.2. For this purpose, introduce special sums over the spherical functions, defined by:

$$S_1(\sigma, \theta) = \sum_{\ell=1}^{\infty} i^{1-\ell} (2\ell+1) h_{\ell}(\sigma) P_{\ell}^1(\cos\theta) = S_{11}(\sigma, \theta) - i S_{12}(\sigma, \theta)$$

$$S_2(\sigma, \theta) = \sum_{\ell=1}^{\infty} i^{-\ell} \frac{(2\ell+1)}{\ell(\ell+1)} h_{\ell}(\sigma) \frac{dP_{\ell}^1(\cos\theta)}{d\theta} = S_{21}(\sigma, \theta) - iS_{22}(\sigma, \theta) \quad (5.6.3)$$

$$S_3(\sigma, \theta) = \sum_{\ell=1}^{\infty} i^{-\ell} \frac{(2\ell+1)}{\ell(\ell+1)} h_{\ell}(\sigma) \frac{P_{\ell}^1(\cos\theta)}{\sin\theta} = S_{31}(\sigma, \theta) - iS_{32}(\sigma, \theta)$$

Sums  $S_{n1}$  are over spherical Bessel functions and sums  $S_{n2}$  are over spherical Neumann functions. Once the functional form of  $S_3$  is known,  $S_2$  follows using the relationship:

$$S_2(\sigma, \theta) = \frac{\partial}{\partial \theta} [\sin\theta S_3(\sigma, \theta)] \quad (5.6.4)$$

To complete all needed information about the radiated field it is also necessary to evaluate the forms:

$$\mathcal{S}_2(\sigma, \theta) = \frac{i}{\sigma} \frac{\partial}{\partial \sigma} [\sigma S_2(\sigma, \theta)] \quad \mathcal{S}_3(\sigma, \theta) = \frac{i}{\sigma} \frac{\partial}{\partial \sigma} [\sigma S_3(\sigma, \theta)] \quad (5.6.5)$$

Combining all the above shows that:

$$\begin{aligned} \sigma E_r &= S_1(\sigma, \theta) e^{-i\Phi} \\ E_{\theta} &= [\mathcal{S}_2(\sigma, \theta) + S_3(\sigma, \theta)] e^{-i\Phi} \\ E_{\phi} &= -i [S_2(\sigma, \theta) + \mathcal{S}_3(\sigma, \theta)] e^{-i\Phi} \end{aligned} \quad (5.6.6)$$

Consider the sums over spherical Bessel functions. The first sum follows by equating the radial components of Eqs. 5.6.1 and 5.6.2; it also follows from Eq. A.27.6:

$$S_{11}(\sigma, \theta) = \sum_{\ell=1}^{\infty} i^{1-\ell} (2\ell+1) j_{\ell}(\sigma) P_{\ell}^1(\cos\theta) = \sigma \sin\theta e^{-i\sigma \cos\theta} \quad (5.6.7)$$

To evaluate the other sums, equate the angular components of Eq. 5.6.1 and Eq. 5.3.1 to obtain:



$$\begin{aligned}
 \cos \theta e^{-i\sigma \cos \theta} &= \sum_{\ell=1}^{\infty} i^{-\ell} \frac{(2\ell+1)}{\ell(\ell+1)} \left[ j_{\ell}(\sigma) \frac{P_{\ell}^1(\cos \theta)}{\sin \theta} + j_{\ell}^{\bullet}(\sigma) \frac{dP_{\ell}^1(\cos \theta)}{d\theta} \right] \\
 e^{-i\sigma \cos \theta} &= \sum_{\ell=1}^{\infty} i^{-\ell} \frac{(2\ell+1)}{\ell(\ell+1)} \left[ j_{\ell}(\sigma) \frac{dP_{\ell}^1(\cos \theta)}{d\theta} + j_{\ell}^{\bullet}(\sigma) \frac{P_{\ell}^1(\cos \theta)}{\sin \theta} \right]
 \end{aligned} \quad (5.6.8)$$

To evaluate the sums, use the identities from Eqs. A.21.1.1 and A.21.1.5:

$$\begin{aligned}
 \frac{d}{d\theta} P_{\ell}^1(\cos \theta) &= \frac{1}{2} [\ell(\ell+1)P_{\ell} - P_{\ell}^2] \\
 \frac{P_{\ell}^1(\cos \theta)}{\sin \theta} &= \frac{1}{2 \cos \theta} [\ell(\ell+1)P_{\ell} + P_{\ell}^2]
 \end{aligned} \quad (5.6.9)$$

Substituting the identities into Eqs. 5.6.8 gives:

$$\begin{aligned}
 \cos \theta e^{-i\sigma \cos \theta} &= \frac{1}{2} \left\{ \sum_{\ell=1}^{\infty} i^{-\ell} (2\ell+1) \left[ j_{\ell}(\sigma) \frac{P_{\ell}(\cos \theta)}{\cos \theta} + j_{\ell}^{\bullet}(\sigma) P_{\ell}(\cos \theta) \right] \right. \\
 &\quad \left. + \sum_{\ell=1}^{\infty} i^{-\ell} \frac{(2\ell+1)}{\ell(\ell+1)} \left[ j_{\ell}(\sigma) \frac{P_{\ell}^2(\cos \theta)}{\cos \theta} - j_{\ell}^{\bullet}(\sigma) P_{\ell}^2(\cos \theta) \right] \right\} \\
 e^{-i\sigma \cos \theta} &= \frac{1}{2} \left\{ \sum_{\ell=1}^{\infty} i^{-\ell} (2\ell+1) \left[ j_{\ell}(\sigma) P_{\ell}(\cos \theta) + j_{\ell}^{\bullet}(\sigma) \frac{P_{\ell}(\cos \theta)}{\cos \theta} \right] \right. \\
 &\quad \left. - \sum_{\ell=1}^{\infty} i^{-\ell} \frac{(2\ell+1)}{\ell(\ell+1)} \left[ j_{\ell}(\sigma) P_{\ell}^2(\cos \theta) + j_{\ell}^{\bullet}(\sigma) \frac{P_{\ell}^2(\cos \theta)}{\cos \theta} \right] \right\}
 \end{aligned} \quad (5.6.10)$$

The two sums on the top lines of both of Eqs. 5.6.10 sum to a known polynomial of trigonometric functions, with the assistance of Eq. 5.6.7. The result is that Eqs. 5.6.10 form two linear, algebraic equations with the sums on the bottom lines of both Eqs. 5.6.10 as unknowns. The equation forms are:

$$f_1(\sigma, \cos \theta) = \frac{1}{2} \left( \frac{x}{\cos \theta} - i y \right) \quad f_2(\sigma, \cos \theta) = -\frac{1}{2} \left( x + \frac{i y}{\cos \theta} \right) \quad (5.6.11)$$

Solving Eq. 5.6.11 and carrying out the details yields the equality:

$$\sum_{\ell=1}^{\infty} i^{-\ell} \frac{(2\ell+1)}{\ell(\ell+1)} j_{\ell}(\sigma) P_{\ell}^2(\cos \theta) = \left\{ \begin{aligned} & -e^{-i\sigma \cos \theta} \left[ 1 + 2i \frac{\cos \theta}{\sigma \sin^2 \theta} \right] \\ & + i \frac{\cos \theta}{\sigma \sin^2 \theta} \left[ 2 \cos \sigma - i \sin \sigma \frac{(1 + \cos^2 \theta)}{\cos \theta} \right] \end{aligned} \right\} \quad (5.6.12)$$

Next, sum over each of Eqs. 5.6.9 after multiplying through by the factor:

$$i^{-\ell} \frac{(2\ell+1)}{\ell(\ell+1)} j_{\ell}(\sigma)$$

In each equation, the sums on the right side are those of Eqs. 5.6.7 and 5.6.12, and give exact values for the sums  $S_{21}$  and  $S_{31}$ . From these sums come exact values for  $\$_{21}$  and  $\$_{31}$ . All sums over spherical Bessel functions are listed in Table 5.6.1.

The sums of Table 5.6.1 evaluated on the positive and negative  $z$ -axes and in the equatorial plane are listed in Table 5.6.2,

---


$$S_{11}(\sigma, \theta) = \sigma \sin \theta e^{-i\sigma \cos \theta}$$

$$S_{21}(\sigma, \theta) = e^{-i\sigma \cos \theta} + \frac{i}{\sigma \sin^2 \theta} \left[ e^{-i\sigma \cos \theta} \cos \theta - (\cos \sigma \cos \theta - i \sin \sigma) \right]$$

$$S_{31}(\sigma, \theta) = -\frac{i}{\sigma \sin^2 \theta} \left[ e^{-i\sigma \cos \theta} - (\cos \sigma - i \sin \sigma \cos \theta) \right]$$

$$\$_{21}(\sigma, \theta) = \cos \theta e^{-i\sigma \cos \theta} + \frac{i}{\sigma \sin^2 \theta} \left[ e^{-i\sigma \cos \theta} - (\cos \sigma - i \sin \sigma \cos \theta) \right]$$

$$\$_{31}(\sigma, \theta) = -\frac{i}{\sigma \sin^2 \theta} \left[ e^{-i\sigma \cos \theta} \cos \theta - (\cos \sigma \cos \theta - i \sin \sigma) \right]$$


---

Table 5.6.1 Closed form solutions for the field sums defined in Eq. 5.6.3, over spherical Bessel functions.

---

1. $S_{11}(\sigma, 0) = S_{11}(\sigma, \pi) = 0$	$S_{11}(\sigma, \pi/2) = \sigma$
2. $S_{21}(\sigma, 0) = \frac{1}{2} \left[ e^{-i\sigma} - \frac{\sin \sigma}{\sigma} \right]$	$S_{21}(\sigma, \pi) = \frac{1}{2} \left[ e^{i\sigma} - \frac{\sin \sigma}{\sigma} \right]$
$S_{21}(\sigma, \pi/2) = \left[ 1 - \frac{\sin \sigma}{\sigma} \right]$	
3. $S_{31}(\sigma, 0) = \frac{1}{2} \left[ e^{-i\sigma} - \frac{\sin \sigma}{\sigma} \right]$	$S_{31}(\sigma, \pi) = -\frac{1}{2} \left[ e^{i\sigma} - \frac{\sin \sigma}{\sigma} \right]$
$S_{31}(\sigma, \pi/2) = -\frac{i}{\sigma} [1 - \cos \sigma]$	
4. $\$_{21}(\sigma, 0) = \frac{1}{2} \left[ e^{-i\sigma} + \frac{\sin \sigma}{\sigma} \right]$	$\$_{21}(\sigma, \pi) = -\frac{1}{2} \left[ e^{i\sigma} + \frac{\sin \sigma}{\sigma} \right]$
$\$_{21}(\sigma, \pi/2) = \frac{i}{\sigma} [1 - \cos \sigma]$	
5. $\$_{31}(\sigma, 0) = \frac{1}{2} \left[ e^{-i\sigma} + \frac{\sin \sigma}{\sigma} \right]$	$\$_{31}(\sigma, \pi) = \frac{1}{2} \left[ e^{i\sigma} + \frac{\sin \sigma}{\sigma} \right]$
$\$_{31}(\sigma, \pi/2) = \frac{\sin \sigma}{\sigma}$	

---

Table 5.6.2 The sums of Table 5.6.1 on the coordinate axes

## 5.7 Evaluation of Sum $S_{12}$ on the Axes

Evaluations of sums over spherical Neumann functions can be made on the axes but not at other angles. The expression for the sum  $S_{12}$ , see Eq. 5.6.3, is:

$$S_{12}(\sigma, \theta) = \sum_{\ell=1}^{\infty} i^{1-\ell} (2\ell+1) y_{\ell}(\sigma) P_{\ell}^1(\cos \theta) \quad (5.7.1)$$

To evaluate this sum on the axes note that since the radial component of the field is proportional to  $\sin \theta$ , it is equal to zero on both the positive and negative  $z$ -axes:

$$S_{12}(\sigma, 0) = S_{12}(\sigma, \pi) = 0 \quad (5.7.2)$$

It remains to evaluate the sum at the equator,  $\theta = \pi/2$ . The series form of the associated Legendre polynomial at  $\theta = \pi/2$  is given in Table A.18.1 and repeated here:

$$P_\ell^1(0) = (-1)^{(\ell-1)/2} \frac{(\ell)!!}{(\ell-1)!!} \delta(\ell, 2n+1) \quad (5.7.3)$$

The Kronecker delta function, with  $n$  representing all integers equal to or greater than zero, shows that the function vanishes for even numbered modes. The series form of the spherical Neumann functions is shown by Eq. A.24.12 and repeated here:

$$y_\ell(\sigma) = - \sum_{s=0}^{\ell-1} \frac{(2\ell-2s-1)!!}{(2s)!!} \sigma^{-\ell-1+2s} - \sum_{s=0}^{\infty} \frac{(-1)^s}{(2s-1)!!} \frac{\sigma^{\ell-1+2s}}{(2\ell+2s)!!} \quad (5.7.4)$$

Combining Eqs. 5.7.1, 5.7.3, and 5.7.4 results in:

$$S_{12}\left(\sigma, \frac{\pi}{2}\right) = - \sum_{\ell; 0; 1}^{\infty} (2\ell+1) \frac{(\ell)!!}{(\ell-1)!!} \left\{ \sum_{s=0}^{\ell-1} \frac{(2\ell-2s-1)!!}{(2s)!!} \sigma^{-\ell-1+2s} + \sum_{s=0}^{\infty} \frac{(-1)^s}{(2s-1)!!} \frac{\sigma^{\ell-1+2s}}{(2\ell+2s)!!} \right\} \quad (5.7.5)$$

Lower limit ' $\ell; 0; 1$ ' indicates the sum is over odd values of  $\ell$  and the lowest value is one. Since only odd modal orders contribute to the sum, by Eq. 5.7.5 only even powers of  $\sigma$  are present and Eq. 5.7.5 has the form:

$$S_{12}\left(\sigma, \frac{\pi}{2}\right) = \sum_{n; -(\ell+1)}^{\infty} A_n \sigma^n \quad (5.7.6)$$

Solving Eq. 5.7.6 to obtain coefficient  $A_n$  results in Eq. 5.7.7:

$$A_n = \left\{ \begin{aligned} & -(-1)^{n/2} \sum_{\ell=0;1}^{n+1} \frac{(2\ell+1)(\ell)!!(-1)^{(1-\ell)/2}}{(\ell-1)!!(\ell+n+1)!!(n-\ell)!!} \\ & - \left( \lim_{L \Rightarrow \infty} \right) \sum_{\ell=0;n+3}^L \frac{(2\ell+1)(\ell)!!(\ell-n-2)!!}{(\ell-1)!!(\ell+n+1)!!} \end{aligned} \right\} \sigma^n \quad (5.7.7)$$

$L$  is the largest modal number present. Consider the coefficients with  $n$  greater than zero. For the special case of coefficient  $A_2$ , the terms equal:

$$\left\{ \frac{3}{8} - \frac{7}{32} - \frac{55}{1024} - \frac{105}{4096} - \frac{1995}{131078} - \frac{5313}{524288} - \frac{243243}{33554452} - \dots \right\} = 0 \quad (5.7.8)$$

The first two terms come from the first sum of Eq. 5.7.7 and the rest from the second sum. Although the equality is correct only in the limit where  $L$  is infinitely large, the series converges rapidly for positive powers of  $\sigma$ , and with  $L$  large but finite the sum approaches zero rapidly.

The coefficients of all other positive powers of  $\sigma$  follow in a similar way, and all of them are equal to zero. Although no individual term is equal to zero each modal order contributes the proper magnitude and phase for the sum to equal zero. Since the total field is equal to zero so is the field energy on the axis. Note that if the magnitudes of all coefficients are changed in a way that preserves recursion relationship Eq. 5.5.15 the field remains equal to zero independently of the magnitude of the coefficients. On the other hand, if any single mode were different from the value of Eq. 5.5.15 the field of that mode would support a large field energy. Should a variation from that value occur the generalized gradient of the added energy is a forcing function that acts until Eq. 5.5.15 is restored; this is a unique characteristic of recursion relationship Eq. 5.5.15.

For negative powers of  $\sigma$ , the series diverges and, therefore, must terminate. With the coefficients of all higher order modes equal to zero, the series is equal to:

$$S_{12}\left(\sigma, \frac{\pi}{2}\right) = - \sum_{\ell=0;n-1}^L (2\ell+1) \frac{(\ell)!!}{(\ell-1)!!} \frac{(\ell+n-2)!!}{(\ell-n+1)!!} \sigma^n \quad (5.7.9)$$

For the special case  $n = 0$  the series of Eq. 5.7.9 is:

$$-\left(\frac{3}{2} + \frac{21}{16} + \frac{165}{128} + \frac{2625}{2048} + \dots\right) \quad (5.7.10)$$

$$= -(1.5 + 1.3125 + 1.2891 + 1.2817 + \dots) = -A_0$$

Each term approaches unity as the modal number increases and  $A_0$  is proportional to  $L$ . Very nearly, for  $L$  much larger than one:

$$A_0 \cong L/2 \quad (5.7.11)$$

For the special case  $n = -2$ , the series is equal to:

$$-\left(3 + \frac{63}{4} + \frac{2475}{64} + \frac{165,375}{2304} + \frac{16,967,475}{147,456} + \dots\right) = -A_2 \quad (5.7.12)$$

$A_2$  is proportional to  $L^3$ . Since a term-by-term expansion shows that  $A_n \approx L^{n+1}$  the sum, evaluated at the equator, is equal to:

$$S_{12}(\sigma, \pi/2) = - \sum_{n=0;e}^{\infty} \frac{A_n}{\sigma^n} \quad (5.7.13)$$

$$A_n = \sum_{\ell=0; n-1}^L \frac{(2\ell+1)\ell!! (\ell+n-2)!!}{(\ell-1)!! (\ell-n+1)!!} \approx L^{n+1}$$

Each coefficient  $A_n$  contains contributions from all modal orders.

In summary, only negative powers of  $\sigma$  are present in the field expression and energy of the radial field component is localized to the source region.

## 5.8 Evaluation of Sums $S_{22}$ and $S_{32}$ on the Polar Axes

The expression for sum  $S_{22}$ , as defined by Eq. 5.6.3, is:

$$S_{22}(\sigma, \theta) = \sum_{\ell=1}^{\infty} i^{-\ell} \frac{(2\ell+1)}{\ell(\ell+1)} y_{\ell}(\sigma) \frac{dP_{\ell}^1(\cos \theta)}{d\theta} \quad (5.8.1)$$

The series form of the associated Legendre polynomial at  $\theta = 0$  and  $\pi$  are shown in Table A.18.1 and repeated here, see also Eq. 5.3.3:

$$\left. \frac{dP_{\ell}^1(\cos \theta)}{d\theta} \right|_{\theta=0} = \frac{\ell(\ell+1)}{2} \text{ and } \left. \frac{dP_{\ell}^1(\cos \theta)}{d\theta} \right|_{\theta=\pi} = (-1)^{\ell} \frac{\ell(\ell+1)}{2} \quad (5.8.2)$$

The expression for sum  $S_{32}$  as defined by Eq. 5.6.3 is:

$$S_{32}(\sigma, \theta) = \sum_{\ell=1}^{\infty} i^{-\ell} \frac{(2\ell+1)}{\ell(\ell+1)} y_{\ell}(\sigma) \frac{P_{\ell}^1(\cos \theta)}{\sin \theta} \quad (5.8.3)$$

The series forms of the associated Legendre polynomial at  $\theta = 0$  and  $\pi$  are shown in Table A.18.1 and repeated here:

$$\left. \frac{P_{\ell}^1(\cos \theta)}{\sin \theta} \right|_{\theta=0} = \frac{\ell(\ell+1)}{2} \text{ and } \left. \frac{P_{\ell}^1(\cos \theta)}{\sin \theta} \right|_{\theta=\pi} = (-1)^{\ell+1} \frac{\ell(\ell+1)}{2} \quad (5.8.4)$$

Comparing axial values of the two sums shows that:

$$S_{22}(\sigma, 0) = S_{32}(\sigma, 0) \text{ and } S_{22}(\sigma, \pi) = -S_{32}(\sigma, \pi) \quad (5.8.5)$$

Because of these equalities, it is only necessary to evaluate one sum on the z-axes. Substituting Eqs. 5.8.4 and the expansion for the spherical Neumann function, Eq. 5.7.4, into Eq. 5.8.3 gives the series expansion:

$$\begin{aligned} S_{32}(\sigma, 0) &= \frac{1}{2} \sum_{\ell=1}^{\infty} i^{-\ell} (2\ell+1) y_{\ell}(\sigma) \\ &= \frac{1}{2} \sum_{\ell=0}^{\infty} i^{-\ell} (2\ell+1) y_{\ell}(\sigma) - \frac{1}{2} y_0(\sigma) = \frac{1}{2} \sum_{\ell=0}^{\infty} i^{-\ell} (2\ell+1) y_{\ell}(\sigma) + \frac{\cos \sigma}{2\sigma} \end{aligned}$$

$$= -\frac{1}{2} \sum_{\ell=0}^{\infty} i^{-\ell} (2\ell+1) \left\{ \sum_{s=0}^{\infty} \frac{(-1)^s}{(2s-1)!!} \frac{\sigma^{\ell-1+2s}}{(2\ell+2s)!!} + \sum_{s=0}^{\ell-1} \frac{(2\ell-2s-1)!!}{(2s)!!} \sigma^{-\ell-1+2s} \right\} + \frac{\cos \sigma}{2\sigma} \quad (5.8.6)$$

For convenience in evaluating the sum, the  $\ell = 0$  term is left in the expansion and subtracted from the total. Both even- and odd-numbered modes are present; even values of  $\ell$  produce odd powers of  $\sigma$  and *vice versa*. Within the curly brackets on the bottom line of Eq. 5.8.6, the upper term contains powers of  $\sigma$  ranging from  $(\ell - 1)$  to  $\infty$ , the lower term contains powers of  $\sigma$  ranging from  $-(\ell + 1)$  to  $(\ell - 3)$ . The upper term contains only positive powers of  $\sigma$  and the lower term contains both positive and negative powers.

Next, let  $n$  be a positive integer and determine the coefficient of  $\sigma^n$ . It is convenient to separate Eq. 5.8.6 into sets of different parity:

$$S_{32} = \left\{ i \frac{(-1)^{n/2}}{2} \sum_{\ell \geq 1}^{n+1} \frac{(2\ell+1)\sigma^n}{(n-\ell)!!(n+\ell+1)!!} + \frac{i}{2} \sum_{\ell \geq n+3}^{\infty} \frac{(-1)^{(\ell-1)/2} (2\ell+1)(\ell-n-2)!! \sigma^n}{(\ell+n+1)!!} \right\} \quad (5.8.7)$$

$$\pm \left\{ \frac{(-1)^{(n-1)/2}}{2} \sum_{\ell \geq 0}^{n+1} \frac{(2\ell+1)\sigma^n}{(n-\ell)!!(n+\ell+1)!!} - \frac{1}{2} \sum_{\ell \geq n+3}^{\infty} \frac{(-1)^{\ell/2} (2\ell+1)(\ell-n-2)!! \sigma^n}{(\ell+n+1)!!} + \frac{\cos \sigma}{2\sigma} \right\}$$

The upper sign of the  $\pm$  sign is to be used at  $\theta = 0$  and the lower sign at  $\theta = \pi$ . Defining  $S_{32}'$  to equal the top row of Eq. 5.8.7 and expanding the series results in:



$n$  even,  $\ell$  odd.

$$S_{32}' = \frac{i(-1)^{n/2}}{2} \left\{ \left[ \frac{3}{(n-1)!!(n+2)!!} + \frac{7}{(n-3)!!(n+4)!!} + \dots + \frac{(2n+3)}{(2n+2)!!} \right] \right. \\ \left. - \left[ \frac{(2n+7)(1)!!}{(2n+4)!!} - \frac{(2n+11)(3)!!}{(2n+6)!!} + \frac{(2n+15)(5)!!}{(2n+8)!!} - \dots \right] \right\} \quad (5.8.8)$$

The bottom row of Eq. 5.8.8 may be evaluated by writing  $(2\ell+1) = (\ell+n+1) + (\ell-n)$  and regrouping the terms as:

$$\left\{ \begin{aligned} & (2n+4) \frac{(1)!!}{(2n+4)!!} + \frac{(1)!!}{(2n+4)!!} \left( 3 - (2n+6) \frac{3}{(2n+6)} \right) \\ & - \frac{(3)!!}{(2n+6)!!} \left( 5 - (2n+8) \frac{5}{(2n+8)} \right) + \dots \end{aligned} \right\} = \frac{1}{(2n+2)!!} \quad (5.8.9)$$

Inserting Eq. 5.8.9 back into Eq. 5.8.8 results in the equation:

$n$  even,  $\ell$  odd.

$$S_{32}' = \frac{i(-1)^{n/2}}{2} \left\{ \begin{aligned} & \frac{3}{(n-1)!!(n+2)!!} + \frac{7}{(n-3)!!(n+4)!!} + \\ & \dots + \frac{(2n+3)}{(2n+2)!!} - \frac{1}{(2n+2)!!} \end{aligned} \right\} \quad (5.8.10)$$

Evaluating Eq. 5.8.10 for the special case of  $n = 0$  gives:

$$\frac{i}{2} \left( \frac{3}{2} - \frac{1}{2} \right) = \frac{i}{2}$$

Repeating the process for the special case of  $n = 2$  results in:

$$-\frac{i}{2} \left( \frac{3}{8} + \frac{7}{48} - \frac{1}{48} \right) = -\frac{i}{4}$$

Repeating the process for all even, positive values of  $n$  equal zero or more then summing results in:

n even,  $\ell$  odd.

$$S_{32} = \frac{i}{2} \cos \sigma \quad (5.8.11)$$

Repeating the process for the opposite parity results in:

n odd,  $\ell$  even.

$$S_{32} = \pm \frac{1}{2} \sin \sigma \quad (5.8.12)$$

Combining results for all non-negative values of n:

Positive powers of  $\sigma$ .

$$S_{32}(\sigma, 0) = \frac{1}{2} \left( i e^{-i\sigma} + \frac{\cos \sigma}{\sigma} \right) \quad S_{32}(\sigma, \pi) = \frac{1}{2} \left( i e^{i\sigma} - \frac{\cos \sigma}{\sigma} \right) \quad (5.8.13)$$

$$S_{22}(\sigma, 0) = \frac{1}{2} \left( i e^{-i\sigma} + \frac{\cos \sigma}{\sigma} \right) \quad S_{22}(\sigma, \pi) = -\frac{1}{2} \left( i e^{i\sigma} - \frac{\cos \sigma}{\sigma} \right)$$

The related sums are obtained by operating on Eqs. 5.8.13 using Eq. 5.6.5:

Positive powers of  $\sigma$ .

$$\mathcal{S}_{32}(\sigma, 0) = \frac{1}{2} \left( i e^{-i\sigma} - \frac{\cos \sigma}{\sigma} \right) \quad \mathcal{S}_{32}(\sigma, \pi) = -\frac{1}{2} \left( i e^{i\sigma} + \frac{\cos \sigma}{\sigma} \right) \quad (5.8.14)$$

$$\mathcal{S}_{22}(\sigma, 0) = \frac{1}{2} \left( i e^{-i\sigma} - \frac{\cos \sigma}{\sigma} \right) \quad \mathcal{S}_{22}(\sigma, \pi) = \frac{1}{2} \left( i e^{i\sigma} + \frac{\cos \sigma}{\sigma} \right)$$

The transcendental functions in Eqs. 5.8.10 and 5.8.11 result in a multimodal sinusoidal wave that propagates away from the source. Each mode contributes the proper magnitude and phase for the infinite sum to equal these specific functions. Although the series terminates at modal number L the series converges rapidly and the results are quite accurate for finite values of L. Note that, as with results obtained using spherical Bessel functions, the magnitude of the first term in each sum is independent of  $\sigma$ . These characteristics are unique properties of recursion relationship Eq. 5.5.15.

The coefficients of negative powers of  $\sigma$  appear only in the second sum of Eq. 5.8.3. Writing negative powers of  $\sigma$  as positive values of  $n$  leaves the equation form:

$$-\frac{1}{2} \sum_{\ell=n-1}^{L+1} i^{-\ell} \frac{(2\ell+1)(\ell+n-2)!!}{(\ell-n+1)!!\sigma^n} \delta(\ell+n, 2q+1)$$

These sums are most easily evaluated by writing  $(2\ell+1) = (\ell-n+1) + (\ell+n)$  then expanding and regrouping. The result is:

$$-\frac{i^{L-n}}{2\sigma^n} \left\{ \frac{(2n-3)!!}{(0)!!} \left( (2n-1) - (2) \frac{(2n-1)}{(2)} \right) - \frac{(2n-1)!!}{(2)!!} \left( (2n+1) - (4) \frac{(2n+1)}{(4)} \right) \right. \\ \left. + \frac{(2n+1)!!}{(4)!!} \left( (2n+3) - (6) \frac{(2n+3)}{(6)} \right) + \dots + \frac{i^{-L+n-2}(L+n)!!}{(L-n-1)!!} \right\}$$

All terms except the last one are equal to zero, leaving only the series remainder:

$$-\frac{i^{-L-1}}{2\sigma^n} \frac{(L+n)!!}{(L-n+1)!!}$$

The full set of solutions for negative powers of  $\sigma$  are:

$$S_{32}(\sigma, 0) = -\frac{i^{-L-1}}{2} \sum_{n=1}^{L+1} \frac{(L+n)!!}{(L-n+1)!!\sigma^n} \quad S_{32}(\sigma, \pi) = -\frac{i^{-L-1}}{2} \sum_{n=1}^{L+1} \frac{(L+n)!!}{(L-n+1)!!\sigma^n} \quad (5.8.15)$$

$$\$_{32}(\sigma, 0) = \frac{i^{-L}}{2} \sum_{n=2}^{L+1} \frac{(n-1)(L+n)!!}{(L-n+1)!!\sigma^{n+1}} \quad \$_{32}(\sigma, \pi) = \frac{i^{-L}}{2} \sum_{n=2}^{L+1} \frac{(n-1)(L+n)!!}{(L-n+1)!!\sigma^{n+1}}$$

Although the magnitude of the modal terms increases with increasing modal number, only the remainder is left and it results from the highest order mode only. Therefore individual modes contribute nothing to the field and are not affected by them, so long as the relationship of Eq. 5.5.15 is maintained. If the relationship is disturbed the disturbing mode will create a field and that

field will generate a radiation reaction force in a direction that reduces the field, thereby minimizing the field energy and maintaining Eq. 5.5.15. Results are shown in Table 5.8.1.

---


$$\begin{aligned}
 S_{22}(\sigma, 0) &= S_{32}(\sigma, 0) = \frac{1}{2} \left( i e^{-i\sigma} + \frac{\cos \sigma}{\sigma} \right) - \frac{i^{-L-1}}{2} \sum_{n=1}^{L+1} \frac{(L+n)!!}{(L-n+1)!! \sigma^n} \\
 \$_{22}(\sigma, 0) &= \$_{32}(\sigma, 0) = \frac{1}{2} \left( i e^{-i\sigma} - \frac{\cos \sigma}{\sigma} \right) + \frac{i^{-L}}{2} \sum_{n=2}^{L+1} \frac{(n-1)(L+n)!!}{(L-n+1)!! \sigma^{n+1}} \\
 S_{22}(\sigma, \pi) &= -S_{32}(\sigma, \pi) = -\frac{1}{2} \left( i e^{i\sigma} - \frac{\cos \sigma}{\sigma} \right) + \frac{i^{L-1}}{2} \sum_{n=1}^{L+1} \frac{(L+n)!!}{(L-n+1)!! \sigma^n} \\
 \$_{22}(\sigma, \pi) &= -\$_{32}(\sigma, \pi) = \frac{1}{2} \left( i e^{i\sigma} + \frac{\cos \sigma}{\sigma} \right) + \frac{i^L}{2} \sum_{n=2}^{L+1} \frac{(n-1)(L+n)!!}{(L-n+1)!! \sigma^{n+1}}
 \end{aligned}$$


---

Table 5.8.1 Field sums over spherical Neumann functions on both the positive and negative z-axes.

## 5.9 Evaluation of Sum $S_{32}$ in the Equatorial Plane

The expression for sum  $S_{32}$ , as defined by Eq. 5.6.3, is:

$$S_{32}(\sigma, \theta) = \sum_{\ell=1}^{\infty} i^{-\ell} \frac{(2\ell+1)}{\ell(\ell+1)} y_{\ell}(\sigma) \frac{P_{\ell}^1(\cos \theta)}{\sin \theta} \quad (5.9.1)$$

We seek to find a simpler expression. At  $\theta = \pi/2$ , the value of the Legendre function is, see Table A.18.1:

$$P_{\ell}^1(0) = i^{1-\ell} \frac{(\ell)!!}{(\ell-1)!!} \delta(\ell, 2q+1) \quad (5.9.2)$$

Substituting Eq. 5.9.2 and the spherical Neumann function, Eq. 5.7.4, into Eq. 5.9.1 gives the expression for the sum at the equator:

$$S_{32}\left(\sigma, \frac{\pi}{2}\right) = i \sum_{\ell=1}^{\infty} \frac{(2\ell+1)(\ell-2)!!}{(\ell+1)!!} \left\{ \sum_{s=0}^{\ell-1} \frac{(2\ell-2s-1)!!}{(2s)!!} \sigma^{-\ell-1+2s} + \sum_{s=0}^{\infty} \frac{(-1)^s}{(2s-1)!!} \frac{\sigma^{\ell-1+2s}}{(2\ell+2s)!!} \right\} \quad (5.9.3)$$

Since only odd orders of  $\ell$  are present, there are only even powers of  $\sigma$  and the sum over the positive powers of  $\sigma$  has the form:

$$S_{32}\left(\sigma, \frac{\pi}{2}\right) = i \sum_{n \in \mathbb{N}} B_n'' \sigma^n \quad (5.9.4)$$

Combining Eqs. 5.9.3 and 5.9.4 gives:

$$B_n'' = (-1)^{n/2} \sum_{\ell \geq 1}^{n+1} \frac{(2\ell+1)(\ell-2)!!(-1)^{(\ell-1)/2}}{(\ell+1)!!(n-\ell)!!(\ell+n+1)!!} + i \sum_{\ell \geq n+3}^{\infty} \frac{(2\ell+1)(\ell-2)!!(\ell-n-2)!!}{(\ell+1)!!(\ell+n+1)!!} \quad (5.9.5)$$

Consider as special cases the coefficients  $B_0''$  and  $B_2''$ . Writing out Eq. 5.9.5 term by term for these cases gives:

$$\begin{aligned} B_0'' &= \left( \frac{3}{2 \times 2} + \frac{7}{4!! \times 4!!} + \frac{11 \times 3^2}{6!! \times 6!!} + \dots \right) = 1 \\ B_2'' &= \left( -\frac{3}{2 \times 4!!} + \frac{7}{4!! \times 6!!} + \frac{11 \times 3^2}{6!! \times 8!!} + \dots \right) = -\frac{1}{6} \end{aligned} \quad (5.9.6)$$

Extending the evaluation to all positive values of  $n$ , then summing gives:

$$S_{32}\left(\sigma, \frac{\pi}{2}\right)_{n \geq 0} = i \frac{\sin \sigma}{\sigma} \quad (5.9.7)$$

To evaluate the coefficients of negative powers of  $\sigma$ , define a new set of coefficients  $B_n$  and write the expansion as:

$$S_{32}\left(\sigma, \frac{\pi}{2}\right)_{n < 0} = i \frac{B_n}{\sigma^n} \quad (5.9.8)$$

Combining Eqs. 5.9.1 and 5.9.8 shows that:

$$B_n = \sum_{\ell=0; n+1}^L \frac{(2\ell+1)(\ell-2)!! (\ell+n-2)!!}{(\ell+1)!! (\ell-n+1)!!} \quad (5.9.9)$$

The coefficients of the first two terms are:

$$\begin{aligned} B_2 &= i(1.31125 + 1.28906 + 1.28174 + 1.27853 + \dots) \approx 5L/8 \\ B_4 &= i(36.09375 + 69.21387 + 106.58936 + 165.99072 + \dots) \approx L^3 \end{aligned} \quad (5.9.10)$$

If  $n$  increases by one the power of  $L$  increases by two.

Combining equatorial values for both positive and negative exponents gives:

$$S_{32}(\sigma, \pi/2) = i \frac{\sin \sigma}{\sigma} + i \sum_{n=2}^{\infty} \frac{B_n}{\sigma^n} \quad (5.9.11)$$

The related sum follows by operating on Eq. 5.9.11 using Eq. 5.6.5:

$$S_{32}(\sigma, \pi/2) = -\frac{\cos \sigma}{\sigma} + \sum_{n=2}^{\infty} \frac{(n-1)B_n}{\sigma^{n+1}} \quad (5.9.12)$$

Each mode contributes just the correct amount so the entire set of positive powers of  $\sigma$  are expressed by the transcendental functions of Eqs. 5.9.11 and 5.9.12; this is another unique property of recursion relationship Eq. 5.5.15.

## 5.10 Evaluation of Sum $S_{22}$ in the Equatorial Plane

The expression for sum  $S_{22}$  as defined by Eq. 5.6.3 is:

$$S_{22}(\sigma, \theta) = \sum_{\ell=1}^{\infty} i^{-\ell} \frac{(2\ell+1)}{\ell(\ell+1)} y_{\ell}(\sigma) \frac{dP_{\ell}^1(\cos \theta)}{d\theta} \quad (5.10.1)$$

We seek to find a simpler expression for the sum. At  $\theta = \pi/2$ , the value of the Legendre function is, see Table A.18.1:

$$\frac{dP_{\ell}^1(0)}{d\theta} = i^{\ell} \frac{(\ell+1)!!}{(\ell-2)!!} \delta(\ell, 2q) \quad (5.10.2)$$

Since the derivatives of odd order Legendre functions, with respect to  $\theta$ , are equal to zero at the equator, only even values of  $\ell$  appear in the summation. Substituting the spherical Neumann function, in the form of Eq. 5.7.4, and Eq. 5.10.2 into Eq. 5.10.1 gives the expression for the sum at the equator:

$$S_{22}\left(\sigma, \frac{\pi}{2}\right) = - \sum_{\ell \in 0}^{\infty} \frac{(2\ell+1)(\ell-1)!!}{(\ell)!!} \left\{ \sum_{s=0}^{\ell-1} \frac{(2\ell-2s-1)!!}{(2s)!!} \sigma^{-\ell-1+2s} + \sum_{s=0}^{\infty} \frac{(-1)^s}{(2s-1)!!} \frac{\sigma^{\ell-1+2s}}{(2\ell+2s)!!} \right\} + \frac{\cos \sigma}{\sigma} \quad (5.10.3)$$

For convenience in evaluating the sum, the  $\ell = 0$  term is added and subtracted. Since only even orders of  $\ell$  are present, only odd powers of  $\sigma$  appear in the sum. The result is:

$$S_{32}\left(\sigma, \frac{\pi}{2}\right) = \sum_{n \in 1}^{\infty} C_n'' \sigma^n + \frac{\cos \sigma}{\sigma} \quad (5.10.4)$$

Comparison of Eq. 5.10.4 with Eq. 5.10.3 shows that:

$$C_n'' = (-1)^{(n-1)/2} \sum_{\ell \in 0}^{n+1} \frac{(2\ell+1)(\ell-1)!!}{(\ell)!!} \frac{(-1)^{\ell/2}}{(n-\ell)!!(n+1)!!} - \sum_{\ell \in n+3}^{\infty} \frac{(2\ell+1)(\ell-1)!!}{(\ell)!!} \frac{(\ell-n-2)!!}{(\ell+n+1)!!} \quad (5.10.5)$$

Evaluation of the special cases  $n = 1$  and  $n = 3$  gives:

$$C_1'' = - \left\{ -\frac{1}{2} + \frac{5}{2!! \times 4!!} + \frac{9 \times 3!! \times 1!!}{4!! \times 6!!} + \dots \right\} = 0$$

$$C_3'' = - \left\{ \frac{1}{3!! \times 4!!} - \frac{5 \times 1!!}{2!! \times 6!!} + \frac{9 \times 3!!}{4!! \times 8!!} + \frac{13 \times 5!! \times 1!!}{6!! \times 10!!} + \dots \right\} = 0 \quad (5.10.6)$$

Extending the evaluation to all positive values of “ $n$ ” then summing give, for positive powers of  $\sigma$ :

$$S_{22}\left(\sigma, \frac{\pi}{2}\right)_{n \geq 0} = \frac{\cos \sigma}{\sigma} \quad (5.10.7)$$

The reduction of Eq. 5.10.3 to this simple form is a unique property of Eq. 5.5.15.

To examine the coefficients for negative powers of  $\sigma$ , define the new coefficients:

$$S_{22}(\sigma, \pi/2)_{n < 0} = - \sum_{n=1}^L \frac{C_n}{\sigma^n} \quad (5.10.8)$$

Combining Eq. 5.10.8 with Eq. 5.10.3 shows that:

$$C_n = \sum_{\ell; n-1}^L \frac{(2\ell+1)(\ell-1)!! (\ell+n-2)!!}{(\ell)!! (\ell-n+1)!!} \quad (5.10.9)$$

Evaluation of the first term gives:

$$C_1 \cong 5L/8 \quad (5.10.10)$$

With each succeeding increase in  $n$ , the power of  $L$  in the approximate equality increases by two.

The total value of the sum is equal to the sum of Eqs. 5.10.8 and 5.10.9:

$$S_{22}\left(\sigma, \frac{\pi}{2}\right) = \frac{\cos \sigma}{\sigma} - \sum_{n=1}^{\infty} \frac{C_n}{\sigma^n} \quad \text{and} \quad S_{22}\left(\sigma, \frac{\pi}{2}\right) = -i \frac{\sin \sigma}{\sigma} + i \sum_{n=1}^{\infty} \frac{(n-1)C_n}{\sigma^{n+1}} \quad (5.10.11)$$

## 5.11 The Axial Fields, Summary

Sums of spherical Hankel functions on the  $+z$ -axis follow from the values for spherical Bessel functions of Table 5.6.2 and the spherical Neumann functions from Sections 5.7 through 5.10. The associated sums follow from the regular sums and Eqs. 5.6.5:



$$S_1(\sigma, 0) = 0$$

$$S_2(\sigma, 0) = e^{-i\sigma} \left( 1 - \frac{i}{2\sigma} \right) - \frac{i^{-L-1}}{2} \sum_{n=1}^{L+1} \frac{(L+n)!!}{(L-n+1)!! \sigma^n} \quad (5.11.1)$$

$$S_3(\sigma, 0) = S_2(\sigma, 0)$$

$$\$2(\sigma, 0) = e^{-i\sigma} \left( 1 + \frac{i}{2\sigma} \right) + \frac{i^{-L}}{2} \sum_{n=2}^{L+1} \frac{(n-1)(L+n)!!}{(L-n+1)!! \sigma^{n+1}}$$

$$\$3(\sigma, 0) = \$2(\sigma, 0)$$

The remainders arise from *the highest order mode only*, and are valid if the recursion relationship of Eq. 5.5.15 holds through order  $L$  and all higher order have zero magnitude. Putting these sums into the field forms of Eq. 5.6.6 and ignoring the remainders gives the electric field intensity on the positive  $z$ -axis:

$$E_r = 0$$

$$E_\theta = 2e^{-i\sigma} e^{-i\phi} \quad (5.11.2)$$

$$E_\phi = -i \, 2e^{-i\sigma} e^{-i\phi}$$

The field is circularly polarized and the magnitude is independent of distance from the source. The time average Poynting vector is:

$$\mathbf{N} = \frac{1}{2} \text{Re}(\tilde{\mathbf{E}} \times \tilde{\mathbf{H}}^*) = -\frac{1}{2\eta} \text{Re}(i\tilde{\mathbf{E}} \times \tilde{\mathbf{E}}^*) \quad (5.11.3)$$

$$\mathbf{N} = \hat{\mathbf{z}} N_z = \frac{4}{\eta} \hat{\mathbf{z}}$$

The axial power density is independent of distance from the source and totally directed in the positive  $z$ -direction.

The remainders in the equatorial plane are quite different from those on the  $z$ -axes; each mode contributes a proportionate share to the whole and fields exist throughout the region. The sums are:

$$\begin{aligned}
S_1(\sigma, \pi/2) &= \sigma + i \sum_{n \geq 0}^L \frac{A_n}{\sigma^n} \\
S_2(\sigma, \pi/2) &= 1 - \frac{i}{\sigma} e^{-i\sigma} + i \sum_{n \geq 1}^L \frac{C_n}{\sigma^n} \\
S_3(\sigma, \pi/2) &= -\frac{i}{\sigma} [1 - e^{-i\sigma}] + \sum_{n \geq 2}^L \frac{B_n}{\sigma^n} \\
S_2(\sigma, \pi/2) &= \frac{i}{\sigma} [1 - e^{-i\sigma}] + \sum_{n \geq 3}^L \frac{(n-1)C_n}{\sigma^{n+1}} \\
S_3(\sigma, \pi/2) &= \frac{i}{\sigma} e^{-i\sigma} - i \sum_{n \geq 2}^L \frac{(n-1)B_n}{\sigma^{n+1}}
\end{aligned} \tag{5.11.4}$$

The letter functions representing the remainders are:

$$\begin{aligned}
A_n &= \sum_{\ell \geq n-1}^L \frac{(2\ell+1)\ell!!}{(\ell-1)!!} \frac{(\ell+n-2)!!}{(\ell-n+1)!!} \\
B_n &= \sum_{\ell \geq n-1}^L \frac{(2\ell+1)(\ell-2)!!}{(\ell+1)!!} \frac{(\ell+n-2)!!}{(\ell-n+1)!!} \\
C_n &= \sum_{\ell \geq n-1}^L \frac{(2\ell+1)(\ell-1)!!}{(\ell)!!} \frac{(\ell+n-2)!!}{(\ell-n+1)!!}
\end{aligned} \tag{5.11.5}$$

Substituting these results into the field forms gives the field:

$$\begin{aligned}
\tilde{E}(\sigma, \pi/2) &= \left[ 1 + i \sum_{n \geq 0}^{\infty} \frac{A_n}{\sigma^{n+1}} \right] e^{-i\hat{\sigma} \hat{r}} \\
&+ \left\{ \sum_{n \geq 2}^{\infty} \frac{B_n}{\sigma^n} + \sum_{n \geq 3}^{\infty} \frac{(n-1)C_n}{\sigma^{n+1}} \right\} e^{-i\hat{\sigma} \hat{\theta}} - i \left\{ 1 + i \sum_{n \geq 1}^{\infty} \frac{C_n}{\sigma^n} - i \sum_{n \geq 2}^{\infty} \frac{(n-1)B_n}{\sigma^{n+1}} \right\} e^{-i\hat{\sigma} \hat{\phi}}
\end{aligned} \tag{5.11.6}$$

With  $O$  representing order, these fields produce the Poynting vector:

$$\mathbf{N}(\sigma, \pi/2) = \frac{1}{\eta} \left\{ O\left(\frac{1}{\sigma^2}\right) \hat{r} + \left[ -1 + O\left(\frac{1}{\sigma^2}\right) \right] \hat{\theta} + O\left(\frac{1}{\sigma^2}\right) \hat{\phi} \right\} \quad (5.11.7)$$

The radial term is an outbound power density proportional to  $B_2/\sigma^2$ . The zenith angle term is a power density of magnitude independent of distance and directed in the positive  $z$ -direction. It describes an energy flow from the lower to the upper hemisphere.

On the negative  $z$ -axis, as it was on the positive one, the remainder is from the highest order mode only and it does not contain contributions from each mode. The other terms are equal to:

$$\begin{aligned} S_2(\sigma, \pi) &= -\frac{i}{2\sigma} e^{-i\sigma} & S_3(\sigma, \pi) &= \frac{i}{2\sigma} e^{-i\sigma} \\ \$2(\sigma, \pi) &= -\frac{i}{2\sigma} e^{-i\sigma} & \$3(\sigma, \pi) &= \frac{i}{2\sigma} e^{-i\sigma} \end{aligned} \quad (5.11.8)$$

Putting these sums into the field forms of Eq. 5.6.6 shows that the electric field intensity and the Poynting vector on the negative  $z$ -axis are equal to zero:

$$\tilde{\mathbf{E}}(\sigma, \pi) = 0 \quad (5.11.9)$$

So long as the recursion relationship of Eq. 5.5.15 holds, any field that exists on the negative  $z$ -axis arises from the remainder of the highest order moment.

These results show that positive powers of the radial terms result in a normalized power density of  $4/\eta$  along the positive  $z$ -axis,  $z$ -directed uniform power density of  $1/\eta$  in the equator, and no power at all along the negative  $z$ -axis. The first order, negative power terms show radially outbound power in the equatorial plane. This result combines with energy conservation to require energy that exits the generating source in the lower hemisphere to pass upward through the equator. By Eq. 5.11.3, all energy ultimately becomes positive  $z$ -directed.

## 5.12 Infinite Radius Radiation Pattern

The teledistant fields of Section 5.11 are coefficients times transcendental terms; half of the terms arise from spherical Bessel functions and half from spherical Neumann functions. Only spherical Neumann functions produce near and far field terms. To extend the axial field expressions over all angles, first note that the fields proportional to spherical Bessel functions are given by Eqs. 5.3.1 and 5.6.1. In the limit of infinite radius, using Eq. A.24.16, the spherical Bessel and Neumann functions satisfy the equality:

$$\lim_{\sigma \Rightarrow \infty} y_\ell(\sigma) = -\frac{dj_\ell(\sigma)}{d\sigma} \quad (5.12.1)$$

The equality permits solving for the full angular expressions for the telefield portion of the sums over spherical Neumann functions. Using Eq. 5.12.1 and adding terms proportional to Bessel and Neumann functions gives the full field over spherical Hankel functions. The functional form is:

$$\lim_{\sigma \Rightarrow \infty} \tilde{\mathbf{E}}(\sigma, \theta, \phi) = \left(1 + i \frac{\partial}{\partial \sigma}\right) \{\text{Eq. 5.6.1}\} \quad (5.12.2)$$

The operation may be applied both to the field forms of Eqs. 5.6.1 and to the sums of Table 5.6.1.

Operating on Eq. 5.6.1 shows that the limiting value of the total teledistant field is:

$$\tilde{\mathbf{E}} = e^{-i\sigma \cos \theta} (1 + \cos \theta) (\hat{r} \sin \theta + \hat{\theta} \cos \theta - i\hat{\phi}); \quad \eta \tilde{\mathbf{H}} = i\tilde{\mathbf{E}} \quad (5.12.3)$$

The result of operating on the sums of Table 5.6.1 is shown in Table 5.12.1.

The electric field intensity also follows from the definitions of Eqs. 5.6.3 through 5.6.6:

$$\begin{aligned} \hat{\mathbf{E}}_r &= e^{-i\sigma \cos \theta} \sin \theta (1 + \cos \theta + i/\sigma) e^{-i\phi} \\ \hat{\mathbf{E}}_\theta &= e^{-i\sigma \cos \theta} \cos \theta (1 + \cos \theta) e^{-i\phi} \\ \hat{\mathbf{E}}_\phi &= -ie^{-i\sigma \cos \theta} (1 + \cos \theta) e^{-i\phi} \end{aligned} \quad (5.12.4)$$

---


$$\begin{aligned}
S_1(\sigma, \theta) &= \sigma \sin \theta \left( 1 + \cos \theta + \frac{i}{\sigma} \right) e^{-i\sigma \cos \theta} \\
S_2(\sigma, \theta) &= e^{-i\sigma \cos \theta} \left( 1 + \cos \theta - \frac{i}{\sigma} \right) + \frac{i}{\sigma \sin^2 \theta} \left[ e^{-i\sigma \cos \theta} - e^{-i\sigma} \right] (1 + \cos \theta) \\
S_3(\sigma, \theta) &= -\frac{i}{\sigma \sin^2 \theta} \left[ e^{-i\sigma \cos \theta} - e^{-i\sigma} \right] (1 + \cos \theta) \\
S_4(\sigma, \theta) &= e^{-i\sigma \cos \theta} \left[ \cos \theta (1 + \cos \theta) + \frac{i}{\sigma} \right] + \frac{i}{\sigma \sin^2 \theta} \left[ e^{-i\sigma \cos \theta} \cos \theta - e^{-i\sigma} \right] (1 + \cos \theta) \\
S_5(\sigma, \theta) &= -\frac{i}{\sigma \sin^2 \theta} \left[ e^{-i\sigma \cos \theta} \cos \theta - e^{-i\sigma} \right] (1 + \cos \theta)
\end{aligned}$$


---

Table 5.12.1 Limiting infinite-radius solutions of sums over spherical Hankel functions, keeping only radial terms with power minus one.

*Listed values are correct only in the limit of infinite radius.*

Comparison shows that the teledistant axial field of Section 5.11, obtained by direct summation, is the same as that of Eq. 5.12.4.

These fields may also be used to construct phasor fields for absorption since the complex conjugate of any electromagnetic phasor field is another electromagnetic phasor field:

Energy emission

$$\hat{\mathbf{E}}(\sigma, \theta, \phi) = e^{-i\sigma \cos \theta} \left\{ \begin{aligned} &\hat{r} \sin \theta (1 + \cos \theta + i/\sigma) \\ &\left( (\hat{\theta} \cos \theta - i\hat{\phi}) (1 + \cos \theta) \right) \end{aligned} \right\} e^{-i\phi} \quad (5.12.5)$$

Energy absorption

$$\hat{\mathbf{E}}(\sigma, \theta, \phi) = e^{i\sigma \cos \theta} \left\{ \begin{aligned} &\hat{r} \sin \theta (1 + \cos \theta - i/\sigma) \\ &\left( (\hat{\theta} \cos \theta + i\hat{\phi}) (1 + \cos \theta) \right) \end{aligned} \right\} e^{i\phi}$$

The fields are circularly polarized. The emission equations describe a wave that exits its source at  $z = 0$  and forms a fully  $z$ -directed plane wave that travels to  $z = +\infty$ . The absorption, complex conjugate, equations describe an oppositely directed plane wave at  $z = \infty$  that travels to a sink at  $z = 0$ . The Poynting vectors are equal to:

$$N_c = \pm \frac{1}{\eta} (1 + \cos \theta)^2 \hat{z} \quad (5.12.6)$$

The upper and lower signs respectively apply for emission and absorption. The radiation pattern is shown in Fig. 5.12.1. The figure is similar to conventional radiation patterns in that the magnitude of the power density at each angle is proportional to the distance from the origin. Unlike other patterns, all energy flows in the direction of the pattern maximum. The result is fully directed, z-oriented power with magnitude that is independent of the distance from the source. It remains to be determined how such a condition is consistent with energy conservation.

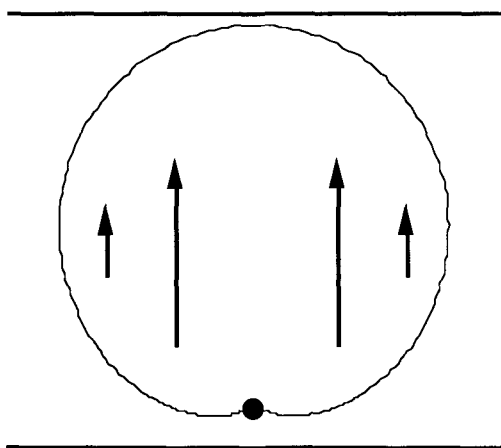


Figure 5.12.1 Radiation Pattern for Fully Directed Radiation.

*Antenna is located at mid-point dot on bottom of the curve. Similar to other radiation patterns field values at a particular angle are proportional to indicated distance from the origin at the lower center of the pattern. Unlike other field patterns, all power flows in the direction of the pattern maximum and, at a specific angle, power density is independent of radius.*

The absorption and emission discussions of Chapter 2 involve structures with ideally conducting surfaces, for which, except for a biconical receiving antenna, the absorbed power is zero. They respond linearly to the incoming plane wave fields of Eqs. 2.1.11, and the powers are given by Eqs. 2.2.7 and 2.14.11. The extinction power is proportional to the first power of the

scattering coefficients,  $\alpha_\ell$  and  $\beta_\ell$ , and the scattered power is proportional to the square of the coefficients. The response of a nonlinear sink is quite different. When triggered by an incoming wave an active sink does more than absorb from the plane wave; in the manner described above it generates near fields that extract energy from the full cross section of the field in the inverse of emission. After the process has begun, the exterior fields at the source are those of Eqs. 5.5.16, not Eqs. 2.1.11. Changing from emission fields to absorption fields is the equivalent of taking the complex conjugate, including changing from Hankel functions of the second kind to those of the first kind.

### 5.13 Self-Consistent Field Analysis

An analytical method that extends the preceding results is the method of self-consistent fields. Self-consistent fields are to electromagnetic fields what a Taylor series expansion is to other mathematical functions. If the fields are continuous through all orders, and if the solution is known exactly at any point, information at that point may be used to construct the field at any other point. For this case, the exact expressions are the telefield terms of Eq. 5.12.4. The method uses continued application of the Maxwell curl equations:

$$\tilde{\mathbf{H}} = \frac{\hbar}{k} \nabla \times \tilde{\mathbf{E}} \quad \tilde{\mathbf{E}} = -\frac{\hbar}{k} \nabla \times \tilde{\mathbf{H}} \quad (5.13.1)$$

The electric field intensity of Eq. 5.12.4 is substituted into the first of Eqs. 5.13.1, which gives a corrected expression for the magnetic field intensity. The corrected magnetic field intensity is substituted into the second of Eqs. 5.13.1, which gives a corrected expression for the electric field intensity. The corrected electric field intensity combines with the first of Eqs. 5.13.1 to yield a further corrected expression for the magnetic field intensity that is, in turn, combined with the second of Eqs. 5.13.1 to yield a further corrected value of the electric field intensity. With each step, the solution becomes more exact and extends to smaller radii. Although labor intensive, the iterative process may be continued as many times as desired to obtain a satisfactory solution. There are inherent difficulties with this technique. Since it only analyzes field symmetries present in the starting

fields, only those symmetries are present in the final one. Iterative errors quickly accumulate if the starting fields are inexact.

Applying the technique to the spherical Bessel function terms simply repeats the terms. The solution is exact and iterations produce no additional terms. Bessel function terms are the first terms inside the brackets of Eqs. 5.13.6-5.13.8; all other terms arise from spherical Neumann functions.

By Eq. 5.12.5 the beginning radial electric field component is:

$$E_r^{(0)} = e^{-i\sigma \cos \theta} \sin \theta (1 + \cos \theta) e^{-i\phi} \quad (5.13.2)$$

Taking iterations begins the expansion at infinity and works towards smaller radius solutions. After completing two full iterations the calculated radial field component is:

$$E_r^{(2)} = e^{-i\sigma \cos \theta} \left\{ \begin{aligned} &\sin \theta (1 + \cos \theta) + \frac{i}{\sigma} \sin \theta (1 + 3 \sin^2 \theta) \\ &+ \frac{1}{\sigma^2} \sin \theta \cos \theta (9 + 6 \sin^2 \theta) \\ &- \frac{i}{\sigma^3} \sin \theta (18 - 30 \sin^2 \theta) + \frac{18}{\sigma^4} \sin \theta \cos \theta \end{aligned} \right\} e^{-i\phi} \quad (5.13.3)$$

Continuing, after completing four full iterations and truncating with the negative fourth power of  $\sigma$ , the radial field component is:

$$E_r^{(4)} = e^{-i\sigma \cos \theta} \left[ \begin{aligned} &\sin \theta (1 + \cos \theta) + \frac{i}{\sigma} \sin \theta (1 + 7 \sin^2 \theta) \\ &+ \frac{1}{\sigma^2} \sin \theta \cos \theta (21 + 54 \sin^2 \theta) \\ &- \frac{i}{\sigma^3} \sin \theta (174 - 30 \sin^2 \theta - 300 \sin^4 \theta) \\ &- \frac{1}{\sigma^4} \sin \theta \cos \theta (642 - 1620 \sin^2 \theta - 840 \sin^4 \theta) \end{aligned} \right] e^{-i\phi} \quad (5.13.4)$$



After eight full iterations, and truncated with the negative fourth power of  $\sigma$ :

$$E_r^{(8)} = e^{-i\sigma \cos \theta} \left[ \begin{aligned} & \sin \theta (1 + \cos \theta) + \frac{i}{\sigma} \sin \theta (1 + 15 \sin^2 \theta) \\ & + \frac{1}{\sigma^2} \sin \theta \cos \theta (45 + 294 \sin^2 \theta) \\ & - \frac{i}{\sigma^3} \sin \theta (966 + 2898 \sin^2 \theta - 5460 \sin^4 \theta) \\ & - \frac{1}{\sigma^4} \sin \theta \cos \theta (14152 + 12462 \sin^2 \theta - 88080 \sin^4 \theta) \end{aligned} \right] e^{-i\phi} \quad (5.13.5)$$

The foregoing series are sufficient to permit generalization to an arbitrary number of iterations. After  $n$  iterations, the three field components generalize to those of Eqs. 5.13.6 through 5.13.8. The equations are expressed as a function of the number of iterations used in the self-consistent field solution. To use the solution, it is necessary to obtain the same expressions as a function of a known physical quantity, for example the number of the largest numbered mode. Establishing a relationship between the fields and those obtained by direct summation is mostly easily done using Eq. 5.13.6.

$$\tilde{E}_r^{(n)} = \sin \theta e^{-i\sigma \cos \theta} \left\{ \begin{aligned} & 1 + \cos \theta + \frac{i}{\sigma} (1 + [2n-1] \sin^2 \theta) \\ & + \frac{1}{\sigma^2} \cos \theta (3[2n-1] + 6[n-1]^2 \sin^2 \theta) \\ & - \frac{i}{\sigma^3} \left( 2[10n^2 - 21n + 11] + 2[8n^3 - 51n^2 + 82n - 39] \sin^2 \theta \right. \\ & \quad \left. - 10[2n^3 - 9n^2 + 13n - 6] \sin^4 \theta \right) \\ & - \frac{1}{4\sigma^4} \cos \theta \left( \begin{aligned} & [224n^3 - 368n^2 + 1672n - 792] \\ & + [81n^4 - 3750n^3 + 41529n^2 - 166950n + 233400] \sin^2 \theta \\ & - [300n^4 - 2760n^3 + 11460n^2 - 29160n + 36480] \sin^4 \theta \end{aligned} \right) \end{aligned} \right\} \quad (5.13.6)$$

$$\tilde{E}_\theta^{(n)} = e^{-i\sigma \cos \theta} \left\{ \begin{aligned} & \cos \theta + \cos^2 \theta + \frac{i}{\sigma} [2n-1] \sin^2 \theta \cos \theta \\ & + \frac{1}{\sigma^2} \left( 2[n-1] + 6[n-1]^2 \sin^2 \theta \cos^2 \theta \right) \\ & - \frac{i}{\sigma^3} \cos \theta \left( \begin{aligned} & 2[4n-5][n-1] + 8[2n^3 - 9n^2 + 13n - 6] \sin^2 \theta \\ & - 10[2n^3 - 9n^2 + 13n - 6] \sin^4 \theta \end{aligned} \right) \\ & - \frac{1}{4\sigma^4} \left( \begin{aligned} & [96n^3 - 432n^2 + 648n - 312] \\ & + [210n^4 - 2524n^3 + 13254n^2 - 37292n + 44352] \sin^2 \theta \\ & - [199n^4 + 2070n^3 - 37339n^2 + 162750n - 232200] \sin^4 \theta \\ & + [300n^4 - 2760n^3 + 11460n^2 - 29160n + 36480] \sin^6 \theta \end{aligned} \right) \end{aligned} \right\} e^{-i\phi} \quad (5.13.7)$$

$$\tilde{E}_\phi^{(n)} = -i e^{-i\sigma \cos \theta} \left\{ \begin{aligned} & 1 + \cos \theta + \frac{i}{\sigma} [2n-1] \sin^2 \theta \\ & + \frac{1}{\sigma^2} \cos \theta \left( [2n-3] + 6[n-1]^2 \sin^2 \theta \right) \\ & - \frac{i}{\sigma^3} \left( \begin{aligned} & [8n^2 - 26n + 23] + [16n^3 - 84n^2 + 140n - 78] \sin^2 \theta \\ & - 10[2n^3 - 9n^2 + 13n - 6] \sin^4 \theta \end{aligned} \right) \\ & + \frac{1}{4\sigma^4} \cos \theta \left( \begin{aligned} & [-96n^3 - 576n^2 + 1200n - 864] \\ & - [220n^4 - 3080n^3 + 20060n^2 - 70960n + 104,400] \sin^2 \theta \\ & + [300n^4 - 2760n^3 + 11460n^2 - 29160n + 36480] \sin^4 \theta \end{aligned} \right) \end{aligned} \right\} e^{-i\phi} \quad (5.13.8)$$

Equating terms proportional to the inverse radius yields the approximate equality:

$$\frac{2i}{\sigma} n = \frac{i}{2\sigma} L \quad (5.13.9)$$

The left side of Eq. 5.13.9 comes from Eq. 5.13.6 and the right side from Eqs. 5.11.6. The equations are equal if:

$$L = 4n \quad (5.13.10)$$

Other term-by-term comparisons between the “L” and “n” expressions yield a similar relationship. Therefore, for equivalent descriptions the number of self-consistent field iterations is one-fourth the maximum modal number of the radiation. This relationship permits writing the full angular dependence of the fields, Eq. 5.13.6-5.13.8, as functions of the maximum modal number.

Incorporating Eq. 5.13.10 into Eqs. 5.13.6, 5.13.7, and 5.13.8, and keeping only the leading terms shows the approximate field set through inverse quartic terms to be:

$$\begin{aligned}
 E_r(\sigma, \theta, \phi) &= e^{-i\sigma \cos \theta} \left\{ \begin{aligned} &\sin \theta + \sin \theta \cos \theta + \frac{L}{2\sigma} \sin^3 \theta + \frac{3L^2}{8\sigma^2} \sin^3 \theta \cos \theta \\ &+ \frac{L^3}{16\sigma^3} \sin^3 \theta (1 - 5 \cos^2 \theta) - \frac{L^4}{1,024\sigma^4} \sin^3 \theta \cos \theta (81 - 300 \sin^2 \theta) \end{aligned} \right\} e^{-i\phi} \\
 E_\theta(\sigma, \theta, \phi) &= e^{-i\sigma \cos \theta} \left\{ \begin{aligned} &\cos \theta + \cos^2 \theta + \frac{L}{2\sigma} \sin^2 \theta \cos \theta + \frac{3L^2}{8\sigma^2} \sin^2 \theta \cos^2 \theta \\ &+ \frac{L^3}{16\sigma^3} \sin^2 \theta \cos \theta (1 - 5 \cos^2 \theta) \\ &- \frac{L^4}{1,024\sigma^4} (210 \sin^2 \theta - 199 \sin^4 \theta + 300 \sin^6 \theta) \end{aligned} \right\} e^{-i\phi} \\
 \tilde{E}_\phi(\sigma, \theta, \phi) &= -ie^{-i\sigma \cos \theta} \left\{ \begin{aligned} &1 + \cos \theta + \frac{L}{2\sigma} \sin^2 \theta + \frac{3L^2}{8\sigma^2} \sin^2 \theta \cos \theta \\ &+ \frac{L^3}{16\sigma^3} \sin^2 \theta (1 - 5 \cos^2 \theta) - \frac{L^4}{1,024\sigma^4} \sin^2 \theta \cos \theta (220 - 300 \sin^2 \theta) \end{aligned} \right\} e^{-i\phi}
 \end{aligned}$$

$$\eta \mathbf{H} = \mathbf{E} \quad (5.13.11)$$

The first term in each field component arises from spherical Bessel functions, all other terms arise from spherical Neumann functions. Although the transcendental propagation term is correct only if L is infinite, in all of these cases with positive powers of  $\sigma$  the series converge so rapidly that L as large as ten appears to be adequate to describe source behavior.

## 5.14 Power and Energy Exchange

To obtain the power and energy in a photon field, begin with the complex Poynting vector. With the fields of Eq. 5.13.11, it may be written as:

$$\mathbf{N}_c = \frac{1}{2} \text{Re}(\tilde{\mathbf{E}} \times \tilde{\mathbf{H}}^*) = -\frac{1}{2\eta} \text{Re}(i \tilde{\mathbf{E}} \times \tilde{\mathbf{E}}^*) \quad (5.14.1)$$

The vector components are:

$$\mathbf{N}_c = \frac{1}{\eta} \text{Re} \left\{ \hat{\rho} (i E_\phi E_\theta^*) + \hat{\theta} (i E_r E_\phi^*) + \hat{\phi} (i E_\theta E_r^*) \right\} \quad (5.14.2)$$

The surface power on a circumscribing sphere surrounding the source follows from the angular components of Eqs. 5.13.11 and 5.14.2.

The real part of the radial component of the Poynting vector for  $L$  large, through quartic terms, is:

$$\begin{aligned} \eta N_r = & 2 \cos^2 \theta + \frac{3L^2}{4\sigma^2} \sin^2 \theta \cos^2 \theta - \frac{L^4}{1,024\sigma^4} \sin^2 \theta [430 - 719 \sin^2 \theta + 600 \sin^4 \theta] \\ & + \cos \theta \left[ \left( 1 + \cos^2 \theta \right) + \frac{L^2}{4\sigma^2} \sin^2 \theta (1 + 2 \cos^2 \theta) + \frac{L^4}{64\sigma^4} \sin^4 \theta (4 - 11 \cos^2 \theta) \right] \\ & \left[ - \frac{L^4}{1024\sigma^4} \sin^2 \theta [430 - 719 \sin^2 \theta + 600 \sin^4 \theta] \right] \end{aligned} \quad (5.14.3)$$

In common with the output powers calculated in Chapters 2 and 3, only products of one Bessel and one Neumann function term integrate to a nonzero value over an enclosing surface. Since all Bessel function terms are teledistant, each surface power term contains at least one teledistant field term. If a source generates the fields of Eq. 5.13.11 without the Bessel terms, the result is standing energy. A plane wave impressed on such a field supplies the leading terms of Eqs. 5.13.11, and may produce an energy exchange.

The power on the surface of a virtual sphere of radius  $\sigma/k$  calculates to be:

$$P_r \cong \frac{4\pi}{\eta k^2} \left( \frac{2\sigma^2}{3} + \frac{L^2}{10} - \frac{1553}{8960} \frac{L^4}{\sigma^2} \right) \quad (5.14.4)$$

All terms of Eqs. 5.14.3 and 5.14.4 are proportional to the teledistant Bessel function. The first term is also proportional to the teledistant Neumann term, the second term to the inverse square Neumann term, and the third term to the inverse quartic Neumann term.

In Chapters 2 and 3, the time-average surface power is supported by the product of field terms each of which is proportional to  $1/\sigma$ , for example Eqs. 3.3.1 and 3.3.2. Since the area increases as  $\sigma^2$ , the product of far field power density and area is independent of distance. The radiation analyzed here is dramatically different. The power from the first term of Eq. 5.14.4 increases with distance as  $\sigma^2$ , the second term is independent of  $\sigma$ , the third term decreases as  $1/\sigma^2$  etc., through higher powers. Yet, energy conservation requires the total value to be independent of distance. This, in turn, requires the energies carried by the higher order terms to transfer to lower order terms as the energy travels outward from the source.

It follows from Eqs. 5.13.11 and 5.14.2 that, through inverse quartic terms, the azimuth-directed portion of the Poynting vector is equal to:

$$\eta N_\theta = - \left\{ \sin\theta(1+\cos\theta)^2 + \frac{L^2}{4\sigma^2} \sin^3\theta(1+3\cos\theta+2\cos^2\theta) \right. \\ \left. + \frac{L^4}{64\sigma^4} \sin^3\theta \left[ 4 - 11\cos^2\theta - \frac{1}{16} \cos\theta(1+\cos\theta)(301-600\cos^2\theta) \right] \right\} \quad (5.14.5)$$

At the equator, this vector component is +z-directed and of magnitude:

$$-\eta N_\theta = \eta N_z = \left\{ 1 + \frac{L^2}{4\sigma^2} + \frac{L^4}{16\sigma^4} \right\} \quad (5.14.6)$$

Equation 5.14.6 shows that energy passes from the lower into the upper hemisphere. This is consistent with energy conservation only if energy that exits the source into the lower hemisphere veers and passes upward.

## 5.15 The Wave Train

The preceding analysis considered only steady state fields, fields that have existed since time  $t = -\infty$ . The wave train, therefore, is infinitely long. Actual wave trains, of course, are finite in length; generating sources start and stop. One estimate of the length of a photon wave train is given in Section 5.2. With a finite wave train, calculated kinematic results are meaningful only for fields that are contained within a sphere, centered on the active region, with a radius equal to the length of the wave train. For a wave train of length  $l$ , if  $W$  is the total radiated energy,  $F$  is the normalizing field constant, Eq. 5.14.4 is the expression for the output power, and letting  $O$  indicate order or the variable,  $W$  is equal to:

$$W \equiv \frac{4\pi(k\ell)^2}{\eta k^2} \int_{\Delta t} dF^2 \left\{ \frac{2}{3} + \frac{L^2}{10(k\ell)^2} - \frac{1553}{8960} \frac{L^4}{(k\ell)^4} + O\left(\frac{L^6}{(k\ell)^6}\right) \right\} \quad (5.15.1)$$

A separate expression for the total output energy follows from Eq. 5.5.17:

$$W = \frac{4\pi}{\eta k^2} \sum_{\ell=1}^L (2\ell+1) \int_{\Delta t} F^2 dt \equiv \frac{4\pi L^2}{\eta k^2} \int_{\Delta t} F^2 dt \quad (5.15.2)$$

Keeping only the lead term of Eq. 5.15.1 and requiring Eqs. 5.15.1 and 5.15.2 to be equal shows that:

$$(k\ell)^2 \equiv 1.5L^2 \quad (5.15.3)$$

This result shows that the normalized wave train length,  $kl$ , is on the same order of magnitude as the maximum modal number of the radiation. For example, if  $L$  were equal to 1000 the wave train would equal about:

$$l \equiv 200\lambda \quad (5.15.4)$$

The estimated length of Eq. 5.15.4 is much less than that obtained for a dipole field generated by a point electron, see Sec. 5.2. However that estimate is based upon the electron as a point charge and oscillations were

produced by oscillations of the entire electronic mass. In this case, the oscillations are within the structure of the electron.

To estimate  $F$ , note that Eq. 5.15.2 is also equal to  $\hbar\omega$ . Making the equality and, to form a definite model, letting  $F$  be a constant magnitude rectangular pulse of width  $\Delta\tau$ , and equal to zero at all other times:

$$F = \sqrt{\frac{3\hbar}{4\epsilon\lambda\tau^3}} \quad (5.15.5)$$

Energy passing through the equator between radius  $a$ , the limit of the active region, and the length  $l$  of the wave train may be obtained by integrating the Poynting vector of Eq. 5.14.6 over the appropriate portion of the equatorial surface. The result is:

$$\begin{aligned} W_z &= \int_{\Delta\tau} d\tau F^2 \frac{2\pi}{\eta k^2} \int_{ka}^{kl} \sigma d\sigma \left\{ 1 + \frac{L^2}{4\sigma^2} + \frac{L^4}{16\sigma^4} + O\left(\frac{L^6}{\sigma^6}\right) \right\} \\ &\equiv \frac{2\pi}{\eta k^2} \int_{\Delta\tau} d\tau F^2 \left\{ \frac{L^2}{4(ka)} + \frac{L^4}{80(ka)^3} + O\left(\frac{L^6}{80(ka)^5}\right) \right\} \end{aligned} \quad (5.15.6)$$

Since the result is positive, energy passes from the lower to the upper hemisphere.

With a wave train containing 200 or more wavelengths, field effects are dominated by the steady state solutions and emission is not just a transient act. The field equations of Eq. 5.13.11 confirm that as the radius increases the energy paths veer towards the  $z$ -direction. When the source is terminated the outermost portion of the wave train is nearly collimated and the ratio of transported energy to transported momentum is only slightly greater than  $c$ . Since the transient solution is not available, whether the transient fields change the near equality with  $c$  to an exact one is unknown.

## 5.16 Multipolar Moments

The purpose of this section is to describe a means by which high-order modes are generated from an initial charge density. Although the magnitudes of the high-order fields are too small to produce the coefficients needed to produce the fields of Eqs. 5.13.11, the needed source symmetry is formed that is, in turn, driven by forces, to be described in the next section, that produce high order terms of significant magnitude.

When a passive, perfectly conducting sphere is immersed in a plane wave, at the surface of the scatterer the magnitudes of the scattered and incident waves are the same, see Eqs. 2.3.7. The equality requires the ratio of field coefficients to be:

$$\frac{\text{Incident field magnitude}}{\text{Scattered field magnitude}} = \frac{(ka)^{2\ell+1}}{(2\ell+1)!!(2\ell-1)!!} \quad (5.16.1)$$

With  $(ka) \ll 1$  the ratio of Eq. 5.16.1 is so small and decreases so rapidly with increasing  $\ell$  that the lowest order terms dominate scattering.

When an atom in a high energy state is immersed in a plane wave, at the surface of the scatterer the magnitude of the scattered wave is much larger than that of the incident wave. For the incident wave coefficients of Eq. 5.3.1 to produce the scattered wave coefficients of Eq. 5.3.2, it is necessary that the ratio of incident to scattered field magnitude be:

$$\frac{\text{Incident field magnitude}}{\text{Scattered field magnitude}} = \frac{(2\ell+1)!!(2\ell-1)!!}{(ka)^{2\ell+1}} \quad (5.16.2)$$

With  $(ka) \ll 1$  the ratio of Eq. 5.16.2 is so large and increases so rapidly with increasing  $\ell$  that the highest order terms dominate emission.

Changing the coefficients Eq. 5.16.1 to those of 5.16.2 is only possible because electron-generated radiation involves much more than scattering. The analysis involves atomic states in unstable equilibrium and radiation reaction forces that far exceed those due to the incident plane wave. To examine a possible source of the driving fields consider an occupied state that supports time-average current and charge densities at all points within the source region. By Eq. 4.5.1 and Eq. 4.5.2 the time-average values of charge and current densities are respectively  $eU^*(\mathbf{r})U(\mathbf{r})$  and



$\frac{\hbar e}{2im} [U^*(\mathbf{r}) \nabla U(\mathbf{r}) - U(\mathbf{r}) \nabla U^*(\mathbf{r})]$ . With biconical receiving antennas, see Section 2.14, by Lenz's law the time changing magnetic field induces currents that generate an opposing field. Quite differently, an intrinsic magnetic moment interacts with the applied magnetic field to generate a field in the direction of the incoming magnetic field.

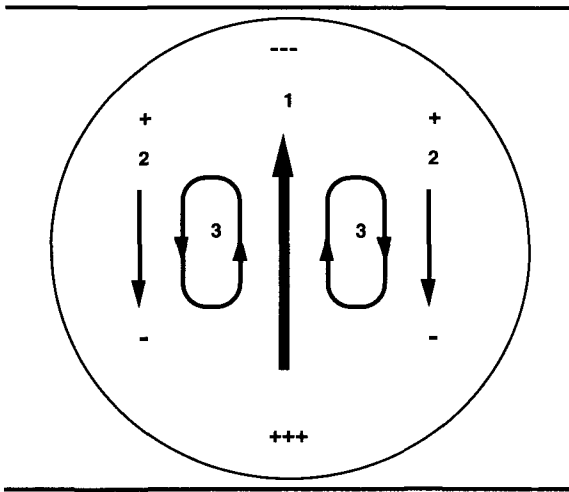


Figure 5.16.1 Source modes resulting from an electric dipole formed within an electric charge distribution.

*Arrows indicate current densities. Current {1} creates a dipole source, Currents {1} and {2} together create an electric octupole source, and Currents {3} create a magnetic quadrupole source. By continuation, this creates all odd numbered TM field sources and all even number TE field sources. With a dual source of a magnetic charge distribution, the result is creation of all even numbered TM field sources and all odd numbered TE field sources.*

Consider a sphere of charge in which the condition  $\nabla \cdot \mathbf{J} = 0$  applies. In Fig. 5.16.1, an applied field drives a dipole mode, as illustrated by the center arrow. Two current options are illustrated by the smaller arrows. Some terminate on the edge of the source, leaving a net charge density that generates an electric octupole field. The interior charge structure drives continuous current loops that generate a magnetic quadrupole field. So long as source constraints permit the charge density to be further subdivided in this way, each current path produces a similar set of higher order modes. The

result is that an oscillating electric dipole moment drives all odd-order electric multipolar moments, TM fields, of the same degree and all even-order magnetic multipolar moments, TE fields, of the same degree.

In a dual manner, using magnetic circuit techniques and an effective magnetic current density, a similar analysis shows that an oscillating magnetic dipole moment drives all even-order TM fields, and all odd-order TE fields of the same degree.

As shown by the multipolar field coefficients for quantized radiation, the field coefficients are proportional to the generating charge times  $ka$  raised to an integer power. The method of calculating moments from source distributions is discussed in the Appendix, Sections A.28 and A.29. Results are that the electric and magnetic multipolar moments of order  $\ell$  are respectively proportional to  $(ka)^\ell$  and  $(ka)^{\ell+1}$ .

Changing from individual charges to charge density permits changing calculation techniques from sums over individual charges to volume integrals over charge distributions. The former is much more difficult than the latter. Electric charge density may be used in local neighborhoods where the ratio of contained charge to the volume of containment is continuous. The discussion associated with Fig. 5.16.1 shows no lower limit to the possible size of current eddies. However, the approach is valid if and only if the charge density is continuous in the neighborhood of a source point, see Section 1.5. We conclude, therefore, that the above arguments apply down to a scale of dimensions on which the use of charge density to determine properties breaks down. Since the order of a radiated mode varies inversely with the physical dimensions of current eddies, the maximum modal number,  $L$ , is determined by lower limit on the physical size of current eddies.  $L$  is determined by the granularity of the electron charge distribution. A fixed array requires  $2^{(L-1)}$  units; if  $L = 1000$  then  $2^{999}$  units are necessary. Yet a single unit that moves rapidly enough can generate the same moment. A necessary axiom is that the moment is enabled by electron nonlocality.

An electrically small scatterer driven by the field of a plane wave was treated in Chapter 2, where it was shown that high-order induced moments and high-order scattering are relatively small. In contrast, the induced sources produce much larger high-order moments. This approach also shows an intrinsic upper limit,  $L$ , to the maximum modal number that depends upon

the dimensional scale of the smallest units of charge and current distributions. If the charge density is continuous ever-larger orders will be driven. The process ceases only when the dimensional scale is so small that granules of charge appear as a three-dimensional mosaic.

## 5.17 Field Stress on the Active Region

As discussed in Sections 1.8, 3.13 and 3.17, Maxwell stress tensor fields accompany electromagnetic fields. An external field intensity that is parallel with or normal to a surface exerts a pressure on that surface directed respectively towards or away from the field. In spherical coordinates, the radial portion of the diagonal components of the stress tensor is:

$$T_{rr} = \frac{\epsilon}{2} (E_r^2 - E_\theta^2 - E_\phi^2) + \frac{\mu}{2} (H_r^2 - H_\theta^2 - H_\phi^2) \quad (5.17.1)$$

If a field exists on one side of the surface, and if there are no fields on the other side, a positive or negative value of  $T_{rr}$  denotes respectively a positive or negative radiation reaction pressure.

To establish stress magnitudes associated with commonly occurring phenomena, consider the solar radiation field on the surface of the earth. The intensity at the equator with a dry atmosphere and the sun directly overhead is about one kW per square meter. The frequency spread is infrared to ultraviolet and it is randomly polarized. Approximate values of electric field intensity and pressure are:

$$E = 27.5 \text{ V/m} \quad \text{and} \quad \frac{\epsilon}{2} E^2 = 3.33 \times 10^{-9} \text{ Pa} \quad (5.17.2)$$

Consider next the pressure on a spherical shell of radius  $a$  that contains a uniformly distributed total inner surface charge of  $-e$  centered about a point charge of  $+e$ . By Coulomb's law the electric field intensity just inside the shell is:

$$E_r = \frac{e}{4\pi\epsilon a^2} \quad (5.17.3)$$

Using Eq. 5.17.1, the Coulomb pressure is:

$$T_{rr} = \frac{e^2}{32\pi^2 \epsilon a^4} \quad (5.17.4)$$

This equation shows that the pressure varies as the inverse fourth power of the radius of the radiating shell. The positive sign indicates that the pressure is directed towards the field, in this case inwardly. If the radius is 'n' times the radius of the first Bohr radius,  $5.29 \times 10^{-11}$  m, the inward pressure is:

$$T_{rr} \cong \left( \frac{1.17}{n^4} \times 10^{12} \right) \text{Pa} \quad (5.17.5)$$

Next, let the shell contain no sources or fields, but the exterior surface supports the surface charge and current densities that generate the fields of Eqs. 5.13.6 through 5.13.8. The total radiation reaction pressure produced by these fields is constant since, like Eqs. 3.17.3 the electric and magnetic fields are sized and phased in a way that the time-dependent portions cancel. However, by Sec. 4.3 the source contains both charge and current densities and electric fields effect charge densities and magnetic fields effect current densities. We define the phase of transcendental functions on the surface of a spherical shell of radius  $a$  to be  $\Phi$  where:

$$\Phi = 2[\omega t - ka \cos \theta - \phi] \quad (5.17.6)$$

Matrix element  $T_{rr}$  calculated from Eqs. 5.13.6 through 5.13.8 is:

$$T_{rr}(ka, \theta, \phi) =$$

$$-\frac{\epsilon}{2} F^2 \left\{ \begin{aligned} & 2\cos^2\theta(1+\cos\theta)^2 + \left[ \frac{3L^2}{2(ka)^2} \right] \sin^2\theta \cos^3\theta(1+\cos\theta) + \frac{L^2}{2(ka)^2} \sin^4\theta \cos^4\theta \\ & + \frac{L^4}{8(ka)^4} \sin^4\theta \cos^2\theta(1-5\cos^2\theta) \\ & + \frac{L^4}{256(ka)^4} \sin^2\theta \cos\theta(1+\cos\theta) \left( 5-10\sin^2\theta-300\sin^4\theta \right) \end{aligned} \right\}$$

$$\begin{aligned}
& + \frac{\epsilon}{2} F^2 \left\{ \begin{aligned} & 2 \sin^2 \theta (1 + \cos \theta)^2 - \frac{L^2}{2(ka)^2} \sin^6 \theta + \frac{3L^2}{2(ka)^2} \sin^4 \theta \cos \theta (1 + \cos \theta) \\ & + \left[ \frac{9L^4}{32(ka)^4} \right] \sin^6 \theta \cos^2 \theta - \frac{L^4}{8(ka)^4} \sin^6 \theta (1 - 5 \cos^2 \theta) \\ & + \frac{L^4}{256(ka)^4} \sin^2 \theta \cos \theta (1 + \cos \theta) (5 - 10 \sin^2 \theta - 300 \sin^4 \theta) \end{aligned} \right\} \cos \Phi \\
& + \frac{\epsilon}{2} F^2 \left\{ \begin{aligned} & \frac{2L}{(ka)} \sin^4 \theta (1 + \cos \theta) + \frac{3L^3}{4(ka)^3} \sin^6 \theta \cos \theta \\ & + \frac{L^3}{4(ka)^3} \sin^4 \theta (1 + \cos \theta) (1 - 5 \cos^2 \theta) \end{aligned} \right\} \sin \Phi
\end{aligned} \tag{5.17.7}$$

The azimuth angle dependence shows that the tensor rotates around the  $z$ -axis twice each field cycle.

The magnitude of coefficient  $\epsilon F^2/2$  follows from Eq. 5.15.4 and Eq. 5.15.5. In the mid-optical range,  $\lambda = 500$  nm, it is:

$$\frac{\epsilon F^2}{2} = 2.37 \times 10^{-8} \text{ Pa} \tag{5.17.8}$$

Combining Eqs. 5.17.7 and Eq. 5.17.8 shows the positive  $z$ -axis pressure to be constant, compressive, and more than 100 times the solar pressure at all radii. There is no pressure on the negative  $z$ -axis.

$$T_{rr}(\sigma, 0, \phi) = -3.80 \times 10^{-7} \text{ Pa} \text{ and } T_{rr}(\sigma, \pi, \phi) = 0 \tag{5.17.9}$$

Figure 5.17.1 shows a plot of total radiation pressure versus zenith angle at the surface of a virtual radiating sphere with radius equal to 1,500,000 Bohr radii, where  $L/(ka) \cong 1$ . This is a radius approximately equal to the length of the wave train, and here the teledistant field terms are dominant. The maximum pressure magnitude is on the positive  $z$ -axis and equal to  $-3.8 \times 10^{-7}$  Pa. This pressure is the mechanism by which the radiation exerts a backward force on the radiator, in accordance with Newton's second law of motion.

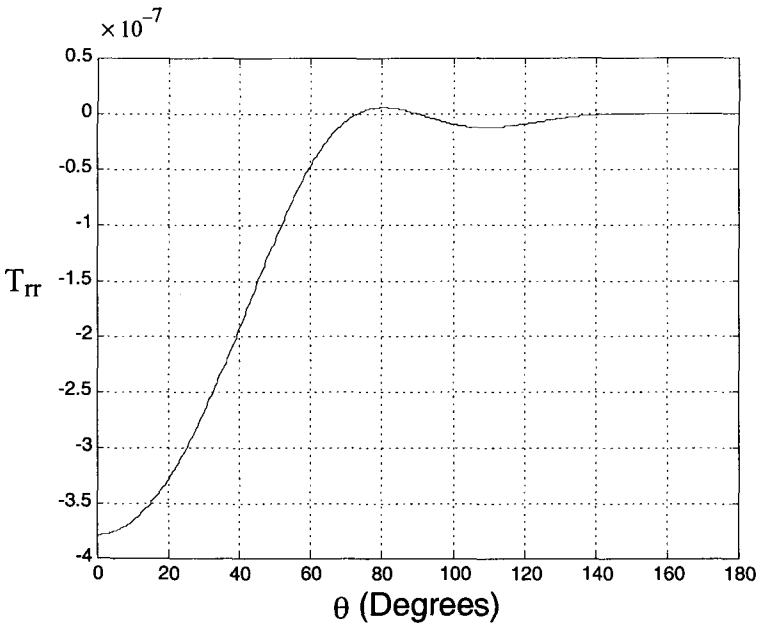


Figure 5.17.1.  $L/(ka) = 1$ , total pressure versus zenith angle.  
*Total pressure on the surface of a radiating sphere with radius equal 1,500,000 Bohr orbits at it generates the fields of Eqs. 5.13.6 through 5.13.8.*

At this radius the Coulomb pressure is about  $2.3 \times 10^{-13}$  Pa. The radiation pressure is greater than the Coulomb pressure by a factor of about 160,000 and greater than the maximum sunlight pressure by a factor of about 10. We conclude that the radiation reaction pressure dominates the dynamics of electron behavior at this radius.

A Mercator projection of the surface pressure showing pressure in the vertical dimension, but limited to half the full azimuth angle for better viewing, is shown in Fig. 5.17.2.

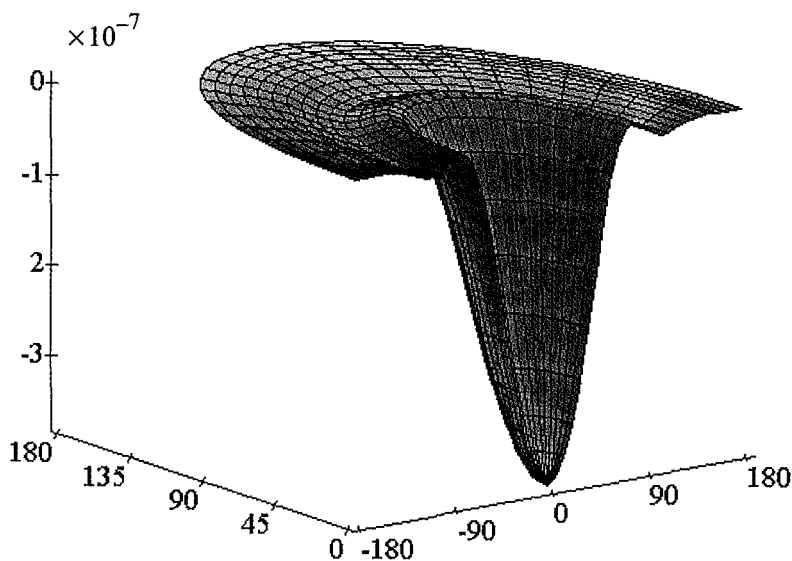


Figure 5.17.2.  $L/(ka) = 1$ , partial three-dimensional view of total pressure versus zenith angle.

*A third dimensional Mercator projection of total radiation pressure on the surface of a radiating sphere with radius equal 1,500,000 Bohr orbits due to the fields of Eqs. 5.13.6 through 5.13.8. Negative values are compressive.*

Figure 5.17.3 shows a plot of only the electric field portion of Eqs. 5.17.6 to 5.17.8. Both the field and this portion of the stress tensor are time dependent. The maximum negative electric pressure is the z-axis value of  $-1.9 \times 10^{-7}$  Pa. The maximum positive pressure is at  $\theta = 67^\circ$ ; it is about half the maximum negative pressure, and oscillates between equal values of compression and expansion. This pressure acts only on electric charge densities, which it drives as part of the coherent generated field.

Figure 5.17.4 shows a three dimensional plot of the pressure magnitudes calculated using Eq. 5.17.7. The upper lobe is compressive and the two lower lobes are expansive.

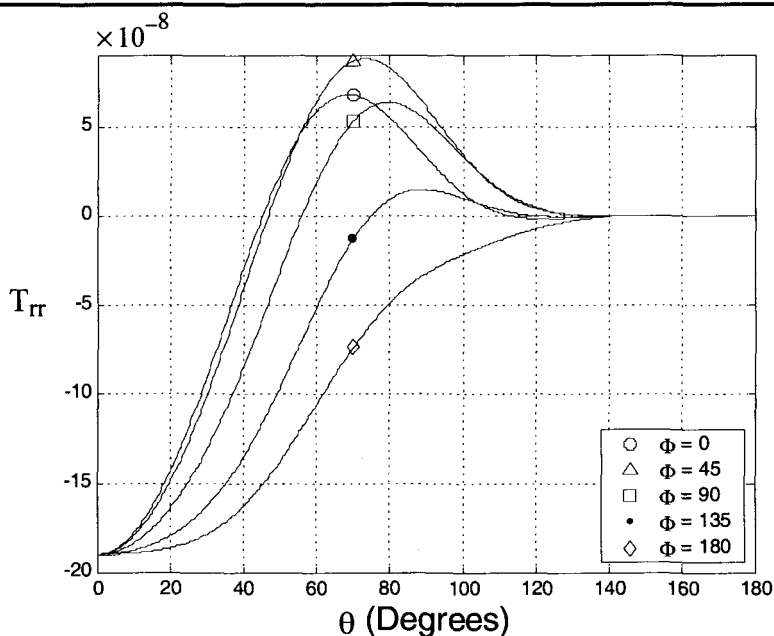


Figure 5.17.3  $L/(ka) = 1$ , electric pressure versus zenith angle.

*Effects on the surface of a radiating sphere with radius equal 1,500,000 Bohr orbits supporting the fields of Eqs. 5.13.6 through 5.13.8. Maximum magnitude is on the positive z-axis. Phase variation with zenith angle is suppressed.*

Although the self consistent field calculations of Sec. 5.13 were truncated at the inverse fourth power of the radius, it is clear from the calculations that continued expansion produces polynomials consisting of trigonometric functions multiplied by  $(L/ka)^{2s}$ , where  $s$  is a positive integer. It is also clear that the multiplying coefficients increase rapidly with increasing values of  $s$ . The series is of the same order as Eq. 5.16.2. Near the outer edge of the original wave train, where the  $L/ka$  ratio is on the order of one, only the teledistant fields are significantly large. Moving inward, as the radius decreases terms with larger values of  $s$  become dominant until the actual radius of the radiating region is reached. The largest value of  $s$  for which we have complete information is four.



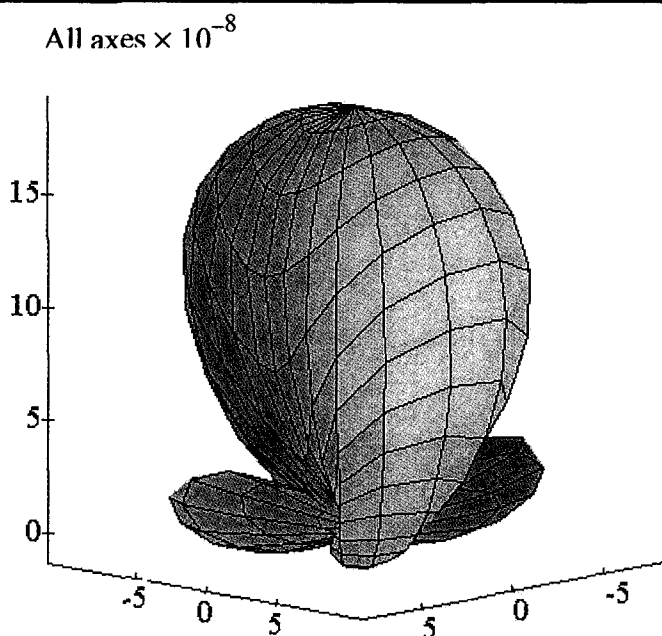


Figure 5.17.4  $L/(ka) = 1$ , a three dimensional plot showing the electrical portion of the same stress tensor magnitude. Phase variation with zenith angle is suppressed.

For the special case  $s = 2$ , Figure 5.17.5 shows the total radiation pressure versus zenith angle at the surface of a virtual radiating sphere with a radius of just one Bohr radius. The maximum pressure magnitude of  $9.0 \times 10^{16}$  Pa is expansive and occurs at zenith angle  $67^\circ$ . The magnitude so dominates the Coulomb force that the size of the radiating eigenstate electron surely undergoes a nova-like expansion of the upper hemisphere once the radiation process begins. Indeed, the pressure is so large that it belies the use of perturbation techniques to calculate radiation effects, as done in Sec. 4.13 and 4.17. The maximum compression is  $-4.2 \times 10^{16}$  Pa and occurs at a zenith angle of  $112^\circ$ . Although expansion of the upper hemisphere is expected, compression is against other atomic forces and hence distortion is less probable.

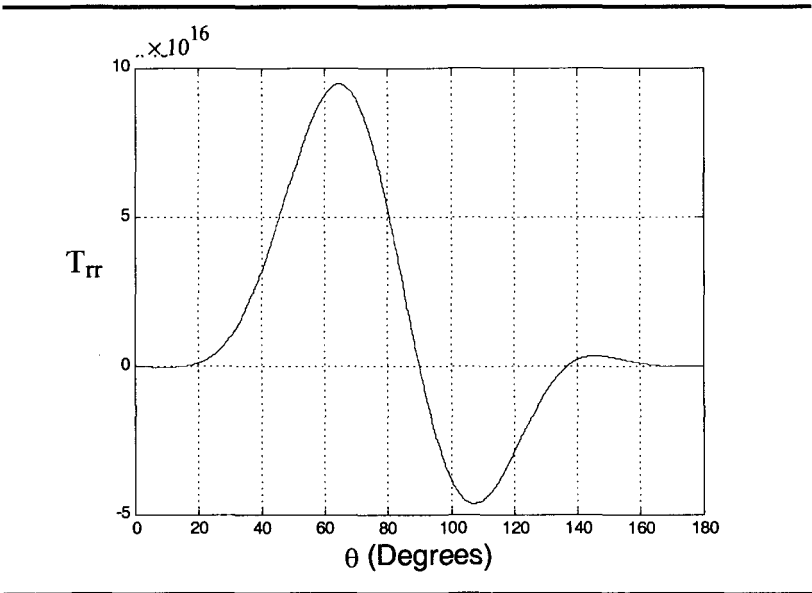


Figure 5.17.5.  $L/(ka) = 15 \times 10^5$ , total pressure versus zenith angle.  
*Total pressure on the surface of a radiating sphere with radius equal one Bohr orbit supporting the fields of Eqs. 5.13.6 through 5.13.8.*

Calculated ratios of radiation-to-Coulomb pressure and radiation-to-solar pressure are listed in Table 5.17.1. At  $\theta = 67^\circ$  the radiation pressure is about 80,000 times the Coulomb pressure and  $10^{25}$  times that of sunlight. The first ratio shows that the Coulomb force is not significant and the second ratio shows sunlight pressure to be trivial.

Radius is one Bohr radius	Pressure ratio Field/Coulomb	Pressure Ratio Field/sunlight
67°	77,000	$27 \times 10^{24}$
112°	-38,000	$-1.4 \times 10^{24}$

Table 5.17.1 Ratio of radiation pressure to Coulomb pressure and to sunlight at a radius of one Bohr orbit.

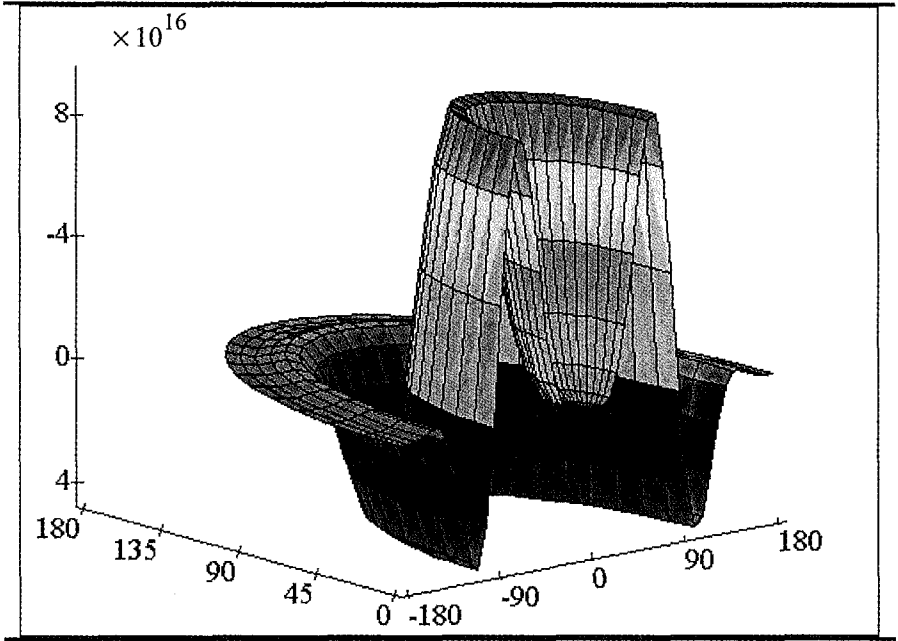


Figure 5.17.6  $L/(ka) = 15 \times 10^5$ , Mercator projection of total pressure versus zenith angle.

*A third dimensional Mercator projection of the total radiation pressure on the surface of a radiating sphere with a radius of one Bohr radius due to the fields of Eqs. 5.13.6 through 5.13.8.*

A Mercator projection of the radiation pressure is illustrated in Fig. 5.17.6. As was the case with Fig. 5.17.2, the  $z$ -axis indicates both magnitude and direction. Positive values represent pressure in the direction of the radiation and *vice versa*.

Figure 5.17.7 shows a plot of electric radiation pressure versus zenith angle at the surface of a radiating virtual sphere the size of the first Bohr radius; at this radius  $L/ka$  equals the number of wavelengths in a wave train. The maximum swing in positive pressure is between zero and  $9.7 \times 10^{16}$  Pa and occurs at a zenith angle of  $67^\circ$ . The maximum swing in negative pressure is between zero and  $-4.2 \times 10^{16}$  Pa and occurs at zenith angle  $112^\circ$ .

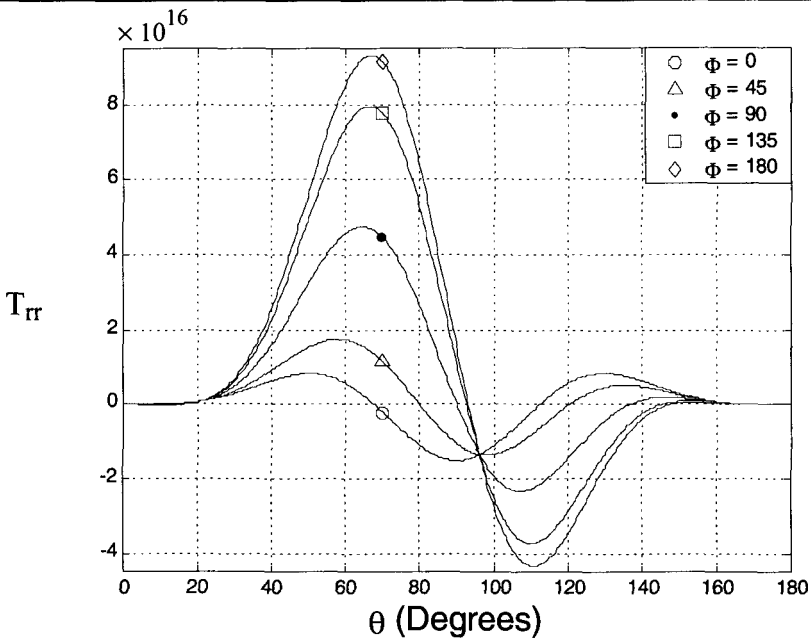


Figure 5.17.7  $L/(ka) = 1.5 \times 10^6$ , electric pressure versus zenith angle.

*Effects on the surface of a radiating sphere with radius equal one Bohr orbit supporting the fields of Eqs. 5.13.6 through 5.13.8. Maximum pressure is about  $9.7 \times 10^6$  Pa. Phase variation with zenith angle is suppressed.*

Figure 5.17.8 is a three dimensional plot of the electrical pressure magnitude at one Bohr radius. The upper and lower lobes represent respectively positive and negative pressure. Lobes on either side are identical and result from the  $2\phi$  angular dependence of the pressure.

To illustrate the importance of the radiation reaction force it was necessary to pick a specific set of examples. Results, however, do not depend upon the particular set chosen. The large radiation reaction pressure-to-Coulomb pressure ratios are robust, and similar results are obtained for any reasonable choice of examples.

It is important to note that the physical origin of the radiation reaction pressure is the standing energy fields that accompany energy exchanges by electrically small radiators. The character and magnitude of the terms make them the primary driving mechanism for quantized transitions. As noted in

earlier sections, although a plane wave contains all needed field symmetries and phases, the input magnitudes of high-order modes are far too small to support the multipolar coefficients of photon radiation. Quite differently, the radiation reaction pressure of the reactive fields meets all requirements. We conclude that atomic transitions consist of a regeneratively driven, nonlocal, eigenstate electron occupying a turbulent region of space that, in the upper hemisphere, may be orders of magnitude larger than the usual size of nascent atoms.

Detailed three-dimensional, time-dependent plots of power, energy, and electromagnetic stress in the vicinity of an atom as it radiates a photon are maintained on website:

<<http://www.ee.psu.edu/grimes/antennas/breakthrough.htm>>

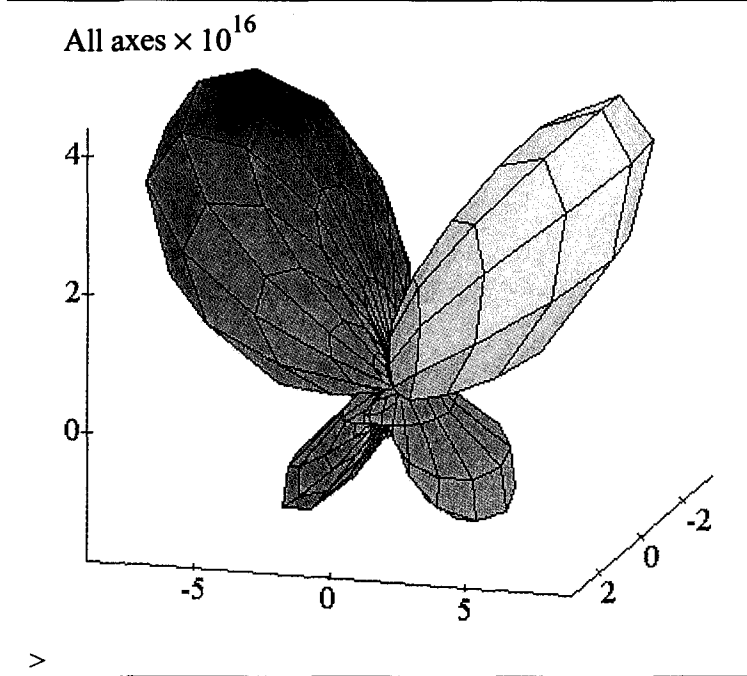


Figure 5.17.8  $L/(ka) = 1.5 \times 10^6$ , three dimensional plot of electric pressure versus zenith angle. Phase variation with zenith angle is suppressed.  
*Effects on the surface of a radiating sphere with radius equal one Bohr orbit supporting the fields of Eqs. 5.13.6 through 5.13.8. Maximum pressure is about  $9.7 \times 10^{16}$  Pa.*

## 5.18 Summary

Radiation onset by a point-electron as it enters an eigenstate generates a standing energy field. That energy field produces an expansive force on the electron in proportion to the inverse square of the electron size, see Sec. 4.2. This is a large force that has not been considered; we postulate that it transforms the electron into an extended, nonradiating, eigenstate electron in dynamic but stable equilibrium. Such an eigenstate electron is an ensemble of evolving charge and current densities. It signifies that the physical significance of  $eU^*(r)U(r)$  lies somewhere between a static charge density and the probability density of a point charge. The electron structure continuously evolves, in response to intrinsic and local forces. For example, interaction between the electron and orbital magnetic moments results in a continuous torque on what might otherwise be a fixed orbital circuit of current.

Energy conservation is applied to the ensemble and results in the Schrödinger time-independent equation, see Sec. 4.3. The method of deriving the equation is similar to methods of thermodynamics in that energy conservation yields ensemble properties although details of a particular ensemble unit are not known.

Emission from a high-energy eigenstate begins after the structure evolves to that needed to generate TE and TM dipole radiation fields with the orientation and phase of Table 3.17.1. Since evolution of the electronic picostructure is not instantaneous, a time delay is expected after the application of an external field before any particular atom ejects a photon. The duration of the delay depends upon the initial structure of that electron and hence is statistical in nature. At some point, the ensemble forms the structure necessary to begin the radiation process. Once begun, the radiation reaction force increases rapidly with modal order and drives all source modes regeneratively. The resulting electromagnetic fields produce the standing energy field of Section 3.17, in which all near field terms are proportional to spherical Neumann functions. When superimposed with an incoming plane wave, which consists solely of spherical Bessel function terms, photon emission occurs with no further time delay.

Full directivity is achieved with spherical modes. A three dimensional plot of the radiation reaction pressure on a rigid, radiating of radius  $a$  at the phase of maximum extensive pressure is shown in Fig. 5.18.1. This extensive pressure is thousands of times larger than the Coulomb attraction pressure.

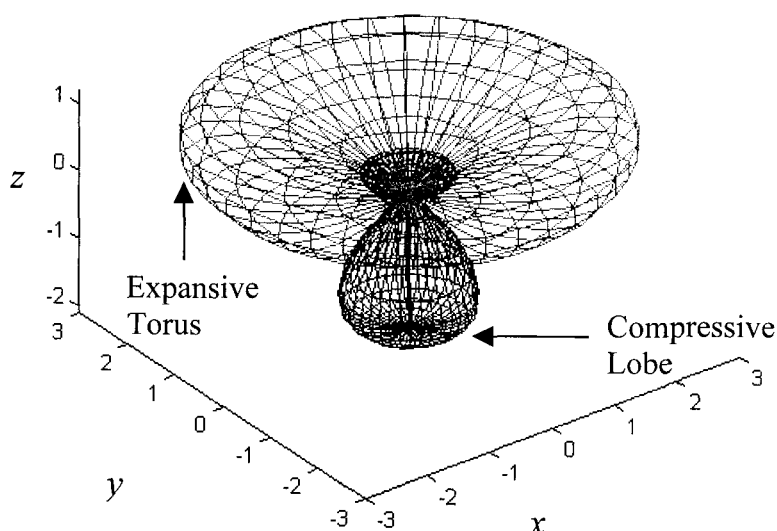


Figure 5.18.1 Electric radiation reaction pressure on a rigid radiating surface. The radius of the radiating surface is at mid-range and phased for maximum upper hemisphere extension. The upper and lower hemispheres show respectively expansive and compressive pressures. Phase variation with zenith angle is suppressed.

Since source build up is nonlinear, the Manley Rowe equations apply and Eqs. 5.1.14 and 5.1.17 correctly predict the observed power-frequency relationships. The nonlinearity voids any possibility of describing the process using equilibrium equations, such as Schrödinger time-independent equation, Eq. 4.3.14, or the Dirac equations; no linear equation can describe such nonlinear events. The time-dependent equation, Eq. 4.5.10, describes near-equilibrium characteristics that are applicable over times long compared with rates of change of the electronic ensemble. It describes events leading up to the transition, and it describes events after the transition, but it does not describe events that occur during the hiatus between periods of equilibrium. A necessary axiom is that the structure of high order multimodal moments is enabled by electron nonlocality.

If energy absorption by an atom was a linear process, see Section 1.13, the incoming energy would be statistically distributed over all available eigenstates. There would be more energy in the lower energy states and less energy in the higher energy states, but all would contain some energy. With

a system that responds nonlinearly, the regenerative process puts energy into a single eigenstate; there is no mixing of nondegenerate atomic states. The probability of an atom being in a single, nondegenerate entry state is one, there is no mixture of states, and hence no wave function collapse during a measurement process.

## References

- R. Becker, *Electromagnetic Fields and Interactions*, trans. by F. Sauter, Dover Publications (1964)
- D.M. Grimes, C.A. Grimes, "A Classical Field Theory Explanation of Photons," in T.W. Barrett, D.M. Grimes, *Advanced Electromagnetism: Foundations, Theory and Applications*, World Scientific (1995) pp. 250-277
- R.F. Harrington, "Effect of Antenna Size on Gain, Bandwidth, and Efficiency," J. Res. National Bureau of Standards vol. 64D, 1-12 (1960)
- J.D. Jackson, *Classical Electrodynamics*, 2<sup>nd</sup> ed., John Wiley (1975)
- L.D. Landau, E.M. Lifshitz, *The Classical Theory of Fields*, Addison-Wesley (1951), trans. By M. Hamermesh
- J.M. Manley, H.E. Rowe, "Some general properties of nonlinear elements, Part I: General energy relations," *Proc. IRE*, vol. 44, pp. 904-913 (1956), and "General energy relations," *Proc. IRE* vol. 47, pp. 2115-2116 (1959)
- W.K.H. Panofsky, M. Phillips, *Classical Electricity and Magnetism*, 2<sup>nd</sup> ed., Addison-Wesley (1962)
- W.R. Smythe, *Static and Dynamic Electricity*, 3<sup>rd</sup> ed., McGraw-Hill (1968)
- J.A. Stratton, *Electromagnetic Theory*, McGraw-Hill (1941)



This page is intentionally left blank

## 6. Epilogue

### 6.1 Historic Background

Particles have played a critical role in the analysis of physical events since Newton (Newton, 1687) examined them in the latter part of the seventeenth century. For the next several centuries studies involving combinations of elastic spheres dominated physics. Consequently electrical problems were first interpreted by analyzing the behavior of charged particles; Maxwell (Maxwell, 1891) used the force between “two very small bodies” to discuss implications of Coulomb’s law. Although Maxwell’s equations showed that fields are essential to explain occurrences that particles alone cannot, still the lore of particles permeated physics at the end of the nineteenth century. Therefore after Thompson (Thompson, 1897) discovered and measured particle-like electrons the idea of electrons as particles was widely accepted, along with the Lorentz (Lorentz, 1909) particle-electron and, later, the Bohr (Bohr, 1913) atomic model. The finely honed and widespread skills of classical mechanics were carried over to quantum effects; even the name “quantum mechanics” is indicative of such an origin.

Building upon his earlier work with particles, Newton (Newton, 1704) compared the propagation of light with that of projectiles. According to him, luminous bodies eject light-making projectiles that continue in flight until acted upon by other objects. Quite differently, Huygens (Huygens, 1678) compared the propagation of light with the propagation of sound through air and waves on water. According to him, light was not a thing but a disturbance that propagated through space. Light is emitted over a spread of angles by a luminous object. It bounces off objects and the total of all bounces off all objects that is intercepted by an observer forms his field of view. After Huygens, more than a century passed before Young in England and, in an arguably unparalleled technical outpouring, Fresnel in France

confirmed that light is propagated as a wave with transverse vibrations and, therefore, two polarizations. (see Born and Wolf, 1965)

The modern theoretical basis for the wave theory of light began with Maxwell (Maxwell, 1891). Hertz (Hertz, 1893), who had earlier discovered the photoelectric effect by showing that ultraviolet light increases current emission from a cathode, was the first to construct a transmitting-receiving pair of electric dipoles. With them, he confirmed that electromagnetic waves carry energy through space. His dipole radiation has rotational symmetry about its axis, a symmetry that Einstein referred to as “spherical” symmetry.

In 1900 Planck (Boorse and Motz, 1966, for example) showed that quantizing electromagnetic energy in units of  $W = \hbar\omega$  accounts for otherwise significant discrepancies between observed and calculated radiation laws. He wrote that a most suitable body for energy exchange seemed to be Hertz’s dipole with its “spherical” waves. He went on to say, “There is one particular question the answer to which will, in my opinion, lead to an extensive elucidation of the entire problem. What happens to the energy of a light-quantum after its emission? Does it pass outwards in all directions, according to Huygens’ wave theory, continually increasing in volume and tending towards infinite dilution? Alternatively, does it, as in Newton’s emanation theory fly like a projectile in one direction only? In the former case the quantum would never again be in a position to concentrate its energy at a spot strongly enough to detach an electron from its atom.” Einstein (Einstein, 1905) used field energy quantization to explain the photoelectric effect. These events rather conclusively showed that electromagnetic energy is exchanged between atoms and free space in quantized units, and this result, in turn, led to a fundamental difficulty. Einstein wrote that quite differently from results of the Maxwell wave equation “monochromatic radiation ... behaves in thermodynamic theoretical relationships *as though it consists* of distinct independent energy quanta of magnitude  $W = \hbar\omega$ .” He later extended Planck’s work (Einstein, 1917) to show that the laws of statistical mechanics require quantized radiant energy exchanges to be accompanied by quantized momentum exchanges,  $p = W/c$ . This, in turn, requires that all of each unit of radiated energy travel in the same direction. He commented: “... (Atomic) emission in spherical waves does not occur, the molecule suffers a recoil of magnitude  $\hbar\omega/c$ . This seems to make a quantum theory of radiation almost unavoidable.” In this way, fully directed emission led to the conclusion light propagates as if it

consists solely of waves and exchanges energy as if it consists solely of particles.

Only a few years after Einstein's "quantized momentum" paper, electrons were shown to support an intrinsic magnetic moment. There was an immediate problem with the result: If the moment arises because the electron charge spins about an axis at a distance equal to the Lorentz electron radius the necessary circumferential speed is many times the speed of light. Then Schrödinger (Schrödinger, 1926) published the equation that now bears his name, followed a few years later by Dirac's equations (see Dirac, 1958). Both the Schrödinger and the Dirac equations correctly describe the behavior of electrons in equilibrium. The Schrödinger equation is correct at non-relativistic electron speeds and the Dirac equations are correct at all speeds; electron spin is inherent to the Dirac equations but must be added in an *ad hoc* way to the Schrödinger equation. Both equations yield the probability that an electron will enter a transition. When it does, the input and output energies and the correct power-frequency relationships result. Both equations treat electrons as waves. Therefore, like light, an electron has historically been thought to have both wave and particle natures.

Schrödinger developed his equation using an analogy with a known relationship between classical mechanics and geometric optics. According to Mehra (Mehra, 1972), Dirac, in the search for his equations: "started playing with equations rather than trying to introduce the right physical idea. A great deal of (the) work is just playing with the equations and seeing what they give." Both Schrödinger's and Dirac's equations, therefore, came without an inherent and obvious physical interpretation. Although results of solving the equations undeniably give correct time-average values of measurable quantities, the question of how to interpret the underlying behavior remains. For example, accelerating charged particles radiate energy; stability requires a closed current loop and/or a spherically symmetric region of charge that pulsates radially. Yet atoms are stable and the Bohr orbit is some 20,000 larger than Lorentz's estimated electron size. Neither of the equations addresses this issue.

Schrödinger (Schrödinger, 1952) expressed concern that quantum jumps occurred in systems described by his *linear* differential equation. Bell (Bell, 1987) quotes Schrödinger as saying: "If we have to go on with these damned jumps, then I'm sorry that I ever got involved." In an attempt to show that what came to be the historic (Copenhagen) interpretation of quantum theory cannot be correct, Schrödinger imagined a cat that might be described by either of two eigenfunction solutions about a single potential. In one

eigenstate, the cat was healthy and, in the other, it was dead (see Penrose, 1989). By the accepted interpretation of quantum theory, the cat is partially in both solutions and thus both dead and alive; only after a measurement is made is the cat one or the other. Although Bohr made the point that a cat, being a large object, is not directly subject to the laws of quantum theory, to many an enigma remained. Dirac (Dirac, 1958) commented on the power-frequency law: "One would expect to be able to include the various frequencies in a scheme comprising certain fundamental frequencies and their harmonics. This is not observed to be the case. Instead, there is observed a new and unexpected connexion between the frequencies." He went on to say that this result is "quite unintelligible from the classical standpoint."

Different opinions about the interpretation of the quantum theory equations led to highly publicized discussions between Einstein and Bohr. Einstein argued that the quantum equations do not supply complete information and hence are incomplete. Bohr argued that the equations are complete and supply all information there is on any level. Currently most theoretical physicists support Bohr's view: the linear differential equations of Schrödinger and Dirac are complete and describe all that can be known about quantum mechanical events. Results of our Chapters 4 and 5 show this viewpoint to be incorrect.

Quantum theory is based upon a number of disparate axioms and, in contrast, electromagnetic field theory rests on only a few. Quantum theory also requires that the classical electromagnetic laws not fully apply within atoms. To some, it seems incongruous that nature should require such disparate and seemingly conflicting bases for such strongly overlapping sciences. To this end, Einstein (Einstein, 1959) wrote that: "I am, in fact, firmly convinced that the essentially statistical character of contemporary quantum theory is solely to be ascribed to the fact that this theory operates with an incomplete description of physical systems." He also said that he had devoted more time to thinking about this than any other subject. Although he believed that the mathematics of quantum theory was uniquely correct, he was bothered, for example, by the statistical nature of radiation onset from an atom that is initially in a high-energy state. He argued that either the atom is stable or it is unstable. If it is stable, it will not spontaneously decay and if it is unstable, it will begin the decay process without a time delay. Yet, atoms are stable until spontaneously undergoing a discontinuous energy drop and emitting a pulse of radiation. He concluded that the wave function description of these events is incomplete. He said: "Assuming the success of

efforts to accomplish a complete physics description, the statistical quantum theory would, within the frame-work of future physics, take an approximately analogous position to statistical mechanics within the framework of classical mechanics. I am rather firmly convinced that the development of theoretical physics will be of this type; but the path will be lengthy and difficult."

While attention was focused on discussions of quantum theory, advances in electromagnetism of ultimate consequence to quantum theory were being made. Mie (Mie, 1908) used the classical wave theory of light and spherical functions to analyze scattering of light by electrically small metallic particles. Forty years later Chu (Chu, 1948) showed emission of electromagnetic energy is necessarily accompanied by a source-associated standing energy. As the size-to-wavelength ratio decreases, the standing energy of radiated mode  $\ell$  increases as the inverse size-to-wavelength ratio raised to the  $(2\ell+1)$  power. Harrington (Harrington, 1960) showed that the maximum possible gain of a single radiated mode is not zero but  $\ell(\ell+1)$ . For atoms of diameter 0.1 nm and light of wavelength 500 nm, the standing energy that, by Chu's calculations, is necessary to support a maximum modal number that, by Harrington's calculations, is necessary to obtain an apparently infinite gain, is so large that the idea of fully directed energy emission is untenable.

During the next decade, Manley and Rowe (Manley and Rowe, 1956) derived the power-frequency relationships produced by nonlinear systems. The result would satisfactorily explain atomic power-frequency relationships if the atomic response was a nonlinear function of the driving force, but the quantum theory equations are linear. During the next decade Bell (Bell, 1964) proved inequalities that subject certain aspects of the philosophical discussions between Bohr and Einstein, as extended by Bohm, to experimental test. In 1981 and 1982 such tests were successfully conducted by Aspect, Grangier, and Roger. Bohm's discussion involves two electrons that have opposite spin but are otherwise in the same state. Results of the Aspect *et al.* experiments are that operating on one electron affects the other *without a measurable time delay* even when the electrons are spaced an arbitrarily large distance apart. The effect is known as electron nonlocality. Adding nonlocality to wave and particle properties shows electrons are even more complex than previously thought.

Since nonlocality does not prove that the quantum theory equations are incomplete, an obvious, widely accepted interpretation is the opposite one:

the quantum theory equations are complete. In Chapters 4 and 5, we supply a counter explanation.

## 6.2 Overview

Because the first analysis of standing energy about an antenna was published in 1948, during the developmental years between 1910 and 1935 the interpreters of modern quantum theory could not have known of its critical importance. Yet theoretical physicists constructed a logically coherent and complete interpretation of quantum mechanics; their success is testimony to the ingenuity of the participating individuals. The conceptual framework, however, comes at a significant cost: it requires rejection of causality in the sense that the dynamical structure of the universe at a given instant does not uniquely determine the dynamical structure at the next instant. We suggest that the non-causal interpretation of quantum theory is required largely because standing energy is ignored in atomic processes

The axioms upon which electromagnetic theory is based show no dependence upon the velocity of an observer, see Chapter 1; a conclusion is that the speed of light in free space is the same in all inertial frames of reference. In free space, the same axioms show no dependence upon the size of an observer; the conclusion appears to be that the equations apply equally well to all sizes. Experimental evidence shows that the axioms upon which electromagnetic theory are based apply equally well from the nanometer scale of electronic devices at least through the scale of galaxies. Yet, it is widely believed that selected parts of electromagnetic field theory break down within atoms. We suggest that the equations apply at least down to the picometer scale of dimensions, without restrictions. Belief to the contrary is caused, in large part, by an insufficient accounting of the affects of standing electromagnetic energy.

It has been recognized for more than seventy years that electrons act, in some circumstances, as a wave and, in other circumstances, as a particle. It has been recognized for nearly twenty years that eigenstate electrons are nonlocal. Although a detailed characterization of a nonlocal electron is unknown, understanding eigenstates requires a detailed analysis of the internal dynamics. Before addressing eigenstate electrons, note that there is a tendency to think that upon going from the macroscopic to the atomic scale of dimensions things will simplify. The notion has no logical or experimental basis. For example, early last century nuclei were considered to

consist of protons and neutrons as basic building blocks; we now know nucleons consist of quarks and gluons. Similarly, an electron is not a simple object and nonlocality seems to suggest that a trapped, stable, eigenstate electron be distributed over the full state independent of its size.

We show that as a Lorentz electron enters an eigenstate, it generates dipole radiation, thereby producing an encompassing electromagnetic energy field. That standing energy, in turn, produces an *expansive* radiation reaction force on the electron, of a magnitude at least as large as the Coulomb binding force, Eq. 4.2.14. Analyses based upon classical electromagnetism show that an expanded charge density has arrays of possible stable modal combinations. We postulate that the expansive radiation reaction force transforms a Lorentz electron into an eigenstate electron consisting of a dynamic ensemble of charge and current densities.

Combining energy conservation with the ensemble yields the Schrödinger wave equation as a statistical descriptor, Section 4.3, but *if and only if the ensemble is in equilibrium*. The linear equations of quantum theory apply to eigenstate electrons that are in equilibrium or in near-equilibrium, but not otherwise. This use of energy conservation applied to an ensemble of objects is very similar to the science of thermodynamics.

Although radiation by a Lorentz electron is, in the main, limited to electric dipole fields, Sections 3.11 and 4.13, radiation from the ensemble is not. If an ensemble structure generates electric dipole radiation, that radiation produces a force that drives higher order radiation of the parity  $E(\theta) = E(-\theta)$ : magnetic quadrupole, electric octupole radiation, etc. Similarly, if an ensemble structure generates magnetic dipole radiation, that radiation produces a force driving higher order radiation of parity  $E(\theta) = -E(-\theta)$ : electric quadrupole, magnetic octupole, etc. Neither set of parities, alone, is resonant. Quite differently, if the structure drives both parities, properly phased and oriented, the system is resonant, Section 3.17. In that case, the radiation reaction force regeneratively builds the radiation level. The reaction force due to this radiation, see Section 5.17, becomes thousands of times larger than the Coulomb binding force and dominates all other forces. One result is a rapid energy change between eigenstates, an energy jump. Another is that the Manley Rowe power-frequency relationships, Section 5.1, apply during the nonlinear process.

The radial components of the steady state photon fields are given by Eqs. 5.6.1 and 5.6.2, and the electric portion of the resulting radiation reaction pressure is shown by Eqs. 5.17.7 and 5.17.8. This radiation pressure is due to the local energy field and, even when truncated with inverse quartic



field terms, is many orders of magnitude larger than the pressure of Coulomb attraction. The sign of the force alternates with time. We expect it to force the radiating electron to undergo nova-like, expansive oscillations in the direction of radiation. Figure 6.2.1 illustrates the time variation of the radiation reaction pressure on a rigid, radiating spherical surface at a few Bohr radii. For clarity, phase dependence upon zenith angle is suppressed. Figure 6.2.1a is drawn for phase zero. The upper hemisphere cap represents an expansive pressure centered about the direction of telefield radiation and the lower hemisphere pressure is compressive. Figure 6.2.1.b shows the pressure at phase  $\pi/5$ . The expansive upper hemisphere pressure is decreased and the compressive lower hemisphere pressure is increased. Figures 6.2.1.c and 6.2.1.d are at phases  $2\pi/5$  and  $3\pi/5$  and entirely compressive. Figure 6.2.1e is at phase  $4\pi/5$ ; the upper hemisphere pressure is small but again expansive. Phase  $\pi$  returns to Fig. 6.2.1a. The configurational sequence is reminiscent of the action of a bellows.

### 6.3 The Radiation Scenario

Classical statistical mechanics analyzes an ensemble of identical particles. The particles are modeled as realistically as possible and there is little or no difficulty interpreting ensemble-averaged results. The state of the ensemble may be specified by the positions and velocities of the component particles, which are sufficient to determine the system energy. With statistical mechanics, studies of complicated systems are accomplished with no knowledge of the precise state of individual particles. The actual state is assumed the most probable state, and if there is full knowledge of an ensemble at a particular instant, its value at the next instant is predictable. A question fundamental to quantum theory is why an individual eigenstate electron acts as a statistical ensemble.

The radiation reaction force, see Eq. 4.2.14, provides at least a partial answer; it is an extensive force of magnitude greater than the attractive Coulomb force. Using an eigenstate ensemble as a physical basis, the Fourier integral transforms of Eqs. 4.3.7 describe the unknown physical realities. To match known experimental results, it is necessary for eigenstate electrons to contain a definite, but unknown, distribution of units of charge and current density; the smallest unit is determined by the discreteness of the charge distribution. The uncertainty of calculated results, Eq. 4.4.7, arises because

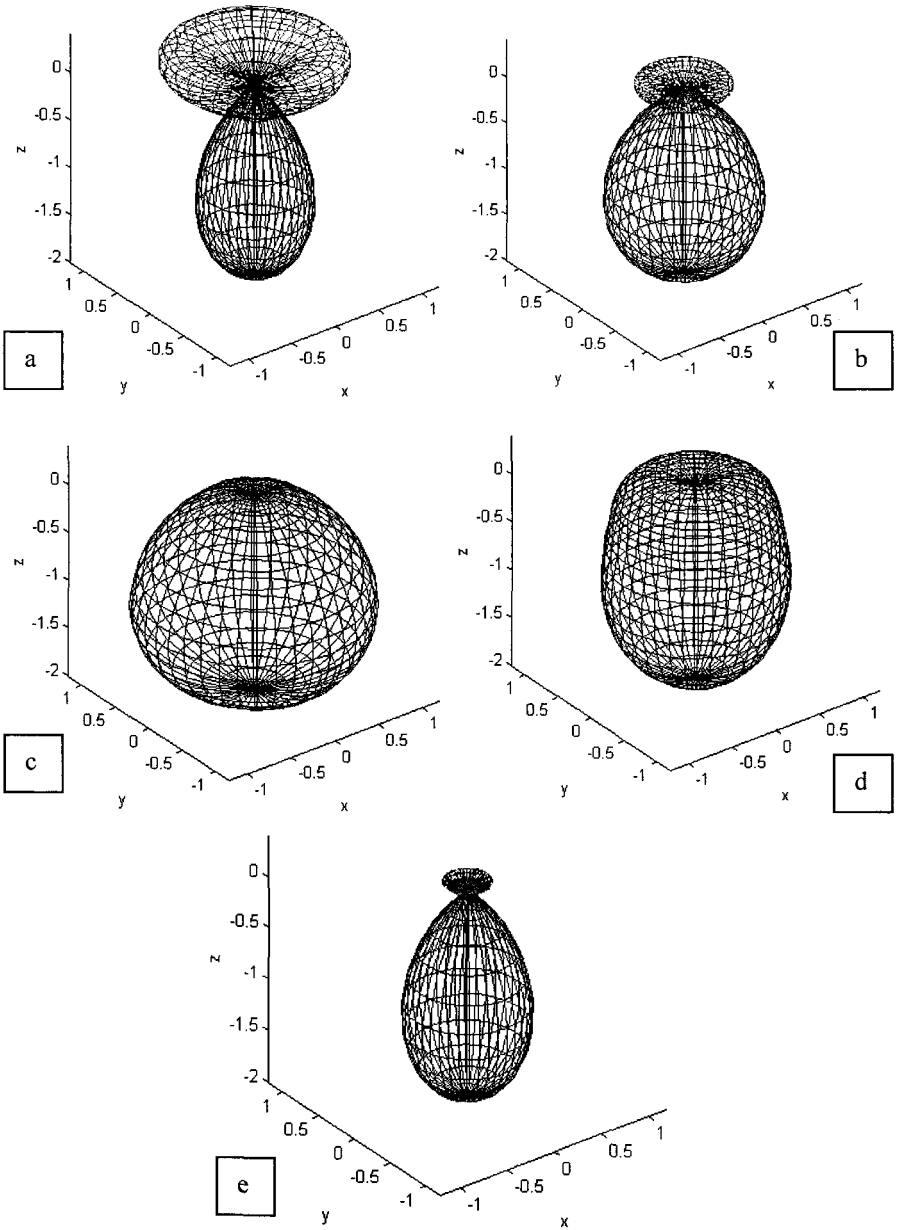


Figure 6.2.1 Time variation of radiation reaction pressure on a radiating electron at a mid-range value of  $L/(ka)$ . Phase variation with zenith angle is suppressed.

of incomplete information about the detailed structure of the charge and current distributions, not because of inherent properties of the distributions themselves. Causality applies in the sense that the detailed structure and kinematics of all charge and current densities at one instant uniquely determine the values at the next instant. Although this difference does not affect expectation values, it has a profound effect upon the interpretational philosophy and the characterization of measurable quantities. Causality also retains Einstein's deterministic view of atoms.

A set of resonant, regeneratively driven electromagnetic field modes, to which Chu's proof of the limiting value of  $Q$  versus electrical size does not apply, is shown in Section 3.17. The field set and certain properties are listed in Table 3.2.1. Section 5.5 and Eq. 5.5.18 show that radiation with the kinematic properties of photons result from imposing energy minimization as a boundary condition on a general multimodal expansion, the field set of Eq. 3.17.4. Therefore, fields with the kinematic properties of photons are resonant and are not subject to Chu's criterion about electrically small radiators. For this reason, large magnitudes of large order radiation modes are supported in the regeneratively driven radiation.

The nonlocal electron and classical electromagnetism not only predict fully directed electromagnetic energy exchanges, but also supply a complete expression for all fields that exist during the transition process. In this sense, the analysis is as complete as the energy exchanges by macroscopic biconical antennas, see Chapter 2. There is no way Einstein could have been aware these results were possible when he wrote that full directivity makes "a quantum theory of radiation almost unavoidable." The electromagnetic background necessary to understand this aspect of the physics was simply not available. The linear equations of quantum theory do not provide a description of the complete electromagnetic radiation. They describe only equilibrated states before and after transitions, Sections 4.3 and 4.5, and the equilibrium dipole moment of interaction between states that, in turn, determines the probability of a transition.

Equilibrium periods, during which the linear quantum theory equations apply, are separated by time hiatuses during which energy exchanges occur. As shown in Chapter 5, the initial radiation produces a radiation reaction force on the source that drives it regeneratively and produces more radiation. The process continues until all available energy is gone and the electron has entered a new energy state. Because the process is nonlinear the Manley Rowe equations apply to the radiation, the energy level changes, and only the initial and final electron states are occupied. There is no mixture of

states; that is, Schrödinger's cat is dead or alive, but not both. There is no way Dirac could know of the time hiatus during which linear equations do not apply when he wrote: "there is observed a new and unexpected connexion between the frequencies." Neither could Schrödinger have known of them when he wrote about "these damned jumps."

A charge with an intrinsic magnetic moment interacts with the closed circuit currents to produce a continuous torque. A continuous torque assures a dynamic configuration. Radiation begins when the ensemble configuration evolves into a configuration set that generates the multipolar moments of Table 3.17.2. For that set of moments, the reactive reaction force of Eq. 4.2.14 is nonexistent, only the real reaction force of Eq. 4.2.7 remains, and hence the regenerative energy exchange of Chapter 5 begins. In accordance with classical statistical mechanics, the initial details of the intra-electron structure and the governing laws determine the onset time of spontaneous decay. With this model, the primary difference between statistical and quantum mechanics is that statistical mechanics, in the main, deals with an ensemble of neutral particles and quantum mechanics does not.

If the length of the emitted, steady state wave train and the upper modal limit of the source fields are both infinite, the field is fully directed and retains its original shape and size over arbitrarily large values of time and distance. However, since both are finite, the size of the calculated steady state wave packet would slowly increase. Although the transient field solution that builds to and from the steady state value is unavailable, it necessarily describes flux closures for steady state flux lines. It is unknown if closures produce a fully directed wave packet; that is, it is unknown if the energy packet arriving from a distant star has the same physical extent it had when emitted or is extended over a larger volume. We know only that the total energy in the coherent wave packet remains constant as it travels through lossless space.

The descriptive transcendental terms in the field equations of Chapter 5 come, bit-by-bit, from each mode, see Eq. 5.8.11 and 5.8.12 for example, and are approached only if the maximum modal number is large. An important question is why the recursion formula of Eq. 5.5.15, the same recursion relationship that applies to spherical Bessel terms in a plane wave, is uniquely correct for quantized radiation. The reasons appear to be that only this particular recursion formula produces a set of z-axis transcendental fields that supports unidirectional energy flow to or from the source, and that only it produces a null for the standing energy. A greater or lesser dependence of modal coefficients upon modal number would result in fields

that depended upon all modes, not just the highest numbered one, see Eq. 5.11.1. For such a case, reactive energy that does not contribute to the regenerative drive would be present and the radiation reaction force of Eq. 4.2.14 would apply, braking power emission. The recursion relationship of Eq. 5.5.15 uniquely accomplishes two things: it avoids the radiation reaction of Eq. 4.2.14 and it meets the requirements of Section 3.17. Only with Eq. 5.5.15 is the radiation reaction force on an electron merely that caused by energy escaping from the system, Eq. 4.2.7.

Spherical Bessel functions give rise only to half the teledistant terms of Eqs. 5.13.6 through 5.13.8, the other half and all other terms come from spherical Neumann functions. Yet, all Poynting vector terms that describe unidirectional energy flow are products of a spherical Bessel term and a spherical Neumann function term. A possible radiation scenario is that the picostructure of an eigenstate evolves to produce the Neumann function terms of Eqs. 5.13.6 through 5.13.8, by which the source is immersed in its own standing energy field with no energy exchange. When an incoming plane wave, totally described by spherical Bessel functions, is applied to the system all needed field forms are present for radiation to occur. The incoming plane wave need only trigger a quantum of energy by providing terms with the needed phases. Planck could not have been aware of this when he wrote of extended photons “a quantum would never again be in a position to concentrate its energy at a spot strongly enough to detach an electron from its atom.”

As described herein, the primary historic obstacle to understanding atomic-level phenomena was that the principals lacked the tools necessary to account for the radiation reaction force of the generated fields, and they used a localized electron model. For these reasons, they were forced to conclude that electromagnetic field theory is not totally applicable within atoms. We show that consistent application of the full equations within atoms, without restrictions, leads to self-consistent results and removes the “strangeness” of quantum theory required by the historic interpretation.

## References

- Aspect, P. Grangier, G. Roger, "Experimental Tests of Realistic Local Theories via Bell's Theorem," *Phys. Rev. Lett.* Vol. 47, 460 (1981) and "Experimental Realization of Einstein-Podolsky-Rosen-Bohm Gedanken Experiment," *Phys. Rev. Lett.* Vol. 49, 92 (1982)
- J.S. Bell, "On the Einstein-Podolsky-Rosen Paradox," *Physics* Vol. 1, pp. 195-200 (1964), see also *Speakable and Unspeakable in Quantum Mechanics*, Cambridge Press (1987)
- N. Bohr, "On the Constitution of Atoms and Molecules," *Phil. Mag.* Vol. 26, 1-19 (1913), Also in *The World of the Atom*, H. A. Boorse and L. Motz, eds., Basic Books (1966) p. 751-765
- M. Born, E. Wolf, *Principles of Optics Electromagnetic Theory of Propagation, Interference and Diffraction of Light*, 3<sup>rd</sup> ed. Pergamon Press (1965)
- L.J. Chu, "Physical Limitations of Omni-Directional Antennas," *J. Appl. Phys.*, vol. 19, 1163-1175 (1948)
- P.A.M. Dirac, *The Principles of Quantum Mechanics*, 4<sup>th</sup> ed., Oxford Press (1958) pp. 1-2
- A. Einstein, "Concerning a Heuristic Point of View About the Creation and Transformation of Light," *Ann. Phys.* vol. 17, 132-148 (1905); also in *The World of the Atom*, H. A. Boorse and L. Motz, eds., Basic Books (1966) p. 544-557
- A. Einstein, "The Quantum Theory of Radiation," *Phys. Z.*, vol. 18, 121-128 (1917); also in *The World of the Atom*, H. A. Boorse and L. Motz, eds., Basic Books (1966) p. 888-901
- A. Einstein, "Reply to Criticisms" in *Albert Einstein, Philosopher and Scientist* (P.A. Schilpp, editor) Harper Torchbooks Science Library (1959) pp. 665-688
- R.F. Harrington, "Effect of Antenna Size on Gain, Bandwidth, and Efficiency," *J. Res. National Bureau of Standards* vol. 64D, 1-12 (1960)
- H. Hertz *Electric Waves: Researches on the Propagation of Electric Action with Finite Velocity Through Space* (1893) Translated by D. E. Jones, Dover Publications (1962)
- C. Huygens, "*Treatise on Light*," (1678) trans. by S.P. Thompson, Dover Publication (1912); also *The World of the Atom*, H. A. Boorse and L. Motz, eds., Basic Books (1966) pp. 69-85
- H.A. Lorentz, *The Theory of Electrons*, (1909) also Dover Publications 2<sup>nd</sup> ed., (1952); also Pais, A., "The Early History of the theory of the Electron: 1897-1947," in *Aspects of Quantum Theory*, A. Salam, P. Wigner, eds., Cambridge Press (1972) pp. 79-93
- J.M. Manley, H.E. Rowe, "Some general properties of nonlinear elements, Part I: General energy relations," *Proc. IRE*, vol. 44, pp. 904-913 (1956), and "General energy relations," *Proc. IRE* vol. 47, pp. 2115-2116 (1959)
- J.C. Maxwell, *A Treatise on Electricity and Magnetism*, 3<sup>rd</sup> ed., (1891) reprint Dover Publications (1954)

- J. Mehra, "'The Golden Age of Theoretical Physics': P. A. M. Dirac's Scientific Work from 1924-1933," in *Aspects of Quantum Theory*, Cambridge Press (1972) p. 45
- G. Mie, "A Contribution to Optical Extinction by Metallic Colloidal Suspensions," *Ann. Physik.* Vol. 25, p. 377 (1908)
- I. Newton, *Mathematical Principles of Natural Philosophy*, (1687) Translated by I.B. Cohen, A. Whitman, Univ. of California Press (1999)
- I. Newton, *Optiks*, (1704); Dover Publications (1952)
- R. Penrose, *The Emperor's New Mind Concerning Computers, Minds, and the Laws of Physics*, Penguin Books (1901)
- M. Planck, "The Origin and Development of the Quantum Theory," Nobel Prize in Physics Address, 1919, in *The World of the Atom*, H. A. Boorse and L. Motz, eds., Basic Books (1966) p. 491-501
- E. Schrödinger, *Ann. Phys.* Vol. 79, p. 489 (1926); also "Wave Mechanics," in *The World of the Atom*, H. A. Boorse and L. Motz, eds., Basic Books (1966) pp. 1060-1076
- E. Schrödinger, "Are There Quantum Jumps?" *Brit. J. for the Phil. of Sci.*, vol. 3, pp. 109-123 and 233-247, (1952)
- J.J. Thompson, "Cathode Rays," *Phil. Mag.* Vol. 44, pp. 293-311 (1897), also *The World of the Atom*, H. A. Boorse and L. Motz, eds., Basic Books (1966) pp. 416-426
- R.C. Tolman, *The Principles of Statistical Mechanics* (1938), reprinted by Dover Publications (1979)

# Appendix

## A.1 Introduction to Tensors

The application of field concepts to classical physics is made easier by the use of tensors. Tensor notation simplifies what would otherwise be tedious notational bookkeeping. The simplest and lowest rank tensor is a scalar, the next higher ranking tensor is a vector, and higher order tensors are referred to simply as tensors:

Rank	
$r = 0$	Scalar
$r = 1$	Vector
$r = 2$	Tensor

Table A.1.1 Properties of Tensors

The number of numbers that it takes to construct a tensor,  $N_0$ , depends upon the rank of the tensor and the number of dimensions. If  $N$  and  $r$  are, respectively, the number of dimensions and the rank, the number of numbers is:

$$N_0 = N^r \tag{A.1.1}$$

Independently of the number of dimensions, a scalar is fully described by a single number. Examples are the speed of light,  $c$ , and electron charge,  $q$ . Scalars have the same value in all inertial frames.

It takes as many numbers as there are dimensions to describe a vector. Example vectors are electric field intensity, velocity, and position. Let vector,  $\mathbf{A}$ , be known in three dimensions. The three numbers represent components along each of the three orthogonal coordinate axes,  $(x_1, x_2, x_3)$ .



If the same vector is determined using a set of axes rotated to new coordinate positions  $(x'_1, x'_2, x'_3)$  the result is the new vector components:

$$\begin{aligned} A'_1 &= A_1 \cos(x'_1, x_1) + A_2 \cos(x'_2, x_1) + A_3 \cos(x'_3, x_1) \\ A'_2 &= A_1 \cos(x'_1, x_2) + A_2 \cos(x'_2, x_2) + A_3 \cos(x'_3, x_2) \\ A'_3 &= A_1 \cos(x'_1, x_3) + A_2 \cos(x'_2, x_3) + A_3 \cos(x'_3, x_3) \end{aligned} \quad (\text{A.1.2})$$

The directional cosine of the angle between axis 'i' in the prime coordinates and axis 'j' in the unprimed coordinates is signified by  $\cos(x'_i, x_j)$ . Making the definition that the direction cosine  $c_{ik} = \cos(x'_i, x_k)$ , Eq. A.1.2 may take the more compact form:

$$A'_j = \sum_{k=1}^3 c_{jk} A_k \quad (\text{A.1.3})$$

It follows that:

$$A_r = \sum_{k=1}^3 c_{kr} A'_k \quad (\text{A.1.4})$$

An example of a second rank tensor is the stress tensor in crystals. Such a tensor transforms between coordinate systems as:

$$T'_{rs} = \sum_{i=1}^3 \sum_{j=1}^3 c_{ri} c_{sj} T_{ij} \quad (\text{A.1.5})$$

The number of direction cosines for a transformation between coordinates systems is the same as the rank of the tensor.

Like all other vectors, a position vector transforms between coordinate frames as:

$$\begin{aligned} x'_1 &= c_{11}x_1 + c_{12}x_2 + c_{13}x_3 \\ x'_2 &= c_{21}x_1 + c_{22}x_2 + c_{23}x_3 \\ x'_3 &= c_{31}x_1 + c_{32}x_2 + c_{33}x_3 \end{aligned} \quad (\text{A.1.6})$$

By definition the rotation matrix is:

$$c_{ij} = \begin{vmatrix} c_{11} & c_{12} & c_{13} \\ c_{21} & c_{22} & c_{23} \\ c_{31} & c_{32} & c_{33} \end{vmatrix} \quad (\text{A.1.7})$$

The length of a differential vector in three dimensions is:

$$(\Delta r)^2 \equiv (\Delta x'_1)^2 + (\Delta x'_2)^2 + (\Delta x'_3)^2 \equiv (\Delta x_1)^2 + (\Delta x_2)^2 + (\Delta x_3)^2 \quad (\text{A.1.8})$$

The transformation equalities derived from Eqs. A.1.8 are:

$$c_{11}^2 + c_{21}^2 + c_{31}^2 = 1 = c_{12}^2 + c_{22}^2 + c_{32}^2 = c_{13}^2 + c_{23}^2 + c_{33}^2 \quad (\text{A.1.9})$$

This may be written as

$$\sum_{i=1}^3 c_{ij}c_{ij} = 1 \quad \text{and} \quad \sum_{i=1}^3 c_{ij}c_{ik} = 0; \quad j \neq k$$

Define the Kronecker delta function to be

$$\delta_{jk} = 1 \quad \text{if } j = k; \quad \delta_{jk} = 0 \quad \text{if } j \neq k \quad (\text{A.1.10})$$

With the definition, the condition on directional cosines may be written more compactly as:

$$\sum_{i=1}^3 c_{ij}c_{ik} = \delta_{jk} \quad (\text{A.1.11})$$

An exercise is to show that

$$\det|c_{ij}| = 1 \quad (\text{A.1.12})$$

Solution: Let the volume of cube  $x_1x_2x_3$  be equal to one. The volume in the transformed coordinates is unchanged by describing it in another frame, so it too is equal to one. The volume is given by:

$$V = \mathbf{x}'_1 \bullet (\mathbf{x}'_2 \times \mathbf{x}'_3) = 1$$

Writing out cross products in terms of directional cosines gives:

$$\mathbf{x}'_2 \times \mathbf{x}'_3 = x_1(c_{22}c_{33} - c_{23}c_{32}) + x_2(c_{33}c_{11} - c_{31}c_{13}) + x_3(c_{11}c_{22} - c_{12}c_{21})$$

From which it follows that:

$$\mathbf{x}'_1 \bullet (\mathbf{x}'_2 \times \mathbf{x}'_3) = \begin{bmatrix} c_{11}(c_{22}c_{33} - c_{23}c_{32}) + c_{12}(c_{23}c_{31} - c_{21}c_{33}) \\ + c_{13}(c_{21}c_{32} - c_{22}c_{31}) \end{bmatrix}$$

The determinant of  $c_{ij}$  is:

$$|c_{ij}| = c_{11}(c_{22}c_{33} - c_{23}c_{32}) + c_{12}(c_{23}c_{31} - c_{21}c_{33}) + c_{13}(c_{21}c_{32} - c_{22}c_{31})$$

Comparison shows that

$$|c_{ij}| = 1$$

## A.2 Tensor Operations

A common summation convention that reduces the number of symbols that would otherwise be required is that if an index occurs twice a summation over all possible values is required. That is:

$$c_{ij}c_{ik} = \delta_{jk} \quad (\text{A.2.1})$$

Consider some arithmetic operations on tensor fields. Tensor addition is defined only for tensors of equal rank; for example, addition of a scalar and a vector is not defined. Addition of tensors of equal rank is by:

$$C_{ij} = A_{ij} + B_{ij} \quad (\text{A.2.2})$$

Proof consists of showing that the sum obeys the coordinate rotation properties of a second rank tensor. In Eq. A.2.2 indices 'i' and 'j' appear only once in each term and, therefore, are running indices. Equation A.2.2 consists of nine separate summations.

Subtraction is accomplished by multiplying  $B_{ij}$  by minus one and adding.

Multiplication is defined between tensors of arbitrary rank. By definition,

$$C_{i..jr..s} = A_{i..j} B_{r..s} \quad (\text{A.2.3})$$

The rank of C is the sum of the ranks of A and B. For example the product of vector  $A_i$  and scalar  $a$  is  $aA_i$ , another vector. The product between two vectors is a second rank tensor, for example the product of  $A_i$  and  $B_j$  is  $C_{ij} = A_i B_j$ , where indices 'i' and 'j' are both running indices;  $C_{ij}$  represents nine numbers.

Division by tensors other than rank zero is not defined.

In addition to these scalar-like arithmetic operations there are operations confined to tensors.

Tensor contraction is accomplished by equating two indices. Equal indices signify a summation and summation results in a tensor reduced in rank by two from the initial one. The process is, therefore, restricted to tensors of rank  $r \geq 2$ . As an example:

$$A'_{rstu} = c_{ri} c_{sj} c_{tk} c_{ul} A_{ijkl} \quad (\text{A.2.4})$$

After equating 's' and 't' and summing:

$$A'_{rssu} = c_{ri} c_{sj} c_{sk} c_{ul} A_{ijkl} \quad (\text{A.2.5})$$

Since:

$$c_{sj} c_{sk} = \delta_{jk} \quad \text{and} \quad A'_{rssu} = c_{ri} c_{ul} A_{ijj\ell} \quad (\text{A.2.6})$$

This is a tensor of rank two less than the starting one.

A common example is the scalar product between two vectors,  $A_i$  and  $B_j$ . To evaluate, begin with the product:

$$C_{ij} = A_i B_j \quad (\text{A.2.7})$$

Equating indices 'i' and 'j' and summing over the indices gives:

$$C_{ii} = A_i B_i = D \quad (\text{A.2.8})$$

The product forms scalar D.

### A.3 Tensor Symmetry

Physically real tensors are either symmetric or antisymmetric. Terms of different symmetry are defined as:

$$\begin{array}{ll} \text{Symmetric tensor} & A_{rstu} = A_{rtsu} \\ \text{Antisymmetric tensor} & A_{rstu} = -A_{rtsu} \end{array} \quad (\text{A.3.1})$$

Symmetric and antisymmetric tensors have, respectively,  $N(N+1)/2$  and  $N(N-1)/2$  terms.

An important special case is a three dimensional tensor of rank two, say  $T_{ij}$ . Such tensors transform as:

$$T'_{ij} = c_{ir} c_{js} T_{rs} \quad (\text{A.3.2})$$

Equation A.3.2 is short hand notation for the nine terms of  $T'_{ij}$ , each of which contains nine separate numbers. For example:

$$T'_{12} = c_{1r} c_{2s} T_{rs} = \left[ \begin{array}{l} c_{11}c_{21}T_{11} + c_{11}c_{22}T_{12} + c_{11}c_{23}T_{13} \\ + c_{12}c_{21}T_{21} + c_{12}c_{22}T_{22} + c_{12}c_{23}T_{23} \\ + c_{13}c_{21}T_{31} + c_{13}c_{22}T_{32} + c_{13}c_{23}T_{33} \end{array} \right] \quad (\text{A.3.3})$$

If  $T_{ij}$  is antisymmetric,  $T_{ij} = -T_{ji}$  and the transformation simplifies to:

$$\begin{array}{l} T'_{23} = c_{11}T_{23} + c_{12}T_{31} + c_{13}T_{12} \\ T'_{31} = c_{21}T_{23} + c_{22}T_{31} + c_{23}T_{12} \\ T'_{12} = c_{31}T_{23} + c_{32}T_{31} + c_{33}T_{12} \end{array} \quad (\text{A.3.4})$$

The proof of Eq. A.3.4 follows by writing out the terms in the form:

$$\begin{aligned} T'_{12} &= \begin{bmatrix} 0 + c_{11}c_{22}T_{12} - c_{11}c_{23}T_{31} \\ -c_{12}c_{21}T_{12} + 0 + c_{12}c_{23}T_{23} \\ +c_{13}c_{21}T_{31} - c_{13}c_{22}T_{23} + 0 \end{bmatrix} \\ &= (c_{11}c_{22} - c_{12}c_{21})T_{12} + (c_{12}c_{23} - c_{13}c_{22})T_{23} + (c_{13}c_{21} - c_{11}c_{23})T_{31} \end{aligned}$$

Similarly:

$$T'_{23} = (c_{21}c_{32} - c_{22}c_{31})T_{12} + (c_{22}c_{33} - c_{23}c_{32})T_{23} + (c_{23}c_{31} - c_{21}c_{33})T_{31}$$

From the determinant:

$$c_{11}(c_{22}c_{33} - c_{23}c_{32}) + c_{12}(c_{23}c_{31} - c_{21}c_{33}) + c_{13}(c_{21}c_{32} - c_{22}c_{31}) = 1$$

Combining this result with  $c_{ij}c_{ik} = \delta_{jk}$  results in:

$$c_{11}c_{11} + c_{12}c_{12} + c_{13}c_{13} = 1$$

The latter two equations combine to show that:

$$c_{11} = (c_{22}c_{33} - c_{23}c_{32}); \quad c_{12} = (c_{23}c_{31} - c_{21}c_{33}); \quad c_{13} = (c_{21}c_{32} - c_{22}c_{31})$$

Substitution of this result back into the expansion results in Eq. A.3.4.

This result shows that an antisymmetric second rank tensor,  $T_{ij}$ , transforms like a vector. It is tempting to call it a vector, but if the coordinate system is switched from a right hand system to a left hand system the components change sign. It is therefore a pseudovector.

## A.4 Differential Operations on Tensor Fields

The gradient operation increases the rank of a tensor by one. As an example, let  $\sigma(\mathbf{r})$  represent a scalar field. Taking the partial differential:

$$\frac{\partial \sigma(\mathbf{r})}{\partial x_i} = V_i \quad (\text{A.4.1})$$

Make the equality:

$$\frac{\partial \sigma(\mathbf{r})}{\partial x_i} = \frac{\partial x'_j}{\partial x_i} \frac{\partial \sigma(\mathbf{r})}{\partial x'_j} = c'_{ij} V_j$$

Combining gives:

$$V_i = c'_{ij} V'_j \quad (\text{A.4.2})$$

Since  $V_i$  transforms as a vector, it is a vector. This gradient operation may be conducted on a tensor of any rank. For example,

$$T_{ij..kl} = \frac{\partial R_{ij..k}}{\partial x_\ell} \quad (\text{A.4.3})$$

The divergence operation decreases the rank of a tensor by one.

$$\sigma(\mathbf{r}) = \frac{\partial V_i}{\partial x_\ell} \quad (\text{A.4.4})$$

To show that  $\sigma(\mathbf{r})$  is a scalar, write it as:

$$\sigma(\mathbf{r}) = \frac{\partial x'_k}{\partial x_i} \frac{\partial (c'_{ij} V'_j)}{\partial x'_k} = c'_{ij} c'_{ik} \frac{\partial V'_j}{\partial x'_k} = \frac{\partial V'_j}{\partial x'_j} = \sigma'(\mathbf{r}) \quad (\text{A.4.5})$$

The divergence operation may be conducted on tensors of any rank.

$$T_{i..j} = \frac{\partial R_{i..jk}}{\partial x_k}, \quad (\text{A.4.6})$$

Proof follows in the same way as for Eq. A.4.4.

The curl operation begins with the vector differential operation:

$$T_{i..j..kn} = \frac{\partial R_{i..j..k}}{\partial x_n} - \frac{\partial R_{i..n..k}}{\partial x_j} \quad (\text{A.4.7})$$

This increases the rank by one. A particularly useful special case is for vectors. Let:

$$T_{in} = \frac{\partial R_i}{\partial x_n} - \frac{\partial R_n}{\partial x_i} \quad (\text{A.4.8})$$

Note that since  $T_{ij}$  is antisymmetric it has  $N(N-1)/2$  independent numbers. In three dimensions, it has three, the same as a vector and we already saw that antisymmetric second rank tensors transform like a vector. Therefore, the curl of a vector changes the vector to an antisymmetric second rank tensor that is pseudovector. The pseudovector acts like a vector in any given coordinate system but changes sign if the systems are changed from a left to right hand system.

- 
- |    |   |
|----|---|
| 1. | $\mathbf{A} \times (\mathbf{B} \times \mathbf{C}) = \mathbf{B}(\mathbf{A} \cdot \mathbf{C}) - \mathbf{C}(\mathbf{A} \cdot \mathbf{B})$  |
| 2. | $\text{grad}(\phi\psi) = \nabla(\phi\psi) = \phi\nabla\psi + \psi\nabla\phi$  |
| 3. | $\text{div}(\phi\mathbf{A}) = \nabla \cdot (\phi\mathbf{A}) = \phi\nabla \cdot \mathbf{A} + \nabla\phi \cdot \mathbf{A}$  |
| 4. | $\text{curl}(\phi\mathbf{A}) = \nabla \times (\phi\mathbf{A}) = \phi\nabla \times \mathbf{A} + \nabla\phi \times \mathbf{A}$  |
| 5. | $\nabla \cdot (\mathbf{A} \times \mathbf{B}) = \mathbf{B} \cdot (\nabla \times \mathbf{A}) - \mathbf{A} \cdot (\nabla \times \mathbf{B})$   |
| 6. | $\nabla \times (\mathbf{A} \times \mathbf{B}) = \mathbf{A}(\nabla \cdot \mathbf{B}) - \mathbf{B}(\nabla \cdot \mathbf{A}) + (\mathbf{B} \cdot \nabla)\mathbf{A} - (\mathbf{A} \cdot \nabla)\mathbf{B}$          |
| 7. | $\nabla(\mathbf{A} \cdot \mathbf{B}) = \mathbf{A} \times (\nabla \times \mathbf{B}) + \mathbf{B} \times (\nabla \times \mathbf{A}) + (\mathbf{B} \cdot \nabla)\mathbf{A} + (\mathbf{A} \cdot \nabla)\mathbf{B}$ |
| 8. | $\nabla^2(1/r) = 0, \text{ if } r > 0$  |
| 9. | $\nabla^2 \mathbf{A} = \nabla(\nabla \cdot \mathbf{A}) - \nabla \times (\nabla \times \mathbf{A})$  |
- 

Table A.4.1 Table of Vector Properties

10.	$\oint \mathbf{A} \cdot d\mathbf{S} = \int (\nabla \cdot \mathbf{A}) dV$
11.	$\oint \phi d\mathbf{S} = \int (\nabla\phi) dV$
12.	$\oint \mathbf{A} \times d\mathbf{S} = -\int (\nabla \times \mathbf{A}) dV$

Table A.4.2 Integrals over closed surfaces



---

13.	$\oint \phi d\ell = \int d\mathbf{S} \times \nabla \phi$
14.	$\oint \mathbf{A} \cdot d\ell = \int (\nabla \times \mathbf{A}) \cdot d\mathbf{S}$

---

Table A.4.3 Integrals over open surfaces

## A.5 Green's Function

The 4-Laplacian of the electromagnetic potential is defined by Eq. 1.5.4, and repeated here:

$$\frac{\partial^2 A_\nu}{\partial X_\beta \partial X_\beta} = -\mu J_\nu \quad (\text{A.5.1})$$

We seek to integrate that differential equation in order to obtain a general expression for the electromagnetic potential itself. For this purpose, it is helpful to define a similar but simpler function, to integrate that function, then to use the integral to obtain an expression for the electromagnetic potential. The function is Green's function  $G(X_\alpha, X'_\alpha)$ . By definition it is:

$$\frac{\partial^2 G(X_\alpha, X'_\alpha)}{\partial X_\beta \partial X_\beta} = -[\delta(X_\alpha - X'_\alpha)]^4 \quad (\text{A.5.2})$$

In Eq. A.5.2, the four-dimensional delta function indicates the Dirac delta. By definition the one dimensional Dirac delta function satisfies the integral relationship:

$$\int f(x) d(x - x') dx = \begin{cases} f(x') \\ 0 \end{cases} \quad (\text{A.5.3})$$

The upper or lower solution applies if the range of integration respectively does or does not include  $x'$ . The integrand magnitude of a Dirac delta function increases without limit and the width  $\Delta x$  decreases without limit in a way that retains a product value of one.

Construct the equation:

$$\int d[g(x) - g(x')] dx = \int \left( \frac{d[g(x) - g(x')]}{dg(x)/dx} \right) dg(x)$$

It follows from the definition of the delta function that

$$\int f(x) d[g(x) - g(x')] dx = \frac{f(x)}{dg(x)/dx} \Big|_{x=x'} \quad (\text{A.5.4})$$

The method used to integrate Eq. A.5.1 is a four-dimensional extension of a common three-dimensional technique. The procedure begins with the quadruple integral:

$$\iiint \left\{ A_\alpha \frac{\partial^2 G}{\partial X_\beta \partial X_\beta} - G \frac{\partial^2 A}{\partial X_\beta \partial X_\beta} \right\} dX_1 dX_2 dX_3 dX_4 = 0 \quad (\text{A.5.5})$$

The equality results since all integrals are evaluated at  $\pm\infty$  and the integrand decreases with distance rapidly enough so the integral is zero at the infinite limits. Substituting Eq. A.5.2 into the first term in the integrand and substituting Eq. A.5.1 into the second gives:

$$A_\alpha(X_\beta) = \mu \iiint J_\alpha(X'_\gamma) G(X'_\gamma, X_\gamma) dX_1 dX_2 dX_3 dX_4 \quad (\text{A.5.6})$$

Since  $J_\alpha(X'_\gamma)$  is known but  $G(X'_\gamma, X_\gamma)$  is not, it is necessary to solve for  $G(X'_\gamma, X_\gamma)$  using Eq. A.5.6 before, in turn, solving for  $A_\alpha(X_\beta)$ . For this purpose, consider an aside on the four dimensional Fourier transform pair:

$$\begin{aligned} F(X_\gamma) &= \left( \frac{1}{2\pi} \right)^2 \iiint H(K_\gamma) e^{-iX_\gamma K_\gamma} dK_1 dK_2 dK_3 dK_4 \\ H(K_\gamma) &= \left( \frac{1}{2\pi} \right)^2 \iiint F(X_\gamma) e^{iX_\gamma K_\gamma} dX_1 dX_2 dX_3 dX_4 \end{aligned} \quad (\text{A.5.7})$$

$K_\gamma$  and  $X_\gamma$  are unknown conjugate variables that are to be determined. Making the definition that:

$$F(X_\gamma) = [\delta(X_\gamma - X'_\gamma)]^4 \quad (\text{A.5.8})$$

Combining Eqs. A.5.7 and A.5.8 results in:

$$\begin{aligned} [\delta(X_\gamma - X'_\gamma)]^4 &= \left(\frac{1}{2\pi}\right)^2 \iiint \int e^{-iK_\gamma(X_\gamma - X'_\gamma)} dK_1 dK_2 dK_3 dK_4 \\ H(K_\gamma) &= \left(\frac{1}{2\pi}\right)^2 e^{iK_\gamma X'_\gamma} \end{aligned} \quad (\text{A.5.9})$$

It is convenient to introduce an additional function,  $g(K_\gamma)$ , defined by the equation:

$$G(X_\gamma, X'_\gamma) = \iiint \int g(K_\alpha) e^{-iK_\gamma(X_\gamma - X'_\gamma)} dK_1 dK_2 dK_3 dK_4 \quad (\text{A.5.10})$$

To solve for the function  $g(K_\gamma)$  consider, as an example, the conjugate pair  $x$  and  $k_x$  to be a single dimension of Eqs. A.5.2 and A.5.9 with the equalities:

$$\begin{aligned} \frac{\partial^2 G(x - x')}{\partial x^2} &= -\delta(x - x') \\ \delta(x - x') &= \left(\frac{1}{2\pi}\right) \end{aligned} \quad (\text{A.5.11})$$

$$G(x, x') = \int g(k_x) e^{-ik_x(x - x')} dk_x$$

Differentiating  $G(x, x')$  twice with respect to  $x$  gives

$$\delta(x - x') = k_x^2 \int g(k_x) e^{-ik_x(x - x')} dk_x \quad (\text{A.5.12})$$

Combining gives:

$$k_x^2 g(k_x) = \frac{1}{2\pi} \quad (\text{A.5.13})$$

Extension to four dimensions gives:

$$g(K_\gamma) = \left(\frac{1}{2\pi}\right)^2 \frac{1}{K_\alpha K_\alpha} \quad (\text{A.5.14})$$

Substituting Eq. A.5.14 back into Eq. A.5.10 results in:

$$G(X_\gamma, X'_\gamma) = \left(\frac{1}{2\pi}\right)^4 \iiint \frac{e^{-iK_\gamma(X_\gamma - X'_\gamma)}}{K_\alpha K_\alpha} dK_1 dK_2 dK_3 dK_4 \quad (\text{A.5.15})$$

It is convenient to use three-dimensional notation to evaluate Eq. A.5.15. For this purpose note that the four variable set  $(x, y, z, ict)$  is complex and, if the exponentials are to remain oscillating functions, it is necessary that the conjugate variable set  $K_\alpha$  also be complex. Writing it as  $(k_x, k_y, k_z, i\omega/c)$  and substituting into Eq. A.5.15 gives:

$$G(X_\gamma, X'_\gamma) = \frac{i}{c} \left(\frac{1}{2\pi}\right)^4 \iiint \frac{e^{-iK_\gamma(X_\gamma - X'_\gamma)}}{k^2 - \omega^2} d\mathbf{k} d\omega \quad (\text{A.5.16})$$

where

$$k^2 = k_x^2 + k_y^2 + k_z^2; \quad d\mathbf{k} = dk_x dk_y dk_z \quad (\text{A.5.17})$$

Equation A.5.16 is the sum of two Cauchy integrals, integrals that may be evaluated by use of the Cauchy integral identity:

$$2\pi i f(z') = \oint \frac{f(z)}{z - z'} dz \quad (\text{A.5.18})$$

Introducing  $p$  as a small, real, positive number used as a construction tool whose value is eventually put equal to zero, Eq. A.5.16 may be written as:

$$G(X_\gamma, X'_\gamma) = \frac{ic}{(2\pi)^4} \iiint d\mathbf{k} \oint \frac{d\omega e^{-iK_\gamma(X_\gamma - X'_\gamma)}}{(\omega - ck - ip)(\omega + ck + ip)}$$

Moving the space portion of the exponential out from under the time-dependent integral results in:

$$G(X_\gamma, X'_\gamma) = \frac{ic}{(2\pi)^4} \iiint d\mathbf{k} e^{-i\mathbf{k} \cdot \mathbf{r}} \oint \frac{d\omega e^{-i\omega(t-t')}}{(\omega - ck - ip)(\omega + ck + ip)} \quad (\text{A.5.19})$$

Restating, the problem is that given an electric charge at  $(\mathbf{r}', t')$  to find the function  $G(X_\gamma, X'_\gamma)$ . The field is zero before the charge is introduced. That is, with  $t'' = t - t'$  all fields are zero for  $t'' < 0$ . The last integral of Eq. A.5.19 may be evaluated first along the real axis and then back around an infinite, complex  $\omega$  path. For  $t'' < 0$  the return path encompasses the lower half-plane, where no poles are enclosed. For  $t'' > 0$  the return path is around the upper half of the complex plane, where two poles are enclosed. Evaluation of the integral gives:

$$\oint \frac{d\omega e^{-i\omega t''}}{(\omega - ck - ip)(\omega + ck + ip)} = 2\pi i \left[ \frac{e^{-it''(ck+ip)}}{2ck} - \frac{e^{-it''(-ck+ip)}}{2ck} \right] = \frac{2\pi}{ck} \sin(ckt'') \quad (\text{A.5.20})$$

Combining Eqs. A.5.20 and A.5.21 gives:

$$G(X_\gamma, X'_\gamma) = \frac{i}{(2\pi)^3} \iiint \frac{1}{k} d\mathbf{k} e^{-i\mathbf{k} \cdot \mathbf{r}} \sin(ckt'') \quad (\text{A.5.21})$$

Next let  $\mathbf{R}$  be the space vector from source point  $\mathbf{r}'$  to field point  $\mathbf{r}$ , and choose it to be in the  $z$ -direction. Then  $\mathbf{k} \cdot \mathbf{r} = kR \cos\theta$  where  $\theta$  is the polar angle. Also, replace  $d\mathbf{k}$  with  $k^2 dk \sin\theta d\theta d\phi$ :

$$G(X_\gamma, X'_\gamma) = \frac{i}{(2\pi)^3} \iiint k dk \sin\theta d\theta d\phi e^{-ikR \cos\theta} \sin(ckt'') \quad (\text{A.5.22})$$

Evaluating the angular integrals over an enclosing sphere gives:

$$G(X_\gamma, X'_\gamma) = \frac{2i}{(2\pi)^2} \int_0^\infty \frac{dk}{R} \sin(kR) \sin(ckt'') \quad (\text{A.5.23})$$

Since the integral of Eq. A.5.23 is an even function of  $k$ , it may, without changing the value of the integral, be replaced by the equation:

$$G(X_\gamma, X'_\gamma) = \frac{i}{8\pi^2 R} \int_{-\infty}^{\infty} dk \left[ e^{-i(\omega t'' - kR)} - e^{i(\omega t'' + kR)} \right] \quad (\text{A.5.24})$$

Equation A.5.10 shows that Eq. A.5.24 is the sum of two Dirac delta functions. The second one is evaluated at advanced time  $t'' < 0$  when there are no charges, and if causality applies all results from it are equal to zero. Working with the retarded time  $t'' > 0$  when there are charges, using Eq. A.5.3 it follows that:

$$\delta(R - ct'') = -\frac{1}{c} \delta(t'' - R/c) \quad (\text{A.5.25})$$

Combining with the first term in the integrand of Eq. A.5.24 gives:

$$G(X_\gamma, X'_\gamma) = \frac{1}{4\pi R c} \delta(t' - R/c) \quad (\text{A.5.26})$$

This completes the derivation of  $G(X_\gamma, X'_\gamma)$ .

## A.6 The Potentials

To obtain potential  $A_\nu$  of a moving charge density, substitute Eq. A.5.26 into Eq. A.5.5. The result is:

$$A_\nu(X_\gamma) = \frac{\mu}{4\pi} \iiint dV' \int dt' \frac{J_\nu(X'_\alpha)}{R(X_\gamma, X'_\gamma)} \delta(t' - R/c) \quad (\text{A.6.1})$$

Distance  $R(X_\gamma, X'_\gamma)$  is the distance between the source and field points. Using Eq. A.5.3 to evaluate Eq. A.6.1 gives:

$$A(\mathbf{r}, t) = \frac{\mu}{4\pi} \iiint \frac{J(\mathbf{r}', t)}{(R - \mathbf{R} \cdot \mathbf{v}/c)} dV'$$

$$\Phi(\mathbf{r}, t) = \frac{\mu}{4\pi} \iiint \frac{\rho(\mathbf{r}', t)}{(\mathbf{R} - \mathbf{R} \cdot \mathbf{v}/c)} dV' \quad (\text{A.6.2})$$

Equation A.6.2 is the final form for the electromagnetic 4-potential of a moving charge. Distance from the point of field emission to the field point when the radiation is received. These are the Liénard-Wiechert potentials.

To obtain the potential  $A_v$  of an oscillating charge density, note that Eq. A.6.2 remains applicable except, for this case, the average velocity of the oscillating charge is zero. The resulting equation is:

$$A_{0v}(\mathbf{r})e^{i\omega t} = \frac{\mu}{4\pi} \int dV' \int dt' \frac{J_{0v}(\mathbf{r}', t')}{R(\mathbf{r}, \mathbf{r}')} \delta(t', t - R/c) \quad (\text{A.6.3})$$

Subscripts “0” indicate the value is independent of time. Applying Eq. A.6.3 to a differential volume in space gives shows that in three dimensions the potentials at position  $\mathbf{r}$  due to a current density are given by:

$$A(\mathbf{r})e^{i\omega t} = \frac{\mu}{4\pi} \int \frac{J(\mathbf{r}')e^{i\omega(t-R/c)}}{R(\mathbf{r}, \mathbf{r}')} dV' \quad (\text{A.6.4})$$

$$\Phi(\mathbf{r})e^{i\omega t} = \frac{1}{4\pi\epsilon} \int \frac{\rho(\mathbf{r}')e^{i\omega(t-R/c)}}{R(\mathbf{r}, \mathbf{r}')} dV'$$

These are the retarded potentials.

## A.7 Equivalent Sources

It is shown in Section 1.10 that the force fields satisfy the partial differential equations:

$$\nabla \times (\nabla \times \mathbf{E}) + \epsilon\mu \frac{\partial^2 \mathbf{E}}{\partial t^2} = 0 \quad \text{and} \quad \nabla \times (\nabla \times \mathbf{B}) + \epsilon\mu \frac{\partial^2 \mathbf{B}}{\partial t^2} = 0 \quad (\text{A.7.1})$$

Other helpful relationships are:

$$\nabla \times (\nabla \times \mathbf{E}) = \nabla(\nabla \cdot \mathbf{E}) - \nabla^2 \mathbf{E} \quad \text{and} \quad \epsilon\mu \frac{\partial^2 \mathbf{E}}{\partial t^2} = -\kappa^2 \mathbf{E} \quad (\text{A.7.2})$$

Combining the two equations shows that:

$$\nabla^2 \mathbf{E} + \kappa^2 \mathbf{E} = 0 \quad \text{and} \quad \nabla^2 \mathbf{B} + \kappa^2 \mathbf{B} = 0 \quad (\text{A.7.3})$$

These are the Helmholtz equations for the field intensities. In rectangular coordinates the form of the vector and scalar Laplacian operators are identical.

The objective is to obtain expressions for the field vectors at any field point,  $\mathbf{r}(x,y,z)$ , external to a field-generating volume as a function of field values on the surface of the volume. The development requires three vector integral equations, the divergence theorem and two related ones. Let  $dS$  represent a scalar differential area on the surface of the volume and  $\mathbf{n}$  be a unit vector directed normal to the surface at the same point. At the surface, fields  $\mathbf{F}$  and  $\phi$  have the continuity properties of electromagnetic fields: they are continuous with continuous first derivatives.

$$\oint dS \cdot \mathbf{F} = \int \nabla \cdot \mathbf{F} dV \quad \oint dS \times \mathbf{F} = \int \nabla \times \mathbf{F} dV \quad \oint \phi dS = \int \nabla \phi dV \quad (\text{A.7.4})$$

Next let  $\phi$  and  $\psi$  each represent scalar fields and construct the function  $\phi \nabla \psi$ . Substituting the new function into the divergence equation gives:

$$\oint \phi \nabla \psi \cdot dS \equiv \int \nabla \cdot (\phi \nabla \psi) dV = \int [\nabla \phi \cdot \nabla \psi + \phi \nabla^2 \psi] dV \quad (\text{A.7.5})$$

Reversing the roles of  $\phi$  and  $\psi$  and subtracting the result from Eq. A.7.5 gives

$$\oint [\phi \nabla \psi - \psi \nabla \phi] \cdot dS = \int [\phi \nabla^2 \psi - \psi \nabla^2 \phi] dV \quad (\text{A.7.6})$$

For the special case of an oscillating charge, the defining equation for Green's function, Eq. A.5.1, in three-dimensional form satisfies an equation similar to that of the Helmholtz wave equation. With point  $\mathbf{r}'(x',y',z')$  representing the source position:



$$\nabla^2 G(\mathbf{r}, \mathbf{r}') + k^2 G(\mathbf{r}, \mathbf{r}') = -\delta(\mathbf{r}, \mathbf{r}') \quad (\text{A.7.7})$$

In free space, the solution is:

$$G(\mathbf{r}, \mathbf{r}') = -\frac{e^{-ik\phi(\mathbf{r}-\mathbf{r}')}}{R(\mathbf{r}, \mathbf{r}')} \quad (\text{A.7.8})$$

The objective is to construct a virtual sphere about a source then to calculate the fields at an arbitrary field point,  $\mathbf{r}(x, y, z)$ , in terms of the fields that exist on the surface of the virtual sphere. In this way, the fields can be obtained without knowledge of the source itself. For this purpose, begin by substituting into Eq. A.7.6 that  $\phi = G$  and  $\psi$  is equal to one component of the electric field intensity. Then repeat twice with  $\psi$  representing the other electric field components and sum over the three equations. The result is the vector form of Eq. A.7.6:

$$\oint \left\{ \mathbf{E}(\mathbf{r}') [\mathbf{n}' \cdot \nabla' G(\mathbf{r}, \mathbf{r}')] - G(\mathbf{r}, \mathbf{r}') [\mathbf{n}' \cdot \nabla'] \mathbf{E}(\mathbf{r}') \right\} dS' \\ = \int \left[ \mathbf{E}(\mathbf{r}') \nabla^2 G(\mathbf{r}, \mathbf{r}') - G(\mathbf{r}, \mathbf{r}') \nabla^2 \mathbf{E}(\mathbf{r}') \right] dV' \quad (\text{A.7.9})$$

Next, let the field point be in the vicinity of the source and construct a virtual sphere with a radius just large enough to contain both source and field points. Substituting Eqs. A.7.3 and A.7.7 into the volume integrals of Eq. A.7.9 results in:

$$\int \mathbf{E}(\mathbf{r}') \delta(\mathbf{r}, \mathbf{r}') dV' = \mathbf{E}(\mathbf{r}) \quad (\text{A.7.10})$$

The second term in the surface integral of Eq. A.7.9 may be written:

$$G(\mathbf{n}' \cdot \nabla') \mathbf{E} = \mathbf{n}' \cdot \nabla' (G\mathbf{E}) - \mathbf{E}(\mathbf{n}' \cdot \nabla' G) \quad (\text{A.7.11})$$

Combining shows that:

$$\mathbf{E}(\mathbf{r}) = \oint \left\{ 2\mathbf{E}(\mathbf{r}') [\mathbf{n}' \cdot \nabla' G(\mathbf{r}, \mathbf{r}')] - [\mathbf{n}' \cdot \nabla'] [G(\mathbf{r}, \mathbf{r}') \mathbf{E}(\mathbf{r}')] \right\} dS' \quad (\text{A.7.12})$$

This equation expresses the field intensity at the field point in terms of field values on the surface of a virtual sphere surrounding both the source and the field. Although Eq. A.7.12 expresses the electric field intensity at the field point in terms of values on the surface of an external virtual sphere, it is not satisfactory since the divergence operation contains derivatives of the electric field intensity.

Next, consider the field point to be outside the virtual sphere and, for completeness construct a second virtual sphere. It is concentric with the first one and of radius large enough to contain both source and field positions, and it contains no other sources. With no sources, the volume integral of Eq. A.7.9 is equal to zero. The integral similar to Eq. A.7.12, for this case, is equal to zero:

$$\oint \{2\mathbf{E}(\mathbf{r}')[\mathbf{r}' \bullet \nabla' G(\mathbf{r}, \mathbf{r}')] - [\mathbf{r}' \bullet \nabla'] [G(\mathbf{r}, \mathbf{r}')\mathbf{E}(\mathbf{r}')] \} dS' = 0 \quad (\text{A.7.13})$$

The integral is taken over both the inner and outer spherical surfaces, with the normal direction always extending outward from the field containing volume. Next, let the radius of the outer surface increase without limit, in which case, as discussed below, the integral over the exterior surface is equal to zero. Comparing Eqs. A.7.12 and A.7.13 then shows that the surface integral over the inner surface is equal to  $-\mathbf{E}(\mathbf{r})$ .

To restate Eq. A.7.12 in a way that involves field vectors only note that the last term of Eq. A.7.13 may be written as a volume integral:

$$\oint \mathbf{r}' \bullet \nabla' (\mathbf{GE}) dS = \int \nabla'^2 (\mathbf{GE}) dV$$

Substitute vector  $(\mathbf{GE})$  into the vector identity:

$$\nabla^2 (\mathbf{GE}) = \nabla [\nabla \bullet (\mathbf{GE})] - \nabla \times [\nabla \times (\mathbf{GE})]$$

Combining and using the second and third integrals of Eqs. A.7.4 to return to surface integrals, Eq. A.7.13 goes to:

$$\oint \{2\mathbf{E}(\mathbf{r}' \bullet \nabla' G) - \mathbf{r}' [\nabla' \bullet (\mathbf{GE})] + \mathbf{r}' \times [\nabla' \times (\mathbf{GE})]\} dS = 0 \quad (\text{A.7.14})$$

Completing both the divergence and curl operations and using the Maxwell equations to substitute for vector operations results in:

$$\oint \{2\mathbf{E}(\mathbf{r}' \bullet \nabla G) - \mathbf{r}'(\mathbf{E} \bullet \nabla G) - \dot{\omega} \mathbf{r}' \times \mathbf{B} + \mathbf{r}' \times (\nabla' G \times \mathbf{E})\} dS = 0 \quad (\text{A.7.15})$$

Substituting for the triple product and simplifying results in:

$$\oint \{-\dot{\omega}(\mathbf{r}' \times \mathbf{B})G + (\mathbf{r}' \bullet \mathbf{E})\nabla' G + (\mathbf{r}' \times \mathbf{E}) \times \nabla' G\} dS = 0 \quad (\text{A.7.16})$$

By Eq. A.7.13, the value of the surface integral is equal to  $-\mathbf{E}(\mathbf{r})$ . However, as defined above the normal is from the field-containing region to the source-containing region. Reversing the direction so the normal extends outward gives:

$$\mathbf{E}(\mathbf{r}) = \oint \{-\dot{\omega}[\mathbf{r}' \times \mathbf{B}(\mathbf{r}')]G(\mathbf{r}, \mathbf{r}') + [\mathbf{r}' \bullet \mathbf{E}(\mathbf{r}')] \nabla' G(\mathbf{r}, \mathbf{r}') + [\mathbf{r}' \times \mathbf{E}(\mathbf{r}')] \times \nabla' G(\mathbf{r}, \mathbf{r}')\} dS \quad (\text{A.7.17})$$

The requirements are that the field point is external to the contained region and the source is fully contained by it.

This equation, when combined with Eq. A.7.8, is the exact expression for the exterior electric field intensity in terms of the surface fields on a source-containing region. It is not necessary to know anything about the source other than it created the surface fields. Although both the external electric field intensity and the fields on the surface are unique, the inverse is not true: the source necessary to produce  $\mathbf{E}(\mathbf{r})$  is not unique.

The corresponding expression for the magnetic flux density follows in a similar way. Carrying out the calculation gives the result:

$$\mathbf{B}(\mathbf{r}) = \oint \{\dot{\omega} \mu \epsilon [\mathbf{r}' \times \mathbf{E}(\mathbf{r}')]G(\mathbf{r}, \mathbf{r}') + [\mathbf{r}' \bullet \mathbf{B}(\mathbf{r}')] \nabla' G(\mathbf{r}, \mathbf{r}') - [\mathbf{r}' \times \mathbf{B}(\mathbf{r}')] \times \nabla' G(\mathbf{r}, \mathbf{r}')\} dS \quad (\text{A.7.18})$$

With static sources Green's function decreases as the inverse of the radius, the electric field intensity decreases as the inverse square of the radius, and the surface area increases as the square of the radius. Therefore in the limit as the radius becomes infinite the contribution to field intensities  $\mathbf{E}(\mathbf{r})$  and  $\mathbf{B}(\mathbf{r})$  due to the outer surface goes to zero. On the other hand, for dynamic sources, Green's function and the electric field intensity both decrease as the inverse of the radius and the surface area increases as the square of the radius. From this point of view, contributions of the outer surface integral to  $\mathbf{E}(\mathbf{r})$  and  $\mathbf{B}(\mathbf{r})$  remain constant in the limit of infinite radius. That the null result remains, however, may be seen by application of

a dynamic boundary condition: The radius of the outer sphere is greater than the speed of light,  $c$ , times whatever time is of interest in the problem. Even with dynamic sources, the outer surface integral has no influence on fields  $\mathbf{E}(\mathbf{r})$  or  $\mathbf{B}(\mathbf{r})$ .

## A.8 A Series Resonant Circuit

An important special case is a series arrangement of inductor  $L$ , resistor  $R$ , and capacitor  $C$ . The differential equation relating the current and voltage is:

$$v(t) = L \frac{di(t)}{dt} + Ri(t) + \frac{1}{C} \int i(t) dt \quad (\text{A.8.1})$$

To obtain the steady state solution define the current in the circuit to be:

$$i(t) = I_0 \cos(\omega t) \quad (\text{A.8.2})$$

Combining Eqs. A.8.1 and A.8.2 shows that the voltage across the circuit is:

$$v(t) = I_0 R \cos(\omega t) - I_0 \left( \omega L - \frac{1}{\omega C} \right) \sin(\omega t) \quad (\text{A.8.3})$$

The power into each element is:

$$p(t) = v_S(t) i(t) \quad (\text{A.8.4})$$

The voltage across the element in question is  $v_S(t)$ . The power into each element is:

$$\begin{aligned} p_L(t) &= -\frac{\omega L I_0^2}{2} \sin(2\omega t) & p_C(t) &= \frac{I_0^2}{2\omega C} \sin(2\omega t) \\ p_R(t) &= \frac{R I_0^2}{2} [1 + \cos(2\omega t)] \end{aligned} \quad (\text{A.8.5})$$

The energy stored in each reactive element is:

$$W_L(t) = \frac{LI_0^2}{4} [1 + \cos(2\omega t)] \quad (A.8.6)$$

$$W_C(t) = \frac{I_0^2}{4\omega^2 C} [1 - \cos(2\omega t)]$$

It would be convenient to relate the voltage and current by a multiplicative constant. Comparing Eqs. A.8.2 and A.8.3 shows that this cannot be done with trigonometric functions. However, adding an imaginary term to Eq. A.8.2 gives the exponential function:

$$i(t) = I_0 [\cos(\omega t) + i \sin(\omega t)] = I_0 e^{i\omega t} \quad (A.8.7)$$

Equation A.8.7 is the phasor form of the current. The phasor form of the circuit voltage is:

$$v(t) = \left[ R + i \left( \omega L - \frac{1}{\omega C} \right) \right] I_0 e^{i\omega t} \quad (A.8.8)$$

By definition, the input impedance,  $Z$ , of the circuit is equal to the complex voltage-to-complex current ratio at the circuit terminals. For this case:

$$Z = R + i \left( \omega L - \frac{1}{\omega C} \right) \quad (A.8.9)$$

Using phasor notation the exponential is suppressed and the reader is supposed to know it should be there. Using phasor notation in this case the current and voltage are:

$$I = I_0 \quad \text{and} \quad V = I_0 \left[ R + i \left( \omega L - \frac{1}{\omega C} \right) \right] \quad (A.8.10)$$

Although phasors provide a constant multiplicative relationship between the current and voltage, other problems arise. Each variable, *i.e.* phasor current and phasor voltage, consists of terms that do and terms that do not represent physical reality, the actual and virtual terms. Separating actual from virtual values in the voltage and current expressions can easily be done since the

actual values appear as real numbers and the virtual values appear as imaginary ones. However, when products are taken things are not so simple. Using power as an example, the product of the phasor current and voltage consists of four types of terms: actual current times actual voltage, actual current times virtual voltage, virtual current times actual voltage, and virtual current times virtual voltage. Of these four products, only the first type represents actuality and only it is desired. The second and third types are multiplied by 'i' and thus may be discarded. The fourth type, however, is a real, unwanted number. Special multiplication rules are necessary to eliminate the fourth type of product.

Consider circuit power as an example. From Eq. A.8.5 the time varying input power is:

$$p(t) = \frac{I_0^2}{2} \left\{ R \left[ 1 + \cos(2\omega t) \right] - \left[ \omega L - \frac{1}{\omega C} \right] \sin(2\omega t) \right\} \quad (\text{A.8.11})$$

By way of contrast consider the product phasor  $P_c = VI^*/2$ :

$$P_c = \frac{I_0^2}{2} \left\{ R + i \left[ \omega L - \frac{1}{\omega C} \right] \right\} \quad (\text{A.8.12})$$

The real and reactive powers shown in Eq. A.8.11 are phased in time quadrature. The real part of  $P_c$  is equal to the time average power. The imaginary part of  $P_c$  is equal to the magnitude of the reactive power. Since the instantaneous value of the power is, in many cases, of no interest, the remaining quantities of interest are both contained in Eq. A.8.12: the time average real power,  $P_{av}$ , and the magnitude of the reactive power,  $P_{re}$ . Because of these relationships, it is common when dealing with power in electrical circuits, to work with the complex power:

$$P_c = P_{av} + i P_{re} \quad (\text{A.8.13})$$

Although the power is complex, it is not a phasor: both real and imaginary parts represent physical reality and there is no virtual part.

## A.9 Q of Time Varying Systems

Q is a dimensionless ratio that describes the quality of anything that oscillates. Although developed for application to a closed system, such as an electrical circuit, a bouncing ball, or a swaying bridge, Q is also useful for dealing with the open system of a radiating antenna. For example, antenna Q is important in communication antennas since modulation is essential, modulation requires a minimum bandwidth, and there is a direct relationship between Q and bandwidth. For high power antennas, Q is a measure of how much energy must be stored about an antenna to obtain the minimum acceptable power output. This is significant in such diverse applications as the decay of atomic states and electrically small, high power antennas used to communicate around the surface of the earth. In nearly all radiation problems, Q is a critical measure of antenna worthiness.

Since only energy within a half wavelength of an antenna can return to it during steady state operation, only this near field energy affects an antenna's input impedance. To the driving terminals of an antenna, energy radiated permanently away from the system is indistinguishable from energy absorbed by a resistor; the power loss is therefore measured as an effective antenna resistance. Since the energy that oscillates to and from an antenna is indistinguishable from reactive energy, the oscillation results in an effective radiation reactance. To the driving circuit, this input impedance is indistinguishable from the input impedance of a properly synthesized closed circuit. Hence, from the point of view of the driving source, an antenna may be replaced by and analyzed as if it were an electric circuit.

Anything that oscillates can be assigned a value of Q. With  $W(t)$  representing the energy stored in the system, the magnitude of the Q of any system is defined to be the dimensionless ratio:

$$Q = \frac{\omega W(t)}{dW(t)/dt} \quad (\text{A.9.1})$$

Q is a measure of how rapidly a system grows or decays. Rewriting Eq. A.9.1 for a lossy system gives:

$$\frac{dW(t)}{dt} = -\frac{\omega}{Q} W(t) \quad (\text{A.9.2})$$

The solution of Eq. A.9.2 is:

$$W(t) = W_0 e^{-\omega t/Q} \quad (\text{A.9.3})$$

$W_0$  is the initial value of energy. As an example, consider a ball bouncing on a smooth, horizontal, surface. In a uniform gravitational field, the energy is proportional to the height and, at maximum height the energy is entirely due to gravity. The maximum height reached by the ball follows the exponential decay of Eq. A.9.3, and the ratio of heights on successive bounces is  $e^{-\omega/Q}$ .

Inductors require a current path and current paths, generally speaking, are also resistive. The ratio of inductance,  $L$ , to resistance,  $R$ , depends upon the nature of the path (the wire) and its geometrical arrangement. Since the peak energy per cycle is equal to the total oscillating energy, a definition derived from Eq. A.9.1 is the peak cyclic value of stored energy-to-average energy loss per radian ratio:

$$Q = \frac{\omega W(t)_{pk}}{p(t)_{av}} \quad (\text{A.9.4})$$

The current and voltage in an RL circuit may be written:

$$\begin{aligned} i(t) &= I_0 \cos(\omega t) \\ v(t) &= I_0 [R \cos(\omega t) - \omega L \sin(\omega t)] \end{aligned} \quad (\text{A.9.5})$$

The power dissipated in the resistor is:

$$p_R(t) = \frac{RI_0^2}{2} [1 + \cos(2\omega t)] \quad (\text{A.9.6})$$

The energy stored in the inductor is:

$$W_L(t) = \frac{LI_0^2}{4} [1 + \cos(2\omega t)] \quad (\text{A.9.7})$$

Combining Eqs. A.9.4, A.9.6, and A.9.7 shows that:



$$Q = \frac{\omega L}{R} \quad (\text{A.9.8})$$

For an RLC circuit, the instantaneous energy-to-time average power ratio is equal to:

$$\frac{\frac{LI_0^2}{4} [1 + \cos(2\omega t)] + \frac{I_0^2}{4C} [1 - \cos(2\omega t)]}{\frac{RI_0^2}{2} [1 + \cos(2\omega t)]} \quad (\text{A.9.9})$$

From Eq. A.9.9 it follows that, if the inductive energy exceeds the capacitive energy, Eq. A.9.8 gives  $Q$ . If the capacitive energy exceeds the inductive energy,  $Q$  is:

$$Q = \frac{1}{\omega RC} \quad (\text{A.9.10})$$

At the resonant frequency, where ‘ $_{av}$ ’ denotes time average values, a commonly used formula is:

$$Q = \frac{2\omega W_{L_{av}}}{P_{av}} \quad (\text{A.9.11})$$

For these simple circuits, values calculated using Eqs. A.9.9, A.9.10, and A.9.11 are equal at resonance. In more complicated circuits where the reactive elements are driven with different phases, Eq. A.9.11 is not exact.

A slightly modified definition that is sometimes used with simple systems is to equate  $Q$  with the tangent of the impedance phase angle. So long as the system frequency is low enough for capacitive effects to be negligible the definition reproduces Eq. A.9.8 for the simple case of an RL circuit. Using all three definitions, results with lossy capacitors are similar to those with lossy inductors. By all three definitions, a capacitor  $C$  in series with resistor  $R$  simply replaces  $\omega L$  by  $1/\omega C$ .

$$Q = 1/(\omega CR) \quad (\text{A.9.12})$$

With an antenna radiating in the steady state since time  $t = -\infty$  there is an infinite amount of energy in the field. The difficulty with calculating  $Q$  is separate the finite field that returns to the source upon shutdown from that which does not. During steady state operation, the magnitudes of the field intensities decrease with increasing radius. The Maxwell stress tensor shows that radiation fields exert an expansive self-pressure equal to the gradient in field energy density. In this way, the tensor describes forces acting to drive the field energy ever outward. However, upon source turnoff, shutdown, the inverse is true. If the fields vanish near the source the tensor describes compressive forces that act to drive the field energy back to the source; it is the returned energy that forms the numerator of the expression for  $Q$ , see Eq. A.9.1.

## A.10 Bandwidth

The normalized bandwidth is defined as the ratio of the frequency difference between the two points at which a resonant circuit drops to half the resonant power (half power points) divided by the resonance frequency.

By definition, the resonance frequency of a series circuit is that frequency at which the reactive power vanishes. From Eq. A.8.3 the input voltage is:

$$v(t) = I_0 R \cos(\omega t) - I_0 \left[ \omega L - \frac{1}{\omega C} \right] \sin(\omega t) \quad (\text{A.10.1})$$

From Eq. A.8.11 the input power is:

$$p(t) = \frac{I_0^2}{2} \left\{ R [1 + \cos(2\omega t)] - \left[ \omega L - \frac{1}{\omega C} \right] \sin(2\omega t) \right\} \quad (\text{A.10.2})$$

The resonance frequency,  $\omega_0$ , is the frequency at which the reactive power vanishes. It is equal to:

$$\omega_0^2 = \frac{1}{LC} \quad (\text{A.10.3})$$

To begin a dimensionless analysis of bandwidth introduce the expressions:

$$\omega_1 = \omega_0(1 + \delta) \text{ and } \omega_2 = \omega_0(1 - \delta) \quad (\text{A.10.4})$$

Frequencies  $\omega_1$  and  $\omega_2$  are the half power frequencies. With no loss of rigor, it is convenient to have the circuit be subject to a constant current input. For that case, the dissipated power drops by half when the real and reactive voltage magnitudes are equal. This occurs for:

$$\frac{\omega_0 L}{R} = \frac{\delta(2 + \delta)}{(1 + \delta)} \cong 2\delta \quad (\text{A.10.5})$$

The bandwidth is  $2\delta\omega_0$ . A result of combining Eqs. A.10.4 and A.10.5 is:

$$Q \cong \frac{1}{2\delta} = \frac{\omega_0}{\omega_1 - \omega_2} \quad (\text{A.10.6})$$

For more complicated circuits, the actual circuit may be replaced by its equivalent Thévenin or Norton circuit and analyzed in a similar way. For structured circuits in which different passive elements have differently phased driving currents the inductive and capacitive energies are not in phase quadrature. The peak value of stored energy contains contributions from both inductors and capacitors.

## A.11 Instantaneous and Complex Power in Radiation Fields

To compare methods of describing power, for steady-state radiation fields return to the Maxwell equations, Eqs. 1.6.8 and 1.6.11:

$$\begin{aligned} \nabla \times \mathbf{E} + \frac{\partial \mathbf{B}}{\partial t} &= 0 & \nabla \cdot \mathbf{B} &= 0 \\ \nabla \times \mathbf{B} - \mu\epsilon \frac{\partial \mathbf{E}}{\partial t} &= \mu\mathbf{J} & \epsilon \nabla \cdot \mathbf{E} &= \rho \end{aligned} \quad (\text{A.11.1})$$

Replacing  $\mathbf{B}$  by  $\mu\mathbf{H}$  and integrating over any closed volume gives:

$$\oint \mathbf{N} \cdot d\mathbf{S} + \int \left( \mu \mathbf{H} \cdot \frac{\partial \mathbf{H}}{\partial t} + \epsilon \mathbf{E} \cdot \frac{\partial \mathbf{E}}{\partial t} \right) dV = - \int \mathbf{E} \cdot \mathbf{J} dV \quad (\text{A.11.2})$$

This is the Poynting theorem. It is a restatement of Eq. 1.9.9 with vector  $\mathbf{N}$  defined by Eq. 1.8.5. The term on the right side of Eq. A.11.2 is power into the system. The volume integral on the left is the rate energy enters the field, and the first term on the left is the rate at which energy leaves through the surface. This interpretation is independent of the wave shape.

When dealing with sinusoidal, steady state radiation it is often convenient to use phasor notation. With  $\exp(i\omega t)$  time dependence the phasor version of Maxwell's equations is:

$$\begin{aligned} \nabla \times \tilde{\mathbf{E}} + i\omega \tilde{\mathbf{B}} &= 0 & \nabla \cdot \tilde{\mathbf{B}} &= 0 \\ \nabla \times \tilde{\mathbf{B}} - i\omega \mu \epsilon \tilde{\mathbf{E}} &= \mu \tilde{\mathbf{J}} & \epsilon \nabla \cdot \tilde{\mathbf{E}} &= \rho \end{aligned} \quad (\text{A.11.3})$$

The integrated results corresponding to Eq. A.11.2 are:

$$\oint \mathbf{N}_c \cdot d\mathbf{S} + \frac{i\omega}{2} \int (\mu \tilde{\mathbf{H}}^2 - \epsilon \tilde{\mathbf{E}}^2) dV = - \frac{1}{2} \int \tilde{\mathbf{E}} \cdot \tilde{\mathbf{J}}^* dV \quad (\text{A.11.4})$$

By definition the complex Poynting vector is:

$$\mathbf{N}_c = \tilde{\mathbf{E}} \times \tilde{\mathbf{H}}^* / 2 \quad (\text{A.11.5})$$

The same volume of integration is chosen for Eq. A.11.4 as was chosen to evaluate Eq. A.11.2. Although the complex Poynting vector is a complex quantity, it is not a phasor, since both real and imaginary parts represent actual quantities.

The real part of the volume integral on the right of Eq. A.11.4 is equal to the time average power into the region. Since the volume integral on the left has no real part, the real part of the surface integral must equal the time average output power through the surface. The volume integral on the left side is  $2\omega$  times the difference between the time average electric and magnetic energies in the volume of integration.

Consider the volume of integration to be spherical, let  $\delta$  be a vanishingly small distance, and place the source currents on the sphere. Consider three

volumes: {1} Inner concentric, virtual spheres containing all radii less than  $a - \delta$ . In this region, there are no sources and all fields are ignored. {2} Concentric spheres of radii within the range  $a \pm \delta$ . In this region are all of the sources. {3} An exterior region containing all radii larger than  $a + \delta$ . In this region, there are fields but no sources.

Since the exterior region contains no currents, within that region the current-containing integral of Eq. A.11.4 is equal to zero. Since the volume integral on the left has no real part the sum of the real part of the surface integral taken at infinity and at  $a + \delta$  is equal to zero. For finite fields, in the limit of infinite radius the imaginary portion of  $N_c$  decreases more rapidly than  $1/r^2$  with increasing radius and, hence, the imaginary part of the surface integral is equal to zero at infinity. Therefore the imaginary part of the surface integral at radius  $a + \delta$  is equal to  $(\omega/2) \times \{\text{the difference between the time average magnetic and electric field energies}\}$  within the volume of integration:

$$\text{Im} \left[ \oint N_c \bullet dS \right]_{a+\delta} = \frac{\omega}{2} \int \left\{ \epsilon \tilde{E} \bullet \tilde{E}^* - \mu \tilde{H} \bullet \tilde{H}^* \right\} dV \quad (\text{A.11.6})$$

Within the source region,  $a \pm \delta$ , since the volume is proportional to  $2\delta$  and there are no singularities in the fields the volume integral on the left of Eq. A.11.4 goes to zero with  $\delta$ . This leaves:

$$\text{Im} \left[ \oint N_c \bullet dS \right] + \frac{1}{2} \text{Im} \left[ \int \tilde{E} \bullet \tilde{J}^* dV \right] = 0 \quad (\text{A.11.7})$$

For simplicity consider the special case where radius  $a \ll \lambda$ , an electrically small antenna. Sources may then be considered as circuit elements and the current containing integral of Eq. A.11.4 may be written as:

$$\frac{1}{2} \int \tilde{E} \bullet \tilde{J}^* dV = \frac{1}{2} \sum_{j=1}^k V_j I_j^* \quad (\text{A.11.8})$$

With more than one current source, unless the sources meet one of the phase conditions of Eqs. 3.1.13 powers do not combine by simple addition.

Therefore, unless that condition is met Eq. A.11.8 does not correctly describe the complex power. If not, the right side of Eq. A.11.4 is not the complex power and, if it is not, neither is the surface integral of Eq. A.11.4.

## A.12 Conducting Boundary Conditions

Let an electric field intensity exist in the vicinity of a smooth boundary about a closed volume that is immersed in the field. The volume is arbitrary in size and shape. Requirements on the volume are that its size be much less than a wavelength, in all three dimensions, and that it includes regions on both sides of the boundary. Apply the condition of Eq. 1.6.8, that:

$$\nabla \cdot \mathbf{E} = \rho/\epsilon \quad (\text{A.12.1})$$

Evaluate the integral of Eq. A.12.1 over the volume in question, with the result:

$$\int \nabla \cdot \mathbf{E} dV = \oint \mathbf{E} \cdot d\mathbf{S} = q/\epsilon \quad (\text{A.12.2})$$

Symbol “q” indicates all charge within the volume. Next, let the dimension normal to the boundary become vanishingly small on both sides of the boundary so the shape approaches that of a disc. The contribution to the surface integral due to electric field intensity normal to the disc is thereby vanishingly small. Thus, only the normal components of the field intensity are of interest, and Eq. A.12.2 goes to:

$$\oint \mathbf{E} \cdot d\mathbf{S} = \rho/\epsilon \quad (\text{A.12.3})$$

Symbol  $\rho$  indicates the charge per unit area at the interface. From Eq. A.12.3, since charge density in free space is equal to zero the normal component of the electric field intensity on any virtual boundary is continuous.

If an electric field intensity existed inside a nearly ideal conductor, it would drive a nearly infinite current density that would, in turn, absorb a nearly infinite amount of power. Therefore an electric field intensity inside an ideal conductor is zero. In turn, if an electric field intensity is applied

normal to the surface of an ideal conductor, by Eq. A.12.3 it is equal to the charge density on the surface normalized by the permittivity of free space.

For a magnetic field intensity, by Eq. 1.6.11:

$$\nabla \times \mathbf{E} = -\frac{\partial \mathbf{B}}{\partial t} \quad (\text{A.12.4})$$

Consider the surface integral of Eq. A.12.4 over an open area that, like the volume of Eq. A.12.1, extends on either side of a smooth boundary. The integral is:

$$\oint \mathbf{E} \cdot d\boldsymbol{\ell} = -\int \frac{\partial \mathbf{B}}{\partial t} \cdot d\mathbf{S} \quad (\text{A.12.5})$$

The symbol  $d\boldsymbol{\ell}$  indicates differential distance along the periphery of the open area. Next, let the dimension normal to the boundary become vanishingly small. In this limit, the open area becomes vanishingly small and since  $\mathbf{B}$  is finite, the entire right side of the equation is vanishingly small. Therefore, the line integral of the electric field intensity around the loop is equal to zero. Since the length of the loop is the same on either side of the boundary, and since  $d\boldsymbol{\ell}$  is oppositely directed on either side, the tangential component of the electric field intensity is continuous through virtual boundaries. At a boundary between free space and a conductor since the electric field component inside the conductor is equal to zero it is also equal to zero just off the conducting surface.

Let  $\mathbf{n}$  be a unit vector normal to a smooth surface. For a virtual surface, the boundary separates regions one and two. For a conducting surface, the field is in the free space region only:

#### Virtual Surface

$$\mathbf{n} \times (\mathbf{E}_1 - \mathbf{E}_2) = 0; \quad \mathbf{n} \cdot (\mathbf{E}_1 - \mathbf{E}_2) = 0 \quad (\text{A.12.6})$$

#### Conducting Surface

$$\mathbf{n} \times \mathbf{E} = 0; \quad \mathbf{n} \cdot \mathbf{E} = \rho_S / \epsilon$$

Consider a closed volume that is immersed in a magnetic field. Like the volume considered for the normal component of the electric field intensity, it may be arbitrary in size and shape. The requirements are that its size be

much less than a wavelength, in all three dimensions, and that it includes regions on both sides of the boundary. Apply the condition of Eq. 1.6.11:

$$\nabla \cdot \mathbf{B} = 0 \quad (\text{A.12.7})$$

Take the volume integral of Eq. A.12.7 over the volume in question, with the result:

$$\oint \mathbf{B} \cdot d\mathbf{S} = 0 \quad (\text{A.12.8})$$

Since Eq. A.12.8 applies to a closed volume, let the dimension normal to the boundary become vanishingly small so the shape approaches that of a disc. It follows that the normal component of  $\mathbf{B}$  is continuous through the boundary. Inside a conductor,  $\mathbf{B}$  is constant since otherwise Eq. A.12.5 shows that it would produce an electric field intensity there. For time varying radiation fields, the normal component of the magnetic field intensity is equal to zero.

By Eq. 1.6.8:

$$\nabla \times \mathbf{B} = \mu\epsilon \frac{\partial \mathbf{E}}{\partial t} + \mu \mathbf{J} \quad (\text{A.12.9})$$

Consider the surface integral of Eq. A.12.9 over an open area that includes a smooth boundary. The integral is:

$$\oint \mathbf{B} \cdot d\boldsymbol{\ell} = \mu\epsilon \int \frac{\partial \mathbf{E}}{\partial t} \cdot d\mathbf{S} + \mu \int \mathbf{J} \cdot d\mathbf{S} \quad (\text{A.12.10})$$

Let the dimension normal to the boundary become vanishingly small. In this limit, the open area becomes vanishingly small and, since  $\mathbf{E}$  is finite, the first term on the right side is vanishingly small, leaving:

$$\oint \mathbf{B} \cdot d\boldsymbol{\ell} = \mu \int \mathbf{J} \cdot d\mathbf{S} = \mu I_S \quad (\text{A.12.11})$$

Symbol  $I_S$  is the total electric current  $I$  that flows through the open area. In free space, there is no current and the line integral of the magnetic field intensity around the loop is equal to zero. Since surface currents may exist on conductors, the tangential component of a time varying magnetic field



just off the surface of a conductor is equal in magnitude and perpendicular in direction to the current per unit length on the surface:

$$n \times \mathbf{B} = \mu \mathbf{I}_S \quad (\text{A.12.12})$$

Summarizing boundary conditions:

Virtual Surface

$$n \times (\mathbf{B}_1 - \mathbf{B}_2) = 0; \quad n \cdot (\mathbf{B}_1 - \mathbf{B}_2) = 0 \quad (\text{A.12.13})$$

Conducting Surface

$$n \times \mathbf{B} = \mu \mathbf{I}_S; \quad n \cdot \mathbf{B} = 0$$

Both field vectors are continuous through a virtual surface. On conducting surfaces the tangential component of the electric field intensity and the normal component of a time varying magnetic field intensity are both equal to zero. Just off the conducting surface, the normal component of the electric field intensity is equal to the surface charge density and the tangential component of the magnetic field is equal to the surface current density in amperes per meter.

## A.13 Uniqueness

If, within a given boundary, a potential reduces to the correct value on the boundary, or to the correct normal derivative of the potential on that boundary, then that potential is unique. This theorem justifies the use of arbitrary solution methods so long as the resulting solution obeys Laplace's equation in the charge-free regions. No matter how the solution is obtained, if it satisfies these conditions the solution is unique.

Taking  $\phi \nabla \phi$  to be a vector field and substituting into the divergence theorem gives:

$$\int \phi \nabla \phi \cdot d\mathbf{S} = \int \nabla \cdot (\phi \nabla \phi) dV = \int [(\nabla \phi)^2 + \phi \nabla^2 \phi] dV \quad (\text{A.13.1})$$

Since Laplace's equation is satisfied, the last term is equal to zero. Suppose  $\phi_1$  and  $\phi_2$  are different potentials that have either equal values of potential or normal derivatives thereof on every conductor in the field:

$$\int (\phi_1 - \phi_2) \nabla(\phi_1 - \phi_2) \cdot d\mathbf{S} = \int [\nabla(\phi_1 - \phi_2)]^2 dV = 0 \quad (\text{A.13.2})$$

Either equality at the conductors requires the surface integral to equal zero. Since the volume integral is equal to zero it follows that the integrand is equal to zero everywhere. Therefore the potential and/or the electric field intensity are equal everywhere in the field and, therefore, the functions are the same.

For time-dependent solutions, it is only necessary to substitute functions  $\psi_1$  and  $\psi_2$  of Section 1.12 into the divergence theorem and repeat the above procedure.

## A.14 Spherical Shell Dipole

Consider a spherical shell of radius  $a$  that supports a static surface electric charge density  $q$ :

$$\rho = \frac{q}{4\pi a^2} \cos \theta \quad (\text{A.14.1})$$

The charge creates an electric field intensity in both the interior and exterior regions about the shell. The form of the external fields follows directly from Eq. 1.12.8, with all coefficients equal to zero except the coefficient with order one and degree zero  $F(1,0)$ . In the limit of zero frequency the external field components are:

$$E_r = \frac{2i}{\sigma^3} F(1,0) \cos \theta \quad E_\theta = \frac{i}{\sigma^3} F(1,0) \sin \theta \quad (\text{A.14.2})$$

The internal fields follow from the same equation set. To avoid functional singularities at the origin with interior region fields it is necessary to replace spherical Hankel functions by spherical Bessel functions. Writing  $F'(1,0)$  as

the internal coefficient, in the limit of zero frequency the internal field components are:

$$E_r = \frac{2}{3} F'(1,0) \cos \theta \quad E_\theta = -\frac{2}{3} F'(1,0) \sin \theta \quad (\text{A.14.3})$$

The boundary conditions on the fields are:

$$\begin{aligned} \frac{q}{4\pi a^2} &= 2\epsilon F(1,0) \left( \frac{i}{(ka)^3} \right) - \frac{2\epsilon}{3} F'(1,0) \\ F(1,0) \left( \frac{i}{(ka)^3} \right) &= -F'(1,0) \frac{2}{3} \end{aligned} \quad (\text{A.14.4})$$

From Eq. A.14.4:

$$iF = \frac{(ka)^3 q}{12\pi\epsilon a^2} \text{ and } F' = -\frac{q}{8\pi\epsilon a^2} \quad (\text{A.14.6})$$

Combining shows the fields to be:

Exterior

$$E_r = \frac{2aq}{12\pi\epsilon r^3} \cos \theta \quad E_\theta = \frac{aq}{12\pi\epsilon r^3} \sin \theta \quad (\text{A.14.7})$$

Interior

$$E_r = -\frac{q}{12\pi\epsilon a^2} \cos \theta \quad E_\theta = \frac{q}{12\pi\epsilon a^2} \sin \theta$$

The interior field is constant, and equal to:

$$E = 2E_z \text{ and } E_z = -\frac{q}{12\pi\epsilon a^2} \quad (\text{A.14.8})$$

The exterior field is that produced by a z-directed electric dipole moment of magnitude:

$$p_z = aq/3 \quad (\text{A.14.9})$$

The energy densities are:

Interior	Exterior	
$W_{dT} = \frac{q^2}{288\pi^2 \epsilon a^4}$	$W_{dT} = \frac{k^6 a^2 q^2}{288\pi^2 \epsilon \sigma^6} (1 + 3 \cos^2 \theta)$	(A.14.10)

The total field energies are:

Interior	Exterior	
$W_T = \frac{q^2}{216\pi \epsilon a}$	$W_T = \frac{q^2}{108\pi \epsilon a}$	(A.14.11)

Equation A.14.11 shows that respectively one third and two thirds of the energy is stored interior and exterior to the shell.

## ***Spherical Harmonics***

### **A.15 Gamma Functions**

Products in which successive factors differ by one occur frequently in the formation of power series. If  $\ell$  is an integer, such products may be expressed as special products of a certain number of integers, beginning with one. The factorial of integer  $\ell$  is, by definition:

$$\ell! = 1 \bullet 2 \bullet 3 \bullet \dots \bullet \ell \quad (\text{A.15.1})$$

It follows that

$$\ell! = \ell(\ell - 1)! \quad (\text{A.15.2})$$

The same symbolism is useful for noninteger numbers,  $v$ . A similar equation is defined:

$$v! = v(v-1)! \quad (\text{A.15.3})$$

Similarly:

$$v(v-1)(v-2)\dots(v-m+1) = \frac{v!}{(v-m)!} \quad (\text{A.15.4})$$

Let  $f(v)$  be any function that satisfies the condition

$$f(v) = vf(v-1) \quad (\text{A.15.5})$$

Taking the ratio of Eq. A.15.5 to A.15.3 shows that:

$$\phi(v) = \frac{f(v)}{v!} = \frac{f(v-1)}{(v-1)!} = \phi(v-1) \quad (\text{A.15.6})$$

It follows that  $\phi(v)$  is a periodic function of period  $v$ .

Euler proposed that the definition of a noninteger factorial be:

$$v! = \int_0^{\infty} t^v e^{-t} dt \quad (\text{A.15.7})$$

This definition is valid over the range

$$-1 < v \leq 0 \quad (\text{A.15.8})$$

Factorial  $v!$  can be evaluated for any value of  $v$  using Eq. A.15.3. For example, if  $-2 < v < -1$  then  $v!$  can be written

$$v! = \frac{(v+1)!}{v+1} = \frac{(v+1)!(v+2)!}{(v+1)(v+2)} = \frac{(v+1)!(v+2)!\dots(v+n)!}{(v+1)(v+2)\dots(v+n)} \quad (\text{A.15.9})$$

Equation A.15.9 shows a simple pole exists for  $v$  equal to a negative integer. Other results of Eq. A.15.7 are that:

$$0! = 1 = 1! \quad (\text{A.15.10})$$

$$\left(-1/2\right)! = \sqrt{\pi} \quad (\text{A.15.11})$$

$$(-v)!(v-1)! = \frac{\pi}{\sin(\pi v)} \quad (\text{A.15.12})$$

The Stirling formula for the approximate value of  $v!$ , in the limit of large values of  $v$ , is:

$$v! \approx \left(\frac{v}{e}\right)^v \sqrt{2\pi v} \quad (\text{A.15.13})$$

A related and frequently recurring product form is with succeeding numbers that differ by two:

$$v(v-2)(v-4)(v-6)\dots$$

The series is denoted by:

$$v!! = v(v-2)(v-4)(v-6)\dots \quad (\text{A.15.14})$$

It follows that for even and odd integers, respectively:

$$(2\ell)!! = 2^\ell (\ell)! \quad \text{and} \quad (2\ell+1)!! = \frac{(2\ell+1)!}{(2\ell)!!} \quad (\text{A.15.15})$$

The left and right equations of Eq. A.15.15 for  $\ell = 0$  show that:

$$(0)!! = 1 \quad \text{and} \quad (1)!! = 1 \quad (\text{A.15.16})$$

Although Eq. A.15.15 is in indeterminate form for  $\ell = -1$ , evaluating the identity:

$$\frac{(\ell)!}{(\ell)!!} = (\ell-1)!! \quad (\text{A.15.17})$$

For  $\ell = 0$ , Eq. A.15.17 shows that

$$(-1)!! = 1 \quad (\text{A.15.18})$$

Table A.15.1 contains a listing of useful and selected sums involving factorials.

---

1.	$2 \sum_{m \geq 0}^{\ell} \frac{(\ell+m-1)!(\ell-m-1)!!}{(\ell+m)!!(\ell-m)!!} U(m) \delta(\ell+m, 2q) = 1$
2.	$\sum_{m \geq 1}^{\ell} \frac{(-1)^{(\ell-m)/2} m(\ell+m-1)!!(\ell-m-1)!!}{(\ell+m)!!(\ell-m)!!} \delta(\ell+m, 2q) = \frac{\ell!!}{(\ell-1)!!}$
3.	$2 \sum_{m \geq 2}^{\ell} \frac{(-1)^{(\ell-m)/2} m^2(\ell+m-1)!!(\ell-m-1)!!}{\ell(\ell+1)(\ell+m)!!(\ell-m)!!} \delta(\ell+m, 2q) = \frac{(\ell-1)!!}{\ell!!}$
4.	$4 \sum_{m=0}^{\ell-1} \frac{(\ell+m)!!(\ell-m)!!}{\ell(\ell+1)(\ell+m-1)!!(\ell-m-1)!!} U(m) \delta(\ell+m, 2q+1) = 1$
5.	$4 \sum_{m=0}^{\ell} \frac{m^2(\ell+m-1)!!(\ell-m-1)!!}{\ell(\ell+1)(\ell+m)!!(\ell-m)!!} \delta(\ell+m, 2q) = 1$
6.	$8 \sum_{m \geq 0}^{\ell} \frac{(-1)^{(\ell-m-1)/2} (\ell+m)!!(\ell-m)!!}{\ell(\ell+1)(\ell+m-1)!!(\ell-m-1)!!} \delta(\ell+m, 2q+1) U(m) = \frac{\ell!!}{(\ell-1)!!}$
7.	$2 \sum_{m \geq 1}^{\ell} \frac{(-1)^{(\ell-m-1)/2} m(\ell+m)!!(\ell-m)!!}{\ell(\ell+1)(\ell+m-1)!!(\ell-m-1)!!} \delta(\ell+m, 2q+1) = \frac{(\ell-1)!!}{\ell!!}$
8.	$2 \sum_{s=0}^{(\ell-m-1)/2} \frac{\ell(-1)^s \delta(\ell+m, 2q+1)}{(\ell+m+2s+1)!!(\ell-m-2s-1)!!} = \frac{1}{(\ell+m-1)!!(\ell-m-1)!!}$

---

Table A.15.1 A Table of Sums over Factorials

## A.16 Azimuth Angle Trigonometric Functions

The solutions of Eq. 1.11.11 are trigonometric functions:

$$\Phi(\phi) = \sum_m [C_m \cos(m\phi) + D_m \sin(m\phi)] \quad (\text{A.16.1})$$

An equally satisfactory solution is:

$$\Phi(\phi) = \sum_m [\hat{C}_m e^{jm\phi} + \hat{D}_m e^{-jm\phi}] \quad (\text{A.16.2})$$

By definition  $j^2 = (-1)$ . For cases of interest here, the azimuth angle occupies the full range of angle from 0 through  $2\pi$ . This condition requires the solution to satisfy the relationship:

$$\Phi(\phi) = \Phi(\phi + 2\pi) \quad (\text{A.16.3})$$

Equations A.16.1 through A.16.3 are jointly satisfied only if  $m$  represents the full range of positive integers, including zero.

The trigonometric functions form an orthogonal set. Trigonometric identities show that:

$$\int_0^{2\pi} \cos(m\phi) \cos(n\phi) d\phi = \frac{1}{2} \int_0^{2\pi} d\phi [\cos((m-n)\phi) + \cos((m+n)\phi)] \quad (\text{A.16.4})$$

Evaluating the integral on the right gives:

$$\int_0^{2\pi} \cos(m\phi) \cos(n\phi) d\phi = \left( \frac{\sin[(m-n)\phi]}{2(m-n)} + \frac{\sin[(m+n)\phi]}{2(m+n)} \right) \bigg|_0^{2\pi} \quad (\text{A.16.5})$$

Since both  $m$  and  $n$  are positive integers, the second term on the right of Eq. A.16.5 is always zero; the first term is also positive unless  $m = n$ , for which case the result is indeterminate. Evaluation may be accomplished by either evaluating the indeterminate or by substituting into the integrand the identity:



$$\cos^2(m\phi) \equiv \frac{1}{2}[1 + \cos(2m\phi)] \quad (\text{A.16.6})$$

Integrating Eq. A.16.6 gives:

$$\int_0^{2\pi} d\phi \cos^2(m\phi) = \frac{1}{2} \int_0^{2\pi} d\phi [1 + \cos(2m\phi)] = \pi \quad (\text{A.16.7})$$

Combining Eq. A.16.5 through A.16.7:

$$\int_0^{2\pi} \cos(m\phi) \cos(n\phi) d\phi = \pi \delta(m, n) \quad (\text{A.16.8})$$

The Kronecker delta function is indicated by  $\delta(m, n)$ . By definition:

$$\delta(m, n) = \begin{cases} 1 & \text{if } m = n \\ 0 & \text{if } m \neq n \end{cases} \quad (\text{A.16.9})$$

It follows in a similar way that:

$$\int_0^{2\pi} \sin(m\phi) \sin(n\phi) d\phi = \pi \delta(m, n) \quad (\text{A.16.10})$$

Also

$$\int_0^{2\pi} \sin(m\phi) \cos(n\phi) d\phi = 0 \quad (\text{A.16.11})$$

Combining Eqs. A.16.8 through A.16.11 gives:

$$\int_0^{2\pi} e^{j(m-n)\phi} d\phi = 2\pi \delta(m, n) \quad (\text{A.16.12})$$

For example, Eq. A.16.12 may be used to evaluate the product function:

$$\begin{aligned} \int_0^{2\pi} e^{j(m-m')\phi} \sin\phi d\phi &= \frac{1}{2j} \int_0^{2\pi} \left( e^{j(m'-m+1)\phi} - e^{j(m'-m-1)\phi} \right) d\phi \\ &= \pi j [\delta(m', m+1) - \delta(m', m-1)] \end{aligned} \quad (\text{A.16.13})$$

It is often convenient to express functions in terms of the order of trigonometric functions. The formulas for going from power to order follow directly from the geometry; all possible combinations are given by the four sums:

$$\cos^{2\ell} \phi \equiv \frac{1}{2^{2\ell}} \left\{ \sum_{k=0}^{\ell-1} \frac{2(2\ell)!}{(2\ell-k)!k!} \cos[2(\ell-k)\phi] + \frac{(2\ell)!}{(\ell!)^2} \right\} \quad (\text{A.16.14})$$

$$\sin^{2\ell} \phi \equiv \frac{1}{2^{2\ell}} \left\{ \sum_{k=0}^{\ell-1} (-1)^{\ell-k} \frac{2(2\ell)!}{(2\ell-k)!k!} \cos[2(\ell-k)\phi] + \frac{(2\ell)!}{(\ell!)^2} \right\} \quad (\text{A.16.15})$$

$$\cos^{2\ell-1} \phi \equiv \frac{4}{2^{2\ell}} \left\{ \sum_{k=0}^{\ell-1} \frac{(2\ell-1)!}{(2\ell-k-1)!k!} \cos[(2\ell-2k-1)\phi] \right\} \quad (\text{A.16.16})$$

$$\sin^{2\ell-1} \phi \equiv \frac{4}{2^{2\ell}} \left\{ \sum_{k=0}^{\ell-1} (-1)^{\ell-k-1} \frac{(2\ell-1)!}{(2\ell-k-1)!k!} \sin[(2\ell-k-1)\phi] \right\} \quad (\text{A.16.17})$$

An expansion for  $1/(\sin\phi)$  is necessary to accomplish needed calculations. To form the expansion, note that since  $1/(\sin\phi)$  is an odd function of  $\phi$  it is expressible as:

$$\frac{1}{\sin\phi} = \sum_{s=1}^{\infty} A_s \sin(2s-1)\phi \quad (\text{A.16.18})$$

To evaluate coefficients  $A_s$ , multiply Eq. A.16.18 by  $\sin(2p-1)\phi$  and integrate over the full range of the variable. The result is:

$$\int_0^{2\pi} d\phi \frac{\sin(2p-1)\phi}{\sin\phi} = \sum_{s=1}^{\infty} A_s \int_0^{2\pi} d\phi \sin[(2s-1)\phi] \sin[(2p-1)\phi] = \pi A_p \delta(p,s) \quad (\text{A.16.19})$$

The left side of Eq. A.16.19 is a periodic trigonometric function for all terms except  $p = 1$  and all periodic terms integrate to zero. This leaves:

$$\int_0^{2\pi} d\phi \frac{\sin(2p-1)\phi}{\sin\phi} = 2\pi \quad (\text{A.16.20})$$

Substituting back into Eq. A.16.18:

$$\frac{1}{\sin\phi} = 2 \sum_{s=1}^{\infty} \sin(2s-1)\phi \quad (\text{A.16.21})$$

A similar sum over cosine terms is equal to zero:

$$\sum_{s=0}^{\infty} \cos[(2s-1)\phi] = 0 \quad (\text{A.16.22})$$

It follows that:

$$\frac{1}{\sin\phi} = 2j \sum_{s=0}^{\infty} e^{-j(2s+1)\phi} \quad (\text{A.16.23})$$

## A.17 Zenith Angle Legendre Functions

The easiest way to obtain the general solution of Eq. 1.11.10 is to first solve the special case  $m = 0$ , for which case the equation is:

$$\frac{d^2\Theta}{d\theta^2} + \cot\theta \frac{d\Theta}{d\theta} + \nu(\nu+1)\Theta = 0 \quad (\text{A.17.1})$$

The character of separation constant  $v$  depends upon the boundary conditions applicable to the region in which the equation is applied. In the case of spherical waves in free space, for example,  $v$  is an integer, and denoted by  $v = \ell$ . For lossless waves in conical structures  $v$  is real and noninteger. If there is loss,  $v$  is imaginary. In this book since only lossless problems are considered  $v$  is real in all cases.

Since Eq. A.17.1 contains a singularity on the polar axes, the character of the functions  $\Theta(\theta)$  in the region away from the axes are of special interest. Rather than go directly to a solution, consider first the solution form in the region of interest. A useful substitution is:

$$\Theta = \frac{1}{(\sin\theta)^{1/2}} \tilde{\Theta} \quad (\text{A.17.2})$$

Differentiating:

$$\frac{d\Theta}{d\theta} = \frac{1}{(\sin\theta)^{1/2}} \frac{d\tilde{\Theta}}{d\theta} - \frac{\cos\theta}{2(\sin\theta)^{3/2}} \tilde{\Theta} \quad (\text{A.17.3})$$

$$\frac{d^2\Theta}{d\theta^2} = \frac{1}{(\sin\theta)^{1/2}} \frac{d^2\tilde{\Theta}}{d\theta^2} - \frac{\cos\theta}{(\sin\theta)^{3/2}} \frac{d\tilde{\Theta}}{d\theta} + \left[ \frac{3\cos^2\theta}{4(\sin\theta)^{5/2}} + \frac{1}{2(\sin\theta)^{1/2}} \right] \tilde{\Theta}$$

Combining Eqs. A.17.1 through A.17.3 gives:

$$\frac{d^2\tilde{\Theta}}{d\theta^2} + \left\{ \left( v + \frac{1}{2} \right)^2 + \frac{1}{4} (1 + \cot^2\theta) \right\} \tilde{\Theta} = 0 \quad (\text{A.17.4})$$

For  $\theta$  near  $\pi/2$ ,  $\cot^2\theta$  is much less than one and Eq. A.17.4 is nearly equal to:

$$\frac{d^2\tilde{\Theta}}{d\theta^2} + \left\{ \left( v + \frac{1}{2} \right)^2 + \frac{1}{4} \right\} \tilde{\Theta} = 0 \quad (\text{A.17.5})$$

Solutions of Eq. A.17.5 are:

$$\Theta(\theta) = \frac{1}{(\sin\theta)^{1/2}} [A_v \cos(\kappa_v\theta) + B_v \sin(\kappa_v\theta)] \quad (\text{A.17.6})$$

By definition:

$$\kappa_v = \left[ \left( v + \frac{1}{2} \right)^2 + \frac{1}{4} \right]^{1/2} \quad (\text{A.17.7})$$

Near the equator the zenith angle functions are trigonometric functions of  $(\kappa_v\theta)$  normalized by the square root of  $\sin\theta$ . The interval over which Eq. A.17.6 is valid increases with increasing values of  $v$ .

To examine the solution near its singularity, begin near the positive  $z$ -axis, where

$$\cot\theta \cong \frac{1}{\theta} \quad (\text{A.17.8})$$

Equation A.17.1 has the form:

$$\frac{d^2\Theta}{d\theta^2} + \frac{1}{\theta} \frac{d\Theta}{d\theta} + v(v+1)\Theta = 0 \quad (\text{A.17.9})$$

Equation A.17.9 is the cylindrical Bessel equation, for which the solution is:

$$\Theta(\theta) = A_v J_0(\beta\theta) + B_v Y_0(\beta\theta) \quad (\text{A.17.10})$$

By definition

$$\beta = [v(v+1)]^{1/2} \quad (\text{A.17.11})$$

$J_0(\beta\theta)$  and  $Y_0(\beta\theta)$  represent, respectively, cylindrical Bessel and Neumann functions of zero order. In the limit as  $\theta$  goes to zero,  $J_0(\beta\theta)$  goes to unity and  $Y_0(\beta\theta)$  becomes logarithmically singular:

$$\Theta(0) = C_v Y_0(0) \quad (\text{A.17.12})$$

By symmetry, near the negative  $z$ -axis the function takes the same form. The local solution is:

$$\Theta(\pi - \theta) = \hat{A}_v Y_0[\beta(\pi - \theta)] + \hat{B}_v J_0[\beta(\pi - \theta)] \quad (\text{A.17.13})$$

Combining shows that:

$$\Theta(\pi) = \hat{D}_v J_0(0) + \hat{C}_v Y_0(0) \quad (\text{A.17.14})$$

It follows that if one solution of Eq. A.17.1 is  $P_v(\cos\theta)$ , the other is  $P_v(-\cos\theta)$ . The first solution is regular on the positive  $z$ -axis and singular on the negative  $z$ -axis and the second solution is singular on the positive  $z$ -axis and regular on the negative  $z$ -axis. Both functions are periodic, see Eq. A.17.6, in the center region. The full solution is:

$$\Theta(\theta) = A_v P_v(\cos\theta) + B_v P_v(-\cos\theta) \quad (\text{A.17.15})$$

For values of  $m$  different from zero it is convenient to rewrite Eq. A.17.1 by introducing the variable  $\chi$  where:

$$\chi = \frac{1}{2}(1 - \cos\theta) = \sin^2(\theta/2) \quad (\text{A.17.16})$$

Derivatives are:

$$\begin{aligned} \frac{d\Theta}{d\chi} &= \frac{d\Theta}{d(\cos\theta)} \frac{d(\cos\theta)}{d\chi} = -2 \frac{d\Theta}{d(\cos\theta)} \\ \frac{d^2\Theta}{d\chi^2} &= \frac{d^2\Theta}{d(\cos\theta)^2} \left[ \frac{d(\cos\theta)}{d\chi} \right]^2 + \frac{d\Theta}{d(\cos\theta)} \frac{d^2(\cos\theta)}{d\chi^2} \end{aligned} \quad (\text{A.17.17})$$

Combining Eqs. A.17.16 and A.17.17 with Eq. A.17.1 gives:

$$\chi(1-\chi)\frac{d^2\Theta}{d\chi^2} + (1-2\chi)\frac{d\Theta}{d\chi} + v(v+1)\Theta = 0 \quad (\text{A.17.18})$$

A power series expansion results in:

$$\begin{aligned} \Theta(\chi) &= \sum_{j=0}^{\infty} a_j \chi^j \\ \frac{d}{d\chi} \Theta(\chi) &= \sum_{j=0}^{\infty} a_j j \chi^{j-1} \\ \frac{d^2}{d\chi^2} \Theta(\chi) &= \sum_{j=0}^{\infty} a_j j(j-1) \chi^{j-2} \end{aligned} \quad (\text{A.17.19})$$

Combining Eqs. A.17.18 and A.17.19 results in the equality:

$$\sum_{j=0}^{\infty} \left[ (j+1)^2 a_{j+1} - j(j+1) a_j + v(v+1) a_j \right] \chi^j = 0 \quad (\text{A.17.20})$$

Since Eq. A.17.20 is an identity in  $\chi$ , the coefficient of each power of  $\chi$  is separately equal to zero. It results in the recursion relationship:

$$\frac{a_{j+1}}{a_j} = \frac{j(j+1) - v(v+1)}{(j+1)^2} \quad (\text{A.17.21})$$

If  $v$  is an integer, the numerator of Eq. A.17.21 is equal to zero at  $v = j$  and the series terminates. Substituting Eq. A.17.21 in the first series of Eqs. A.17.19 results in the solution:

$$P_v(\cos \theta) = \sum_{j=0}^{\infty} \frac{(-1)^j (v+j)!}{(j)!^2 (v-j)!} \sin^{2j} \left( \frac{\theta}{2} \right) \quad (\text{A.17.22})$$

$P_v(-\cos \theta)$  is also a solution; changing the sign in Eq. A.17.17 gives:

$$\chi = \frac{1}{2} (1 + \cos \theta) = \cos^2 (\theta/2) \quad (\text{A.17.23})$$

Combining Eqs. A.17.22 and A.17.23 gives the second solution:

$$P_v(-\cos \theta) = \sum_{j=0}^{\infty} \frac{(-1)^j (v+j)!}{(j)!^2 (v-j)!} \cos^{2j} (\theta/2) \quad (\text{A.17.24})$$

Neither Eq. A.17.22 nor Eq. A.17.24 is a totally even or odd function of  $\theta$ . Since it is convenient to work with equations of definite parity, it is convenient to define the new functions:

$$\begin{aligned} L_v(\cos \theta) &= \frac{1}{2} \{ P_v(\cos \theta) + P_v(-\cos \theta) \} \\ M_v(\cos \theta) &= \frac{1}{2} \{ P_v(\cos \theta) - P_v(-\cos \theta) \} \end{aligned} \quad (\text{A.17.25})$$

The functional symmetry is:

$$L_v(\cos \theta) = L_v(-\cos \theta); \quad M_v(\cos \theta) = -M_v(-\cos \theta) \quad (\text{A.17.26})$$

Since the regions of convergence for  $P_v(\cos \theta)$  are  $-1 < \cos \theta \leq 1$  or  $0 \leq \theta < \pi$ , the region of convergence for  $L_v$  and  $M_v$  are  $0 < \theta < \pi$ .

## A.18 Legendre Polynomials

To solve problems with the  $z$ -axis is included in the region where a solution is necessary, all functions must remain bounded at the endpoints:  $0 \leq \theta \leq \pi$ . This happens only if separation constant  $n$  is an integer and the series



solution of Eq. A.17.21 terminates. For that case, both Eqs. A.17.22 and A.17.24 remain bounded on both the  $\pm z$ -axes, but are not independent. Since the product  $\ell(\ell+1)$  is the same for  $\ell = n$  as it is for  $\ell = -(n+1)$ , solutions are the same for the range of integers respectively from 0 to  $+\infty$  and from  $-1$  to  $-\infty$ . Therefore, only positive values of  $\ell$  need be considered.

To characterize Legendre polynomials, it is more convenient to redo the expansion than to work from the existing solutions. For this purpose, rewrite Eq. A.17.1 by replacing noninteger  $\nu$  by integer  $\ell$  and defining  $\chi = \cos\theta$ , to obtain:

$$(1-\chi^2)\frac{d^2\Theta}{d\chi^2} - 2\chi\frac{d\Theta}{d\chi} + \ell(\ell+1)\Theta = 0 \quad (\text{A.18.1})$$

The power series expansion is:

$$\begin{aligned} \Theta(\chi) &= \sum_{j=0}^{\infty} a_j \chi^j \\ \frac{d\Theta(\chi)}{d\chi} &= \sum_{j=0}^{\infty} a_j j \chi^{j-1} \\ \frac{d^2\Theta(\chi)}{d\chi^2} &= \sum_{j=0}^{\infty} a_j j(j-1) \chi^{j-2} \end{aligned} \quad (\text{A.18.2})$$

Combining gives:

$$\sum_{j=0}^{\infty} [(j+1)(j+2)a_{j+2} - j(j+1)a_j + \ell(\ell+1)a_j] \chi^j = 0 \quad (\text{A.18.3})$$

Combining:

$$\frac{a_{j+2}}{a_j} = \frac{j(j+1) - \ell(\ell+1)}{(j+1)(j+2)} \quad (\text{A.18.4})$$

Combining Eq. A.18.4 with the expansion for  $\Theta(\chi)$ :

$$\Theta_{\ell}(\chi) = a_0 \sum_{j=0}^{\infty} \frac{(-1)^j \chi^{2j} (\ell)!! (\ell + 2j - 1)!!}{(2j)! (\ell - 1)!! (\ell - 2j)!!} \quad (\text{A.18.5})$$

Examples are:

$$\Theta_0(\chi) = a_0; \quad \Theta_1(\chi) = a_0(1 - 3\chi^2); \quad \Theta_2(\chi) = a_0 \left( 1 - 10\chi^2 + \frac{35}{3}\chi^4 \right) \quad (\text{A.18.6})$$

$a_0$  is an arbitrary constant and is redefined for each value of  $\ell$  to make  $\Theta_{\ell}(0) = 1$ . With that definition, functions  $\Theta_{\ell}(\chi)$  are defined to be Legendre polynomials of the first kind, and indicated by  $P_{\ell}(\cos\theta)$ . Therefore  $P_{\ell}(\chi)$  is given by the series:

$$P_{\ell}(\chi) = \frac{1}{2^{\ell}} \sum_{s=0}^{[\ell/2]} \frac{(-1)^s}{s!} \frac{(2\ell - 2s)!}{(\ell - s)! (\ell - 2s)!} \chi^{\ell - 2s} \quad (\text{A.18.7})$$

The symbol  $[\ell/2]$  indicates the largest integer contained in  $\ell/2$ . From Eq. A.18.7, it follows that:

$$P_{\ell}(1) = 1; \quad P_{2\ell+1}(0) = 0; \quad P_{2\ell}(0) = (-1)^{\ell} \frac{(2\ell - 1)!!}{(2\ell)!!}; \quad P_{\ell}(-\chi) = (-1)^{\ell} P_{\ell}(\chi)$$

Values of the important functional combinations on the axes are shown in Table A.18.1.

	$P_{\ell}(\cos\theta)$	$\frac{dP_{\ell}^1(\cos\theta)}{d\theta}$	$\frac{P_{\ell}^1(\cos\theta)}{\sin\theta}$
$\theta=0$	1	$\frac{1}{2} \ell(\ell+1)$	$\frac{1}{2} \ell(\ell+1)$
$\theta=\pi$	$(-1)^{\ell}$	$\frac{1}{2} \ell(\ell+1)(-1)^{(\ell+1)/2}$	$\frac{1}{2} \ell(\ell+1)(-1)^{(\ell-1)/2}$
$\theta=\pi/2$	$i^{\ell} \frac{(\ell-1)!!}{\ell!!} \delta(2q, \ell)$	$i^{\ell} \frac{(\ell+1)!!}{(\ell-2)!!} \delta(2q, \ell)$	$i^{\ell-1} \frac{(\ell)!!}{(\ell-1)!!} \delta(2q+1, \ell)$

Table A.18.1 Values of Selected Functions on the Axes

For even values of  $\ell$ , the expansion may be written:

$$P_\ell(\chi) = \frac{1}{2^\ell(\ell)!} \frac{d^\ell}{d\chi^\ell} \sum_{s=0}^{\ell} \frac{(-1)^s(\ell)!}{(s)!(\ell-s)!} \chi^{2\ell-2s} \quad (\text{A.18.8})$$

The binomial expansion is:

$$(\chi^2 - 1)^\ell = \sum_{s=0}^{\ell} \frac{(-1)^s(\ell)!}{(s)!(\ell-s)!} \chi^{2\ell-2s} \quad (\text{A.18.9})$$

Combining results gives another expression for Legendre polynomials:

$$P_\ell(\chi) = \frac{1}{2^\ell(\ell)!} \frac{d^\ell}{d\chi^\ell} (\chi^2 - 1)^\ell \quad (\text{A.18.10})$$

Equation A.18.10 is the Rodrigues formula for Legendre polynomials.

Comparison using Eqs. A.17.27 and Eq. A.18.9 shows, for integer orders:

$$L_{2\ell}(\chi) = P_{2\ell}(\chi); \quad M_{2\ell+1}(\chi) = P_{2\ell+1}(\chi) \quad (\text{A.18.11})$$

The second integer-order solution to Eq. A.18.1 is commonly defined as:

$$Q_v(\chi) = \frac{\pi}{2\sin(v\pi)} [P_v(\chi) \cos(v\pi) - P_v(-\chi)] \quad (\text{A.18.12})$$

$Q_v(\chi)$  is obviously a solution of the Legendre differential equation and, when  $v$  is equal to integer  $\ell$ ; it is in indeterminate form. Differentiating numerator and denominator then letting  $v$  become an integer:

$$\begin{aligned} Q_\ell(\chi) &= \lim_{v \Rightarrow \ell} \frac{1}{2\cos(v\pi)} \left[ -\pi \sin(v\pi) P_v(\chi) + \cos(v\pi) \frac{dP_v(\chi)}{dv} - \frac{dP_v(-\chi)}{dv} \right] \\ &= \frac{1}{2} \left\{ \frac{dP_v(\chi)}{dv} - \frac{dP_v(-\chi)}{dv} \right\}_{v=\ell} \end{aligned} \quad (\text{A.18.13})$$

Using Eq. A.18.13, the functions at the lowest three orders are:

$$\begin{aligned} Q_0(\chi) &= \ln[\cot(\theta/2)] \\ Q_1(\chi) &= (\cos\theta) \ln\left(\cot\frac{\theta}{2}\right) - 1 \\ Q_2(\chi) &= \frac{1}{2}(3\cos^2\theta - 1) \ln\left(\cot\frac{\theta}{2}\right) - \frac{3}{2}\cos\theta \end{aligned} \quad (\text{A.18.14})$$

Comparison with the noninteger functions, Eq. A.18.12, shows that:

$$\begin{aligned} Q_{2\ell}(\chi) &= \frac{\partial M_v(\chi)}{\partial v} \Big|_{v \Rightarrow 2\ell} \\ Q_{2\ell+1}(\chi) &= \frac{\partial L_v(\chi)}{\partial v} \Big|_{v \Rightarrow 2\ell+1} \end{aligned} \quad (\text{A.18.15})$$

In this work, we are concerned only with the zero order function  $Q_0(\chi)$ .

## A.19 Associated Legendre Functions

Associated Legendre functions are solutions for the extended case  $m > 0$ . The Legendre differential equation, Eq. 1.11.10, may be rewritten as:

$$\left(1 - \chi^2\right) \frac{d^2 \Theta}{d\chi^2} - 2\chi \frac{d\Theta}{d\chi} + \left[ v(v+1) - \frac{m^2}{(1 - \chi^2)} \right] \Theta = 0 \quad (\text{A.19.1})$$

Solutions are most easily obtained by starting with the  $m = 0$  equation and differentiating  $m$  times to obtain:

$$\left(1 - \chi^2\right) \frac{d^{m+2} \Theta}{d\chi^{m+2}} - 2(m+1)\chi \frac{d^{m+1} \Theta}{d\chi^{m+1}} + [v(v+1) - m(m+1)] \frac{d^m \Theta}{d\chi^m} = 0 \quad (\text{A.19.2})$$

Introducing construction function  $W(\theta)$  and solving for the first two derivatives:

$$\Theta(\theta) = W(\theta) \sin^m \theta$$

$$\frac{d\Theta}{d\chi} = \frac{dW}{d\chi} \sin^m \theta - mW \sin^{m-2} \theta \cos \theta$$

$$\frac{d^2\Theta}{d\chi^2} = \frac{d^2W}{d\chi^2} \sin^m \theta - 2m \frac{dW}{d\chi} \sin^{m-2} \theta \cos \theta + m(m-2)W \sin^{m-4} \theta \cos^2 \theta - mW \sin^{m-2} \theta \quad (\text{A.19.3})$$

Substituting Eqs. A.19.3 into Eq. A.19.1 for the special case  $m = 0$  results in:

$$\frac{d^2W}{d\chi^2} \sin^2 \theta - 2(m+1) \frac{dW}{d\chi} \cos \theta + [v(v+1) - m(m+1)]W = 0 \quad (\text{A.19.4})$$

For the special case where  $v = \ell$ , an integer, comparison of Eqs. A.19.2 and A.19.4 shows that  $W$  is given by:

$$W_\ell(\theta) = \frac{d^m P_\ell(\cos \theta)}{d\chi^m} \quad (\text{A.19.5})$$

Since Eq. A.19.5 satisfies the associated Legendre differential equation, the solution of that equation is:

$$\Theta(\theta) = P_\ell^m(\cos \theta) = \sin^m \theta \frac{d^m P_\ell(\cos \theta)}{d\chi^m} \quad (\text{A.19.6})$$

The equality holds for all integer orders,  $\ell$ , and degrees,  $m$ . Combining Eq. A.19.6 with the Rodrigues formula shows that the corresponding expression for associated Legendre functions is:

$$P_\ell^m(\chi) = \frac{1}{(2\ell)!!} (1-\chi^2)^{m/2} \frac{d^{\ell+m}}{d\chi^{\ell+m}} (\chi^2-1)^\ell \quad (\text{A.19.7})$$

## A.20 Orthogonality

An integral relationship for products of Legendre polynomials follows directly from the differential equation, Eq. A.19.1, for integer orders. Multiplying the differential equation by another Legendre polynomial of the same degree but unspecified order gives:

$$\int_{-1}^1 P_n^m(\chi) \left\{ \frac{d}{d\chi} \left[ (1-\chi^2) \frac{d^2 P_\ell^m}{d\chi^2} \right] + \left[ \ell(\ell+1) - \frac{m^2}{(1-\chi^2)} \right] P_\ell^m \right\} d\chi = 0 \quad (\text{A.20.1})$$

To evaluate the left side, integrate the first term once by parts. The result is:

$$\int_{-1}^1 \left\{ (1-\chi^2) \frac{dP_\ell^m}{d\chi} \frac{dP_n^m}{d\chi} + \left[ \ell(\ell+1) - \frac{m^2}{(1-\chi^2)} \right] P_\ell^m P_n^m \right\} d\chi = 0 \quad (\text{A.20.2})$$

Next exchange positions of  $\ell$  and  $n$ , repeat the process, and subtract the second integral from the first. The result is:

$$[\ell(\ell+1) - n(n+1)] \int_{-1}^1 P_\ell^m(\chi) P_n^m(\chi) d\chi = 0 \quad (\text{A.20.3})$$

The result shows that the associated Legendre polynomials form an orthogonal set.

To evaluate the integral with  $\ell = n$ , put  $I_1$  equal to the integral:

$$I_1 = \int_{-1}^1 [P_\ell^m(\chi)]^2 d\chi \quad (\text{A.20.4})$$

Combining Eqs. A.19.7 and A.20.4:

$$I_1 = \frac{(-1)^m}{[(2\ell)!!]^2} \int_{-1}^1 d\chi \frac{d^{\ell+m}}{d\chi^{\ell+m}} (\chi^2 - 1)^\ell \left[ (\chi^2 - 1)^m \frac{d^{\ell+m}}{d\chi^{\ell+m}} (\chi^2 - 1)^\ell \right] \quad (\text{A.20.5})$$

Integrating by parts  $\ell + m$  times leaves:

$$I_1 = \frac{1}{[(2\ell)!!]^2} \int_{-1}^1 d\chi \left\{ (1-\chi^2)^\ell \frac{d^{\ell+m}}{d\chi^{\ell+m}} \left[ (\chi^2-1)^m \frac{d^{\ell+m}}{d\chi^{\ell+m}} (\chi^2-1)^\ell \right] \right\} \quad (\text{A.20.6})$$

Only the highest power of  $\chi$  survives the indicated differentiation operations:

$$\begin{aligned} \frac{d^{\ell+m}}{d\chi^{\ell+m}} \left[ (\chi^2-1)^m \frac{d^{\ell+m}}{d\chi^{\ell+m}} (\chi^2-1)^\ell \right] &= \frac{d^{\ell+m}}{d\chi^{\ell+m}} \left[ \chi^{2m} \frac{d^{\ell+m}}{d\chi^{\ell+m}} \chi^{2\ell} \right] \\ &= \frac{(2\ell)!}{(\ell-m)!} \frac{d^{\ell+m}}{d\chi^{\ell+m}} \chi^{\ell+m} = \frac{(2\ell)!(\ell+m)!}{(\ell-m)!} \end{aligned} \quad (\text{A.20.7})$$

Combining Eqs. A.20.6 and A.20.7 leaves:

$$I_1 = \frac{(2\ell)!(\ell+m)!}{[(2\ell)!!]^2 (\ell-m)!} \int_{-1}^1 d\chi (1-\chi^2)^\ell \quad (\text{A.20.8})$$

Using the binomial expansion, Eq. A.18.9, and integrating:

$$I_1 = \frac{2(-1)^\ell (2\ell-1)!! (\ell+m)!}{(2\ell)!! (\ell-m)!} \sum_{s=0}^{\ell} \frac{(-1)^s \ell!}{s! (\ell-s)! (2\ell-2s+1)} \quad (\text{A.20.9})$$

The sum may be written in closed form as:

$$I_1 = \frac{2}{(2\ell+1)} \frac{(\ell+m)!}{(\ell-m)!} \quad (\text{A.20.10})$$

Combining Eqs. A.20.3 and A.20.10 gives the orthogonality relationship for associated Legendre polynomials:

$$I_1 = \int_{-1}^1 P_\ell^m(\chi) P_n^m(\chi) d\chi = \frac{2}{(2\ell+1)} \frac{(\ell+m)!}{(\ell-m)!} \delta(\ell, n) \quad (\text{A.20.11})$$

A similar integral, the value of which follows by a slight extension of the above, is:

$$I_2 = \int_{-1}^1 P_\ell^m(\chi) P_\ell^{m+2s}(\chi) d\chi = (-1)^s \frac{2}{(2\ell+1)} \frac{(\ell+m)!}{(\ell-m-2s)!} \quad (\text{A.20.12})$$

## A.21 Recursion Relationships

It is helpful to compile a table of identities involving associated Legendre polynomials. A convenient starting point for determining the recursion relationships is Eq. A.18.7. For the case that  $\ell$  is odd the upper limit is  $(\ell-1)/2$ . Substituting  $p = (\ell-1-2s)/2$  into the equation yields:

$$P_\ell(\chi) = \frac{\chi(-1)^{(\ell-1)/2}}{2^\ell} \sum_{p=0}^{(\ell-1)/2} \frac{(-1)^p (\ell+1+2p)!}{(2p+1)! \left(\frac{\ell-1-2p}{2}\right)! \left(\frac{\ell+1+2p}{2}\right)!} \chi^{\ell-2s} \quad (\text{A.21.1})$$

Rewrite the equation as:

$$P_\ell(\chi) = (-1)^{(\ell-1)/2} \frac{(\ell)!!}{(\ell-1)!!} \sum_{s=0}^{(\ell-1)/2} \frac{(-1)^s \chi^{2s+1} (\ell+2s)!! (\ell-1)!!}{(2s+1)! (\ell)!! (\ell-1-2s)!!} \quad (\text{A.21.2})$$

For the case of  $\ell$  even, the upper limit is  $\ell/2$ . In a similar way the equation goes to:

$$P_\ell(\chi) = (-1)^{\ell/2} \frac{(\ell-1)!!}{(\ell)!!} \sum_{s=0}^{\ell/2} \frac{(-1)^s \chi^{2s} (\ell-1+2s)!! (\ell)!!}{(2s)! (\ell-1)!! (\ell-2s)!!} \quad (\text{A.21.3})$$

With Eq. A.21.3, replace  $\ell$  by  $(\ell+1)$  and write out the first few terms, then repeat with  $\ell$  replaced by  $(\ell-1)$ . The resulting series are:



$$P_{\ell+1}(\chi) = (-1)^{(\ell+1)/2} \frac{(\ell)!!}{(\ell+1)!!} \left\{ 1 - \frac{\chi^2}{2!} \frac{(\ell+2)!!}{(\ell)!!} \frac{(\ell+1)!!}{(\ell-1)!!} + \frac{\chi^4}{4!} \frac{(\ell+4)!!}{(\ell)!!} \frac{(\ell+1)!!}{(\ell-3)!!} - \dots \right\}$$

$$P_{\ell-1}(\chi) = (-1)^{(\ell-1)/2} \frac{(\ell-2)!!}{(\ell-1)!!} \left\{ 1 - \frac{\chi^2}{2!} \frac{(\ell)!!}{(\ell-2)!!} \frac{(\ell-1)!!}{(\ell-3)!!} + \frac{\chi^4}{4!} \frac{(\ell+2)!!}{(\ell-2)!!} \frac{(\ell-1)!!}{(\ell-5)!!} - \dots \right\}$$

These expressions combine to form the indicated sum:

$$\begin{aligned} \ell P_{\ell-1}(\chi) + (\ell+1) P_{\ell+1}(\chi) &= (-1)^{(\ell-1)/2} \frac{(2\ell+1)(\ell)!!}{(\ell-1)!!} \left\{ \frac{\chi^2}{1!} - \frac{\chi^4}{3!} (\ell+2)(\ell-1) + \dots \right\} \\ &= (-1)^{(\ell-1)/2} \frac{(2\ell+1)(\ell)!!}{(\ell-1)!!} \sum_{s=0}^{(\ell-1)/2} \frac{(-1)^s \chi^{2s+2} (\ell+2s)!! (\ell-1)!!}{(2s+1)(\ell)!! (\ell-1-2s)!!} \end{aligned} \quad (\text{A.21.4})$$

Combining Eqs. A.21.3 and A.21.5 results in:

$$(2\ell+1)\chi P_{\ell}(\chi) = \ell P_{\ell-1}(\chi) + (\ell+1) P_{\ell+1}(\chi) \quad (\text{A.21.5})$$

Proofs for even values of  $\ell$  follow in a parallel way and give the same result. Equation A.21.5 is the first recursion relationship.

The same technique with the indicated operations results in the second recursion relationship:

$$(2\ell+1)P_{\ell}(\chi) = \frac{dP_{\ell+1}(\chi)}{d\chi} - \frac{dP_{\ell-1}(\chi)}{d\chi} \quad (\text{A.21.6})$$

The integral expression of Eq. A.21.7 follows from Eq. A.21.6:

$$\int P_{\ell}(\chi) d\chi = \left[ \frac{P_{\ell+1}(\chi) - P_{\ell-1}(\chi)}{(2\ell+1)} \right] \quad (\text{A.21.7})$$

Differentiating Eq. A.21.5 by  $\chi$  and adding  $\ell \times$  Eq. 21.6 gives:

$$(\ell+1)P_{\ell}(\chi) = \frac{dP_{\ell+1}(\chi)}{d\chi} - \chi \frac{dP_{\ell}(\chi)}{d\chi} \quad (\text{A.21.8})$$

Differentiating Eq. A.21.8  $m$  times, multiplying through by  $\sin^{m+1}\theta$ , and using Eq. A.19.7 gives:

$$P_{\ell+1}^{m+1}(\chi) = \chi P_{\ell}^{m+1}(\chi) + (\ell + m + 1) \sin \theta P_{\ell}^m(\chi) \quad (\text{A.21.9})$$

A series of identities follows by mixing and matching. Selected ones are listed in Table A.21.1.

---

1.	$\frac{dP_{\ell}^m}{d\theta} = \frac{1}{2}[(\ell + m)(\ell - m + 1)P_{\ell}^{m-1} - P_{\ell}^{m+1}]$
2.	$\frac{mP_{\ell}^m}{\sin \theta} = \frac{1}{2}[(\ell + m)(\ell - m + 1)P_{\ell-1}^{m-1} + P_{\ell-1}^{m+1}]$
3.	$\sin \theta \frac{dP_{\ell}^m}{d\theta} = \frac{1}{2\ell + 1}[\ell(\ell - m + 1)P_{\ell+1}^m - (\ell + m)(\ell + 1)P_{\ell-1}^m]$
4.	$\cos \theta P_{\ell}^m = \frac{1}{2\ell + 1}[(\ell - m + 1)P_{\ell+1}^m + (\ell + m)P_{\ell-1}^m]$
5.	$P_{\ell}^{m+1} = 2m \cot \theta P_{\ell}^m - (\ell + m)(\ell - m + 1)P_{\ell}^{m-1}$
6.	$(\ell - m + 1)P_{\ell+1}^m = (2\ell + 1) \cos \theta P_{\ell}^m - (\ell + m)P_{\ell-1}^m$
7.	$(2\ell + 1) \sin \theta P_{\ell}^m = P_{\ell+1}^{m+1} - P_{\ell-1}^{m+1}$
8.	$P_{\ell+1}^{m+1} = \cos \theta P_{\ell}^{m+1} + (\ell + m + 1) \sin \theta P_{\ell}^m$
9.	$P_{\ell-1}^{m+1} = \cos \theta P_{\ell-1}^{m+1} - (\ell - m) \sin \theta P_{\ell}^m$
10.	$\frac{dP_{\ell}^m}{d\theta} = m \cot \theta P_{\ell}^m - P_{\ell}^{m+1}$
11.	$\frac{dP_{\ell}^m}{d\theta} = -m \cot \theta P_{\ell}^m + (\ell + m)(\ell - m + 1)P_{\ell}^{m-1}$

---

Table A.21.1 A Table of Identities for Legendre functions

Associated Legendre functions have even or odd parity, respectively, if the sum  $(\ell + m)$  is even or odd:

$$P_{\ell}^m(\chi) = (-1)^{\ell+m} P_{\ell}^m(-\chi) \quad (\text{A.21.10})$$

Let  $\delta$  be a Kronecker delta and let  $q$  equal any of the field of positive integers, including zero. At  $\theta = \pi/2$ , the equator, functional values are:

$$P_{\ell}^m(0) = (-1)^{(\ell-m)/2} \frac{(\ell+m+1)!}{(\ell-m)!} \delta(2q, \ell+m) \quad (\text{A.21.11})$$

$$\left. \frac{d^r}{d\theta^r} P_{\ell}^m(\cos \theta) \right|_{\frac{\pi}{2}} = P_{\ell}^{m+r}(0) \quad (\text{A.21.12})$$

In the tables to follow, order is  $\ell$ , degree is  $m$ , and  $\chi = \cos \theta$ . Polynomials are even or odd functions of  $\chi$  as  $(\ell+m)$  is even or odd, respectively; absence of a superscript indicates degree 0. Normalization is chosen to make  $P_{\ell}(1) = 1$ .

Table A.21.2 contains values of associated legendre polynomials. Useful recursion relationships for constructing the table are:

$$P_{\ell}^m(\chi) = \frac{1}{\ell-m} \left[ (2\ell-1)\chi P_{\ell-1}^m(\chi) - (\ell-1+m)P_{\ell-2}^m(\chi) \right]$$

$$P_{\ell}^m(\chi) = \left[ 2(m-1)\cot \theta P_{\ell}^{m-1}(\chi) - (\ell-1+m)(\ell+2-m)P_{\ell}^{m-2}(\chi) \right]$$

$$P_{\ell}^1(\chi) = -\frac{dP_{\ell}}{d\theta}$$

The sum of all coefficients in the expansion for  $P_{\ell}^m(\chi)$  is

$(\ell+m)!/2^m(m)!(\ell-m)!$ . To normalize, multiply each associated Legendre function by  $\sqrt{(2\ell+1)(\ell-m)!/2(\ell+m)!}$ .

Table A.21.3 contains values of spherical angular function  $dP_{\ell}^m/d\theta$ , based upon the relationship:

$$dP_{\ell}^m/d\theta = -m \cot \theta P_{\ell}^m + (\ell+m)(\ell-m+1)P_{\ell}^{m-1} = m \cot \theta P_{\ell}^m - P_{\ell}^{m+1}$$

$\ell$	$\mathbf{m} = 0$ , Values for $P_\ell(1)$	$\mathbf{m} = 1$ , Values for $P_\ell^1(\chi)$
0	1	
1	$\chi$	$\sin\theta$
2	$\frac{1}{2}(3\chi^2 - 1)$	$3\chi\sin\theta$
3	$\frac{\chi}{2}(5\chi^2 - 3)$	$\frac{3}{2}(5\chi^2 - 1)\sin\theta$
4	$\frac{1}{8}(35\chi^4 - 30\chi^2 + 3)$	$\frac{5\chi}{2}(7\chi^2 - 3)\sin\theta$
5	$\frac{\chi}{8}(63\chi^4 - 70\chi^2 + 15)$	$\frac{15}{8}(21\chi^4 - 14\chi^2 + 1)\sin\theta$
6	$\frac{1}{16}(231\chi^6 - 315\chi^4 + 105\chi^2 - 5)$	$\frac{21\chi}{8}(33\chi^4 - 30\chi^2 + 5)\sin\theta$
7	$\frac{\chi}{16}(429\chi^6 - 693\chi^4 + 315\chi^2 - 35)$	$\frac{7}{16}(429\chi^6 - 495\chi^4 + 135\chi^2 - 5)\sin\theta$
8	$\frac{1}{16}(6435\chi^8 - 12012\chi^6 + 6930\chi^4 - 1260\chi^2 + 35)$	$\frac{9\chi}{128}(715\chi^6 - 1001\chi^4 + 385\chi^2 - 35)\sin\theta$
9	$\frac{\chi}{16}(12155\chi^8 - 25740\chi^6 + 18018\chi^4 - 4620\chi^2 + 315)$	$\frac{45}{128}(2431\chi^8 - 4004\chi^6 + 2002\chi^4 - 308\chi^2 + 7)\sin\theta$

Table A.21.2a Table of Associated Legendre Polynomials,  $P_\ell^m(\chi)$

$\ell$	$m = 2$ , Values for $P_\ell^2(\chi)$	$m = 3$ , Values for $P_\ell^3(\chi)$
2	$3\sin^2\theta$	
3	$15\chi\sin^2\theta$	$15\sin^3\theta$
4	$\frac{15}{2}(7\chi^2 - 1)\sin^2\theta$	$105\chi\sin^3\theta$
5	$\frac{105\chi}{2}(3\chi^2 - 1)\sin^2\theta$	$\frac{105}{2}(9\chi^2 - 1)\sin^3\theta$
6	$\frac{105}{8}(33\chi^4 - 18\chi^2 + 1)\sin^2\theta$	$\frac{315\chi}{2}(11\chi^2 - 3)\sin^3\theta$
7	$\frac{63\chi}{8}(143\chi^4 - 110\chi^2 + 15)\sin^2\theta$	$\frac{315}{8}(143\chi^4 - 66\chi^2 + 3)\sin^3\theta$
8	$\frac{315}{16}(143\chi^6 - 143\chi^2 + 33\chi^2 - 1)\sin^2\theta$	$\frac{3465\chi}{8}(39\chi^4 - 26\chi^2 + 3)\sin^3\theta$
9	$\frac{495\chi}{16}(221\chi^6 - 273\chi^2 + 91\chi^2 - 7)\sin^2\theta$	$\frac{3465}{16}(221\chi^4 - 195\chi^4 + 39\chi^2 - 1)\sin^3\theta$

Table A.21.2b Table of Associated Legendre Polynomials,  $P_\ell^m(\chi)$

$\ell$	$m = 4,$ Values for $P_\ell^4(\chi)$	$m = 5,$ Values for $P_\ell^5(\chi)$
4	$105\sin^4\theta$	
5	$945\chi\sin^4\theta$	$945\sin^5\theta$
6	$945(11\chi^2 - 1)\sin^4\theta/2$	$10395\chi\sin^5\theta$
7	$3465\chi(13\chi^2 - 3)\sin^4\theta/2$	$10395(13\chi^2 - 1)\sin^5\theta/2$
8	$10395(65\chi^4 - 26\chi^2 + 1)\sin^4\theta/8$	$135135\chi(5\chi^2 - 1)\sin^5\theta/2$
9	$135135\chi(17\chi^4 - 10\chi^2 + 1)\sin^4\theta/8$	$135135(85\chi^4 - 30\chi^2 + 1)\sin^5\theta/8$

Table A.21.2c Table of Associated Legendre Polynomials,  $P_\ell^m(\chi)$ 

$\ell$	$m = 6,$ Values for $P_\ell^6(\chi)$	$m = 7,$ Values for $P_\ell^7(\chi)$
6	$10395\sin^6\theta$	
7	$135135\chi\sin^6\theta$	$135135\sin^7\theta$
8	$135135(15\chi^2 - 1)\sin^6\theta/2$	$2027025\chi\sin^7\theta$
9	$675675\chi(17\chi^2 - 3)\sin^6\theta/2$	$2027025(17\chi^2 - 1)\sin^7\theta/2$

Table A.21.2d Table of Associated Legendre Polynomials,  $P_\ell^m(\chi)$ 

$\ell$	$m = 8,$ Values for $P_\ell^8(\chi)$	$m = 9,$ Values for $P_\ell^9(\chi)$
8	$2027025\sin^8\theta$	
9	$34459425\chi\sin^8\theta$	$34459425\sin^9\theta$

Table A.21.2e Table of Associated Legendre Polynomials,  $P_\ell^m(\chi)$

$m = 0$ , Values of  $dP_\ell/d\theta = -P_\ell^1$  are listed above in Table A.21.2.a

$\ell$	$m = 1,$ $dP_\ell^1/d\theta = -\cot\theta P_\ell^1 + \ell(\ell+1)P_\ell$	$m = 2,$ $dP_\ell^2/d\theta = -2\cot\theta dP_\ell^2 + (\ell-1)(\ell+2)dP_\ell^1$
1	$\chi$	
2	$3(2\chi^2 - 1)$	$6\chi\sin\theta$
3	$\frac{3}{2}\chi(15\chi^2 - 11)$	$15(3\chi^2 - 1)\sin\theta$
4	$\frac{5}{2}(28\chi^4 - 27\chi^2 + 3)$	$30\chi(7\chi^2 - 4)\sin\theta$
5	$\frac{15\chi}{8}(105\chi^4 - 126\chi^2 + 29)$	$\frac{105}{2}(15\chi^4 - 12\chi^2 + 1)\sin\theta$
6	$\frac{21}{8}(198\chi^6 - 285\chi^4 + 100\chi^2 - 5)$	$\frac{105\chi}{4}(99\chi^4 - 102\chi^2 + 19)\sin\theta$
7	$\frac{7\chi}{16}(3003\chi^6 - 5049\chi^4 + 2385\chi^2 - 275)$	$\frac{63}{8}(1001\chi^6 - 1265\chi^4 + 375\chi^2 - 15)\sin\theta$
8	$\frac{9}{16}(5720\chi^8 - 11011\chi^6 + 6545\chi^4 - 1225\chi^2 + 35)$	$\frac{315\chi}{8}(286\chi^6 - 429\chi^4 + 176\chi^2 - 17)\sin\theta$
9	$\frac{45\chi}{16}(21879\chi^8 - 47464\chi^6 + 34034\chi^4 - 8932\chi^2 + 623)$	$\frac{495}{16}(1989\chi^8 - 3458\chi^6 + 1820\chi^4 - 294\chi^2 + 7)\sin\theta$

Table A.21.3a Table of Spherical Angular Function  $dP_\ell^m/d\theta$

$\ell$	$m = 3,$ $dP_\ell^3/d\theta = -3 \cot \theta P_\ell^3 + (\ell - 2)(\ell + 3)P_\ell^2$	$m = 4,$ $dP_\ell^4/d\theta = -4 \cot \theta P_\ell^4 + (\ell - 3)(\ell + 4)P_\ell^3$
3	$45\chi \sin^2 \theta$	
4	$105(4\chi^2 - 1)\sin^2 \theta$	$420\chi \sin^3 \theta$
5	$315\chi(15\chi^2 - 7)\sin^2 \theta/2$	$945(5\chi^2 - 1)\sin^3 \theta$
6	$945(22\chi^4 - 15\chi^2 + 1)\sin^2 \theta/2$	$945\chi(33\chi^2 - 13)\sin^3 \theta$
7	$315\chi(1001\chi^4 - 902\chi^2 + 141)\sin^2 \theta/8$	$3465(91\chi^4 - 54\chi^2 + 3)\sin^3 \theta/2$
8	$10395(104\chi^6 - 117\chi^4 + 30\chi^2 - 1)\sin^2 \theta/8$	$10395\chi(130\chi^4 - 104\chi + 14)\sin^3 \theta/2$
9	$10395\chi(663\chi^6 - 897\chi^4 + 325\chi^2 - 27)\sin^2 \theta/16$	$135135(153\chi^6 - 155\chi^4 + 35\chi^2 - 1)\sin^3 \theta/8$

Table A.21.3b Table of Spherical Angular Function  $dP_\ell^m/d\theta$



$\ell$	$m = 5$ $dP_\ell^5/d\theta = -5 \cot \theta P_\ell^5 + (\ell - 4)(\ell + 5)P_\ell^4$	$m = 6$ $dP_\ell^6/d\theta = -6 \cot \theta P_\ell^6 + (\ell - 5)(\ell + 6)P_\ell^5$
5	$4725\chi \sin^4 \theta$	
6	$4725(6\chi^2 - 1)\sin^4 \theta$	$62370\chi \sin^5 \theta$
7	$10395\chi(91\chi^2 - 31)\sin^4 \theta/2$	$135135(7\chi^2 - 1)\sin^5 \theta$
8	$135135(40\chi^4 - 21\chi^2 + 1)\sin^4 \theta/2$	$810810\chi(10\chi^2 - 3)\sin^5 \theta$
9	$675675\chi(153\chi^4 - 110\chi^2 + 13)\sin^4 \theta/8$	$2027025(51\chi^4 - 24\chi^2 + 1)\sin^5 \theta/2$

Table A.21.3c Table of Spherical Angular Function  $dP_\ell^m/d\theta$ 

$\ell$	$m = 7$ , $dP_\ell^7/d\theta = -7 \cot \theta P_\ell^7 + (\ell - 6)(\ell + 7)P_\ell^6$	$m = 8$ , $dP_\ell^8/d\theta = -8 \cot \theta P_\ell^8 + (\ell - 7)(\ell + 8)P_\ell^7$
7	$945945\chi \sin^6 \theta$	
8	$2027025(8\chi^2 - 1)\sin^6 \theta$	$16216200\chi \sin^7 \theta$
9	$2027025\chi(153\chi^2 - 41)\sin^6 \theta$	$34459425(9\chi^2 - 1)\sin^7 \theta$

Table A.21.3d Table of Spherical Angular Function  $dP_\ell^m/d\theta$

$\ell$	$m = 9,$
	$dP_\ell^9/d\theta = -9 \cot \theta P_\ell^9 + (\ell - 8)(\ell + 9)P_\ell^8$
9	$310134825\chi \sin^8 \theta$

Table A.21.3e Table of Spherical Angular Function  $dP_\ell^m/d\theta$ 

## A.22 Integrals of Legendre Functions

Integrals of different functional combinations of Legendre polynomials are needed. Consider, for example, the integral:

$$I_3 = m \int_0^\pi \frac{d}{d\theta} (P_\ell^m P_n^m) d\theta = 0 \quad (\text{A.22.1})$$

The equality follows since the integrand is a perfect differential and  $P_\ell^m(\pm 1) = 0$  for  $m > 0$ .

Consider the integral:

$$I_4 = \int_0^\pi \left\{ \frac{dP_\ell^m}{d\theta} \frac{dP_n^m}{d\theta} + \frac{m^2 P_\ell^m P_n^m}{\sin^2 \theta} \right\} \sin \theta d\theta \quad (\text{A.22.2})$$

The first term in the integrand may be written:

$$\frac{dP_\ell^m}{d\theta} \frac{dP_n^m}{d\theta} = \frac{1}{\sin \theta} \frac{d}{d\theta} \left[ \sin \theta P_\ell^m \frac{dP_n^m}{d\theta} \right] - \frac{P_\ell^m}{\sin \theta} \frac{d}{d\theta} \left[ \sin \theta \frac{dP_n^m}{d\theta} \right]$$

The second term in the integrand, after using the differential equation, may be written:

$$\frac{m^2 P_\ell^m P_n^m}{\sin^2 \theta} = \frac{P_\ell^m}{\sin \theta} \frac{d}{d\theta} \left[ \sin \theta \frac{dP_n^m}{d\theta} \right] + n(n+1) P_n^m P_\ell^m$$

Combining results in:

$$I_4 = \int_0^\pi \sin\theta d\theta \left\{ \frac{1}{\sin\theta} \frac{d}{d\theta} \left[ \sin\theta P_\ell^m \frac{dP_n^m}{d\theta} \right] + \ell(\ell+1) P_\ell^m P_n^m \right\} \quad (\text{A.22.3})$$

The first term is an exact differential that integrates to zero, leaving:

$$I_4 = \ell(\ell+1) \int_0^\pi \sin\theta d\theta P_\ell^m P_n^m = \frac{2\ell(\ell+1)(\ell+m)!}{(2\ell+1)(\ell-m)!} \delta(\ell, n) \quad (\text{A.22.4})$$

Consider the integral

$$I_5 = \int_0^\pi \cos\theta \sin\theta d\theta \left\{ \frac{dP_\ell^m}{d\theta} \frac{dP_n^m}{d\theta} + \frac{m^2 P_\ell^m P_n^m}{\sin^2\theta} \right\} \quad (\text{A.22.5})$$

The procedure is similar to that for  $I_5$ . Replace the first term using the differential equation, sum, and partially integrate once to obtain:

$$I_5 = \int_0^\pi \sin\theta d\theta \left\{ \left[ \sin\theta P_\ell^m \frac{dP_n^m}{d\theta} \right] + \ell(\ell+1) \cos\theta P_\ell^m P_n^m \right\}$$

Combining with recursion relationships, Table A.21.1.3 and A.21.1.4, shows that:

$$I_5 = \int_0^\pi \sin\theta d\theta P_\ell^m \left[ \frac{\ell(\ell-m+1)(\ell+2)}{(2\ell+1)} P_{\ell+1}^m + \frac{(n+m)(n^2-1)}{(2n+1)} P_{n-1}^m \right]$$

Evaluation using Eq. A.20.11 gives:

$$I_5 = \left[ \frac{2\ell(\ell+2)(\ell+m+1)!}{(2\ell+1)(2\ell+3)(\ell-m)!} \delta(\ell, \ell+1) + \frac{(n^2-1)(n+m)!}{(2n-1)(2n+1)(n-m-1)!} \delta(\ell, n-1) \right] \quad (\text{A.22.6})$$

Consider the integral

$$I_6 = \int_0^{\pi} \sin^2 \theta d\theta \frac{d}{d\theta} (P_{\ell}^m P_n^m) \quad (\text{A.22.7})$$

Expanding the differential and using recursion relationship Table A.21.1.3 results in:

$$I_6 = \int_0^{\pi} \sin \theta d\theta \left\{ P_{\ell}^m \left[ \frac{n(n-m+1)}{(2n+1)} P_{n+1}^m - \frac{(n+m)(n-1)}{(2n+1)} P_{n-1}^m \right] \right. \\ \left. + P_n^m \left[ \frac{(\ell-m+1)}{(2\ell+1)} P_{\ell+1}^m - \frac{(\ell+m)(\ell-1)}{(2\ell+1)} P_{\ell-1}^m \right] \right\}$$

Term by term evaluation shows that:

$$I_6 = 0 \quad (\text{A.22.8})$$

Consider the integral

$$I_7 = \int_0^{\pi} \sin^2 \theta d\theta \left[ \frac{dP_{\ell}^m}{d\theta} \frac{dP_n^{m+1}}{d\theta} + \frac{m(m+1)}{\sin^2 \theta} P_{\ell}^m P_n^{m+1} \right] \quad (\text{A.22.9})$$

Substituting the differential equation into the first term, summing, and taking one partial integration results in:

$$\int_0^{\pi} \sin \theta d\theta P_n^{m+1} \left\{ -\cos \theta \frac{dP_{\ell}^m}{d\theta} + \left[ \ell(\ell+1) \sin \theta + \frac{m}{\sin \theta} \right] P_{\ell}^m \right\}$$

After using the recursion relationship of Table A.21.1.10 on the first term then summing the curly bracket becomes:

$$\left\{ [\ell(\ell+1) + m] \sin \theta P_{\ell}^m + \cos \theta P_{\ell}^{m+1} \right\}$$

With the use of the recursion relationships of Tables A.21.1.4 and A.21.1.7 the bracket becomes:

$$\left\{ P_{\ell+1}^{m+1} \left[ \frac{\ell(\ell+2)}{(2\ell+1)} \right] - P_{\ell-1}^{m+1} \left[ \frac{(\ell-1)(\ell+1)}{(2\ell+1)} \right] \right\}$$

Putting the bracket back under the integral sign and integrating gives:

$$I_7 = \frac{2\ell(\ell+2)(\ell+m+2)!}{(2\ell+1)(2\ell+3)(\ell-m)!} \delta(n, \ell+1) - \frac{2(\ell-1)(\ell+1)(\ell+m)!}{(2\ell-1)(2\ell+1)(\ell-m-2)!} \delta(n, \ell-1) \quad (\text{A.22.10})$$

Consider the integral

$$I_8 = \int_0^\pi \sin \theta d\theta \left( (m+1) P_\ell^{m+1} \frac{dP_n^m}{d\theta} + m P_n^m \frac{dP_\ell^{m+1}}{d\theta} \right) \quad (\text{A.22.11})$$

This may be rewritten as:

$$\int_0^\pi d\theta \left( \sin \theta P_\ell^{m+1} \frac{dP_n^m}{d\theta} + m \sin \theta \frac{d}{d\theta} [P_n^m P_\ell^{m+1}] \right)$$

Integrating the perfect differential by parts gives:

$$\int_0^\pi \sin \theta d\theta P_\ell^{m+1} \left( \frac{dP_n^m}{d\theta} - m \cot \theta P_n^m \right) = - \int_0^\pi \sin \theta d\theta P_\ell^{m+1} P_n^{m+1}$$

The second equality is in the proper form to use Table A.21.1.10. The result is:

$$I_8 = - \frac{2}{(2\ell+1)} \frac{(\ell+m+1)!}{(\ell-m-1)!} \delta(\ell, n) \quad (\text{A.22.12})$$

Similarly, except using Table A.21.1.11, integrals with  $(m-1)$  replacing  $(m+1)$  may be evaluated, and are listed in Table A.22.1.

1. 
$$I_{\ell\ell} = \int_0^\pi P_\ell^m P_n^m \sin\theta d\theta = \frac{2(\ell+m)!}{(2\ell+1)(\ell-m)!} \delta(\ell, n)$$
2. 
$$\int_0^\pi P_\ell^m P_\ell^{m+2s} \sin\theta d\theta = \frac{2(-1)^s}{(2\ell+1)} \frac{(\ell+m)!}{(\ell-m-2s)!}$$
3. 
$$m \int_0^\pi \frac{d}{d\theta} (P_\ell^m P_n^m) d\theta = 0$$
4. 
$$m \int_0^\pi \frac{d}{d\theta} (P_\ell^m P_n^m) \cos\theta d\theta = \frac{2m(\ell+m)!}{(2\ell+1)(\ell-m)!} \delta(\ell, n)$$
5. 
$$\int_0^\pi \frac{d}{d\theta} (P_\ell^m P_n^m) \sin^2\theta d\theta = 0$$
6. 
$$\int_0^\pi \left[ \frac{dP_\ell^m}{d\theta} \frac{dP_n^m}{d\theta} + \frac{m^2 P_\ell^m P_n^m}{\sin^2\theta} \right] \sin\theta d\theta = \frac{2\ell(\ell+1)(\ell+m)!}{(2\ell+1)(\ell-m)!} \delta(\ell, n)$$
7. 
$$\int_0^\pi \left[ \frac{dP_\ell^m}{d\theta} \frac{dP_n^m}{d\theta} + \frac{m^2 P_\ell^m P_n^m}{\sin^2\theta} \right] \cos\theta \sin\theta d\theta = \left\{ \begin{array}{l} \frac{2\ell(\ell+2)(\ell+m+1)!}{(2\ell+1)(2\ell+3)(\ell-m)!} \delta(n, \ell+1) \\ + \frac{2(\ell-1)(\ell+1)(\ell+m)!}{(2\ell-1)(2\ell+1)(\ell-m-1)!} \delta(n, \ell-1) \end{array} \right\}$$
8. 
$$\int_0^\pi \left[ \frac{dP_\ell^m}{d\theta} \frac{dP_n^{m+1}}{d\theta} + \frac{m(m+1)P_\ell^m P_n^{m+1}}{\sin^2\theta} \right] \sin^2\theta d\theta = \left\{ \begin{array}{l} \frac{2\ell(\ell+2)(\ell+m+2)!}{(2\ell+1)(2\ell+3)(\ell-m)!} \delta(n, \ell+1) \\ - \frac{2(\ell-1)(\ell+1)(\ell+m)!}{(2\ell-1)(2\ell+1)(\ell-m-2)!} \delta(n, \ell-1) \end{array} \right\}$$
9. 
$$\int_0^\pi \left[ \frac{dP_\ell^m}{d\theta} \frac{dP_n^{m-1}}{d\theta} + \frac{m(m-1)P_\ell^m P_n^{m-1}}{\sin^2\theta} \right] \sin^2\theta d\theta = \left\{ \begin{array}{l} -\frac{2\ell(\ell+2)(\ell+m)!}{(2\ell+1)(2\ell+3)(\ell-m)!} \delta(\ell, n+1) \\ + \frac{2(\ell-1)(\ell+1)(\ell+m)!}{(2\ell-1)(2\ell+1)(\ell-m)!} \delta(\ell, n-1) \end{array} \right\}$$
10. 
$$\int_0^\pi P_\ell^m (\cos\theta) \sin^{\ell+1}\theta d\theta = (-1)^{(\ell-m)/2} \frac{2^{\ell+1}(\ell)! (\ell+m)!}{(2\ell+1)!} \delta(\ell+m, 2q)$$
11. 
$$\int_0^\pi \left( (m+1)P_\ell^{m+1} \frac{dP_n^m}{d\theta} + mP_n^m \frac{dP_\ell^{m+1}}{d\theta} \right) \sin\theta d\theta = -\frac{2}{(2\ell+1)} \frac{(\ell+m+1)!}{(\ell-m-1)!} \delta(\ell, n)$$
12. 
$$\int_0^\pi \left( (m-1)P_\ell^{m-1} \frac{dP_n^m}{d\theta} + mP_n^m \frac{dP_\ell^{m-1}}{d\theta} \right) \sin\theta d\theta = -\frac{2}{(2\ell+1)} \frac{(\ell+m)!}{(\ell-m)!} \delta(\ell, n)$$

Table A.22.1 Table of Integrals of Legendre Polynomials

## A.23 Integrals of Fractional Order Legendre Functions

The Legendre differential equation of fractional order is:

$$\frac{1}{\sin\theta} \frac{d}{d\theta} \left( \sin\theta \frac{d\Theta_v^m(\cos\theta)}{d\theta} \right) + \left( v(v+1) - \frac{m^2}{\sin^2\theta} \right) \Theta_v^m = 0 \quad (\text{A.23.1})$$

Functions  $\Theta_v^m(\cos\theta)$  represent  $L_v^m(\cos\theta)$ ,  $M_v^m(\cos\theta)$ , or any linear combination thereof. Useful boundary conditions are:

$$M_v^m(\cos\theta)|_{\theta=\psi} = 0 \quad \text{and} \quad \frac{dL_v^m(\cos\theta)}{d\theta}|_{\theta=\psi} = 0 \quad (\text{A.23.2})$$

This evaluation of integrals over noninteger order Legendre functions includes the boundary conditions of Eqs. A.23.2.

Consider the integral

$$I_9 = \int_{\psi}^{\pi-\psi} \sin\theta d\theta \left( \frac{dM_v^m}{d\theta} \frac{dP_n^m}{d\theta} + \frac{m^2 M_v^m P_n^m}{\sin^2\theta} \right) \quad (\text{A.23.3})$$

The evaluation procedure is to use the differential equation and rewrite the first term as:

$$\frac{dM_v^m}{d\theta} \frac{dP_n^m}{d\theta} = \frac{1}{\sin\theta} \frac{d}{d\theta} \left( \sin\theta M_v^m \frac{dP_n^m}{d\theta} \right) - \frac{M_v^m}{\sin\theta} \frac{d}{d\theta} \left( \sin\theta \frac{dP_n^m}{d\theta} \right) \quad (\text{A.23.4})$$

The first term on the right side of Eq. A.23.4 forms a perfect differential and, after imposing Eq. A.23.2, the integral of that differential is equal to zero. With the differential equation substituted into the remaining term, the result is:

$$I_9 = n(n+1) \int_{\psi}^{\pi-\psi} M_v^m P_n^m \sin\theta d\theta \quad (\text{A.23.5})$$

To evaluate Eq. A.23.5, since  $M_v^m(\cos\theta)$  has odd parity and  $P_n^m(\cos\theta)$  is even or odd as  $(n+m)$  is even or odd, the integral vanishes if  $(n+m)$  is even. If  $(n+m)$  is odd, repeat the procedure used in Eq. A.20.1 through A.20.3. The result is:

$$I_9 = \int_{\psi}^{\pi-\psi} M_v^m P_n^m \sin\theta d\theta = \left\{ \frac{\sin\theta \left[ P_n^m \frac{dM_v^m}{d\theta} - M_v^m \frac{dP_n^m}{d\theta} \right]}{n(n+1) - v(v+1)} \right\}_{\psi}^{\pi-\psi}$$

After imposing the boundary condition of Eq. A.23.2:

$$\int_{\psi}^{\pi-\psi} M_v^m P_n^m \sin\theta d\theta = -2 \sin\psi \left\{ \frac{P_n^m(\cos\psi) \frac{dM_v^m(\cos\psi)}{d\theta}}{n(n+1) - v(v+1)} \right\} \delta(n, 2q+1) \quad (\text{A.23.6})$$

The integer 'q' represents any positive integer, including zero.

The next integral to be evaluated is:

$$I_{10} = \int_{\psi}^{\pi-\psi} \sin\theta d\theta \left( \frac{dL_{\mu}^m}{d\theta} \frac{dP_n^m}{d\theta} + \frac{m^2 L_{\mu}^m P_n^m}{\sin^2\theta} \right) \quad (\text{A.23.7})$$

The same technique that was applied to Eq. A.23.2 when applied to Eq. A.23.7 results in:

$$I_{10} = \mu(\mu+1) \int_{\psi}^{\pi-\psi} L_{\mu}^m P_n^m \sin\theta d\theta \quad (\text{A.23.8})$$

The same technique applied to Eq. A.23.4 results in:



$$I_{10} = \int_{\psi}^{\pi-\psi} L_{\mu}^m P_n^m \sin \theta d\theta = 2 \sin \psi \left\{ \frac{L_{\mu}^m(\cos \psi) \frac{dP_n^m(\cos \psi)}{d\theta}}{n(n+1) - \mu(\mu+1)} \right\} \delta(n, 2q) \quad (\text{A.23.9})$$

It follows at once from the parity of the functions that the integral:

$$I_{11} = \int_{\psi}^{\pi-\psi} \sin \theta d\theta \left( \frac{dM_v^m}{d\theta} \frac{dL_{\mu}^m}{d\theta} + \frac{m^2 M_v^m L_{\mu}^m}{\sin^2 \theta} \right) = 0 \quad (\text{A.23.10})$$

Consider the integral

$$I_{12} = \int_{\psi}^{\pi-\psi} \sin \theta d\theta \left( \frac{dM_v^m}{d\theta} \frac{dM_{\mu}^m}{d\theta} + \frac{m^2 M_v^m M_{\mu}^m}{\sin^2 \theta} \right) \quad (\text{A.23.11})$$

The same technique applied to Eq. A.23.2 results in:

$$I_{12} = v(v+1) \int_{\psi}^{\pi-\psi} \sin \theta d\theta M_v^m M_{\mu}^m \quad (\text{A.23.12})$$

The same technique applied to Eq. A.23.4 results in:

$$\int_{\psi}^{\pi-\psi} M_v^m M_{\mu}^m \sin \theta d\theta = \left\{ \frac{\sin \theta \left[ M_{\mu}^m \frac{dM_v^m}{d\theta} - M_v^m \frac{dM_{\mu}^m}{d\theta} \right]}{\mu(\mu+1) - v(v+1)} \right\}_{\psi}^{\pi-\psi}$$

The boundary condition shows that the result is zero unless  $\mu(\mu+1) - v(v+1)$ . For that case, evaluating the indeterminate form gives:

$$I_{12} = \int_{\psi}^{\pi-\psi} M_{\nu}^m M_{\mu}^m \sin \theta d\theta = \frac{2 \sin \psi}{2\nu+1} \left[ \frac{\partial M_{\nu}^m(\cos \psi)}{\partial \nu} \frac{\partial M_{\nu}^m(\cos \psi)}{\partial \theta} \right] \delta(\nu, \mu) \quad (\text{A.23.13})$$

The delta function indicates a Kronecker delta function with a noninteger argument.

Consider the integral

$$I_{13} = \int_{\psi}^{\pi-\psi} \sin \theta d\theta \left( \frac{dL_{\nu}^m}{d\theta} \frac{dL_{\mu}^m}{d\theta} + \frac{m^2 dL_{\nu}^m dL_{\mu}^m}{\sin^2 \theta} \right) \quad (\text{A.23.14})$$

In a way similar to the earlier integrals:

$$I_{13} = \mu(\mu+1) \int_{\psi}^{\pi-\psi} \sin \theta d\theta L_{\nu}^m L_{\mu}^m \quad (\text{A.23.15})$$

$$I_{13} = \int_{\psi}^{\pi-\psi} L_{\nu}^m L_{\mu}^m \sin \theta d\theta = -\frac{2 \sin \psi}{2\mu+1} \left[ L_{\mu}^m(\cos \psi) \frac{\partial^2 L_{\mu}^m(\cos \psi)}{\partial \nu \partial \theta} \right] \delta(\nu, \mu) \quad (\text{A.23.16})$$

Results are summarized in Table A.23.1.

## ***Spherical Bessel Functions***

### **A.24 The First Solution Form**

Since the radial differential equation, Eq. 1.11.7, is independent of separation parameter  $m$ , so are the solutions. The spherical Bessel differential equation with separation parameter  $\nu$  is:

$$\frac{1}{\sigma^2} \frac{d}{d\sigma} \left( \sigma^2 \frac{dR}{d\sigma} \right) + \left( 1 - \frac{\nu(\nu+1)}{\sigma^2} \right) R = 0 \quad (\text{A.24.1})$$

- 
1. 
$$I_{vn} = \int_{-\psi}^{\psi} M_v^m P_n^m \sin \theta d\theta = -2 \sin \psi \left\{ \frac{P_n^m(\cos \psi) \frac{dM_v^m(\cos \theta)}{d\theta} \Big|_{\theta=\psi}}{n(n+1) - v(v+1)} \right\} \delta(m+n, 2q+1)$$
  2. 
$$\int_{-\psi}^{\psi} \left( \frac{dM_v^m}{d\theta} \frac{dP_n^m}{d\theta} + \frac{m^2 M_v^m P_n^m}{\sin^2 \theta} \right) \sin \theta d\theta = n(n+1) I_{vn}$$
  3. 
$$K_{\mu n} = \int_{\psi}^{\pi-\psi} L_{\mu}^m P_n^m \sin \theta d\theta = 2 \sin \psi \left\{ \frac{L_{\mu}^m(\cos \psi) \frac{dP_n^m(\cos \psi)}{d\theta}}{n(n+1) - \mu(\mu+1)} \right\} \delta(n, 2q)$$
  4. 
$$\int_{\psi}^{\pi-\psi} \left( \frac{dL_{\mu}^m}{d\theta} \frac{dP_n^m}{d\theta} + \frac{m^2 L_{\mu}^m P_n^m}{\sin^2 \theta} \right) \sin \theta d\theta = \mu(\mu+1) I_{\mu n}$$
  5. 
$$\int_{\psi}^{\pi-\psi} \left( \frac{dM_v^m}{d\theta} \frac{dL_{\mu}^m}{d\theta} + \frac{m^2 M_v^m L_{\mu}^m}{\sin^2 \theta} \right) \sin \theta d\theta = 0$$
  6. 
$$I_{vv} = \int_{\psi}^{\pi-\psi} M_v^m M_{\mu}^m \sin \theta d\theta = \frac{2 \sin \psi}{2v+1} \left[ \frac{\partial M_v^m(\cos \psi)}{\partial v} \frac{\partial M_v^m(\cos \psi)}{\partial \theta} \right] \delta(v, \mu)$$
  7. 
$$\int_{\psi}^{\pi-\psi} \left( \frac{dM_v^m}{d\theta} \frac{dM_{\mu}^m}{d\theta} + \frac{m^2 M_v^m M_{\mu}^m}{\sin^2 \theta} \right) \sin \theta d\theta = v(v+1) I_{vv}$$
  8. 
$$K_{\mu\mu} = \int_{\psi}^{\pi-\psi} L_v^m L_{\mu}^m \sin \theta d\theta = -\frac{2 \sin \psi}{2\mu+1} \left[ L_{\mu}^m(\cos \psi) \frac{\partial^2 L_{\mu}^m(\cos \psi)}{\partial v \partial \theta} \right] \delta(v, \mu)$$
  9. 
$$\int_{\psi}^{\pi-\psi} \left( \frac{dL_v^m}{d\theta} \frac{dL_{\mu}^m}{d\theta} + \frac{m^2 L_v^m L_{\mu}^m}{\sin^2 \theta} \right) \sin \theta d\theta = \mu(\mu+1) K_{\mu\mu}$$
- 

Table A.23.1 Table of Integrals, Noninteger Order Legendre Functions

Equation A.24.1 is a second order equation and has two independent solutions. Because of a singularity at the origin, solutions are satisfied over the region  $0 < \sigma \leq \infty$ . For the range of solutions in which  $\sigma^2 \gg v(v+1)$ , the differential equation goes to:

$$\frac{1}{\sigma^2} \frac{d}{d\sigma} \left( \sigma^2 \frac{dR(\sigma)}{d\sigma} \right) + R(\sigma) = 0 \quad (\text{A.24.2})$$

Solutions of Eq. A.24.2 are:

$$R(\sigma) = \frac{C_1}{\sigma} \cos \sigma + \frac{C_2}{\sigma} \sin \sigma \quad (\text{A.24.3})$$

$C_1$  and  $C_2$  are constants of integration. This is the asymptotic limit for large radius.

To obtain solutions valid at all radii, use a power series expansion to solve differential Eq. A.24.1. The series and its first two derivatives are:

$$R_v(\sigma) = \sum_{s=0}^{\infty} a_s \sigma^{s+p}$$

$$\frac{dR_v(\sigma)}{d\sigma} = \sum_{s=0}^{\infty} (s+p) a_s \sigma^{s+p-1} \quad (\text{A.24.4})$$

$$\frac{d^2 R_v(\sigma)}{d\sigma^2} = \sum_{s=0}^{\infty} (s+p)(s+p-1) a_s \sigma^{s+p-2}$$

Substituting Eqs. A.24.2 into Eq. A.24.1 and solving leads to:

$$\left\{ \begin{aligned} & [p(p+1) - v(v+1)] a_0 \sigma^{p-2} + [(p+1)(p+2) - v(v+1)] a_1 \sigma^{p-1} \\ & + \sum_{s=0}^{\infty} \{ [(s+p+2)(s+p+3) - v(v+1)] a_{s+2} + a_s \} \sigma^{s+p} \end{aligned} \right\} = 0 \quad (\text{A.24.5})$$

Since the series of Eq. A.24.5 is an identity in  $\sigma$ , the coefficient of each power of  $\sigma$  is separately equal to zero. There are but two nontrivial ways that the coefficients of  $\sigma^{p-2}$  and  $\sigma^{p-1}$  can both be equal to zero. One is if  $a_0$  is equal to zero and  $(p+1)(p+2) = v(v+1)$ . The other is if  $a_1$  is equal to zero and  $p(p+1) = v(v+1)$ . Arbitrarily making the second choice, the condition that  $p(p+1) = v(v+1)$  is met either of two ways:  $p = v$  or  $p = -(v+1)$ ; these choices determine the two independent solutions.

For the case  $p = v$  the portion of Eq. A.24.5 in the curly brackets is zero, and results in the recursion relationship:

$$\frac{a_{s+2}}{a_s} = -\frac{1}{(s+2)(2v+s+3)} \quad (\text{A.24.6})$$

This relationship, after redefining the dummy index, leads to the functional form of the radial function  $R_v(\sigma)$ :

$$R_v(\sigma) = a_0 \sum_{s=0}^{\infty} \frac{(-1)^s (2v+1)!!}{2^s s! (2v+2s+1)!!} \sigma^{v+2s} \quad (\text{A.24.7})$$

Making the definition that  $a_0 = 1/(2v+1)!!$  the result is the function:

$$j_v(\sigma) = \sum_{s=0}^{\infty} \frac{(-1)^s}{2^s s! (2v+2s+1)!!} \sigma^{v+2s} \quad (\text{A.24.8})$$

Functions  $j_v(\sigma)$  are the spherical Bessel functions of order  $v$ . The functional limit at small values of  $\sigma$  follows from Eq. A.24.8, and is equal to:

$$\lim_{\sigma \Rightarrow 0} [j_v(\sigma)] = \frac{\sigma^v}{(2v+1)!!} \quad (\text{A.24.9})$$

For the case  $p = -(v+1)$ , the last term of Eq. A.24.5 results in the recursion relationship:

$$\frac{a_{s+2}}{a_s} = \frac{1}{(s+2)(2v-s-1)} \quad (\text{A.24.10})$$

This relationship leads directly to the series solution:

$$y_v(\sigma) = \frac{a_0}{\sigma^{v+1}} \left\{ \begin{aligned} &1 + \frac{\sigma^2}{2(2v-1)} + \frac{\sigma^4}{2 \cdot 4(2v-1)(2v-3)} + \dots + \frac{\sigma^{2p}}{(2p)!!(2v-1) \dots (2v-2p-1)} + \dots \\ &+ \frac{\sigma^{2(v-1)}}{(2v-2)!!(2v-1)!!} - \frac{\sigma^{2v}}{1 \cdot (2v)!!(2v-1)!!} + \frac{\sigma^2}{3 \cdot (2v+2)!!(2v-1)!!} - \dots \end{aligned} \right\} \quad (\text{A.24.11})$$

The series is monotone for  $s$  less than  $v$  and oscillatory for  $s$  greater than  $v$ . The combination is readily described by separate sums over the monotone and oscillatory portions. After using the definition  $a_0 = 1/(2v+1)!!$  and again redefining the dummy index:

$$y_v(\sigma) = - \sum_{s=0}^{[v]} \frac{(2v-2s-1)!!}{(2s)!! \sigma^{v+1-2s}} - \sum_{s=0}^{\infty} \frac{(-1)^s}{(2s-1)!!} \frac{\sigma^{v-1+2s}}{(2v+2s)!!} \quad (\text{A.24.12})$$

The symbol  $[v]$  indicates the largest integer less than  $v$ . The first sum of Eq. A.24.12 describes a monotone power series with inverse powers of  $v$ , powers that range upward from  $-(v+1)$  to  $(v+1)$  and a second sum that represents an alternating series with positive powers of  $v$ . The sums are the spherical Neumann functions; Eq. A.4.12 shows the functional small argument limit of  $j_v(\sigma)$  to be:

$$\lim_{\sigma \Rightarrow 0} [y_v(\sigma)] = - \frac{(2v-1)!!}{\sigma^{v+1}} \quad (\text{A.24.13})$$

For integer orders,  $v$  equal integer  $\ell$ , and  $\sigma \gg 1$ , the functions are determined by Eqs. A.24.8 and the second of Eqs. A.24.12:

$$j_{\ell}(\sigma) = \sum_{s=0}^{\infty} \frac{(-1)^s}{(2s)!!(2\ell+2s+1)!!} \sigma^{\ell+2s} \quad (\text{A.24.14})$$

$$y_{\ell}(\sigma) \equiv - \sum_{s=0}^{\infty} \frac{(-1)^s}{(2s-1)!!(2\ell+2s)!!} \sigma^{\ell-1+2s}$$

Term-by-term comparison of the series representation of Eqs. A.24.3 and A.24.14 shows that:

$$\begin{aligned} \lim_{\sigma \Rightarrow \infty} j_{\ell}(\sigma) &= \frac{1}{\sigma} \cos \left[ \sigma - \frac{\pi}{2}(\ell+1) \right] \\ \lim_{\sigma \Rightarrow \infty} y_{\ell}(\sigma) &= \frac{1}{\sigma} \sin \left[ \sigma - \frac{\pi}{2}(\ell+1) \right] \end{aligned} \quad (\text{A.24.15})$$

Using Eq. A.24.15, it follows that the Bessel and Neumann functions are related as:

$$\begin{aligned} \lim_{\sigma \Rightarrow \infty} \left\{ j_{\ell}(\sigma) = \frac{1}{\sigma} \frac{d}{d\sigma} [\sigma y_{\ell}(\sigma)] \right\} \\ \lim_{\sigma \Rightarrow \infty} \left\{ y_{\ell}(\sigma) = -\frac{1}{\sigma} \frac{d}{d\sigma} [\sigma j_{\ell}(\sigma)] \right\} \end{aligned} \quad (\text{A.24.16})$$

## A.25 The Second Solution Form

If the separation constant is an integer, the spherical Bessel differential equation, Eq. 1.11.7, is given by:

$$\frac{1}{\sigma^2} \frac{d}{d\sigma} \left( \sigma^2 \frac{dR}{d\sigma} \right) + \left( 1 - \frac{\ell(\ell+1)}{\sigma^2} \right) R = 0 \quad (\text{A.25.1})$$

Solutions follow that are more convenient to use than Eqs. A.24.8 and A.24.12. Integer solutions, valid over the range  $0 < \sigma < \infty$ , may be obtained by removing the value at infinity before obtaining a detailed

solution. To remove the value at infinity, note that as the radius becomes infinite Eq. A.25.1 approaches:

$$\frac{d^2 R_\ell(\sigma)}{d\sigma^2} + R_\ell(\sigma) = 0 \quad (\text{A.25.2})$$

If Eq. A.25.2 were an exact solution, the result would be exponential with constant coefficients. Although Eq. A.25.2 is not exact, it is helpful to write Eq. A.24.3 in the form:

$$R_\ell(\sigma) = F_\ell(\sigma)e^{-i\sigma} + G_\ell(\sigma)e^{i\sigma} \quad (\text{A.25.3})$$

A requirement is that at large radii  $F_\ell(\sigma)$  and  $G_\ell(\sigma)$  vary much less rapidly with increasing radius than do the exponentials. Also since  $F_\ell(\sigma)$  and  $G_\ell(\sigma)$  are complex conjugates it is only necessary to solve for one of them.

A convenient method of obtaining them is with a power series expansion. The series and the first two derivatives are:

$$\begin{aligned} R_\ell(\sigma) &= F_\ell(\sigma)e^{-i\sigma}; & \frac{dR_\ell(\sigma)}{d\sigma} &= \left[ \frac{dF_\ell(\sigma)}{d\sigma} - iF_\ell(\sigma) \right] e^{-i\sigma} \\ \frac{d^2 R_\ell(\sigma)}{d\sigma^2} &= \left[ \frac{d^2 F_\ell(\sigma)}{d\sigma^2} - 2i \frac{dF_\ell(\sigma)}{d\sigma} - F_\ell(\sigma) \right] e^{-i\sigma} \end{aligned} \quad (\text{A.25.4})$$

Substituting Eqs. A.25.4 into Eq. A.25.1 results in the differential equation:

$$\frac{d^2 F_\ell(\sigma)}{d\sigma^2} + 2\left(\frac{1}{\sigma} - i\right) \frac{dF_\ell(\sigma)}{d\sigma} - \left(\frac{2i}{\sigma} + \frac{\ell(\ell+1)}{\sigma^2}\right) F_\ell(\sigma) = 0 \quad (\text{A.25.5})$$

The most convenient method of solving Eq. A.25.5 is with a power series expansion. The series and the first two derivatives are:

$$F_\ell(\sigma) = \sum_{s=0}^{\infty} a_s \sigma^{s+p}$$



$$\frac{dF_\ell(\sigma)}{d\sigma} = \sum_{s=0}^{\infty} (s+p)a_s\sigma^{s+p-1}$$

$$\frac{d^2F_\ell(\sigma)}{d\sigma^2} = \sum_{s=0}^{\infty} (s+p)(s+p-1)a_s\sigma^{s+p-2}$$
(A.25.6)

Inserting Eqs. A.25.6 into Eq. A.25.5 and gathering similar powers of  $\sigma$  result in:

$$\left\{ \frac{p(p+1) - \ell(\ell+1)}{\sigma^{p-2}} + \sum_{s=0}^{\infty} \sigma^{s+p+1} \times \{a_{s+1}[(s+p+1)(s+p+2) - \ell(\ell+1)] - 2i\dot{a}_s(s+p+1)\} \right\} = 0$$
(A.25.7)

Since the series is an identity, the coefficient of each power of  $\sigma$  is separately equal to zero. It follows from the  $\sigma^{p-2}$  term that either  $p = \ell$  or  $p = -(\ell + 1)$  and it follows from the square brackets that:

$$\frac{a_{s+1}}{a_s} = \frac{2i(s+p+1)}{(s+p+1)(s+p+2) - \ell(\ell+1)}$$
(A.25.8)

With the option  $p = \ell$ , in the limit as  $\sigma$  becomes infinite Eq. A.25.8 goes to:

$$\lim_{s \Rightarrow \infty} \left( \frac{a_{s+1}}{a_s} \right) = \frac{2i}{s}$$
(A.25.9)

Equation A.25.9 is also the limiting form for a series expansion of  $\exp(2i\sigma)$ .

Therefore, since  $F_\ell(\sigma)$  varies more slowly with  $\sigma$  than  $e^{-i\sigma}$ , the recursion relationship of Eq. A.25.8 is not an acceptable solution. Returning to the option that  $p = -(\ell + 1)$ , Eq. A.25.7 goes to:

$$\frac{a_{s+1}}{a_s} = \frac{2i(\ell-s)}{(s+1)(2\ell-s)}$$
(A.25.10)

Since the progression of Eq. A.25.10 terminates at  $s = \ell$  the power series truncates to a polynomial of highest order  $\ell$ . The general term is:

$$\frac{a_{s+1}}{a_s} = \frac{(2i)^s \ell! (2\ell - s)!}{s! (2\ell)! (\ell - s)!} \quad (\text{A.25.11})$$

The series results in solution  $R_\ell(\sigma)$  where:

$$R_\ell(\sigma) = \frac{e^{-i\sigma}}{\sigma} \sum_{s=0}^{\ell} \frac{(2i)^s \ell! (2\ell - s)!}{s! (2\ell)! (\ell - s)!} a_0 \quad (\text{A.25.12})$$

To characterize the solution substitute  $p = \ell - s$ , rewrite Eq. A.25.12 as a sum over  $p$ , then change the dummy index back to  $s$ . The result is:

$$R_\ell(\sigma) = a_0 \frac{e^{-i\sigma}}{\sigma} \frac{\ell! (2i)^\ell}{(2\ell)!} \sum_{s=0}^{\ell} \frac{(\ell + s)!}{s! (\ell - s)!} \left( \frac{1}{2i\sigma} \right)^s \quad (\text{A.25.13})$$

With the definition that  $a_0 = i(2\ell - 1)!!$ , the full solution is the function  $h_\ell(\sigma)$  where:

$$h_\ell(\sigma) = \frac{i^{\ell+1} e^{-i\sigma}}{\sigma} \sum_{s=0}^{\ell} \frac{(\ell + s)!}{s! (\ell - s)!} \left( \frac{1}{2i\sigma} \right)^s \quad (\text{A.25.14})$$

Function  $h_\ell(\sigma)$  is a spherical Hankel function of the second kind. The real part is a spherical Bessel function and the negative of the imaginary part is a spherical Neumann function. By definition:

$$h_\ell(\sigma) = j_\ell(\sigma) - iy_\ell(\sigma) \quad (\text{A.25.15})$$

The complex conjugate of Eq. A.25.14 is the second independent solution of the equation. It is a spherical Hankel function of the first kind. In this work, we shall be concerned only with Hankel functions of the second kind.

For vanishingly small values of  $\sigma$ , the dominant term in Eq. A.25.14 is:

$$\lim_{\sigma \Rightarrow 0} [h_\ell(\sigma)] = \frac{i(2\ell-1)!!}{\sigma^{\ell+1}} \quad (\text{A.25.16})$$

As the radius increases without limit, the dominant term is:

$$\lim_{\sigma \Rightarrow \infty} [h_\ell(\sigma)] = \frac{i^{\ell+1}}{\sigma} e^{-i\sigma} \quad (\text{A.25.17})$$

Equation A.25.17 shows that as the radius increases without limit the function  $[\sigma h_\ell(\sigma)]$  does not approach a limit. For those cases where it is necessary to impose a limit condition, it is necessary to use the solutions of Section A.24. For all other cases, the above form is convenient and applicable.

## A.26 Tables of Spherical Bessel, Neumann, and Hankel Functions

To evaluate spherical Bessel, Neumann, and Hankel functions, it is helpful to factor each function into rational and transcendental parts. We introduce rational functions  $A_\ell(\sigma)$  and  $B_\ell(\sigma)$ . In these terms the functions of Eqs. A.25.14 and A.25.15 are:

$$\begin{aligned} j_\ell(\sigma) &= \frac{1}{\sigma} \{B_\ell(\sigma) \cos \sigma + A_\ell(\sigma) \sin \sigma\} \\ y_\ell(\sigma) &= \frac{1}{\sigma} \{-A_\ell(\sigma) \cos \sigma + B_\ell(\sigma) \sin \sigma\} \\ h_\ell(\sigma) &= \frac{1}{\sigma} \{B_\ell(\sigma) + iA_\ell(\sigma)\} e^{-i\sigma} \end{aligned} \quad (\text{A.26.1})$$

Comparison of the equations shows, with  $q$  equal to any integer, that:

$$\begin{aligned}
 A_\ell(\sigma) &= \sum_{s=0}^{\ell} \frac{(\ell+s)!}{s!(\ell-s)!} \left(\frac{1}{2\sigma}\right)^s (-1)^{(\ell-s)/2} \delta(\ell+s, 2q) \\
 B_\ell(\sigma) &= \sum_{s=0}^{\ell} \frac{(\ell+s)!}{s!(\ell-s)!} \left(\frac{1}{2\sigma}\right)^s (-1)^{(\ell-s+1)/2} \delta(\ell+s, 2q+1)
 \end{aligned}
 \tag{A.26.2}$$

Comparison of the equations shows values of the letter functions. The primary recursion relationship used to develop the table follows from Eq. A.24.6:

$$j_{\ell+2}(\sigma) = \frac{2\ell+3}{\sigma} j_{\ell+1}(\sigma) - j_\ell(\sigma) \tag{A.26.3}$$

Important related functions are obtained by operating on the radial function to obtain the special function:

$$h_\ell^\bullet(\sigma) = \frac{1}{\sigma} \frac{d}{d\sigma} [\sigma h_\ell(\sigma)] \tag{A.26.4}$$

Similarly to Eq. A.26.1, the related functions factor into rational and transcendental parts:

$$\begin{aligned}
 j_\ell^\bullet(\sigma) &= \frac{1}{\sigma} \{D_\ell(\sigma) \cos \sigma + C_\ell(\sigma) \sin \sigma\} \\
 y_\ell^\bullet(\sigma) &= \frac{1}{\sigma} \{-C_\ell(\sigma) \cos \sigma + D_\ell(\sigma) \sin \sigma\} \\
 h_\ell^\bullet(\sigma) &= \frac{1}{\sigma} \{D_\ell(\sigma) + \mathcal{C}_\ell(\sigma)\} e^{-i\sigma}
 \end{aligned}
 \tag{A.26.5}$$

Term-by-term comparison shows that:

$$\frac{dA_\ell(\sigma)}{d\sigma} = B_\ell(\sigma) + C_\ell(\sigma) \quad \frac{dB_\ell(\sigma)}{d\sigma} = D_\ell(\sigma) - A_\ell(\sigma) \tag{A.26.6}$$

It follows upon combining Eq. A.26.4 with Eqs. A.24.9 and A.24.13 that in the limit of a vanishingly small radius:

$$\lim_{\sigma \Rightarrow 0} j_{\ell}^{\bullet}(\sigma) = \frac{(\ell+1)\sigma^{\ell-1}}{(2\ell+1)!!} \quad \lim_{\sigma \Rightarrow 0} y_{\ell}^{\bullet}(\sigma) = \frac{\ell(2\ell-1)!!}{\sigma^{\ell+2}} \quad (\text{A.26.7})$$

It follows similarly upon combining Eq. A.26.4 with Eqs. A.24.15 that in the limit of an infinitely large radius:

$$\begin{aligned} \lim_{\sigma \Rightarrow \infty} j_{\ell}^{\bullet}(\sigma) &= -\frac{1}{\sigma} \sin \left[ \sigma - \frac{\pi}{2}(\ell+1) \right] \\ \lim_{\sigma \Rightarrow \infty} y_{\ell}^{\bullet}(\sigma) &= \frac{1}{\sigma} \cos \left[ \sigma - \frac{\pi}{2}(\ell+1) \right] \end{aligned} \quad (\text{A.26.8})$$

$\ell$	$A_{\ell}(\sigma)$	$B_{\ell}(\sigma)$	$C_{\ell}(\sigma)$	$D_{\ell}(\sigma)$
1		0	0	1
0				
1	$1/\sigma$	-1	$-1/\sigma^2+1$	$1/\sigma$
2	$3/\sigma^2-1$	$-3/\sigma$	$-6/\sigma^3+3/\sigma$	$6/\sigma^2-1$
3	$15/\sigma^3-6/\sigma$	$-15/\sigma^2+1$	$-45/\sigma^4+21/\sigma^2-1$	$45/\sigma^3-6/\sigma$
4	$105/\sigma^4-45/\sigma^2+1$	$-105/\sigma^3+10/\sigma$	$-420/\sigma^5+195/\sigma^3-10/\sigma$	$420/\sigma^4-55/\sigma^2+1$

Table A.26.1 Table of Values of the Radial Letter Functions

$$\begin{aligned} A_5 &= 945/\sigma^5 - 420/\sigma^3 + 15/\sigma \\ B_5 &= -945/\sigma^4 + 105/\sigma^2 - 1 \\ C_5 &= -5(9!!)/\sigma^6 + 2205/\sigma^4 - 120/\sigma^2 + 1 \\ D_5 &= 5(9!!)/\sigma^5 - 630/\sigma^3 + 15/\sigma \end{aligned}$$

---


$$A_6 = (11!!)/\sigma^6 - 5(9!!)/\sigma^4 + 210\sigma^2 - 1$$

$$B_6 = -(11!!)/\sigma^5 + 1260/\sigma^3 - 21/\sigma$$

$$C_6 = -6(11!!)/\sigma^7 + 31(9!!)/\sigma^5 - 1680/\sigma^3 + 21/\sigma$$

$$D_6 = 6(11!!)/\sigma^6 - 8505/\sigma^4 + 231/\sigma^2 - 1$$

---


$$A_7 = (13!!)/\sigma^7 - 6(11!!)/\sigma^5 + 3150/\sigma^3 - 28/\sigma$$

$$B_7 = -(13!!)/\sigma^6 + 17,325/\sigma^4 - 378/\sigma^2 + 1$$

$$C_7 = -7(13!!)/\sigma^8 + 43(11!!)/\sigma^6 - 26,775/\sigma^4 + 406/\sigma^2 - 1$$

$$D_7 = 7(13!!)/\sigma^7 - 131,670/\sigma^5 + 4662/\sigma^3 - 28/\sigma$$

---


$$A_8 = (15!!)/\sigma^8 - 7(13!!)/\sigma^6 + 5(11!!)/\sigma^4 - 630/\sigma^2 + 1$$

$$B_8 = -(15!!)/\sigma^7 + 2(13!!)/\sigma^5 - 6930/\sigma^3 + 36/\sigma$$

$$C_8 = -8(15!!)/\sigma^9 + 57(13!!)/\sigma^7 - 46(11!!)/\sigma^5 + 8190/\sigma^3 - 36/\sigma$$

$$D_8 = 8(15!!)/\sigma^8 - 17(13!!)/\sigma^6 + 7(11!!)/\sigma^4 - 666/\sigma^2 + 1$$

---


$$A_9 = (17!!)/\sigma^9 - 8(15!!)/\sigma^7 + 7(13!!)/\sigma^5 - 13,860/\sigma^3 + 45/\sigma$$

$$B_9 = -(17!!)/\sigma^8 + 35(13!!)/\sigma^6 - (13!!)/\sigma^4 + 990/\sigma^2 - 1$$

$$C_9 = -9(17!!)/\sigma^{10} + 9(17!!)/\sigma^8 - 70(13!!)/\sigma^6 + 17(11!!)/\sigma^4 - 1035/\sigma^2 + 1$$

$$D_9 = 9(17!!)/\sigma^9 - 22(15!!)/\sigma^7 + 11(13!!)/\sigma^5 - 15,840/\sigma^3 + 45/\sigma$$


---

Table A.26.1 Table of Values of the Radial Letter Functions (cont.)

---

1.	$dA_\ell/d\sigma = C_\ell + B_\ell$	$dB_\ell/d\sigma = D_\ell - A_\ell$
2.	$A_{\ell-1} + A_{\ell+1} = \frac{2\ell+1}{\sigma} A_\ell$	$B_{\ell-1} + B_{\ell+1} = \frac{2\ell+1}{\sigma} B_\ell$
3.	$\ell A_{\ell-1} - (\ell+1)A_{\ell+1} = (2\ell+1) \left[ \frac{dA_\ell}{d\sigma} - \frac{A_\ell}{\sigma} - B_\ell \right]$ $\ell B_{\ell-1} - (\ell+1)B_{\ell+1} = (2\ell+1) \left[ \frac{dB_\ell}{d\sigma} - \frac{B_\ell}{\sigma} + A_\ell \right]$	
4.	$dA_\ell/d\sigma = -\frac{\ell}{\sigma} A_\ell + A_{\ell-1} + B_\ell$	$dB_\ell/d\sigma = -\frac{\ell}{\sigma} B_\ell + B_{\ell-1} - A_\ell$
5.	$dA_\ell/d\sigma = \frac{\ell+1}{\sigma} A_\ell - A_{\ell+1} + B_\ell$	$dB_\ell/d\sigma = \frac{\ell+1}{\sigma} B_\ell - B_{\ell+1} - A_\ell$
6.	$C_\ell = -\frac{\ell}{\sigma} A_\ell + A_{\ell-1} = \frac{\ell+1}{\sigma} A_\ell - A_{\ell+1}$ $D_\ell = -\frac{\ell}{\sigma} B_\ell + B_{\ell-1} = \frac{\ell+1}{\sigma} B_\ell - B_{\ell+1}$	
7.	$dC_\ell/d\sigma = -\left[ 1 - \frac{\ell(\ell+1)}{\sigma^2} \right] A_\ell + D_\ell$ $dD_\ell/d\sigma = -\left[ 1 - \frac{\ell(\ell+1)}{\sigma^2} \right] B_\ell - C_\ell$	
8.	$A_\ell D_\ell - B_\ell C_\ell = 1$	
9.	$A_\ell B_{\ell-1} - A_{\ell-1} B_\ell = 1$	$C_\ell D_{\ell-1} - C_{\ell-1} D_\ell = -\left( 1 + \frac{\ell^2}{\sigma^2} \right)$
	$A_{\ell+1} D_\ell - B_{\ell+1} C_\ell = \frac{\ell+1}{\sigma}$	$A_\ell D_{\ell+1} - B_\ell C_{\ell+1} = \frac{\ell+1}{\sigma}$
10.	$A_{\ell+2} B_\ell - A_\ell B_{\ell+2} = \frac{2\ell+3}{\sigma}$ $C_{\ell+2} D_\ell - C_\ell D_{\ell+2} = \frac{\ell+3}{\sigma} \left( 1 - \frac{(\ell+1)\ell+2}{\sigma^2} \right)$	

---

Table A.26.2 Radial Function Identities

- 
11.  $\left( A_\ell^2 - B_\ell^2 - C_\ell^2 + D_\ell^2 \right)$   

$$= \int d\sigma \left\{ 4(A_\ell - D_\ell)(B_\ell + C_\ell) - 2(A_\ell C_\ell - B_\ell D_\ell) \frac{\ell(\ell+1)}{\sigma^2} \right\}$$
  
 $\left( A_\ell^2 + B_\ell^2 + C_\ell^2 + D_\ell^2 \right)$   

$$= \int d\sigma \left\{ 2(A_\ell C_\ell + B_\ell D_\ell) \frac{\ell(\ell+1)}{\sigma^2} \right\}$$
12.  $(A_\ell B_\ell - C_\ell D_\ell)$   

$$= -\int d\sigma \left\{ \left[ (A_\ell - D_\ell)^2 + (B_\ell + C_\ell)^2 \right] + (A_\ell D_\ell + B_\ell C_\ell) \frac{\ell(\ell+1)}{\sigma^2} \right\}$$
  
 $(A_\ell B_\ell + C_\ell D_\ell)$   

$$= \int d\sigma \left\{ -A_\ell^2 + B_\ell^2 - C_\ell^2 + D_\ell^2 \right\} + (A_\ell D_\ell + B_\ell C_\ell) \frac{\ell(\ell+1)}{\sigma^2}$$
13.  $(A_\ell C_\ell - B_\ell D_\ell)$   

$$= \int d\sigma \left\{ \left[ -(A_\ell - D_\ell)^2 + (B_\ell + C_\ell)^2 \right] + (A_\ell^2 - B_\ell^2) \left( \frac{\ell(\ell+1)}{\sigma^2} \right) \right\}$$
  
 $(A_\ell C_\ell + B_\ell D_\ell)$   

$$= \int d\sigma \left\{ \left( -A_\ell^2 - B_\ell^2 + C_\ell^2 + D_\ell^2 \right) + (A_\ell^2 + B_\ell^2) \left( \frac{\ell(\ell+1)}{\sigma^2} \right) \right\}$$
14.  $\left[ A_\ell D_\ell + B_\ell C_\ell - (-1)^\ell \right]$   

$$= \int d\sigma \left\{ -2(A_\ell - D_\ell)(B_\ell + C_\ell) + 2A_\ell B_\ell \left( \frac{\ell(\ell+1)}{\sigma^2} \right) \right\}$$
15.  $\frac{d}{d\sigma} (A_\ell A_n + B_\ell B_n + C_\ell C_n + D_\ell D_n)$   

$$= \frac{1}{\sigma^2} \left[ \ell(\ell+1)(A_\ell C_n + B_\ell D_n) + n(n+1)(A_n C_\ell + B_n D_\ell) \right]$$


---

Table A.26.2 Radial Function Identities (cont.)



- 
16. 
$$\begin{aligned} \frac{d}{d\sigma} (A_\ell B_n - B_\ell A_n + C_\ell D_n - D_\ell C_n) \\ = \frac{1}{\sigma^2} [\ell(\ell+1)(A_\ell D_n - B_\ell C_n) - n(n+1)(A_n D_\ell - B_n C_\ell)] \end{aligned}$$
17. 
$$\begin{aligned} \frac{d}{d\sigma} (A_\ell C_n - C_\ell A_n + B_\ell D_n - D_\ell B_n) \\ = \frac{1}{\sigma^2} [n(n+1) - \ell(\ell+1)](A_\ell A_n + B_\ell B_n) \end{aligned}$$
18. 
$$\begin{aligned} \frac{d}{d\sigma} (A_\ell C_n + C_\ell A_n - B_\ell D_n - D_\ell B_n) \\ = \left\{ \begin{aligned} &\frac{1}{\sigma^2} [n(n+1) - \ell(\ell+1)](A_\ell A_n + B_\ell B_n) \\ &+ 2(A_\ell D_n + A_n D_\ell + B_\ell C_n + B_n C_\ell) + \\ &\quad - 2(A_\ell A_n - B_\ell B_n - C_\ell C_n + D_\ell D_n) \end{aligned} \right\} \end{aligned}$$
19. 
$$\begin{aligned} \frac{d}{d\sigma} (A_\ell B_n + B_\ell A_n - C_\ell D_n - D_\ell C_n) \\ = \left\{ \begin{aligned} &\frac{1}{\sigma^2} [\ell(\ell+1)(A_\ell D_n + B_\ell C_n) + n(n+1)(A_n D_\ell + B_n C_\ell)] \\ &+ 2(A_\ell D_n + A_n D_\ell + B_\ell C_n + B_n C_\ell) + \\ &\quad - 2(A_\ell A_n - B_\ell B_n - C_\ell C_n + D_\ell D_n) \end{aligned} \right\} \end{aligned}$$
20. 
$$\frac{d}{d\sigma} \left( \frac{A_\ell B_\ell}{A_\ell^2 - B_\ell^2} \right) = \frac{(A_\ell^2 + B_\ell^2)}{(A_\ell^2 - B_\ell^2)^2} \left[ 1 - (A_\ell^2 + B_\ell^2) \right]$$


---

Table A.26.2 Radial Function Identities (cont.)

$\ell$	$[A_\ell D_\ell + B_\ell C_\ell - (-1)^\ell]$
1.	$2/\sigma^2;$
2.	$36/\sigma^4 - 18/\sigma^2;$
3.	$1350/\sigma^6 - 720/\sigma^4 + 72/\sigma^2$
4.	$88200/\sigma^8 - 49350/\sigma^6 + 6000/\sigma^4 + 200/\sigma^2$
5.	$8930250/\sigma^{10} - 5159700/\sigma^8 + 699300/\sigma^6 - 31500/\sigma^4 + 450/\sigma^2$
6.	$1296672300/\sigma^{12} - 766215450/\sigma^{10} + 111370140/\sigma^8 - 5900580/\sigma^6$ $+ 123480/\sigma^4 - 882/\sigma^2$

Table A.26.3 Radial Dependence of  $[A_\ell D_\ell + B_\ell C_\ell - (-1)^\ell]$

$\ell$	$[A_\ell C_\ell - B_\ell D_\ell]$
1	$-1/\sigma^3 + 2/\sigma$
2	$-18/\sigma^5 + 33/\sigma^3 - 6/\sigma$
3	$-675/\sigma^7 + 1250/\sigma^5 - 276/\sigma^3 + 12/\sigma$
4	$-44100/\sigma^9 + 83475/\sigma^7 - 20220/\sigma^5 + 1300/\sigma^3 - 20/\sigma$
5	$-4465125/\sigma^{11} + 8533350/\sigma^9 - 2201850/\sigma^7$ $+ 169470/\sigma^5 - 4425/\sigma^3 + 30/\sigma$
6	$-648336150/\sigma^{13} + 1247555935/\sigma^{11}$ $- 335975850/\sigma^9 + 28797930/\sigma^7$ $- 961380/\sigma^5 + 12201/\sigma^3 - 42/\sigma$

Table A.26.4 Radial Dependence of  $[A_\ell C_\ell - B_\ell D_\ell]$

$\ell$	$[A_\ell C_\ell + B_\ell D_\ell]$
1	$-1/\sigma^3$
2	$-18/\sigma^5 - 3/\sigma^3$
3	$-675/\sigma^7 - 90/\sigma^5 - 6/\sigma$
4	$-44100/\sigma^9 - 4725/\sigma^7 - 270/\sigma^5 - 10/\sigma^3$
5	$-4465125/\sigma^{11} - 396900/\sigma^9 - 18900/\sigma^7 - 630/\sigma^5 - 15/\sigma^3$
6	$-648336150/\sigma^{13} - 49116375/\sigma^{11} - 1984500/\sigma^9 - 56700/\sigma^7 - 1260/\sigma^5 - 21/\sigma^3$

Table A.26.5 Radial Dependence of  $[A_\ell C_\ell + B_\ell D_\ell]$ 

$\ell$	$2(A_\ell - D_\ell)(B_\ell + C_\ell)$
1	0
2	$36/\sigma^5$
3	$2700/\sigma^7 - 360/\sigma^5$
4	$264000/\sigma^9 - 65100/\sigma^7 + 1800/\sigma^5$
5	$35271500/\sigma^{11} - 11510100/\sigma^9 + 642600/\sigma^7 - 6300/\sigma^5$
6	$6483361500/\sigma^{13} - 2436172200/\sigma^{11} + 189162540/\sigma^9$ $- 3969000/\sigma^7 + 17640/\sigma^5$

Table A.26.6 Radial Dependence of  $2(A_\ell - D_\ell)(B_\ell + C_\ell)$ 

$\ell$	$(A_\ell - D_\ell)^2 - (B_\ell + C_\ell)^2$
1	$-1/\sigma^4$
2	$-36/\sigma^6 - 9/\sigma^4$
3	$-2025/\sigma^8 + 1440/\sigma^6 - 36/\sigma^4$
4	$-176400/\sigma^{10} + 174825/\sigma^8 - 14400/\sigma^6 + 100/\sigma^4$
5	$-22325625/\sigma^{12} + 26195400/\sigma^{10} - 3316950/\sigma^8 + 81900/\sigma^6 - 225/\sigma^4$
6	$-3890016900/\sigma^{14} + 5058986625/\sigma^{12} - 802531800/\sigma^{10} + 32345224/\sigma^8 - 335160/\sigma^6 + 441/\sigma^4$

Table A.26.7 Radial Dependence of  $(A_\ell - D_\ell)^2 - (B_\ell + C_\ell)^2$

$\ell$	$(A_\ell - D_\ell)^2 + (B_\ell + C_\ell)^2$
1	$1/\sigma^4$
2	$36/\sigma^6 + 9/\sigma^4$
3	$2025/\sigma^8 + 360/\sigma^6 + 36/\sigma^4$
4	$176400/\sigma^{10} + 23625/\sigma^8 + 1800/\sigma^6 + 100/\sigma^4$
5	$22325625/\sigma^{12} + 2381400/\sigma^{10} + 141750/\sigma^8 + 6300/\sigma^6 + 225/\sigma^4$
6	$3890016900/\sigma^{14} + 343814625/\sigma^{12} + 16669800/\sigma^{10}$ $+ 593224/\sigma^8 + 17640/\sigma^6 + 441/\sigma^4$

Table A.26.8 Radial Dependence of  $(A_\ell - D_\ell)^2 + (B_\ell + C_\ell)^2$ 

## A.27 Sums Over Spherical Bessel Functions

Any electromagnetic field may be expressed as the product of spherical Bessel, Neumann, Hankel functions of  $\sigma$ , or linear combinations thereof, times linear combinations of Legendre functions of  $\theta$ , times linear combinations of trigonometric functions of azimuth angle  $\phi$ .

A particularly useful function is a  $z$ -directed plane wave:  $e^{-ikz} = e^{-i\sigma \cos\theta}$ . It follows that functions with  $m = 0$  are present, and there is no dependence upon  $\phi$ . Since the function is regular on the  $z$ -axis, only spherical Bessel functions are present. The result, expressed using spherical coordinates, is the general solution form expressed as a sum over the single product:

$$e^{-i\sigma \cos\theta} = \sum_{\ell=0}^{\infty} a_\ell j_\ell(\sigma) P_\ell(\cos\theta) \quad (\text{A.27.1})$$

The objective is to evaluate each of the infinite number of constants  $a_\ell$ . To do so, multiply both sides by  $P_n(\cos\theta)$  and integrate over the full range of zenith angle. The result is:

$$\frac{2j_\ell(\sigma)}{(2\ell+1)} a_\ell = \int_0^\pi \sin\theta d\theta P_\ell(\cos\theta) e^{-i\sigma \cos\theta} \quad (\text{A.27.2})$$

Differentiating both sides  $\ell$  times with respect to  $\sigma$  then going to the limit of vanishing small radius, see Eq. A.24.7, gives:

$$\frac{2a_\ell i^\ell}{(2\ell+1)} \frac{\ell!}{(2\ell+1)!!} = \int_0^\pi \sin\theta d\theta P_\ell(\cos\theta) \cos^\ell \theta \quad (\text{A.27.3})$$

The integral is listed in Table A.22.1.10. Doing the integration and solving for  $a_\ell$  gives:

$$a_\ell = i^{-\ell} (2\ell+1) \quad (\text{A.27.4})$$

Combining Eq. A.27.1 with A.27.4 gives:

$$e^{-i\sigma \cos\theta} = \sum_{\ell=0}^{\infty} i^{-\ell} (2\ell+1) j_\ell(\sigma) P_\ell(\cos\theta) \quad (\text{A.27.5})$$

Other related sums follow from Eq. A.27.5. Differentiating both sides of Eq. A.27.5 with respect to  $\theta$  and using Table A.21.1.10 gives:

$$\sigma e^{-i\sigma \cos\theta} = \sum_{\ell=1}^{\infty} i^{1-\ell} (2\ell+1) j_\ell(\sigma) \frac{P_\ell^1(\cos\theta)}{\sin\theta} \quad (\text{A.27.6})$$

Evaluating Eq. A.27.1 on the positive  $z$ -axis gives the three series:

$$e^{-i\sigma} = \sum_{\ell=0}^{\infty} i^{-\ell} (2\ell+1) j_\ell(\sigma) \quad (\text{A.27.7})$$

$$\sin\sigma = \sum_{\ell=0;1}^{\infty} (-1)^{(\ell-1)/2} (2\ell+1) j_\ell(\sigma)$$

$$\cos \sigma = \sum_{\ell \in 0}^{\infty} (-1)^{\ell/2} (2\ell + 1) j_{\ell}(\sigma)$$

Subscripts “o;1” and “e;0” indicate respectively odd integers beginning with one and even integer beginning with zero.

Evaluation of Eqs. A.27.5 and A.27.6 at  $\theta = \pi/2$ , see Table A.18.1, gives:

$$1 = \sum_{\ell \in 0}^{\infty} (2\ell + 1) \frac{(\ell - 1)!!}{(\ell!!)^2} j_{\ell}(\sigma) \quad (\text{A.27.8})$$

$$\sigma = \sum_{\ell \in 1}^{\infty} (2\ell + 1) \frac{(\ell)!!}{(\ell - 1)!!^2} j_{\ell}(\sigma)$$

Application of Eq. A.26.4 to Eqs. A.27.8 results in:

$$\frac{1}{\sigma} = \sum_{\ell \in 0}^{\infty} (2\ell + 1) \frac{\ell!!}{(\ell!!)^2} j_{\ell}^{\bullet}(\sigma) \quad (\text{A.27.9})$$

$$1 = \sum_{\ell \in 1}^{\infty} \frac{(2\ell + 1)}{2} \frac{\ell!!}{(\ell - 1)!!^2} j_{\ell}^{\bullet}(\sigma)$$

Use of Eq. A.7.6 to integrate Eq. A.27.5 over  $\theta$  gives:

$$\left[ \frac{e^{-i\sigma \cos \theta}}{\sigma} \right]_{\theta_1}^{\theta_2} = \sum_{\ell=0}^{\infty} i^{-\ell-1} j_{\ell}(\sigma) [P_{\ell+1}(\cos \theta) - P_{\ell-1}(\cos \theta)]_{\theta_1}^{\theta_2} \quad (\text{A.27.10})$$

Evaluation of Eq. A.27.10 between limits  $\theta = \pi$  and  $\pi/2$  gives:

$$\left( \frac{1 - e^{i\sigma}}{\sigma} \right) = \sum_{\ell=0}^{\infty} i^{-\ell-1} j_{\ell}(\sigma) [P_{\ell+1}(0) - P_{\ell-1}(0)] - j_0(\sigma) \quad (\text{A.27.11})$$

Evaluation of Eq. A.27.11 between limits  $\theta = \pi/2$  and 0 gives:

$$\left( \frac{e^{-i\sigma} - 1}{\sigma} \right) = -ij_0(\sigma) - \sum_{\ell=0}^{\infty} i^{\ell-1} j_{\ell}(\sigma) [P_{\ell+1}(0) - P_{\ell-1}(0)] \quad (\text{A.27.12})$$

Subtracting Eq. A.27.11 from Eq. A.27.12 gives:

$$\frac{\cos \sigma - 1}{\sigma} = \sum_{\ell=0}^{\infty} (2\ell+1) \frac{(\ell-1)!}{(\ell-1)!!(\ell+1)!!} j_{\ell}(\sigma) \quad (\text{A.27.13})$$

The operation of Eq. A.26.4 results in:

$$\frac{\sin \sigma}{\sigma} = \sum_{\ell=0}^{\infty} (2\ell+1) \frac{(\ell-1)!}{(\ell-1)!!(\ell+1)!!} j_{\ell}^{\bullet}(\sigma) \quad (\text{A.27.14})$$

Evaluating Eq. A.27.6 on the positive z-axis gives

$$\sigma e^{-i\sigma} = \frac{1}{2} \sum_{\ell=1}^{\infty} i^{1-\ell} (2\ell+1) \ell(\ell+1) j_{\ell}(\sigma) \quad (\text{A.27.15})$$

The exponential breaks into the two equations:

$$\sigma \cos \sigma = \frac{1}{2} \sum_{\ell \geq 1} (-1)^{(\ell-1)/2} (2\ell+1) \ell(\ell+1) j_{\ell}(\sigma) \quad (\text{A.27.16})$$

$$\sigma \sin \sigma = \frac{1}{2} \sum_{\ell \geq 2} (-1)^{\ell/2} (2\ell+1) \ell(\ell+1) j_{\ell}(\sigma)$$

Table A.27.1 contains a listing of sums over different functions of spherical Bessel functions.

- 
1. 
$$e^{-i\sigma \cos \theta} = \sum_{\ell=0}^{\infty} i^{-\ell} (2\ell+1) j_{\ell}(\sigma) P_{\ell}(\cos \theta)$$
  2. 
$$\sigma \sin \theta e^{-i\sigma \cos \theta} = \sum_{\ell=1}^{\infty} i^{1-\ell} (2\ell+1) j_{\ell}(\sigma) P_{\ell}^1(\cos \theta)$$
  3. 
$$\frac{1 - \cos \sigma}{\sigma} = \sum_{\ell \geq 1} (2\ell+1) \frac{(\ell-2)!!}{(\ell+1)!!} j_{\ell}(\sigma)$$
  4. 
$$\frac{\sin \sigma}{\sigma} = \sum_{\ell \geq 1} (2\ell+1) \frac{(\ell-2)!!}{(\ell+1)!!} j_{\ell}^{\bullet}(\sigma)$$
  5. 
$$1 = \sum_{\ell \geq 0} (2\ell+1) \frac{(\ell-1)!!}{\ell!!} j_{\ell}(\sigma)$$
  6. 
$$\frac{1}{\sigma} = \sum_{\ell \geq 0} (2\ell+1) \frac{(\ell-1)!!}{(\ell)!!} j_{\ell}^{\bullet}(\sigma)$$
  7. 
$$\sigma = \sum_{\ell \geq 1} (2\ell+1) \frac{(\ell)!!}{(\ell-1)!!} j_{\ell}(\sigma)$$
  8. 
$$1 = \sum_{\ell \geq 1} \frac{(2\ell+1)}{2} \frac{(\ell)!!}{(\ell-1)!!} j_{\ell}^{\bullet}(\sigma)$$
  9. 
$$\sigma e^{-i\sigma} = \frac{1}{2} \sum_{\ell=1}^{\infty} i^{1-\ell} (2\ell+1) \ell (\ell+1) j_{\ell}(\sigma)$$
  10. 
$$(2 - i\sigma) e^{-i\sigma} = \frac{1}{2} \sum_{\ell=1}^{\infty} i^{1-\ell} (2\ell+1) (\ell+1) j_{\ell}^{\bullet}(\sigma)$$
- 

Table A.27.1 Table of Sums over Spherical Bessel Functions



## *Multipolar Sources*

### A.28 Static Scalar Potentials

To examine physical sources of TM modal coefficients  $F(\ell, m)$ , it is convenient to start with the static scalar potential field,  $\Phi(\mathbf{r})$ . By Eq. 1.5.4 the differential equation that governs the scalar potential is:

$$\nabla^2 \Phi = \rho/\epsilon \quad (\text{A.28.1})$$

By this equation the scalar potential has a spatial curvature only where electric charges exist and a field function exists only if the curvature is other than zero. It follows that static scalar potentials arise only from electric charges.

To characterize such potentials we establish an origin near or in a region that contains static electric charges. Based upon that origin, the coordinates within the charged region are  $\mathbf{r}(x, y, z)$ . The field points at which the potential is to be evaluated are  $\mathbf{r}(x, y, z)$ . The field point may be either interior or exterior to the charge-containing region. The distance from the source to the field point is  $R$  where, by definition:

$$R(\mathbf{r}, \mathbf{r}) = \left[ (x - x)^2 + (y - y)^2 + (z - z)^2 \right]^{1/2} \quad (\text{A.28.2})$$

The potential at a field point was previously calculated, see Eq. 1.5.9, and is given by:

$$\Phi(\mathbf{r}) = \frac{1}{4\pi\epsilon} \int \frac{\rho(\mathbf{r})}{R} dV \quad (\text{A.28.3})$$

It is convenient to work with distance from the origin to the field point,  $\mathbf{r}$ , but the function in the denominator of Eq. A.28.3 is the distance from the differential source point to the field point,  $R$ . To replace  $1/R$  by a function of  $1/r$ , use the Taylor series expansion:

$$\frac{1}{R} = \left\{ \frac{1}{r} + x_i \frac{\partial}{\partial x_i} \left( \frac{1}{R} \right)_r + \frac{1}{2} x_i x_j \frac{\partial}{\partial x_i} \frac{\partial}{\partial x_j} \left( \frac{1}{R} \right)_r + \frac{1}{6} x_i x_j x_k \frac{\partial}{\partial x_i} \frac{\partial}{\partial x_j} \frac{\partial}{\partial x_k} \left( \frac{1}{R} \right)_r + \frac{1}{24} x_i x_j x_k x_m \frac{\partial}{\partial x_i} \frac{\partial}{\partial x_j} \frac{\partial}{\partial x_k} \frac{\partial}{\partial x_m} \left( \frac{1}{R} \right)_r + \dots \right\} \quad (\text{A.28.4})$$

Placing the expansion of Eq. A.28.4 into Eq. A.28.3 results in the desired form:

$$\Phi(r) = \frac{1}{4\pi\epsilon} \left\{ \left( \frac{1}{r} \right) \int \rho(r) dV + \frac{\partial}{\partial x_i} \left( \frac{1}{R} \right)_r \int x_i \rho(r) dV + \frac{1}{2} \frac{\partial}{\partial x_i} \frac{\partial}{\partial x_j} \left( \frac{1}{R} \right)_r \int x_i x_j \rho(r) dV + \frac{1}{6} \frac{\partial}{\partial x_i} \frac{\partial}{\partial x_j} \frac{\partial}{\partial x_k} \left( \frac{1}{R} \right)_r \int x_i x_j x_k \rho(r) dV + \dots \right\} \quad (\text{A.28.5})$$

The first term of Eq. A.28.5 has a first order singularity at the origin:

$$\Phi_0(r, \theta, \phi) = \frac{1}{4\pi\epsilon} \frac{q}{r} \quad \text{where} \quad q = \int \rho(r) dV \quad (\text{A.28.6})$$

Succeeding terms have successively higher order singularities. Fields associated with succeeding singularities are generated by equal values of positive and negative charge, spaced incremental distances apart. The total potential is the sum of that from each charge and, in the limit as the inter-charge spacing goes to zero, the mathematical affect on the potential is the same as obtained by differentiating with respect to  $x_i$ . For example, for the special case of charge separation  $z_0$  all differentials in Eq. A.28.5 are  $z$ -directed.

Consider the multipolar electric moment of a charge distribution with  $\ell$  displacements. The moment is of order  $\ell$  and degree  $m$ :

$$p_\ell^m = \int \rho(r) x_i x_j \dots x_k dV \quad (\text{A.28.7})$$

Moments are designated by the number of charges involved; moment  $p_\ell^m$ , where  $\ell$  is the order, is formed by  $2^\ell$  charges. Charges are arrayed according to the coefficients of a binomial expansion of the same order. Let a total of  $(\ell-m)$  displacements be  $z$ -directed, let  $s$  of them be  $x$ -directed, and of them  $(m-s)$  be  $y$ -directed.

Easily verified equalities satisfied by the Legendre polynomials are:

$$P_\ell(\cos\theta) = \frac{1}{\ell!} \frac{\partial^\ell}{\partial z^\ell} \left( \frac{1}{R} \right)_r \quad (\text{A.28.8})$$

$$P_\ell^1(\cos\theta) \sin\phi = \frac{1}{(\ell-1)!} \frac{\partial^\ell}{\partial y \partial z^{\ell-1}} \left( \frac{1}{R} \right)_r$$

Consider, as examples, structures that generate the lowest order multipolar moments. A dipole consists of two discrete charges: charge  $q$  at  $z_0/2$  and charge  $-q$  at  $-z_0/2$ ; the volume integral, Eq. A.28.7, over order one is  $qz_0$  and over any even order is zero. A linear quadrupole consists of four discrete charges: charges  $q$  at  $+z_0$  and  $-z_0$  and charge  $-2q$  at the origin; the volume integral over order two is  $2qz_0^2$  and over any odd order is zero. A linear octupole consists of eight discrete charges: charge  $q$  at  $3z_0/2$ ,  $-3q$  at  $z_0/2$ ,  $3q$  at  $-z_0/2$ ,  $-q$  at  $-3z_0/2$ . For a source of order three, the volume integral is  $qz_0^3/4$ . The same integral over any even order is zero. The volume integral over order one is zero but the volume integral for odd orders greater than three is not zero.

In all cases, the volume integral of Eq. A.28.7 is zero if the charge distribution and the displacements have opposite parity. It is also equal to zero if there are fewer charges than the number of displacements. In all other cases, the integral is non-zero. Tables A.28.1 and A.28.2 show some basic features of common multipolar electric moments. In each table column one shows the order of the source. Column two shows the discrete charge distribution that generates that order of singularity. Column three shows the volume integral of Eq. A.28.7. Column four shows the lowest non-vanishing order of the potential. With the aid of the static portion of Eq. A.28.6, column five shows the radial components of the generated electric field intensity. Table A.28.1 is for only  $z$ -directed displacements and Table A.28.2

is for one  $y$ - and  $(\ell-1)$   $z$ -directed displacements. Table A.28.1 uses scalar charge  $q$  as the unit cell and Table A.28.2 uses a  $y$ -directed dipole as the unit cell.

The scalar potential of an arbitrary charge distribution is the simple sum of values obtained from each moment:

$$\Phi(r, \theta, \phi) = \frac{1}{4\pi\epsilon} \sum_{\ell=0}^{\infty} \sum_{m=-\ell}^{\ell} \frac{p_{\ell}^m}{r^{\ell+1}} P_{\ell}^m(\cos \theta) e^{-jm\phi} \quad (\text{A.28.9})$$

This is the static scalar potential at an arbitrary, exterior field point due to the charge distribution.

The radial component of the electric field intensity follows from Eq. A.28.9 with the aid of the static portion of Eq. 1.6.3, and is equal to:

$\ell$	Charge Sites	$p_{\ell}$	$4\pi\epsilon\Phi_{\ell}(r, \theta)$	$4\pi\epsilon E_{r\ell}(r, \theta)$
0	+q at 0	q	$\frac{q}{r}$	$\frac{q}{r^2}$
1	-q at $-z_0/2$ +q at $z_0/2$	$p_1 = qz_0$	$\frac{p_1}{r^2} P_1(\cos \theta)$	$\frac{2p_1}{r^3} P_1(\cos \theta)$
2	+q at $-z_0$ -2q at 0 +q at $z_0$	$p_2 = 2p_1 z_0$ $= 2qz_0^2$	$\frac{p_2}{r^3} P_2(\cos \theta)$	$\frac{3p_2}{r^4} P_2(\cos \theta)$
3	-q at $-3z_0/2$ ; +3q at $-z_0/2$ ; -3q at $z_0/2$ +q at $3z_0/2$	$p_3 = 3p_2 z_0$ $= 6qz_0^3$	$\frac{p_3}{r^4} P_3(\cos \theta)$	$\frac{4p_3}{r^5} P_3(\cos \theta)$
4	+q at $-2z_0$ -4q at $-z_0$ +6q at 0 -4q at $z_0$ ; +q at $2z_0$	$p_4 = 4p_3 z_0$ $= 24qz_0^4$	$\frac{p_4}{r^5} P_4(\cos \theta)$	$\frac{5p_4}{r^6} P_4(\cos \theta)$

Table A.28.1 Electrostatic Potentials of a Linear Array of Sources,  $\ell$  Charges Spaced Distance  $z_0$  Apart

$\ell$	Charge and Sites	$p_\ell^1$	$\frac{4\pi\epsilon\Phi_\ell^1(r,\theta,\phi)}{\sin\phi}$	$\frac{4\pi\epsilon E_{r\ell}(r,\theta,\phi)}{\sin\phi}$
1	+q at $y_0/2$ -q at $-y_0/2$	$p_1^1 = qy_0$	$\frac{p_1^1}{r^2} P_1^1(\cos\theta)$	$\frac{2p_1^1}{r^3} P_1^1(\cos\theta)$
2	+q at $(y_0+z_0)/2$ -q at $(-y_0+z_0)/2$ +q at $-(y_0+z_0)/2$ -q at $(y_0-z_0)/2$	$p_2^1 = p_1^1 z_0$	$\frac{p_2^1}{r^3} P_2^1(\cos\theta)$	$\frac{3p_2^1}{r^4} P_2^1(\cos\theta)$
3	+q at $(y_0\pm 2z_0)/2$ -2q at $y_0/2$ +2q at $-y_0/2$ -q at $(-y_0\pm 2z_0)/2$	$p_3^1 = 2p_2^1 z_0$	$\frac{p_3^1}{r^4} P_3^1(\cos\theta)$	$\frac{4p_3^1}{r^5} P_3^1(\cos\theta)$
4	+q at $\pm(y_0+3z_0)/2$ -3q at $\pm(y_0+z_0)/2$ -q at $\pm(y_0-3z_0)/2$ 3q at $\pm(y_0-z_0)/2$	$p_4^1 = 3p_3^1 z_0$	$\frac{p_4^1}{r^5} P_4^1(\cos\theta)$	$\frac{5p_4^1}{r^6} P_4^1(\cos\theta)$

Table A.28.2 Electrostatic Source Potentials, One  $y_0$  and  $(\ell-1) z_0$  Charge Spacings

$$E_r(r,\theta,\phi) = \frac{1}{4\pi\epsilon} \sum_{\ell=0}^{\infty} \sum_{m=-\ell}^{\ell} \frac{(\ell+1)p_\ell^m}{r^{\ell+2}} P_\ell^m(\cos\theta) e^{-jm\phi} \quad (\text{A.28.10})$$

Connection between the coefficients of Eqs. 1.12.7 and those of Eqs. A.28.10 is by direct comparison. In the limit as the frequency goes to zero, combining Eqs. 1.12.7 and A.24.13 gives:

$$E_r(r,\theta,\phi) = - \sum_{\ell=0}^{\infty} \sum_{m=0}^{\ell} r^{-\ell} F(\ell, m) \ell(\ell+1) \frac{(2\ell-1)!!}{\sigma^{\ell+2}} P_\ell^m(\cos\theta) e^{-jm\phi} \quad (\text{A.28.11})$$

Direct comparison of Eq. A.28.10 with A.28.11 shows that:

$$F(\ell, m) = -\frac{1}{4\pi\epsilon} \frac{i^\ell k^{\ell+2} p_\ell^m}{\ell(2\ell-1)!!} \quad (\text{A.28.12})$$

For the special case of a  $z$ -directed electric dipole of moment  $m_1$ , it follows from the third row of Table A.28.1 that:

$$\Phi_1 = \frac{p_1 \cos \theta}{4\pi\epsilon r^2} \quad \text{and} \quad E_r = \frac{2p_1 \cos \theta}{4\pi\epsilon r^3} \quad (\text{A.28.13})$$

## A.29 Static Vector Potentials

To examine physical sources of TE modal coefficients  $G(\ell, m)$ , it is convenient to start with the vector scalar potential field,  $\mathbf{A}(\mathbf{r})$ . By Eq. 1.5.4 the differential equation that governs the vector potential is:

$$\nabla^2 \mathbf{A}(\mathbf{r}) = \mu \mathbf{J}(\mathbf{r}) \quad (\text{A.29.1})$$

By this equation the vector potential has a non-zero spatial curvature only where electric currents exist. Since a field function cannot exist unless, somewhere, the curvature is not zero, it follows that static vector potentials arise only from electric currents.

Although the formal descriptions of the scalar and vector potential are similar, the sources are not. Static scalar potentials arise from stationary electric charges and vector potentials arise from moving ones. The integrated form of Eq. A.29.1 follows from Eq. 1.5.8. With  $\mathbf{J}(\mathbf{r})$  representing a continuum charge distribution it is:

$$\mathbf{A}(\mathbf{r}) = \frac{\mu}{4\pi} \oint \frac{\mathbf{J}(\mathbf{r})}{R(\mathbf{r}, \mathbf{r})} dV \quad (\text{A.29.2})$$

Combining the Taylor distance expansion of Eq. A.28.4 with Eq. A.29.2 gives:

$$\mathbf{A}(\mathbf{r}) = \frac{\mu}{4\pi} \left\{ \left( \frac{1}{R} \right)_r \int \mathbf{J}(\mathbf{r}) dV + \left( \frac{\partial}{\partial x_i} \frac{1}{R} \right)_r \int x_i \mathbf{J}(\mathbf{r}) dV + \frac{1}{2} \left( \frac{\partial}{\partial x_i} \frac{\partial}{\partial x_j} \frac{1}{R} \right)_r \int x_i x_j \mathbf{J}(\mathbf{r}) dV + \frac{1}{6} \left( \frac{\partial}{\partial x_i} \frac{\partial}{\partial x_j} \frac{\partial}{\partial x_k} \frac{1}{R} \right)_r \int x_i x_j x_k \mathbf{J}(\mathbf{r}) dV \right\} \quad (\text{A.29.3})$$

Consider a filamentary current of magnitude  $I$  that is located in the  $xy$  plane at  $z = 0$ . The current is at radius  $a$  and flows in the  $\hat{\phi}$  direction. By Eq. A.29.1, the potential component in a particular direction is proportional to the current in that direction and there is no  $z$ -component of the current. Therefore, there is no  $z$ -component of the potential. Since the current has rotational symmetry about the  $z$ -axis, there is no loss of generality in placing the field point in the  $xz$ -plane,  $(x_0, 0, z_0)$ . With the differential source at position  $a(\hat{x}\cos\phi + \hat{y}\sin\phi) = x\hat{x} + y\hat{y}$  the source to field distance is  $R = [(x_0 - x)^2 + y^2 + z_0^2]^{1/2}$ . By Eq. A.29.2 the zero order vector potential is:

$$\mathbf{A}_0(\mathbf{r}) = \frac{\mu I}{4\pi r} \int_0^{2\pi} a(-\hat{x}\sin\phi + \hat{y}\cos\phi) d\phi = 0 \quad (\text{A.29.4})$$

To evaluate the first order vector potential of the current loop, note the partial derivatives:

$$\frac{\partial}{\partial x} \left( \frac{1}{R} \right)_r = \frac{1}{r^2} \sin\theta, \quad \frac{\partial}{\partial y} \left( \frac{1}{R} \right)_r = 0;$$

The first order vector potential is:

$$\mathbf{A}_1(\mathbf{r}) = \frac{\mu}{4\pi} \frac{\sin\theta}{r^2} \int_0^{2\pi} a \cos\phi \cdot I(-\hat{x}\sin\phi + \hat{y}\cos\phi) \cdot a d\phi = \frac{\mu I \pi a^2}{4\pi} \frac{\sin\theta}{r^2} \hat{\phi} \quad (\text{A.29.5})$$

Since the field point is in the  $xz$ -plane, the  $y$ -direction of Eq. A.29.5 generalizes to the  $\phi$  direction.

To evaluate the second order vector potential, note the partial derivatives:

$$\frac{\partial^2}{\partial x^2} \left( \frac{1}{R} \right)_r = \frac{1}{r^3} (3 \sin^2 \theta - 1); \quad \frac{\partial^2}{\partial x \partial y} \left( \frac{1}{R} \right)_r = 0 \quad \frac{\partial^2}{\partial y^2} \left( \frac{1}{R} \right)_r = -\frac{3}{r^3}$$

The second order vector potential is:

$$\mathbf{A}_2(\mathbf{r}) = \frac{\mu}{4\pi} \left\{ \begin{aligned} & \frac{1}{r^3} (3 \sin^2 \theta - 1) \int_0^{2\pi} a^2 \cos^2 \phi \bullet \mathbf{I}(-\hat{x} \sin \phi + \hat{y} \cos \phi) \bullet d\phi \\ & - \frac{3}{r^3} \int_0^{2\pi} a^2 \sin^2 \phi \bullet \mathbf{I}(-\hat{x} \sin \phi + \hat{y} \cos \phi) \bullet d\phi \end{aligned} \right\} = 0 \quad (\text{A.29.6})$$

Since all integrals vanish, so does the potential of this and all other even orders.

To evaluate the third order vector potential, note the partial derivatives:

$$\begin{aligned} \frac{\partial^3}{\partial x^3} \left( \frac{1}{R} \right)_r &= \frac{3}{r^4} \sin \theta (5 \sin^2 \theta - 3); & \frac{\partial^3}{\partial x^2 \partial y} \left( \frac{1}{R} \right)_r &= 0; \\ \frac{\partial^3}{\partial x \partial y^2} \left( \frac{1}{R} \right)_r &= -3 \frac{\sin \theta}{r^4}; & \frac{\partial^3}{\partial y^3} \left( \frac{1}{R} \right)_r &= 0 \end{aligned}$$

The third order vector potential is:

$$\mathbf{A}_3(\mathbf{r}) = \frac{\mu \mathbf{I}}{24\pi} \left\{ \begin{aligned} & 3 \frac{a^4}{r^4} \sin \theta (5 \sin^2 \theta - 3) \int_0^{2\pi} (-\sin \phi \hat{x} + \cos \phi \hat{y}) \cos^3 \phi d\phi \\ & - 9 \frac{a^4}{r^4} \sin \theta \int_0^{2\pi} (-\sin \phi \hat{x} + \cos \phi \hat{y}) \cos \phi \sin^2 \phi d\phi \end{aligned} \right\} \quad (\text{A.29.7})$$

Evaluation of the integrals gives:



$$A_3(r) = \frac{3\mu I \pi a^4 \hat{\phi}}{32\pi r^4} \sin\theta (5\sin^2\theta - 4) \quad (\text{A.29.8})$$

The radial component of the magnetic field follows by adding Eqs. 1.2.17, A.29.5, and A.29.8:

$$B_{r1} = \frac{2\mu I \pi a^2 \cos\theta}{4\pi r^3} = \frac{2\mu I \pi a^2}{4\pi r^3} P_1(\cos\theta) \quad (\text{A.29.9})$$

$$B_{r3} = \frac{3\mu I \pi a^4 \cos\theta (5\cos^2\theta - 3)}{8\pi r^5} = \frac{3\mu I \pi a^4}{4\pi r^5} P_3(\cos\theta) \quad (\text{A.29.10})$$

The magnetic dipole moment of the loop is, by definition:

$$\mathbf{m}_1 = m_1 \hat{z} = \pi a^2 I \hat{z} \quad (\text{A.29.11})$$

For non-circular loops, with  $S$  representing the planar area of the closed current, the definition generalizes to:

$$m_1 = IS \quad (\text{A.29.12})$$

It follows from Eqs. A.29.5 and A.29.11 that the dipole potential is expressible as:

$$A_1(r) = \frac{\mu}{4\pi} \mathbf{m}_1 \times \left( \frac{\hat{r}}{r^2} \right) \quad (\text{A.29.13})$$

For the special case of a  $z$ -directed magnetic dipole of moment  $m_1$ , combining Eqs. A.29.9, A.29.12 and A.29.13 gives:

$$A_1 = \frac{\mu m_1 \sin\theta}{4\pi r^2} \hat{\phi} \quad \text{and} \quad B_r = \frac{2\mu m_1 \cos\theta}{4\pi r^3} \quad (\text{A.29.14})$$

The electric field of Eq. A.28.13 and the magnetic field of Eq. A.29.9 are identical in form. Therefore, field form cannot be used to determine whether a magnetic source consists of separated magnetic monopoles or a current loop. In other words, the role played by a current loop in determining the

vector potential is the same as that played by separated charges in determining scalar potential.

Extension to higher order moments follows similarly to the dipole case. An electric quadrupole consists of two superimposed sets of separated electric charges and a magnetic quadrupole consists of two superimposed sets of separated current loops. With linear displacements, current loops follow the same rule as electric moments with one lateral and  $(\ell-1)$  linear displacements. Results for several orders are compiled in Tables A.29.1 and A.29.2.

Tables A.29.1 and A.29.2 display features of multipolar magnetic moments. In each case, column one shows the order of the source. Column two shows the discrete current distributions that generate that order of singularity. Column three shows the value of the volume integrals that appear in Eq. A.29.3. Column four shows the lowest order derived potentials. Column five shows the radial components of the generated electric field intensity. Table A.29.1 is based upon a  $z$ -directed loop and Table A.28.2 is based upon a  $y$ -directed loop. In both cases, all displacements are  $z$ -directed.

Equating the field value of Eq. A.29.10 with the octupole moment of Table A.29.1 shows that the octupole moment of a circular current loop is:

$$m_3 = \frac{3I\pi a^4}{4} \quad (\text{A.29.15})$$

The value of odd, higher order moments follow similarly.

Contrasting Tables A.28.1, A.28.2, A.29.1, and A.29.2 shows that Tables A.28.1 and A.29.1 have identical structures, quite different potentials, and identical force fields; the same is true of Tables A.28.2 and A.29.2. Since there are electric monopoles but not magnetic monopoles, the  $\ell = 0$  case occurs only in Table A.28.1. For all higher order modes, Tables A.28.1 and A.29.1 have  $z$ -directed dipoles as the unit cell. Tables A.28.2 and A.29.2 have  $y$ -directed dipoles as the unit cell, with identical structures except the source structure of Table A.28.1, order  $\ell$ , is the same as that of Table A.29.1, order  $(\ell+1)$ .

All orders and degrees of any source may be described similarly to those of the tables. The result is the radial component of the static magnetic field component of arbitrary order:

$\ell$	Loop Direction, Sites	$m_\ell$	$4\pi A_{\phi\ell}(r, \theta)/\mu$	$4\pi B_{r\ell}(r, \theta)/\mu$
1	$\uparrow\uparrow$ at 0	$m_1 = IS_0$	$\frac{m_1}{r^2} \sin\theta$	$\frac{2m_1}{r^3} P_1(\cos\theta)$
2	$\downarrow\downarrow$ at $-z_0/2$ $\uparrow\uparrow$ at $+z_0/2$	$m_2 = 2m_1 z_0$	$\frac{m_2}{2r^3} 3\sin\theta\cos\theta$	$\frac{3m_2}{r^4} P_2(\cos\theta)$
3	$\uparrow\uparrow$ at $-z_0$ $2\downarrow\downarrow$ at 0 $\uparrow\uparrow$ at $-z_0$	$m_3 = 3m_2 z_0$	$\frac{m_3}{2r^4} \sin\theta(5\cos^2\theta - 1)$	$\frac{4m_3}{r^5} P_3(\cos\theta)$
4	$\downarrow\downarrow$ at $-3z_0/2$ $3\uparrow\uparrow$ at $-z_0/2$ $3\downarrow\downarrow$ at $z_0/2$ $\uparrow\uparrow$ at $3z_0/2$	$m_4 = 4m_3 z_0$	$\frac{5m_4}{32r^5} \sin\theta(7\cos^3\theta - 3\cos\theta)$	$\frac{5m_4}{r^6} P_4(\cos\theta)$

Table A.29.1 Magnetostatic Vector Potentials and Radial Fields of Sources,  $z$ -Directed Current Loops of Area  $S_0$  with  $(\ell-1)z_0$  Separations.

Arrows indicate direction of the unit cell magnetic dipole moment.

$$B_r(r, \theta) = \frac{\mu}{4\pi} \sum_{\ell=0}^{\infty} \sum_{m=-\ell}^{\ell} \frac{(\ell+1)m_\ell^m}{r^{\ell+2}} P_\ell^m(\cos\theta) e^{-jm\phi} \quad (\text{A.29.16})$$

Similarly with the case of the electric field, in the limit as the frequency goes to zero the radial component of the magnetic field of Eq. 1.12.7 goes to:

$$B_r = \frac{j}{c} \sum_{\ell=0}^{\infty} \sum_{m=0}^{\ell} i^{-\ell} G(\ell, m) \ell(\ell+1) \frac{(2\ell-1)!!}{\sigma^{\ell+2}} P_\ell^m(\cos\theta) e^{-jm\phi} \quad (\text{A.29.17})$$

Combining Eqs. A.29.15 and A.29.17 gives:

$$G(\ell, m) = -\frac{\eta}{4\pi} \frac{i^\ell \kappa^{\ell+2} m_\ell^m}{\ell(2\ell-1)!!} \quad (\text{A.29.18})$$

$\ell$	Loop Direction, Sites	$m_\ell^1$	$4\pi A_\ell(r, \theta, \phi)/\mu$	$\frac{4\pi B_{r\ell}(r, \theta, \phi)}{\mu \sin\phi}$
1	$\Rightarrow$ at 0	$m_1^1 = IS_0$	$\frac{\mu m_1^1}{4\pi r^2} (\hat{\theta} \cos\phi - \hat{\phi} \cos\theta \sin\phi)$	$\frac{2m_1^1}{r^3} P_1^1(\cos\theta)$
2	$\Leftarrow$ at $-z_0/2$ ; $\Rightarrow$ at $+z_0/2$	$m_2^1 = m_1^1 z_0$	$\frac{m_2^1}{r^3} \begin{bmatrix} (-\hat{r} \sin\theta + 2\hat{\theta} \cos\theta) \cos\phi \\ -\hat{\phi} (3\cos^2\theta - 1) \sin\phi \end{bmatrix}$	$\frac{3m_2^1}{r^4} P_2^1(\cos\theta)$
3	$\Rightarrow$ at $z_0/2$ $2 \Leftarrow$ at 0 $\Rightarrow$ at $z_0/2$	$m_3^1 = 2m_2^1 z_0$	$\frac{3m_3^1}{8r^4} \begin{bmatrix} -2\hat{r} \sin\theta \cos\theta \cos\phi \\ +\hat{\theta} (3\cos^2\theta - 1) \cos\phi \\ -\hat{\phi} (5\cos^2\theta - 3) \cos\theta \sin\phi \end{bmatrix}$	$\frac{4m_3^1}{r^5} P_3^1(\cos\theta)$
4	$\Leftarrow$ at $-3z_0/2$ $3 \Rightarrow$ at $-z_0/2$ $3 \Leftarrow$ at $+z_0/2$ $\Rightarrow$ at $+3z_0/2$	$m_4^1 = 3m_3^1 z_0$	$\frac{m_4^1}{2r^5} \begin{bmatrix} 3\hat{r} (1 - 5\cos^2\theta) \sin\theta \cos\phi \\ +4\hat{\theta} (5\cos^2\theta - 3) \cos\theta \cos\phi \\ -\hat{\phi} \begin{pmatrix} 35\cos^4\theta \\ -30\cos^2\theta + 3 \end{pmatrix} \sin\phi \end{bmatrix}$	$\frac{5m_4^1}{r^6} P_4^1(\cos\theta)$

Table A.29.2 Magnetostatic Vector Potentials and Radial Fields of Sources,  $y$ -Directed Current Loops of Area  $S_0$ ,  $(\ell-1)z_0$  Separations.*Arrows indicate direction of the unit cell magnetic dipole moment.*

## References

- W. Kaplan, *Advanced Calculus*, Addison-Wesley (1952)  
J.D. Jackson, *Classical Electrodynamics*, 2<sup>nd</sup> ed., John Wiley (1975)  
T.W. Körner, *Fourier Analysis*, Cambridge University Press (1988)  
R.B. Leighton, *Principles of Modern Physics*, McGraw-Hill (1959)  
P.M. Morse, H. Feshbach, *Methods of Theoretical Physics*, McGraw-Hill (1953)  
W.K.H. Panofsky, M. Phillips, *Classical Electricity and Magnetism*, 2<sup>nd</sup> ed., Addison-Wesley, (1962)  
S.A. Schelkunoff, *Advanced Antenna Theory*, John Wiley (1952)  
S.A. Schelkunoff, *Applied Mathematics for Engineers and Scientists*, 2<sup>nd</sup> ed., Van Nostrand (1965)  
R.. Scott, *Linear Circuits*, 2<sup>nd</sup> ed, Addison-Wesley (1962)  
W.R. Smythe, *Static and Dynamic Electricity*, 3<sup>rd</sup> ed., McGraw-Hill (1968)  
M.E. VanValkenburg, *Network Analysis*, 3<sup>rd</sup> ed., Prentice Hall (1974)  
J.R. Wait, *Electromagnetic Wave Theory*, Harper & Row (1985)

# Index

## A

absorbed power, 43, 92, 96, 103, 289  
 absorption cross section, 92, 107  
 accelerating charge, 16, 191, 319  
 acceleration, 16, 17, 21, 24, 193, 194, 198  
 active region, 297, 298, 302  
 Aharonov-Bohm effect, 1  
 anechoic chamber, 180, 185  
 angular momentum, 154, 165, 191, 193,  
     212, 213, 215, 223, 234, 235, 260, 261,  
     263  
 antisymmetric, 12, 15, 236, 237, 238,  
     336, 337, 339  
 antisymmetric wave function, 236, 237,  
     238, 239  
 aperture, 53, 54, 64, 66, 67, 72, 76, 96  
 Aspect, 321  
 associated Legendre function, 29, 31, 33,  
     38, 215, 383, 384, 389, 390  
 asteroid, 2  
 atomic stability, xiii, xv, 193  
 attenuator, 182  
 axial field, 283, 288

## B

back-scatter, 44, 45  
 bandwidth, 128, 129, 252, 315, 354, 357,  
     358  
 Bell, 319, 321  
 Bessel differential equation, 40, 405, 410  
 Bessel function, 29, 31, 33, 38, 49, 56,  
     57, 79, 80, 87, 96, 100, 133, 264, 265,  
     267, 269, 277, 283, 287, 291, 294, 295,

296, 313, 327, 328, 365, 376, 377, 405,  
 408, 410, 413, 414, 423, 426, 427  
 biconical antenna, xv, 52, 53, 68, 70, 71,  
     76, 119, 133, 157, 177, 192, 326  
 biconical receiving antenna, xiv, 91, 95,  
     143, 289, 300  
 biconical transmitting antenna, 52, 70, 77,  
     78, 79, 95, 143  
 Bohm, 1, 321  
 Bohr, 317, 320, 321  
 Bohr magneton, 235  
 Bohr orbit, 231, 254, 305, 306, 307, 309,  
     311, 312, 319  
 Bohr radius, 218, 303, 304, 308, 309,  
     310, 311  
 boundary condition, xvi, 28, 30, 31, 34,  
     47, 52, 54, 60, 61, 62, 64, 65, 94, 95,  
     96, 99, 100, 101, 106, 230, 245, 326,  
     351, 361, 364, 366, 375, 402, 403, 404  
 boundary value, xiv, 37, 221

## C

cap, 73, 74, 76, 97, 107, 108  
 cap current, 107, 108  
 cap currents, 108  
 cat, 319, 320, 327  
 Cauchy integral, 343  
 causality, vi, 322, 326, 345  
 caustic, 265  
 centrifugal force, 191  
 characteristic frequency, 239  
 characterization, 172, 179, 185, 190, 322,  
     326  
 charge density, xv, 9, 12, 54, 62, 199,  
     200, 203, 206, 221, 238, 299, 300, 301,  
     302, 323, 345, 346, 361, 362, 364, 365

Chu, 131, 133, 135, 136, 138, 140, 142,  
 143, 152, 187, 189, 321, 326  
 Chu's limit, 189  
 circularly polarized, 33, 140, 160, 161,  
 163, 164, 165, 176, 189, 254, 260, 266,  
 284, 288  
 circulator, 179, 180, 182, 189  
 classical mechanics, 213, 317, 319, 321  
 closed system, 245, 354  
 coherent wave train, 251  
 complementary current, 61  
 complete, v, xiv, xvi, 27, 28, 30, 34, 52,  
 56, 95, 105, 192, 197, 205, 214, 221,  
 229, 234, 320, 321, 322, 326, 349  
 complex power, xiv, xv, 76, 77, 78, 113,  
 115, 117, 123, 124, 125, 126, 131, 140,  
 152, 353, 358, 361  
 complex Poynting vector, 41, 75, 88, 118,  
 295, 359  
 conducting boundary conditions, 34, 61,  
 62, 95, 361  
 conducting surface, 157, 289, 362, 364  
 cone-cap junction, 73, 97  
 conjugate variable, 202, 203, 341, 343  
 constant current source, 96  
 constant voltage source, 96  
 Coulomb field, 223  
 Coulomb force, xv, 191, 196, 198, 199,  
 308, 309, 323, 324  
 Coulomb pressure, xvi, 302, 305, 309,  
 311  
 Coulomb trapping pressure, 245  
 Coulomb's law, 1, 302, 317  
 current densities, xv, 62, 73, 96, 97, 106,  
 155, 168, 198, 199, 200, 208, 299, 300,  
 303, 313, 323, 326  
 current density, 9, 12, 15, 45, 54, 62, 73,  
 106, 107, 206, 207, 301, 324, 346, 361,  
 364  
 current eddies, 301  
 current loop, 54, 158, 300, 319, 434, 436,  
 437, 438, 439

## D

deductive approach, 1, 13  
 degenerate, 211, 212, 315

difference and sum frequencies, 245  
 dipole antenna, 157, 170, 174, 179, 181  
*dipole antenna*, 173  
 dipole selection rules, 231  
 Dirac, xvi, 191, 193, 203, 234, 242, 243,  
 314, 319, 320, 327, 340, 345  
 Dirac delta function, 242, 340, 345  
 directed power, 91, 93, 147, 174  
 direction cosine, 5, 332  
 directivity, v, xiii, 258, 326  
 driving phase, 182, 184  
 dual, 35, 139, 141, 158, 165, 191, 300,  
 301  
 dynamic equilibrium, 192  
 dynamic variable, 202

## E

eigenfunction, 209, 210, 211, 212, 220,  
 221, 222, 223, 224, 225, 228, 229, 235,  
 319  
 eigenstate, vi, xiii, xv, xvi, 192, 198, 199,  
 200, 208, 211, 212, 240, 245, 249, 260,  
 313, 314, 320, 322, 323, 324, 328  
 eigenstate electron, xiii, 192, 199, 260,  
 308, 313, 322, 323, 324  
 eigenvalues, 62  
 Einstein, 240, 242, 258, 318, 319, 320,  
 321, 326  
 electric moment, 158, 183, 184, 429, 430,  
 437  
 electrically long antenna, 78  
 electrically short antenna, xiii, 77  
 electrodynamics, 1, 9, 193  
 electromagnetic mass, 21  
 electromagnetic potential, 340  
 electron model, 192, 198, 205, 328  
 electron spin, 203, 234, 319  
 electron stream, 239  
 electrostatic force, 192, 200, 213  
 electrostatic potential, 199, 431  
 elliptical orbit, 191  
 embodiment, 142, 184, 190  
 energy absorption, 231, 314  
 energy conservation, xv, 55, 145, 199,  
 203, 228, 246, 286, 289, 296, 313, 323  
 energy emission, 231, 321

energy quanta, 318  
 energy-to-momentum ratio, 111  
 equivalent circuit, 132, 133, 134, 136,  
   139, 140, 142, 152, 167  
 exclusion principle, 192, 238  
 expectation value, 200, 201, 204, 205,  
   206, 326  
 exterior coefficient, 69  
 exterior mode, 66, 68, 96, 107  
 exterior region, 53, 54, 55, 65, 75, 100,  
   360, 365  
 extinction cross section, 44, 49, 50, 92  
 extinction momentum, 50  
 extinction power, 43, 44, 46, 92, 94, 96,  
   109, 289

## F

FDTD, 172, 173, 185, 187  
 feed network, 172, 179  
 field coefficient, 56, 59, 82, 86, 98, 104,  
   106, 167, 185, 299, 301  
 field energy, xiii, xv, 24, 35, 130, 131,  
   170, 254, 272, 279, 318, 354, 357  
 field stress, 302  
 field-associated energy density, 147  
 forbidden, 228  
 forward-scatter, 45  
 Fourier integral, 26, 200, 205, 209, 324  
 Fourier integral transform, 200, 205, 209,  
   324  
 Fourier transform pair, 341  
 Fresnel, 317

## G

gain, xiii, 160, 161, 258, 260, 265, 321  
 gamma function, 367  
 gamma power, 123  
 Gaussian wave function, 203, 205  
 generalized force, 131  
 generalized force and flow, 131, 138, 196  
 generator, 172, 179, 180, 189  
 geometric cross section, 43, 44, 46, 49,  
   91, 92  
 g-factor data, 193  
 gluons, 323

Grangier, 321  
 Green's function, 340, 347, 350

## H

half power point, 129, 357  
 Hamiltonian operator, 208, 223, 225, 226,  
   236  
 Hankel function, 29, 33, 40, 55, 75, 87,  
   99, 143, 158, 259, 263, 264, 283, 287,  
   288, 290, 365, 413, 414, 423  
 Hansen, 30, 31  
 Hansen's method, 31  
 harmonic oscillator equation, 127  
 Harrington, 258, 260, 321  
 Helmholtz equation, 27, 31, 347  
 Hertz, 239, 318  
 historic interpretation, v, xiii, 196, 319,  
   328  
 homogeneous equation, 127  
 homogeneous Maxwell equations, 14, 22  
 Huygens, 317, 318  
 hydrogen atom eigenfunction, 220, 222

## I

incomplete, 192, 205, 320, 321, 326  
 input admittance, 53, 59, 60, 61, 139  
 input impedance, 70, 71, 75, 103, 115,  
   128, 129, 131, 133, 134, 139, 140, 147,  
   152, 172, 180, 352, 354  
 input reactance, 119, 133, 135, 142  
 instantaneous power, 122, 123, 124, 173,  
   174, 175  
 integral equation, 65, 101, 347  
 integrating oscilloscope, 179  
 inter-element phasing, 176  
 Interior currents, 108  
 interior mode, 68, 73, 96  
 interior region, 54, 56, 73, 75, 99, 100,  
   108, 365

## K

kinematic properties, xvi, 22, 154, 200,  
   260, 265, 326



kinematic variable, 198  
 Kirchhoff circuit laws, 117  
 Kronecker delta function, 81, 90, 271,  
 333, 372, 405

## L

Laplacian, 10, 12, 28, 213, 214, 340, 347  
 Laplacian operator, 213, 347  
 Legendre function, 29, 30, 31, 33, 38, 54,  
 55, 56, 63, 65, 66, 67, 68, 79, 99, 106,  
 215, 221, 279, 281, 282, 374, 383, 384,  
 389, 390, 397, 402, 406, 423  
 Legendre polynomial, 40, 72, 79, 97, 221,  
 271, 274, 379, 380, 381, 382, 385, 386,  
 387, 393, 397, 401, 430  
 Lenz's law, 97, 107, 108, 300  
 Liénard-Wiechert potentials, 346  
 line admittance, 58, 59, 60  
 linearly polarized, 53, 162, 163, 176  
 local coupling, 184  
 Lorentz, 5, 317, 319, 323  
 Lorentz contraction, 4, 9  
 Lorentz frame, 8  
 Lorentz radius, 193, 253, 319  
 Lorentz transformation, 3, 5

## M

magnetic current density, 301  
 magnetic moment, xv, 97, 108, 161, 165,  
 183, 184, 191, 193, 223, 234, 235, 300,  
 313, 319, 327, 437  
 magnetic potential, 1  
 magnetostatic vector potential, 438, 439  
 Manley, xvi, 321, 323  
 Manley Rowe equations, xvi, 245, 314,  
 326  
 many-electron problem, 236  
 matrix element, 5, 155, 227, 228, 231,  
 303  
 Maxwell, 317, 318  
 Maxwell curl equation, 30, 290  
 Maxwell equations, 1, 14, 16, 22, 34, 52,  
 193, 349, 358, 359  
 Maxwell stress tensor, 17, 19, 155, 167,  
 302, 357

Mehra, 319  
 Method of Moments, 184  
 Mie, 321  
 Mie region, 50  
 Minkowski force, 7  
 modal coefficient, xiv, 67, 68, 118, 259,  
 327, 428, 433  
 modal coupling, 73, 188  
 modal impedance, 132  
 MoM, 184  
 momentum densities, 200  
 momentum space, 202, 204  
 monochromatic radiation, 318  
 monopole, 221, 436, 437  
 multi-element antenna, 176  
 multipolar electric moment, 429, 430  
 multipolar expansion, xvi, 117, 143  
 multipolar moments, 299, 301, 327, 430  
 multipolar sources, 428

## N

network analyzer, 179, 180, 182  
 Neumann function, 29, 31, 33, 56, 57, 79,  
 133, 263, 264, 265, 267, 270, 271, 274,  
 279, 282, 283, 287, 291, 294, 295, 296,  
 313, 328, 377, 409, 410, 413, 414, 423  
 Newton, 317, 318  
 Newton's law, 7, 21, 304  
 nonhomogeneous Maxwell, 14  
 nonhomogeneous Maxwell equations, 14,  
 22  
 non-ionizing transition, 225  
 nonlinear, v, xiii, xvi, 211, 246, 247, 248,  
 250, 260, 290, 314, 321, 323, 326  
 nonlinear source, 250  
 nonlocal, v, xiii, xvi, 191, 321, 322, 323,  
 326  
 normalized bandwidth, 357  
 Norton circuit, 358  
 nova-like expansion, 308  
 nucleons, 323  
 numerical solution, 52

## O

occupied state, 223, 299

oil droplet, 198  
 omnidirectional, 143, 170  
 operator form, 202, 212, 213, 228, 229  
 optical region, 50  
 orthogonal, 28, 65, 66, 67, 68, 96, 163,  
 176, 210, 211, 236, 331, 371, 385, 386

## P

parasitic coupling, 182  
 parity, 56, 86, 144, 275, 277, 323, 379,  
 389, 403, 404, 430  
 permeability, 10  
 permittivity, 11, 247, 362  
 perturbation, 223, 229, 231, 308  
 perturbation equation, 229  
 phase shifter, 172, 182  
 phase-quadrature, 115, 176  
 photo effect, 239  
 photocurrent, 239, 240  
 photoelectric effect, 242, 318  
 photon, vi, xv, xvi, 245, 251, 252, 260,  
 265, 295, 297, 313, 326, 328  
 Planck, 258, 318, 328  
 Planck's constant, 199, 203, 249  
 point mass, 234  
 power splitter, 172  
 power-frequency relationships, v, xiii,  
 xvi, 245, 250, 314, 319, 321, 323  
 Poynting vector, 19, 41, 45, 75, 76, 88,  
 118, 120, 144, 147, 150, 160, 162, 194,  
 258, 259, 261, 284, 286, 288, 295, 296,  
 298, 328, 359  
 Poynting's theorem, 41  
 principal current, 61  
 probability coefficient, 226, 229  
 probability coefficients, 229  
 probability density, 203, 236, 313  
 projectile, 317, 318  
 proper time, 6, 15

## Q

quadrilateral symmetry, 221  
 quantum electrodynamic, 193  
 quantum theory operator, 210, 213  
 quarks, 323

quasi-continuum, 240, 241, 242

## R

radar cross section, 44, 51  
 radiation pattern, 53, 151, 258, 287, 289  
 radiation Q, 127, 130, 131, 172, 177, 178,  
 179, 182, 183, 184, 187, 188, 251, 254,  
 255  
 radiation reaction force, v, xv, xvi, 191,  
 194, 195, 196, 197, 198, 245, 279, 299,  
 313, 323, 324, 326, 328  
 radiation reaction pressure, xvi, 155, 157,  
 158, 167, 169, 302, 303, 311  
 rank, 12, 17, 19, 331, 332, 334, 335, 336,  
 337, 338, 339  
 Rayleigh region, 50  
 reactive energy, 137, 174, 192, 195, 197,  
 328, 354  
 reactive radiation reaction force, 195,  
 196, 198  
 recursion relation, 263, 264, 272, 277,  
 281, 284, 286, 327, 328, 378, 387, 388,  
 390, 398, 399, 408, 412, 415  
 reflected waveform, 180, 182  
 related functions, 57, 256, 415  
 remainder, 278, 284, 285, 286  
 remarkable stability, 191, 192, 193  
 requires, v  
 resonance, 70, 129, 133, 134, 135, 167,  
 265, 356, 357  
 resonant antenna, 77  
 retarded potentials, 346  
 rigid surface, 168  
 ring charge, 74  
 Ritz power-frequency, xvi  
 Rodrigues formula, 382, 384  
 Roger, 321  
 Rowe, xvi, 321, 323

## S

scattered field, 40, 45, 49, 87, 92, 93, 95,  
 103, 299  
 scattered power, 40, 43, 44, 45, 91, 92,  
 290  
 scattering cross section, 43, 49, 91, 110

scattering parameters, 43, 180, 182  
 Schrödinger, xv, xvi, 198, 199, 203, 205,  
     206, 208, 213, 223, 225, 228, 234, 245,  
     313, 314, 319, 320, 323, 327  
 Schrödinger equation, 198, 199, 203, 205,  
     206, 208, 213, 223, 228, 245, 319  
 self-consistent field analysis, 290  
 separation constant, 28, 29, 30, 33, 214,  
     215, 375, 379, 410  
 singlet, 221  
 solar radiation, 302  
 source region, 53, 54, 273, 299, 360  
 source turn-off, 173, 175, 176, 177, 179,  
     180, 187  
 source-associated energy density, 146  
 source-free region, 24, 33  
 spherical scatter, 43, 47, 87, 91, 92  
 spherical wave, 318  
 spin wave function, 236  
 stable arrays, 198  
 standing energy density, 145, 151  
 Stark effect, 223  
 state value, 175, 210, 211, 212, 218, 221,  
     327  
 static scalar potentials, 428, 433  
 static vector potential, 433, 438, 439  
 statistical mechanics, 198, 199, 318, 321,  
     324, 327  
 Stirling formula, 369  
 stopping potential, 239  
 stored energy, 135, 137, 355, 358  
 stress tensor, 17, 19, 155, 167, 302, 306,  
     308, 332, 357  
 string theory, 193  
 surface current density, 54, 62, 73, 106,  
     364  
 surface currents, 45, 96, 108, 130, 363  
 surface power, 90, 120, 131, 258, 295,  
     296  
 surface tension, xv, 198  
 symmetric, 17, 19, 108, 183, 236, 237,  
     238, 319, 336  
 symmetric wave function, 236, 237, 238  
 symmetry, 1, 5, 33, 47, 52, 53, 54, 55, 56,  
     98, 99, 107, 117, 118, 213, 221, 236,  
     237, 238, 258, 260, 299, 318, 336, 377,  
     379, 434

## T

Taylor series expansion, 290, 428  
 TE coefficient, 54  
 TE mode, 39, 40, 82, 87, 97, 98, 106,  
     118, 119, 122, 138, 139, 140, 141, 142,  
     143, 158, 255, 257, 258, 298  
 telefield, 266, 287, 290  
 TEM mode, 53, 56, 57, 60, 61, 107, 143  
 TEM transmission line, 60  
 tensor contraction, 335  
 tensor field, 302, 334, 337  
 tensor introduction, 331  
 tensor operations, 334  
 tensor symmetry, 336  
 terminal pair, xiv, 143  
 terminator admittance, 59  
 thermodynamic, xv, 199, 200, 208, 313,  
     318, 323  
 Thévenin circuit, 115, 358  
 Thompson, 317  
 thrust, 50, 92  
 time dilatation, 4  
 time-dependent equation, xv, 206, 208,  
     314  
 time-dependent Schrödinger equation,  
     205, 228  
 time-independent equation, 207, 313, 314  
 time-independent Schrödinger equation,  
     198, 205, 208  
 TM mode, 40, 53, 61, 83, 87, 106, 107,  
     119, 122, 123, 138, 139, 141, 142, 143,  
     245, 256  
 torque, xv, 191, 313, 327  
 transient-capturing oscilloscope, 179  
 transition, vi, xv, xvi, 3, 10, 208, 225,  
     228, 231, 234, 240, 241, 245, 250, 254,  
     260, 311, 314, 319, 326  
 transmitting antenna, 52, 53, 70, 74, 75,  
     77, 78, 79, 95, 96, 98, 111, 143  
 trapping potential, 223  
 trigonometric function, 29, 80, 96, 246,  
     268, 307, 352, 371, 373, 374, 376, 423  
 triplet, 221  
 truncation, 69, 70  
 turnstile antenna, 173, 176, 177, 178, 179,  
     182, 183

**U**

Uncertainty Principle, 203, 205, 252

uniqueness, 266, 364

Uniqueness Theorem, 266

**V**

virtual shell, 133, 192

virtual sphere, 75, 88, 131, 156, 157, 167,  
172, 173, 174, 175, 184, 196, 259, 295,  
310, 348, 349, 360

virtual surface, 41, 92, 107, 157, 362, 364

**W**

wave equation, xv, 203, 318, 323, 347

wave train, 251, 252, 253, 254, 297, 298,  
307, 310, 327

waveform generator, 180

**Y**

Yee cell, 185

Young, 317

**Z**

Zeeman effect, 223

This book presents a rigorous application of modern electromagnetic field theory to atomic theory. The historical view of quantum theory was developed before four major physical principles were known, or understood. These are (1) the standing energy that accompanies and encompasses electromagnetically active, electrically small volumes, (2) the power–frequency relationships in nonlinear systems, (3) the possible directivity of modal fields, and (4) electron nonlocality. The inclusion of

## THE ELECTROMAGNETIC ORIGIN OF QUANTUM THEORY AND LIGHT

these four effects yields a deterministic interpretation of quantum theory that is consistent with those of other sciences; the quixotic axioms of the historically accepted view of quantum theory are not needed. The new interpretation preserves the full applicability of electromagnetic field theory within atoms, showing that the status of all physical phenomena — including that within atoms — at any instant does completely specify the status an instant later.